Rapporter och meddelanden nr 87



14th

Salt Water Intrusion Meeting

·SWIM·96·

16–21 June 1996
Malmö · Sweden

Convened by the Swedish IHP-Committee at the Natural Science Research Council, and organized in co-operation with the Geological Survey of Sweden, Land and Water Resources at the Royal Institute of Technology, Swedish Nuclear Fuel and Waste Management Co, and VBB Viak Consulting Engineering Firm

SGU
Sveriges Geologiska Undersökning
Geological Survey of Sweden

Uppsala 1996

Rapporter och meddelanden nr 87



14th Salt Water Intrusion Meeting

·SWIM·96·

16–21 June 1996
Malmö · Sweden

Convened by the Swedish IHP-Committee at the Natural Science Research Council, and organized in co-operation with the Geological Survey of Sweden, Land and Water Resources at the Royal Institute of Technology, Swedish Nuclear Fuel and Waste Management Co, and VBB Viak Consulting Engineering Firm

SGU
Sveriges Geologiska Undersökning
Geological Survey of Sweden

Uppsala 1996

ISBN 91-7158-572-9
ISSN 0349-2176

© Sveriges Geologiska Undersökning
© *Geological Survey of Sweden*

Printed by Gotab, Stockholm 1996

CONTENTS

Preface 5
Previous SWIM meetings 6
Sponsors 6
Photos 7

Introduction

J. van Dam — Salt Water Intrusion; Analysis, Research Needs and Opportunities 9

Basic theories – mathematical modelling

G.H.P. Oude Essink, R.H. Boekelman — Problems with large-scale modelling of salt water intrusion in 3D 16

S. Oswald, C. Schwarz, W. Kinzelbach — Benchmarking in numerical modelling of density driven flow 32

J. van Esch, A. Stakelbeek — Density depended groundwater flow near deepwell infiltration systems, Modelling aspects 41

T.N. Olsthoorn — Variable density groundwater flow modelling with MODFLOW 51

P. Vogel, K. Schelkes — Modelling of brine transport in an aquifer crossing the Gorleben salt dome: Influence of initial conditions and hydrogeological settings 61

A. Yakirevich, V. Borisov, S. Sorek — A quasi three-dimensional approach for simulating water flow and solute transport in the vadoze zone and aquifer 71

Hydrochemical characterization, chemical mixing and tracing of salt water

G. Jacks, K. Rajagopalan — Effects of past change on hydrochemistry and hydraulics in two large aquifers in S and SE Asia 79

Y. Yechieli, D. Ronen, A. Vengosh — ^{14}C study of groundwater at the fresh-saline water interface of the Mediterranean Coastal Plain aquifer in Israel 84

B. Olofsson — Salt groundwater in Sweden — Occurence and origin 91

M. Laaksoharju, C. Skårman — Multivariate mixing calculations used to trace modern Baltic Sea water intrusion at Äspö, Sweden 101

N. Karahanoglu — Use of principal component analysis in hydro-geochemical characterization of an aquifer along the Mediterranean coast of Turkey 103

Y. Yurtsever — Isotope applications in the study of processes and dynamics of groundwater salinization 111

T. Tadolini, M. Spizzico, D. Sciannamblo — Groundwater flow circuits in the Salentine karstic aquifer (Apulia, Italy) as defined by the analysis of radon concentrations 121

Investigation methodologies

W. De Breuck — Future research on coastal aquifers 126

L. Eriksson — Direct current through saline rock 130

K.–P. Sengpiel — Improved delineation of saline groundwater by airborne electromagnetics 137

J.-P. Groeztner, A. Rogge, P.-C. Scherler — Interaction of salt/fresh water flow and hydrochemical zoning in an aquifer in the Pyrmont area, SW Lower Saxony 146

L. Lebbe, E. van Houtte, F. Vanlerberghe, W. de Breuck — Quality evolution of fresh and salt groundwater pumped near a drainage canal in the Western Flemish coastal plain 157

P. J. Stuyfzand — Salinization of drinking water in the Netherlands: anamnesis, diagnosis and remediation 168

Salinization due to irrigation, road salts, waste deposits — its prevention, control and remediation

H. Gökçekus, W. Doyurans — Degradation of groundwater quality in the Güzelyurt basin, Northern Cyprus 178

J. Lindbergh, B. Olofsson, T. Gumbrich — Risk mapping of groundwater salinization using Geographic Information Systems 188

D. Ortlam — The method of pollution–tracer to measure lowest groundwater velocities in the city of Bremen 198

D. Ortlam, M. Sauer — Geogene and anthropogene salinization—phenomenons in the groundwater of Bremen 207

J. Aaltonen, G. Blomqvist — Repeatability of geoelectrical investigations 217

C. Fabricius, B. Olofsson — Salinization of private wells from de–icing chemicals — A pilote project in central Sweden 220

Regional and local case studies

M. D. Fidelibus, L. Tulipano — Regional flow of intruding sea water in the carbonate aquifers of Apulia 230

S.J.A. van Baalen, J. C. de Ruiter — The combination of the Stuyfzand-classification and Fuzzy C-Means clustering in a hydrogeochemical systems analysis of the IJssel valley, The Netherlands 241

K. Wichmann, A. Grube — Groundwater salinization in Northern Germany – New developments in research 251

G. Pranzini, A. Bencini — Groundwater salinization in southern Tuscany (Italy) 261

K. Walraevens, N. El Halimi, A. Chaouni Alia, E. Beeuwsaert, W. De Breuck — Hydrogeological and hydrochemical study of the coastal plains of Saidia and Bou–Areg (North-Eastern Morocco) 271

S. A. Sadeg, N. Karahanoglu, — Simulation of seawater intrusion in Libya 281

G.H.P. Oude Essink — Impact of sea level rise on Dutch groundwater regimes 288

S. Follin — On the simulation of saline intrusion for repository performance assessment 300

List of participants 314

SWIM programme 318

PREFACE

The 14th Salt Water Intrusion Meeting held in Malmö, Sweden, 16–21 June 1996 brought together more than 60 experts from 12 countries sharing salt water problems.

SWIM´96 started with an opening ceremony including a welcome from Bo Leander, the chairman of the organizing committee, a welcome and a formal opening by the County Governor Ann-Cathrine Haglund and introductions by Professor Malin Falkenmark and Professor Jan van Dam.

The aim of the SWIM´96 was the exchange of experience and the information on a variety of aspects such as intrusion of sea water in coastal areas, occurrence and origin of relict salt water, pollution of fresh water aquifers from road salts, industries and waste deposits, methodologies for evaluation and prognoses of salinization of aquifers, methods of tracing salt water wells and methods for mitigation of salt water problems.

After the meeting in Malmö a field excursion was arranged to the southeastern part of Sweden and the Äspö Hard Rock Laboratory. The research in the Äspö HRL is focused on questions concerning the Precambrian bedrock and its condition for hosting a nuclear fuel waste repository. In particular movement and chemical composition of the groundwater are studied in-situ. The facility consists of a reseach village and a tunnel 3,600 metres in length down to a depth of 450 metres. In the new report *10 years of research*, that was presented to the participants, most of the main results from Äspö are shown.

The UNESCO Interdisciplinary Working Group for "Coasts and Small Islands" had placed a meeting in connection with the conference. Some of the SWIM-participants joined the two days meeting.

The SWIM´96 was convened by the Swedish National Committee for International Hydrological Programme at the Natural Science Research Council and organized in co-operation with the Geological Survey of Sweden, Land and Water Resources at Royal Institute of Technology, the Swedish Nuclear Fuel and Waste Management Co and VBB Viak Consulting Engineering Firm.

During the conference and the excursion all the participants stayed at the same hotel which made it easier for the important social contacts. Many different common activities such as dining together and the receptions contributed to the SWIM-feeling.

This volume contains the papers and posters presented at the SWIM´96 and we hope it will help to preserve the achievements of the meeting.

August 1996

Organizing Committee for SWIM´96

Bo Leander Chairman	Iréne Johansson, Executive Secretary of IHP
Lars O. Ericsson	Ove Gustafsson
Carl-Fredrik Müllern	Bo Olofsson

Salt Water Intrusion Meetings

1968		Hannover, Germany
1970	May	Vogelenzang, The Netherlands
1972	June	Copenhagen, Denmark
1974	August	Ghent, Belgium
1977	April	Medmenham, England
1979	October	Hannover, Germany
1981	September	Uppsala, Sweden
1983	May	Bari, Italy
1986	May	Delft, The Netherlands
1988	May	Ghent, Belgium
1990	May	Gdansk, Poland
1992	November	Barcelona, Spain
1994	June	Cagliary, Italy
1996	June	Malmö, Sweden

SWIM'96

SPONSORS

Department of Environmental and Public Health Protection, Malmö
Department of Land and Water Resources, KTH, Stockholm
Department of Public Works, Malmö
Freds Trend, Malmö
Geological Survey of Sweden
Geotec
Gothenburg Biscuit
Kemira Kemwater AB
Malmbergs i Yngsjö AB
PL-Photo, Malmö
Swedish National Committee for IHP
Swedish Nuclear Fuel and Waste Management Co
The City of Malmö
The Town of Kalmar
Vattenteknik AB
VBB Viak AB



1. Poster session



2. Underground visit, 450 m below sea level, at Äspö Hard Rock Laboratory.



3. Discussions the day after an important football game.



4. Malmö City Hall banquet.



5. Dinner at the Malmö Town Hall Cellar.



6. Dutch collegial discussion.

Salt Water Intrusion; Analysis, Research Needs and Opportunities

prof.dr.ir. J.C. van Dam
emeritus professor of Delft University of Technology
Delft, the Netherlands

Looking backward

The first SWIM took place in 1967 in Hanover, very informal, at the initiative of the late dr. Richter of the Bundesanstalt für Bodenforschung, presently Bundesanstalt für Geowissenschaften und Rohstoffe. Only three countries were represented, Germany (ca. 12), the Netherlands (3) and Denmark (1). Dr. Richter and his co-workers were confronted with the problem of salt water intrusion in the northern part of the Federal Republic of Germany and some of his co-workers had experiences abroad. Rightly he felt that an exchange of experiences would be useful. We decided that such a meeting should be repeated some two years later. The second meeting took place in the Netherlands in 1970. Since then more and more European countries became involved, and with intervals of two and incidentally 2½ years we had a SWIM. This term was introduced by prof. De Breuck who organized the fourth SWIM in Ghent, Belgium. There was always a country, sometimes even more than one, which volunteered to organize the next SWIM. So, after several meetings around the North Sea, we met also near the Baltic Sea, in Uppsala, and in Gdansk, and the Adriatic Sea, in Bari, and the Mediterranean in Barcelona and Cagliari. The papers presented did not only relate to Europe. Some European participants presented their experiences in other continents and incidentally we had participants from other continents, with and without papers. They were and are still most welcome. Time and again we concluded that we should continue. The number of participants was rarely below fifty and never over hundred. With these numbers it was possible to have good discussions during the meetings and moreover to have good personal contacts. The SWIM-participants have become good friends and young coming men came in and felt at ease in this informal group. Though we have seen great developments in the investigations and research, the practical problems have increased considerably during the past decades. This is due to increased abstraction of fresh groundwater and the delayed effects thereof.

From the very beginning the contributions to the SWIM in the form of papers and posters have been subdivided into, mostly, six categories, which can roughly be described as follows:

- cases,
- geophysical methods,
- hydrochemical and isotope studies,
- modelling,
- prevention, control and remediation,
- special subjects, such as studies on the (changing) sub-soil properties, other sources of salt, non-conventional techniques of salt water intrusion abatement (e.g. with electric currents) or fresh water recovery from submarine springs in karstic areas.

As, in this keynote, I would like to present my views on the future rather than to look back, I will be brief in my review of the past and give only very concise comments on what we have heard and seen in these categories during the past decades, just as a starting point for my prophecies about the future.

Category 1, "Cases", has always been well represented. Interesting, but often ending with problems and not always with solutions, which was not always possible, either by lack of data or uncertainty, or simply because the situation was spoiled and could not be restored for technical or economic reasons.

Category 2, "Geophysical methods", was usually small. Electrical resistivity prospecting was known and applied from the very beginning. We have seen improvements in geophysical well-logging and the introduction of electromagnetic methods, which are easy to carry out, but have another resolution than the electrical resistivity methods.

Category 3, "Hydrochemical and isotope studies", was there from the very beginning. In the beginning the number of papers was modest. The number of elements considered was only small and the conclusions that could be drawn and have been drawn were only limited. At present this is a category of big growth.

Category 4, "Modelling", shows even more growth. In the first SWIM we saw sets of differential equations for fresh and saline groundwater in one-dimensional horizontal flow in steady state with a sharp interface. As analytical solutions were either impossible or too complex the differential equations were solved numerically by the first computers. No need to say that the computer technique has developed progressively and that two-dimensional transient problems with gradually varying densities are common practice now and that realization of the dream of models which can handle 3D transient cases with gradually varying densities and even accounting for chemical reactions is not far off. In the mean time a new approach, the analytic element technique, has come up and will compete with the customary finite difference and finite element methods.

Category 5, "Prevention, control and remediation", is perhaps the most important one because, in contrast to the categories 2, 3 and 4 which are the more scientific ones, this relates to the practical application of measures and their results. Perhaps our group hosted more scientists than practitioners, because this important category is somewhat lagging behind.

Category 6, "Special subjects", has always been small and diverse, but interesting.

It should also be noted here that the legislative and socio-economic aspects have rarely been discussed here and if so, it was only as a side-aspect.

Looking forward

After the foregoing concise description of the development and the present state in the six categories, we will now see what the prospects are.

Without adequate human interference the practical problems will increase for the following two reasons. The increase of the world population and the growing water demand per capita makes that more fresh groundwater is needed. This alone makes the problem of salt water intrusion even more pressing than at present. The second reason is that even without any further increase of the abstraction of fresh groundwater and reclamation of new land in coastal areas, the present situations will generally continue to deteriorate for a long time ahead due to the time lag between previous and ongoing causes and their effects. Even in case the present situation just continues, the ultimate dynamic equilibrium will often be unacceptable. Then, wells and well-fields will have to be abandoned. This implies that measures have to be taken, based on the lessons learned so far, on the results of field studies and on calculations. Thus more work of the same nature. This makes that any measure that leads to better, faster and/or cheaper results is welcome. This holds primarily for the exploitation of the groundwater, but evidently also for the preceding studies and their scientific bases.

Research needs and opportunities

Climate change and sea level rise

In the past the climate has changed continuously and slowly. This holds also for the natural recharge of groundwater. The relative movement of the mean sealevel with respect to the land surface is partly due to climate changes and partly due to tectonic forces. Due to the delayed effects of these slow natural processes in terms of the distribution of fresh and saline groundwater, a state of dynamic equilibrium has not yet been reached in many cases. At present the climate change is strongly believed to be accelerated due to human activities. Despite the fact that, world-wide, much attention is paid to climate change and its direct consequences, little attention has been paid, so far, to the impacts of changes in the water balance terms and in sea level rise on the groundwater regime in coastal areas and small islands. Though the impacts of such changes will take place gradually, their delayed effects can be considerable in the distant future. Therefore it is recommended to start, now already, studies for orientation on what might happen in terms of salt water intrusion and on the sensitivity of the results for the underlying assumptions, the uncertainty in the (geo)hydrologic data and the stresses by human activities. The results of such studies indicate where to concentrate upon in data collection and groundwater monitoring.

Time lags

As was mentioned before, the time lag between cause (groundwater abstraction, landreclamation) and effect (salt water intrusion) can be great, in the order of decades or even centuries. This has two aspects. A favourable one is that there is mostly no immediate danger and thus time for study and for implementation of measures, which however entails the danger that such studies are postponed too long. The other side of the medal is the unfavourable fact that the effects of countermeasures or compensating measures will also be delayed. If such measures are taken late they should be more rigourous; if they are taken too late the situation may even be spoiled. Restoration may still be possible, but only after reduction or even interruption of the abstraction of fresh groundwater and/or relocation of groundwater abstraction works, which is at least costly. This leads to the recommendation to study the present transient situation and, based on the results, to design and execute adequate measures.

Sustainability

The term sustainability, introduced in 1987, in the Brundtland report, is not sharply defined because it relates to an infinite variety of subjects and conditions, but yet the principle is well understood. It can also be applied to the dynamic equilibrium between fresh and saline groundwater. In any particular situation with a known natural recharge, supplemented or not by artificial recharge, one can never abstract more than the mean annual recharge. The fraction of the total mean annual recharge that can be abstracted sustainably depends on the location of the abstraction wells in relation to the geometry of the aquifer and on the variation of the rates of recharge and abstraction over the year and even from year to year. The greater the mean rate of abstraction the smaller the volume of fresh groundwater in store and the greater the risk of failure in periods of small recharge and/or great demand. This leads to an interesting problem of risk assessment, followed by a decision problem. If a decision is made where the required mean volume of fresh groundwater in store is smaller than the present volume, the difference can partly be consumed, which is acceptable mining. The other part will disappear as discharge by natural outflow. In the opposite situation, where the present volume of fresh groundwater in store is smaller than the required mean volume, the aquifer should be restored by increased rates of (artificial) recharge. It may be clear that the choice to be made requires

calculations, based on data which must first be collected if not yet available. The result will certainly be rewarding for the society and give satisfaction to the various scientists who study this optimization problem.

Storage

The mentioned optimization problem will be even more complex and interesting in case the annual cycles of abstraction and recharge (including artificial recharge) are out of phase because of seasonal variations of the demand (irrigation, tourism) and the available quantity of water of good quality for artificial recharge (if any). Then the volume of fresh water in store will vary over time, either regularly or irregularly. These changes manifest themselves by fluctuations of the phreatic groundwater tables and even more by vertical displacements of the transition zones between the fresh groundwater and the underlying saline groundwater. These displacements lead to a higher degree of mixing of the fresh and saline groundwater in the transition zone, unavoidably resulting in a percentage of loss of the recharged fresh water. The results of some interesting experiments have already been reported in previous SWIM's. These results are certainly dependent on the variations of the abstraction and recharge regimes and on the local subsoil properties. So, in my view, there will be ample scope for more such experiments and studies under various conditions.

Conjunctive use of surface and groundwater

In the light of the foregoing considerations with respect to the fluctuations over time of demand and recharge and the resulting fluctuations in storage of fresh groundwater it may be worthwile to study conjunctive use of surface and groundwater. This widens the scope of the groundwater experts, who then have to cooperate with surface water experts and with systems experts who can assist in the determination of optimal solutions. One step further and we enter the domains of integrated water management and environmental issues. These will be left out of consideration in this lecture.

Skimming wells

Skimming wells have been applied where the thickness of the fresh groundwater lens is only thin, which is mostly the case in local lenses of small lateral extent. In such cases skimming wells were applied in reaction to upconing of saline groundwater in wells which were to heavily pumped. Thus the application of skimming wells is based on the practical experience that in such cases it is better to pump at moderate or low rate in a great many of wells at short spacings and at small rates of pumping than in only few wells at greater distances and at high pumping rates. This experience should be kept in mind when projecting new well-fields under such circumstances.

Scavenger wells

Scavenger wells are applied to abstract saline groundwater below the interface or transition zone with the pumped fresh groundwater in the upper part of the same aquifer. When pumping the saline groundwater at a properly adjusted rate, upconing of saline groundwater under and into the fresh water wellscreen is avoided. This is a good solution, provided that the vertical distribution of the salinity is continuously monitored and the ratio of the pumping rates of the fresh and the saline water are adjusted accordingly. A practical problem might be how to dispose of the saline water, as the local water authorities may not allow the discharge of saline groundwater into fresh surface waters and saline surface waters may be too far away. Desalting could be a technical solution, but it is

questionable whether the costs are justified. So far only few applications of scavenger wells to control the salinity distribution under a pumped well have been reported. In cases of scarcity of fresh water it may in some places become necessary to resort to scavenger wells. The exploitation of such wells must be based on continuous monitoring and will be a matter of practical adjustment rather than of scientific research.

Abstraction of saline groundwater

In contrast to scavenger wells, which are applied in combination with individual abstraction wells and which are effective below and in the immediate vicinity of such wells, the designation "abstraction of saline groundwater" relates to large scale abstraction of saline groundwater in thick and large aquifers. By drawing down the piezometric level of the saline groundwater by pumping, the piezometric level of a thick layer of fresh groundwater in the upper part of the same aquifer will also be drawn down. This implies that the seaward gradient of the fresh water head will decrease and therewith the outflow of fresh groundwater, which otherwise is a loss. The gain is the recovery of fresh groundwater which would otherwise be lost. The price to be paid for it is the installation, exploitation and maintenance of the deep wells for the salt water abstraction. Again the disposal or desalting of the saline groundwater is a matter of serious concern. In case of desalting the products are an additional source of fresh water and a much smaller volume of highly concentrated brine. An interesting problem will be to optimize the location and the capacity of the abstraction wells in particular cases. So far no practical cases have come to my knowledge. The more pressing the demand for fresh water, the more the abstraction of saline groundwater will come to the fore as a possible means to increase the exploitable fresh water resources.

Modelling

After the foregoing review of the achievements in this category one may question when and in what stage this development comes to an end. With the rapidly increasing capacities and speeds of the computers we will soon be in a position that the bottle-neck is no longer in the computer capacity but in the available data and the uncertainty of the many types of spatially varied input data. This is not as bad a situation as it looks like. When making different assumptions for the missing or uncertain data one can check the sensitivity of the model solutions for the various parameters and thus learn where to concentrate the field-work on. This can save a lot on the expenditure for the high costs of boreholes, pumping tests, etc. and to a lesser extent of the less expensive geophysical exploration techniques.

Geographical Information Systems

Geographical Information Systems (GIS) have been developed during the last two decades for application in a large variety of subjects. As in saltwater intrusion problems both the input and the output data are geographically distributed, GIS appeared to be a useful tool for our problems as well. This is an opportunity. The latest development is a coupling of a GIS with a numerical groundwater model or, in our case a salt water intrusion model.
Several cases have already been reported and undoubtedly this will soon become current practice.

Artificial neural networks

Like GIS, artificial neural networks (ANN) are a new opportunity. The rather sophisticated theory of ANN has been developed only recently in the domain of artificial intelligence. An ANN is trained to reproduce a given set of output vectors for a corresponding set of input vectors. These vectors may represent values of physical parameters (e.g. flows) or patterns of numbers (e.g time series). ANN are able to simulate almost any complex physical system, even if the governing equations of the system are not well defined. If a relationship between input and output data is unknown, but acknowledged to exist, an ANN can be trained to learn that relationship to a high degree of accuracy. So ANN might compete with traditional (geo)hydrologic modelling. This opportunity should be further explored in order to be able to judge whether this is the case indeed, to what extent, under what conditions and what limitations there are.

Chemical composition, trace elements and isotopic properties

As mentiond before studies of the chemical composition and isotopic properties of groundwater have been presented from the very beginning of the SWIM. Since then the number of elements, trace elements and isotopes studied has increased due to improved resolution of existing and new detection methods. The results can learn us from where the sampled water originates, how old it is and what exchange processes have taken place. The results should, of course, be in agreement with the present and past flow patterns and with the results of the numerical modelling of the groundwaterflow. If so the different methods of study corroborate one another. Regrettably this was and is not yet always the case. Therefore it is necessary to analyse the reasons for such discrepancies before any definitive conclusion can be drawn. The results of such studies can lead not only to better and correct pictures of the situations under consideration, but also to improvement of the different methods of investigation.

Remote sensing

Remote sensing has first been developed for military purposes. As such the techniques and results were classified. Since the late sixties remote sensing has become available for civil applications as well and since then the resolution of the various techniques has increased considerably. It is true that remote sensing gives images of the land and water surfaces and not directly of the subsoil, our domain. However the features of the surface: topography, drainage patterns, geologic structures such as faults, and the vegetation give at least some indication of what structures and conditions one may expect in the subsoil and incidentally even in terms of the depth and/or the salinity of the groundwater. In speakers view this additional information is not yet fully utilized in field studies. Therefore it is strongly recommended to take advantage of this source of additional information.

Socio-economic aspects and communication

Salt water intrusion can have great socio-economic aspects. For instance, if wells have to be abandoned because of upconing of salt groundwater there is not only damage through loss of invested capital but also the socio-economic aspect that the water supply for domestic use, agriculture or industry is in danger. Failures which have occurred could have been prevented by proper measures in terms of land use planning and rules for proper groundwater management. Therefore it is necessary that the various experts

- cooperate to describe the present situation and to develop plans for restoration, where needed, and exploitation and control of the groundwater systems, and

- subsequently convince the gouverning authorities to ensure the execution of their proposals as an investment to garantee a sustainable exploitation of the groundwater resources.

Opportunities

It is not surprising that recently a number of initiatives has been launched (not yet implemented!) to pay more attention and to take action to prevent and where necessary to restore situations where the limits of sustainability have been exceeded. To mention a few:

a. Two years ago, at the 13th SWIM, in Cagliary, mr. Pallas of FAO and myself reported about an expert meeting held in 1993 in Cairo, at the initiative of FAO, to draw attention to the problem of salt water intrusion, its technical, legislative and socio-economic aspects, which resulted in a recommendation to install pilot projects where all relevant aspects could be studied, resulting in practical solutions. This of course requires funds and time. The funds should be provided by all interested parties and not only or predominantly by organizations as FAO and UN.

b. The recently launced EC plan to set up a Task Force "Environment. Water", which has a budget and intends to work along the following four foreseen axes:
   - fight against pollution,
   - rational use of water,
   - fight against structural deficits,
   - prevention and management of crises (e.g. droughts).

   The Task Force will work out the plan.

c. The new UNESCO programmes "Environment and Development in Coastal Regions and Small Islands" (of UNESCO's Division of Hydrology) and "Maintaining and Managing Coastal Ecosystem Productivity for the Sustainable Development of Human Communities" (of UNESCO's Human Habitat Unit) offer a nice opportunity to bring together hydrologists, urban sociologists, architects and townplanners and to draw their attention to, among others, the problem of salt water intrusion and how to prevent it. To that aim UNESCO invited some experts from those circles to attend the present SWIM and to engage a dialogue with SWIM and SWIMers.

These are opportunities which we, the SWIM-community, should pick up. We, scientists and some practitioners, should present our gospel to a wide audiance and convince colleagues from other disciplines and decisionmakers that it pays off to invest in measures to prevent further salt water intrusion and to restore situations which have already been spoiled or are on the way to be spoiled and thus to take the necessary technical and legislative measures, based on field investigations and research.

SWIMeetings

Coming to the end of this keynote-lecture do I need to ask whether we should have come to an end with SWIM? I do hope and expect to have convinced you that there is still a long way to go for us, but also to widen our scope in the sence that we should present our results and messages better to those who need them and who do not always realize that there exist salt water intrusion problems, but fortunately also solutions.

Problems with large-scale modelling of salt water intrusion in 3D

G.H.P. Oude Essink and R.H. Boekelman
e-mail: g.oude.essink@ct.tudelft.nl and r.boekelman@ct.tudelft.nl
Delft University of Technology, Faculty of Civil Engineering,
Hydrology & Ecology Group, P.O. Box 5048, 2600 GA Delft, the Netherlands

Abstract

In this paper, the restrictions of three-dimensional (3D) modelling of salt water intrusion in large-scale coastal (homogeneous) aquifers are discussed. Computer codes, of which the solution of the advection-dispersion equation is based on standard finite element or finite difference techniques, cannot yet be applied to model large-scale coastal aquifers. The reason is that these codes must satisfy a condition of spatial discretization, characterized by the so-called grid Peclet number. This number imposes that the dimension of the grid block should be not greater than a few times the magnitude of the longitudinal dispersivity, as otherwise numerical dispersion will occur. In addition, stand-alone personal computers are not yet fast enough to execute models with several hundreds of thousands of grid blocks. Finally, reliable and sufficient groundwater data, required for calibration and verification, are not available in most cases. In conclusion, 3D-modelling of salt water intrusion in large-scale coastal aquifers is technically possible within some years, though the availability of data will always restrict practical applications to a certain extent.

1. Introduction

In this keynote-paper, the following topics should be discussed: intrusion of seawater, basic theories, analytical approaches, hydrodynamics, steady-unsteady state solutions, and finally, mathematical modelling. It is, however, not possible to treat all these topics within a concise paper. Therefore, only one topic, which is becoming more and more relevant, is discussed extensively: *problems with three-dimensional modelling of salt water intrusion in large-scale coastal aquifers.* Large-scale coastal aquifers are defined here as aquifer systems along the coast of several tens to a few hundreds of square kilometres. In these systems, mostly non-uniform density distributions occur.

Developments in modelling are mainly caused by the (still ongoing) breakthroughs in computation technologies and the increased possibilities of personal computers. The devices and tools, such as sophisticated graphical modules, pre- and postprocessors, are already available on the market. Now, knowledge on and experience with 3D-modelling must follow. In addition, many geo(hydro)logic events in coastal aquifers where mostly non-uniform density distributions occur should nowadays be simulated more accurately than they have been simulated up to now. For instance, the effect of different deep-well infiltration scenarios or the salinisation of fresh groundwater resources due to overpumping should not be simulated anymore with only (3D) sharp interface models or 2D solute transport models. Instead, 3D-modelling of salt water intrusion, which is based on density dependent groundwater flow and solute transport, is required.

Some people may think that around the turn of the millennium, the possibility to model, to simulate and to visualise 3D flow of groundwater and 3D transport of salt and other hydrochemical constituents is common practice. However, the near future is probably less favourable, because, in practice, 3D-modelling of salt water intrusion in large-scale coastal aquifers is restricted. In this paper, aspects of the three most important restrictions are discussed. First of all, in order to suppress *numerical dispersion*, which occurs in solutions techniques with the standard finite element method (fem) and the standard finite difference method (fdm), the dimension of the grid block must be small. This means that large-scale geometries can only be modelled with an enormous amount of grid blocks. Second, 3D-modelling of large-scale geometries is restricted by the memory allocation and the speed of the computer: this is called the *computer problem*[1]. Third, there is the *data availability problem*, as 3D-modelling requires a large amount of data sets for calibration and verification, whereas reliable data sets are, in practice, rare.

[1]Note that we are talking about the problems for geo(hydro)logists in daily practice. This means that personal computers are in question instead of (fast) workstations, supercomputers or even Cray computers.

In section 2, different types of salt water intrusion models are discussed. In section 3, the mathematical formulation of salt water intrusion is given by means of the solute transport equation. In section 4, some solution techniques are summarized. In section 5, some 3D salt water intrusion models are shortly discussed. Then, the discussion follows on the three problems: the numerical dispersion problem in section 6; the computer problem in section 7; and the data availability problem in section 8. Finally, some conclusions are drawn.

2. Types of salt water intrusion models

In the past, the behaviour of density dependent groundwater flow has been investigated by means of analogue models as well as by means of analytical models. However, since computers appeared on the scene, mathematical models[2] gained ground. At present, a large number of mathematical models is available, capable of handling fresh and saline groundwater flow in aquifer systems. The U.S. Geological Survey is the leading institute in developing 2D and 3D groundwater flow models. Important distributors of affordable computer codes are, among others, the International Ground Water Modeling Center [IGWMC: Golden, U.S.A., 1995] and the Scientific Software Group, Washington D.C., U.S.A. [1995]. Reviews of literature on fresh and saline groundwater and available computer codes and models are given in e.g. Reilly & Goodman [1985], Custodio *et al.* [1987], Strack [1989] and Maidment [1993]. Obviously, all preceding SWIM-proceedings comprise a large number of case studies with different kinds of models.

2.1 Two-dimensional versus three-dimensional models

Two-dimensional groundwater flow models, which also simulate solute transport, require quite some effort before they are completely understood. Although they can be applied in various situations, the practical application is rather limited. The most important restriction of these models is obviously that only cross-sections can be simulated. Therefore, a proper cross-section should be carefully selected.

In many cases, however, groundwater flow perpendicular to the coastline is disturbed in such a way that the schematisation and modelling of the actual situation by a cross-section cannot be allowed any more. Such situations occur for instance in polder areas where the controlled phreatic groundwater levels lead to radial flow patterns, at areas with complex geohydrologic geometries or in the vicinity of singular wells where groundwater is extracted or infiltrated. Under those circumstances, 3D-models should be applied to simulate density dependent groundwater flow. Obviously, 3D-models naturally require even more effort to be understood, implemented and utilised effectively than 2D-models. For instance, the problems that arise to visualise 3D groundwater flow and solute transport on a 2D (color) monitor should not be underestimated. Moreover, the *numerical dispersion problem* will also restrict the practical application of 3D salt water intrusion models (see section 7 for further discussion). The application of these 3D-models on a broad scale is still at an early stage of development.

2.2 Sharp interface model versus solute transport model

Sharp interface models are based on the assumption that a sharp interface between fresh and saline groundwater represents the actual situation. This is the well-known *Badon Ghyben-Herzberg principle*. The straightforward sharp interface models can be applied as an educational means to gain a clear insight in the behaviour of fresh and saline groundwater in coastal aquifer systems. As such, sharp interface models are still widely applied, which can be deduced from many papers, presented during the preceding Salt Water Intrusion Meetings. Nevertheless, restrictions on the applicability of the principle should be considered:

a. First, the principle only approximates the actual occurrence of fresh, brackish and saline groundwater in the subsoil. In fact, the brackish zone between fresh and saline groundwater should only be schematised by a sharp interface when the maximum thickness of the brackish zone is in the order of several metres only. This condition applies only in rare situations where the freshwater lens is evolved by natural recharge, as occurs in sand-dune areas or in (coral) islands.

[2] *"A mathematical model simulates groundwater flow indirectly by means of a governing equation ··· to represent the physical processes that occur in the system."* [Anderson & Woessner, 1992].

b. Second, the principle assumes a hydrostatic equilibrium, whereas in reality the aquifer system might considerably deviate from this equilibrium situation. In those cases, e.g. in freshwater bodies near the shoreline, the Badon Ghyben-Herzberg principle should not be applied, because the computed position of the sharp interface significantly deviates from the actual position as the coast is approached.

In many coastal aquifer systems, a relatively broad transition zone between fresh, brackish and saline groundwater is present because of various processes during geological history. In addition, the transition zone is also increasing as a result of the circulation of brackish water due to inflow of saline groundwater, the tidal regime and human activities, such as (artificial) recharge and groundwater extraction at high and variable rates. Under such conditions, more sophisticated models are required than just models with expressions for sharp interfaces: namely models which take into account variable densities. In this paper, these models are referred to as *solute transport models* or *salt water intrusion models*. They apply the advection-dispersion equation to convert solute concentration (or total dissolved solids) to density. They are able to simulate, among others, changes in solute concentration (e.g. near pumping wells due to upconing), changes in volumes of freshwater in sand-dune areas and changes in the salinity of seepage in low-lying polder areas. As solute transport models usually apply numerical schemes, they can also be utilized to simulate aquifer systems with complex geohydrologic geometries and inversions of fresh and saline groundwater.

3. Mathematical formulation of solute transport

The three-dimensional equation for solute transport in homogeneous isotropic porous media can be written as follows:

$$\frac{\partial C}{\partial t} = \frac{\partial}{\partial x_i}(D_{ij}\frac{\partial C}{\partial x_j}) - \frac{\partial}{\partial x_i}(C\,V_i) + \frac{(C - C')\,W}{n_e} + \frac{\Psi}{n_e} \qquad (1)$$

where

- C = concentration of the dissolved solutes ($M\,L^{-3}$),
- t = time (T),
- D_{ij} = coefficient of hydrodynamic dispersion (see section 6) ($L^2\,T^{-1}$),
- $V_i = q_i/n_e$ = effective velocity of the groundwater in the direction of x_i ($L\,T^{-1}$),
- C' = concentration of the dissolved solutes in a source or sink ($M\,L^{-3}$),
- $W(x,y,z,t)$ = general term for sources and sinks (T^{-1}),
- n_e = effective porosity of the medium ($-$),
- Ψ = chemical reaction source or sink per unit volume ($M\,L^{-3}\,T^{-1}$). It includes equilibrium-controlled sorption or exchange and first-order irreversible rate (radioactive decay) reactions.

Equation 1 is called the *solute transport equation*, the *advection-dispersion equation* or the *transport-dispersion equation*. The first term on the right hand side represents the change in concentration of solutes due to hydrodynamic dispersion. The second term represents the effect of advective transport which is the movement of solutes attributed to transport by flowing groundwater. The third term represents the contribution and removal of solutes due to fluid sources and sinks, whereas the fourth term represents chemical reactions. With regard to the transport of a conservative solute, viz. salt, Ψ is assumed to be equal to zero.

4. Solution techniques

Various solution techniques have been developed to solve both the groundwater flow equation and the (complicated) solute transport equation. Computer codes with suitable solution techniques are already available since at least two decades. In this paper, some solution techniques will be mentioned briefly:

- Analogue method
  Analogue models have been applied to investigate the behaviour of density dependent groundwater. Analogue models are based on the fact that several physical processes are governed by equations that are similar to the equations of groundwater flow. As such, these processes are analogous with groundwater flow. If such a process can easily be realized and measured, it can be applied to study groundwater flow in a specific situation through interpretation and translation of the physical constants towards groundwater flow constants. Unfortunately, in most cases analogue models cannot be applied for simulating the movement of contaminants in groundwater. Well-known analogues are the Hele Shaw model, the membrane model, the thermal model and the electric model.

- Analytical method
  Analytical models[3] are based on (e.g. Laplace) transformations and the hodograph method (by means of conformal mapping). In addition, an effective approach was to derive analytical formulas from analogous physical processes. The similarity between groundwater flow and conduction of heat in solids appeared to be very convenient [e.g. Carslaw & Jaeger, 1959]. In this physical process, several analytical solutions are similar to those for groundwater flow in aquifers. The application of analytical models is limited as analytical solutions are only available for relatively simple problems (e.g. homogeneous aquifers, 1D or 2D, steady-state, sharp interface). Unfortunately, analytical solutions are very rarely available for problems with density dependent groundwater flow, of which the solute transport is governed by means of the advection-dispersion equation. Such a rare case is Henry's problem [1964], where saline water intrudes in a hypothetical rectangular aquifer and merges by a constant dispersion coefficient. Henry's case is a benchmark for 2D groundwater flow models that can simulate solute transport and density flow [Segol, 1994][4].

- Analytical element method
  This method is based on the theory of Strack [1989]. Analytical solutions are determined for head and discharge that satisfy the governing flow equations and specified boundary conditions within the aquifer. The most important advantage over conventional numerical methods is its lack of a fixed grid. As such, it is possible to extend the model any distance to incorporate regional features without sacrificing accuracy in the area of interest. Moreover, refinement of the discretization and zooming into a local problem can easily be accomplished.

- Finite difference method (fdm)
  This well-known method is one of the oldest and most widely used methods. It is based of the Taylor series expansions in order to determine approximations of the first and the second derivatives of the parameter in question. This method is not often used for solving the advection-dispersion equation because numerical dispersion can easily develop in the finite difference scheme[5]. For more information, see Konikow & Bredehoeft [1978]; and Kinzelbach [1987a].

- Finite element method (fem)
  This numerical method (already applied in the early 1950's to problems of solid mechanics) is a very well-known method to solve the governing partial differential equations. An advantage of this method is that it is easier to change a finite element grid than a finite difference grid, because the nodes can be added very easily in the finite element grid without redesigning the entire grid. As such, a fem is preferred to a fdm, if the exact representation of the boundaries is important. It goes beyond the scope of this paper to describe this method, however, relevant information can be found in Zienkiewicz [1971]; Pinder & Gray [1977]; Kinzelbach [1987a] and Bear & Verruijt [1987].

- Method of characteristics
  This method can be applied in salt water intrusion problems to solve the (hyperbolic) advection-

[3] Also the vortex theory has an analytic character. It solves groundwater flow in combination with a sharp interface.

[4] It appears that currently no method has succeeded in reproducing Henry's steady state solution. Henry solved the equations with the Galerkin technique by using Fourier series. The inaccuracies of Henry's results are probably a consequence of the limited computer facilities at the time [Segol, 1994].

[5] There appear to be (five point) finite difference schemes which also take into account the second order approximation. As such, numerical dispersion and oscillations do not occur.

dispersion equation for groundwater flow. By decoupling the advective and the dispersive component of the equation, and solving them sequentially, numerical dispersion can be suppressed to a large extent. Moving points are introduced in this method, namely particles, that can be traced through the flow field within the stationary coordinates of the finite difference grid. This process is called *particle tracking*. For more information, see Garder, Peaceman & Pozzi [1964]; Konikow & Bredehoeft [1978]; and Kinzelbach [1987a, 1987b].

- Random walk method
  The random walk method also uses the particle tracking method. Each particle represents a fixed mass of pollutant. Both the advective and the dispersive transport are represented by particle movements. The first step in the procedure is to follow particles along the direction of the flow field while the second step consists of adding a random movement by means of statistical properties in order to take into account the dispersive transport. Only the superposition of the particle paths and the counting of mass reveals the concentrations in each grid cell of the overlain grid. The random walk method can be used to simulate groundwater contaminant transport at great Peclet numbers (see section 6.1). An advantage of this method is that particles are only introduced where contaminants are present. For more information, see Kinzelbach [1987a, 1987b]; and Uffink [1990].

It appears that most of the salt water intrusion models are based on the fem or the fdm. At present, however, the method of characteristics and the random walk method come to the front. These methods can more easily simulate the flow of groundwater in combination with the (complicated) transport of solutes without (numerical) dispersion problems (this problem will be discussed in section 6).

5. Three-dimensional salt water intrusion models

There are already quite a few 3D computer codes available which can cope with salt water intrusion in coastal aquifers. Here, a selection of some codes is given:

- HST3D [Kipp, 1986] is a 3D finite difference code that can simulate heat and solute transport. Ossenkoppele [1993] showed that modelling the sand-dune area of Amsterdam Waterworks along the Dutch coast (dimensions: 12,000 · 20,000 m^2 by 160 m) with HST3D appeared to be rather complicated. Large dispersivities (e.g. α_L=200 m) had to be applied as otherwise the solute transport equation does not converge to a solution. As a consequence of simulations with great dispersivities, excessive hydrodynamic dispersion created extensive and unrealistic brackish zones which do not agree with the actual situation.

- SWICHA [Huyakorn *et al.*, 1987; Lester, 1991] is a 3D finite element code. It can simulate variable density fluid flow and solute transport processes in saturated porous media. The applications range from simple one-dimensional to complex three-dimensional, coupled flow and solute transport. The groundwater flow and solute equations are solved by the Galerkin technique. An implicit Picard iterative scheme is applied to treat the nonlinearity of the problems. For a transient solution of the seawater intrusion problem, the Crank-Nicholson time step scheme is applied to handle the temporal discretization. Spatial discretization is performed using rectangular or triangular elements. The solute transport equation may not converge to a solution, if a so-called *critical Peclet number* is exceeded in a grid block. In order to solve this problem, SWICHA offers a trick at the user's option: numerical dispersion (the so-called *artificial dispersion*) is added to the solute transport equation matrix. Then, spatial oscillations are suppressed and the critical Peclet number is no longer exceeded in that grid block. Subsequently, the solution will converge. It appears that convergence difficulties especially occur when small dispersivities are used, unless: (1) a lot of artificial dispersion is added to the matrix (then, the overall dispersion is great again), or (2) the grid is refined to avoid local numerical oscillations which come with the Galerkin technique.

- METROPOL [Sauter *et al.*, 1993] (**ME**thod for the **TR**ansport **O**f **POL**lutants) simulates 3D groundwater flow with varying density and simultaneous transport of contaminants. It is based on the finite element method. METROPOL is developed by the Dutch National Institute of Public

Health and Environmental Protection RIVM. It has been applied to simulate safety assessments of the geological disposal of radionuclear waste in (high-brine) salt formations.

- MVAEM [Strack, 1995] is the analytical element model MLAEM which has recently been extended with a variable density module. MVAEM is now able to calculate the 3D-water pressure distribution, on condition that the 3D-density distribution within an aquifer is given. De Lange [1996] has applied the analytical element method to develop the NAtional GRoundwater Model (NAGROM) for density dependent aquifer systems in the Netherlands. Note that, at present, MVAEM has some drawbacks. First, it is not (yet) possible to simulate hydrodynamic dispersion and anisotropy. Second, it is still a steady-state model for the simulation of density-dependent groundwater flow. The displacement of the points with densities through the known velocity distributions is not solved yet. As such, salt water intrusion as a function of time can not be simulated. Third, it appears that the so-called multiquadric-biharmonic interpolator, which is used to provide the initial 3D-density distribution within an aquifer (by means of two parameters (Δ and h_{scale})) and to control the smoothness and the spatial behaviour of the distribution, may not be robust enough to produce reliable 3D-density distribution under all circumstances [van Gerven & de Lange, 1994].
- SWIFT [Ward, 1991] (**S**andia **W**aste-**I**solation **F**low and **T**ransport model) is a 3D-model to simulate groundwater flow, heat (energy), brine and radionuclide transport in porous and fractured media [Maidment, 1993]. The equations for flow, heat and brine are coupled by fluid density, viscosity and porosity. The equations are solved by the finite difference method.

6. The numerical dispersion problem

Numerical approximations of the derivatives of the nonlinear solute transport equation may introduce *truncation errors* and *oscillation errors* (see figure 1). As such, these errors limit the techniques that solve the partial differential equation. The truncation error has the appearance of an additional dispersion-like term, the so-called *numerical dispersion*, which may dominate the numerical accuracy of the solution. *Oscillations* may occur in the solution of the solute transport equation as a result of over and undershooting of the solute concentration values. If the oscillation reaches unacceptable values, the solution may even become unstable.

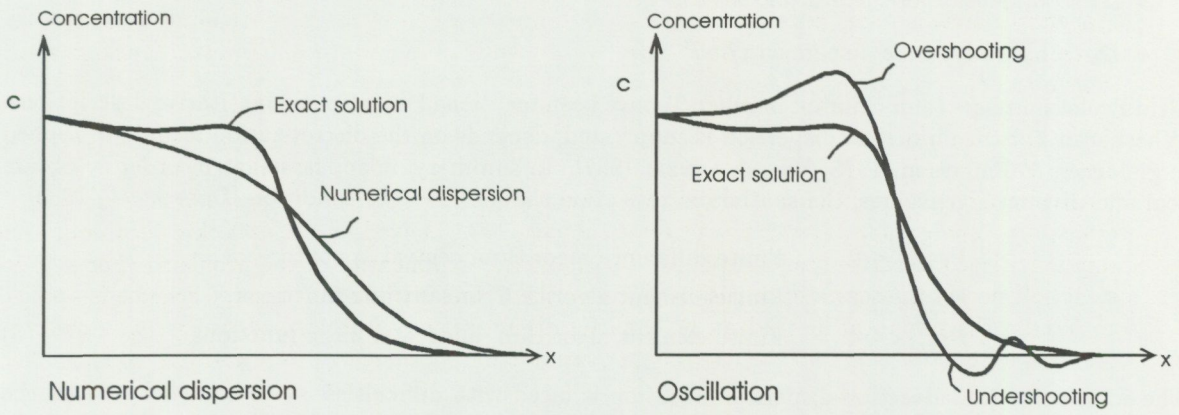


Figure 1: Schematisation of numerical dispersion and oscillation.

There is a close relation between numerical accuracy (numerical dispersion) and stability (oscillation) [Peaceman, 1977; Pinder & Gray, 1977]. In fact, numerical dispersion acts to stabilize the solution of the solute transport equation. Numerical dispersion spreads the sharp front by generating a solution which applies a greater dispersion than the hydrodynamic dispersion. In order to suppress the numerical dispersion, the numerical scheme (spatial as well as temporal) can be adapted. Meanwhile, this scheme may lead to over and undershooting, and subsequently, oscillation may be amplified. For these reasons,

the discretization scheme should be chosen carefully in order to control both numerical accuracy and stability. In this paper, the interest is focussed on the spatial discretization which is largely responsible for the numerical dispersion.

6.1 Analysis of the truncation error

In order to quantify numerical accuracy, an *eigenvalue analysis* of the advection-dispersion equation should be performed[6]. Such an analysis will demonstrate the importance of the dimension of the grid block [see e.g. Frind & Pinder, 1983]. Which of the terms of the advection-dispersion equation is more dominant depends on the relative size of the advective and dispersive fluxes at the level of the discretization element [Kinzelbach, 1987a]. The grid Peclet number can be applied to assess the most dominant process. For small grid Peclet numbers ($Pe_{grid} < 1$) the dispersive fluxes (viz. the parabolic nature of the advection-dispersion equation) prevails, whereas for great grid Peclet numbers ($Pe_{grid} > 2$) the advective fluxes (the hyperbolic nature) dominates. In field problems, advective transport of solute mostly dominates over dispersive transport. Numerical solving (by means of standard fem and fdm) of an equation with a hyperbolic nature is more difficult than solving an equation with a parabolic nature.

A one-dimensional schematisation of the standard advection-dispersion equation is often applied to demonstrate, in case of the finite difference method[7], in a simple way the principle of assessing truncation errors [e.g. Bear & Verruijt, 1987]. Approximations of the first-order derivatives generate errors in the order of magnitude of the second-order derivatives. This is shown by using Taylor series expansions [e.g. Lantz, 1971; INTERCOMP, 1976; Bear & Verruijt, 1987]. The truncation errors depend on the chosen numerical approximation scheme (e.g. backward, central or forward difference in space and time). For the analysis of the truncation error, the so-called *grid Peclet number* Pe_{grid} is defined:

$$Pe_{grid} = \left| \frac{V \Delta x}{D_h} \right| \tag{2}$$

where

- Pe_{grid} = grid Peclet number $(-)$,
- V = effective velocity of groundwater $(L\,T^{-1})$,
- Δx = dimension of the grid block (L),
- D_h = hydrodynamic dispersion $(L^2\,T^{-1})$.

Grid Peclet numbers (and Courant numbers[8]) have been mentioned in various quantitative descriptions. Whether or not the numerical dispersion is suppressed, depends on the discretization technique applied [e.g. Jensen & Finlayson, 1978; Voss & Souza, 1987]. In summary, it appears that in order to obtain real and distinct eigenvalues, the spatial discretization should meet the condition [Daus *et al.*, 1985]:

$Pe_{grid} \leq 2$	Finite difference algorithm, central in space	
$Pe_{grid} \leq 2$	Finite element algorithm, linear basic functions	
$Pe_{grid} \leq 4$	Finite element algorithm, quadratic basic functions	(3)

The solution of the advection-dispersion equation is faced with difficulties, since models based on the standard fem and fdm may yield unreliable results if the spatial discretization conditions are not met. Both widely used methods have in common that they produce poor results at great (grid) Peclet numbers. As such, it is peculiar that this well-known fact does not have a broader attention in numerical modelling practices of groundwater contaminant transport [Uffink, 1990].

---

[6] In addition, a stability analysis should determine the stability condition [e.g. Peaceman, 1977].

[7] The analysis of (truncation and oscillation) errors caused by numerical dispersion and oscillation by means of central finite difference approximations for the fdm is similar for the fem [Pinder & Gray, 1977; Kinzelbach, 1987a].

[8] The Courant condition Co, $\frac{V \Delta t}{\Delta x}$, is physically interpreted as the ratio of the advective transport distance during one time step to the spatial discretization.

6.2 The dispersion coefficient

Hydrodynamic dispersion D_h is defined as the combined effect of two processes, mechanical dispersion and molecular diffusion:

$$D_h = D_m + D_d \tag{4}$$

where

- D_m $(L^2\,T^{-1})$ = mechanical (or convective) dispersion coefficient. This process is caused by velocity variations at the microscopic scale. The spreading depends on both fluid flow and the characteristics of the pore system through which the flow takes place,
- D_d $(L^2\,T^{-1})$ = molecular diffusion coefficient. This process is caused by the random movement of molecules in a fluid and depends on concentration gradients, the properties of the fluid and the soil.

Under normal groundwater flow conditions, molecular diffusion is of marginal importance with respect to mechanical dispersion. The subdivision of the hydrodynamic dispersion into mechanical dispersion and molecular diffusion is artificial. The mechanical dispersion coefficient, which is a second-rank symmetrical tensor, can be defined for an isotropic aquifer in terms of two constants:

$$\begin{aligned} D_L &= \alpha_L\,|V| \\ D_T &= \alpha_T\,|V| \end{aligned} \tag{5}$$

where

- α_L = longitudinal dispersivity of the aquifer (L),
- α_T = transversal dispersivity of the aquifer (L).

The exact determination of the hydrodynamic dispersion is very difficult, if not impossible, as it depends on many features (e.g. scale effect, fingering, transient effects [Anderson & Woessner, 1992]). In fact, the more one knows about the hydraulic conductivity and porosity distribution, and subsequently, the exact velocity distribution, the more the hydrodynamic dispersion value will converge to the value of molecular diffusion. As such, one should model the heterogeneous and anisotropic medium as accurately as possible. However, as it is not possible to determine the exact hydraulic conductivity distribution as well as the velocity distribution, the exact value of the dispersion coefficient can not be given. For this reason, the mechanical dispersion, which is inserted in the model, may (somewhat) be increased to take into account these uncertainties in the subsoil parameters. The less one knows, the higher the model dispersivities must be.

Gelhar *et al.* [1992] reviewed 59 different field sites in order to classify the dispersivity data into three reliability classes. The representative scale of the cases ranges from 10^{-1} to 10^5 m. They found that for these cases, the longitudinal dispersivity ranges from 10^{-2} to 10^4 m. In conclusion, the variation in dispersivity reflects the influence of different degrees of aquifer heterogeneity at different field sites. They concluded that in general, longitudinal dispersivities in the lower part of the indicated range are more likely to be realistic for field applications. Therefore, the so-called *scale-dependency* of dispersivities ($\alpha_L = 0.1\,L$, where L is the traveled distance of the contaminant), determined from field data, should be reviewed critically. Furthermore, they indicated that there is a need for long-term, very large-scale experiments extending to several kilometres.

In contrast with some field sites in especially the U.S.A. (see, e.g., the cases in Gelhar *et al.*, 1992), the best estimates of the longitudinal dispersivities in Dutch and Belgian large-scale aquifer systems with Holocene and Pleistocene deposits of marine and fluviatile origin appear to yield rather small values. This observation is based on various case studies, such as Lebbe [1983], Kooiman *et al.* [1986], Stuyfzand [1991]; Walraevens *et al.* [1993]; and Oude Essink [1993]. For instance, computations have indicated that if a great hydrodynamic dispersion (that means great dispersivities) is simulated during long simulation times, unrealistic solutions are generated [Oude Essink, 1996]. In figure 2, the effect of the longitudinal dispersivity α_L is evaluated by comparing the results of simulations with four different

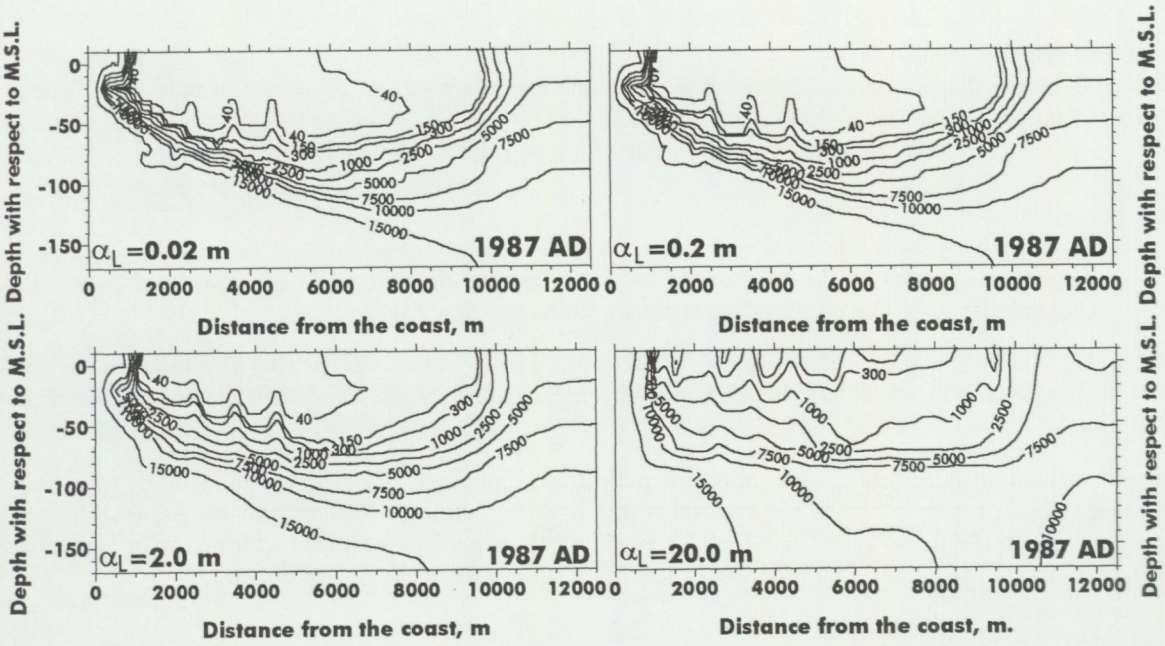


Figure 2: Chloride distributions (in $mg\ Cl^-/l$) in 1987 in a cross-section of the sand-dune area of Amsterdam Waterworks, the Netherlands, calculated with MOC [Konikow & Bredehoeft, 1978] (adapted for density differences to model vertical cross-sections [Oude Essink, 1996]) for four different longitudinal dispersivities: α_L=0.02 m, α_L=0.2 m, α_L=2.0 m and α_L=20.0 m. A thick freshwater lens is only simulated for small dispersivities.

values of α_L: 0.02 m, 0.2 m, 2.0 m and 20.0 m. The chloride distributions of the cross-section are given after a simulation time of 134 years: from 1854 till the end of 1987. The cross-section is situated in a sand-dune area along the Dutch coast where a freshwater lens has been formed. The calculated chloride distribution matches the observed distribution best if small longitudinal dispersivities are applied, namely α_L=0.02 m and α_L=0.2 m. By contrast, the case with α_L=2.0 m shows a freshwater lens that is too thin, whereas the case with α_L=20.0 m does not simulate a freshwater lens any more: the aquifer system only consists of a large brackish zone. This situation does not occur in reality.

6.3 The dimension of the grid block

If mechanical dispersion dominates over molecular diffusion, the hydrodynamic dispersion D_h in equation 2 can be expressed as $D_h = \alpha_L |V|$, and thus, equation 3 becomes:

$$\begin{aligned} \Delta x &\leq 2\,\alpha_L \quad && \text{Finite difference algorithm, central in space} \\ \Delta x &\leq 2\,\alpha_L \quad && \text{Finite element algorithm, linear basic functions} \\ \Delta x &\leq 4\,\alpha_L \quad && \text{Finite element algorithm, quadratic basic functions} \end{aligned} \tag{6}$$

Note that there are acceptable solutions obtained with values up to $\Delta x < 10\,\alpha_L$[9]. As such, this restriction is not very compulsory. Under those circumstances, the solution can still be satisfactory though in some places over and undershooting (viz. oscillation) may occur.

From the formulations in equation 6 can be deduced that the application to model salt water intrusion in large-scale coastal aquifers is restricted for 3D computer codes which are based on the standard fdm and fem (see figure 3). Because, as a matter of fact, the restriction means that the dimension of the grid block may not be larger than four times the magnitude of the longitudinal dispersivity. Unfortunately, the longitudinal dispersivity is for many aquifer systems in the order of (at maximum) metres, and thus the dimension of the grid block should also be in the order of (tens) of metres. Consequently, a very large number of grid blocks is necessary to model large-scale areas of various square kilometres. For the

[9]Sudicky [1989] even obtained highly accurate solutions for grid Peclet numbers in excess of 30 for the finite element method, based on a Laplace transformation of the temporal derivatives.

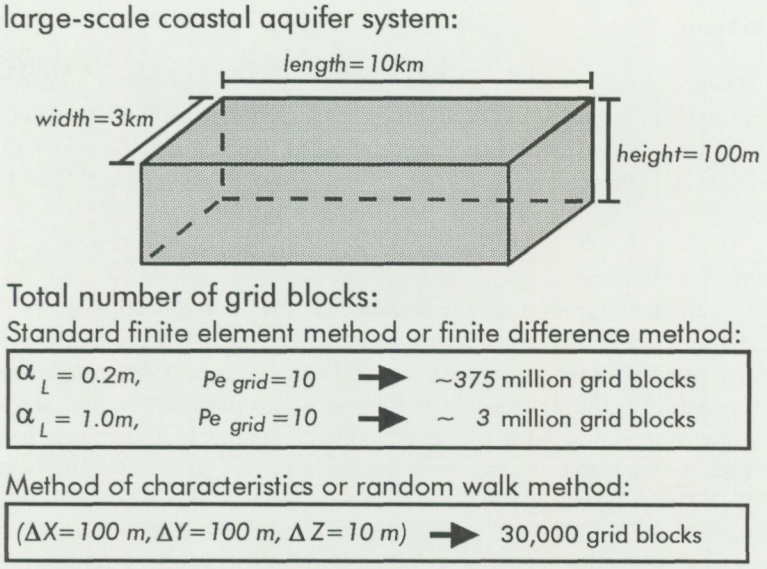


Figure 3: Effect of the longitudinal dispersivity α_L on the total number of grid blocks which are required to simulate a large-scale coastal aquifer by means of a model based on the standard finite element or finite difference method and a model based on the method of characteristics or the random walk method (viz. no effect of α_L !).

time being, the allowed number of grid blocks is restricted by computer memory capacity and execution time. In conclusion, when standard fdm and fem are applied, 3D-modelling of salt water intrusion of coastal aquifer systems is, for the time being, only possible on the scale of small geometries, such as small islands.

6.4 Remedy for the numerical dispersion problem

To avoid the numerical dispersion problems associated with standard finite element and finite difference solutions of the advection-dispersion equations, particle tracking solutions should be used, such as the method of characteristics (particle tracking for advection with a finite difference solution of the dispersion part) or the random walk method (to reproduce a Gaussian distribution of particles to simulate dispersion). As such, we think that an interconnected model of the well-known MODFLOW [McDonald & Harbaugh, 1984] and MT3D [Zheng, 1990] can avoid the numerical dispersion problem (see figure 3). MODFLOW is the most widely used groundwater flow model in the world. A recently (1994) released model is the modular 3D transport model called MT3D that is completely compatible with MODFLOW. MT3D applies the method of characteristics, the modified method of characteristics or a hybrid of these two methods. It is developed to simulate solute transport[10] without the complications of heat and density effects. However, the combined model can be made suitable for simulating density dependent groundwater flow by adapting the original model of MODFLOW with an additional term to the vertical Darcian specific discharge in the groundwater flow equation, the so-called *buoyancy* or *vertical density gradient velocity*. This adaption has already been executed with success for the 2D-model MOC [Lebbe, 1983; Oude Essink, 1996]. Schaars [1996] already adapted MODFLOW for density differences by converting, with the help of the MATLAB (a package that is able to manipulate and present matrices), the standard subsoil parameters to density dependent subsoil parameters (based on an article of Maas & Emke [1989]). At present, that model still steady-state, thus salt water intrusion as a function of time cannot yet be simulated.

In addition, research is taken place to develop more effective solution techniques based on the finite element method with the purpose to reduce numerical dispersion [Sudicky, 1989; Esch, van, personal communication, 1996].

[10]Note that MT3D is not free of errors: it appears that the error in the solute mass balance is not yet of minor importance.

7. The computer problem

Until some years ago, 3D-modelling of salt water intrusion in large-scale coastal aquifers was not really possible due to shortcomings in computer possibilities[11]. Two major reasons restricting the application are the memory problem (limited memory to store data of a 3D-model) and the speed problem (limited computer speed to execute a (transient) 3D-model). It is common knowledge that this situation is changing very fast.

7.1 The memory problem

A computer system with sufficient *random access memory* (RAM) is required to store data and arrays during the execution of the model. Until a few years ago, most FORTRAN compilers accessed only 640 Kb of RAM, which is the standard memory limit of DOS. As such, the possibility to store large amounts of data was limited. So, the arrays which represent the parameters and the number of grid blocks should not be dimensioned too large. The problem of insufficient memory has recently been solved. Since the late 1980's, much more memory is available on the personal computer: the so-called *Extended Memory RAM* (EM RAM). Executables of computer codes can address this EM RAM beyond the usual 640 Kb RAM-limit of DOS through sophisticated compilers (e.g. the Lahey Fortran compiler F77L-EM/32 in combination with the Lahey/Ergo/Phar-Lab 386 Operating System). As such, even stand-alone personal computers can accommodate a much larger number of grid blocks than under 640 Kb of conventional RAM.

Table 1 gives the number of elements or grid blocks of some computer codes. For instance, originally, the number of grid cells in MOC[12] [Konikow & Bredehoeft, 1978] was 400 (20 by 20 grid cells) which required about 302 Kb of RAM. As the maximum number of grid cells under 640 Kb of RAM was only 900 grid cells (591 Kb of RAM), the application of MOC for large-scale geometries was rather limited. Even more data must be stored for 3D-models. For instance, Navoy [1991] applied 52,470 grid blocks to model an area of 60 $km \cdot 45\ km$ with MODFLOW (5 layers, 106 columns and 99 rows). The sand-dune area of Amsterdam Waterworks in the Netherlands, which has a geometry of 19,000 m · 12,000 m by 160 m, has been schematised by 40,000 grid blocks using MODFLOW [Schaars, 1996], and by 11,408 grid blocks using HST3D and METROPOL [Ossenkoppele, 1993]. In order to model a large-scale geometry with the dimensions 10,000 m · 20,000 m by 150 m with MODFLOW (adapted and interconnected with MT3D, see subsection 6.4), 300,000 grid blocks with a dimension[13] of 100 m · 100 m · 10 m are required. As such, the memory to store data must increase significantly: up to several tens of Mb of RAM. Nowadays, the EM RAM in a computer can be increased without high costs. For instance, 4 Mb of EM RAM costs only ± 130 US$ (summer 1996[14]). Standard computer systems contain several (tens of) Mb of EM RAM, so the memory problem has been disposed for 2D and some 3D problems. Anyway, now (1996), the application on a broad scale of 3D-models for extensive and complex geometries is still in an early stage.

7.2 The speed problem

The length of time necessary to execute the computations with the computer program for a given set of input data of a geohydrologic problem is the so-called *execution time*. This execution time depends on four factors:

a. the speed of the computer

   Table 2 illustrates how some types of computer systems perform. The difference in MHz does not matter much. As can be seen, the new computer systems with faster processors (disk-speed) open the application of 3D-modelling of large-scale geometries.

b. the size of the model

   The number of grid blocks and type of the governing equations being solved determines the size

[11] Three-dimensional modelling of oil and gas reservoir behaviour by the petroleum industry is already taking place for many years: apparently, the benefit of predicting reliable oil and gas reservoir has been higher.

[12] Nowadays, MOC is also called USGS 2-D TRANSPORT.

[13] Note that at areas where changes in the future salinity distribution are limited, the grid may be more coarse, which will reduce the number of grid blocks.

[14] In September 1995, 4 Mb of EM RAM cost ± 260 US$, whereas in spring 1990, it cost ± 2500 US$!

Table 1: The number of elements or grid blocks of executable computer codes depends on the free Extended Memory RAM (EM RAM) of the computer [source: Scientific Software Group, 1995]. Note that, e.g., in an 8 Mb EM RAM computer, only some 7 Mb is free for memory allocation.

Computer code	Extended Memory RAM (Mb)	Number of (2D) elements or (3D) grid blocks
MOC (2D), adapted* for density differences by Oude Essink [1996]	†0.3	‡400
	†0.6	900
	3.5	10000
	6.7	20000
	16.4	50000
MOCDENSE (2D)♡	2.5	2500
SUTRA (2D)•	4	1300
	8	2175
	16	6525
HST3D (3D)	4	2500
	8	7000
	16	14000
MODFLOW (3D)	◇4	60000

*: MOC (USGS 2-D TRANSPORT) is adapted to simulate salt water intrusion in vertical cross-sections [Oude Essink, 1996].
†: under 640 Kb of conventional RAM, the standard memory limit of DOS.
‡: in the case with 400 grid cells, the number of particles per grid cell is 8, whereas for the other cases the number of particles is 9.
♡: MOCDENSE [Sanford & Konikow, 1985] is an adapted version of MOC, developed for vertical cross-sections (it is based on pressures).
•: the main reason for this small number of grid cells relative to MOC is that SUTRA [Voss, 1984] has to allocate arrays for additional subsoil characteristics.
◇: it is also possible to apply a virtual memory system, which uses disk storage to supplement the computer's memory. Note, however, that then the computer speed will drop significantly.

Table 2: Execution time of different computer systems (processors) with different MHz on a benchmark problem [Anderson & Woessner, 1992].

Computer system	Execution time	Speed (relative to PC)
PC	$49^m\ 43^s$	1
XT	$26^m\ 13^s$	1.9
286 (AT)	$7^m\ 7^s$	7.0
386 16 MHz	$5^m\ 8^s$	9.7
386 25 MHz	$5^m\ 2^s$	9.9
486 25 MHz	$1^m\ 40^s$	29.8
486 33 MHz	$1^m\ 16^s$	39.3
486 50 MHz†	$\pm\ 1^m$	49.7
Pentium 120 MHz†	$\pm\ 16^s$	186.4

†: based on the author's own experience.

of the model. The larger the number of grid blocks, the longer the execution time will be.

c. the efficiency of the compiler

To execute the model, an executable file of the computer code must be produced by an appropriate compiler. A compiler reads the source code and generates machine language statements for the computer hardware. Some compilers go through commands and information more efficiently than others. For example, the Lahey Fortran compiler (e.g. F77L-EM/32) is capable of a very rapid compilation of FORTRAN-codes. This compiler could already address the Extended Memory

RAM at least since the end of the 1980's.

d. the type of the output device

Some models ask for keyboard input during the execution or frequently write to the screen printer or even an output file. These actions increase the execution time (massive output files of several Mb's may increase the execution time substantially). The output devices can be reduced by setting the printing options to minimal output.

8. The data availability problem

Obviously, a numerical model, which is applied to simulate groundwater flow and solute transport in a coastal aquifer, must be calibrated and verified with available groundwater data in order to prove its predictive capability, accuracy and reliability. Examples of groundwater data are subsoil parameters (e.g. the hydraulic conductivity, the exact position of aquitards; the effective porosity; the anisotropy, and the hydrodynamic dispersion), groundwater extraction rates, and salinity and piezometric level distributions as a function of space and time. Regrettably, in many cases reliable and sufficient data are scarce. The availability of enough reliable data is obviously even more pinching for 3D-models than for 2D-models. As such, the application of 3D computer codes is restricted seriously.

8.1 Upscaling of data from 1D and 2D to 3D

In fact, the collection of data is one- or two-dimensional. Geohydrologic information is mostly obtained from a point source (e.g. groundwater level from a observation well) or from a line source (geohydrologic information from a geohydrologic column). This information must be extrapolated or interpolated to a 3D distribution of subsoil parameters. This upscaling obviously faces some difficulties.

8.2 Long time series of hydrochemical constituents

Another problem is that the calibration of groundwater flow models with salinities changing over time and space is still rather laborious. As the flow of groundwater and subsequently the transport of hydrochemical constituents are slow processes, it takes quite some years before a salinisation can be detected. As such, relative long time series of monitored salinities (of some tens of years or even more) are necessary in order to accurately calibrate 3D salt water intrusion in large-scale coastal aquifers. Unfortunately, these time series are available only occasionally and reliable measurements are scarce in many cases. As a consequence, the calibration will be less reliable. One has to collect many data during many years before a good calibration can be achieved.

8.3 Remedy for the data availability problem

The collection and the analysis of reliable groundwater data should be intensified, varying from subsoil parameters to records of solute concentrations and piezometric levels as functions of time and space. The present salinisation process should be monitored as a function of time to detect long-term changes. The geometry and geohydrologic parameters of the coastal aquifer systems should be determined and described, particularly for those aquifer systems which are vulnerable and sensitive to natural and man-induced processes.

To solve the data availability problem to a certain extent, so-called *Geohydrologic Information Systems* can be very useful. In these systems, all relevant geohydrologic data can be stored. By analysing these systems, areas with a lack of data can be detected immediately. In 1990, research institutes, governmental organizations and drinking water companies in the Netherlands started the development of a so-called REgional Geohydrologic Information System (REGIS). In REGIS, a database is available to supply all types of relevant geohydrologic information, such as geo-electric data, groundwater levels (observation well data), chemical data, geohydrologic columns, topographic information, pumping and borehole test data, locations of contaminants, etc. Now, the system is operational and has already proven to be profitable.

Conclusions

Though 3D-modelling of salt water intrusion in large-scale coastal aquifers is technically possible, a number of practical problems arise.

First of all, to suppress truncation and oscillation errors in the solution of the advection-dispersion equation, models based on the standard fem or fdm should satisfy the condition that the spatial discretization (that is the dimension of the grid block) should not be greater than a few times the magnitude of the (longitudinal) dispersivity that represents hydrodynamic dispersion. When the dimension of the aquifer system in question is large and the (longitudinal) dispersivity is small (e.g. in the order of decimetres for Holocene and Pleistocene deposits of marine and fluviatile origin), the dimensions of the grid blocks must be in the order of (tens of) metres. This condition of spatial discretization considerably restricts the practical application of 3D computer codes with dispersive solute transport, such as HST3D, SWICHA and METROPOL, to simulate 3D salt water intrusion in large-scale coastal (homogeneous) aquifers. However, an interconnected model of MODFLOW (adapted for simulating density dependent groundwater flow) and the transport model MT3D will probably avoid the numerical dispersion problem.

Second, the required number of grid blocks to model large-scale coastal (homogeneous) aquifers is enormous, e.g. of several hundreds of thousands of grid blocks. Nowadays, the (personal or mini) computer which is applied to execute a model with this number of grid blocks is still not fast enough, but it will be within a few years. The memory allocation is no problem any more, as computers with some tens of Mb of Extended Memory RAM are already available on a large scale.

Third, the large number of groundwater data, required for calibration and verification, are not yet available in most cases. As such, data collection should be intensified. However, we have to accept that the collection of data will always lag behind the developments in computer possibilities.

References

ANDERSON, M.P. & WOESSNER, W.W. 1992. Applied groundwater modeling. Simulation of flow and advective transport. *Academy Press, Inc., San Diego.*

BEAR, J. & VERRUIJT, A. 1987. Modeling Groundwater Flow and Pollution. *D. Reidel Publishing Company, Dordrecht, the Netherlands. 414 p.*

CARSLAW, H.S. & JAEGER, J.C. 1959. Conduction of Heat in Solids. *Oxford University Press, London.*

CUSTODIO, E. & BRUGGEMAN, G.A. (eds). 1987. Groundwater Problems in Coastal Areas. *Studies and Reports in Hydrology. UNESCO, International Hydrological Programme, Paris.*

DAUS, A.D., FRIND, E.O. & SUDICKY, E.A. 1985. Comparative error analysis in finite element formulations of the advection-dispersion equation. *Adv. in Water Resour., 8: 86-95.*

ESCH, J.M. VAN. 1996. *Delft Geotechnics. P.O. Box 69, 2600 AB Delft, the Netherlands.*

FRIND, E.O. & PINDER, G.F. 1983. The principle direction technique for solution of the advection-dispersion equation. *Proc. 10^{th} IMACS World Congress on Systems Simulation and Scientific Computation, Concordia University, Montreal, Canada, Aug. 1982. pp. 305-313.*

GARDER, A.O., Jr., PEACEMAN D.W. & POZZI, A.L., Jr. 1964. Numerical calculation of multidimensional miscible displacement by the method of characteristics. *Soc. of Petroleum Eng. J., 4 (1): 26-36.*

GELHAR, L.W., WELTY, C. & REHFELDT, K.R. 1992. A Critical Review of Data on Field-Scale Dispersion in Aquifers. *Water Resour. Res., 28 (7): 1955-1974.*

GERVEN, M.W., VAN & LANGE, W.J., DE. 1994. Experiences with the new variable density module of MLAEM in a well-defined test area. *Proc. 13^{th} Salt Water Intrusion Meeting, Cagliari, Italy, 5-10 June 1994. (in press).*

HUYAKORN, P.S., ANDERSEN, P.F., MERCER, J.W. & WHITE, H.O., Jr. 1987. Saltwater Intrusion in Aquifers: Development and Testing of a Three-Dimensional Finite Element Model. *Water Resour. Res., 23*

(2): 293-312.

IGWMC. 1995. Ground-water software catalog. Summer. *International Ground Water Modeling Center. Colorado School of Mines, Golden, CO 80401-1887, U.S.A.*

INTERCOMP. 1976. A model for calculating effects of liquid waste disposal in deep saline aquifers. *Resource Development and Engineering, Inc. U.S.G.S. Water-Resources Investigations Report 76-96, 263 p.*

JENSEN, O.K. & FINLAYSON, B.A. 1978. Solution of the convection-diffusion equation using a moving coordinate system. *Second Int. Conf. on Finite Elements in Water Resour., Imperial College, London, July. pp. 4.21-4.32.*

KINZELBACH, W.K.H. 1987a. Numerische Methoden zur Modellierung des Transports von Schadstoffen im Grundwasser. (In German.) *Schriftenreihe GWF Wasser-Abwasser. Band 21. R. Oldenbourg Verlag GmbH, Munchen.*

KINZELBACH, W.K.H. 1987b. Methods for the simulation of pollutant transport in ground water. A model comparison. In: *Proc. Solving Ground Water Problems With Models. Conference and Exposition. Vol. 1, Denver Colorado, U.S.A., Feb. 1987. pp. 656-675.*

KIPP, K.L. Jr. 1986. HST3D. A Computer Code for Simulation of Heat and Solute Transport in Three-dimensional Groundwater Flow Systems. *IGWMC, International Ground Water Modeling Center. U.S.G.S. Water-Resources Investigations Report 86-4095.*

KONIKOW, L.F. & BREDEHOEFT, J.D. 1978. Computer model of two-dimensional solute transport and dispersion in ground water. *U.S.G.S. Techniques of Water-Resources Investigations, Book 7, Chapter C2, 90 p.*

KOOIMAN, J.W. 1989. Modelling the salt-water intrusion in the dune water-catchment area of the Amsterdam Waterworks. *Proc. 10^{th} Salt Water Intrusion Meeting, Ghent, Belgium, May 1988. pp. 132-142.*

LANTZ, R.B. 1971. Quantitative Evaluation of Numerical Diffusion (Truncation Error). *Transactions AIME, Soc. of Petroleum Eng. J., 251: 315-320.*

LANGE, W., DE. 1996. Groundwater modeling of large domains with analytic elements. *Ph.D. thesis. Delft University of Technology. 237 p.*

LEBBE, L.C. 1983. Mathematical model of the evolution of the fresh-water lens under the dunes and beach with semi-diurnal tides. *Proc. 8^{th} Salt Water Intrusion Meeting, Bari, Italy. Geologia Applicata e Idrogeologia, Vol. XVIII, Parte II: 211-226.*

LESTER, B. 1991. SWICHA. A Three-Dimensional Finite-Element Code for Analyzing Seawater Intrusion in Coastal Aquifers. *Version 5.05. GeoTrans, Inc., Sterling, Virginia, U.S.A. IGWMC, International Ground Water Modeling Center, Delft, the Netherlands. 178 p.*

MAAS, C. & EMKE, M.J. 1989. Solving varying density groundwater problems with a single density computer program. *Proc. 10^{th} Salt Water Intrusion Meeting, Ghent, Belgium, May 1988. pp. 132-142.*

MAIDMENT, D.R. (ed). 1993. Handbook of Hydrology. *McGraw-Hill, Inc.*

MCDONALD, M.G. & HARBAUGH, A.W. 1984. A modular three-dimensional finite-difference ground-water flow model. *U.S.G.S. Open-File Report 83-875, 528 p.*

NAVOY, A.S. 1991. Aquifer-estuary interaction and vulnerability of groundwater supplies to sea level rise-driven saltwater intrusion. *Ph.D. thesis. Pennsylvania State University, U.S.A. 225 p.*

OSSENKOPPELE, H. 1993. Modelling the distribution and the movement of fresh, brackish and saline groundwater in the sand-dune area of Amsterdam Waterworks. (in Dutch). *M.Sc. thesis at the Delft University of Technology, the Netherlands. 84 p.*

OUDE ESSINK, G.H.P. 1993. A sensitivity analysis of the adapted groundwater model MOC. *Proc. 12^{th} Salt Water Intrusion Meeting, Barcelona, Spain, Nov. 1992. pp. 407-420.*

OUDE ESSINK, G.H.P. 1996. Impact of sea level rise on groundwater flow regimes. A sensitivity analysis for the Netherlands. *Ph.D. thesis. Delft University of Technology. 411 p.*

PEACEMAN, D.W. 1977. Fundaments of numerical reservoir simulation. *Developments in Petroleum Science 6, Elsevier Scientific Publishing Company, Amsterdam.*

PINDER, G.F. & GRAY, W.G. 1977. Finite element simulation in surface and subsurface hydrology. *Aca-*

demic Press, 295 p.

REILLY, Th.E. & GOODMAN, A.S. 1985. Quantitative analysis of saltwater-freshwater relationships in groundwater systems – a historical perspective. *J. of Hydrol., 80: 125-160.*

SANFORD, W.E. & KONIKOW, L.F. 1985. MOCDENSE. A two-constituent solute-transport model for ground water having variable density. *U.S.G.S. Water-Resources Investigations Report 85-4279.*

SAUTER, F.J., LEIJNSE, A. & BEUSEN, A.H.W. 1993. METROPOL. User's Guide. *Report number 725205.003. National Institute of Public Health and Environmental Protection. Bilthoven, the Netherlands.*

SCHAARS, F. 1996. Implementation of a method for spatial modelling of simultaneous flow of fresh, brackish and saline groundwater in the sand-dune area of Amsterdam Waterworks. (in Dutch). *M.Sc. thesis at the Delft University of Technology, the Netherlands. 102 p.*

SCIENTIFIC SOFTWARE GROUP. 1995. Catalog Environmental Software & Publications. 1995-1996. *P.O. Box 23041, Washington, D.C., 20026-3041, U.S.A.*

SEGOL, G. 1994. Classic groundwater simulations. Proving and improving numerical models. *Prentice-Hall, Inc. New York. 531 p.*

STRACK, O.D.L. 1989. Groundwater Mechanics. *Prentice Hall, New Jersey, U.S.A. 732 p.*

STRACK, O.D.L. 1995. A Dupuit-Forcheimer model for three-dimensional flow with variable density. *Water Resour. Res., 31 (12): 3007-3017.*

STUYFZAND, P.J. 1991. Composition, genesis and quality variations of shallow groundwater in coastal dunes. (in Dutch). *KIWA SWE-91.008, 175 p.*

SUDICKY, E.A. 1989. The Laplace Transform Galerkin Technique: a time-continuous finite element theory and application to mass transport in groundwater. *Water Resour. Res., 25 (8): 1833-1846.*

UFFINK, G.J.M. 1990. Analysis of dispersion by the random walk method. *Ph.D. thesis. Delft University of Technology. 150 p.*

VOSS, C.I. 1984. SUTRA – A finite element simulation for saturated-unsaturated, fluid-density-dependent ground-water flow with energy transport or chemically reactive single-species solute transport. *U.S.G.S. Water-Resources Investigations Report 84-4369, 409 p.*

WALRAEVENS, K., LEBBE, L.C., *et al.* 1993. Salt/fresh-water flow and distribution in a cross-section at Oostduinkerke (Western Coastal Plain of Belgium). *Proc. 12th Salt Water Intrusion Meeting, Barcelona, Spain, Nov. 1992. pp. 407-420.*

WARD, D.S. 1991. Data Input for SWIFT/386, version 2.50. *Geotrans Technical Report, Sterling, Va.*

ZIENKIEWICZ, O.C. 1971. The finite element method in engineering science. *McGraw-Hill, London, 521 p.*

ZHENG, C. 1990. MT3D. A modular three-dimensional transport model. *S.S. Papadopolous and Associates, Bethesda, Md.*

Benchmarking in Numerical Modelling of Density Driven Flow

Sascha Oswald, Carsten Schwarz and Wolfgang Kinzelbach
Institute of Hydromechanics and Water Recources Management,
Swiss Federal Institute of Technology
ETH Hönggerberg, CH-8093 Zürich, Switzerland

For the prediction of density driven flow in aquifers one has to rely on numerical codes developed for that purpose. To prove the capability and reliability of these codes benchmark tests are necessary. This study is concerned with benchmarking for density effects due to the influence of salt water, in both two and three dimensions.

Henry's problem

For the problem of seawater intrusion in a coastal aquifer *Henry* (1964) presented a two-dimensional case, for which a semi-analytic steady-state solution exists. Henry's problem has been widely used as a benchmark for density driven flow codes. However, this problem is not sensitive to the performance of transport codes with respect to consistency of velocities and description of small transition zones (*Voss and Souza*, 1987). Recent results and our own calculations show that beyond this deficiency even the utilisation of the Boussinesq approximation and the use of relatively coarse grids do not affect the results significantly. The previously observed differences between model results and the semi-analytic solution of Henry seems to be irrelevant since *Segol* (1994) presented a revised calculation of the semi-analytic solution (Fig. 1a).

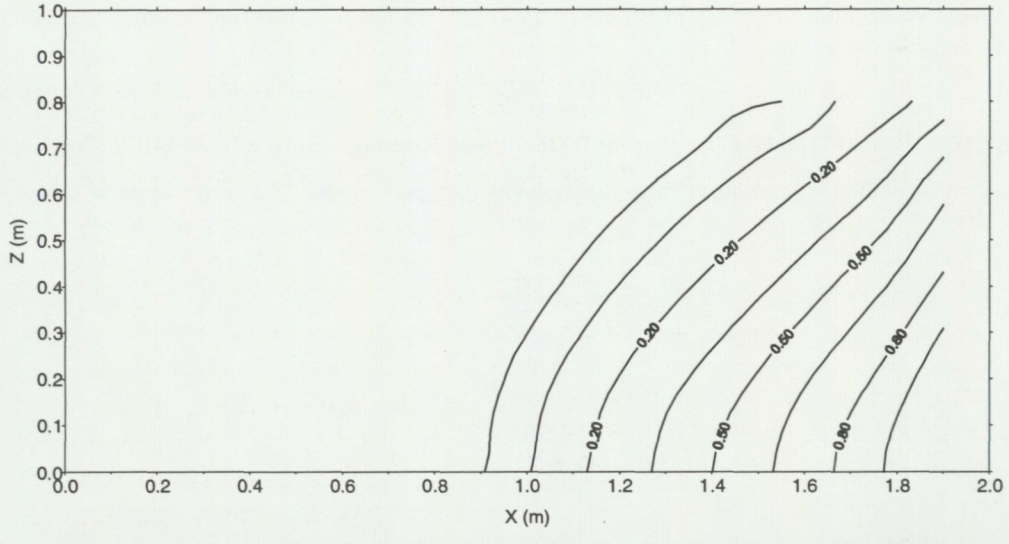


Fig. 1 Salt concentration isolines of the revised semi-analytic solution of the Henry problem (Segol, 1994); inflow from the left, fixed seawater concentration at the right, diffusion coefficient $D = 18.86 \times 10^{-6}$ m^2/s.

In the numerical calculations four different codes were used for comparison purposes:

- FEFLOW (*Diersch*, 1994): Galerkin finite elements (FE), extended Boussinesq approximation
- MARCEAU (*Oltean et al.*, 1994): mixed hybrid FE for flow and dispersion, discontinuous FE for advection
- SALTFLOW (*Frind and Molson*, 1994): rectangular FE, explicit advection term
- ug (*Bastian et al.*, 1995): finite volumes, multigrid solver

The solutions obtained with these codes all match Segol's revised solution very closely, provided the appropriate diffusion coefficient is used. The isochlors evaluated with the four different codes are virtually identical to each other and to the semi-analytic solution (see Fig. 1b). Increasing the resolution of the grid does not change the results any more and also the velocity field, in most cases a more sensitive measure, is not a sensitive indicator of model inaccuracy here. If the seaside boundary conditions for concentrations are modified (in comparison to Henry's problem) to describe a more realistic situation the agreement between the models still prevails.

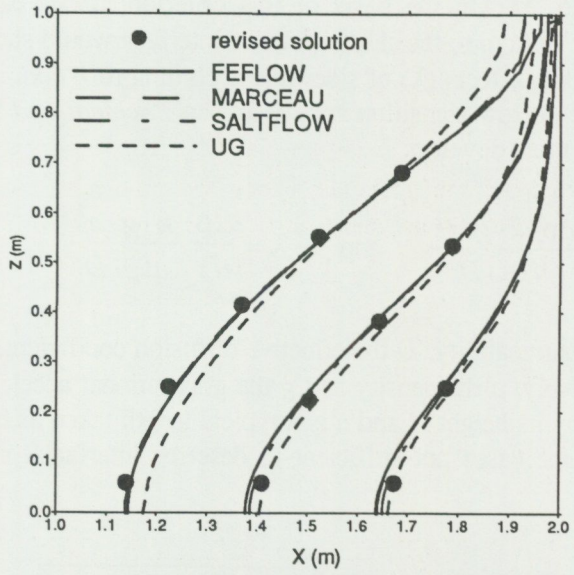


Fig. 1b Comparison of calculated isochlors with the revised solution obtained by Segol (1994). Isochlor values are 20%, 50% and 80% of seawater concentration.

Since the Henry problem can only be used as a benchmark to a very limited extent, more complex, maybe three-dimensional situations of seawater intrusion, have to be considered, i.e. layered or locally heterogeneous aquifers, time-dependent freshwater discharge and/or pumping wells. This types of more realistic problems have been looked into on the field scale, e.g. by *Frind* (1982, 1994), *Huyakorn* (1987) or *Xue* (1995). However, the advantage of having a semi-analytic solution to compare with is lost, and hence one has to use consecutive refinement or comparison with possibly incomplete field data to judge the quality of results. Another widespread benchmark test, the Elder problem (*Elder*, 1967), is indeed more complex due to its unstable nature, but it is only two-dimensional and can only be checked against experimental data of density flow caused by temperature differences.

Miscible density fingering

A second objective of this study is to model saltwater flow driven by density effects on a local scale in a case, in which the results of numerical modelling can be compared to well-controlled laboratory experiments. The physical phenomenon studied is the development of saltwater fingers in a saturated porous medium without change of total salt mass and possibly including the influence of heterogeneities.

The experimental set-up consisted of a container with impervious boundaries filled with glass beads as a porous medium. In the upper central part of the homogeneous bead packing, a heterogeneity was introduced by embedding a more permeable blockshaped zone. An unstable saltwater/freshwater layering serves as initial condition (see Fig. 2). It was produced by removing a thin plastic sheet separating the salt and fresh water zones at time t=0. The inner size of the cube-shaped container was 240 mm along each edge. The upper third was filled with a salt solution of concentration c = 3 g/l. The highly permeable zone was 40 mm by 40 mm in the horizontal directions and 160 mm in the vertical direction.

The value of the nondimensional Rayleigh number (*Ra*) (for a horizontally infinite, homogeneous porous medium) exceeded $4\pi^2$ (Eq. 1). On the basis of this criterion in our case even a salt distribution increasing linearly from the bottom to the salt/freshwater interface would show instability. The Rayleigh number including the damping effects (λ) of sidewalls according to *Wooding* (1959) is also larger than its critical value due to the narrow transition zone (see also *Bachmat and Elrick*, 1970). Hence, some kind of convective mixing must develop.

$$Ra = \frac{\Delta\rho \cdot k \cdot g \cdot H}{n \cdot \mu \cdot D} \quad \text{and} \quad \lambda = \frac{d\rho}{dz} \cdot \frac{k \cdot g \cdot a^2}{\mu_m \cdot D} \tag{1}$$

where n is porosity, k the permeability, D the effective diffusion coefficient, μ and μ_m the viscosity and the mean viscosity respectively, ρ the density and g the gravitational acceleration. The geometry of the container is characterised by its height H and a is a typical length taken as half the width. The Rayleigh number is, however, in some cases not sufficient to describe interfacial stability (*Schincariol et al.*, 1994).

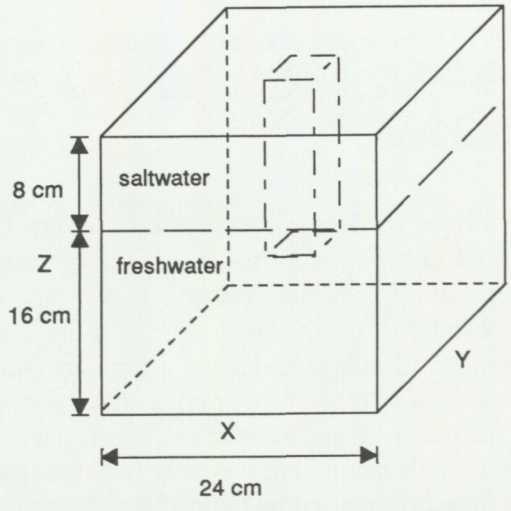


Fig. 2 Set-up for fingering experiments with unstable saltwater/freshwater layering.

We used a nuclear magnetic resonance apparatus to get time-dependent concentration data in three dimensions. Copper sulphate ($CuSO_4$) was added to the saltwater as a paramagnetic tracer in low concentration to get a linear signal-to-concentration relation. The magnetic resonance imaging (MRI) was performed in slices of 5 mm thickness with an image plane resolution of 2.34 mm using a spin-echo imaging sequence.

After removing the separating plastic sheet, the denser saltwater flows downward forming fingers, while the fresh water is forced to go up in a similar way. Additionally, there is mixing by diffusion and dispersion. The built-in block of higher permeability acts as a preferential location for finger flow (see Fig. 3). Starting out with a very small size the fingers do not only grow in length but also in width. The latter phenomenon is caused by dispersion and the coalescence of smaller fingers. Also tipsplitting is visible. The primary and quickest flow of saltwater takes place in the highly permeable zone accompanied by upward freshwater fingers in the same zone. In the low permeability region fingering is observed over the whole horizontal plane. Their development, however, is significantly slower. Hence the convective, vertical mixing by the miscible fingering is dominated by the heterogeneity, although this zone is small in size compared to the whole cross-section. Although the extension of the highly permeable zone in the vertical direction was limited, the vertical finger movement was not stopped when the finger reached the bottom of this zone. Finger width increased still further.

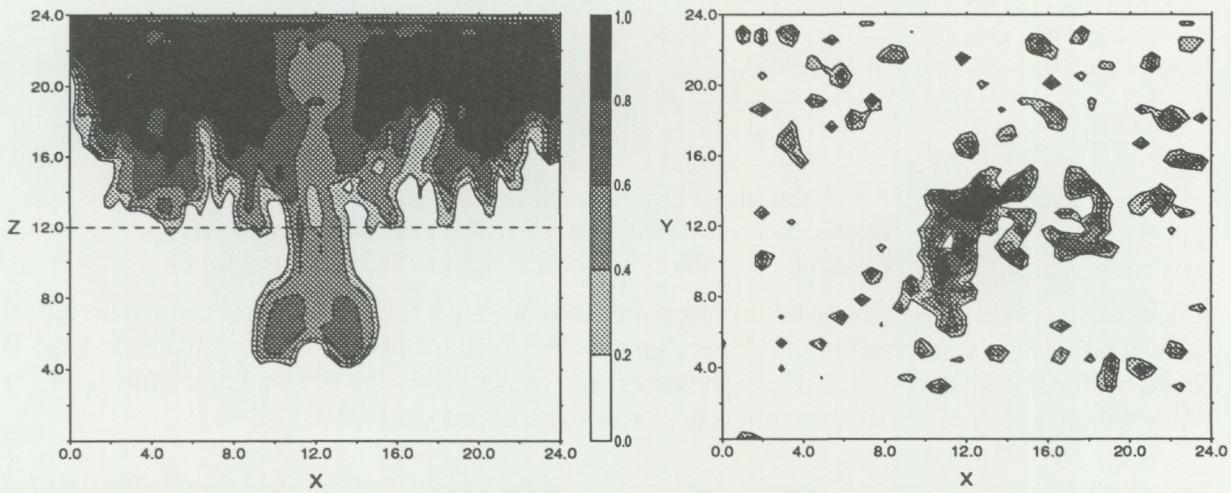


Fig. 3 Fingering of saltwater in unstable layering with central heterogeneity (a) Vertical centre plane, permeability ratio of 5.1, after 176 minutes; (b) Horizontal plane, permeability ratio of 3.2, 4 cm below initial interface as indicated in 3a (dotted line), after 166 minutes.

Benchmarking on the basis of this unstable type of flow phenomenon has to be different from the usual comparison of local concentrations, heads, or velocities applied in stable problems. A comparison between model and measured data has to focus on the generic properties such as the geometry of the basic evolving flow pattern. What can be compared are quantities such as finger growth speed, finger size (as done by *Manickam and Homsy*, 1995) and spatial frequencies or onset of fingering and fingering modes as a function of the Rayleigh number. To reproduce these features is a challenge for numerical flow codes and modelling, yet it presents the most sensitive test whether the physical nature of the problem is captured by the model.

An example of the results of numerical simulation of the experiment discussed above is shown in Fig 4. We used the code SALTFLOW (*Frind and Molson*, 1994). This code was able to reproduce the development of fingers in the highly permeable heterogeneity starting with a sharp initial interface

between saltwater and freshwater. But it did not show any fingering in the outer, low permeable part of the porous medium.

This is due to several reasons. Firstly, the actual initial perturbations of the interface (caused by pulling out the plastic sheet) and the unavoidable small variations of permeability and porosity in the physical model, which constitute the origin of fingers, were not taken into account. Further, the density gradient at the front may be reduced in the model due to limited resolution.

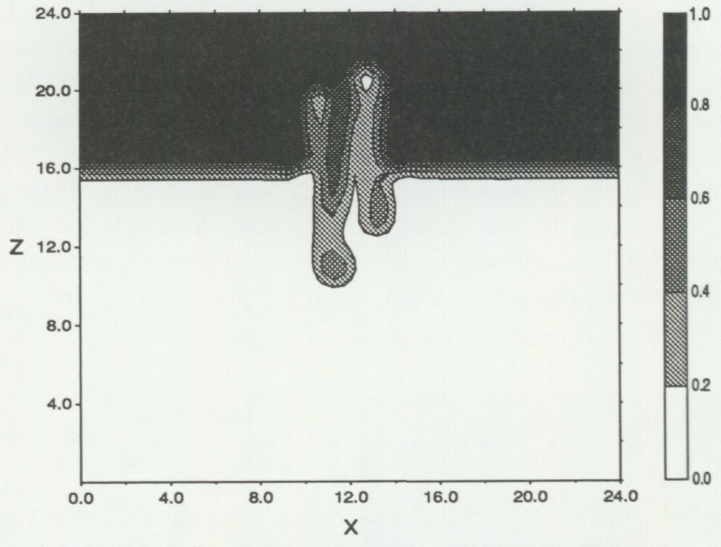


Fig. 4 Calculated concentration in the central vertical cross-section; permeability ratio 5.1, after 173 minutes.

A comparison of the finger length development of the central finger (Fig. 5) indicates that the numerical calculation is able to reproduce the correct growth rate of the finger, but a much longer time is necessary for fingering to start. Both, experimental and numerical results show a linear growth rate of finger length, which coincides with results of similar experiments (*Pearl*, 1993).

Applying a small perturbation of the salt concentration to the initial interface could shorten the time lag of finger initialisation, provided it has an appropriate wavelength. In this case, too, there is no finger growth in the outer part of the model yet. The main problem in modelling finger development is to obtain the observed onset of fingering. This demands a very high degree of grid resolution in the interface region, use of an appropriate initial perturbation and numerical codes, which do not suppress or smear out small differences in concentration or head. On the other hand, the simulation of finger growth after initiation seems to be possible.

Apart from its use in the validation of codes, density flow and fingering on a small scale is of interest in itself, because it may influence flow and transport also on a larger scale by increasing - or in some cases even decreasing - vertical mixing, particularly under heterogeneous conditions. Hence, investigating fingering in laboratory experiments and numerical simulation should help to find an appropriate way to account for the subscale effects in large scale modelling using effective parameters.

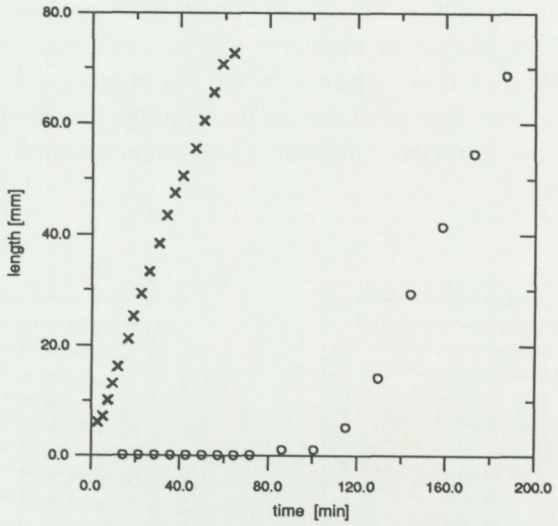


Fig. 5 Finger growth of central finger: Comparison between experimental data (denoted by crosses) and numerical simulation (denoted by circles).

Proposed benchmark

To have a benchmark test, which does not demand as much from the transport code and the physical modelling approach as the fingering example, we suggest another problem case (see Fig. 6). It starts from a stable sharp interface saltwater/freshwater layering with no inflow. The change in salt distribution and flow field under the influence of a constant influx/discharge of freshwater presents a situation useful for benchmarking. This problem is not only closely related to the situation of transient mixing of freshwater with saltwater in case of seawater intrusion, but also to salinization of an aquifer in the neighbourhood of a salt dome.

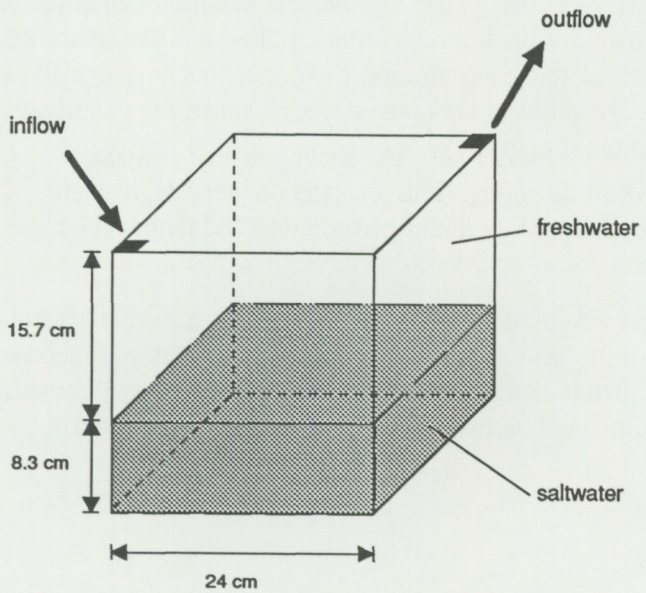


Fig. 6 Saltwater pool at the bottom of an impervious container with inflow and outflow at top corners.

As numerical calculations indicate there can be different flow patterns depending on the physical parameters: In the case of high freshwater discharge and low salt concentration the saltwater can be displaced easily by the freshwater flow, whereas in the opposite case a saltpool will remain at the bottom. Inside the saltwater zone one or more eddies develop driven by the flow field above the interface. Now, the saltwater is transported upward by dispersion and diffusion only, thus forming a transition zone (Fig.7a and b).

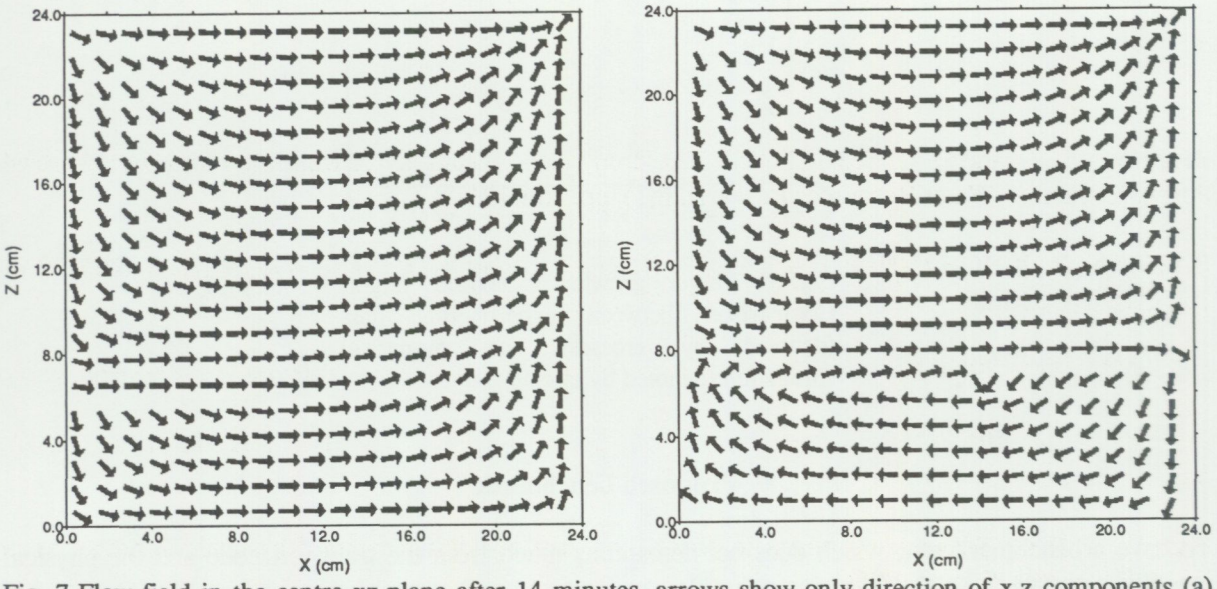


Fig. 7 Flow field in the centre xz-plane after 14 minutes, arrows show only direction of x,z components (a) initial salt concentration at the bottom is 100 g/l, total inflow/outflow is 0.1 l/min. (b) initially saturated brine (300 g/l) at the bottom, same inflow/outflow as in (a).

In contrast to the Henry problem, here the time evolution of an already existing saltwater layer after introduction of a freshwater inflow is studied. No nontrivial steady state solution exists. This choice takes into account that the insensitivity of the Henry problem is not only caused by the stability of the stratification but also by the fact that in this steady state situation numerical diffusion does not play a role. Additionally the possibility of different resulting flow and concentration patterns depending on inflow, dispersion, and initial salt concentration provide a tool to judge the capabilities of transport codes in this benchmark. The problem set-up is also well-suited for investigation with MRI as was the case in the fingering example shown above.

Conclusions

The Henry problem can only be used as a very weak benchmark for the general capabilities of transport codes for density driven flow. To validate such codes comparison with generic properties of fingering phenomena can be used, also in three dimensions. A time-dependent, three-dimensional, stably layered problem with external inflow and outflow could be a promising benchmark.

Acknowledgements

This work is financially supported by the GRS, Cologne. We want to thank Dr. G. Brix (German Cancer Research center DKFZ, Department of Radiological Diagnostic and Therapy, Heidelberg, Germany) and Andrea Greiner (Inst. of Environmental Physics, Heidelberg, Germany) for their contributions in performing the MRI measurements and Philippe Ackerer/Anis Younes (Inst. de Mécanique des Fluides, Strassbourg, France) and Gabi Beddies (Inst. for Computer Applications, Stuttgart, Germany) for their calculations of the Henry problem.

References

BACHMAT, Y., and D. E. ELRICK, 1970: Hydrodynamic Instability of Miscible Fluids in a Vertical Porous Column, - Water Resources Research 6(1), pp. 156-171.

BASTIAN, P., K. JOHANNSEN, N. NEUSS, H. RENTZ-REICHERT, Ch. WAGNER, G. WITTUM, 1995: ug 3.0, tutorial, revised version (April 1995), Stuttgart, Germany.

DIERSCH, H.-J., 1994: FEFLOW User's Manual Version 4.2, WASY GmbH, Berlin, Germany.

ELDER, J- W., 1967: Transient convection in a porous medium, - J. Fluid Mechanics, vol. 27(3), pp. 609-623.

FRIND, E.,1982: Seawater Intrusion in continuous coastal aquifer-aquitard systems, - Advances in Water Resources, 5, pp. 89-96.

FRIND, E., and J. MOLSON, 1994: SALTFLOW 2.0 user guide, Waterloo Centre for Groundwater Research, Canada.

HENRY, H., 1964: Effects of dispersion on saltwater encroachment in coastal aquifers, Sea Water in Coastal Aquifers, - Geological Survey Water-Supply Paper 1613-C, pp. C70-C84.

HUYAKORN, P.S., et al., 1987: Saltwater Intrusion in Aquifers: Development and Testing of a Three-Dimensional Finite Element Model, - Water Resources Research 23(2), pp. 293-312.

MANICKAM, O., and G. M. HOMSY, 1995: Fingering instabilities in vertical miscible displacement flows in porous media, - J. Fluid Mechanics, vol. 288, pp. 75-102.

OLTEAN, C., et al. 1994: Solute Transport in 3D Laboratory Model through an homogeneous porous medium: Behaviour of Dense Phase and Simulation, - Computational Methods in Water Resources X, pp. 521-528, Kluwer academic publishers, Dordrecht, The Netherlands.

PEARL, Z., et al., 1993: Nuclear Magnetic Resonance Imaging of Miscible Fingering in Porous Media, - Transport in Porous Media (12), pp. 107-123.

SCHINCARIOL, R. A., et al., 1994: On the generation of instabilities in variable density flow, - Water Resources Research 30(4), pp. 913-927.

SEGOL, G., 1994: Classic Groundwater Simulations, PTR Prentice Hall, New Jersey.

VOSS, C., and W. SOUZA, 1987: Variable Density Flow and Solute Transport Simulation of Regional Aquifers Containing a Narrow Freshwater-Saltwater Transition Zone, - Water Resources Research 23(10), pp. 1851-1866.

WOODING, R. A., 1959: The stability of a viscous liquid in a vertical tube containing a porous material, - Proc. Royal Society, Ser. A, 252, pp. 102-134.

XUE, Y., et al., 1995: A three-dimensional miscible transport model for seawater intrusion in China, - Water Resources Research 31(4), pp. 903-912.

Density dependent groundwater flow near deepwell infiltration systems, Modelling aspects

J.M. van Esch
Delft Geotechnics, P.O. Box 69, 2600 AB Delft, The Netherlands
Delft University of Technology, P.O. Box 5048, 2600 GA Delft, The Netherlands

A. Stakelbeek
Water Supply Company of North Holland, P.O. Box 5, 2060 BA Bloemendaal, The Netherlands

In this article a coupled flow-transport model is presented by which the time dependent behaviour of the brackish zone between salt and fresh groundwater can be simulated. The model will be used to optimize the balance between groundwater infiltration and abstraction as it takes place in deepwell infiltration systems, under the restriction that low concentration of salt makes the abstracted water useless for drinking water production. Although it can be shown that the model presented here gives promising results, it has to be adjusted to be useful in engineering practice. Some suggestions are given to reduce computational time and use of memory.

Introduction

The dune area along the North sea coast in the north-western part of the Netherlands is one of the most valuable natural areas in this country. To keep the groundwater, for ecological reasons, at an adequately high level, groundwater abstraction has been reduced in the last 30 years from about 20 Mm^3/year to about 2 Mm^3/year. This reduction of the abstraction of natural groundwater has been compensated by an artificial recharge system, which has become the predominant production method in the western part of Holland. Particularly the method of deep-well infiltration is winning ground because its slight spacial demands combined with small eco-hydrological impact.

PWN, Water Supply Company of North Holland, has been operating a deep-well infiltration system since the beginning of 1990. Its capacity is 5 Mm^3/year. The infiltration is carried out by means of 20 infiltration wells into an aquifer 50 to 100 metres below sea level. Abstraction is carried out by 12 abstraction wells in the same aquifer in which the infiltration wells are situated. This semi-confined aquifer is bounded at the lower side by a thin silty layer, under which the groundwater is brackish. An overinfiltration of 10% is maintained to avoid upconing of the brackish groundwater under the abstraction wells. Salt concentrations higher than 200 mg/l make the abstracted water unsuitable for drinking water production.

Recently a research project has been started for the development of a numerical model, by which low salinities can be predicted for this really three dimensional and time dependent problem. The model will be calibrated by hydraulic head measurements and resistivity measurements of electrode cables which are placed under the abstraction wells and in infiltration wells at several locations. The model will be used to optimize the balance between infiltration and abstraction. Further an estimation can be made of the length of the period the groundwater abstraction can be continued, when the infiltration is interrupted in the case of a calamity. If this period turns out to be sufficient long then the deep-well infiltration system will be an important reserve storage, when the surface water used for infiltration is polluted.

Basic equations

In this paragraph the main equations that form the coupled flow-transport model will be given by which the time dependent behaviour of the brackish zone can be simulated. For it is assumed that the equations are known to most of the readers, the equation will be presented in a short form, for details see [Bear 1972 and Bear Verruijt 1987].

The flow equation follows from Darcy's law and continuity of mass:

$$\frac{\partial(\rho n)}{\partial t} = \rho(\alpha+n\beta_p)\frac{\partial p}{\partial t}+\rho n\beta_c\frac{\partial c}{\partial t} = \nabla\cdot\left(\frac{\rho K}{\mu}\cdot(\nabla p+\rho g)\right) \qquad (1)$$

where the pressure p is the basic variable. The time dependent terms are all on the left hand side, ρ represents the fluid density, n is the porosity of the soil matrix and t is the time. The coefficient α accounts for the deformation of the solid matrix and follows from a linear state equation $\alpha = dn/dp$. The β_p coefficient accounts for the compression of the fluid and follows from the state equation $\beta_p = 1/\rho\cdot\partial\rho/\partial p$. The coefficient β_c describes the relation $\beta_c = 1/\rho\cdot\partial\rho/\partial c$. At the right-hand side K is the second-order intrinsic permeability tensor, μ is the dynamic viscosity and **g** the gravity constant.

The mass-transport equation, where the salt concentration c is the basic variable, reads:

$$R\frac{\partial c}{\partial t} = -\nabla\cdot(vc)+\nabla\cdot(\boldsymbol{D}\cdot\nabla c) \qquad (2)$$

where R is called the retardation factor due to adsorption, which assumes a constant state of equilibrium between the concentration in the fluid c and the concentration at the solid matrix c'. The partitioning coefficient between these concentrations is called the linear equilibrium isotherm $K = c'/c$. The retardation factor can be written as: $R = 1 + (1-n)/n\cdot K$. The first term at the right hand side represents the transport by convection, **v** is the real pore velocity vector of the fluid. The second term represents the dispersion part, where **D** is the second order dispersion tensor.

The fluid velocity in the pores follows from the Darcy velocity and is written as:

$$v = -\frac{K}{n\mu}\cdot(\nabla p+\rho g) \qquad (3)$$

For an isotropic medium the dispersion tensor equals:

$$\boldsymbol{D} = (d+\alpha_t|v|)\boldsymbol{I}+(\alpha_l+\alpha_t)\frac{\boldsymbol{v}\boldsymbol{v}^T}{|v|} \qquad (4)$$

The unit tensor is denoted by **I**, d represents the molecular diffusion coefficient. The two parameters α_l and α_t in this expression are the longitudinal and transverse dispersivity, respectively. In a homogeneous medium they both are of the order of the pore size. For a practical situation the dispersivities are dominated by variations in the velocity field, mainly due to variations in the intrinsic permeability field. Both the velocity field and the dispersion field can be calculated from the flow equation. The longitudinal dispersivity is usually much larger than the transverse dispersivity.

For the case of coupled flow the fluid density and fluid viscosity are assumed to be some function of the pressure and the concentration.

The state equation $\rho = \rho(p,c)$ linearized around the point $\rho_0 = \rho(p_0,c_0)$ for the fluid density is written as:

$$\rho = \rho_0\{1+\beta_p(p-p_0)+\beta_c(c-c_0)\} \tag{5}$$

where ρ_0 is a reference value for the fluid density at pressure p_0 and concentration c_0. The coefficients β_p and β_c indicate the change in fluid density as a function of pressure and concentration, respectively. The coefficients are defined by $\beta_p = 1/\rho \cdot \partial\rho/\partial p$ and $\beta_c = 1/\rho \cdot \partial\rho/\partial c$.

The state equation for the dynamic fluid viscosity $\mu = \mu(p,c)$ is linearized in the same manner, leading to:

$$\mu = \mu_0\{1+\gamma_p(p-p_0)+\gamma_c(c-c_0)\} \tag{6}$$

where μ_0 is a reference value for the viscosity at pressure p_0 and concentration c_0. The coefficients γ_p and γ_c specify the change in viscosity relative to the pressure and concentration change and are defined by $\gamma_p = 1/\mu \cdot \partial\mu/\partial p$ and $\gamma_c = 1/\mu \cdot \partial\mu/\partial c$.

Equations 1 to 6 form the coupled flow-transport model. A unique solution for a practical problem can be found under specific initial and boundary conditions.

Numerical model

The solution of equations 1 and 2 is approximated by the finite element method. According to this method the computational domain is subdivided in a large number of elements. The basic variables (pressure and concentration) are calculated in the nodal points of the mesh. Inside the element the values of these variables can be obtained by interpolation using the shape function. In this paper isoparametric 4 nodded quadrilateral and 8 nodded hexahedral elements are used, for 2D and 3D simulations respectively. Soil properties are taken constant within an element, the mesh is fixed in space (Eulerian description) which seems to be physically reasonable. Velocity vectors and dispersion tensor values are computed in the interpolation points, (Gauss points).

A sequential solution scheme is employed for solving the sets of equations 1 and 2 [Huyakorn and Pinder 1983]. At first the flow equation is solved using an estimate of the concentration field. Then the mass equation is solved using the computed velocity field. This procedure is repeated for the same time increment until concentration and pressure stabilize. The numerical formulation for both sets of equations is found using the Galerkin formulation [Bathe 1996 and Zienkiewics 1977]. The Galerkin method is a special case of the method of weighted residuals where the weight functions are chosen equal to the shape functions.

A consistent formulation for the flow equation has been found by order reduction of the gravitation field. A lumped mass formulation has been employed to increase the stability of the mass transport equation. The set of linear equations for pressures has a sparce symmetric coefficient matrix and is solved by the ordinary conjugate gradient method [Press ea., 1988]. The second set contains a sparce but asymmetric matrix of coefficients and is solved using the biconjugate gradient method.

Preliminary results

As a demonstration some simulation results are shown in figures 1 to 5. In these figures iso-concentration lines are drawn, the upmost isoline corresponds to a concentration 0.1, the lowest line corresponds to a concentration 0.9. The problem concerns a homogeneous layer with a source

of 0.33 m^2/d at the right boundary and a sink of equal size at the left side. The layer has a length of 30 m and a height of 10 m. To the upper boundary of the layer an atmospheric pressure condition is imposed, all other boundaries are impermeable. Initially the lower half of the domain has a concentration 1 which corresponds to salt water with a density of 1025 kg/m^3. The upper half has a concentration 0 which corresponds to fresh water with a fluid density of 1000 kg/m^3. The permeability of the porous medium is 1 m/d, the dynamic viscosity is assumed to be constant and has a value of 10^{-3} Pas, the porosity is 0.4.

Figure 1 shows the results of a 2D simulation the dispersivities are α_l = 1 m, α_t = 0.5 m. Upconing takes place at the left side of the domain. The salt water zone is pushed down at the right size, however initially dispersion dominates convection and low concentrations are found upstream.

The results of a 2D simulation with a longitudinal dispersivity of 0.5 m and a transverse dispersivity of 0.1 m are shown in figure 2. For this case the brackish zone remains limited in size.

The results of the model are compared with the results of a sharp interface model. The result of the sharp interface model GAMMA [Verruijt 1996] are given in figure 3. This model is based on the same flow equation, fluid densities are kept constant for each element however.

Figure 4 displays a vertical section of a 3D model for longitudinal and transverse dispersivities of respectively α_l = 1 m, α_t = 0.5 m. The infiltration and abstraction rates are 0.33 m^3/d, the computational domain is extended in the third direction to 5 m. Upconing is less severe under these conditions as can be expected.

Finally the results of a decoupled simulation are presented in figure 5, dispersivities now are again α_l = 1 m, α_t = 0.5 m. For this simulation fluid density is assumed to be independent of the concentration. As a result of this, upconing will be greater; the driving force downward is not present.

Conclusions

For a sharp interface problem the time scale and length scale differ from a coupled convection-dispersion problem. Sharp interface models show less upconing at the same time, this is partially the result of the smaller density force at low concentrations that counteracts the abstraction force. For early time steps a decoupled convection-diffusion model for which the density effect is not part of the problem gives a better estimate than a sharp interface approach.

The finite element formulation demonstrated in this paper is suitable for solving density dependent groundwater flow problems. Three dimensional calculations however require a lot of internal computer memory and calculation times may be long. For the presented case of a strip of 30 meters long 10 meters high and 5 meters of with, 10 Mb memory was required an the calculation time was about 5 hours (on a 100 MHz Pentium PC) till the equilibrium state was almost reached at 1000 days. Comparing the results with the two dimensional simulation it must be noted that one has to be very careful in applying two dimensional models for a really three dimensional problem.

Coupled convection-diffusion problems with fresh water on top of a salt water zone, differ numerically from uncoupled convection-diffusion problems for transport of a pollutant. In zones where the convection is small, diffusion will be small too, the front remains steep giving rise to numerical oscillations. These oscillations may be suppressed by using a lumped mass formulation, however numeric simulations showed that the mesh size must be smaller than 5 times the lowest dispersivity coefficient (according to the Peclet number, the Courant number may be used to determine the time step size). The finite element method seems to be very efficient for three

dimensional modelling of groundwater flow problems, as it is possible to refine the mesh in parts of the computational domain where large gradients are expected.

To reduce calculation times and to limit memory requirements, an Arbitrary Lagrangian-Eulerian (ALE) description is proposed. Pressures and velocities will be calculated for a fixed Eulerian mesh. Soil parameters are kept constant within an element which seems physically right. Concentrations however will be calculated for a moving Lagrangian mesh, displacement of the mesh nodes account for the convection part of the transport equation. Local refinement of the mesh in the front between salt and fresh water may be necessary for reasons of accuracy.

Practically dispersion is dominated by variations in the convection field due to heterogenities in the soil properties and temporal variations in the boundary conditions. As these variations are unknown dispersion accounts for a statistical process. It is assumed that dispersion will be the main contributor to mixing and the development of the brackish zone, this process will be studied by physical models as well. Temperature effects might be important too, the model will be extended to account for these effects. A sensitivity study has to show which of the processes are most important for modelling an abstraction-infiltration problem. A faster model may be derived using this knowledge.

REFERENCES

Bathe K.J., 1996: Finite element procedures in engineering analysis, Prentice Hall, Englewood Cliffs.

Bear J., 1972: Dynamics of fluids in porous media, Dover Publications inc., New York.

Bear J., Verruijt A., 1987: Modelling groundwater flow and pollution, Reidel, Dordrecht.

Huyakorn P.S., Pinder G.F., 1983: Computational methods in subsurface flow, Academic Press, New York.

Press h.w., ea., 1988: Numerical recipes in C, 2d ed., Cambridge University Press, New York.

Verruijt A., 1996: Gamma, A computer model for interface flow, Delft University of technology, Delft.

Verruijt A., 1996: Displacement of an interface between fresh and salt groundwater, Delft.

Zienkiewics O.C., 1977: The finite element method, 3d ed., McGraw-Hill, London.

FIGURE 1, 2D simulation results (α_l = 1 m, α_t = 0.5 m)

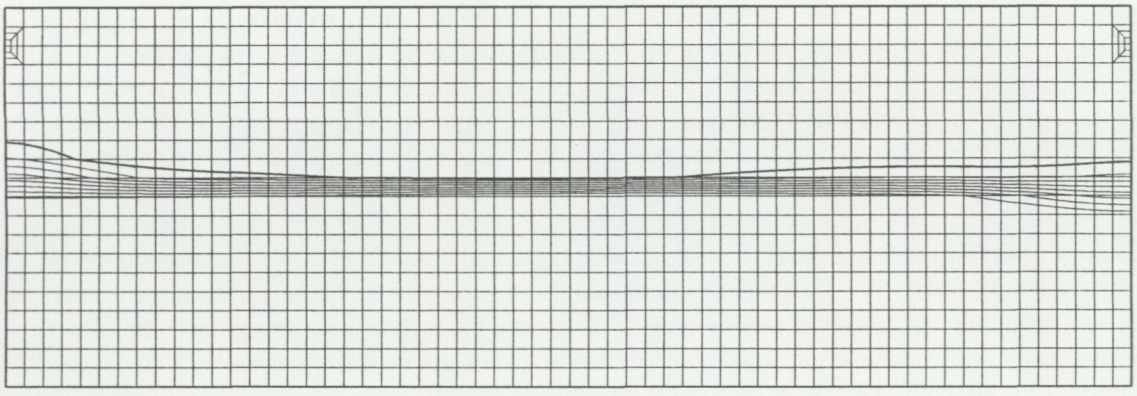


figure 1a, t = 10 days

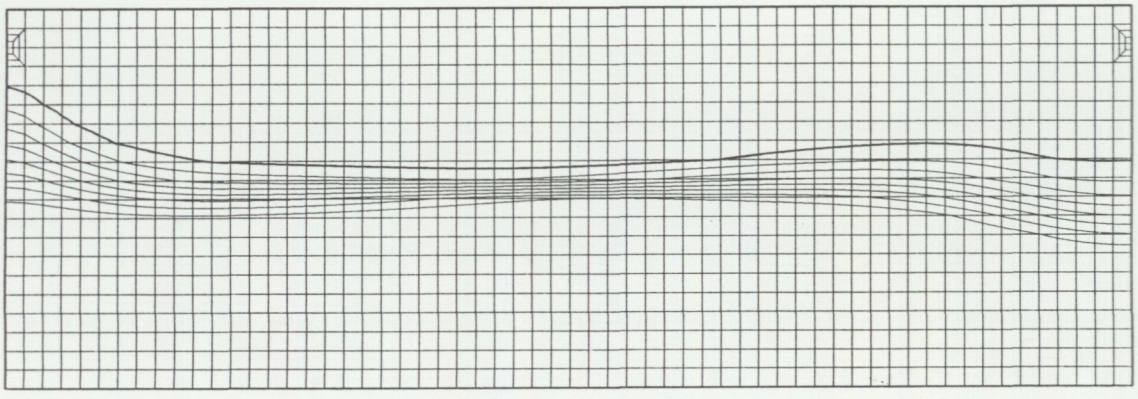


figure 1b, t = 50 days

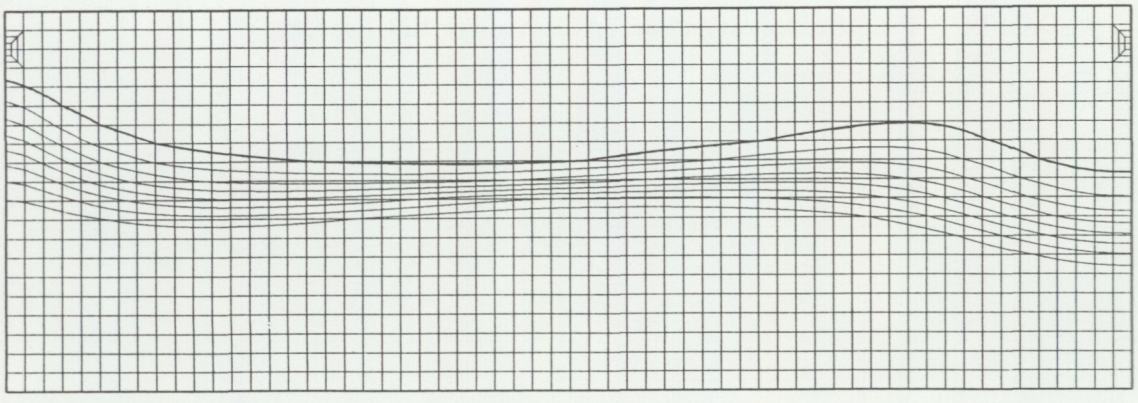


figure 1c, t = 100 days

FIGURE 2, 2D simulation results (α_l = 0.5 m, α_t = 0.1 m)

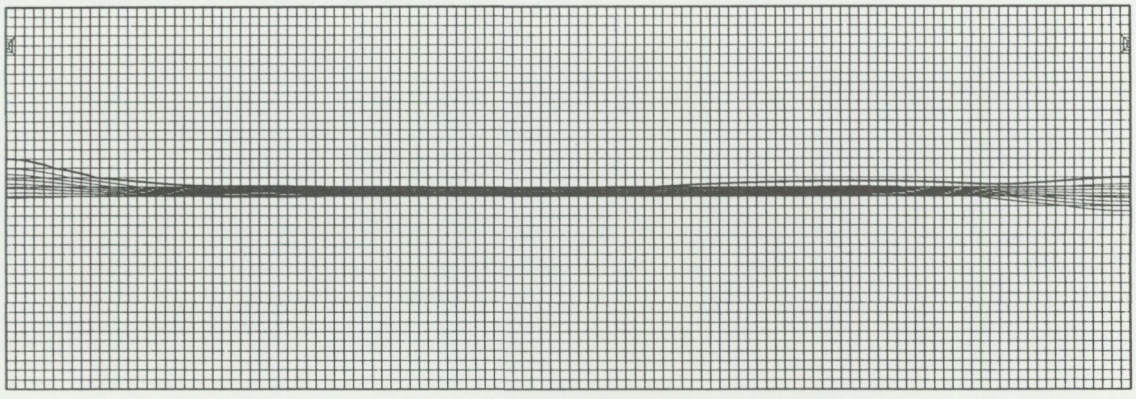


figure 2a, t = 10 days

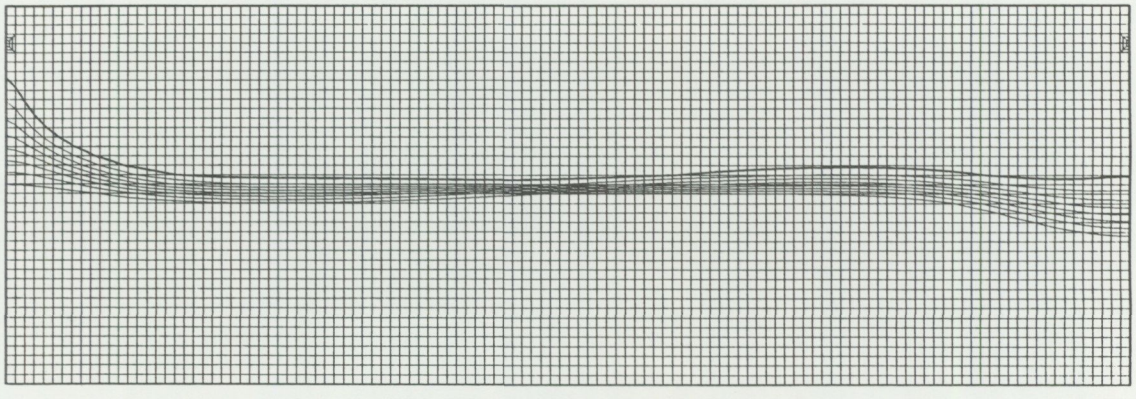


figure 2b, t = 50 days

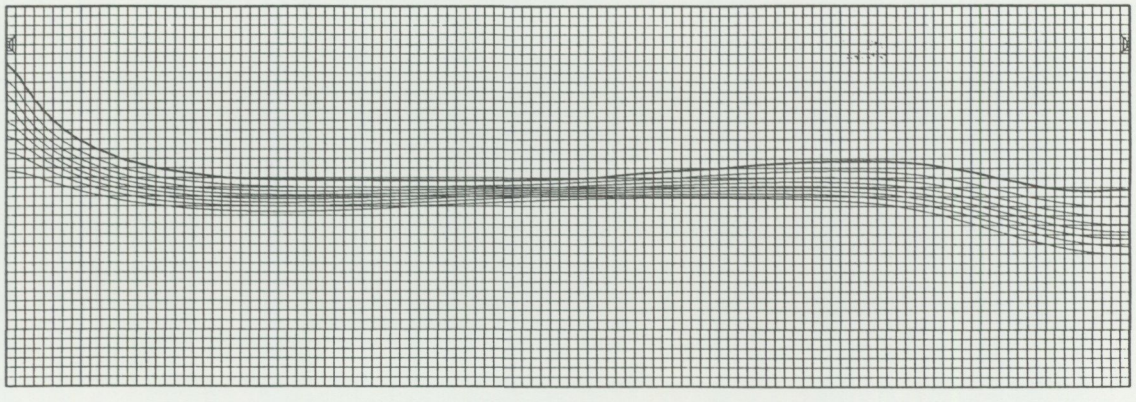


figure 2c, t = 100 days

FIGURE 3, 2D simulation results sharp interface model

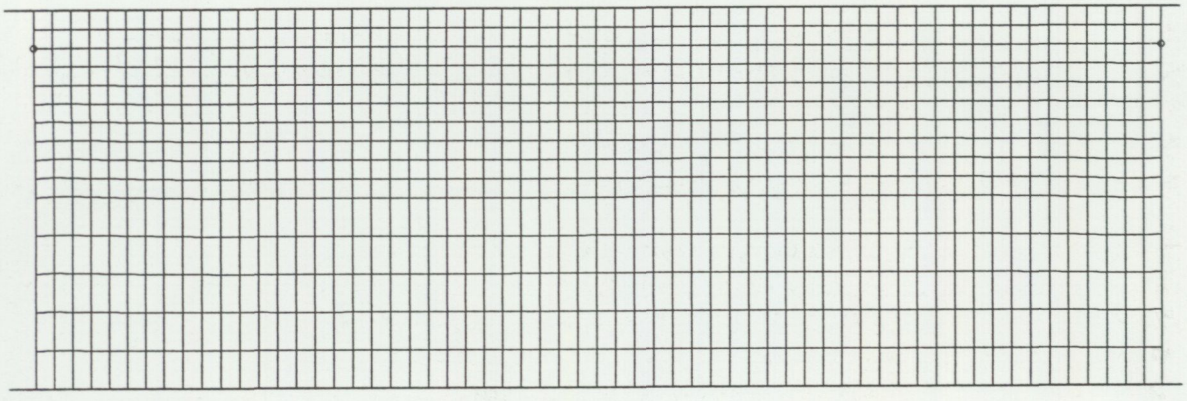


figure 3a, t = 10 days

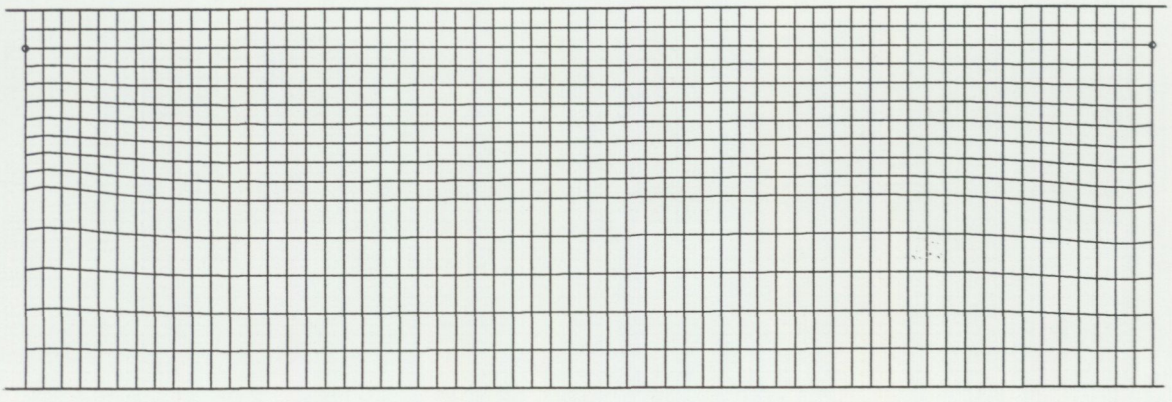


figure 3b, t = 50 days

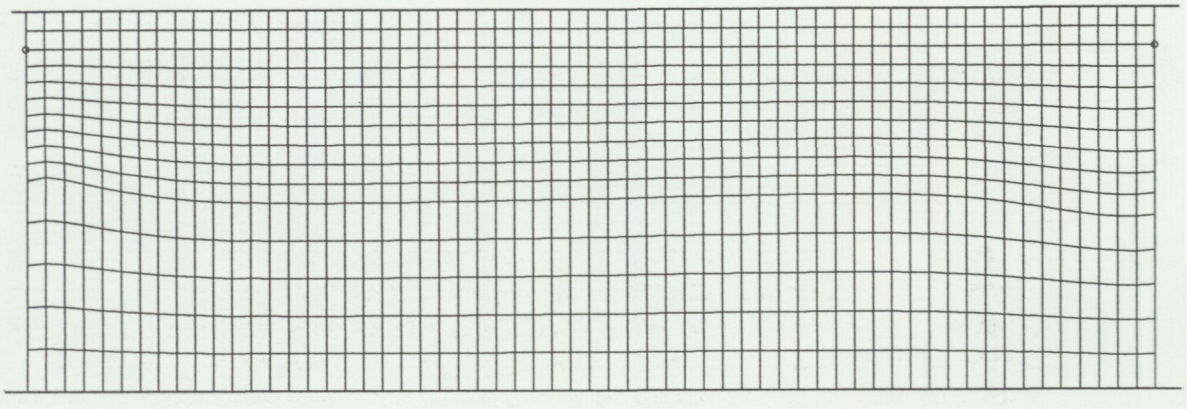


figure 3c, t = 100 days

FIGURE 4, 3D simulation results (α_l = 1 m, α_t = 0.5 m)

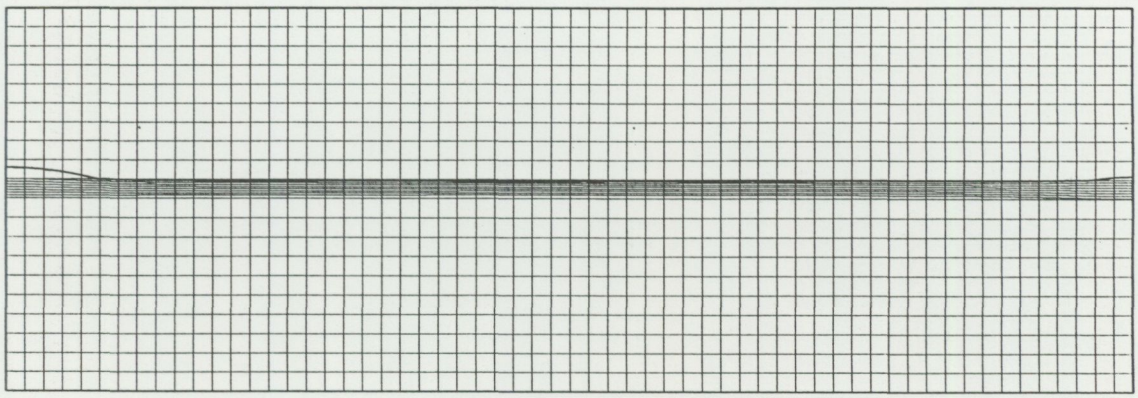


figure 4a, t = 10 days

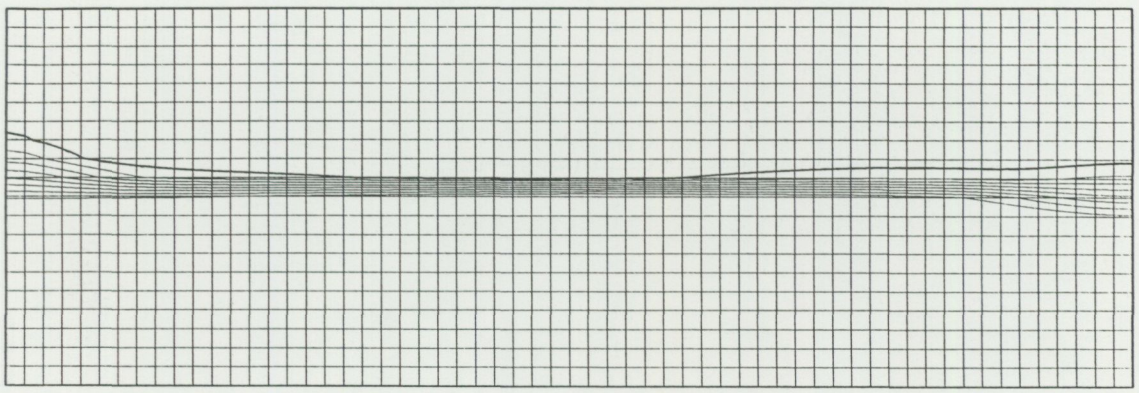


figure 4b, t = 50 days

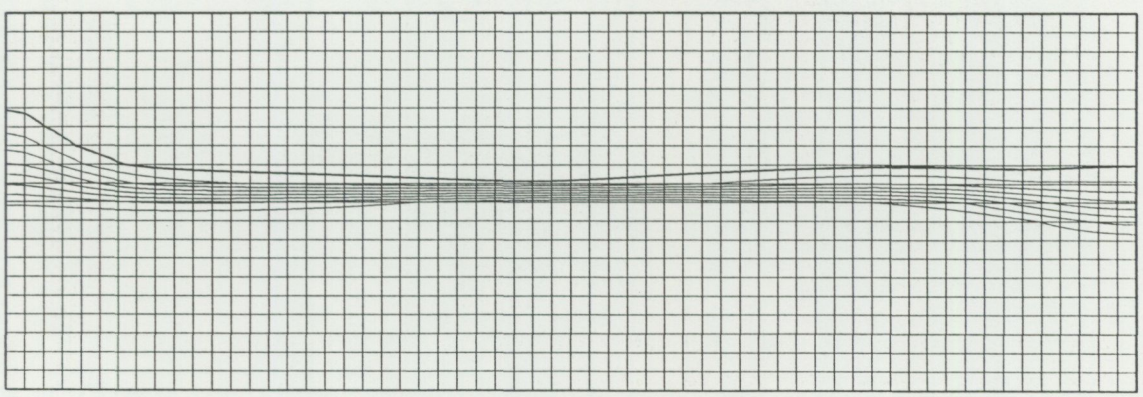


figure 4c, t = 100 days

FIGURE 5, 2D decoupled simulation results (α_l = 1 m, α_t = 0.5 m)

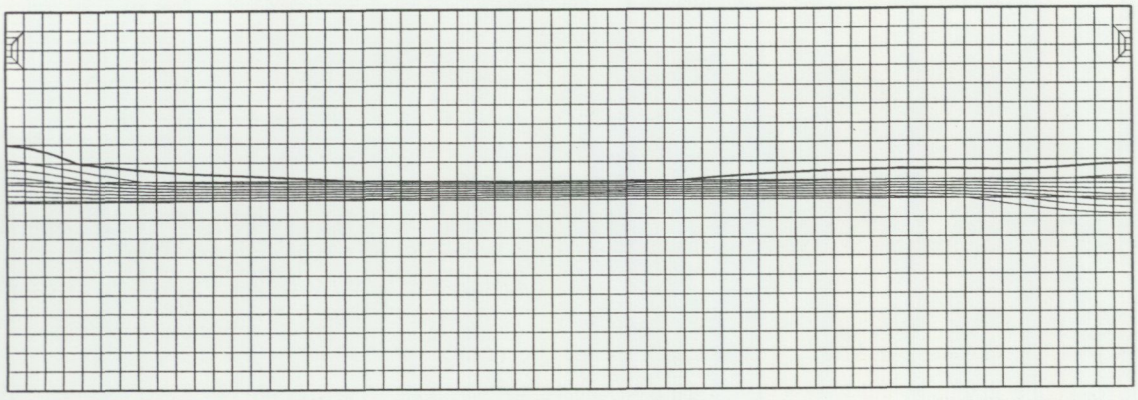


figure 5a, t = 10 days

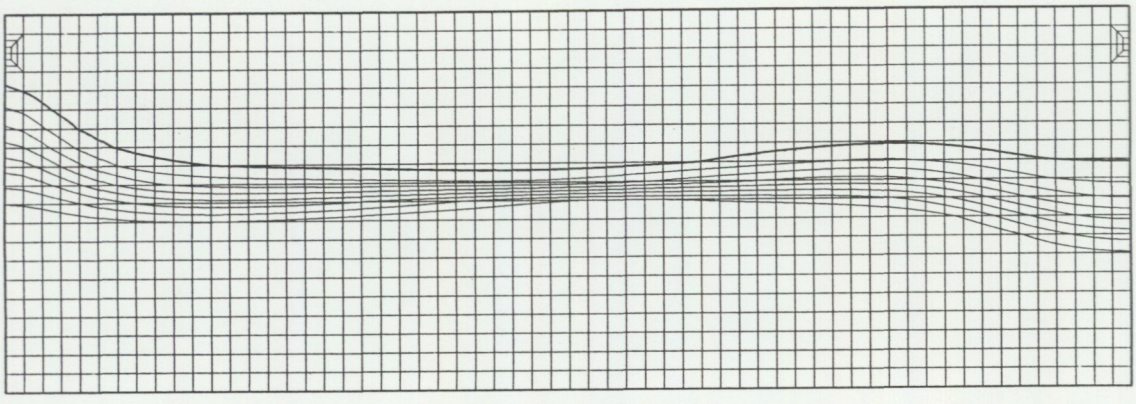


figure 5b, t = 50 days

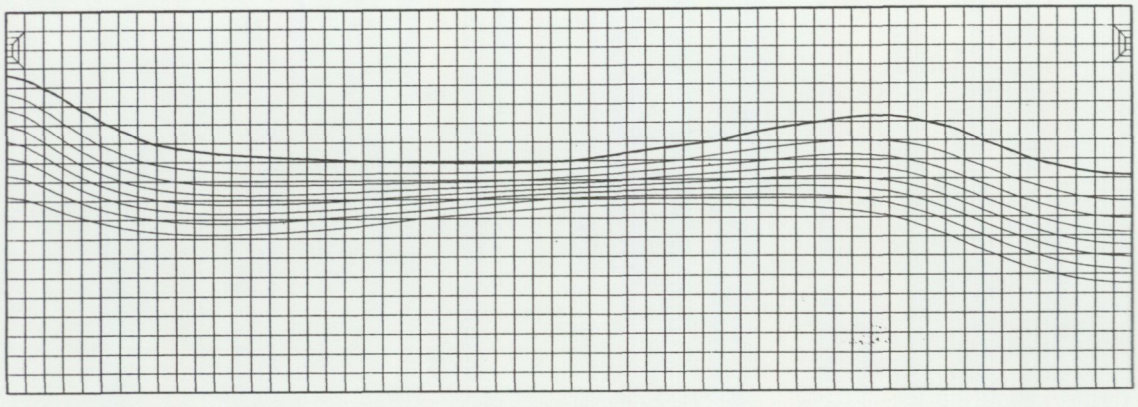


figure 5c, t = 100 days

Variable density groundwater flow modelling with MODFLOW

T.N.Olsthoorn,
Amsterdam Water Supply, Vogelenzangseweg 21, 2114 BA Vogelenzang, The Netherlands
Tel: +31-23-5233569, Fax:+31-23-5281460, E-mail: t.olsthoorn@gw.amsterdam.nl

Variable density flow of groundwater can be computed by a general purpose groundwater model such as the block-centred finite-difference model MODFLOW. Density effects are accounted for by source terms that can be computed in advance. After correcting the computed intercell flows for the density effect, general purpose flow line or particle transport models such as MODPATH or MT3D can be used to generate streamlines and particle transport for the variable density situation.

Others, (Maas and Emke, 1988, Strack, 1995) have been successful in modelling regional variable density flow by means of single density models. Contrary to their work, fresh water heads are now used instead of pressures. This has many advantages in every day hydrologic practice. Further, fresh-water heads are considered easier to understand and applied in a finite difference model such as MODFLOW than the discharge potential developed by Strack for his analytical model MVAEM (1995).

Basics

In Darcy's law for volumetric three-dimensional groundwater flow under variable density conditions the flux, v [L/t], is be expressed in terms of pressure, p [F/L^2], the intrinsic permeability κ [L^2], the fluid viscosity μ [Ft/L^2] and the specific fluid weight γ [F/L^3], the latter being the negative z-derivative of the hydrostatic pressure Γ [F/L^2]:

$$v_x = -\frac{\kappa_x}{\mu}\frac{\partial p}{\partial x}\;; \qquad v_y = -\frac{\kappa_y}{\mu}\frac{\partial p}{\partial y}\;; \qquad v_z = -\frac{\kappa_z}{\mu}\left(\frac{\partial p}{\partial z}+\gamma\right) = -\frac{\kappa_z}{\mu}\left(\frac{\partial (p-\Gamma)}{\partial z}\right) \tag{1}$$

Note that the vertical coordinate, z [L], is taken positive in upward direction. The hydrostatic pressure, Γ [F/L^2], is defined in terms of the specific fluid weight, γ [M/L^3], as follows:

$$\Gamma = \int_{z_0}^{z} (-\gamma)\,dz \quad \rightarrow \quad \gamma = -\frac{\partial \Gamma}{\partial z} \tag{2}$$

In the sequel we'll use the fresh-water head, ϕ [L] and the hydrostatic fresh-water head, G [L], rather than pressure, p, and hydrostatic pressure, Γ. By definition:

$$\phi = \frac{p}{\gamma_0} + z\;; \qquad G = \frac{\Gamma}{\gamma_0} + z \tag{3}$$

where γ_0 [M/L^3] is fixed and set conveniently equal to the specific weight of fresh water. The hydrostatic fresh-water head, G [L], is the perfect analog of the hydrostatic pressure, Γ [F/L^2]. It is alternatively and often conveniently defined directly in terms of γ as:

$$G=\frac{\Gamma}{\gamma_0}+z \;=\; -\int_0^z \frac{\gamma}{\gamma_0}dz+z \;=\; -\int_0^z (\frac{\gamma}{\gamma_0}-1)dz \qquad (4)$$

Note that both the fresh-water head and the hydrostatic fresh-water head are easily understandable physical entities. The first one being the measured head if the piezometer tube were filled over its full height with water of specific weight γ_0, the latter can be seen as the fresh-water head in case that "no water were flowing" relative to some reference level taken z=0 here for convenience. Since the density distribution is considered given, the hydrostatic fresh-water head can be computed in advance.

Filling in $p = \gamma_0(\phi - z)$ in the Darcy equations above, we obtain the Darcy equations in terms of fresh water heads:

$$v_x=-k_x\frac{\partial\phi}{\partial x}\;; \qquad v_y=-k_y\frac{\partial\phi}{\partial y}\;; \qquad v_z=-k_z(\frac{\partial\phi}{\partial z}+\frac{\gamma}{\gamma_0}-1)= -k_z(\frac{\partial(\phi-G)}{\partial z}) \qquad (5)$$

in which the usual permeabilities, k [L/t], replace the coefficients $\kappa\gamma_0/\mu$. Both forms of Darcy's equations are perfectly analogous. Note that the combined term $\Phi=\phi-G$ is called the environmental head after De Wiest (1969), because it produces the vertical flow in density situations if differentiated with respect to z.

Horizontal flow in MODFLOW cells

In density flow computations the head and the flows may be strongly dependent on the density distribution of the fluid. The water may flow to the right in the top of an aquifer and at the same time to the left at its bottom. Hence we have to consider the gradient variation even within model cells. The block centred finite difference model only computes heads at the centre of each cell. So we must consider the head variation relative to the value at the cell centre.

We obtain the head at some height ,z ,above or below the cell centre, z=M, by integrating the vertical head gradient given by Darcy (eq. 5) accordingly:

$$\frac{\partial\phi}{\partial z}=-\frac{v_z}{k_z}+\frac{\partial G}{\partial z} \quad\rightarrow\quad \phi_z=\phi_M+G_z-G_M-\int_M^z\frac{v_z}{k_z}dz \qquad (6)$$

Within a model cell k_z is considered constant, while v_z is considered to vary only with z and so it vanishes when the head is differentiated with respect to x or y in order to compute the horizontal flow components a elevation z. Hence the horizontal x-component of the groundwater flow at elevation z is expressed in the head at the cell centre and the hydrostatic fresh-water head:

$$v_x=-k_x\frac{\partial\phi_M}{\partial x}-k_x\frac{\partial(G_z-G_M)}{\partial x} \qquad (7)$$

In order to obtain the horizontal flow, Q_x [L3/t], in x-direction through a model cell of given height Δz [L] (fig. 1), we integrate v_x over the full height of the cell and multiply by the cell width Δy [L]:

$$Q_x = \Delta y \int_{z_B}^{z_T} v_x(z)dz = -k_x \Delta y \Delta z [\frac{\partial \phi_M}{\partial x} + \frac{\partial (\overline{G} - G_M)}{\partial x}] \quad (8)$$

Where the $\overline{G}$ denotes the average hydrostatic head taken at the x-location over the full height of the cell. Hence $\overline{G}$-G_M represents the deviation of the average hydrostatic fresh-water head over the height of the model cell from its value at half the height of the cell. This term is zero if the density is constant over the cell height, because in that case the hydrostatic fresh-water head is a linear function of z at any location.

Between the midpoints of two adjacent model cells A and C (fig. 1) Q_x is considered constant, $Q_{AC}=Q_x$, only to jump at the cell centers. So, to express the horizontal flow in the heads in the cell centers, we integrate the head gradients between these two points A and C, passing through the points BL and BR at the left- and right-hand side of the cell wall, B, between the two cells (fig. 2). Note that, while Δz may vary from cell to cell, Δx and Δy are constant per column and row:

$$Q_{AC} \int_A^C \frac{1}{k_x \Delta y \Delta z} dx = -\int_A^C \frac{\partial \phi_M}{\partial x} dx - \int_A^C \frac{\partial (\overline{G} - G_M)}{\partial x} dx \quad (9)$$

This yields:

$$Q_{AC} = C_{AC} [(\phi_A - \phi_C) - (\phi_{BL} - \phi_{BR}) + (\overline{G_A} - G_A) - (\overline{G_{BL}} - G_{BL}) + (\overline{G_{BR}} - G_{BR}) - (\overline{G_C} - G_C)] \quad (10)$$

Where C_{AC} [L2/t] is the MODFLOW conductance (McDonald and Harbaugh, 1988):

$$C_{AC} = \Delta y \ / \ [\frac{\Delta x_A / 2}{k_A \Delta z_A} + \frac{\Delta x_C / 2}{k_C \Delta z_C}] \quad (11)$$

The fresh-water head difference ϕ_{BL}-ϕ_{BR} has to be evaluated with care, because the hydrostatic fresh water head doesn't have to be continuous across the cell wall. Neglecting the resistance against vertical flow in this cell boundary plane we can express this term in terms of precalculated hydrostatic fresh-water heads (fig. 2):

$$\phi_{BR} - \phi_{BL} = (G_{BR} - G_{MR}) - (G_{BL} - G_{ML}) = \Delta G_{BR} - \Delta G_{BL} \quad (12)$$

So finally we have, in a most general sense, the following expression for the horizontal volumetric flow between adjacent cells A and C, as shown in fig. 2:

$$Q_{AC} = C_{AC} (\phi_A - \phi_C) + C_{AC} [(\overline{G_A} - G_A) - (\overline{G_C} - G_C) - (\overline{G_{BL}} - G_{BL}) + (\overline{G_{BR}} - G_{BR}) - (\Delta G_{BL} - \Delta G_{BR})] \quad (13)$$

The first term on the right hand side represents the effect of the fresh water head on the flow, the second part

represents the effect of density variations. The latter is a fixed value, since the all hydrostatic fresh-water heads are assumed to be given. If brought to the left side of the equation it represents a fixed source term to be added to other fixed source terms before running the model. If left at the right hand side of the equation, as in the above form, it represents a correction on the horizontal flow computed by the model, in order to obtain the true volumetric flow between the cells A and C. Clearly, the same equation holds true in both the x and y directions.

PRACTICAL SIMPLIFICATION: Often, one will be tempted to simplify the model by assuming either a single density value in each cell or a density distribution that is independent of x,y within each cell, for instance by assuming a cell-wise horizontal interface between fresh and salt water. In such cases we have:

$$(\overline{G_A}-G_A)=(\overline{G_{BL}}-G_{BL}) \quad and \quad (\overline{G_C}-G_C)=(\overline{G_{BR}}-G_{BR}) \tag{14}$$

so that then all terms that express the difference between de height-averaged hydrostatic head and their value at half the cell's height vanish. This leaves us with:

$$Q_{AC}=C_{AC}\,(\phi_A-\phi_C)-C_{AC}\,(\Delta G_{BL}-\Delta G_{BR}) \tag{15}$$

The right term can be elaborated explicitly in the special case of a single density per cell or per layer as was used by Maas and Emke (1988). We can, however, in all cases just as well precalculate G and use that.

If we assume within each cell a density that is independent of x,y and at the same time adopt a regular model mesh, such that the tops and bottoms of the cells in a model layer all match, then the horizontal flow between two adjacent cells simplifies to the equation for the fresh-water model (refer to eq. 12):

$$Q_x=C_{AC}\,(\phi_A-\phi_C) \tag{16}$$

Use of one density per layer can often be achieved by splitting model layers in sublayers at planes separating zones of constant but distinct density, such as the interface between fresh and salt water (Maas and Emke, 1988). Use of a single density per cell is often acceptable with small salinity gradients. We tend to use cell-wise horizontal interface or simply use the given full equation for horizontal flow. In any case, it should be noted that all terms comprising the specific fluid weight, γ, and hence the hydrostatic fresh-water head, G, can be computed in advance.

Vertical flow

To discretize the equation for vertical flow, we integrate the head gradient of the vertical flow equation (eq. 5) between the centres of two cells situated above one another (fig. 3).

$$\int_{z_A}^{z_B}\frac{v_z}{k_z}dz=-\int_{z_A}^{z_B}\frac{\partial\Phi}{\partial z}dz=-\int_{z_A}^{z_B}\frac{\partial(\phi-G)}{\partial z}dz \tag{17}$$

If we consider the three different permeabilities between point A and B as shown in fig. 3, we obtain:

$$v_z \left(\frac{\Delta z_A/2}{k_{z_A}} + \frac{D}{k_z} + \frac{\Delta z_B/2}{k_{z_B}}\right) = (\phi_A - \phi_B) - (G_A - G_B) \qquad \textbf{(18)}$$

or, for the total volumetric flow $Q_{AB} = \Delta x \Delta y \, v_z$

$$Q_{AB} = C_{AB}(\phi_A - \phi_B) - C_{AB}(G_A - G_B) \qquad \textbf{(19)}$$

in which C_{AB} [L2/t] is the vertical MODFLOW conductance or leakance (McDonald and Harbaugh, 1988):

$$C_{AB} = \Delta x \Delta y \; / \; \left[\frac{\Delta z_A/2}{k_{z_A}} + \frac{D}{k_z} + \frac{\Delta z_B/2}{k_{z_B}}\right] \qquad \textbf{(20)}$$

Like the horizontal flow, the first term of the equation represents the vertical flow computed by the model, while the second term is a density source term, if brought to the left side of this equation. So, it has to be added to the other ordinary source terms (such as wells) before running the model. The right-hand term has to be subtracted from the flows calculated by the model in order to obtain the true flow, Q_{AB}, for the variable density case. Note that the right hand term is zero in the fresh-water part of the model.

Water balance for a model cell

Providing indices N,E,S,W,T,B to indicate the cell to the North, East, South, West, Top and Bottom of the considered cell, we write down the water balance of a MODFLOW cell:

$$Q_E + Q_N + Q_W + Q_S + Q_T + Q_B + Q_G + Q = 0. \qquad \textbf{(21)}$$

In which the index "G" stands for all indirect, that is, head dependent "general head boundaries", including rivers and drains:

$$Q_G = \sum_{j=1}^{m} [C_j(G_j - G_0)] \qquad \textbf{(22)}$$

Where the index "0" denotes the considered cell and C_j is the corresponding conductance. The sum is taken over all external heads connected to the considered cell. Q is the total direct input for the cell. Note that all values are taken positive if their direction is inward, that is, when they raise the head in the cell that is being considered.

Because all hydrostatic fresh-water head terms are considered to be known in advance, they can be put to the right hand side of the above cell balance (eq. 21), together with the direct inputs (wells). Filling in the formulas for horizontal and vertical flow (eqs. 13 and 17), we obtain in the most general case:

$$
\begin{aligned}
&C_E\phi_E+C_N\phi_N+C_W\phi_W+C_S\phi_S+C_T\phi_T+C_B\phi_B+\sum C_G\phi_G \\
&-(C_E+C_N+C_W+C_S+C_T+C_B+\sum C_G)\,\phi_0 \quad = \\
&\quad -C_E((\overline{G_E}-G_E)-(\overline{G_0}-G_0)-(\overline{G_{EE}}-G_{EE})+(\overline{G_{E0}}-G_{E0})-(\Delta G_{EE}-\Delta G_{E0})) \\
&\quad -C_N((\overline{G_N}-G_N)-(\overline{G_0}-G_0)-(\overline{G_{NN}}-G_{NN})+(\overline{G_{N0}}-G_{N0})-(\Delta G_{NN}-\Delta G_{N0})) \\
&\quad -C_W((\overline{G_W}-G_W)-(\overline{G_0}-G_0)-(\overline{G_{WW}}-G_{WW})-(\overline{G_{W0}}-G_{W0})-(\Delta G_{WW}-\Delta G_{W0})) \\
&\quad -C_S((\overline{G_S}-G_S)-(\overline{G_0}-G_0)-(\overline{G_{SS}}-G_{SS})-(\overline{G_{S0}}-G_{S0})-(\Delta G_{SS}-\Delta G_{S0})) \\
&\quad +C_T(G_T-G_0) \\
&\quad +C_B(G_B-G_0) \\
&\quad +\sum C_G(G_G-G_0) \\
&\quad -Q
\end{aligned}
\qquad (23)
$$

The index "0" to denotes the considered cell. The index "EE" denotes the East-side of the boundary plane between the considered cell and its eastern neighbour; the index "E0" denotes the boundary plane between the eastern cell and the considered cell at the side of the considered cell. "E" is replaced accordingly by "N", "W" and "S".

The left hand side of eq. 23 represents the internal structure of the finite difference model, i.e. MODFLOW, and the right-hand side represents its source terms. So we can obtain the fresh-water head under variable density conditions by using the right-hand side as the source term and running our ordinary ground-water model.

Boundary conditions

Direct boundary flows from or to wells are unchanged in the variable density situation. Given heads must be specified in terms of fresh-water heads. Boundaries with horizontal flow require v_z to be zero and so the head must equal the hydrostatic fresh-water head but for a constant:

$$
\frac{\partial\phi}{\partial z}=\frac{\partial G}{\partial z} \quad \rightarrow \quad \phi=G+Constant \qquad (24)
$$

Horizontal boundaries that are closed also have a zero vertical flow component. This is achieved here by a using a boundary flow equal to $-k_z\partial G/\partial z$

$$
v_z=-k_z\frac{\partial\Phi}{\partial z}=-k_z\frac{\partial(\phi-G)}{\partial z}=0 \quad \rightarrow \quad -k_z\frac{\partial\phi}{\partial z}=-k_z\frac{\partial G}{\partial z} \qquad (25)
$$

Hence, the model must be given the right-hand term as a source term at this boundary in order for it to be impermeable. This, however, is automatically guaranteed by proper computation of the vertical density source terms.

Use of the equations

The density source terms are composed of contributions from all cell faces (E, N, W, S, T, B) and different kind of general head boundaries. These individual components are computed first and put in a budget file to be used later to correct the intercell flows before applying MODPATH or MT3D. Then the terms for each cell are summed and merged into the well input file. Finally, MODFLOW is run to obtain the fresh-water heads for the variable density case.

In many cases this is all we need, since fresh-water heads are exactly what we need in the fresh-water part

of the model. They are also correct for the saline part, but as is generally the case with density flow, interpretation in terms of flow is somewhat more complicated.

Also, the flows in the fresh water part of the model are immediately usable. Hence transport models will produce the right results in this part of the model right away. But the intercell flows in the saline part of the model have to be corrected before MODPATH and MT3D yield the correct particle transport. All we have to do before using MODPATH or MT3D is to subtract the corresponding density source term components from the computed intercell flows residing in the budget file freshly computed by MODFLOW.

Rapid modelling of variable density flow

There are several tricks to have MODFLOW itself compute and output its conductances and density source terms by using proper initial heads and run MODFLOW with zero iterations. Limited space allows only to indicate this here. For instance, if the density can be simplified as independent on x,y within a model cell, and we use a regular model mesh, such that the tops and bottoms of the cells in a layer match exactly, the former water balance equation reduces to:

$$\begin{aligned} &C_E\Phi_E+C_N\Phi_N+C_W\Phi_W+C_S\Phi_S+C_T\Phi_T+C_B\Phi_B+\sum C_G\Phi_{G_C} \\ &-(C_E+C_N+C_W+C_S+C_T+C_B+\sum C_G)\Phi_0 \quad = \\ &\qquad +C_T(G_T-G_0)+C_B(G_B-G_0)+\sum C_G(G_G-G_0)-Q \end{aligned} \tag{26}$$

This allows very easy computation of variable density flow, since the right-hand source terms can now be readily computed by the model itself. This is achieved by first setting Q=0, then making $C_E=C_N=C_W=C_S=0$ and finally running MODFLOW with zero iterations, with the initial heads and external heads (rivers and so on) the precomputed hydrostatic fresh-water head, G. This makes the left-hand side of the above equation equivalent to the right-hand side. Thus the model itself will produce the density-source terms specified at the right-hand side of the above equation in MODFLOW's budget file. After totalling them per cell and adding them to the other source terms (wells, i.e. the given Q-values) the model is run a second time to compute the wanted fresh-water heads throughout the model for the variable density situation. The new intercell flows are stored in MODFLOW's the budget file. They have to be corrected before using MODPATH or MT3D by subtracting the source density terms stored in the first budget file.

Hence solving a variable density groundwater problem in the case of a regular mesh and a single density per model cell is reduced to running the model twice. If the mesh is not regular, but the density is constant per layer, the model has to be run three times. (This may not only be true for a regular and easily understood finite difference model such as MODFLOW, but just as well for any finite element model, which we leave to be proved by others.). In more general cases the easiest way will be to compute these terms by a separate program. Note that the conductances can be obtained from MODFLOW using initial heads such that the head difference between adjacent cells in x, y and z direction always equals unity.

Example

Simple examples, concerning flow in a vertical cut, have already been given by Olsthoorn (1996). So here a more complicated example is presented to demonstrate the potential of the method. Here we show the applications applied on the MODFLOW model of the Amsterdam dune area (Olsthoorn e.a. 1993, Kamps and Olsthoorn, 1996) that contains 13 layers, i.e. 7 aquifers and 6 aquitards.

The cells of a layer do not match in height, but we assume, just for this example, that the density within a cell only depends on z, (such as a piecewise horizontal interface or a single density per cell). Hence, all horizontal density terms containing an overlined (i.e. height averaged) hydrostatic fresh-water head vanish from the general water balance equation. For now we assume a sharp interface crossing a great number of cells. This sharp interface allows easy precomputation of the hydrostatic fresh water head, G, everywhere in the model. It equals the depth below the interface times (γ/γ_0-1) .

Figure 4 shows a west-east cross section running from the North Sea in the west 4.4 km land inward, showing the computed fresh water heads and the wells. (The dark skyline is the dry part of the phreatic top aquifer). Above the interface the fresh-water head isolines directly show the flow situation; below it, the effect of density on the fresh-water head is manifest. There the flowlines will not be perpendicular to the isolines.

Figure 5 shows the flow situation and the layers. The arrows have been computed by MODPATH, they are in fact small pathlines of 100 days duration starting at equidistant locations with an arrow head placed at 100 days (i.e. at the end of the path). The result is a clear flow picture, clarifying among others the predominant vertical flow through the aquitards. Before running MODPATH the intercell flows in the budget file have been corrected by the density flow source terms. Clearly, below the interface the flow is no longer perpendicular to the fresh-water heads.

Of course, cells that are intersected by the interface cannot within MODFLOW reveal the details of the density flow within them. However the total flow over each cell boundary is always correct. Still, more detail can be obtained by splitting layers of interest or by applying the horizontal gradient for height z above the centre of the cell using the details of the density distribution, as given in equation 7.

We use Matlab (see http://www.mathworks.com on the world wide web for details) to compute the hydrostatic fresh water heads and the density source terms directly from the data. Matlab is efficient in handling matrices and so to compute coefficients from a block-shaped model such as MODFLOW. Matlab is also used to alter the budget file by subtracting the density source terms from it before running MODPATH. (You may E-mail me for the Matlab mfiles). Visualization is done conveniently in Visual MODFLOW (see Scientific Software Catalogue) from which the figs. 4 and 5 were produced as well. Using Matlab our basic data are immediately shaped into Visual MODFLOW files. These are somewhat easier to handle than those of MODFLOW, while an import phase is omitted. Visual MODFLOW produces the needed MODFLOW and MODPATH files, launches the latter models and reads their results back in for visualization.

It is concluded that the method is practical and works well in complex three-dimensional situations. It could be readily implemented in a MODFLOW-module if someone were willing to invest some time to realise it. The next step to be developed would be the movement of the density along with the water flows.

REFERENCES

MAAS, C. & EMKE M.J. (1988). Solving varying density groundwater problems with a single density computer program. In De Breuck W. & L. Walschot (Eds) Proceedings of the 10 th salt water intrusion meeting, SWIM, Ghent, Belgium, 1988. Ghent: Natuurwetenschappelijk Tijdschrift 1989, Vol 70, 1988, p143-154.

MCDONALD M.G. & HARBAUGH, A.W. (1988) A modular three-dimensional finite difference groundwater flow model. USGS Techniques of Water Resources Investigations Report, Book 6, Chapter 1.

OLSTHOORN T.N. (1996) Dichtheidsberekeningen met een standaard grondwatermodel (Density calculations with a standard Groundwater model. Journal Stromingen, June 1996, in press. (In Dutch)

OLSTHOORN, T.N., KAMPS P.T.W.J. & DROESEN W.J. (1993) Groundwater modelling using a GIS at the Amsterdam Water Supply: In HydroGIS 93, Proceedings of the Vienna Conference, April 1993, IAHS publ. 211, p665-674.

SCHAARS, F. (1996) Implementation of a method for spatial modelling of simultaneous flow of fresh, brackish and saline groundwater in the Amsterdam Dune Area. Amsterdam Water Supply, Hydrology Section, Msc. Thesis, 101p, (In Dutch)

STRACK, O.D.L. (1995) A Dupuit-Forchheimer model for variable density flow. Water ResourcesResearch, Dec. 1995.

DE WIEST, R.J.M. (1969) Fundamental principles of groundwater flow. In: Flow through porous media, p1-51, Academic Press, London.

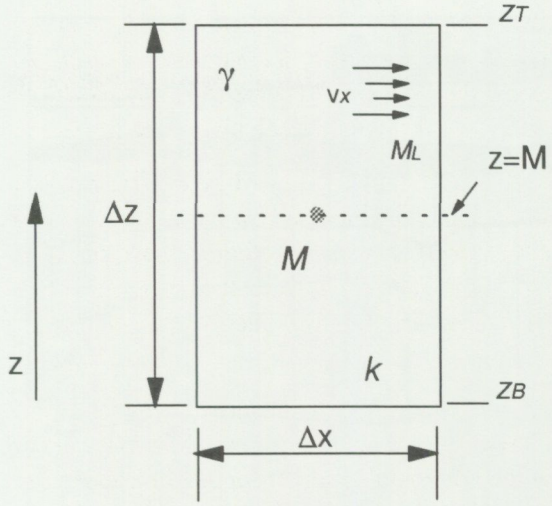
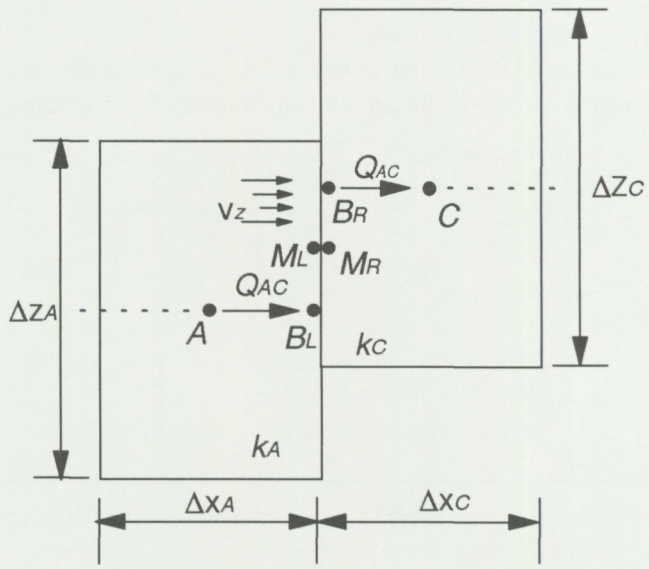


Fig. 1: Single MODFLOW cell, in vertical cross section

Fig. 2: Horizontal flow between two MODFLOW cells of different height.



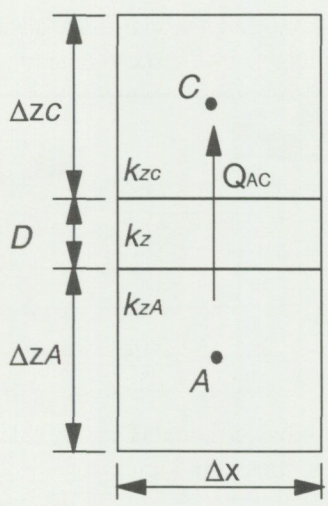
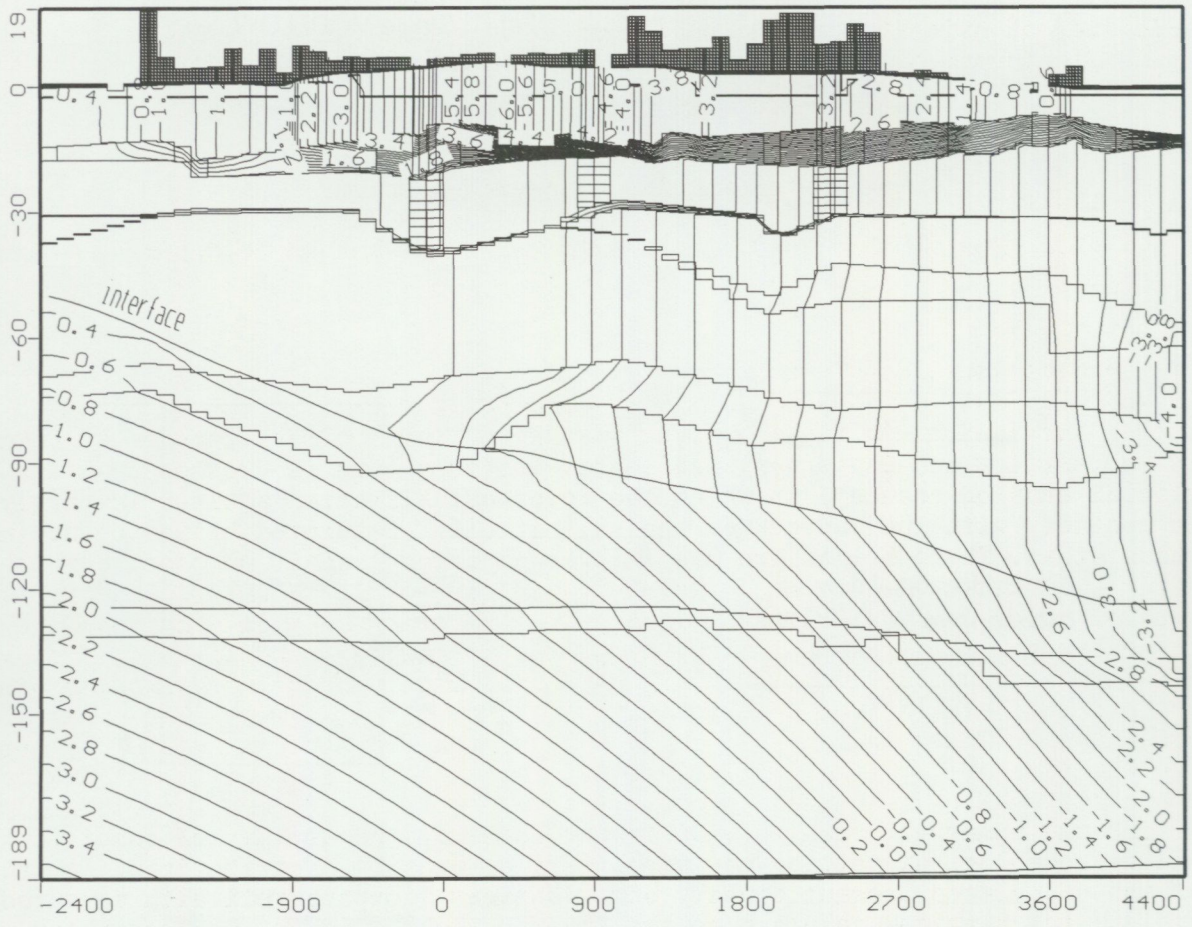
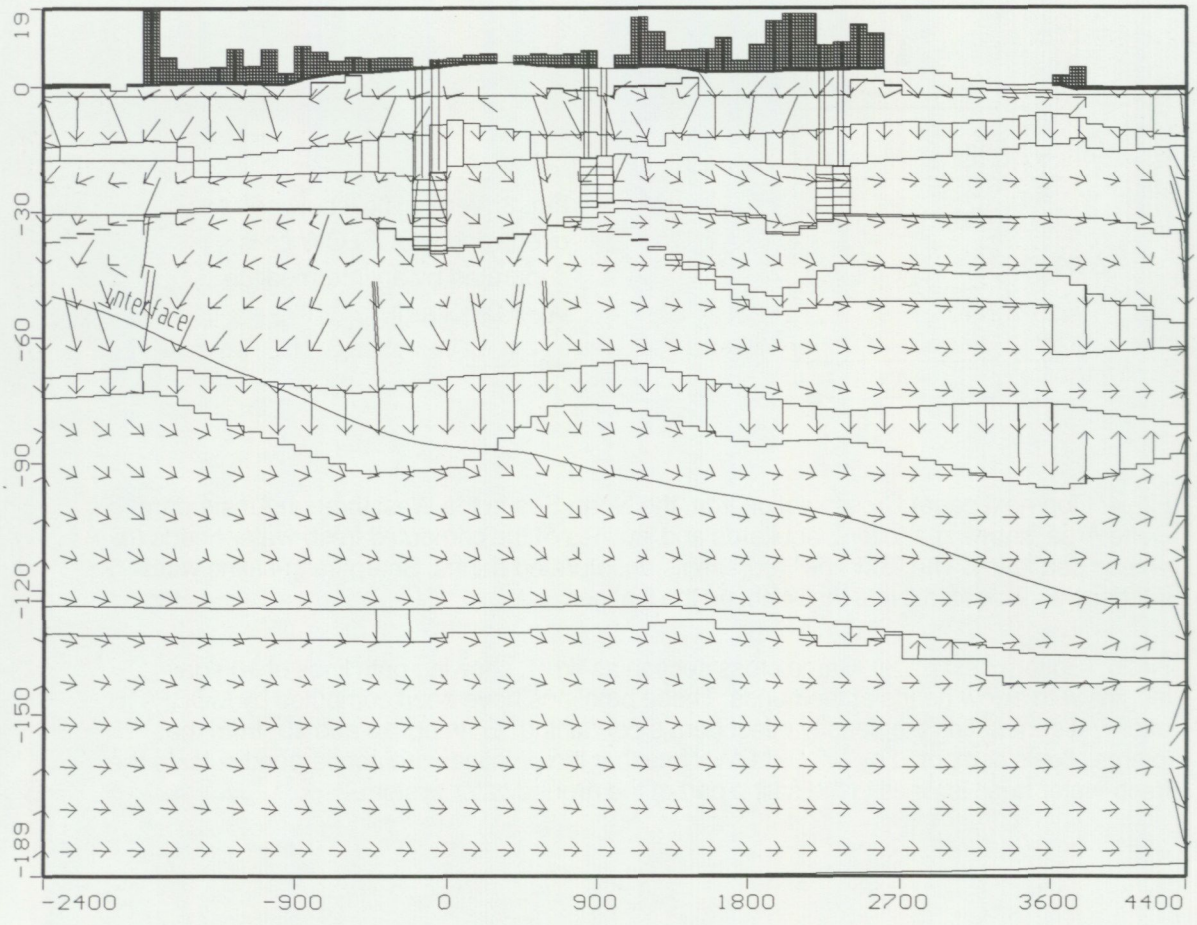


Fig. 3: Vertical flow between two overlaying MODFLOW cells, separated by an intermediate layer (aquitard).

Fig. 4: (Top next page) Cross section from the North Sea in the West through Amsterdam Dune Area, showing aquifers, aquitards and isolines of the computed fresh-water heads (m +mean sea level). The "Sky line" represents unsaturated dunes. Sharp fresh-saline water interface as indicated. Note the effect on the isolines.

Fig. 5: (Bottom next page) Same cross section as fig. 4, showing path lines of 100 day lengths with arrow heads at their ends. These pathlines have been computed by MODPATH, after first subtracting the density effect (terms containing "G" in eq. 10 and 19) from the intercell flows computed by MODFLOW. Note that the pathlines are not perpendicular to the fresh-water head isolines in the saline part of the groundwater system.


19
0
-30
-60
-90
-120
-150
-189
-2400
-900
0
900
1800
2700
3600
4400
Interface


19
0
-30
-60
-90
-120
-150
-189
-2400
-900
0
900
1800
2700
3600
4400
Interface

Modelling of brine transport in an aquifer crossing the Gorleben salt dome: Influence of initial conditions and hydrogeological settings

Peter Vogel & Klaus Schelkes
Federal Institute for Geosciences and Natural Resources (BGR)
P.O. Box 510153, 30631 Hannover, Federal Republic of Germany

The Gorleben salt dome, in the northeastern part of Lower Saxony in Germany, is under investigation as a candidate site for the final disposal of radioactive waste. The multiple-aquifer system in the sediments above the dome is in Tertiary and Quaternary sediments. The salt dome is crossed by a subglacial erosion channel, in which the lowermost Elsterian aquifer is partly in contact with the caprock or the salt itself. Saturated brines occur in these areas. These brines are overlain by a narrow transition zone in which water salinities decrease to that of brackish or fresh water. Numerical studies based on a generalized hydrogeological cross-section were conducted to determine the transient density distribution and the associated flow field in the subglacial erosion channel. The objective of these studies was to determine the effect of different hydrogeological settings and initial conditions. The transient simulations were assumed to start 10 000 years ago at the end of the last ice age. Both the initial condition and the shape of the Elsterian channel outlet to a deep Tertiary aquifer strongly affect the numerical results. Different combinations of initial conditions and hydrogeological setting may yield similar density distributions. A few of the calculated present density distributions compare well with measured field data. A unique solution to the inverse problem is not yet possible.

Introduction

In this paper, interest is focused on transient two-dimensional numerical modelling of a generalized hydrogeological cross-section along an erosion channel crossing the Gorleben salt dome. The objective was to calibrate the numerical model on the basis of the present groundwater density distribution. Paleoclimatic and hydraulic arguments yield a reasonable estimate of the rather unknown salinity distribution at the end of the last ice age to serve as initial condition. Steady-state conditions have not been reached in this groundwater system. Some of the predicted present density distributions achieve a good fit to measured density data along the entire lenth of the channel.

Hydrogeological situation

The Gorleben salt dome, in the northeastern part of Lower Saxony in Germany, is under investigation as a candidate site for the permanent disposal of radioactive waste. This salt dome is approximately 14 km long, up to 4 km wide, and its base is at a depth of more than 3000 m. Hydrogeological studies have been conducted in an area of about 300 km^2 around the salt dome for site characterization and long-term safety assessments. Numerous experiments have been carried out in the Gorleben area to obtain information about the hydrogeology, hydraulic parameters, and groundwater movement. A good picture of the hydrogeological situation has been obtained from these studies (Vierhuff, 1984; Fielitz et al., 1984).

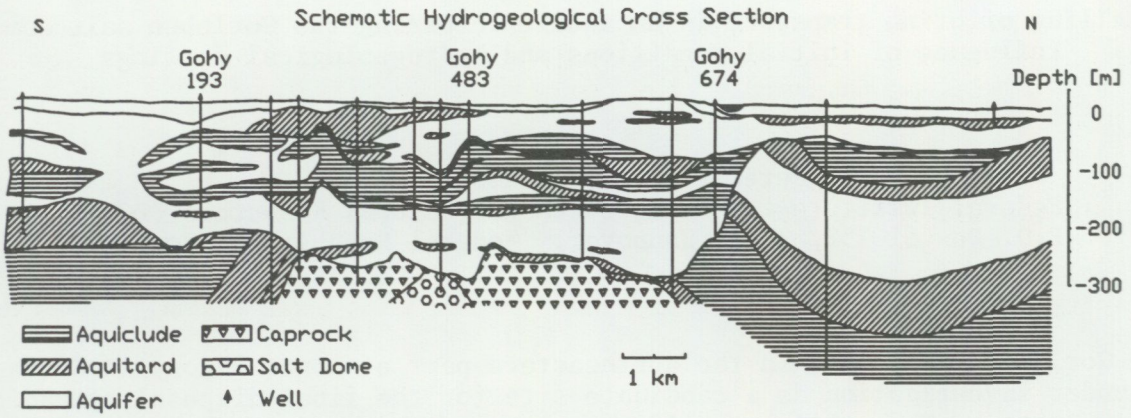


Fig. 1. Schematic hydrogeological cross-section along the Gorleben erosion channel.

Tertiary and Quaternary sediments above the Gorleben salt dome form a multiple-aquifer system up to 300 m thick. The lowermost aquifer consists of Miocene lignite-bearing sands or Elsterian sandy, gravelly deposits in subglacial erosion channels. One such channel, the so-called Gorleben erosion channel, which is more than 10 km long and 1 - 2 km wide, crosses the salt dome from south to north. This erosion channel is locally deeper than 275 m below m.s.l. and extends down to the cap rock and in some places down to the salt itself (cf. Fig. 1). The channel contains fairly thick, sandy sediments with interbedded lenses of till; these sediments are overlain by a complex of silt and clay up to 110 m thick, the Lauenburg Clay Complex. It almost completely covers the channel aquifer above the salt dome, nearly isolating it hydraulically from the shallower aquifers.

The land surface is quite flat with elevation differences of 5 - 15 m between gentle hills and the receiving streams. Below the higher elevations south of the dome, the groundwater table is about 8 m higher than the level of the discharge areas. The groundwater flows from the slightly elevated areas towards the surrounding lower regions, infiltrating almost to the salt dome at 200 - 250 m depth, where saline water is found.

Throughout the study area, the freshwater body is underlain by rather saline water. The salt content usually increases with depth. Fig. 2 (left) shows the density of water samples from the "Gorleben channel" as a func-

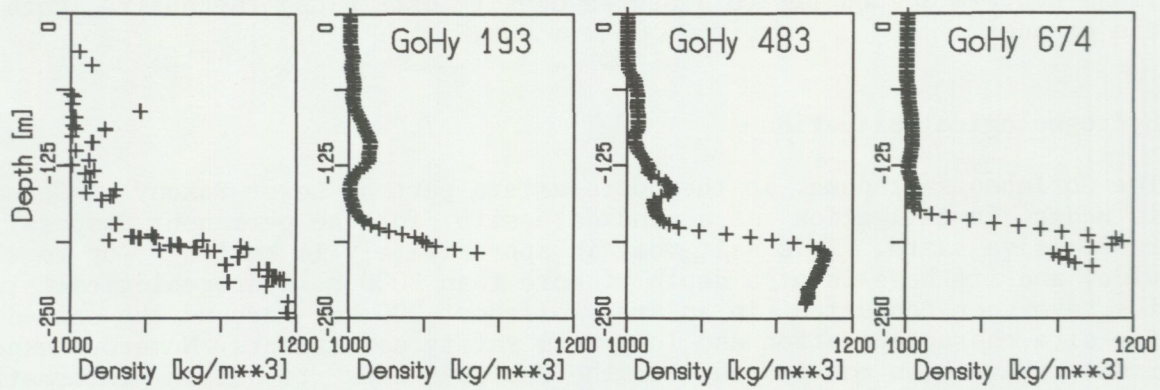


Fig. 2. Groundwater density measured on water samples (leftmost) and groundwater density logs for the wells GoHy 193, GoHy 483, and GoHy 674.

tion of depth. Induction logs were run in a number of the deeper observation wells to determine the groundwater density distribution (Ochmann & Fielitz, 1993). As an example, the groundwater density logs for three wells located on the above-mentioned cross-section are depicted in Fig. 2.

The general density distribution with depth can be characterized as follows: Groundwater mineralization increases slowly from the groundwater table down to a depth of 160 - 170 m below m.s.l. Between 170 and 200 m below m.s.l. there is a very steep increase in density from 1020 to about 1170 kg/m³. Below this transition zone highly saline water, in some places saturated brine, is found.

Simulation set-up

The schematic hydrogeological cross-section depicted in Fig. 1 was derived from the results of the hydrogeological investigation program, but it has been modified for the purpose of this numerical 2D modelling to incorporate recharge effects in the southern part of the cross-section. This modified hydrogeological cross-section served as a basis for the numerical model.

The simulated domain has a length of 16 400 m and extends from 15 m above m.s.l. down to a depth of 380 m below m.s.l. The finite element mesh employed in the simulations comprises about 4000 nodes (cf. Fig. 3).

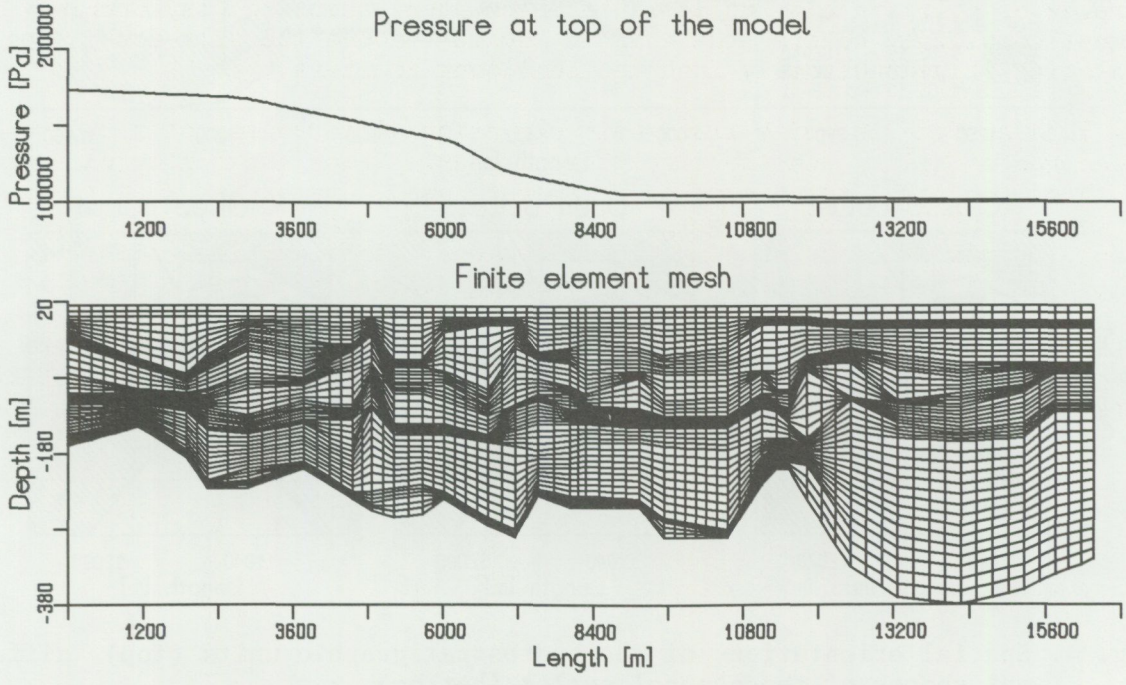


Fig. 3. Finite element mesh and pressure at top of the model.

Boundary conditions for groundwater flow and solute transport equations were chosen according to the hydrogeological situation. The pressure was fixed at the top of the cross-section to simulate the topography of the water table (top of Fig. 3). No fluid flow occurs across any other boundary. A solute concentration corresponding to that of saturated brine was assumed

along part of the bottom of the cross-section to represent the contact with the salt dome. Neither lateral boundary represents a flux boundary for solute transport. A solute concentration of zero, corresponding to fresh water, was specified along the top of the cross-section for fluid entering the system. No restriction was imposed on the solute concentration of the fluid leaving the system (i.e., free outflow).

Fluid densities were allowed to vary linearly between 1000 and 1200 kg/m^3 for solute mass fractions of 0.0 - 0.285. These values correspond to fresh water and saturated brine, respectively.

A diffusion coefficient of 10^{-9} m^2/s was used. Trial simulations showed that even small transverse dispersivities will spread any plume vertically through the entire thickness of the aquifer system within a geologically rather short time. It was also found that the system is relatively insensitive to changes in longitudinal dispersivity. Therefore, longitudinal dispersivity in each finite element was set to half of the element size and a transverse dispersivity of 0 m was employed (cf. Frind et al., 1989).

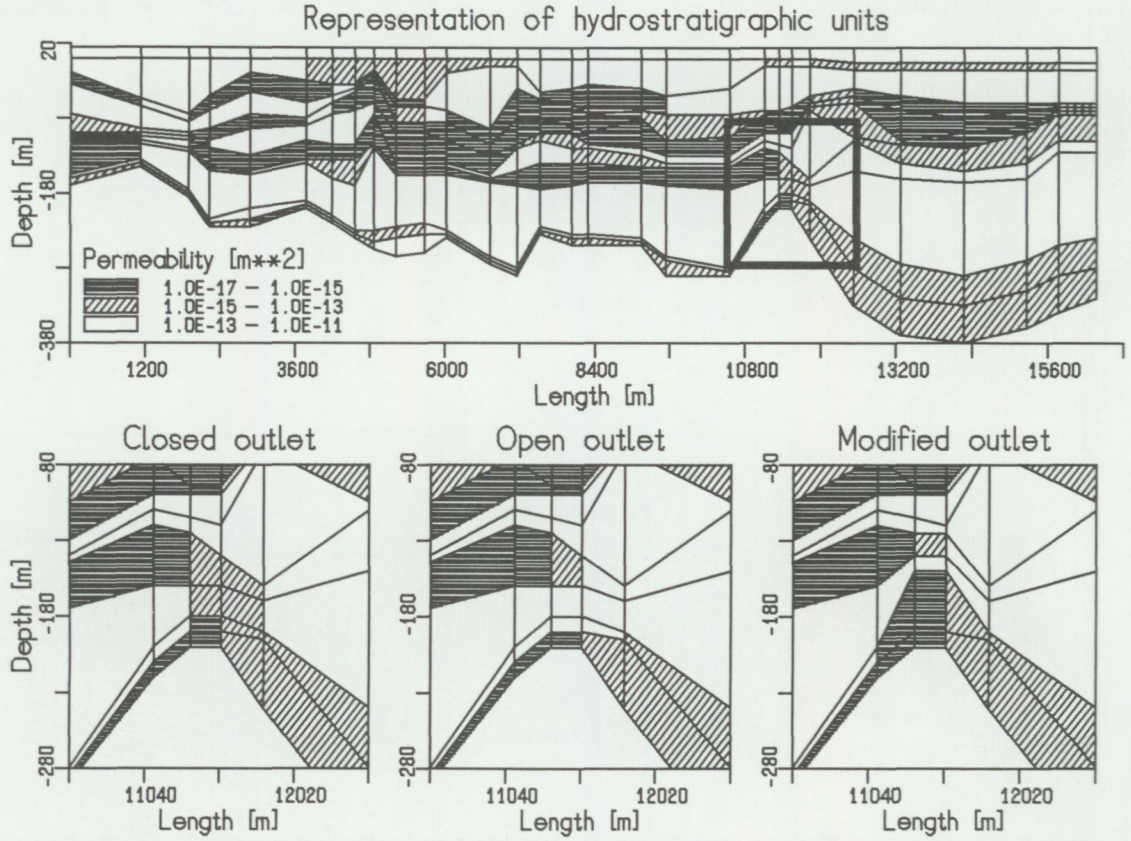


Fig. 4. Spatial orientation of the hydrostratigraphic units (top), different shapes of the channel outlet (bottom).

The numerical model can generally be characterized as a two-aquifer system consisting of aquifers, aquitards, and aquicludes with permeabilities of 10^{-12} m^2, 10^{-14} m^2, and 10^{-16} m^2, respectively, all three with a porosity of 0.2. Fig. 4 (top) depicts the permeability and spatial orientation of the hydrostratigraphic units. In the left part of the model (up to kilometer 11.5), three main layers can be distinguished. The upper one represents

the post-Elsterian aquifer system. It overlies a low-permeability zone, the Lauenburg Clay Complex. The high-permeability region below that represents the Elsterian erosion channel aquifer. At its base, contact with the diapir is assumed between kilometer six and kilometer ten. The framed area in Fig. 4 (top) depicts the northern channel outlet. Three configurations of this outlet that are equally possible within the range of currently known hydrogeological data were considered. These configurations differ in the shape and size of the channel outlet and are zoomed in Fig. 4 (bottom). The case of the closed outlet is shown in Fig. 4 (bottom left). In contrast, highly permeable elements provide a hydraulic connection to the north in the case of the open channel outlet. The hydraulic connection between the erosion channel aquifer and the area to the north is reduced in size and shifted upward for the case of the modified channel outlet. These differences in the channel outlet are the only differences between the three model geometries considered in the following discussion.

Modelling the salt water system

Numerical calculations were performed employing the SUTRA code (Voss, 1984). The objective of the investigations was to test the sensitivity of parameters and structural geometries, and to obtain a density distribution that is at least similar to the present one.

One of the main assumptions is that the present density distribution has developed since the late Pleistocene. Therefore, an important question was whether the present density distribution can be approximated by a steady-state solution. The answer had already been obtained in previous studies (Vogel et al., 1993; Schelkes & Vogel, 1993). The transient behaviour of the calculated salinity distribution indicates that steady-state conditions have not yet been reached in the observed groundwater system. The initial salinity distribution and the modelled time period strongly affect the simulation results.

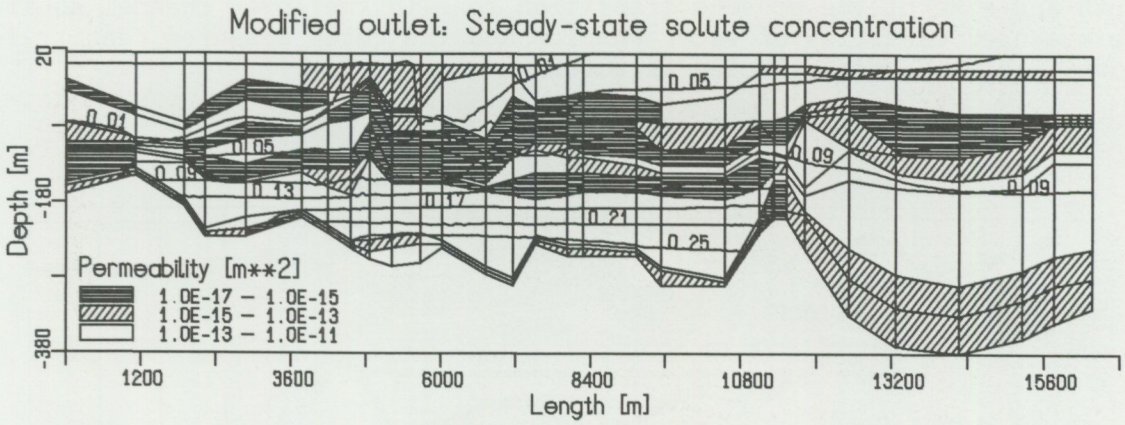


Fig. 5. Calculated steady-state concentration.

To verify this result for the cross-section under investigation, the steady-state salinity distribution was approximated by long-term transient simulations. The results of the numerical modelling are depicted in Fig. 5. Apart from a freshwater lens in the recharge area, brackish water is found up to the top of the model. Instead of the observed steep density increase within a small transition zone, the results exhibit an only moderate

salinity increase spread over the entire thickness of the lower channel aquifer. This confirms the earlier results that the observed density distribution cannot be obtained by a steady-state solution.

Therefore, a transient solution method was selected. This requires the setting of the initial conditions and the time period to be modelled. With respect to the paleoclimatic history, it was assumed that the simulations start at the end of the last ice age, approximately 10 000 years ago, and end at the present. This assumption requires a reasonable estimate of the rather unknown former density distribution to serve as an initial condition. On the basis of the hypothesis that the groundwater was mainly at rest during the last ice-age, the estimated initial density distributions were assumed to be hydraulically stable, i.e., density increases with depth. Due to dissolution, saturated brines were assumed to prevail at least in that area where the groundwater is in contact with the diapir. The present density distribution is characterized by deep brines in the lowermost channel aquifer, overlain by a transition zone with water salinities decreasing to that of brackish or fresh water. Therefore, it seemed reasonable to start the simulation runs with initial solute concentrations that exhibit a similar characteristic feature.

All initial conditions investigated assume saturated brine at the base with freshwater conditions prevailing throughout the remaining modelled area. A small horizontal transition zone separates the two regions. The depth of this narrow transition zone was varied in a series of simulation runs. Saturated brines always prevail at the base of the lower channel aquifer. Depending on the depth of the transition zone and the depth of the channel outlet in some cases, the brine/freshwater interface was extended to the north, where field data on groundwater densities are not yet available. Fig. 6 presents a schematic sketch of the initial density distributions. The different positions of the transition zone are indicated by thick lines.

For each of the three model geometries, the conditions from 10 000 years ago to the present were simulated. Special care was taken to match the depth and size of the present transition zone in the lower channel aquifer. The measured densities of water samples and the three measured density logs shown in Fig. 2 were selected as reference.

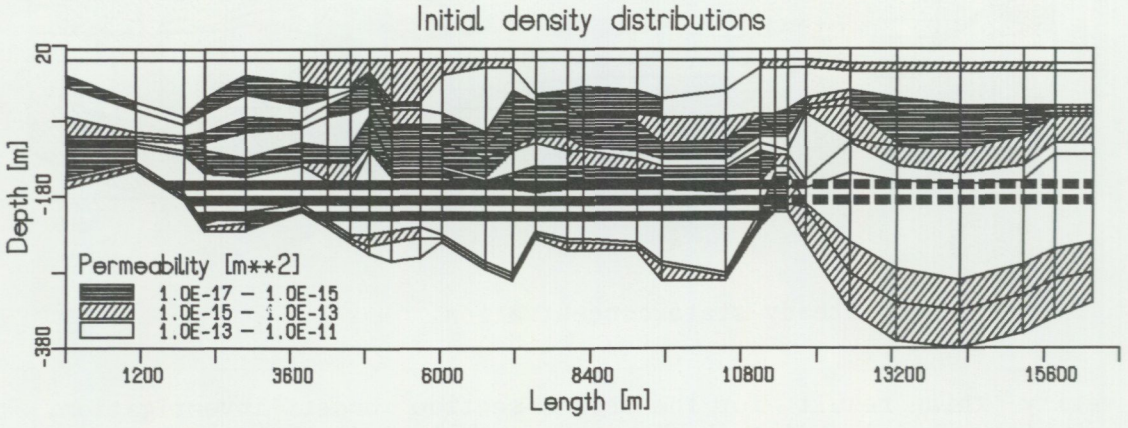


Fig. 6. Schematic sketch of initial conditions indicating positions of the brine/freshwater transition zone.

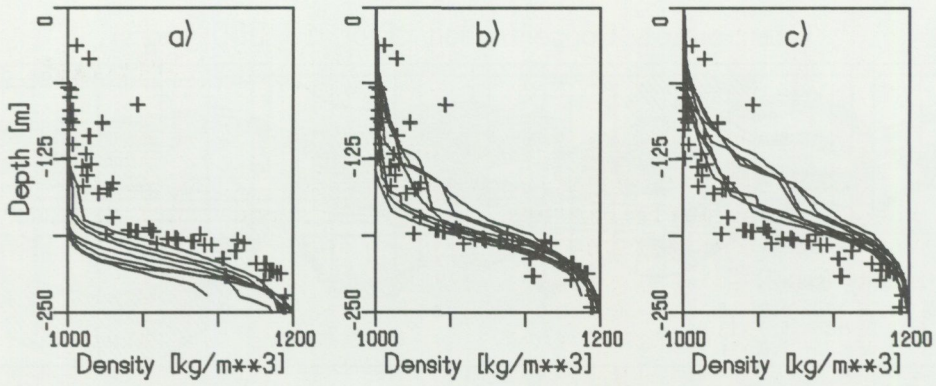


Fig. 7. Comparison of measured water samples densities with calculated density distributions employing different initial conditions. The initial brine/freshwater transition zone is a) in lower, b) in medium, c) in upper position.

Vertical density distributions at equally spaced locations between kilometers 4.5 and 10.5 in the model were compared with the densities of the water samples. These calculated densities are shown as solid lines together with the measured water densities in Fig. 7. All simulations that employ the initial brine/freshwater interface in the lowermost position predict a depth of the transition zone below the observed one (Fig. 7a). Similarly, all simulations that employ the initial brine/freshwater interface in the uppermost position predict a depth of the transition zone above the observed one (Fig. 7c). Thus, the range of possible initial conditions could be reduced. Only those cases were investigated further that start from a

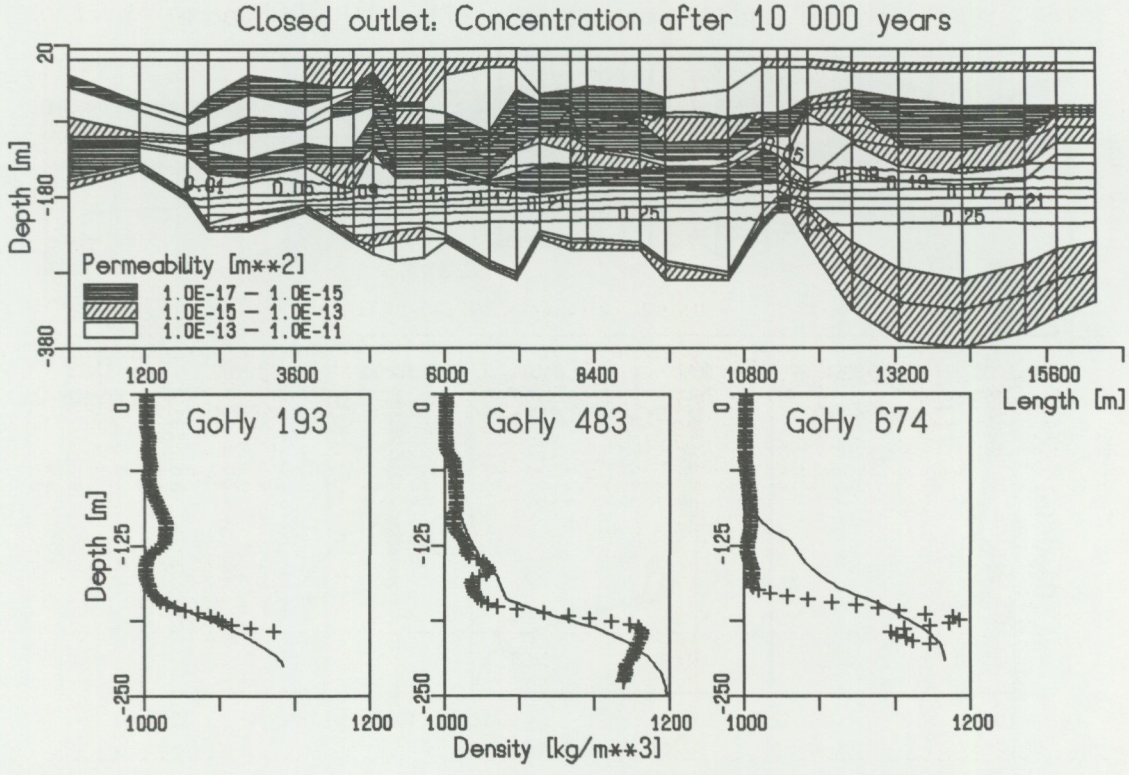


Fig. 8. Closed channel outlet: Calculated solute concentration (top), comparison of measured and calculated density logs (bottom).

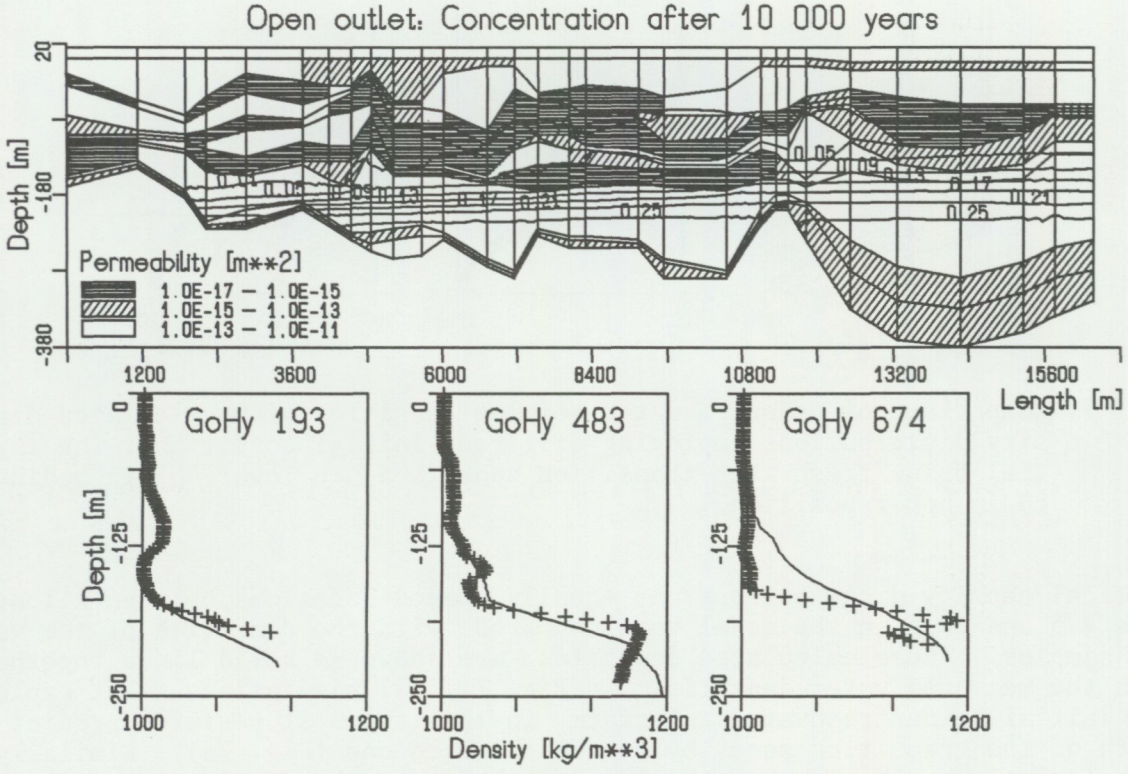


Fig. 9. Open channel outlet: Calculated solute concentration (top), comparison of measured and calculated density logs (bottom).

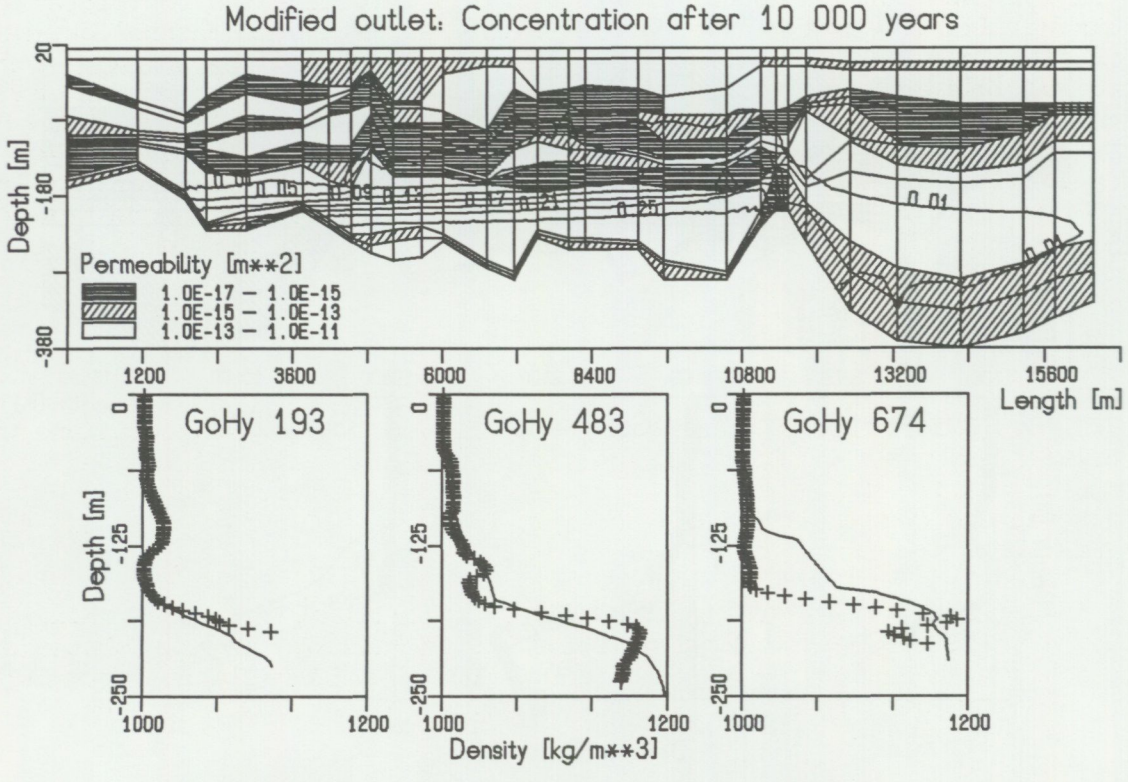


Fig. 10. Modified channel outlet: Calculated solute concentration (top), comparison of measured and calculated density logs (bottom).

somewhat medium depth of the initial brine/freshwater interface and yield results similar to those in Fig. 7b.

However, plots like in Fig. 7 do not allow decisions to be made about which is the best fit. Hence, a more detailed criterion had to be provided for the further investigations. The three wells GoHy 193, GoHy 483, and GoHy 674 are located exactly on the cross-section under investigation. They are spaced over the entire length of the channel (Fig. 1) and there are measured density logs available for these wells (Fig. 2). Therefore, the next step was to achieve a fit of the calculated density distributions to the measured density logs at these three well locations.

For this purpose, the previous estimates of suitable initial conditions were gradually improved. A set of initial conditions was thus obtained that all fit the simulation results to the measured density logs. These initial conditions have in common the initial depth of the brine/freshwater interface, but they differ in its lateral extent. Figs. 8 to 10 present the best-fit results for each of the model geometries. The predicted solute distributions are shown at the top. A comparison of the three measured density logs with the simulation results (solid lines) is presented at the bottom. Generally, measured and calculated densities are in fairly good agreement for wells GoHy 193 and GoHy 483 and are in still acceptable agreement for well GoHy 674. The results for the three model geometries are very similar to each other. Hence, a set of solutions is obtained that compare more or less favourably to the measured density logs but the best of them cannot yet be established.

The lateral extent of the initial brine/freshwater interface is easily inferred from the plots of the calculated solute distributions in Figs. 8 to 10. In the case of the modified outlet, this interface was restricted to the channel itself. In the cases of the closed and the open channel outlets, the initial interface was extended to the right (i.e., to the north). Comparison of calculated and measured groundwater densities north of the channel could help reduce ambiguity in the simulation results. Although there is considerable groundwater density data available for the erosion channel and surrounding area, the current database does not yet provide information on groundwater densities further to the north. This lack of information is one of the reasons why a unique solution to the inverse problem cannot be given at present.

REFERENCES

FIELITZ, K., GIESEL, W., SCHELKES, K. & SCHMIDT, G., 1984: Calculations of Groundwater Movement and Salt Transport in the Groundwater of the Sedimentary Cover of the Gorleben Salt Dome. - Proc. Int. Symp. on Groundwater Utilisation and Contaminant Hydrogeology, Montreal, Canada, Vol. II, pp. 383-392. AECL.

FRIND, E.O., DUYNISVELD, W.H.M., STREBEL, O. & BÖTTCHER, J., 1989: Simulation of Nitrate and Sulfate Transport and Transformation in the Fuhrberger Field Aquifer, Hannover, Germany. In H.E. Kobus & W. Kinzelbach: Proc. Int. Symp. on Contaminant Transport in Groundwater, Stuttgart, Germany, pp. 97 - 104. - Balkema. Rotterdam, Brookfield.

OCHMANN, N. & FIELITZ, K., 1993: Estimation of Horizontal and Vertical Groundwater Flow from Well-Logging and Pressure Data in Groundwater of Variable Density above a Salt Dome. In E. Custodio & A. Galofré: Study and

Modelling of Salt Water Intrusion into Aquifers, Proc. 12th Salt Water Intrusion Meeting, Barcelona, pp. 23-34. - CIMNE. Barcelona.

SCHELKES, K. & VOGEL, P., 1993: Paleohydrogeological Information as an Important Tool for Groundwater Modeling of the Gorleben Site. In: Paleohydrogeological Methods and their Applications, pp. 237-250. - OECD. Paris.

VIERHUFF, H., 1984: Hydrogeological Investigations in the Area of the Gorleben Salt Dome. - Proc. Int. Symp. on Groundwater Utilisation and Contaminant Hydrogeology, Montreal, Canada, Vol. II, pp. 573-579. AECL.

VOGEL, P., SCHELKES, K. & GIESEL, W., 1993: Modeling of Variable-Density Flow in an Aquifer Crossing a Salt Dome - First Results. In E. Custodio & A. Galofré: Study and Modelling of Salt Water Intrusion into Aquifers, Proc. 12th Salt Water Intrusion Meeting, Barcelona, pp. 359-369. - CIMNE. Barcelona.

VOSS, C.I., 1984: Sutra: A Finite-Element Simulation Model for Saturated Unsaturated, Fluid-Density-Dependent Ground-Water Flow with Energy Transport or Chemically-Reactive Single Species Solute Transport. - USGS Water Resour. Invest. Rep. 84-4369.

A quasi three-dimensional approach for simulating water flow and solute transport in the vadose zone and phreatic aquifer

A. Yakirevich, V. Borisov, and S.Sorek
Water Resources Research Center, J. Blaustein Institute for Desert Research
Ben-Gurion University of the Negev, Sede Boker Campus, 84990, Israel

Movement of solutes through the vadose zone and groundwater is of increasing concern because of environmental problems. Many theoretical models describing flow, solute transport and physico-chemical processes in soil, have been developed in recent years. Fully 3-D saturated-unsaturated flow and transport models (e.g., Panday *et al.*, 1993) give the full simulation extent of the problem. However, they require considerable computation time and thus their use for management problems is usually restricted. To circumvent these difficulties, the dimension of the equations is reduced to quasi three-dimensional case. Quasi three-dimensional models of flow for heterogeneous multiaquifer systems were developed by Bredehoeft and Pinder (1970), Herrera and Yates (1977), Neuman *et al.* (1982), etc. Pikul *et al.* (1974) coupled the one-dimensional Richards equation in vertical direction for the unsaturated zone with the one-dimensional Boussinesq equation in the horizontal direction for the phreatic aquifer. In order to link the rate of drainage out of the saturated zone to the change of height of the water table, Pikul *et al.* (1974) had to introduce the concept of the dynamic storage coefficient. As was noted by Vachaud and Vauclin (1975), such an approach is physically incorrect, and the use of a linked system of equations resting on the concept of storage coefficient may not yield simplification. Another recent development is given by Kool *et al.* (1994) which is a three-dimensional composite approach for subsurface flow and transport. However, this model considers steady state flow conditions and ignores the saturation variation in the vadose zone and in the capillary fringe above the phreatic surface.

In this paper we present a quasi three-dimensional model of flow based on coupling of the one-dimensional Richards equation in the unsaturated zone and the plane two-dimensional flow equation in the saturated zone. This is similar to the model developed by Pikul *et al.* (1974), but does not require the introduction of the storage coefficient. A three-dimensional transport equation is used to simulate the movement of solutes.

Governing equations

The motion of water in the unsaturated-saturated zone of soil can be described by the 3-D Richards equations. Let us introduce the following simplified assumptions to reduce the problem to a quasi 3-D case: 1) The flow in the unsaturated zone is in the vertical direction only; 2) Water is practically incompressible and soil matrix is rigid; 3) The Dupuit assumption of the essentially horizontal flow is valid in the saturated zone.

The equation that describes the phreatic surface reads

$$h(x,y,t) - z = 0 \tag{1}$$

where h is the elevation of the phreatic surface, x and y are the planar coordinates, z is the vertical coordinate (positive upward), and t is time.
In the unsaturated zone the model is presented by series of vertical 1-D Richards equations evaluated at points throughout the areal plane, i.e.

$$c\frac{\partial \psi}{\partial t} = \frac{\partial}{\partial z}\left(K_{zz}\frac{\partial \psi}{\partial z} + K_{zz} \right) \tag{2}$$

where c is the water capacity, ψ is the matric pressure head, and K_{zz} is the vertical component of **K**, the hydraulic conductivity tensor.

The 2-D averaged flow equation for the saturated zone can be obtained by integrating the 3-D flow equation over the vertical direction (Bear and Verruijt, 1987)

$$\int_{\eta(x,y)}^{h(x,y,t)} (\nabla \cdot \mathbf{q} + I) dz = 0 \tag{3}$$

where η is the elevation of the bottom of the aquifer, $\mathbf{q}$ is the water flux vector, and I is an internal sink-source term. By employing Leibnitz rule we write (3) in the form

$$\nabla' \cdot (h-\eta)\tilde{\mathbf{q}}' + \mathbf{q}|_h \cdot \nabla(z-h) - \mathbf{q}|_\eta \cdot \nabla(z-\eta) + \tilde{I} = 0 \tag{4}$$

where

$$\tilde{\mathbf{q}}' = \frac{1}{h-\eta}\int_\eta^h \mathbf{q}' dz \quad \text{and} \quad \tilde{I} = \int_\eta^h I dz$$

in which $(\,)'$ denotes a property defined only in the xy-plane. The $\mathbf{q}|_h$ and $\mathbf{q}|_\eta$ denote the water flux vectors at the phreatic surface and at the aquifer bottom, respectively. The first term in (4) can be presented as (Bear and Verruijt, 1987)

$$\nabla' \cdot (h-\eta)\tilde{\mathbf{q}}' = -\nabla' \cdot \left[\mathbf{K}'(h-\eta)\nabla' h\right] \tag{5.1}$$

Taking into account that the normal fluxes at both sides of the phreatic surface (1) are equal, we write

$$-K_{zz}\left(\frac{\partial \psi}{\partial z} + 1\right)\Big|_{z=h^+} = \mathbf{q}|_{h^-} \cdot \nabla(z-h) \tag{5.2}$$

The last term in (4) we present in the form

$$\tilde{I} = -\sum_l P_w(x_l, y_l, t)\delta(x-x_l, y-y_l) \tag{5.3}$$

where P_w is the rate of the flux source located at a point (x_l, y_l) and δ is the Dirac delta function. The water flux at the bottom of the aquifer, $\mathbf{q}|_\eta$, can be either prescribed, or calculated using known head values at the top of the underlying confined aquifer (Bear and Verruijt, 1987). In view of (5), we rewrite (4) in the form

$$-K_{zz}\left(\frac{\partial \psi}{\partial z} + 1\right)\Big|_{z=h} = \nabla' \cdot \left[\mathbf{K}'(h-\eta)\nabla' h\right] + \mathbf{q}|_\eta \cdot \nabla(z-\eta) + \sum_l P_w(x_l, y_l, t)\delta(x-x_l, y-y_l) \tag{6}$$

The main difference of (6) from the Boussinesq equation for a leaky-phreatic aquifer, is that it does not contain a term with specific yield and a source term for natural replenishment. However it explicitly models a vertical flux at the phreatic surface. We note, that (6) refers to a nonsteady state, since ψ, the matric pressure head, is a function of time. The position of the moving phreatic surface is found by

$$\psi(x,y,z,t)\big|_{z=h} = 0 \tag{7}$$

As a result, we decompose the 3-D flow problem to a 1-D vertical direction presented by (2) for the unsaturated zone, and to 2-D horizontal plane for the saturated zone presented by (6).

The transport of contaminant species is described by the advection-dispersion equation

$$\frac{\partial(\theta C_i)}{\partial t} + \rho_s(1-n)\frac{\partial F_i}{\partial t} = \nabla\cdot(\mathbf{D}_i\theta\nabla C_i - \mathbf{q}C_i) - \sum_m \mu_{im} + \sum_l \left[\tilde{C}_{wi}H(P_w) - C_i H(-P_w)\right] P_w(x_l,y_l,t)\delta(x-x_l, y-y_l, z-z_l) \tag{8}$$

where C_i and F_i are the concentration of the ith component in the liquid and on the adsorbed phases, respectively, ρ_s is the solid phase density, n is soil porosity, θ is the soil water content, $\mathbf{D}_i$ is the apparent dispersion tensor, μ_{im} is the sink-source term associated with the mth transformation reaction, e.g. decay, mineralization, immobilization etc., $\tilde{C}_{wi}$ is the concentration of the ith component in the injected water, and H is the Heaviside step function.

Numerical algorithm

To solve (2) and (6) to (8), we had implemented a finite differences grid in a three-dimensional space. We solved (2) along the vertical coordinate z at every J nodal point situated at (x_j, y_j) on the horizontal plane. Equation (6) is considered as the lower boundary condition for (2). The RHS of (6) is approximated by finite differences on a horizontal part of the 3-D grid.

The algorithm for solving (2) and (6) to (8) is described as follows:
1) Use the prescribed distribution of capillary pressure head $\psi(z_i, t^k)$ at the previous time level t^k and at each node J situated at (x_j, y_j) to find the height Z_J at which $\psi(Z_J, t^k) = 0$. Knowing this height, constitutes the phreatic surface h_J at every node J (i.e., $h_J(x_j, y_j, t^k)=Z_J$).
2) Calculate the RHS of (6) using h_J. This will constitute the flux at the phreatic surface, which is the lower boundary for the solution of (2). This boundary condition can also be projected from the phreatic surface to the bottom of the aquifer, since the vertical component of Darcy's velocity is constant in the saturated zone when considering the 1-D Richards equation.
3) Given also the boundary condition at the soil surface, solve for $\psi(z_i, t^{k+1})$ using (2).
4) Evaluate the vertical component of Darcy's velocity in the unsaturated zone, and the vertical and horizontal components of the Darcy's velocity in the saturated zone, at the t^{k+1} time level.
5) Solve the three-dimensional transport problem (3), at the t^{k+1} time level.
Since (2) and (6) are nonlinear, an iterative procedure is required.

The vertical component of the water flux in the saturated zone can be approximately found by integrating the equation of continuity from the bottom to the top of the aquifer (Polubarinova-Kochina, 1977; Strak, 1984), i.e.,

$$q_z = \int (\nabla'\cdot\mathbf{q}' + I)dz + A \tag{9}$$

where A is a constant which can be found using the value of the water flux at the bottom of the aquifer.

To introduce the soil water retention curve and the unsaturated hydraulic conductivity we refer to the van Genuchten's relations (van Genuchten, 1980), namely

$$S_e = \left[1 + (-\alpha\psi)^{n_v}\right]^m \tag{9}$$

$$K = K_s S_e^{0.5}\left[1 - \left(1 - S_e^{1/m}\right)^m\right]^2 \tag{10}$$

where $S_e = (\theta - \theta_r)/(\theta_s - \theta_r)$, θ_r is irreducible water content, θ_s is the water content at saturation, K_s is the saturated hydraulic conductivity of the soil, α and n_V are model parameters, and m=1-1/ n_V.

Examples

To test the ability of the model to simulate flow and transport in the unsaturated zone and in the phreatic aquifer, we compared the model's quasi 2-D predictions with those obtained by a fully 2-D unsaturated-saturated flow and transport equations which were simulated by the SUTRA (Voss, 1984) and 2DSOIL (Pachepsky et. al., 1993) numerical codes. Note, that the flow in the unsaturated zone is vertical only, while in the saturated zone it is essentially horizontal. Therefore, we consider, for the quasi 2-D case, these two direction as the principal axes of the dispersion (i.e., D_{xz}=D_{zx}=0). This allows us to use the Operator Splitting Methods to solve a 2-D transport equation (Samarsky, 1977). The two remaining components are given by (Bear and Verruijt, 1987)

$$D_{xx} = D_m\tau_c + \left(\alpha_T V_z^2 + \alpha_L V_x^2\right)/V \quad \text{and} \quad D_{zz} = D_m\tau_c + \left(\alpha_L V_z^2 + \alpha_T V_x^2\right)/V \tag{11}$$

where D_m is molecular diffusion coefficient, τ_c is tortuosity factor, α_L and α_T are the longitudinal and the transverse dispersivities of soil, respectively, V_x,, V_z and $V\left(=\sqrt{V_x^2 + V_y^2}\right)$ are the horizontal and vertical components of the average water velocity vector and its module, respectively.

In all examples, we considered a homogeneous isotropic porous media and the transport of a single solute without any chemical reaction.

1. *Spread of the groundwater 'stripe'*

The groundwater level at the initial time is given as a step function

$$h(x,t_0) = h_0 \quad \text{if } |x| \geq R, \text{ and } h(x,t_0) = h_0 + \Delta h \text{ if } |x| < R \tag{12}$$

where h_0 and the step $\Delta h \times R$ are prescribed. The analytical solution of the linearized 1-D Boussinesq equation for this case, has the form (Polubarinova- Kochina, 1977) of

$$h(x,t) = h_0 + \frac{\Delta h}{2}\left(\operatorname{erf}\frac{R-x}{2\sqrt{at}} + \operatorname{erf}\frac{R+x}{2\sqrt{at}}\right) \tag{13}$$

where $a = K_s/\left(S_y\tilde{h}\right)$, S_y is the specific yield and $\tilde{h}$ is the average groundwater level.

We carried out simulations for the silt loam GE 3 soil (van Genuchten, 1980) for which θ_s=0.369, θ_r=0.131, K_s=0.0496 m/day, α=0.423 m^{-1} and n_V=2.06. The longitudinal and transversal dispersivities were α_L=1.0 m and α_T=0.1 m, respectively. The simulated domain was presented by a

rectangle of height 4 m (from bottom of the aquifer to the soil surface) and 40 m length. The assigned initial conditions were h_0= 2.0 m, $\Delta h = 0.5$ m, and R=5.0 m. We note the symmetry of (13) at x=0, hence, accordingly the $\partial h/\partial x = 0$ condition was assigned. No flow condition was also specified at z=0 and z=4 m. At x=40 m we prescribed a constant head h=2 m. The initial solute concentration was set to be C_0=1 for $0 \le x \le R$ and $h_0 \le z \le h_0 + \Delta h$, and C_0=0 elsewhere. A finite differences grid of 17×17 nodes was used to solve the quasi 2-D (QUASI2D) problem. An equivalent finite elements grid was implemented for simulation with SUTRA and 2DSOIL. The time step increased by a factor of 1.1 starting from 10^{-6} day. The simulated groundwater level, on the basis of (2) and (6), was between the analytical solution of the linearized Boussinesq equation and the numerical solution of the 2-D Richards equation, however, closer to the latter one (Fig. 1a). The simulated distribution of the water content in the unsaturated zone was consistent with the one obtained on the basis of the 2-D Richards equation. The concentration obtained by the quasi 2-D approach and the fully 2-D flow and transport, were also in good agreement (Fig. 1b).

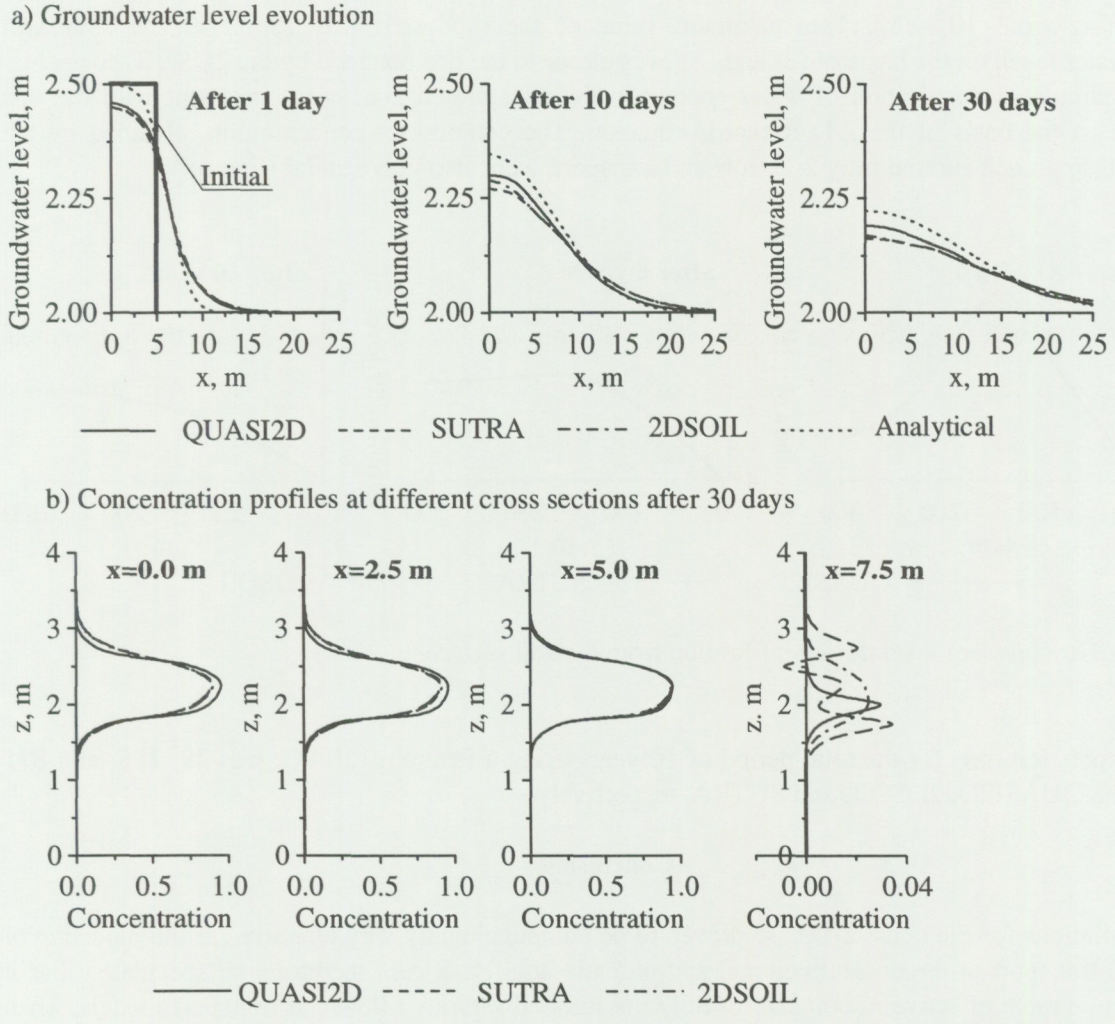


Figure 1. Groundwater level (a) and concentration profiles (b) for the problem of the 'stripe' spread.

The computation time for the period of 30 days using a Pentium/120 PC, was **12**, **60**, and **600** sec for the QUASI2D, 2DSOIL and SUTRA, respectively.

2. *Infiltration from the soil surface*

A problem of time dependent water infiltration and solute transport through the soil surface was considered. The simulations were carried out for the Guelph loam soil (van Genuchten, 1980) for which θ_s=0.520, θ_r=0.218, K_s=0.316 m/day, α=1.15 m^{-1}, n_V=2.03. The longitudinal and transversal dispersivities were α_L=5.0 m and α_T=1.0 m, respectively. The simulated domain was presented by a rectangle of height 10 m (from bottom of the aquifer to the soil surface) and 300 m length. Initial groundwater level was h_0= 4 m. Initial solute concentration was equal to zero. The flux boundary condition was assigned at the soil surface for the segment $110<x<170$ m. During the first 3 years, the intensity of the flux was 2 mm/day with a concentration of the solute in water equal to 1; during the next 3 years, these were 0.2 mm/day and 0, respectively; and during the last 4 years, no flow condition was implemented. The boundary conditions h=4.0 m for flow and $\partial C/\partial x = 0$ for transport, were assigned at x=0 m. The remaining part of the boundary was subject to no flow boundary condition. A finite differences grid of 16 × 18 nodes was used to solve the quasi 2-D problem. An equivalent finite elements grid was implemented for simulation with SUTRA and 2DSOIL. The time step increased by a factor of 1.5 starting from 10^{-6} day. The maximum value of the time step was 10 days. The simulated groundwater level, on the basis of (2) and (6), was closer to the one obtained by the 2DSOIL code (Fig. 2). The simulated distribution of water content in the unsaturated zone was consistent with the one obtained on the basis of the 2-D Richards equation. The contours of concentration, obtained by the quasi 2-D approach and the fully 2-D flow and transport, were also very similar (Fig. 3).

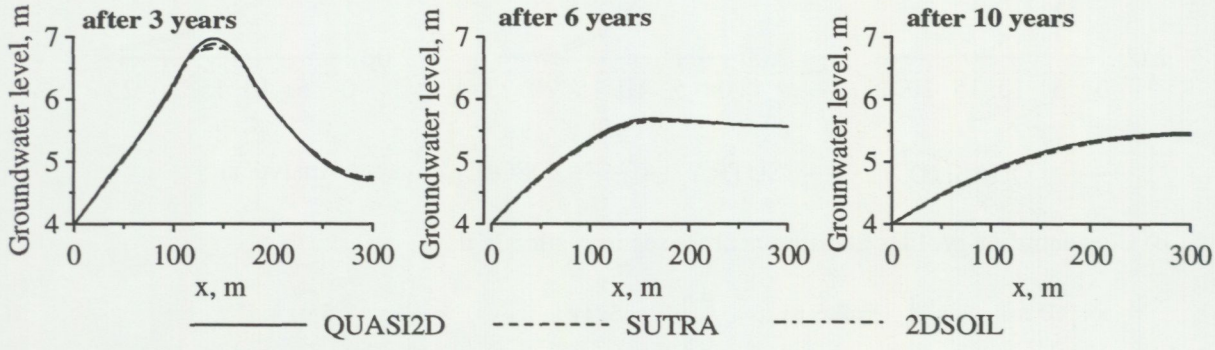


Figure 2. Groundwater level during infiltration from the soil surface.

The computation time for the total period of 10 years using a Pentium/120 PC, was **29**, **155**, and **871** sec for the QUASI2D, 2DSOIL and SUTRA, respectively.

Conclusion

The simulations for the quasi 2-D case proved to be computationally very effective for the modeling of flow and transport in the unsaturated soil and phreatic aquifer. It can, therefore, be speculated that it will even be more effective in compare to fully unsaturated-saturated flow and transport models, when considering the 3-D case. Limitations of the developed approach are that they assume a 1-D flow in the vadose zone and refers to small slopes of the phreatic surface. However, this model can be used for reliable solution of field scale flow and transport problems.

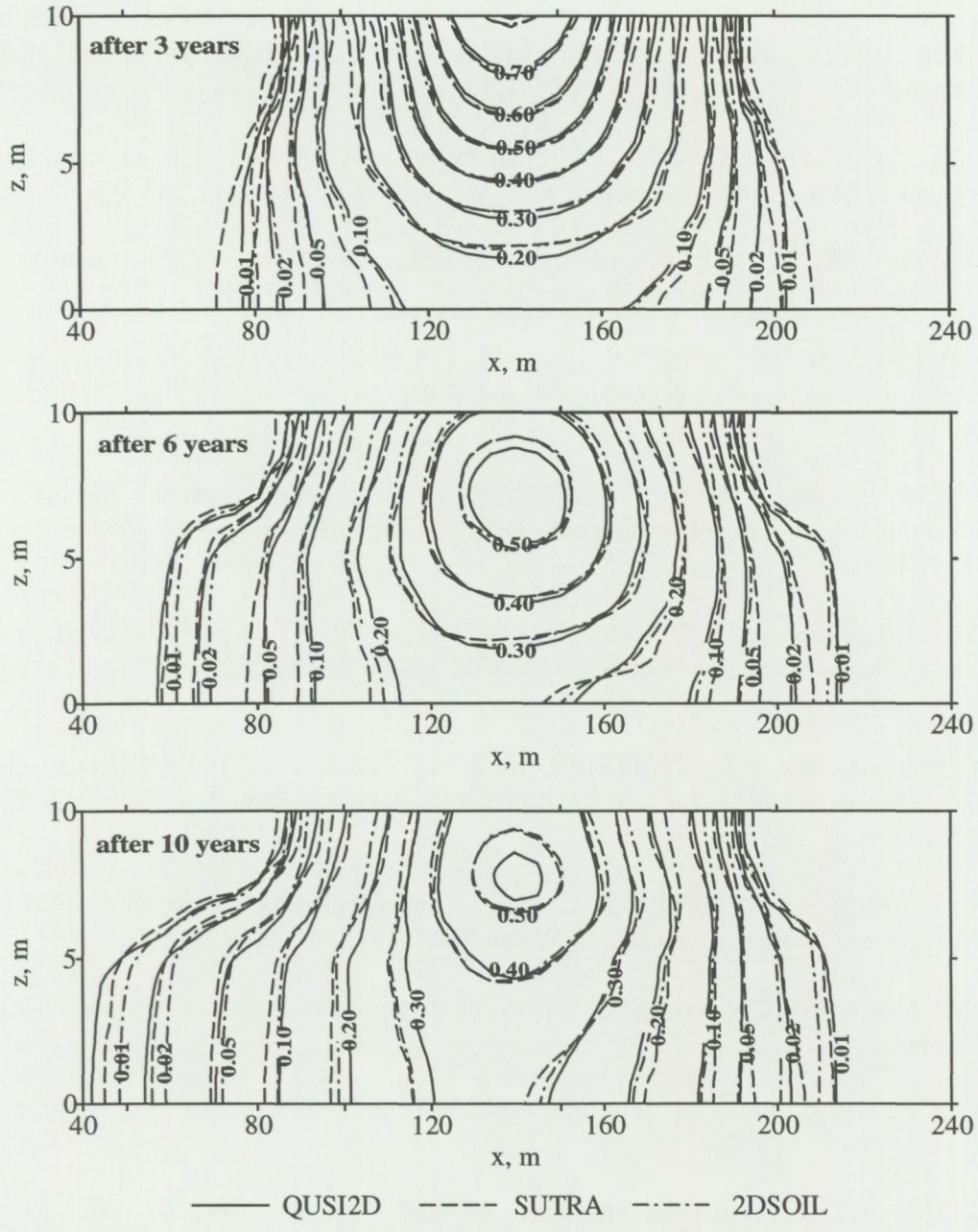


Figure 3. Contours of the solute concentration during infiltration from the soil surface.

Acknowledgments. Drs. Yakirevich and Sorek wish to thank the Rashi Foundation for providing funding to conduct this research.

REFERENCES

BEAR, J. & VERRUIJT, A., 1987: Modeling groundwater flow and pollution., pp. 414 - D. Reidel Publishing Company.

BREDEHOEFT, J.D. & PINDER, G.F., 1970: Digital analysis of areal flow in multiaquifer groundwater system: A quasi-three-dimensional model. - Water Resour. Res., 6, pp. 883-888.

HERRERA, I. & YATES, R., 1977: Integrodifferential equations for systems of leaky aquifers and applications, 3, A numerical method of unlimited applicability. - Water Resour. Res., 13, pp. 725-732.

KOOL, J.B., HUYAKORN, P.S., SUDICKY, E.A. & SALEEM, Z.A., 1994: A composite modeling approach for subsurface transport of degrading contaminants from land disposal sites. - J. Contam. Hydrol., 17, pp. 69-90.

NEUMAN, S.P., PRELLER, C. & NARASIMHAN, T.N., 1982: Adaptive explicit-implicit quasi three-dimensional finite element model for flow and subsidence in multiaquifer systems. - Water Resour. Res., 18, pp. 1551-1561.

PACHEPSKY, Ya., TIMLIN, D., ACOCK, B., LEMMON, H. & TRENT, A., 1993: 2DSOIL-A new modular simulator of soil and root processes. - USDA-ARS, System Research Lab., 209 pp., Beltsville, MD.

PANDAY, S., HUYAKORN, P.S., THERRIEN, R, & NICHOLS, R.L., 1993: Improved three-dimensional finite element techniques for field simulations of variably saturated flow and transport. - J. Contam. Hydrol., 12, pp. 3-33.

PIKUL, M.F., STREET, R.L. & REMSON, I., 1974: A numerical model based on coupled one-dimensional Richards and Boussinesq equations. - Water. Resour. Res., 10, pp. 295-302.

POLUBARINOVA-KOCHINA, P.Ya., 1977: Theory of groundwater motion. - Nauka, 664 pp., Moscow (in Russian).

SAMARSKY, A.A., 1977: Theory of finite differences schemes. - Nauka, 656 pp., Moscow (in Russian)

STRAK, O.D.L., 1984: Three dimensional streamlines in Dupuit-Forchhimer models. - Water. Resour. Res., 20, pp. 812-822.

VACHAUD, G. & VAUCLIN, M., 1975: Comments on 'A numerical model based on coupled one-dimensional Richards and Boussinesq equations' by Mary F. Pikul, Robert L. Street, and Irwing Remson. - Water. Resour. Res., 11, pp. 506-509.

VAN GENUCHTEN, M.T., 1980: A Closed form equation for predicting the hydraulic conductivity of unsaturated soil. - Soil Sci. Soc. Am. J., 44, pp. 892-898

VOSS, C. I., 1984: A finite-element simulation model for saturated-unsaturated, fluid-density-dependent ground-water flow with energy transport or chemically-reactive single-species solute transport: - U.S. Geol. Surv. Water Resour. Investig. Report No. 84-4369, 409 pp., Reston, VA.

Effects of Past Climate Change on Hydrochemistry and Hydraulics in two Large Aquifers in S and SE Asia

G. Jacks [1] and K. Rajagopalan [2]
[1] Div. of Land & Water Resources, Royal Inst. of Technology, S-100 44 Stockholm, Sweden
[2] Central Ground Water Board, T. Nagar, Madras 600 017, Tamil Nadu, India

S and SE Asia are densely populated and this refers in particular to the fertile delta plains of the major rivers. Several megacities and their supply areas are situated in or close to the deltas. Hanoi lies in the Red River delta, Ho Chi Minh City in the fringe of the Mekong delta, Bangkok on the Chao Phrya delta, Rangoon in the Irrawaddy delta and Dhaka and Calcutta in the Ganga-Brahmaputra delta. The water requirement is large, both for water supply and for irrigation. The extensive aquifers underlying the delta are attractive both for water supply and irrigation. The groundwater is often of a good quality and the investments for utilising it is very reasonable. This has led to overdraft resulting in deterioration of quality and settling of the ground (Ramnarong, 1991).

The delta areas are built up by complex sediments ranging in age from the Tertiary until recent. Depending on variations in the past climate they consist of alternating layers of finer and coarser sediments reaching thicknesses of several hundred to even several thousand metres.

The coastal Kerala aquifers

Hydrogeology

The coastal plain in Kerala in SW India is underlain by sediments ranging in thickness up to about 400 m and width up to 50 km (Fig. 1). The oldest sediments are of Tertiary age and the coastal strip is covered by recent sand-dunes (Nair & Rao, 1980). The sediments are relatively much more extensive than the size of the river catchments indicate. This is due to the tilting over of the Indian peninsula towards the East as a consequence of tectonic movements brought about by the collision of the peninsula with the Eurasian continent and the uplift of the Himalayas. This means that the Peistocene and Holocene sediments are thin on the West coast of the peninsula while they are rather much thicker on the East coast.

Four aquifers are distinguishable, from below the Vaikom, the Quilon, the Warkali aquifers and the recent sand-dunes. The three lower aquifers are confined towards the coastline. Especially the Warkali aquifer is subject to a considerable withdrawal, lowering the head below the sea level in the area south of Alleppey. Worries are raised about the possibility of seawater intrusion (Gottshalk et al., 1988).

Hydrochemistry

There is a clear zonation in the water quality from south towards north along the coast in the Warkali aquifer (Fig. 1). In the south Ca-HCO_3-waters dominate, turning into a Na-HCO_3-type of water south of Alleppey before the dominance of brackish Na-Cl-waters comes north of the Vembanad lake (Subramanian, 1980). The pattern is similar in the Vaikom aquifer, however shifted a bit southwards.

This looks like a fresh water flushing of a formerly saline aquifer with a natural softening through ion-exchange resulting in the Na-HCO_3-waters (Fig. 2) (Mercado, 1985; Appelo, 1994). The flushing should then proceed in a SE to NW direction. This interpretation is, however, clearly contradicted by the low heads existing in parts of the area (Gottshalk et al., 1988).

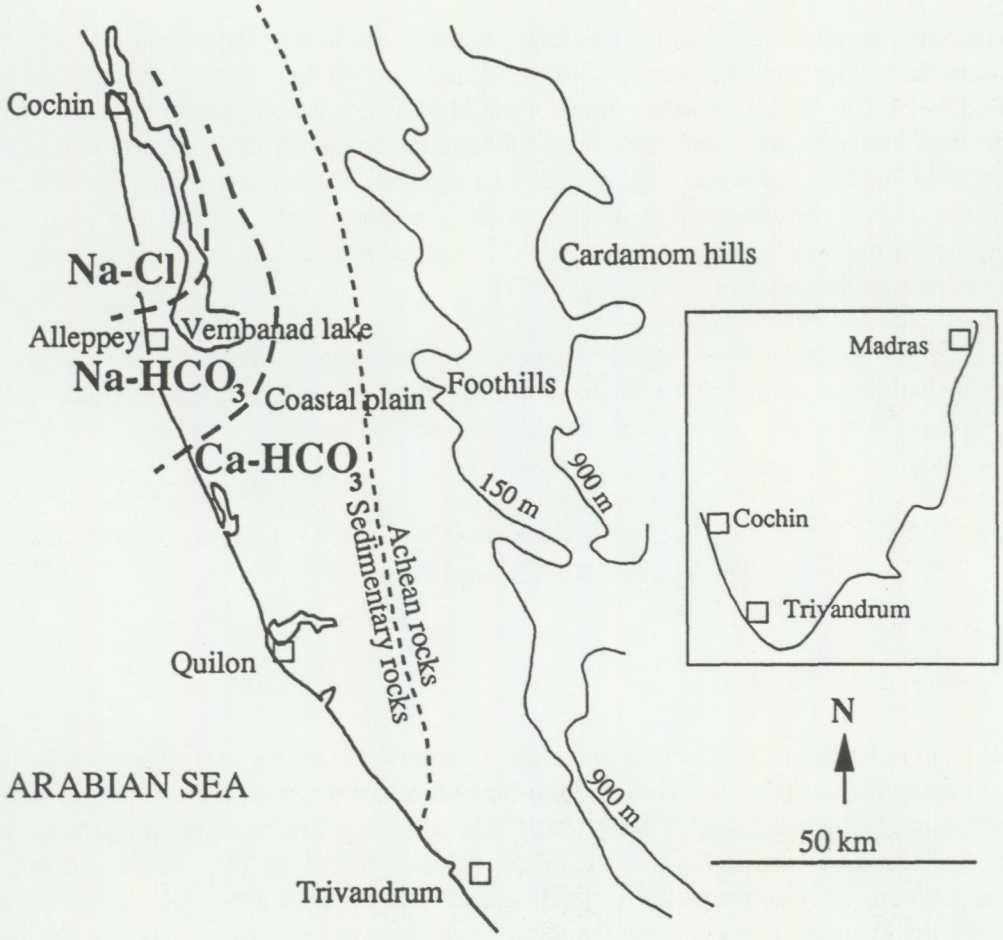


Fig. 1. Zonation of groundwater chemistry in the Warkali aquifer in the coastal Kerala plain, SW India.

The past seawater levels may give the key for interpreting the hydrochemical pattern as well as it may explain the apparent inconsistencies between the water chemistry and the present low heads. The Flandrian transgression was rather small on the Indian West coast (Pirazzoli, 1991). The seawater level during the Pleistocene were about 120 m below the present sea surface, pushing the shoreline about 60-70 km offshore from the present one (Pirazzoli, 1991). This would during a few thousand years have given good opportunities for recharge and flushing of the aquifers (Fig. 3). The reason why the flushing has proceeded from the south may be due to the rather thin cover in the southeast by laterites giving less resistance to recharge than the more impermeable and clayey cover northwards.

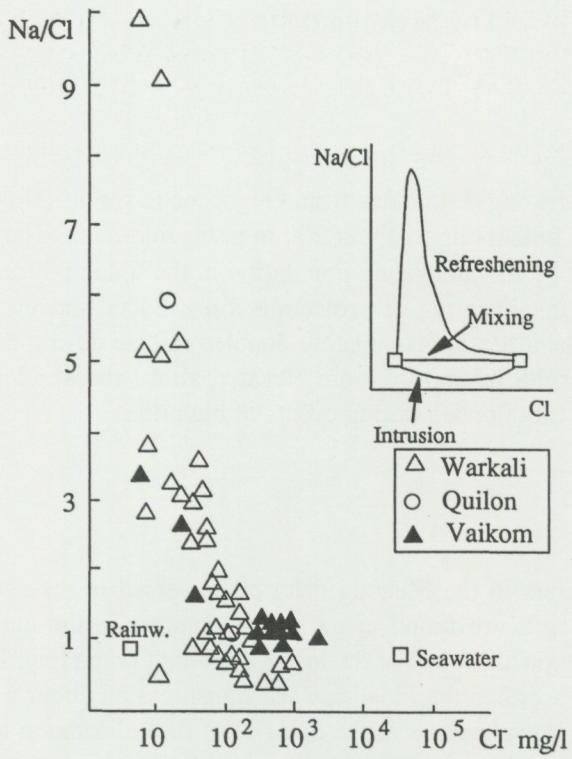


Fig. 2. Na/Cl ratios versus chlorinity for the Kerala coastal aquifers indicating both fresh water flushing and intrusion (graph after the design of Mercado, 1985).

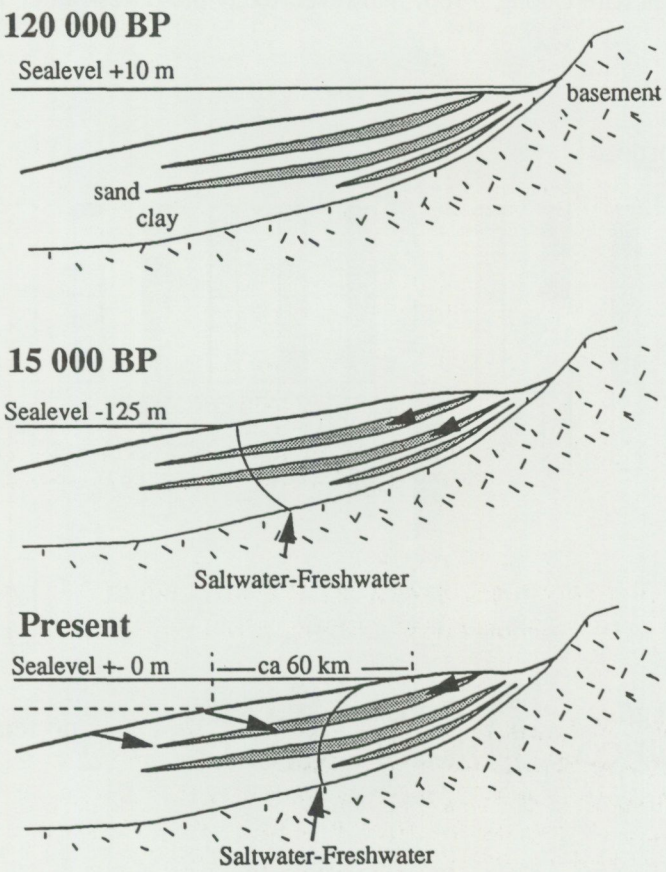


Fig. 3. Hypothetical groundwater flow pattern in the Kerala aquifers as influenced by the sea level changes.

The Mekong delta

Hydrogeology

The on shore sediments in the Mekong delta dates from Oligocene to recent (United Nations, 1986). The Pleistocene sediments are thick, amounting to about 200 m in the mid-delta. The Holocene sediments are also thick, a fact brought about by the increasing population in the upland during the last few thousand years, resulting in the gradual disappearing of protecting forest cover and increased erosion (Nguyen Kim Cuong, 1989). Thus the delta has approximately doubled in size during the last 4000 years. This has also meant that the outer delta is slightly more elevated above the sea level than the inner delta which is the area which is generally flooded during events of high tide.

Hydrochemistry

The water qualities in the aquifers in the Mekong delta are inversed in the sense that the most saline groundwater with more than 3 g/L are found in the upper aquifers in the inner delta while the fresh waters of generally Na-HCO_3-type are found in the lower aquifers (Tran Hong Phu, 1990) (Fig. 4). The salinity in the upper aquifers is ascribed the Flandrian sea transgression about 6 000 years ago (Nguyen Kim Cuong, 1989). Due to the low elevation in the inner delta the salinisation has mainly hit the upper aquifers in the inner delta, seen to the left in Fig. 4. The fresh groundwater in the lower aquifers is of ^{14}C-ages more than 10 000 years and this may be a similar phenomenon as in the Kerala aquifers, being flushing during the Pleistocene period with a seawater level of about 120 m below the present one. It is inferred from offshore drilling for hydrocarbons that freshwater may be present 20-50 km offshore in these aquifers (Nguyen Kim Cuong, 1986). However, today these freshwater aquifers are considered

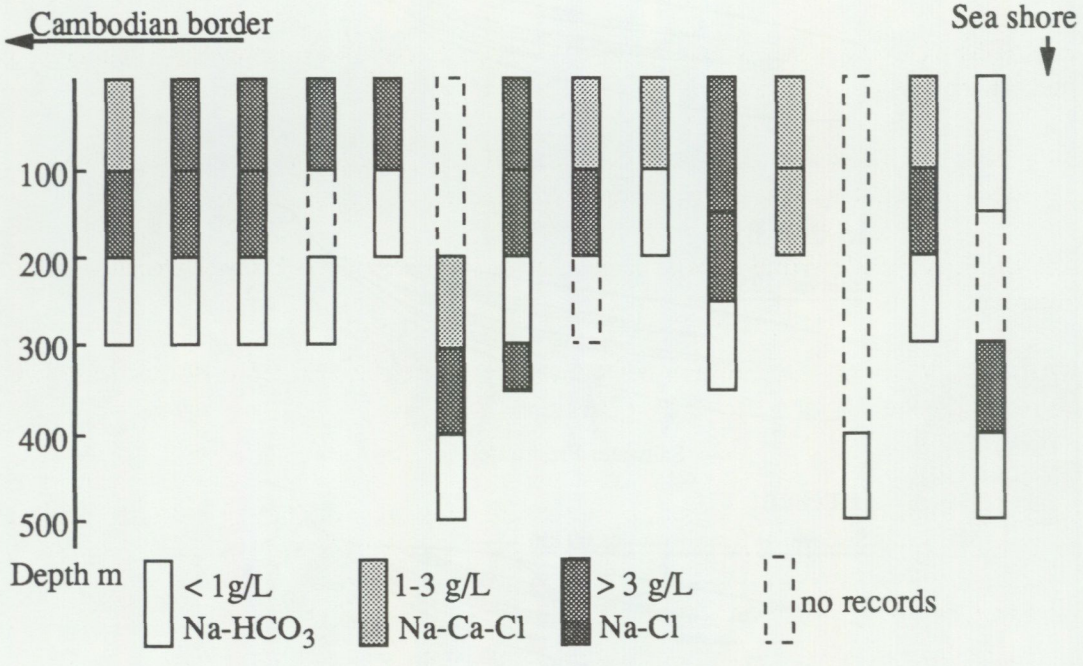


Fig. 4. Sections of water quality from wells in the Mekong delta from close to the Cambodian border downstream to the sea shore. Modified after Tran Hong Phu (1990). The low salinity waters are of the Na-HCO_3-type, the medium saline ones are of a mixed Na-Ca-Cl-type while the most saline are of the Na-Cl-type.

to be quite stagnant which warrants the conservative attitude adopted for their use by the Vietnamese legislation, not allowing them to be used for irrigation, only for domestic water supply.

Conclusions

The two examples given here reflects the complexity of the hydrogeology in the delta areas. They have a four-dimensional character, three in space and one in time. It is essential to consider this in order to be able to exploit the groundwater in a sustainable way. For the Mekong delta a very conservative legislation has been adopted, allowing the use of groundwater only for domestic water supply, not for irrigation. A similar approach may be warranted in other areas as well. A network for hydrogeologists and hydrochemists working in these areas would be useful to transfer experience from one area to another, shedding light on similarities as well as on differences between sites. Another urgent task is to share the knowledge with decision makers, water users and legislators.

REFERENCES

APPELO, C. A. J., 1994: Cation and proton exchange, pH variations, and carbonate reactions in a freshening aquifer. - Water Resources Research 30, pp. 2793-2805.

GOTTSHALK, L., KRASOVSKAIA, I. & LANGSHOLT, L. 1988: Application of groundwater models to the Kerala Coastal Zone. - Central Ground Water Board of India, Report Coastal Kerala Project.

MERCADO, A.,1985: The use of hydrogeochemical patterns in carbonate sand and sandstone aquifers to identify intrusion and flushing of saline water. - Ground Water 23, pp. 635-645.
NAIR, K. M. & RAO, M. R., 1980: Stratigraphic analysis of the Kerala basin. - Geology and Geomorphology of Kerala, Geol. Survey of India, Spec. Publ. No 5, pp. 1-8.

NGUYEN KIM CUONG, 1986: Origin of groundwater in the Mekong plain and outstanding problems. - 1st Conf. on the Geology of Indochina, Ho Chi Minh City, Vol 2.

NGUYEN KIM CUONG, 1989: History of Red River Plain development after Flandrian sea transgression. - Abstract, Int. Seminar on Quaternary Geology and Human Survival 7-13 Oct., Hanoi.

PIRAZZOLI, P. A., 1991: World atlas of Holocene sea level changes. - Elsevier Oceanography Series 58, Amsterdam.

RAMNARONG, V., 1991: Groundwater contamination. - Workshop on Groundwater Monitoring and Evaluation. Vinh Long, Vietnam, 22-25 Nov. 1991.

TRAN HONG PHU, 1990: Alteration of chemical characteristics of groundwater along downward direction in the Mekong Delta. - Workshop on Groundwater Monitoring Khon Kaen, Thailand 9-13 Nov. 1990. Mekong Committee Report.

SUBRAMANIAN, P., 1980: Groundwater resources of the Cochin-Shertallai area, Kerala. - In Geology and Geomorphology of Kerala, Geol. Survey of India, Spec. Publ. No 5, pp. 107-110.

UNITED NATIONS, 1986: ESCAP atlas of stratigraphy VI. - Mineral Resources Development Series No 54.

Preliminary ^{14}C study of groundwater at the fresh-saline water interface of the Mediterranean Coastal Plain Aquifer in Israel

Yoseph Yechieli: Geological Survey of Israel, 30 Malkhei Israel St. Jerusalem 95501, Israel.
Daniel Ronen: Department of Environmental Sciences and Energy Research, The Weizmann Institute of Science, Rehovot 76100, Israel.
Avner Vengosh: Hydrological Service, P.O. Box 6381, Jerusalem 91063, Israel.

ABSTRACT

^{14}C and tritium contents of saline and fresh groundwaters from the interface zone of the Coastal Plain aquifer of Israel were analysed. The low tritum values in most of the saline waters rule out penetration of present-day sea water. Preliminary ^{14}C results of saline groundwater (most of samples with values of about 50 PMC) also suggests that they are not modern sea water, although their locations are near the sea shore (100 m to 500 m). The problems involved in ^{14}C dating of penetrating sea water are discussed. Low ^{14}C content was found in several freshwater samples. The data suggest that (a) flow of fresh water from the aquifer to the sea is, in some cases, restricted and (b) the location of the fresh - saline water interface is not in equilibrium with the present level of the Mediterranean Sea.

INTRODUCTION

The intrusion of sea water into coastal aquifers is a well known process that leads to groundwater salinization to levels above drinking and irrigation water standards. It has been observed that the chemical composition of saline water at the fresh - saline water interface can be different from that of sea water (Vengosh et al., 1991). This phenomenon, attributed to be the result of subsurface storage of evaporated brines, calls into question the dynamics of the sea water - fresh water contact in coastal aquifers. More specifically it raises the question of whether: (1) there is a synchronic response between the changes in sea level and groundwater levels, and (2) the chemical composition of water at the interface zone is a result of mixing of the two presently existing saline and fresh water end members.

Kapuler and Bear (1970) suggested that the coastal plain aquifer of Israel is in a direct connection with the sea whereas Kolton (1988) has argued that in some locations the deeper sub-aquifers are not presently hydraulically connected to the sea. The elucidation of the nature of the fresh - saline water interface is of both scientific and practical interest since the nature of the fresh water - salt water contact will eventually define the pumping regime of coastal aquifers. In this paper we use tritium and ^{14}C isotopes to date saline water from the fresh - saline water interface. It is suggested that the apparent ages of the saline and fresh groundwater will assist in evaluating the residence time of saline waters in the aquifer and the dynamics of their inland penetration.

THE COASTAL PLAIN AQUIFER OF ISRAEL

The Coastal Plain Aquifer of Israel is basically a phreatic aquifer, located along the Mediterranean coast (Fig. 1). It varies in width from 7 km in the north to 20 km in the south; its thickness decreases eastwards from 200 m near the coastline to a few metres at the foothills of the Judea Mountains. The aquifer (the Kurkar Group) consists of interlayered sandstone, calcareous sandstone (arenites - kurkar), siltstone, red loam (Hamra), and marine clays of Pleistocene age, which overly impervious marine clays of Pliocene age (the Saqiye Group). In the west, up to 5 to 8 km from the coastline, interveing clay layers divide the aquifer in to four to six sub-aquifers (Fig. 2). Some of these sub-aquifers are confined (Weisbrod, 1993). In the central and eastern areas, the aquifer is composed mainly of sand and sandstone and is phreatic.

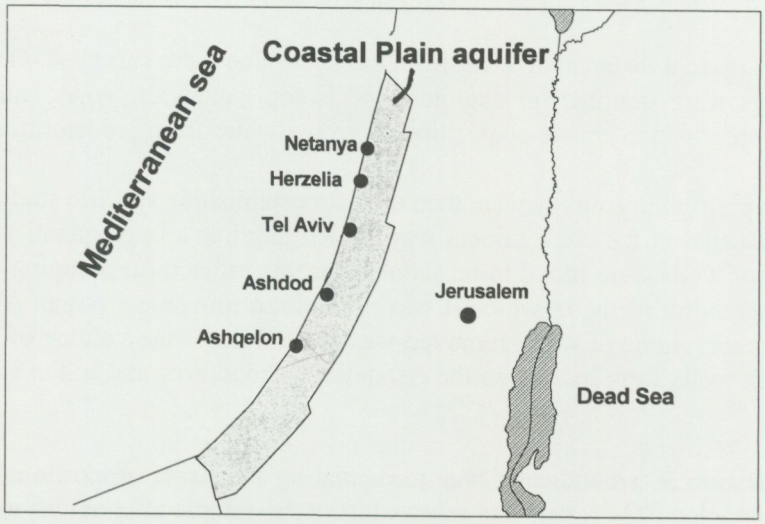


Fig. 1. Location map of the Coastal Plain Aquifer.

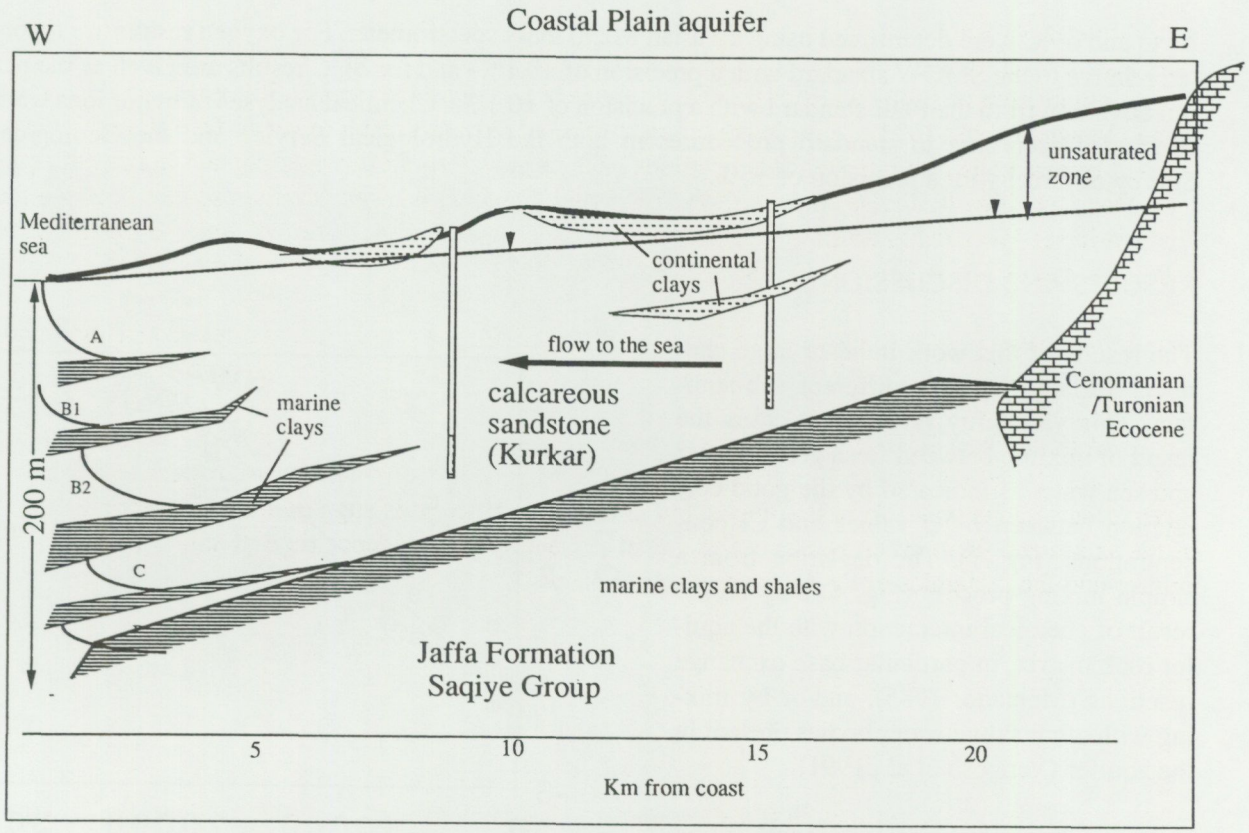


Fig. 2. Schematic hydrogeological cross section of the Coastal Plain Aquifer.

SAMPLING SITES AND ANALYTICAL METHODS

All existing wells up to a distance of 1 km from the shore line were surveyed. Groundwater from different sub-aquifers were sampled for chemical and isotopic analysis. Water samples were collected with a 700 cc sampler which enable acquisition of groundwater from predetermined depths.

The results of the preliminary survey were then used for establishing specific study areas. Since the ^{14}C analysis was conducted in the conventional way, which requires a large quantity of water (about 100 liters), two types of wells were found to be suitable for this project: (a) pumping wells in the Tel Aviv area, and (b) observation wells, in which it was possible to immerse a pump. All wells were purged before sampling; the volume of water removed was about 3 times the volume of the water in the well pipe. The research wells were located in the Ashqelon-Ashdod area and in the Herzelia-Netanya area (Fig. 1).

The ^{14}C concentration in groundwater was measured by means of proportional counters on ethane produced from extracted CO_2 which was released from the sample after acidifying with HCl. The ^{14}C concentrations are expressed as PMC (Percent Modern Carbon). For tritium analysis, the water samples were first enriched by electrolysis and then mixed with scintillation liquid and measured in an LKB 1220 Quantulus scintillation counter. The purpose of the enrichment was to reduce the counting errors to 0.3–0.5 T.U. Tritium concentrations are expressed in Tritium Units (1 T.U. corresponds to a tritium/hydrogen atom ration of 10^{-18}).

$\delta^{18}O$ and $\delta^{13}C$ were determined using a Varian M250 mass spectrometer. For oxygen results are reported relative to the SMOW standard with a precision of ±0.1 ‰ and for $\delta^{13}C$ results are given as the per mil deviation from the PDB standard with a precision of ±0.1 ‰. Chemical analyses of major ions were conducted according to standard procedures in both the Hydrological Service and the Geological Survey of Israel with a precision of ±5%.

RESULTS AND DISCUSSION

The results of this work indicate large chemical variability in the different sub-aquifers. This variability is in many cases the result of mixture between fresh groundwater and sea water as indicated by the good correlation between $\delta^{18}O$ values and Cl concentrations (Fig. 3). The deviation from a simple mixing process (Fig. 4) may be the result of chemical interaction with the aquifer rock matrix, in particular base exchange reactions (Mercado, 1985), and/or by mixing with other saline water bodies present in the aquifer (Vengosh et al., 1991).

Tritium concentrations in most saline groundwaters were low (<3 T.U.) indicating that they are not the result of penetration of recent sea water. The variable tritium concent in the different sub-aquifers reflects the difference in the rate of groundwater recharge (Fig. 5).

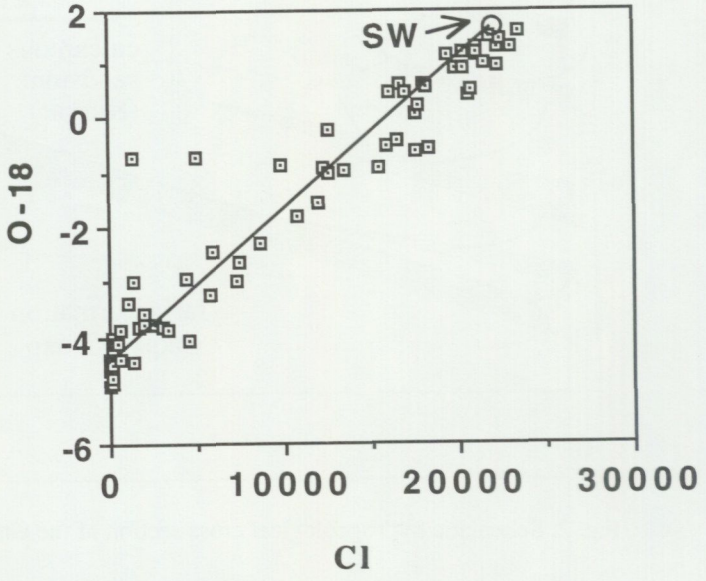


Fig. 3. Cl concentrations versus $\delta^{18}O$ in groundwater from observation wells in the interface zone of the coastal plain aquifer. Also shown is the mixing line between fresh water and sea water.

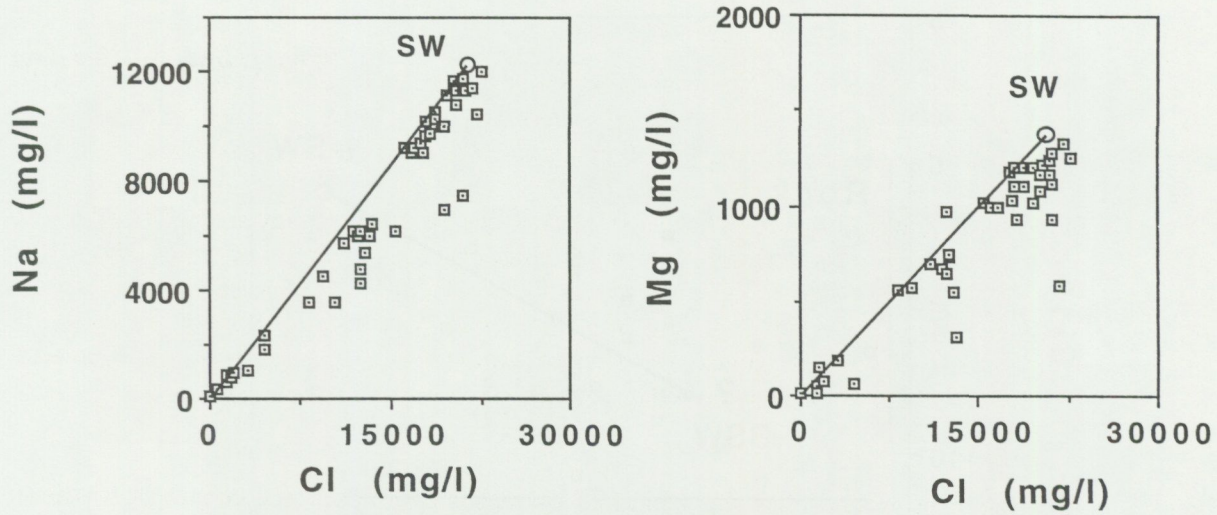


Fig. 4. Na and Mg versus Cl concentrations in groundwater from observation wells in the coastal plain aquifer. Also shown is the mixing line between fresh water and sea water.

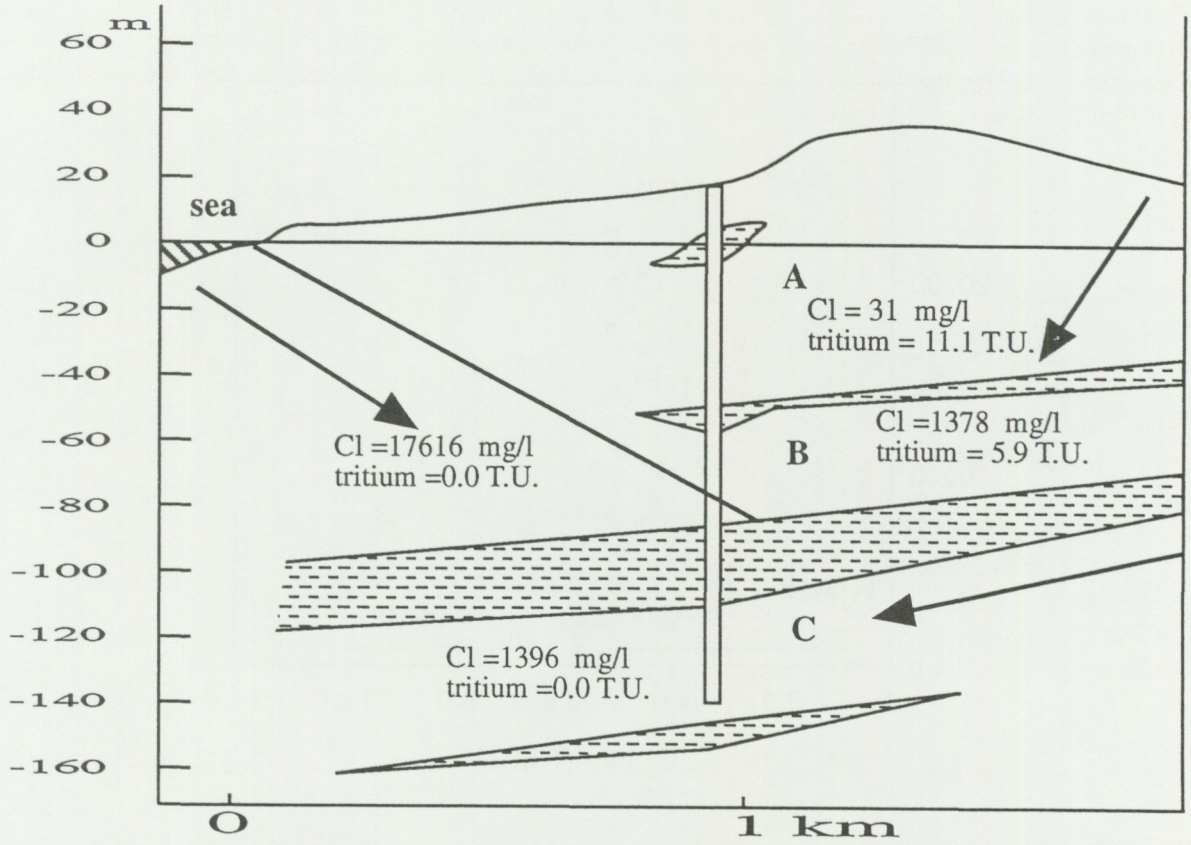


Fig. 5. Schematic cross section of the coastal plain aquifer 5 km south of Ashqelon. The arrows denote the direction of flow of the different water bodies. Note the differences in Cl and tritium concentrations between the adjacent sub-aquifers (denoted by A, B and C).

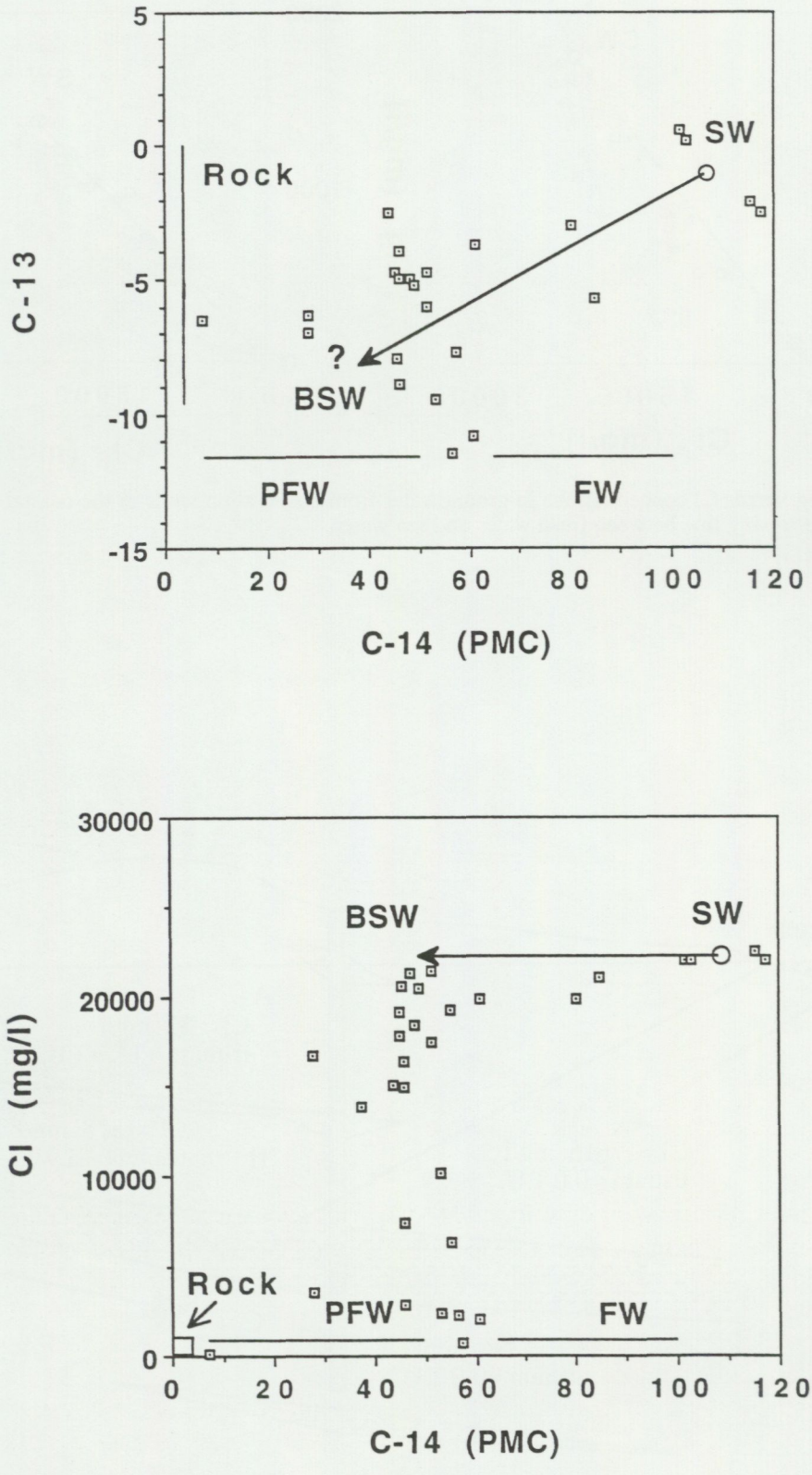


Fig. 6. ^{14}C concentration versus Cl concentration and $\delta^{13}C$ in groundwater from all studied wells (including pumping and observation wells). Also shown are the possible end-members that determine the final composition of groundwater: SW - sea water; BSW - sea water in the sediment at the bottom of the sea; FW - present fresh water; PFW - paleo fresh water (^{14}C = 7-45 PMC); Rock - typical values of calcareous sandstone (Magaritz, 1973).

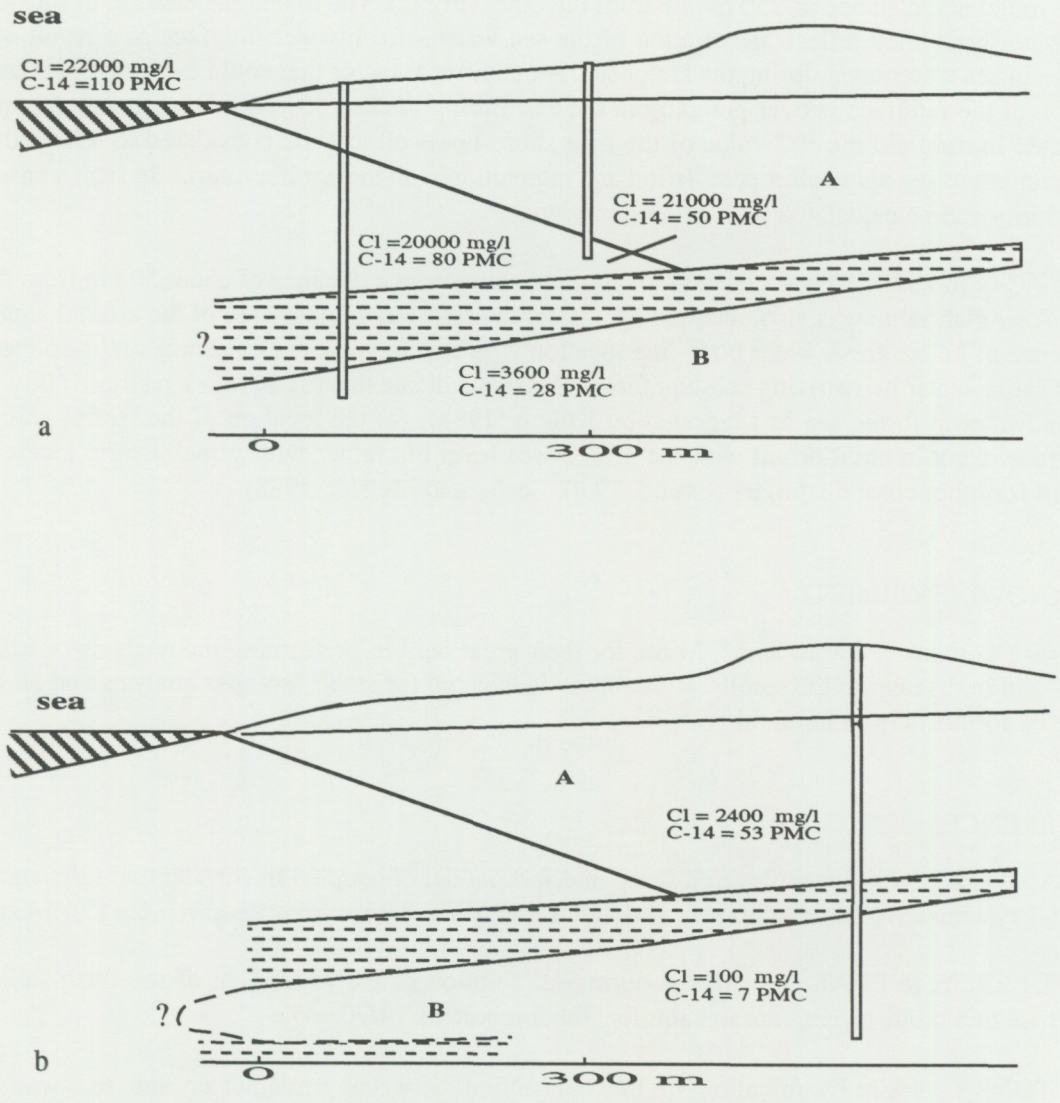


Fig. 7. Schematic cross sections of the coastal plain aquifer in Herzelia (a) and Netanya (b). Note the differences in Cl and 14C concentrations in the different sub-aquifers.

The ^{14}C in saline groundwaters was generally < 50 PMC (much lower than the concentration in modern sea water, 100–115 PMC) giving an age of thousands of years. This age should be considered a preliminary estimate for the following reasons: (1) the initial ^{14}C content of interstitial water in the sediment at the bottom of the sea is difficult to establish since the ^{14}C content of the solid carbonate matrix and the organic matter is unknown and it is reasonable to assume that it decreases with depth, (2) the amount of organic carbon in the sediments, their variation with depth and their ^{13}C values are not known (Fig. 6), and therefore, the ^{14}C of interstitial water resulting from the interaction with "dead" rocks (containing no ^{14}C) cannot be corrected according to the $\delta^{13}C$ values as is normally done for fresh groundwater, (3) the ^{14}C of the fresh water end member may be highly variable, and (4) according to available data (Magaritz, 1973) the ^{13}C of the calcareous sandstone in the aquifer is not uniform, varying from 0 to -10‰.

Within a same sub-aquifer and along a horizontal stream line an interesting case was detected in the Netanya area where two water bodies having similar Cl content and an age difference of 4000 years

were found at a distance of 250 m one from the other (Fig. 7). The inland penetration of the 4000 year old water body may reflect penetration of the sea water - fresh water interface as a result of the increase in sea water level during the Holocene. An additional factor that could enhance the inland penetration of the interface is over pumping in the east during the last 50 years. Where such a sequence is detected in the field the ^{14}C value of the near shore-line well may be considered to reflect the initial ^{14}C content of sea water after percolation and interaction with the aquifer matrix. In such a case the age variability can be calculated with better confidence.

Low ^{14}C (7 to 28 PMC) was detected for some fresh water at a distance of about 500 m from the shore line. A similar value was also obtained by Weisbrod (1993) in another area of the coastal aquifer. The presence of an old fresh water body in a location where saline water is expected, and also the presence of saline water in overlying sub-aquifers in the area indicate that (a) there is a restricted flow of fresh groundwater in to the sea as suggested by Kolton (1988); (b) the location of the fresh - saline water interface is not in equilibrium with the present sea level but rather with some historic levels, as suggested for other coastal aquifers (Essaid, 1990; Leahy and Meisler, 1988).

ACKNOWLEDGEMENT

We wish to thank I. Carmi and J. Mintz for their great help in performing the analysis of tritium and C-14 and in discussing the results. R. Selinkov is thanked for stable isotopes analysis and H. Hemo is thanked for his help in the field.

REFERENCES

ESSAID, H.I., 1990: A multilayered sharp interface model of coupled freshwater and saltwater flow in coastal systems: Model development and application. Water Resources Research, 26 (7): 1431–1454.

KAPULER, Y. & BEAR, J., 1970: A numerical solution of the movement of the fresh-saline water interface in a multi-layered coastal aquifer. Tahal report 01/74/70.

KOLTON, Y., 1988: Examination of the connection between groundwater and sea water in the Pleistocene aquifer in the continental shelf of the Mediterranean sea coast in Central Israel. Tahal report 01/88/31.

LEAHY, P. & MEISLER, H., 1988: Effect of eustatic sea level changes on the position of saltwater-freshwater transition zone in the coastal plain aquifer system of New Jersey. EOS 69 (16): 356.

MAGARITZ, M., 1973: Isotopic composition of oxygen and carbon in carbonatic rocks from Israel. Ph.D. thesis, Weizmann Institute of Science, Rehovot.

MERCADO, A., 1985: The use of hydrogeochemical patterns in carbonate sand and sandstone aquifers to identify intrusion and flushing old saline water. Groundwater 23:635–644.

VENGOSH, A., SRARINSKY, A., MELLOUL, A., FINK, M. & ERLICH, S., 1991: Salinization of the coastal aquifer water by Ca-chloride solutions at the interface zone, along the Coastal Plain of Israel. Hydrological Service report Hydro/20/1991.

WEISBROD, N., 1993: Hydraulic connections in the groundwater system of the Kurkar Group, Coastal Plain, Israel. M.Sc. thesis, Hebrew University, Rehovot.

Salt Groundwater in Sweden - Occurrence and Origin

Bo Olofsson
Division of Land and Water Resources, Royal Institute of Technology, S-100 44 Stockholm, Sweden

Abstract

The aims of this paper are to give a general regional description of the distribution of salt groundwater in Sweden and to discuss the origin of the salt. Data from the Well Record Section at the Geological Survey of Sweden (SGU) has been compiled, expecially from six counties in central Sweden. Pore water from marine clays has been chemically compared to salt groundwater from drilled wells. The project shows that more than 20% of all wells in the six counties in central Sweden have an increased content of chloride in relation to the natural deposition from precipitation. A strict correlation between salinization and areas beneath the highest marine shore level from previous stages of the development of the Baltic sea, clearly points out fossil seawater trapped in marine clays or in rock fractures beneath the clays as the main natural source of salt in crystalline rock areas. This type of salinization is probably restricted to the upper part (<700 m) of the rock. Locally, other sources of salt water are prevailing, such as salt water intrusion from the sea within a narrow zone, usually less than 100 m from the shore, and formation salts in some sedimentary rock areas. At deep levels in crystalline rock (>1000 m) salt brines are found, probably at increasing depth with increasing distance from the present sea. Such brines may be of hydrothermal origin. In addition to these natural salt sources, locally a considerable salinization of groundwater from anthropogenic sources occur, especially from de-icing road salts. A raised chloride content and an increased hardness of the groundwater can be seen along major roads in Sweden.

Introduction

Salt groundwater is a wellknown problem in the world, usually along the coastal areas. Before nineteen-seventies salt groundwater was sporadically described in Swedish literature. Most notes of salt groundwater concern sedimentary basins (Erdmann, 1911, Tullström, 1955, Pousette & Möller, 1972, Möller et al, 1981). However, such areas only cover a minor part of Sweden. From old crystalline rock areas, salt groundwater was early reported by Olberg (1854), who described salt springs in western Sweden and Svenonius (1918) who noticed salt groundwater in a drilled well not far from Lake Vänern, southwestern Sweden.

Valuable information of the occurrence of deep salt groundwater in sweden has been collected from about ten sites in Sweden, which have been investigated within the Swedish nuclear waste repository project (Laurent, 1982, Smellie & Wikberg, 1989, Arad, 1991).

More comprehensive studies of the occurrence of salt groundwater in Sweden, based on information from the well record section at the Geological Survey of Sweden (SGU) are given by Knutsson & Fagerlind (1977), Lindewald (1985) and Olofsson (1994).

The aims of this paper are to give additional data regarding the occurrence of salt groundwater wells in Sweden and to discuss possibly sources of the salt in relation to recently carried out investigations.

Methods of investigation

From the middle of the nineteen-seventies information from the construction of drilled wells in Sweden regarding capacity, localization, depth and geology have been stored at SGU. Some of these well records include chemical analyses of the groundwater. Analysis of 13 000 well records in Sweden has recently been carried out (Olofsson, 1994). The present project comprises analyses of chemistry using

5-6000 of the chemical analyses stored at SGU. Data has been compiled from 6 different counties in south and central Sweden; the counties of Stockholm, Uppland, Östergötland, Gotland, Örebro and Göteborg-Bohuslän. Among the well records, analyses with a chloride content exceeding 100 mg/l were selected and information regarding geology, topography and distance from seashore and de-icing salted roads were collected from maps for these sites in order to evaluate the chemical variations in relation to natural geological and hydrogeological conditions. In order to evaluate the contribution of salts to the bedrock aquifers from marine clays, pore water in clays in the vicinity of some salt wells, have been pressed out and chemically compared to the well water. Sampling of groundwater has also been carried out in 93 wells within 300 m from roads in the county of Västmanland, central Sweden, on which de-icing salts have been used, in order to clarify the impact on groundwater from roads.

The occurrence of salt groundwater wells in Sweden

A compilation of chloride analyses from almost 13 000 well records stored at SGU indicates that the salt groundwater occurs along the whole Swedish coastline as well as within a 200 km wide zone in central Sweden, from Lake Mälaren in eastern Sweden, through Lake Vättern and Lake Vänern to the Swedish west coast, **figure 1.**

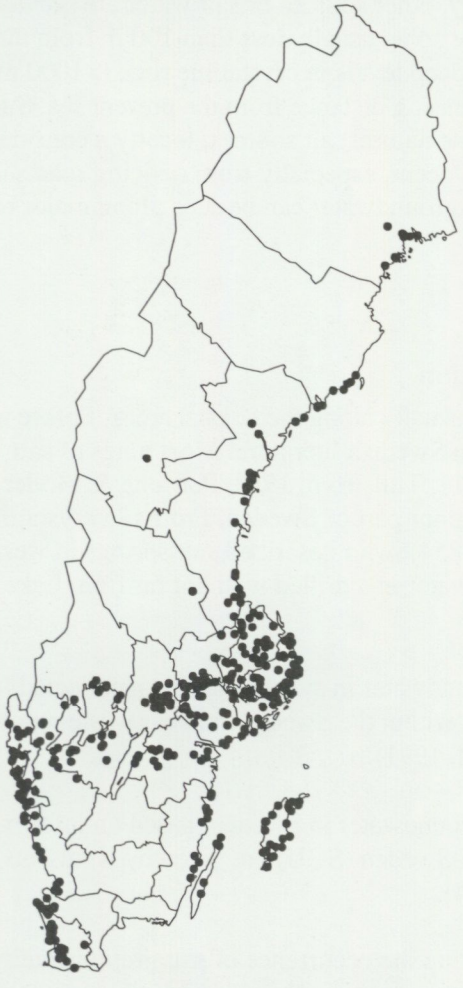


Figure 1 *Salt groundwater (>300 mg Cl/l) in Sweden (data collected from SGU)*

In total approximately 17% of the wells at SGU show a raised content of chloride, which here is defined as a chloride content exceeding 50 mg Cl/l. The chloride content of the precipitation, which is the main natural chloride source in Sweden, varies between 0.2 mg/l in the northernmost part of Sweden, where the wet deposition is small, to 10 mg/l at the Swedish west coast (Granat, 1990). The dry deposition of chloride is much more difficult to estimate. However, measurements of throughfall in a forested terrain, compared to open terrain show that the value of dry deposition is 50-100% of the wet deposition in the northern Sweden and 100-300% of the wet deposition in southern Sweden (Lövblad et al, 1992).

A rough estimation of the present situation in Sweden shows that more than 60 000 wells in Sweden may be affected by other salt sources than from precipitation (Olofsson, 1994). The salt content in 13 000 of these wells may exceed the taste limit of salt (app. 300 mg Cl/l). However, these figures give not a true picture of the present situation, since they principally only reflect the chemical composition of the aquifer at the time of the construction of the wells. Analyses of well records stored at the health administrations of the municipalities, indicate an increased number of salt affected wells (in total 20-30%), compared to the well record section at SGU (Lindell, 1987, Olofsson, 1990).

In the six counties, which have been more closely studied, the percentage of salt affected wells varies from 17% in the county of Örebro to as much as 61% on the island of Gotland, **table 1**. Taste of salt

usually occurs in 2-6% of the wells, except on the island of Gotland where the taste limit exceeds in as much as 25% of the wells. As can be seen in **figure 2**, the distribution of the salt affected wells is highly varying. In the county of Uppland, which consists of a flat crystalline bedrock surface, partly covered by a thin layer of clay, the distribution of salt wells is spread over the whole county, whereas in the county of Örebro, the salt affected wells are more concentrated to the eastern part where the area consists of clays covering a flat surface of sedimentary rocks.

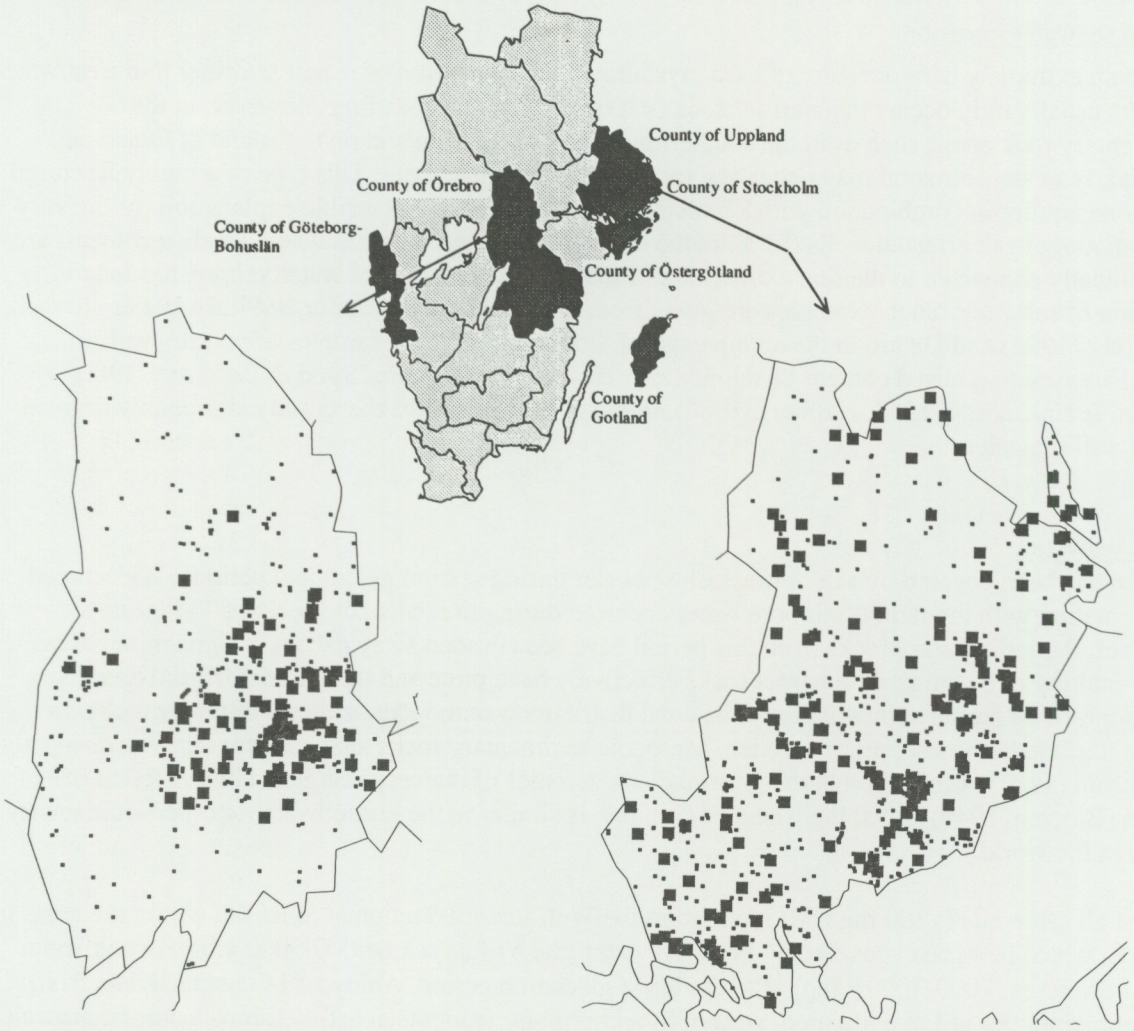


Figure 2 *Location of six detailed studied counties in the south and central Sweden as well as examples of distribution of salt water affected wells (>50 mg Cl/l, black boxes) compared to all wells with chemical analyses at SGU (small black dots) from two of these counties (Uppsala and Örebro).*

Table 1 *Chloride contents of groundwater in six counties in Sweden.*

County	No of wells	>50 mg Cl/l	>100 mg Cl/l	>300 mg Cl/l	>1000 mg Cl/l
All six counties	4980	20.7 %	11.2 %	4.1 %	1.0 %
Stockholm	2046	18.9 %	9.7 %	2.9 %	0.7 %
Uppsala	887	21.2 %	12.0 %	4.2 %	0.7 %
Östergötland	787	17.4 %	7.8 %	2.2 %	0.6 %
Gotland	149	61.1 %	43.0 %	25.5 %	9.4 %
Göteborg-Bohuslän	570	23.5 %	13.2 %	5.8 %	1.4 %
Örebro	540	17.8 %	9.6 %	3.7 %	0.7 %

Origin of salt groundwater

The origin of the salt groundwater in Sweden has been discussed among others by Lindewald (1981,1985), Nordstrom et al (1989), Arad (1991), Kökeritz (1993) and Olofsson (1994). Several sources have been proposed such as intrusion of seawater in coastal areas, fossil seawater, water-rock interaction, freezing of seawater as well as anthropogenic sources (e.g. leakage from waste deposits and de-icing salts on roads).

Recent seawater intrusion

Due to an extremely heterogeneity of hard crystalline rocks, intrusion of recent seawater into freshwater aquifers usually only occurs in a narrow zone (<100 m) along the coastline. However, in the sedimentary rock areas, such as in the southernmost part of Sweden and on the island of Öland and Gotland, seawater intrusion may occur at a far distance from the shore. This type of a highly fractured limestone aquifer in combination with karstic structures may be one plausible explanation for the very high amount of salt affected wells (61%) in the county of Gotland. In areas where sandy sediments are hydraulically connected to the sea, extraction of freshwater for municipal water supply, has led to intrusion of seawater. Such examples are given from Stafsnäs (Tilly-Leander, 1994, Huber & Lundqvist, 1995) and Dalarö in the archipelago of Stockholm. Many examples of private wells in coastal areas with a raised content of salinity are described in literature (Sund & Bergman, 1980, Gewers & Håkansson, 1988, Hallberg, 1986). In many of these wells, the salinity is probably derived from fossil seawater.

Fossil seawater

Sweden has been covered by salt or brackish seawater during several geological periods. Widespread sedimentation with interstitial salt pore water occurred during the Paleozoic period 570-400 m.y. However, the sedimentary rocks from this period have been eroded away except in some minor areas where faulting or covering with harder rocks effectively have protected the sediments from erosion. Sandstone-filled fractures now indicate the areal distribution of the Paleozoic sedimentary rocks. In Scania, the southernmost part of Sweden, Mesozoic sedimentary rocks also indicate salt water stages. Nordstrom (1983) points out that the general characteristics of the very salt groundwater found in Scania (Brotzen, 1949) and at the island of Gotland, is similar to the groundwater in other sedimentary basins in the world.

Almost all salt wells (>300 mg Cl/l) reported to the Well Record Section at SGU fall within the areas in Sweden, which have been covered by brackish water (the Yoldia sea, 10000-9000 y.b.p) or salt water (the Litorina sea, 7000-3000 y.b.p) after the latest glaciation period. Analyses of chemical data from four municipalities at Lake Mälaren, west of Stockholm, far from the coastline, show a similar amount of salt affected wells as in coastal municipalities within the county of Stockholm (Assad & Salih, 1989).

Areas below the highest marine shore level have a large frequency of marine clays. In order to evaluate a correlation between pore water in clays and the chemical composition of the groundwater in some very salt drilled wells (>1000 mg Cl/l) in eastern central Sweden, the pore water from different depths was pressed out of the clay. The chemical composition of the pore water has been compared to the salt groundwater pumped up from the wells, **figure 3 A-C**.

The comparison shows that moderate saline water from the wells (<700 mg Cl/l) can be partly explained by leakage from the marine clays, whereas the deeper and strongly saline groundwater, which was mobilized by pumping, indicates another source. The chloride content was also three times higher (up to 9000 mg/l) than the chloride content of the present Baltic sea.

Water-rock interaction

Water-rock interaction has been proposed as a source of the salt groundwater. The Br/Cl-ratio of the solutes in fluid inclusions matches the ratio of the groundwater in the granite at the research mine

Stripa, central Sweden (Nordström et al, 1989, a,b) and at Finnsjön, central eastern Sweden (Puigdomènech & Nordstrom, 1987).

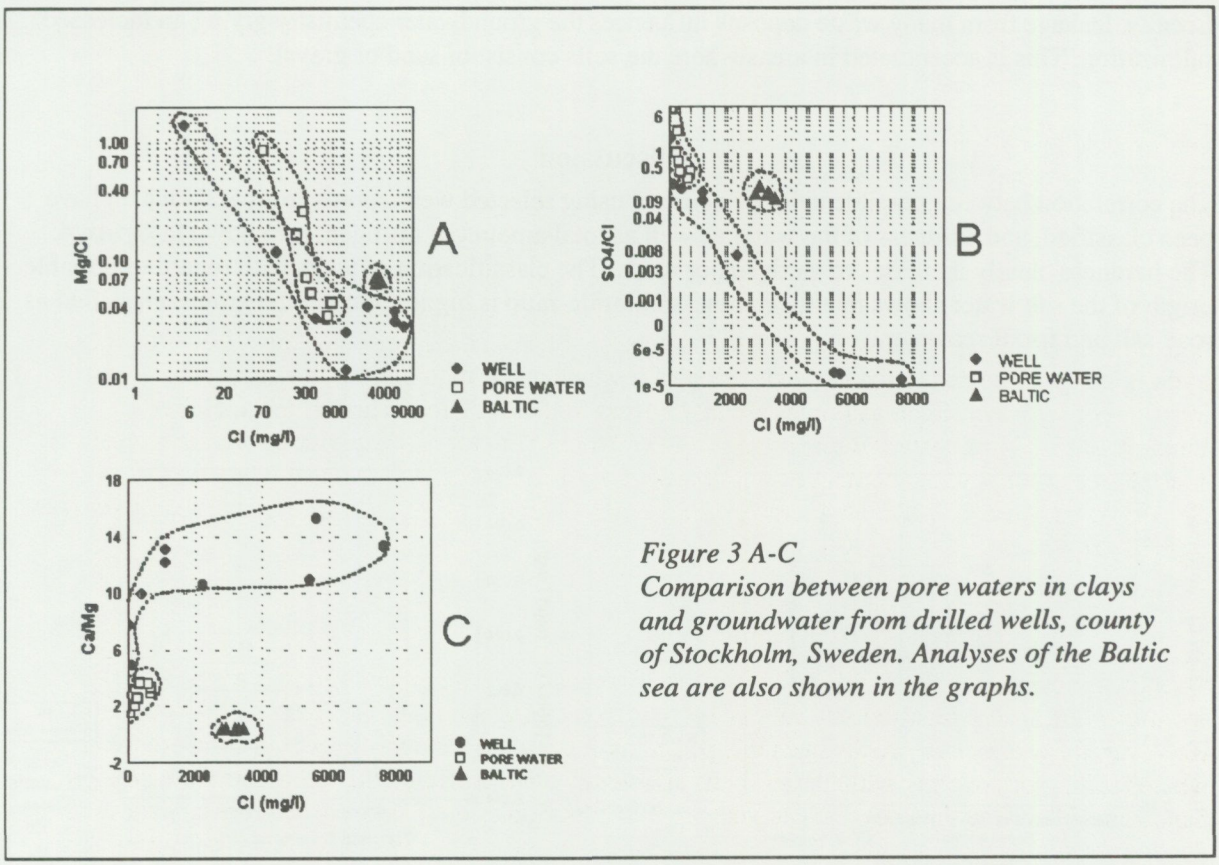


Figure 3 A-C
Comparison between pore waters in clays and groundwater from drilled wells, county of Stockholm, Sweden. Analyses of the Baltic sea are also shown in the graphs.

Freezing of seawater

Herud et al (1990) and Bein & Arad(1992) have suggested freezing of seawater as a conceivable explanation for the formation of deep salt groundwater in Sweden.

Anthropogenic sources

De-icing salts on road have been suggested as an important chloride-source in groundwater supply in Finland and Canada. In Sweden some early investigations on the impact of de-icing salts on groundwater were carried out around the nineteen-eighties (Bäckman, 1980). Locally, unprotected storages of road salts have caused salinization of wells (Müllern & Eriksson, 1981). Comprehensive studies of a municipal well, located in the vicinity of the main road E4 at Upplands Väsby, north of Stockholm, have revealed that the groundwater in the sandy aquifer is strongly affected by infiltrated de-icing salts (Maxe et al, 1993). Water sampling and analyses of groundwater along major roads in the county of Västmanland, central Sweden, have shown that almost 40% of the wells exhibit an increased content of chloride. This figure is much higher than data regarding the chloride content collected from the Well Record Section at SGU, which represents the situation when the well was constructed (Fabricius & Olofsson, 1996). The hardness of the groundwater close to roads is also usually much higher, which can be explained by intensive ion exchange with release of calcium when large amount of sodium-chloride is added to the soils.

Analysis of variance (ANOVA) using classified well records with a chloride content exceeding 100 mg/l, collected from the six counties, shows that groundwater close to roads represents the group with the highest hardness.

Water chemical sampling and analyses in about 100 wells along the major road E20, east of Lake Vänern, in the county of Skaraborg, central Sweden, have shown that about 50% of the sampled wells within 100 m from the road showed a raised content of chloride (Jansson, 1996).

Locally, leakage from many waste deposits influences the groundwater chemistry giving an increased salinization. This is accentuated in areas where the soils consist of sand or gravel.

Discussion

The correlation between possible chloride sources, using selected well records from SGU which have been classified, and hardness of the water as well as total amount of nitrogen, are shown in **figure 4**. The hardness clearly increases towards major roads. The classification of wells with regard to possible origin of the salt water shows that the hardness/chloride-ratio is highest among the groups classified as road salt and fossil seawater.

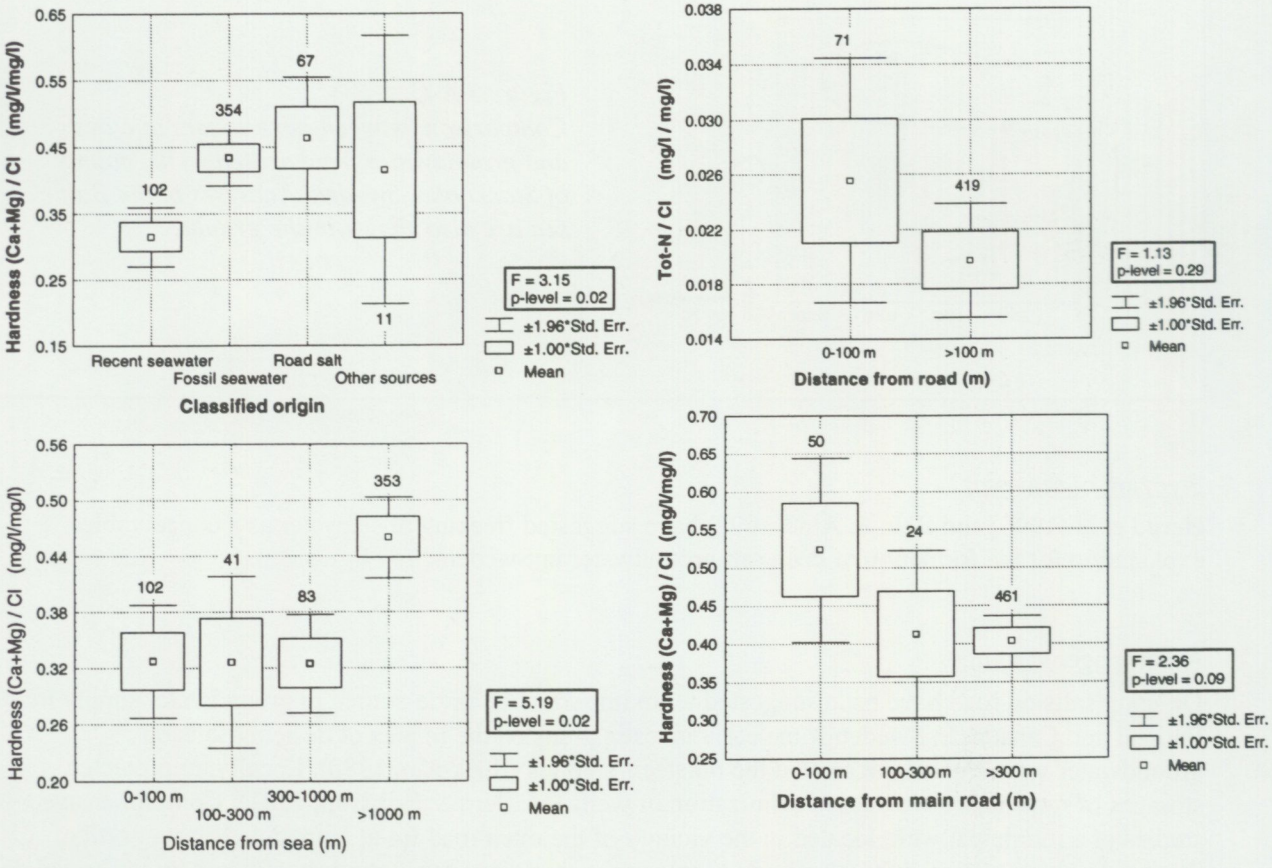


Figure 4 *ANOVA, showing the variation of hardness and nitrogen in relation to some probably sources of chloride. Based on classified well records from SGU.*

The spatial distribution of salt water wells in Sweden, clearly points out a strong connection to the brackish and salt marine environment after the latest glaciation period. The strong correlation (so far without exceptions) can only be explained either by the capture of seawater in rock fractures and pores in marine clays or by the fact that the marine clays act as an effective protection from flushing by fresh water. However, if other major sources of the salts, such as water-rock interaction, which has been proposed a.o. by Nordstrom et al (1989,a ,b) or old Paleozoic pore water could be preserved in crystalline rocks, salt groundwater should have been frequently found also in other areas, such as in the

Storsjön basin, west central Sweden or in central Småland (south Sweden). Also in the many deep drilled wells in Sweden (<800m), which have been carried out within the investigation programme for the final nuclear waste repository, salt groundwater at depth has only been registrered in boreholes below the highest marine shore level. In the three studied areas above this boarder, Taavinunnanen, Svartboberget and Klipperås, only fresh groundwater was found, **figure 5**.

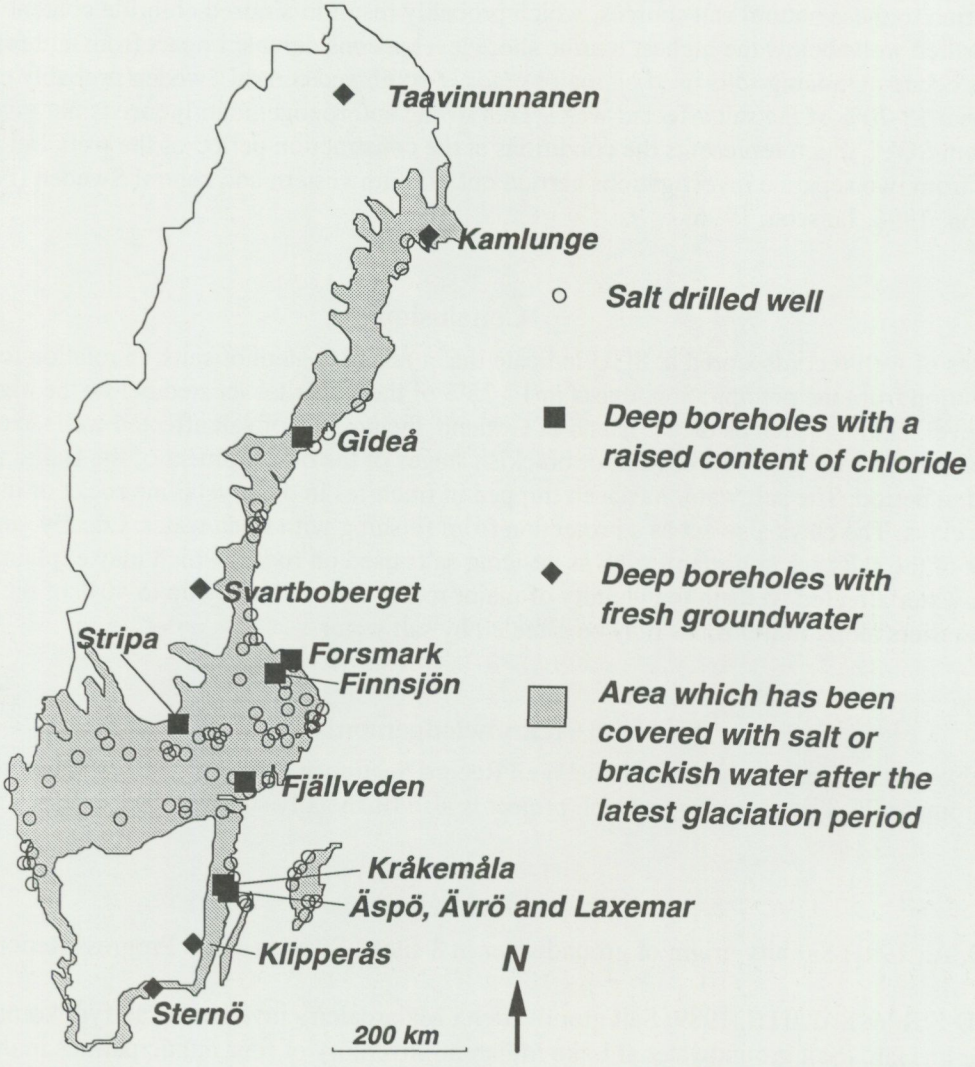


Figure 5 *Localization of deep drilled boreholes within the final nuclear waste repository project in Sweden. The highest marine shore level and the occurrence of salt drilled wells among well records at SGU, is also presented in the graph.*

Although most of the salt wells can be explained by the Holocene marine environment, some other sources of the salt must exist:

The very high salinity on the island of Gotland (>60 000 mg Cl/l) and in Scania (>150 000 mg Cl/l) (Brotzen, 1949) as well as the presence of many salt wells registrered in the southwestern part of Scania, must be a result of formation salts (such as salt minerals or very salt pore waters) connected with the sedimentary rocks prevailing in these areas.

Very high salinity has also been registrered at very deep levels in crystalline rocks (>1000 m) at Laxemar, south eastern Sweden, and at a depth of more than 4000 m in the deep Siljan borehole (central Sweden). Probably, brines exist at increasing depths, from the recent coastline where this type of water is found at depths more than 800 m, to the central part of Scandinavia, where the extremely saline water is found several tousand metres below the land surface. The origin of these brines may be of hydrothermal processes, indicating stagnant flow conditions at these depths.

In addition to these natural salt sources, which probably result in a raised chloride content in about 20% of all drilled wells below the highest marine shore level, a considerable impact from anthropogenic sources occurs. De-icing salts used on major roads in south and central Sweden probably explain additional 15-20% of the salt affected wells. This strong anthropogenic influence is not given by the data from SGU, which represents the conditions at the construction period of the well, but it is mainly shown from two separate investigations carried out in southwestern and central Sweden (Fabricius & Olofsson, 1996, Jansson, 1996).

Conclusions

Analyses of well records stored at SGU indicate that a raised content of salts, in relation to the contribution from the precipitation, exists in 17-25% of the well sites located below the highest marine shore level. Locally, such as on the island of Gotland, the amount of salt affected wells exceeds 61%. Most of the salt wells derive from salt or brackish stages of the development of the Baltic after the latest glaciation period. The salt water has been trapped in fractures in the crystalline rocks or in pores in the marine clays. The clays also act as a protection from flushing with fresh water. Locally, anthropogenic sources of the salts are important, such as de-icing salts used on roads, which may explain 15-20% of the salt water affected wells in the vicinity of major roads. Hence, locally up to 40% of the wells in small aquifers along major roads may be affected by salt water.

Acknowledgements

Groundwater chemical analyses from the Well Record Section at SGU has been supplied by Sten Sandström, SGU. The on-going research project is also financially supported by research funds at SGU.

References

ARAD, A., 1991: Salinity origin of groundwater in 8 sites - Sweden. SKB Progress Report 91-09.

ASSAD Z R. & SALIH S, 1989: Salt grundvatten i Mälardalen - inventering av fyra kommuner i Stockholms län. (Salt groundwater at Lake Mälaren - inventory of four municipalities in the county of Stockholm). MSc thesis, at Div. of Land and Water Resources, KTH, Stockholm, Sweden.

BEIN, A.& ARAD, A., 1992: Formation of saline groundwaters in the Baltic region through freezing of seawater during glacial periods. Journal of Hydrology, vol 140, pp 75-87.

BROTZEN, F., 1949: De geologiska resultaten från borrningarna vid Höllviken, del II, undre kritan och trias. (Geological results from drilling at Höllviken, part 2, lower Cretaceous and Triassic rocks). SGU, ser C, no 505.

BÄCKMAN, L., 1980: Vintervägsaltets miljöpåverkan.(Environmental impact of de-icing salts). National Road and Traffic Research Institute (VTI), report no 197, Linköping.

ERDMANN, E., 1911: De Skånska stenkolsfälten och deras tillgodogörande. Geologisk och teknisk beskrivning. (The hard coal areas of Scania. Geological and technical description). SGU, ser Ca, no 6.

FABRICIUS, C.& OLOFSSON, B., 1996: Salinization of private wells from de-icing chemicals - a pilot project in central Sweden. SWIM-proceedings, Malmö 1996 (this report).

GEWERS, K.& HÅKANSSON, P., 1988: Saltvatteninträngning i brunnar i kustnära områden - en studie av två öar i Norrtälje kommun. (Salt water intrusion in coastal areas - a study of two islands in the municipality of Norrtälje.) MSc thesis at Div. of Land and Water Resources, Trita-Kut no 3041, Stockholm.

GRANAT, L., 1990: Luft- och nederbördskemiska stationsnätet inom PMK. Rapport från verksamheten 1990. (Network for measurement of chemistry in Air and precipitation within PMK, 1990). National Swedish Environment Protection Board, Report no 3942.

HALLBERG, U., 1986: Analys av en saltvattenbrunn in Stockholms skärgård. (Analysis of a salt well in the archipelago of Stockholm). MSc thesis at Dept. of Physical Geography, University of Stockholm.

HERUD, B., STARINSKY, A., KATZ, A.& BEIN, A., 1990: The role of seawater freezing in the formation of subsurface brines. Geochimica et Cosmochimica Acta, vol 54, pp 13-21.

HUBER, A. & LUNDQVIST, A., 1995: Application of geophysical methods in salt water intrusion detection in a coastal aquifer system. Msc thesis at Div. of Land and Water Resources, KTH, Report series 1995:7.

JANSSON, K., 1996: Salt i grundvatten - metod för bedömning av saltvattenursprung. (Salt in groundwater - method for evaluation of origin). Swedish National Road Administration, report 1995:68.

KNUTSSON, G.& FAGERLIND, T., 1977: Grundvattentillgångar i Sverige (Groundwater resources in Sweden). SGU, Rapporter och Meddelanden, no 9.

KÖKERITZ, K., 1993: Ursprung hos salt grundvatten - exempel från Stockholms län. (Origin of salt groundwater - example from the county of Stockholm). MSc thesis at Div. of Land and Water Resources, KTH, Trita-Kut 93:3059.

LAURENT, S.,1982: Analysis of groundwater from deep boreholes in Kråkemåla, Sternö and Finnsjön, SKBF/KBS, Technical Report 82-23.

LINDELL A, 1987: Salt grundvatten i kustnära områden. Delrapport. En analys av läget i Stockholms län. (Salt groundwater in coastal areas, analysis from the county of Stockholm). Report, Stockholm county administration and Div. of Land and Water Resources, KTH, Stockholm.

LINDEWALD, H., 1985: Salt grundvatten i Sverige. (Salt groundwater in Sweden). SGU, Rapporter och Meddelanden no 39, Uppsala.

LÖVBLAD, G., ANDERSEN, B., JOFFRE, S., PEDERSEN, U., HOVMAND, M. & REISSELL, A., 1992: Mapping deposition of sulphur, nitrogen and base cations in the Nordic countries. Swedish Environmental Research Institute (IVL), report B1055, 1992-06-25.

MAXE, L., KNUTSSON, G., OLOFSSON, B.& JACKS, G., 1994: Analys och utvärdering av saltets ursprung i Hammarby reservvattentäkt, Upplands Väsby kommun, Stockholm län. (Analysis of the origin of the salt at Hammarby waterworks). Report, Div of Land and Water Resources, KTH, Stockholm.

MÜLLERN, C-F.& ERIKSSON, L., 1981. Testing VLF-resistivity measurements in order to locate saline groundwater. Salt Water Intrusion Meeting (SWIM-81). Rapporter och meddelanden no 27, pp 91-100.

MÖLLER, Å., ENGQVIST, P.& ANDERSSON, J-E., 1981: Hydrogeologiska förhållanden inom Östergötlands sedimentära berggrund (Hydrogeological conditions within the sedimentary bedrock of Östergötland). SGU, ser Ag no 10.

NORDSTROM, K., 1983: Saline waters. in Allard, B., Larson, S.Å., Tullborg, A-L., Wikberg, P., 1983. Chemistry of deep groundwaters from granitic bedrock. SKBF/KBS Technical Report 83-59.

NORDSTROM, D. K., BALL, J., DONAHOE, R. & WHITTEMORE, D., 1989A: Groundwater chemistry and water-rock interactions at Stripa. Geochimica et Cosmochimica Acta, vol 53, s 1727-1740.

NORDSTROM, D. K., LINDBLOM, S., DONAHOE, R. & BARTON, C., 1989B: Fluid inclusions in the Stripa granite and their possible influence on the groundwater chemistry. Geochimica et Cosmochimica Acta, vol 53, s 1741-1755.

OLBERG, E.W., 1854: Om Torpa och Torps saltkällor (Saline springs at Torpa). Öfvers. af K.Vet.Akad. Förh., pp 81 and 219.

OLOFSSON B, 1990: Salt grundvatten. (Salt groundwater) Berg- & Dalbladet, no 2, p 10-19.

OLOFSSON, B., 1994: Salt groundwater in Sweden. *In*. Olofsson B (ed) Salt groundwater in the Nordic countries. Nordic Hydrological Programme (NHP), Report no 35, s 19-35.

POUSETTE, J. & MÖLLER, Å., 1972: Ölands hydrogeologi - en översikt (Hydrogeology of Öland). SGU, ser C no 670.

PUIGDOMÈNECH, I. & NORDSTROM, K., 1987: Geochemical interpretation of groundwaters from Finnsjön, Sweden. SKB Technical Report 87-15.

SMELLIE, J. & WIKBERG, P., 1989: Hydrochemical investigations at Finnsjön, Sweden. *In* Ahlbom, K., Smellie, J. (eds). Characterization of fracture zone 2, Finnsjön study-site. Swedish Nuclear Fuel and Waste Management Company (SKB), Technical Report no 89-19.

SUND, B. & BERGMAN, G., 1980: Saltvatteninträngning i bergborrade brunnar. Swedish Environmental Research Institute /IVL), Report no B584.

SVENONIUS, F., 1918: Om Mariebergsproblemet (About the Marieberg problem). The Geological Society of Sweden, GFF, vol 40, no 2, pp 92-98.

TILLY-LEANDER, L., 1994: Salt groundwater in Värmdö, county of Stockholm - a case study. *In*. Olofsson B (ed) Salt groundwater in the Nordic countries. Nordic Hydrological Programme (NHP), Report no 35, s 111-116

TULLSTROM, H., 1954: Hydrogeologiska förhållanden inom Slite köping på Gotland (Hydrogeological conditions at Slite, Gotland). SGU ser C no 538.

Multivariate mixing calculations used to trace modern Baltic Sea water intrusion at Äspö, Sweden

Marcus Laaksoharju and Christina Skårman
GeoPoint AB, Sollentunavägen 63, S-19140 SOLLENTUNA, Sweden

The Swedish Äspö Hard Rock Laboratory (HRL) is located under a small island off the Baltic coast approximately 350km south of Stockholm. The Äspö HRL was initiated by the Swedish Nuclear Fuel and Waste Management Company (SKB). Äspö is being investigated because it geologically represents a variety of typical granitic crystalline bedrock environments in Sweden designated as suitable host rocks for the final disposal of radioactive waste.

Many boreholes have been used to evaluate the geological, hydrogeological and hydrogeochemical character of the Äspö area. In order to establish the mixing portions in the groundwater a *Multivariate Mixing Model* was constructed (Laaksoharju et al. 1994). The model describes how large portions of a particular type of water are needed in order to explain the chemical composition of the observed water. The mixing processes are inherently very complex and include multi end-member mixing processes. A multivariate method called Principal Component Analysis (PCA) was therefore used. The strength of this approach is that all variables in a data matrix can be examined simultaneously. Greater resolution is possible and the character of the data in a general data matrix is therefore more easily identified than using univariate analysis, where only one variable is compared at a time. The major components Cl, Ca, Na, Mg, K, SO_4 HCO_3 and the isotopes ^{2}H, ^{18}O and ^{3}H were used in the Principal Component Analysis. It is important to note that both conservative and non-conservative elements were used. This is possible since conservative or non-conservative behaviour in one or several of the variables can be tracked by PCA.

The result of the analysis and the identified end-members are shown in Figure 1. The selected end-members represent extreme waters found in the Äspö area. The *Glacial* end-member has been determined as an old glacial water based on the stable isotope values which indicate cold climate recharge (^{18}O= -15.8 SMOW) (Smellie and Laaksoharju, 1992). *Deep Saline* water represents a brine type of water found at 1700m depth, *Baltic sea* water represents modern Baltic sea water. *Modified Baltic Sea* water represents Baltic sea water which has been modified by chemical process such as sulphate reduction. *Shallow* water represents relatively modern non saline groundwater.

The five identified end-members form a pentagon. The observations within the pentagon can by definition be described by the selected end-members. The co-ordinates for the observations are given by the first and second Principal Component respectively (Comp 1 and Comp 2 in Figure 1). The scales in Figure 1 are linear and the distance from any observation to the five end-members can be calculated by using simple trigonometric functions ie, the pentagon is used as a phase diagram. The distance is equivalent to the mixing ratios of any water observed in the system. The exact mixing portions of any groundwater sample can be calculated.

Infiltration of modern Baltic Sea during the construction of the underground laboratory has been modelled (Figure 1) as an example of how the method can be

Infiltration of modern Baltic Sea during the construction of the underground laboratory has been modelled (Figure 1) as an example of how the method can be applied. By using the described technique the mixing portions for all the observations at Äspö can be calculated and the feasible end-members can be identified (Laaksoharju and Skårman, 1995).

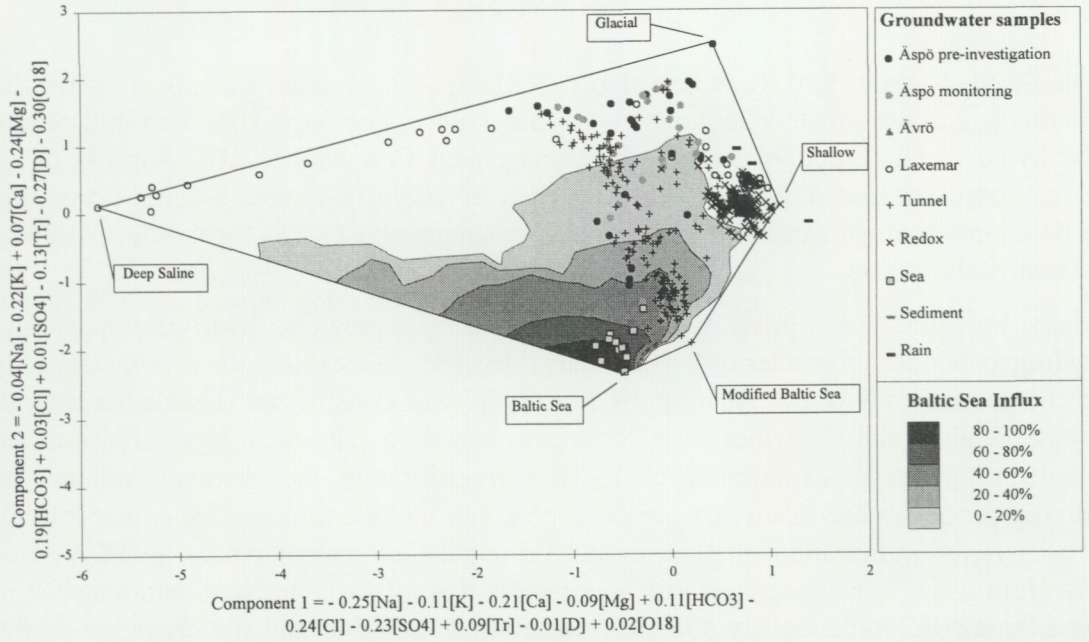


***Figure 1**: Principal Component plot used for identifying end-members in the Äspö area and to calculate the influx in portions of 100-80%, 80-60%, 60-40%, 40-20% and 20-0% of modern Baltic Sea water. The position of the selected end-members are shown in the figure. Between the five end-members lines are drawn so that a pentagon is formed. The observations within the pentagon can by definition be described by the selected end-members. The pentagon is used as a phase diagram. The mixing ratios of any observed water can be calculated.*

Acknowledgements

This study was supported by Swedish Nuclear Fuel and Waste Management Company (SKB). The support and many suggestions from Dr. Peter Wikberg, SKB are especially acknowledged.

References

Smellie, J. and Laaksoharju, M., (1992). The Äspö hard rock laboratory: final evaluation of the hydrogeochemical pre investigations in relation to existing geologic and hydraulic conditions, Swedish Nuclear Fuel and Waste Management Company (SKB) publication TR 92-31. SKB, PO Box 5864, S-102 48 Stockholm, Sweden.

Laaksoharju, M., Smellie, J., Nilsson, A-C. and Skårman, C., (1994). The Laxemar deep borehole KLX02: Groundwater sampling and chemical characterisation. Swedish Nuclear Fuel and Waste Management Company (SKB) publication TR 95-05. SKB, PO Box 5864, S-102 48 Stockholm, Sweden.

Laaksoharju M, Skårman C, (1995). Groundwater sampling and chemical characterisation of the HRL tunnel at Äspö, Sweden. SKB-Progress report (in progress).

Use of Principal Component Analysis in hydro-geochemical characterization of an aquifer along the Mediterranean coast of Turkey

Nurkan Karahanoglu

Department of Geological Engineering, Middle East Technical University
06 531, Ankara, TURKEY

This paper presents a research about statistical evaluation of water quality samples by using the method of Principal Component Analysis. Chemical analyses of the water samples collected from an aquifer in the Mediterranean coast of Turkey were used as input data in which the major anions and cations, pH, Electrical conductivity, Transmissivity and Lithology were considered as variables. Statistical analyses were aimed at investigating interrelations and similarities between the variables, studying hydro-geochemistry of the groundwater system and determining the most effective components in the multivariate data set. Additionally the effect of time was searched by using reduced data sets in order to lead the analysis towards saltwater intrusion in the region. As a result of the analyses correlation coefficients were calculated for different data sets and their transient variations were evaluated. Principal component analysis delineated two groups of water samples as those coming from saltwater and freshwater origins.

Introduction

Starting with Ghyben-Herzberg in late 1800s, the problem of seawater intrusion has been introduced into the literature and in recent years it became one of the major problems in coastal aquifers. Due to gentle behavior of the dynamic equilibrium between freshwater and saltwater these aquifers are under continual danger of seawater contamination. Increased water demand in resort regions triggers movement of seawater to intrude into aquifers and change freshwater quality. This requires optimal management of coastal aquifers which are to be guided by quality monitoring.

Hydrogeochemical investigations of coastal aquifers could yield valuable information about relations between seawater and freshwater in such regions. Careful analysis of the physical and chemical quality parameters and their spatial and temporal distributions is quite helpful in defining the level of seawater contamination. Analysis of water samples, collected from coastal aquifers could well be used to detect probable trends of deteriorating water quality. This brings interpretation of a multivariate dataset which includes distribution of the physical and chemical variables for multitude number of water samples. Classical methods, like Scholler graphs and Piper diagrams, were successfully used in interpreting quality datasets, however, such methods can no longer be applicable for analyzing multivariate datasets where both the physical and chemical variables are included for large numbers of water samples. Multivariate statistical methods, take their roles in performing such tasks and they are found to be very powerful.

Several studies can be mentioned where statistical methods have been extensively applied to analyze multivariate data sets in different fields of the earth sciences (Davis, 1986; Rock, 1988; Helsel and Hirsch, 1992, Brown, 1993; Istok et.al., 1993; Wen and Kung, 1993). In recent years several statistical applications have been noted as focused on the topics related with the environmental problems (Geiss et.al., 1991; Melloul and Collin, 1992; Xhoffer et.al., 1991; Sodestrom, 1992; Pohlmann, 1993; Zitko, 1994; Melloul, 1995).

Xhoffer and others (1991) accomplished a principal component analysis to study characterization of individual aerosol particles over the North Sea and the English channel. The samples were clustered by using the principal component analysis as, the marine-derived samples, CaSO4-rich samples and those related to high silica and sulphur abundance. Geiss and others (1991) performed a multivariate correlation analysis and compared time series of heavy metal concentrations at two points of a river.

They concluded that correlation analysis proved to be a useful tool for investigating internal and external connections of time and distance series. Melloul and Collin (1992) pointed the vital and complementary role of the Principal Component analysis in evaluating multivariate data sets of groundwater samples, especially in identification of relevant groups of water and the factors that bring about a change in their quality. They conducted a hydrogeochemical research in water quality factor identification and used the principal components to identify relevant water chemistry types and the factors that cause a change in water quality in the Dan metropolitan region of the coastal plain aquifer of Israel. Brown (1993) applied correlation, principal component and multiple regression analyses to laboratory chemical and petrographic data to assess the usefulness of these techniques in evaluating physical and hydraulic properties of carbonate rock aquifers in Pennsylvania. Zitko (1994) proved the usefulness of the principal component analysis in the examination of enzyme induction and contaminants, heavy metals in sediments and mussels, metals in sediments and corals, survey of organochlorine compounds in fish. He concluded that principal component analysis could provide a deeper insight into the structure of the data and help reaching conclusions those were not immediately obvious. Melloul (1995) developed a methodology to investigate the Nubian sandstone aquifer beneath the Sinai Peninsula (in Egypt) and the Negev Desert (in Israel) by using the principal component analysis. He emphasized that the method successfully utilized the principal component analysis in the description of a complex flow system, in the delineation of optimal operational zones, and in the characterization of groundwater flow paths.

In view of these studies, hydro-geochemistry of a coastal aquifer in Turkey has been investigated by using the principal component analysis in order to define saltwater and freshwater interactions in the region. Erzin groundwater basin is located along the Mediterranean coast (Fig. 1) and supplies freshwater to continuously increasing water demand of the irrigation. In respect to its potential the aquifer needs to be thoroughly investigated to clarify recent indications of water quality deterioration. For this purpose chemical analysis of the water samples, collected from three springs and 161 water wells during different observation periods, and some physical parameters of the aquifer were studied (Karahanoglu et al., 1995). A multivariate data set was formed with variables of major anion and cation concentrations, pH and electrical conductivity (EC) values, transmissivity and type of screened lithologies. In this form the data matrix collects spatial and temporal variations related to unknown number of combinations between physical and chemical variables, which are responsible from this realization. It would be almost impossible to interpret such a data set and uncover hidden interrelations between so many variables without using statistical techniques.

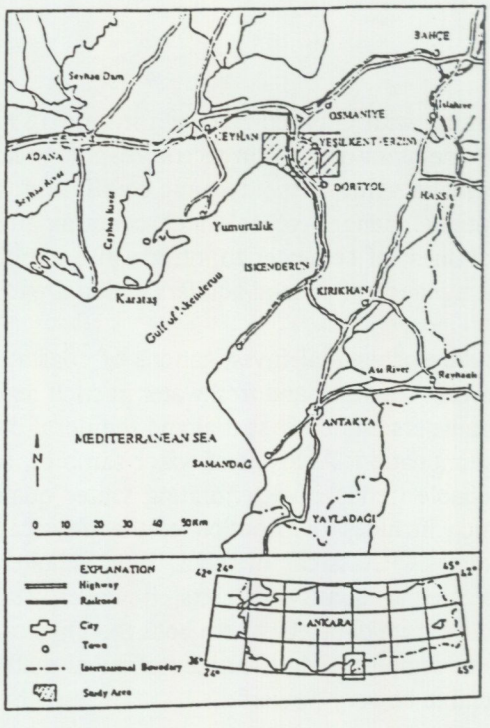


Fig. 1. Location map of the study area.

Hydrogeological setting of the study area

Owing to its great potential, Erzin aquifer has been extensively studied for the geological and hydrogeological aspects (Türkmen et.al., 1974; Doyuran, 1982). The basin was simulated for the flow mechanism (Karahanoglu et al., 1986) and a numerical model was proposed for the coupled mechanism of fluid flow and saltwater intrusion (Emekli et al., 1996).

The Erzin groundwater basin is formed of Tertiary and Quaternary deposits and stores water under unconfined conditions. Geological map of the area shows that impervious ophiolitic series form the basement and boundary along the eastern part. The northern boundary is occupied by well-cemented and well-compacted Miocene sandstone, conglomerate and marl alternations. These impervious units are unconformably covered by a thick conglomerate deposit with highly fractured and jointed nature. The estimated thickness of the conglomerate is about 1500 m and it forms the major aquifer where the hydraulic conductivities range between 10-50 m/day. In the northern and northwestern part of the Erzin plain olivine basalts are located and they show excellent storage and conduit properties. These basalts form the most productive aquifer in the basin and the hydraulic conductivities range between 50-150 m/day. The conglomerate and the basalt aquifers are estimated to be hydraulically connected (Doyuran, 1982) and these units supply water by means of 161 wells and three springs throughout the basin (Fig. 2).

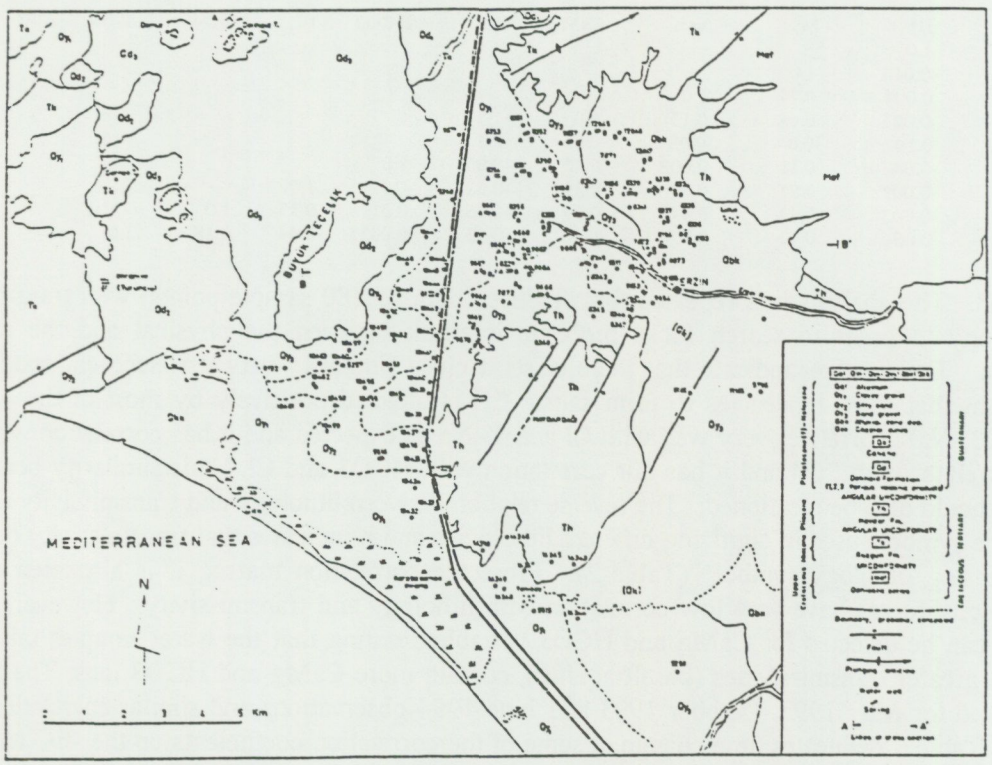


Fig. 2. Geological Map of the Erzin Plain Groundwater Basin and the water wells.

Method of Study

Samples have been collected from the water wells and springs and they have been analyzed for the major anions and cations as well as their pH and EC (electrical conductivity) values. Transmissivity coefficients and type of the screened lithologies were also collected for some of the wells. In this form a data matrix was formed by using chemical analysis of the samples and some of the physical parameters of the Erzin groundwater basin. This yields a multivariate data set with 316 number of observations for the variables of pH, EC, NaK, CaMg, CO3, HCO3, Cl, SO4, % Na, Trans (Transmissivity) and Lith (Lithology). In this form, the raw data includes all kind of information related to spatial and temporal variations which might result from unknown number of combinations between the variables. In order to interpret such a complex data set Principal Component Analysis was applied in order to uncover hidden interrelations between so many variables.

In the analysis the data matrix is manipulated to evaluate cumulative variances, the eigenvalues and the eigenvectors for extracting the principal components. These principal components (new set of variables) are formed by linear combination of the original variables according to their loadings on the cumulative variance. In the procedure they are determined by using the correlation matrices, and the coefficients of each principal component are evaluated accordingly. Hence the method aims at determining minimum number of such components that would account for most of the variance in the raw data (Davis, 1986).

Analyses begun with calculating the correlation coefficients in order to detect similarities between the variables. For this purpose the data set was separated into subgroups and the coefficients were calculated accordingly. Table 1 shows the correlations between the variables compiled for 1964-68

Table 1. Correlation coefficients for 1964-1968 data set.

	pH	EC	NaK	CaMg	CO3	HCO3	Cl	SO4	%Na
pH	1.0								
EC	-0.016	1.0							
NaK	0.004	0.77	1.0						
CaMg	-0.025	0.65	0.13	1.0					
CO3	0.14	-0.04	-0.08	0.03	1.0				
HCO3	-0.04	0.31	0.008	0.42	-0.05	1.0			
Cl	-0.002	0.82	0.79	0.39	-0.03	-0.19	1.0		
SO4	-0.003	0.60	0.44	0.50	-0.06	0.01	0.35	1.0	
%Na	0.06	0.40	0.77	-0.16	-0.12	0.0025	0.44	0.18	1.0

observation. The analysis was repeated for a reduced data set (80 sample points) with transmissivity and lithology in order to search for a probable interlink between the physical and the chemical parameters. These values indicate that there exists a close similarity between electrical conductance and the ions that show tendencies to form salts. EC is affected positively by most of the variables except CO3; NaK correlates very well with Cl and % Na as expected and it has correlation with SO4; CaMg correlates with SO4 and it has fair correlation with HCO3 and Cl. Fair similarity between Cl and SO4 should also be mentioned. The reverse relation between lithology and transmissivity is due to order of the symbols used in digitizing different lithologies and it indicates that transmissivity decreases with increasing lithology symbol (Table 2). From the correlation matrix, it is also seen that the chemical constituents have very low correlation with lithology and transmissivity. However, a weak similarity can be detected for CaMg and HCO3 variables, stating that the water samples taken from wells with greater transmissivities (basalt aquifer), contain more CaMg and HCO3 ions. The analysis was repeated for May 1993, October 1993 and June 1994 observations and similar correlations were obtained. Table 3 delineates time change of some of the correlation coefficients on the EC and NaK basis. It is interesting that on EC basis the correlation coefficients with NaK,

Table 2. Correlation coefficients for the selected samples with transmissivity and screened lithology.

	pH	EC	NaK	CaMg	HCO3	Cl	SO4	%Na	Trans	Lith
pH	1.0									
EC	-0.27	1.0								
NaK	-0.13	0.84	1.0							
CaMg	-0.31	0.71	0.24	1.0						
HCO3	-0.22	0.17	-0.16	0.48	1.0					
Cl	-0.18	0.89	0.89	0.47	-0.21	1.0				
SO4	-0.24	0.65	0.55	0.47	-0.09	0.48	1.0			
%Na	-0.05	0.51	0.80	-0.11	-0.08	0.54	0.32	1.0		
Trans	-0.05	0.18	0.008	0.29	0.33	0.06	0.04	-0.12	1.0	
Lith	0.02	-0.15	0.02	-0.28	-0.31	-0.06	0.08	0.17	-0.64	1.0

CaMg, Cl, and %Na increase, whereas the coefficients with HCO3 and SO4 decrease with time. This should point that the contribution of NaK and Cl ions (seawater constituents) to Electrical Conductivity (EC) of the water samples becomes more effective than that of HCO3 and SO4 ions (freshwater constituents). A similar trend is found for the coefficients computed on the NaK basis,

Table 3. Variation of correlation coefficients with time for different variable couples.

	NaK	CaMg	HCO3	Cl	SO4	%Na
EC						
1964-68	0.77	0.65	0.31	0.82	0.60	0.40
May 1993	0.71	0.92	0.19	0.82	0.18	0.52
Oct 1993	0.86	0.82	0.13	0.88	0.003	0.73
June 1994	0.89	0.83	-0.09	0.92	0.03	0.76
NaK						
1964-68		0.13	0.008	0.79	0.44	0.77
May 1993		0.38	-0.49	0.96	-0.31	0.96
Oct 1993		0.43	-0.26	0.99	-0.29	0.95
June 1994		-0.49	-0.51	0.99	-0.31	0.97

where the correlation coefficient with Cl increases to 0.99, however correlation with HCO3 and SO4 depict a decreasing trend from 1964-68 to June 1994. This could mean that due to seawater intrusion effect, the probability of NaK ion to form a compound with Cl becomes greater than the probability of forming NaK-HCO3 and NaK-SO4 compounds.

Principal Component Analysis

Principal component analysis formed two principal components for each data group by combining the original variables. Table 4 lists the principal components and the related contributions of the

Table 4. Principal component weights for different data sets.

Variable	1964-1968		May 1993		October 1993		June 1994		DATATL	
	PC-1	PC-2	PC-1	PC-2	PC-1	PC-2	PC-1	PC-2	PC-1	PC-2
EC	0.510	0.165	0.408	0.381	0.461	0.265	0.433	0.289	0.493	0.096
NaK	0.471	-0.301	0.498	-0.088	0.488	-0.101	0.480	-0.009	0.464	-0.183
CaMg	0.289	0.591	0.264	0.546	0.281	0.588	0.246	0.559	0.295	0.395
HCO3	-0.077	0.504	-0.190	0.533	-0.074	0.574	-0.237	0.539	0.013	0.463
Cl	0.457	-0.167	0.500	0.016	0.490	-0.078	0.479	0.040	0.462	-0.083
SO4	0.348	0.195	-0.134	0.466	-0.119	0.430	-0.155	0.538	0.358	0.038
%Na	0.312	-0.461	0.459	-0.219	0.459	-0.232	0.460	-0.144	0.322	-0.297
Lith									-0.051	-0.498
Trans									0.075	0.492

variables. Study of the table shows that the principal components (PC-1 and PC-2) are formed by different contributions. For 1964-68 data group, EC, NaK and Cl have more contributions to the first principal component (PC-1) whereas the second component (PC-2) is heavily weighted by CaMg and HCO3 ions. Transmissivity and lithology have no contribution to the first principal component (PC-1), whereas the transmissivity is found to have the maximum weight on the second principal component (PC-2) in addition to CaMg and HCO3 ions. May 1993, October 1993 and June 1994 data sets yield similar results with slight deviations. In general the first principal component (PC-1), is majorly contributed by EC, NaK, Cl and Na% and CaMg, HCO3 and SO4 repeatedly form the majority in the second principal component (PC-2).

Overall evaluation of the components delineates that some of the variables are interrelated. The first principal component (PC-1) collects the variables which are either seawater constituents (NaK, Cl, Na%) or those affected by seawater (EC); the second component (PC-2) shows that major contributions come from land-derived ions (CaMg, HCO3, SO4).

Fig. 3 is constructed to show scatter of the 1964-68 group data with respect to the first (PC-1) and the second principal components (PC-2). On the same graph the original variables are represented by lines, which reflect how each variable contributes to the components. Analysis of the variable lines indicates that there exist close relations between CaMg - HCO3 and NaK - Cl couples. SO4 and EC lie in between these implying that the electrical conductivity is affected by both of these couples. This plot supports to verify the above classification of the water samples, as two distinctive groups of CaMg and HCO3, and NaK and Cl variables are easily identified.

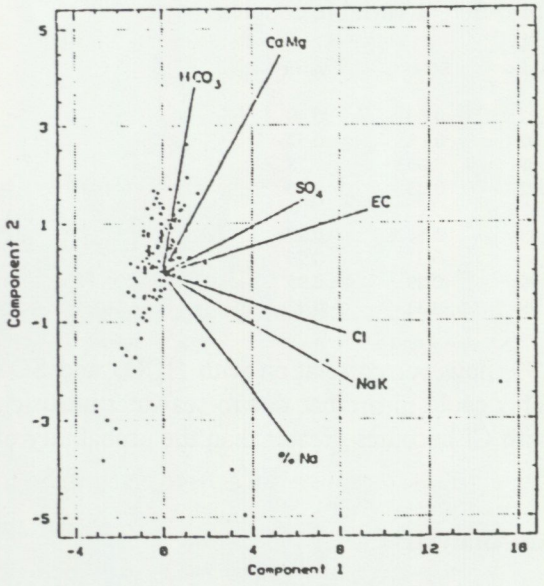


Fig. 3. Scatter of 1964-68 group data.

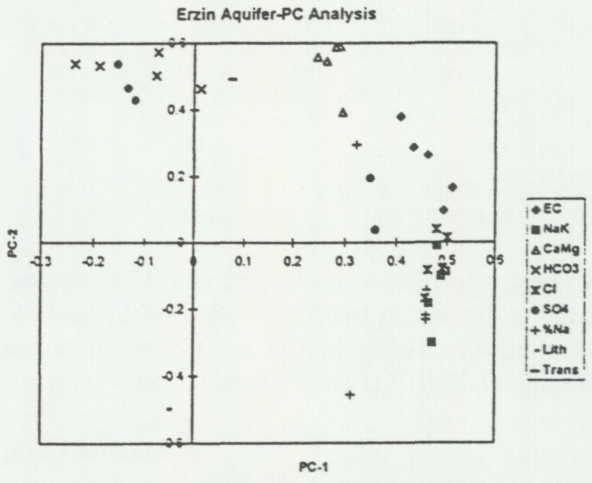


Fig. 4. Principal component weights.

A composite figure is formed to compare different data sets in terms of their component weights (Fig. 4). Principal component weights of the individual variables are grouped in this figure and sub-regions are defined. NaK, Cl, and CaMg variables define smaller areas due to their smaller variances in time. SO4 was dominantly controlled by the first principal component (PC-1) in 1964-68 group, whereas for the last three data groups it becomes majorly controlled by the second principal component (PC-2). Minor contribution of the first principal component on HCO3 variable loses its effect for the last three data groups. This simply means that HCO3 and SO4 ions become majorly controlled by the second principal component in recent observations. It is also observed that NaK - Cl and CaMg - HCO3 groups are located at the two extreme ends with EC sub-region in between. It is interesting that similar behavior is detected in the correlation analysis that verifies these relations.

Contributions of the lithology and transmissivity on the principal components were investigated by constructing a scatterplot with reduced data set (Fig. 5). It is found that majority of the sampling wells collect around the second component (PC-2) axis, and a few wells deviate from the major group. On the same graph the data points were replaced by corresponding lithologies and two different sub-groups were identified. These groups are formed by the wells tapping basalt formations and by those wells, which tap from conglomerate type lithologies. Wells screened to basalt have greater contributions to the second principal component since the basalt has higher coefficients of transmissivities (Fig. 3). The negative contribution of conglomerate-tapping wells to the second principal component is due to negative correlation between Lith and Trans variables (Table 4).

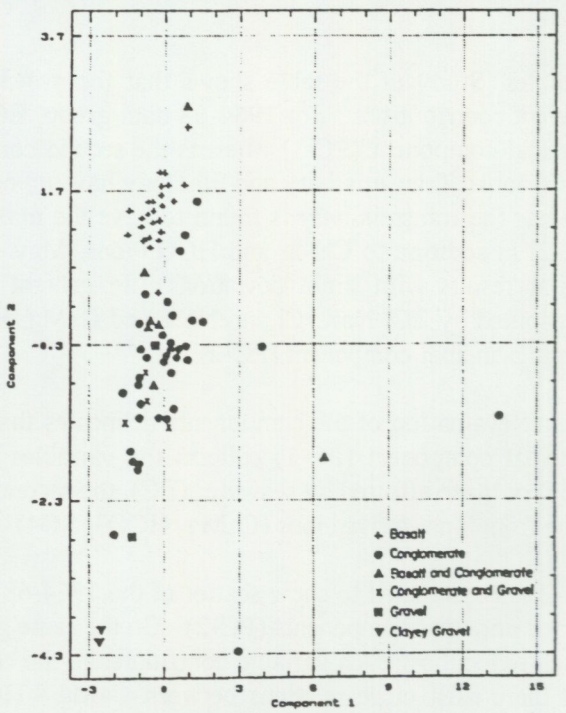


Fig. 5. Scatterplot for reduced dataset.

Conclusions

In this research the Erzin plain groundwater basin (Turkey) was extensively studied to investigate hydrogeochemistry of the aquifer and clarify interrelation between seawater and freshwater in the region. The research was accomplished by applying the correlation and the principal component analysis in order to identify seawater intrusion problem in the area. As a result of the investigation the following conclusions were drawn:

- Correlation analysis showed that some of the major ions have significant correlation and these correlations follow temporal change in the Erzin aquifer. This change is quite clear for NaK, Cl, HCO3 and SO4 ions. Correlation of the first two ions with the electrical conductance increases with time whereas the correlation of the next two follows a decreasing trend. This explains that NaK and Cl ions take the majority in controlling the electrical conductance of the water samples. CaMg is also determined as effective for controlling the electrical conductivity however its time change is not so clear. Among the variables pH and CO3 were determined to have random behavior and they have no correlation with the other variables. Screened lithologies and the transmissivities were determined to be strongly correlating. On the other hand the weak correlation of CaMg and HCO3 ions with lithology and transmissivity, indicated that these ions are contributed from the aquifer formation.

- Principal component analysis determined that two new variables (principal components) could explain variations in the water samples as effectively as the entire data set. These principal components were formed from the combination of EC, NaK, Cl, % Na for the first one and CaMg, HCO3 and SO4 for the second. This simply groups the original variables as a combination affected by seawater and a combination of freshwater constituents. The analysis also yielded that lithology and transmissivity had no contribution to the first principal component, whereas transmissivity had the greatest contribution to the second principal component. Principal component analysis clearly categorized two major clusters of water samples depending on the type of lithology. In the first cluster water samples from the basalt formation are collected, and in the second water samples from conglomerate type lithologies are gathered.

- Application of the above methods proved that great complexity of the water samples of the Erzin aquifer could be clarified by using multivariate data interpretation techniques. This research defined and extracted hidden interrelations between the original variables, which had important role on the present geochemical state of the aquifer. It is mathematically found that there exists an interrelation between seawater and freshwater in the region, and this is an early indication that the basin is being contaminated by seawater.

REFERENCES

BROWN, C.E., 1993: Use of principal components, correlation and stepwise multiple regression analyses to investigate selected physical and hydraulic properties of carbonate-rock aquifers. -J. Hydrology, 147, pp. 169-195.

DAVIS, J.C., 1986 : Statistics and data analysis in Geology. - 2nd edition, John Wiley and Sons, 646 pp. NewYork.

DOYURAN, V., 1982: Geological and hydrogeological features of Erzin and Dörtyol plains. - Bull. Geological Society of Turkey, 25, pp.151-160.

EMEKLİ, N., KARAHANOGLU, N., YAZICIGİL, H., DOYURAN, V., 1996: Numerical simulation of saltwater intrusion in Erzin groundwater basin, Turkey. - Water Environment Research, (in press).

GEISS, S., EINAX, J., DAMZER, K., 1991: Multivariate analysis and its application in environmental analysis. - Analytica Chimica Acta, 242, 1, pp.5-9.

HELSEL, D.R., & HIRSCH, R.M., 1992: Statistical methods in water resources. - Elsevier, 522 pp. Amsterdam.

ISTOK, J.D., SMYTH, J.D., FLINT, A.L., 1993: Multivariate geostatistical analysis of groundwater contamination: A case history. - Ground Water, 31, 1, pp. 63-74.

KARAHANOGLU, N., DOYURAN, V., & SUVAGONDHA, F., 1986: Finite element model for the Erzin (Hatay) groundwater basin. - Bull. Geological Society of Turkey, 26, pp.53 -60.

KARAHANOGLU, N., YAZICIGİL, H., DOYURAN, V., EMEKLİ, N., HALLAJİ, K., 1995: Finite element simulation of saltwater-freshwater interface in coastal aquifers. - Project Final Report, YBAG-0074, The Scientific and Technical Research Council of Turkey (in Turkish). 288 pp. Ankara.

MELLOUL, A., 1995: Use of principal component analysis for studying deep aquifers with scarce data - Application to the Nubian sandstone aquifer, Egypt and Israel. - Hydrogeology Journal, 3, 2, pp. 19-39.

MELLOUL, A., & COLLIN, M., 1992: The principal component statistical method as a complementary approach to geochemical methods in water-quality factor identification-An application to the coastal plain aquifer of Israel. - J. Hydrology, 140, 1-4, pp. 49-73.

POHLMANN, H., 1993: Geostatistical modeling of environmental data. - Catena, 20, 1-2, pp.191-198.

ROCK, N.M.S., 1988: Numerical geology; in Lecture notes in Earth Sciences. - Battacharji, S., Friedman, G.M., Nuegebouer, H.J., and Seilacher, A., (eds), Springer Verlag,, 427 pp. Heidelberg.

SODERSTROM, M., 1992: Geostatistical modeling of salinity as a basis for irrigation management and crop selection- A case study in central Tunisia. - Environmental Geology and Water Sciences, 20, 2, pp.85-92.

TÜRKMEN, G., ERTÜRK, A., & TÜRKMAN, M., 1974: Dörtyol-Erzin plain hydrogeological investigation report. - Turkish Hydraulics Works, Ankara, Turkey (in Turkish), 76 pp. Ankara.

WEN, X.H., & KUNG, C.S., 1993: Stochastic simulation of solute transport in heterogeneous formations: A comparison of parametric and nonparametric geostatistical approaches. - Ground Water, 31, 6, pp. 953-965.

XHOFFER, C., BERNARD, P.,VANGRIEKEN, R., & VANDERAUWERA, L., 1991: Chemical characterization and source apportionment of individual aerosol particles over the North Sea and the English Channel using multivariate techniques. - Environmental Science and Technology, 25, 8, pp.1470-1478.

ZITKO, V., 1994: PC analysis in the evaluation of environmental data. - Marine Pollution Bulletin, 28, 12, pp.718-722.

Isotope Applications in the Study of Processes and Dynamics of Groundwater Salinization

Y. Yurtsever
Department of Research and Isotopes
International Atomic Energy Agency (IAEA)
Wagramer strasse 5, P.O.Box: 100, A-1400 Vienna, Austria

Abstract

Naturally occurring stable isotopes of Oxygen and Hydrogen (^{18}O and ^{2}H) are often indicators of the origin (genesis) of groundwater, and they can be used effectively in identification of salinity sources and/or differentiation between various processes that may be involved in groundwater salinization. The stable isotopic composition of sea water is significantly different to that of freshwater resources and provides a conservative label for tracing of sea water mixing with groundwater. Furthermore, evolution of stable isotopic composition of groundwater due to different salinization processes (i.e mineral dissolution, leaching of salt formations, re-cycling of irrigation water, etc.) exhibit characteristic features as a means of studying salinization processes.

Environmental radioactive isotopes of ^{3}H and ^{14}C, with their known time-dependent input concentrations in groundwater systems, facilitate investigating the dynamics of the water salinization and estimating relevant time-parameters involved.

The paper summarizes basic concepts of natural isotope applications for the above purposes and provides summary results from isotope field investigations conducted by the IAEA in the West Asia region related to groundwater salinization.

Introduction

Methodologies based on the use of isotopes in a wide spectrum of hydrological problems encountered in water resources assessment, development and management activities are already an established scientific discipline recognized as "Isotope Hydrology".

During the last three decades, the International Atomic Energy Agency (IAEA) has been directly involved in efforts directed towards research and development of isotope techniques in water sciences, their actual field applications, and has acted as an international scale focal point for dissemination of information and promoting their wider scale use, within the framework of its activities related to peaceful nuclear applications.

Contributions of isotope methods in water resources can be grouped into the following general categories:

- **Determination of physical parameters** related to flow, its dynamics and structure of the hydrological system,

- **Process Tracing** - delineation of processes involved in circulation of water and mass transport of dissolved constituents,

- **Identification of origin (genesis)** of water,

- **Component Tracing** - determination of pathways and mixing ratios of component flows,

- **Study of "Time-scale"** of hydrological events.

Isotopes that are naturally produced and incorporated into the hydrological cycle, are referred to as "Environmental Isotopes". Temporal and/or spatial variations of concentration of these isotopes in the hydrological cycle cannot be controlled and they are governed by natural processes.

Natural isotopes commonly employed for hydrological applications are the heavy isotopes of the elements oxygen (^{18}O); hydrogen (^{2}H - deuterium, ^{3}H - tritium); and carbon (^{13}C, ^{14}C -radiocarbon). Of these, ^{18}O, ^{2}H and ^{13}C are stable isotopes; whereas ^{3}H and ^{14}C are radioactive, with half-life values of 12.43 and 5730 years, respectively [1]. Spatial and/or temporal variations of stable isotopes in hydrological systems are the result of isotope fractionation that accompanies physical, chemical and biological processes taking place in nature. Variations of ^{18}O and ^{2}H are mainly governed by isotopic fractionation during evaporation and condensation processes, so that water molecules with different isotopic species are preferentially removed from one phase to another due to differences in their partial vapor pressures. Consequently, freshwater exhibits stable isotope content governed by the history of its origin and processes during its formation [2]. The isotopic changes thus induced, are a conservative property of the water. Radioactive isotopes of ^{3}H (tritium) and ^{14}C (radiocarbon), with their known input concentrations in the hydrological cycle (both natural and anthropogenic origin) also provide a label for different water bodies. The unique radioactive decay property of these isotopes, particularly of radiocarbon with a steady-state input concentration, also facilitate time-domain estimation to be made of the physical parameters related to circulation dynamics of water in hydrological systems, and particularly in groundwater.

Specific types of information that can be obtained from applications of natural isotopes in groundwater systems are:

- system boundaries, hydraulic discontinuities and stratification,
- origin (genesis) of water and hydraulic interconnections between surface and groundwater or between different aquifer units,
- process and rate of replenishment of groundwater,
- source and process of groundwater salinization and its dynamics,
- travel times involved in groundwater flow, covering a time scale of up to 40 000 years,
- parameters related to mass transport characteristics.

Isotopic composition of oceans are rather uniform, and they exhibit slightly enriched concentration of stable isotopes (^{18}O and ^{2}H) as a result of surface evaporation which preferentially removes heavier isotopic species into the vapor phase. Freshwater derived from precipitation will always have lower stable isotopic composition than that of sea water. The tritium content of sea water is in the range of 10-20 Tritium Units (TU) in the northern hemisphere and around 5 TU in the southern

hemisphere. (1 TU corresponds to a concentration of one tritium atom per 10^{18} atoms of Hydrogen). Average radiocarbon (^{14}C) concentration of ocean water was about 85 pmc (percent modern carbon) prior to the thermonuclear period (1953-1963) and about 95 pmc at the ocean surface. (radiocarbon concentration is expressed as percent of pre-industrial radiocarbon concentration of the atmospheric CO_2 defined as 100 %). Groundwater concentration of both these isotopes, however, may be much higher or lower than the sea water concentration, governed by the distribution of travel times in the system. Most of the paleaowaters encountered in regional coastal aquifer systems, and particularly deep confined aquifers in arid and semi-arid regions, will not contain any tritium and will exhibit rather lower concentrations of radiocarbon.

Isotope applications in groundwater salinization

Temporal and spatial variations of the above cited natural isotopes and the significant difference often encountered between the isotopic concentration of sea water and groundwater, together with characteristic isotopic evolution patterns associated with different salinization processes provide an effective tracing tool for investigating water salinization sources, processes and dynamics. Basic characteristics related to evolution of stable isotopic concentrations for sea water-freshwater mixing and other salinization processes are schematically shown in Fig.-1 as ^{18}O and ^{2}H relationship, which forms the basis for stable isotope applications for this purpose.

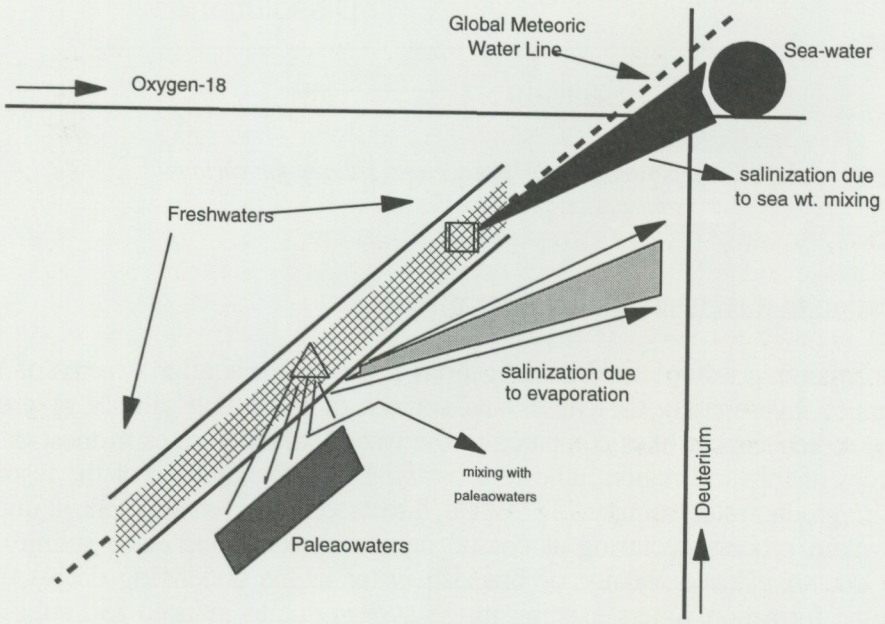


Figure-1. Evolution of stable isotopic composition of water for different water salinization processes

In studies dealing with water salinization, it is often more appropriate to consider both the isotopic and chemical evolution. Chloride ion concentration is often used as indicator of salinity, as it is one of the most conservative tracer in this regard. Such an approach will provide the basis for distinction to be made of different salinization processes. Typical relationships between stable isotope composition and salinity for different salinization processes are shown in Fig.-2. In the case of

salinity increase due to mineralization resulting from water-rock interactions (dissolution) or leaching of salt formations, stable isotope content of the water is not affected while the salinity of water increases.

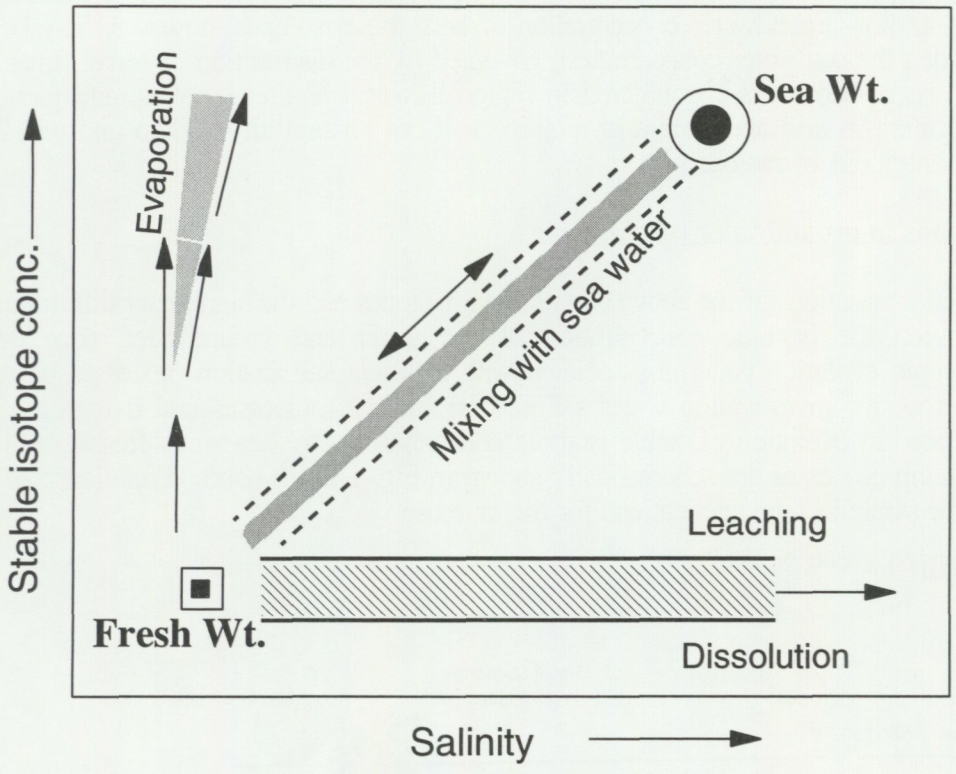


Figure-2. Relationship between stable isotope and salinity for various salinization processes

Example of application to a regional aquifer system

IAEA has been implementing isotope field investigations in the major aquifer systems of West Asia region with the aim of investigating the causes and sources of increasing salinity of groundwater. Existing data on the replenishment rates compared to the water extraction rates in most of the major groundwater resources of this arid region indicate substantial over-exploitation of the resources with resulting increase in groundwater salinity [3]. While direct sea-water encroachment due to over-exploitation is the main process occurring at coastal aquifer systems, increased salinity in inland aquifers should be due to induced leakage of brackish water in the underlying deeper aquifers or displacement of saline formation waters existing in the system due to induced hydraulic conditions through exploitation. Main geological features of the aquifer systems in the West Asia region are shown in Fig.-3 [4], and the range of salinity observed in the aquifers being extensively exploited are given in Table-1 [3].

Long-term mean (weighted by amount) value of the stable isotopic composition of precipitation from selected meteorological stations in the region [5] as an indicator of the expected isotope composition of groundwater replenished under present climatic conditions together with the stable isotopic concentration of sea water in Mediterranean Sea and Persian Gulf are given in the ^{18}O-^{2}H plot of Fig.-4. Since the expected isotope content of groundwaters in the region is significantly different than that of the sea water (Fig.-4), survey of isotope content in the aquifer systems would enable the

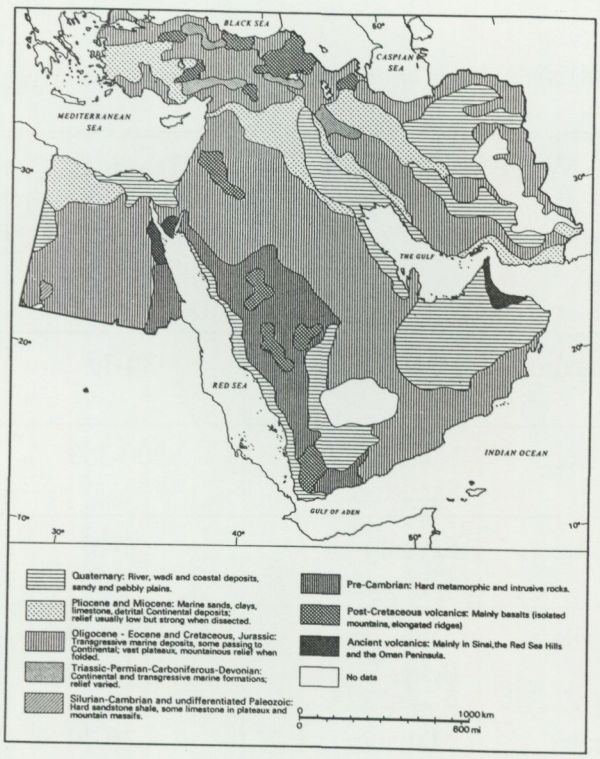


Figure-3. Geological settings of main aquifer systems in West Asia

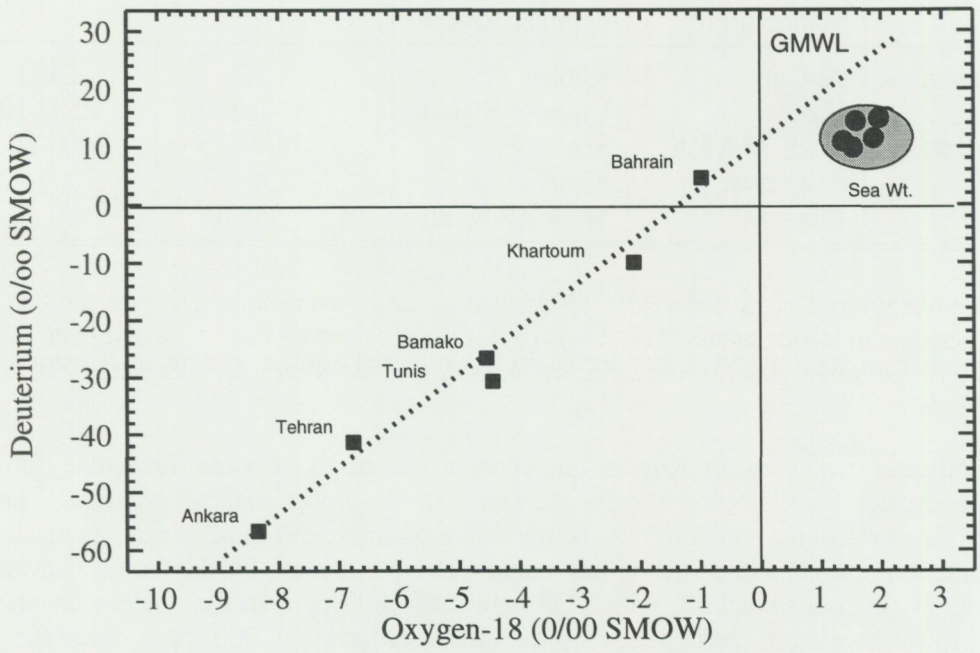


Figure-4. Long-term mean values of isotopic composition of precipitation in the region and isotope concentration of Mediterranean sea and Persian Gulf

Table-1 *Present salinity levels in major aquifers in the region*

COUNTRY	Brackish Water Location	Aquifers	Depth to Aquifers from ground (m)	Total Dissolved Solid (TDS-ppm)
Bahrain	Main Island of Bahrain	Khober	30-39	2200-8400
Egypt	Bahr El Baqar Sinai	Nubian Sandstone	200-300	1000-7000
Lebanon	Coastal regions	Recent Alluvium	5-10	1000-3000
Jordan	Jordan valley Azraq W.Dhuleil Wadi Araba	Alluvium Belqa-B2 Basalt Alluvium	0-100 10-50 10-60 30-70	> 5000
Kuwait	Soleibeyah Shagayah Wafra Abdali	Kuwait Gr. Khobar Umm Er Rhadu.	30-100	2800-5300
Qatar	Northern prov. Southern Prov.	Rusait Umm er Rhadu.	20-80	2000-2500
Saudi Arabia	Al-Qatif Hufuf Wadi Al-Mish Al-Quawayah Rus-south	Khobar Umm er Rhadu. Saq Khuff Wadi Alluvium	130 240-350 170-325 90-170 40-70	2450 2500-10 000 2000-10 000 2000-57 000

study of the sources/causes of increased salinity.

Data obtained from such a survey conducted in the regional aquifer system in Kuwait is presented as an example.

Main groundwater resources in Kuwait are encountered in the Eocene limestone formation of Dammam formation overlain by Mio-Pleistocene Kuwait group shallow aquifers. Three distinct aquifer units separated by aquitards are being exploited since 1960, at steady increasing rate and present extraction rate is around 170 million cubic meter per annum. Quality of groundwater in these aquifer units is generally brackish, with TDS values of 3000 ppm in the south west and gradually increasing towards eastern part, reaching to values around 50 000 ppm near the coast [6]. Groundwater salinity variations in the lower Dammam aquifer is shown in Fig.-5, and the general east-west hydrogeological cross-section is given in Fig.-6. Isotope sampling of wells tapping different aquifer units were carried out to study the genesis of saline waters and their hydraulic interconnections as the possible cause of increasing salinity in the shallow Kuwait group aquifer. The location of sampled wells are shown in Fig.-6.

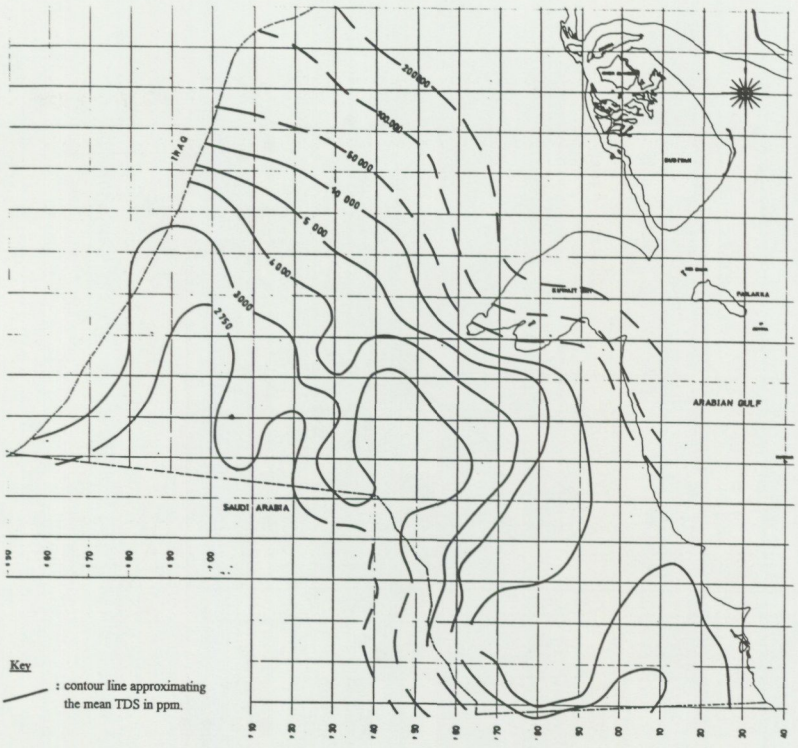


Figure-5. Salinity variations in Dammam aquifer in Kuwait

Results of stable isotope analyses are shown as 18O-2H plot of Fig.-7, where the isotope content of the Dammam group in Saudi Arabia [7] providing main lateral recharge to the aquifers in Kuwait is also shown. Under present climatic conditions, direct recharge to the upper aquifer from precipitation is minimal, if any. The line representing the Local Meteoric Water line on Fig.-6 is derived from the long-term isotope data available on monthly precipitation at Bahrain which has a slope of eight and deuterium excess value (intercept) of +14.6 [5].

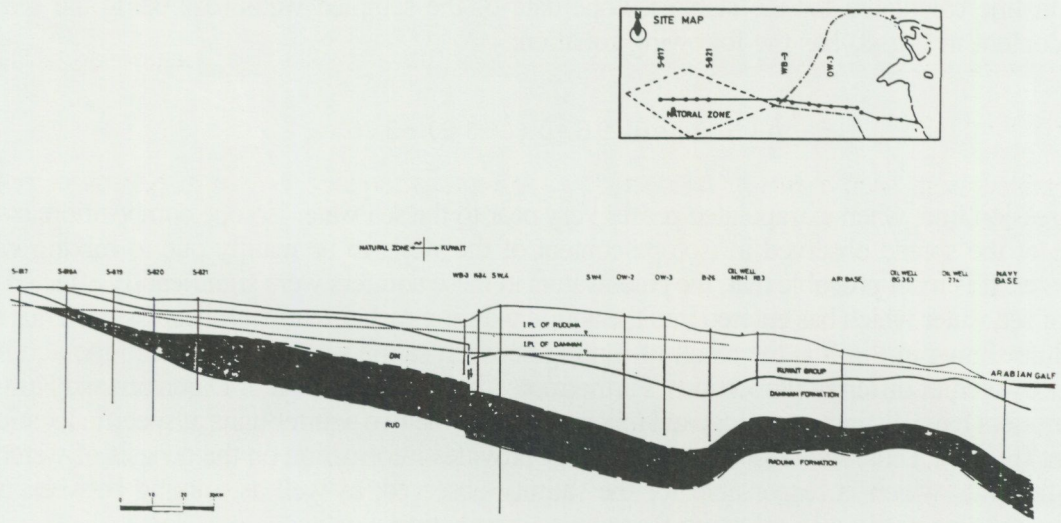


Figure-6. East-West hydrogeological cross-section of the aquifer systems

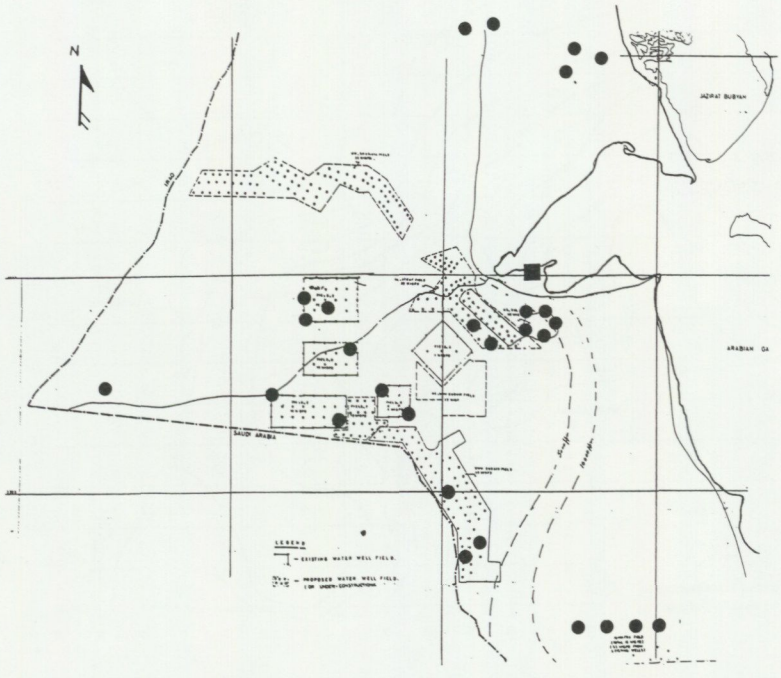


Figure-7. Location of sampled wells in the study area

Stable isotope data of both Dammam and Kuwait Group aquifers (Fig.-8) exhibit characteristic features of paleaowaters, with lower deuterium excess values as compared to the isotope content expected for meteoric waters under present climatic conditions in the region. None of the sampled wells, except the shallow freshwaters in the northern part, contain tritium. Radiocarbon dating of selected wells indicate the waters to have an age in the range of 17000 to 27000 years. Stable isotope data given in Fig.-8, together with the results of radiocarbon dating is clear evidence of the groundwaters within both Dammam and Kuwait Group aquifers to have been replenished during earlier pluvial periods, with very limited replenishment at the present, if any. The least-square regression line calculated for the stable isotope data of the sampled wells (excluding the sea water isotope content in Fig.-8) has the following equation:

$$\delta(H\text{-}2) = 6.95 * \delta(O\text{-}18) - 3.6$$

This regression line, when extrapolated passes very near to the sea water isotope composition, as an evidence of the spread observed in isotope content of the wells to be mainly due to mixing with saline water. It is most probable that, the paleowaters in these aquifers were significantly effected by mixing of sea water which has entered into the aquifers during earlier marine transgression. Thus the mixing line shown in Fig-8 is the result of mixing between saline water intruded into the aquifers and groundwater, at different proportions. Furthermore, the isotope content of Dammam and Kuwait Group aquifers have distinct grouping, and mixing between the two aquifer units at specific locations is evident (Fig.-8). Thus, stable isotope data clearly provides information on the genesis of water in the aquifer units which is responsible for the salinity observed, as well as, mixing between two aquifer units to be partly also affecting the salinity distribution.

Salinity versus Oxygen-18 content of the sampled wells are shown in Fig.-9, where the above depicted mixing processes are also evident.

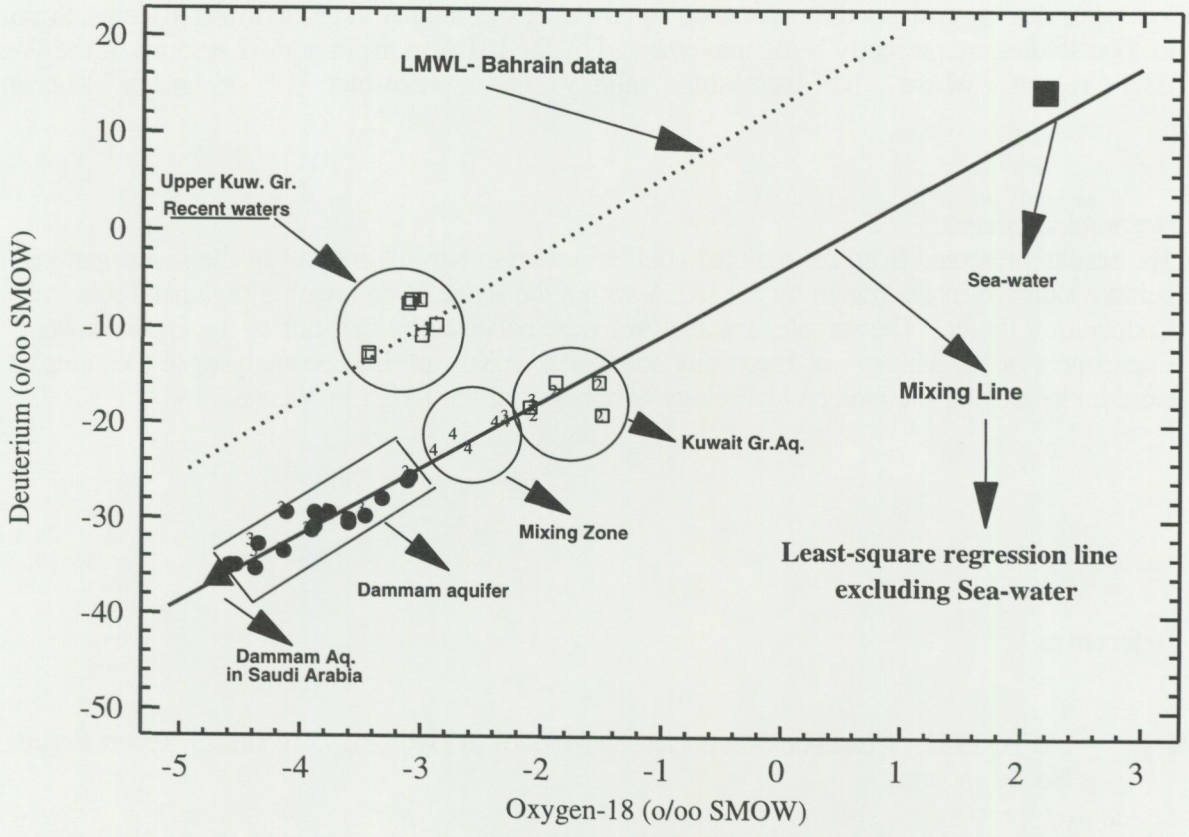


Figure-8. Stable isotope content of sampled wells

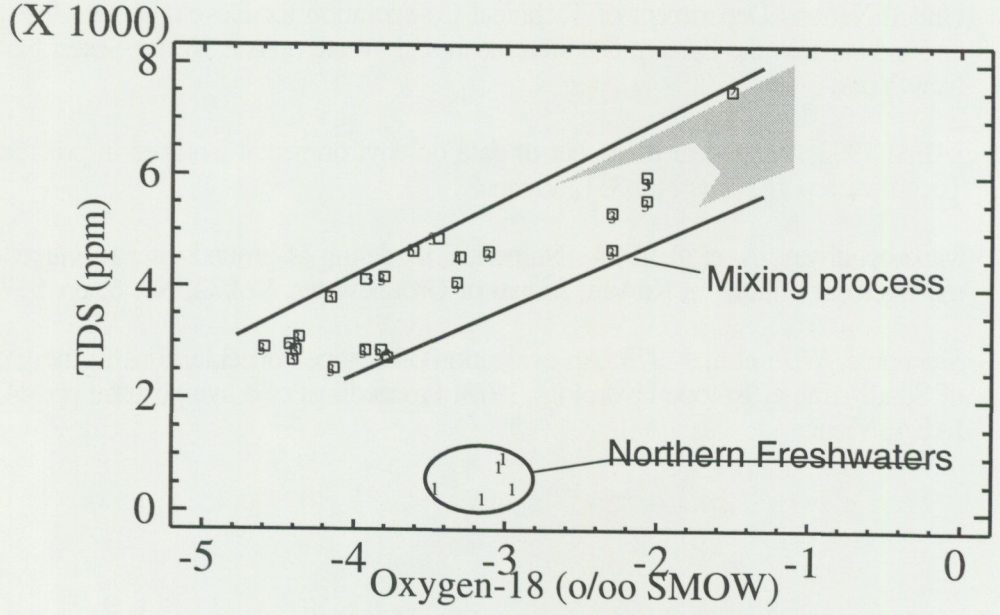


Figure-9. Salinity - Stable isotope relationship for the wells

The example presented above illustrates the capabilities and applications of isotope methodologies to studies dealing with sources, processes and dynamics of salinity in groundwater systems. Similar isotope studies are presently being implemented by the IAEA in major aquifer systems of the West Asia region, where the increasing salinity of groundwater is of major concern.

Acknowledgements:
The results presented from the regional aquifer system in Kuwait are part of the investigations being conducted in the region by the IAEA within the scope of an ongoing regional Technical Cooperation Project. The samples for analyses were collected by the staff of the Groundwater Department of the Ministry of Electricity and Water in Kuwait. Isotope analyses of the samples were undertaken at the Isotope Hydrology Laboratory of the IAEA in Vienna.

References

[1] IAEA, 1983 : Guidebook on nuclear techniques in Hydrology, Technical Report Serires No. 91, Vienna.

[2] IAEA, 1981 : Stable isotope hydrology - Deuterium and Oxygen-18 in the water cycle, Technical report series No. 210, Vienna.

[3] United Nations Economic and Social Commission for Western Asia, 1996 : Assessment of water quality in the ESCWA region, New York.

[4] United Nations Department of Technical Co-operation for Development, 1982 : Groundwater in the Eastern Mediterranean and Western Asia, Water Series No.9, New York.

[5] IAEA, 1992 : Statistical treatment of data on environmental isotopes in precipitation, Technical report series No. 331, Vienna.

[6] Mukhopadhyay, A. et al, 1994 : Numerical modeling of groundwater resources management options in Kuwait, Jounal of Groundwater, Vol.32, No. 6, pp. 917-928.

[7] Shampine, W.J., et al., 1978: An evaluation of isotope concentartions in the groundwater of Saudi Arabia, Isotope Hydrology 1978, Proceedings of a symposium, pp. 443-463, IAEA, Vienna.

GROUNDWATER FLOW CIRCUITS IN THE SALENTINE KARSTIC AQUIFER (APULIA, ITALY) AS DEFINED BY THE ANALYSIS OF RADON CONCENTRATIONS

T. Tadolini - M. Spizzico - D. Sciannamblo
Istituto di Geologia Applicata e Geotecnica, Politecnico di Bari, Italia

ABSTRACT

Surveys carried out in a large portion of the coastal carbonate aquifer in the Salentine Peninsula showed that ^{222}Rn is always present in the groundwater, though with a very broad range of concentrations. The observed concentrations were found to be correlated with the presence, within the aquifer, of "terra rossa" which, as already pointed out in previous works, contains fairly large amounts of ^{226}Ra.

Groundwater circulation and storage are determined by the state of fissuring and karstification of the carbonate aquifer and by the presence of more or less important amounts of "terra rossa". Big karst conduits and large cavities that contain this kind of residual material play an important role in the process of waters enrichment with radon. The research reported in this paper has showed that radon concentrations are instrumental in providing useful information on subterranean water circuits ending up in coastal springs, as well as on the aquifer's state of karstification.

1. FOREWORD

Investigations carried out to date in the Puglia region to check for the presence of natural radioactive isotopes in groundwaters circulating inside carbonate aquifers have shown that radon, a radioactive gas, is always present, though at widely differing concentration levels. In particular, it has been found that wherever groundwater is sampled, this gas always occurs at concentrations ranging from a few pCi/l to some thousand pCi/l.

In earlier studies such presence was correlated mainly to groundwater flow velocity (Cotecchia 1977). However, it has been shown lately that the observed variability of concentrations over time is caused by different processes originating from the hydrological cycle as well as from natural phenomena (Tadolini et *al.*,1994-a) and from water withdrawals while the "terra rossa", which is a residual product of carbonate rock weathering, actually represents the main source of ^{222}Rn; in Puglia, this kind of material is widely distributed both at the soil surface and in depth and contains significant amounts of radionuclides (Tadolini Spizzico,1996).

It is well known that the state of fissuring and karstism in carbonate formations is often attended by the presence of "terra rossa" that may affect two important hydrogeological parameters namely, permeability and water storage.

2. INVESTIGATIONS

Radon was employed as an indicator in this study which was aimed at seeking correlations between the occurrence of "terra rossa" on the one hand and groundwater flow velocity, the carbonate aquifer's permeability and its state of fissuring and karstism, on the other hand.

Radon has a half-life of 3.8 days while the Salentine karstic groundwater has an especially long residence time owing to the fact that flow velocity is extremely low, just about a few dozen centimetres per day (Cotecchia, 1977; Cotecchia et *al.*, 1989)

The study covered groundwater circulating in a vast portion of the Salentine Peninsula coastal carbonate aquifer which is characterized by a generally high degree of fissuring and karstism though it may vary widely at sites from very high to just negligible values.

In order to simplify the interpretation of the very special hydrogeological environment discussed here, the permeability characters are expressed in terms of the specific yields observed by test pumping a large number of boreholes; higher specific yields are usually due to a higher state of rock fissuring and karstism, hence to a higher degree of permeability.

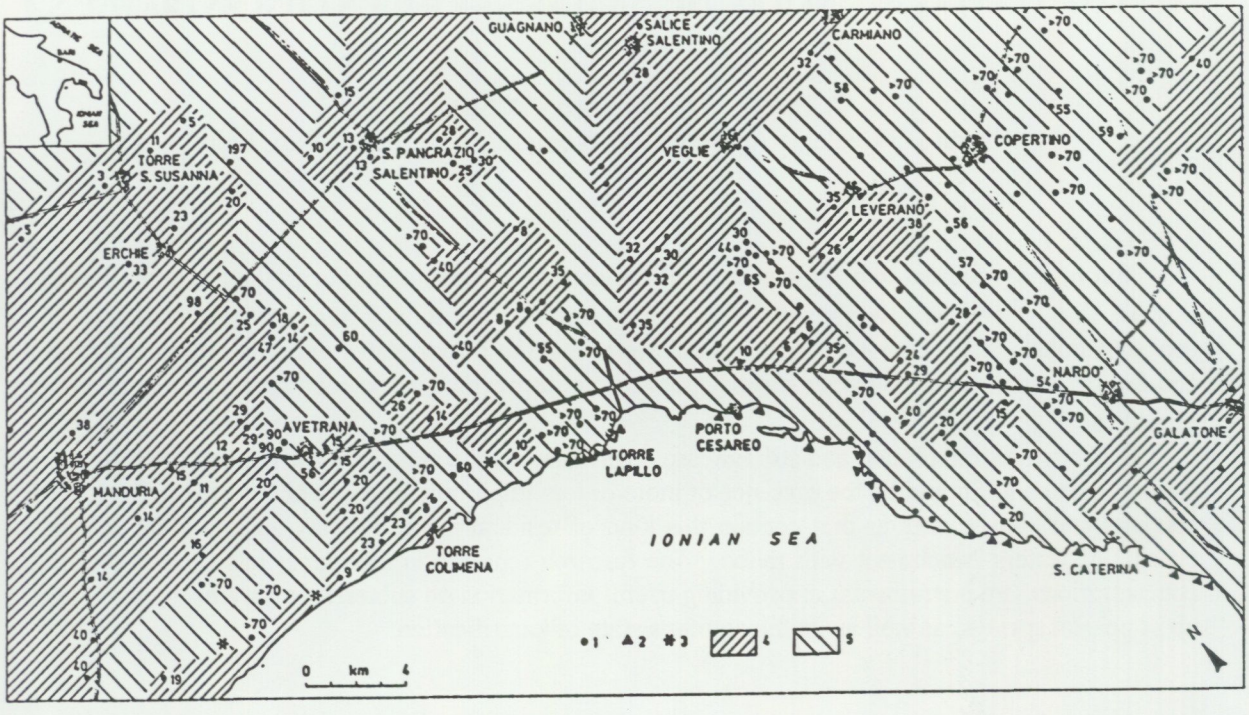


Fig. 1- Specific discharge (Qsp) values distribution (1: well; 2 coastal spring; 3: suaberial outflow; 4: Qsp < 50 l/s • m; 5: Qsp > l/s • m).

The map in figure n. 1 highlights areas with distributions of specific yields below and above 50 l/s.m. , respectively. Noteworthy, these distributions correlate well with the area's typical tectonic-stratigraphic features (Tadolini et *al.*, 1995).

As shown in figure n. 1, the most outstanding permeability factors along the coastline are revealed by the presence of a large number of springs.

The study area presents a variety of karst forms, sinkholes and dolinas, which, thanks to natural and/or man-induced leaching, contribute to making the "terra rossa" penetrate from the land surface, where it occurs in varying amounts over more or less widespread areas, down to different depths. Surface distribution of "terra rossa" can also depend on local farming practices: this residual carbonate rock material is collected, transported, handled and distributed on the soil, then used by peasants to grow some particular crops.

Two different types of symbols in figure n. 2 denote two fields, for different distributions of ^{222}Rn concentration values, below or above 270 pCi/l respectively, as measured in groundwater samples taken dynamically. Still other symbols denote water points at which radon values are higher than 600 pCi/l, with peaks of up to 3400 pCi/l.

The aquifer can be characterized by correlating the observed variety in radon concentrations, to its different states of fissuring and karstification.

Radon concentrations in waters sampled from coastal springs were found to be well correlated with those measured in boreholes drilled just inland from the coastline, despite the obvious fact that they are diluted in seawater (Tadolini et *al.*, 1994-b).

This was confirmed by the observed relationship of salt contents and corresponding radon cncentrations between boreholes and springs supplied by the same water like, for example, the spring at Torre Castiglione (^{222}Rn=960 pCi/l; T.D.S. 8.5 g/l) and the corresponding inland borehole (^{222}Rn=1610 pCi/l; T.D.S. 4.91 g/l), or in other similar circumstances.

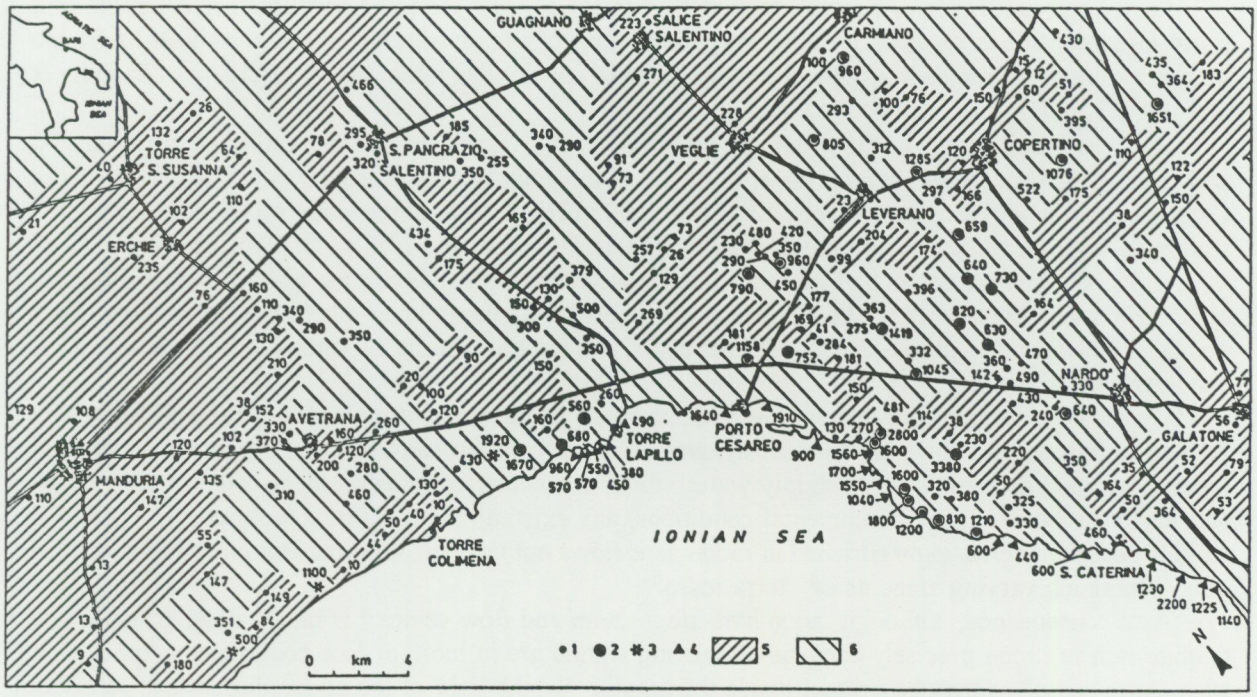


Fig. 2 - ^{222}Rn values concentration (1: well; 2: well with ^{222}Rn concentration > 600 pCi/l; 3: subaerial outflow; 4: coastal spring; 5: ^{222}Rn < 270 pCi/l; 6: ^{222}Rn > 270 pCi/l).

3. RESULTS

Areal distributions of radon concentration values can be correlated with the aquifer's hydrodynamic characteristics, as expressed in terms of specific yelds; such features derive not only from the rock's state of fissuring and degree of karstification, but also from the more or less conspicuous, yet widespread, presence of "terra rossa".

The data collected and processed for the purpose of this work show that, in the area just off Avetrana, radon concentrations are comparatively high while specific yelds are rather low. In the light of the information given above, this may be due to a significant presence of "terra rossa" that obstructs the cracks and fills the cavities so that permeability in that portion of the aquifer is markedly reduced.

Permeability is fairly high (Qsp>100 l/s.m) in the vicinity of Torre S. Susanna whereas radon concentration (<70pCi/l) is rather low: this means that in those parts of the aquifer where the state of fissuring and karstification is more developed, "terra rossa" is present in correspondingly lower amounts.

In the coastal strip west of Torre Columena, seaward outflows of karstic groundwater are strongly conditioned by the last patches of Calabrian clays presented all over the Tarantine Ionian Arc. Such stratigraphic conditions cause ground waters to flow along lines running practically parallel to the coast, then out into the sea at sites where the described impervious formation is no longer present.

It is worth noting that where the water heads are comparatively high and the thickness of the impervious clay layer is rather small, springs may develop because the impervious roof of a particular portion of the aquifer has been burst open. Examples of this kind are the Chidro and the Boraco springs located several dozen meters seaward from the coast (Cotecchia et *al.*, 1973).

In the inland area between Torre Columena and Torre Lapillo, where groundwater flows under moderately confined conditions and seawater ingression is rather strong, both specific yelds and radon concentrations are low (Tadolini et *al.*, 1995).

Conversely, specific yelds are low and radon concentrations are high between Torre Santa Susanna and San Pancrazio Salentino where the rock is heavily fissured and karstified and there are remarkably rich "terra rossa" deposits.

Lastly, groundwater is heavily drained by coastal springs scattered between Torre Lapillo and Porto Cesareo: this is revealed by observing the pattern of the piezometric surface as well as by the presence of many significant groups of springs some of which yield rather heavy discharges (Tadolini et *al.*, 1995; Tadolini et *al.*, 1996).

Radon concentrations in the grouped outflows in the vicinity of Torre Lapillo are between 500 and 600 pCi/l; instead, the submarine springs along the coastal stretch from Porto Cesareo to Santa Caterina show values ranging between 1200 and 1600 pCi/l. Inland, at the water points covered by this study, the corresponding values were as follows: 600 to 700 pCi/l and 1300 to 2800 pCi/l.

Along the coast east of S. Caterina, radon concentrations in submarine springs are remarkably high (2200 pCi/l); but could not be compared with those of the coastal belt due to lack of suitable water points. However, at about 2 km off the coast, where the aquifer's permeability is low, radon concentration is also low.

Given the environmental setting described above, a particular hydroisotopic cycle can be briefly defined as follows: as rainwater flows away over soils that contain "terra rossa", it becomes enriched in radon. As soon as it turns into "supply water" for groundwater replenishment, it conveys both radon and, under favourable geoenvironmental conditions, any existing "terra rossa"; groundwater inside the aquifer becomes increasingly enriched in radon as it flows out through subterranean cracks and cavities often containing varying amounts of "terra rossa"

As a consequence, although radon half-life is brief and flow velocity is rather slow, groundwater is quite rich in radon precisely because circulating waters are in more or less continuous contact with such "terra rossa" as may be present inside the aquifer. In the light of the above discussion, precisely the latter circumstance suggests that the various radon concentrations observed in this study basically depend on the existence of the karstic phenomenon, hence on the occurrence of "terra rossa" that is more or less copiously and variously distributed inside the aquifer.

With a higher degree of karstification, hence in the presence of big karst conduits and extended cavities with "terra rossa" deposits, very large water volumes are often directly in contact with the "terra rossa".

Lastly, radon concentrations measured in flowing coastal springwaters reveal another peculiar feature of the study area: inland sea water intrusions penetrate from below, not laterally, except in a few rather well-defined portions of the aquifer, generally without seaward outflows.

Work carried on with MURST 60%-40% and CNR-CE.RI.S.T. financial support.

REFERENCES

COTECCHIA V. (1977) - Studi e ricerche sulle acque sotterranee e sull'intrusione marina in Puglia (Penisola Salentina)" Ist. Ric. sulle Acque del CNR. Quaderni de "La Ricerca Scientifica", n. 20, Roma.

COTECCHIA V., SPIZZICO M., TADOLINI T., TINELLI R. (1989) - Variazioni nel tempo della concentrazione del Radon nelle acque di falda circolanti nell'acquifero costiero salentino. Geol. Appl. e Idrogeol., vol. XXIV, Bari.

COTECCHIA V., TADOLINI T., TAZIOLI G.S., TULIPANO L. (1973) - Studio idrogeologico della zona della sorgente Chidro (Taranto). 2° Conv. Int. sulle Acque Sott., Palermo.

TADOLINI T., SPIZZICO M. (1996) - The influence of "terra rossa" on radon contents in water: Experimental correlations in laboratory. In corso di pubblicazione su Hydrogeology Journal.

TADOLINI T., SPIZZICO M., SCIANNAMBLO D. (1994) - Variazioni di concentrazione del radon nelle acque di una sorgente costiera subaerea e nord di Brindisi. Soc. Geol. It., 77a Riunione Estiva, Congr. Naz. "Geologia delle aree di avampaese", Bari

TADOLINI T., SPIZZICO M., SCIANNAMBLO D. (1994) - Variation over the time of Radon concentration in a portion of the coastal groundwater at N-E of S. Vito dei Normanni (Brindisi-Italy). 13th Salt Water Intrusion Meeting SWIM, Cagliari.

TADOLINI T., SCIANNAMBLO D., SDAO F., SPIZZICO M. (1995) - Sulle possibilità di recupero di efflussi idrici in aree costiere della zona compresa tra T. Columena e P. Cesareo (Lecce)". "2° Conv. Naz. sulla Protezione e Gestione delle Acque sotterranee: Metodologie, Tecnologie e Obiettivi, vol. 1, pg. 61-68 Nonantola (Modena).

TADOLINI T., SPIZZICO M., SCIANNAMBLO D. (1996) - Karst groundwater outflows along the coastal area between T. Columena and Porto Cesareo (Lecce, Southern Italy) and their possible use. Int. Conf. on Karst Fractured Aquifers Vulnerability and Sustainability, Katowice - Ustrom, POLAND.

FUTURE RESEARCH ON COASTAL AQUIFERS

W. de Breuck
Geologisch Instituut S8, Krijgslaan 281, B-9000 Gent, Belgium

All over the world mankind has always been attracted by the sea because of the abundance of food and the transport and trade facilities and tourism. Hence coastal regions are very densely populated areas. One of the essential needs is water, not only for drinking but also for industrial and agricultural activities. Besides in many countries tourism is highly developed requiring huge amounts of water in some seasons. Coastal aquifers often provide a substantial amount of the water needed. In some areas they form the sole resource of water. The proper management of this valuable resource requires a thorough understanding of the delicate balance between fresh and salt water. Too often people realize too late that wells and land are salinized by mismanagement.

Groundwater in coastal aquifers is in a constant but very slow evolution controlled by the geological conditions of the area. The fresh-/salt-water distribution is in a dynamic equilibrium. Any human interference will change this equilibrium but the consequences may only be felt decades later. It is well known that overdrawing in coastal aquifers has caused the salinization of the wells and sometimes the abandonment of large tracts of coastal areas by shortage of good quality water. The reclamation of marsh lands and the subsequent drainage have a long-term salinization effect on the groundwater. Therefor a thorough knowledge of the hydrogeology of coastal aquifers in general and a detailed field survey of every area, where groundwater will be affected in particular is needed if the groundwater resources are to be exploited. Besides human works but also natural events at large distances may influence groundwater conditions in coastal areas.The Aswan dam is changing the fresh-/salt-water situation in the Nile delta in a slow but drastic way.

In most cases no investigation of the salinization of a region is made until the groundwater conditions have become alarming and even dramatic. Since hydrogeological processes evolve

very slowly, remediation will take a long time to provide results if economically feasible at all. Many examples of inadequate management of the groundwater conditions in our countries may be quoted. At present the general situation is known but more research is needed even in countries where already much information is available. Before undertaking remediation measures one should have a thorough knowledge of the situation; otherwise remedies however costly may increase rather than solve the problem.

Recently G.OUDE ESSINK, in his doctoral thesis on the impact of sea level rises on groundwater flow regimes (1996) demonstrated that even without a future sea level rise the salinization process in the subsoil of the Netherlands will continue as a delayed effect of both past and present human activities. In the southern part of Noord-Holland the reclamation of the low-lying Haarlem lake polder in the middle of the 19th century has generated a salt water encroachment in the deep aquifers of at least 1 km a year.

One of the conclusions of ESSINK's study is the recommendation to collect more data of hydraulic parameters, solute concentrations and piezometric levels. This is remarquable since the Netherlands have a longstanding record of collecting data on and observing the groundwater conditions. But even so the author concluded that he did not have enough reliable information for accurately modeling the groundwater conditions in several crucial areas of the Netherlands.

The voluminous work on "Groundwater problems in coastal areas" by CUSTODIO and BRUGGEMAN as a UNESCO report (1987) covers many aspects of the present knowledge of the relationship between fresh and salt water in coastal aquifers drawing information from experiences in many parts of the world. It also generates questions which call for more scientific research and more field investigation.

More research is needed to explain the interaction between water and sediment, especially the clayey part, since the latter plays an important role in the composition of the water as well as the hydraulic behaviour of the formation. Goldenberg and Mandel at the 10th SWIM presented some information on their experiences on reducing the permeability of a sediment by air injection and thus hindering salt-water encroachment. The phenomenon of ion exchange in clayey material has been widely studied but in relationship to groundwater quality evolution and groundwater movement research could provide some very interesting results. Isotopic investigations have been reported in the past but a systematic inclusion of stable as well as radioactive isotope research in ongoing studies may contribute to a better understanding of the salinization/freshening processes. Much research is to be done in the field of modeling of hydrogeochemical conditions and processes.

Considerable attention has been paid to calculations and modeling but much effort will still be needed to develop accessible tridimensional models of groundwater flow accounting for density differences and mass transport. But modeling should be based upon reliable field data. These can only be acquired by an intensive field investigation. In this domain the geophysical methods, which complement the drilling operations, are receiving a renewed interest. During the latest SWIM's few but interesting contributions have been presented. Recent developments in the field of resistivity/conductivity surveying are very promising. At a previous SWIM SENGPIEL presented the results of an airborne electromagnetic survey in Pakistan, whereby fresh-/salt-water conditions were mapped. This method may contribute to a better and faster delineation of the fresh-/salt-water interface. The concept of combining resistivity sounding and traversing can be realized by a multi-electrode approach as proposed by the LUND IMAGING SYSTEM (ABEM). It provides an automatic data acquisition and software for the handling and the representation of the data. Data acquisition is performed by a cable containing a large series of electrodes, which can be combined in different arrays, each entailing its own geometrical factor and determining its apparent exploration depth. The results can be represen-

ted as a pseudodepth section providing a qualitative image of the resistivity distribution and hence the groundwater quality conditions.

A field experience of combined fresh- and salt-water pumping may provide interesting results not only from a scientific but also from a practical viewpoint. By extracting and evacuating salt water at a reasonable cost from a salinized area fresh water resources may be exploited and increased at the same time. The first results may be reported on at the next SWIM.

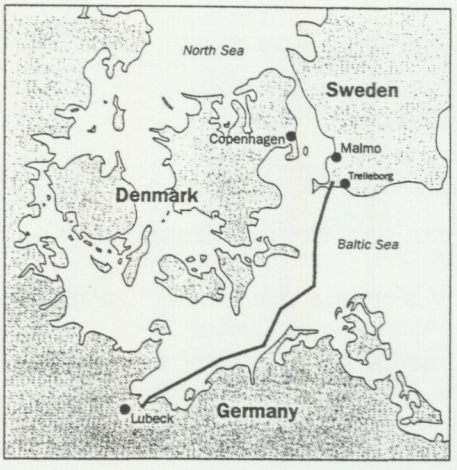
In general a better dating availability will help to explain the long tem evolution of aquifers regarding their flow as well as their chemical behaviour. Dating groundwater under beaches may provide information on the short term salinization process.

More and faster progress will be made if, as in the past some steps have set, exchange and cooperation between researchers and laboratories could be intensified. In well investigated regions complementary methods could be tested and applied in such a way that these methods could be calibrated and additional information on the region could be gained.

As a sequel to the work of Custodio and Bruggeman one could think of elaborating a practical manual for groundwater management in coastal aquifers destined for technicians and local government officials.

DIRECT CURRENT THROUGH SALINE ROCK.

Leif Eriksson, Geological Survey of Sweden,
box 670, S-75128 Uppsala, Sweden.



ABSTRACT

The geological conditions for an effective electrical grounding at large depths are often favourable because of a lower earth resistivity resulting from a higher salt content.
A new type of ground electrode installed in a 550 m deep bore hole is under test in the Baltic Cable HVDC transmission system in Scania in the south of Sweden.
The deep hole electrode has the advantage of low grounding resistance, low ground surface voltages and thereby a reduced risk for corrosion of buried metal structures in the surroundings.

In the last few years a lot more knowledge has been acquired regarding salt groundwater, especially in connection with radwaste investigations in Finland and Sweden. Within the Research and Development Programme at the Geological Survey of Sweden numerous tests have been carried out in order to find out whether it is possible to measure the depth to salt groundwater both in sedimentary and crystalline bedrock using electrical, as well as electromagnetical, soundings. The results are promising. The picture is becoming rather clear that deep groundwater is saline everywhere, but the interface between fresh and salt groundwater, which is often rather sharp, is situated at different depths in different areas.

The experience from investigations around various HVDC projects, and direct studies of the adjacent potentials have confirmed these observations. The Baltic Cable deep hole grounding is an illuminating case.

1. INTRODUCTION

Effective ground electrodes in HVDC transmission systems are of primary concern to suppliers and utilities for many reasons. A low electrode resistance reduces the power loss and the DC potentials at the surface of the earth. Low electric earth surface potentials and potential gradients diminish the risk of interference, e.g. increased corrosion on burried metallic structures due to DC earth current. Existing HVDC ground electrodes are located in remote areas often at a distance of several tens of kilometers from the converter station itself due to the risk of interference.
Significant advantages can be achieved, when electrodes of low resistance are located in low resistivity earth layers. This results in low DC electric potentials and potential gradients at the surface of the earth;

* the electrode can be located closer to the converter station
* shorter electrode line
* reduced power loss
* reduced interference in the vicinity of the electrode
* further opportunities to use monopolar HVDC transmission.

The main objective of this project has been to design and test a new type of HVDC ground anode installed in a bore hole of 550 m depth at the site of the Baltic Cable HVDC converter station in the far south of Sweden, where favourable conditions for a deep grounding point was found.
The project is a joint venture between ABB Power Systems, Vattenfall Transmission, Baltic Cable and Statnett SF. Consultants have been SGU and Vattenfall Hydro Power. STRI (Swedish transmission Research Institute) is managing the project.
The test electrode was installed in the borehole in June 1994 and was taken into operation for the first time at the end of January 1995.
The electrode is in fact located within the HVDC station area and connected in parallel to the ordinary sea electrode located about 23 km from the HVDC station.

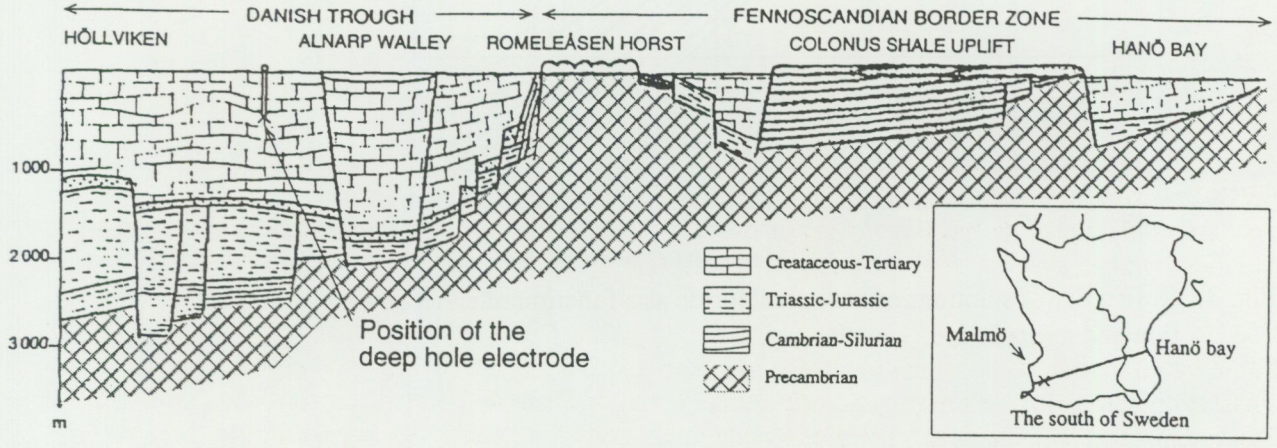


Fig. 2 Cross section through the fossile-bearing bedrock of Skåne

2. GEOLOGICAL CONDITIONS IN SKÅNE

Fig. 2 shows a section through the fossile-bearing bedrock in Skåne, the southernmost province of Sweden (1). This delineates a several kilometer deep sedimentary bedrock characterized by relatively young and thus porous rocks covering the crystalline basement. This type of bedrock occurs commonly in large areas of the world and represents the dominating situation in Europe, for example.
Porous sedimentary bedrocks are well suited to electrical grounding because of their content of electrolyte, i.e., salty water. The resistivity of the electrolyte present in the close vicinity of the grounding point, i.e., out to some hundred meters, is the primary determining factor for the resistance of the grounding point. As the diagram in Fig. 3 shows, this resistivity is determined by salt content and temperature and in this particular case (appr. 1 % NaCl and 10 °C) it can be just below 1 Ωm.
Regarding actual earth deposits it can be said that their resistivity depends on the content of electrolyte and its salinity. On land down to about 100 m (depending on the groundwater level above sea level) the electrolyte consists of fresh water, which means that sand and gravel have a resistivity between 100 and 500 Ωm. whereas clay can be between 10 and 100 Ωm. In exeptional cases, salty electrolytes are present resulting from seawater penetration or from relict saltwater deposits.
Below an often rather thin earth layer usually less than 10 m in depth one meets the initial bedrock consisting of limestone. Its resistivity is also determined by the porosity and the salinity of the electrolyte. The resistivity can be calculated by means of Archies law if the porosity and resistivity of the electrolyte are known, see Fig. 4. If the electrolyte consists of freshwater, the resistivity is of the order of 50 - 100 Ωm.

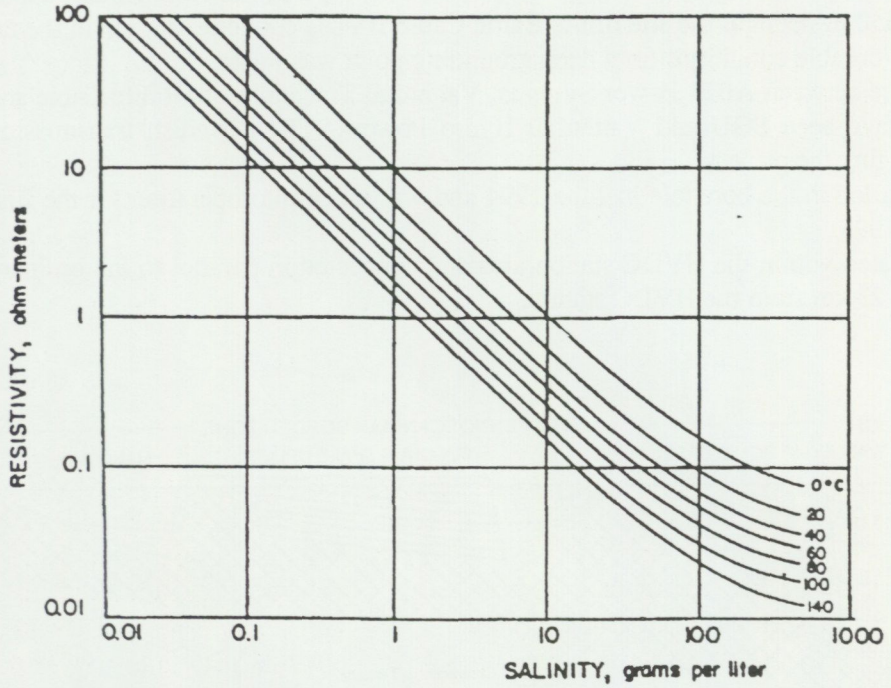


Fig. 3 Resistivity of solutions of sodium chloride as a function of concentration and temperature.

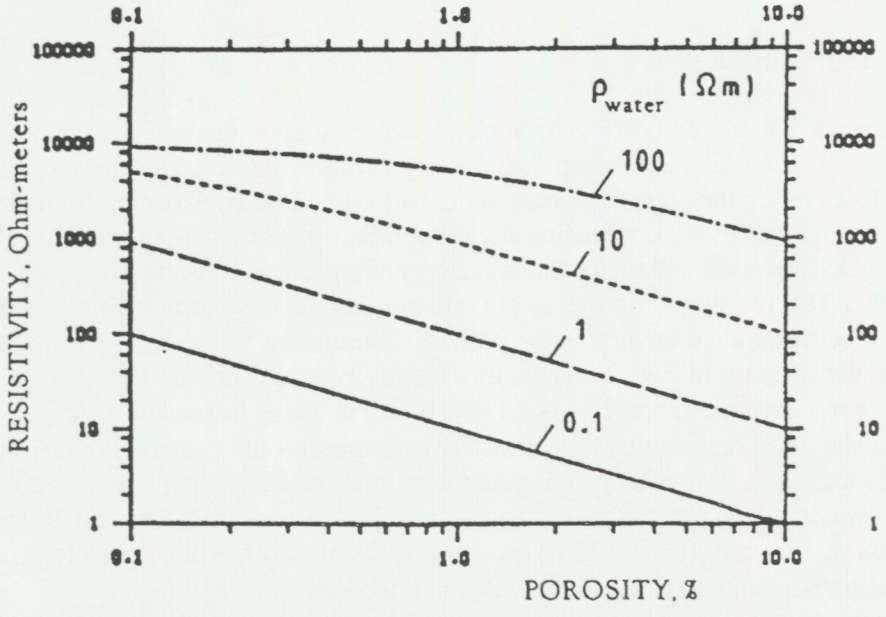


Fig. 4 Resistivity of the bedrock as function of porosity and the resistivity of the electrolyte.

At larger depths the salinity and the porosity can rise to very high values. In the lowest part of the limestone (Cenoman), there exist remarkably high salt contents (10 - 15 %) and also high porosities, which can be over 30 %. Since the temperature increases with depth by some 20 °C per kilometer, the resistivity will decrease for that reason too.
In connection with such projects as prospecting for oil, SGU and OPAB have drilled a large number of deep bore holes in the far south of Sweden. Bore hole loggings show that resistivity at somewhat deeper levels in the limestone is of the order of 5 - 10 Ωm but taken in the Cenoman horizon at deeper level (1200 m in Höllviken) the value is 0.1 - 1 Ωm. Some of the deepest holes continue down through the sedimentary bedrocks and into the crystalline basement, which of course has a considerably lower porosity, perhaps only of the order of 0.1 %, but has a salt saturated electrolyte and therefore a resistivity as low as 300 - 500 Ωm.

At a very early stage it was proposed by SGU that one of these existing bore holes, that is not in use at present, should be utilized for grounding, or at least for tests of deep grounding in parallel with those tests that were conducted in cooperation between SGU and Vattenfall Västsverige. In some introductory tests the grounding resistance of the steel casing of some of the deeper holes were measured according to the Bolzman methode, resulting in resistances of 0.1 - 0.2 Ω. However, the resistance of the long steel casing itself was included in these measurements and it was obvious that the major part of the current was leaving the casing at minor depths. It should therefore be possible to consider a shorter bore hole, but yet have a sufficiently low grounding resistance.

In order to gain information about variations in resistivity in the upper part down to a depth of 250 m, where old bore hole loggings started, electrical soundings were carried out with current electrodes gradually separated up to a maximum half distance of 320 m. Results show that fresh water has displaced salt water down to 60 m depth, where the resistivity decreases from 200 Ωm to appr. 20 Ωm and gradually decreases further to 5 - 10 Ωm. See Fig. 5. It can be concluded that a deep hole grounding means that a low resistivity bedrock which is not affected by fresh water can be used as the location for a ground electrod.

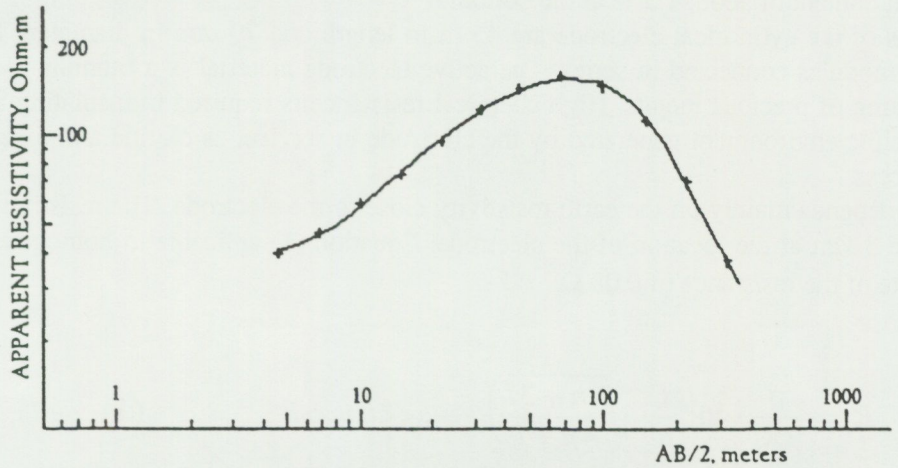


Fig. 5 Resistivity as function of depth from electrical sounding in Håslöv.
(AB/2= half distance between current electrodes)

Layer	Resist. [Ωm]	Thickn. [m]	Depth [m]
1	36.59	5.5	5.5
2	247.82	55.1	60.6
3	17.84		

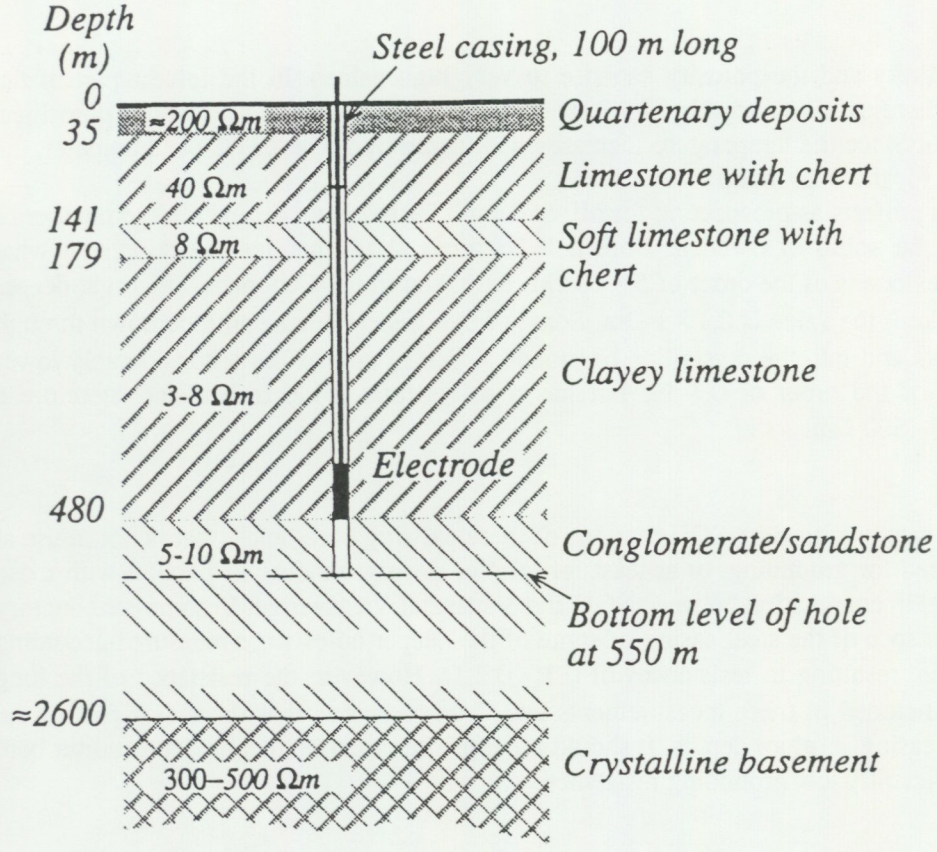


Fig. 6 Resistivities, earth layers and location of the electrode in the bore hole.

3. ELECTRODE DESIGN

The bore hole is 550 m deep, and drilled by means of a 96 mm bore except for the first 100 m where a steel casing of 139 mm diameter is inserted in order to stabilize the bore hole. The bore hole is naturally filled with water with salt content of about 1.5 % at the bottom.

The principal dimensions of the cylindrical electrode are 45 m in length and 70 mm in diameter. The electrode consists of 34 modules connected in series. The active electrode material is a titanium mesh with a special oxide coating of precious metals. High chemical resistance is required in insulating and other materials due to acidic environment generated by the electrode in service, as clorine and oxygen result from the anod process.

The electrode resistance depends mainly on the earth resistivity close to the electrode. The resistivivity is measured to be around 3 Ωm at the location of the electrode. Equation (1) aplicable to homogenous earth gives a first estimate of the resistance of 0.08 Ω.

$$R = \frac{\rho}{2\pi l} \cdot \ln\left(\frac{l}{a} \cdot \sqrt{\frac{4h+3l}{4h+l}}\right) \qquad a<<l,\ h>>a \qquad (1)$$

where ρ is the earth resistivity, l the electrode length, a the electrode radius and h the distance from the surface of the earth to the top of the electrode [2]. If l is small compared to h as in this case the square root expression is close to one.

Measurement of the electrode resistance where the sea electrode was used as counter electrode shows an electrode resistance of 0.086 Ω. The resistance of the deep hole electrode and the sea electrode together was 0.12 Ω. If cable resistances are included, the total resistance of the deep hole electrode (0.11 Ω) is considerably lower than the resistance of the sea electrode (0.38 Ω) due to long sea electrode cables (two in parallel, 23 km each)

4. POTENTIAL DISTRIBUTION

Compared to electrodes at the surface, the deep hole electrode gives lower potentials on the earth surface in an area relatively close to the electrode (in this particular case up to some km). The size of the area is mainly depending on the depth to the electrode. See Fig. 7 which for simplicity's sake concerns a case with homogeneous earth.

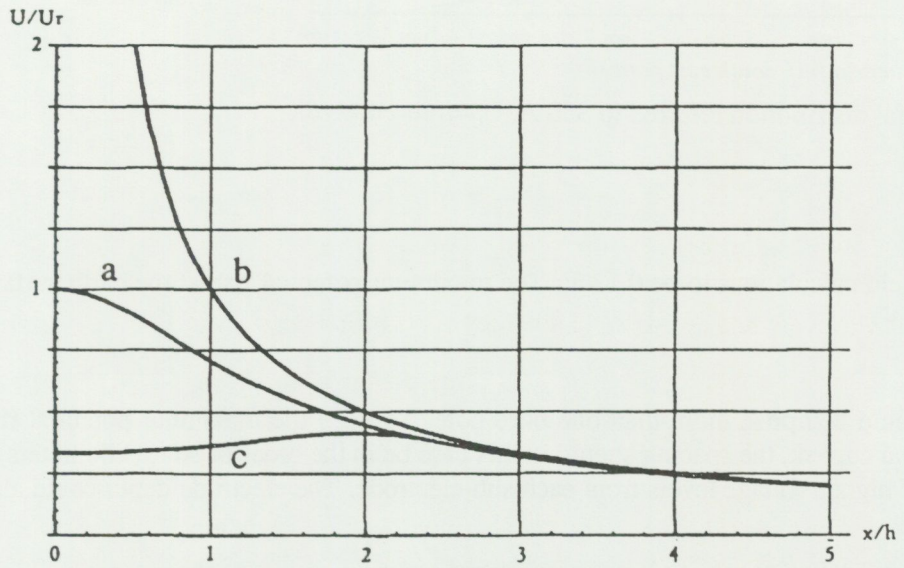


Fig. 7 Potential distributions at the surface of a homogeneous earth. x=horizontal distance, U_r=maximum voltage in case a.

a. Electrode at depth h
b. Electrode at the surface
c. Four sub-electrodes at depth h, separated a distance of 4h (placed in the corners of a square)

A relatively thin top layer (a fresh water layer) of larger resistivity will, however, not significantly increase the potentials at the surface around the deep hole electrode. If instead the electrode is placed in that surface layer, then the potentials within a distance of about 2d, where d is the depth of the surface layer, are very sensitive to the surface layer resistivity and the potentials are increased markably as the resistivity goes up (2).

The potential distribution was measured using the successive voltage drop methode, which simply consists of measuring voltages between successive pairs of points on the earth surface. The potential to a reference level can then be obtained by summation of the measured voltages. Measurements were carried out up to a distance of 3.6 km along available roads out from the electrode site. Fig. 8 shows the result of the measurements referred to an electrode current of 350 A. The potential at 3.6 km is

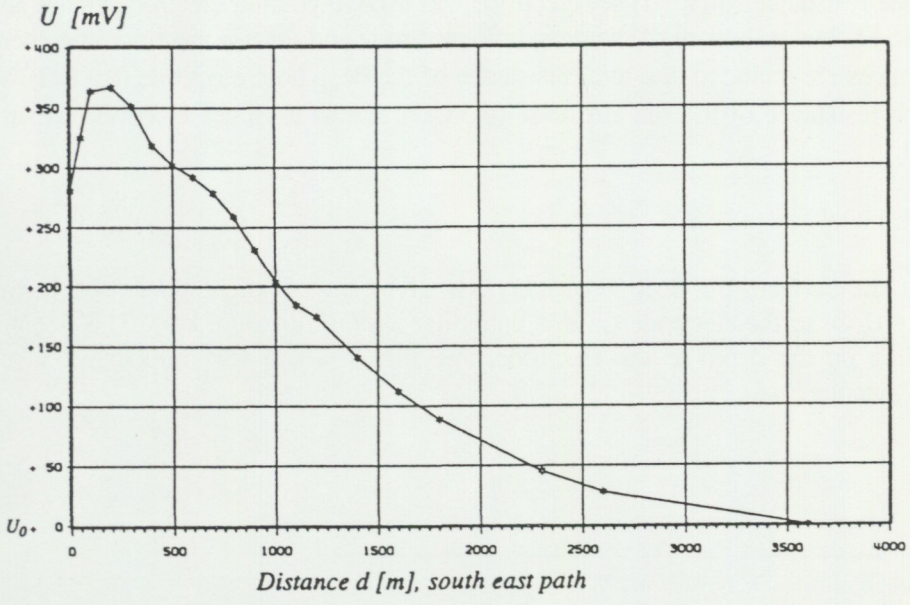


Fig. 8 Measured potential distribution referred to 350 A. U_0=reference voltage at 3.6 km.

estimated from electric field calculations to be 0.13 V. The maximum potential rise at the earth surface is thus 0.37 + 0.13 = 0.5 V.

A full scale electrode would comprise more than one bore hole. To keep the maximum potential rise down despite a higher total current, the spacing should in this case be in the order of some kilometers to avoid coinciding areas of higher voltage levels from each sub-electrode. The electrode depth could also be increased.

REFERENCES

(1) Frede´n, C., (Ed) and Geological Survey of Sweden, 1994: National Atlas of Sweden, Geology,

(2) Kimbark, E., 1971: Direct Current Transmission, Vol. 1 Wiley, New York.

Improved Delineation of Saline Groundwater by Airborne Electromagnetics

Klaus-Peter Sengpiel
Federal Institute for Geosciences and Natural Resources (BGR)
Postfach 510153, D–30631 Hannover, Germany

Measuring principles

For several decades d.c. resistivity soundings have been used to provide valuable information for groundwater surveys. Only very recently have electromagnetic (EM) induction methods begun to provide similar standards of data evaluation, particularly in resolving resistivities and thicknesses of a layered halfspace from survey data. EM methods have the advantage that neither transmitters nor receivers require galvanic contact with the ground. Therefore, they can be moved during measurement and operated at considerable height above ground surface. For helicopter applications, transmitters and receivers are housed in a towed missile ("bird"), where they are spaced only a few meters apart. The bird is flown at a height of about 30 m above ground, providing a depth of investigation of up to 150 m with standard equipment.

BGR operates a helicopter-borne Dighem-III system as shown in the sketch (Fig. 1). The system is flown at a speed of up to 150 km/h. The primary magnetic field oscillates at three frequencies simultaneously, normally 380, 3 600 and 32 000 Hz, in order to induce current systems which are centered at different depths. The current density is a function of the ground conductivity; therefore, good conductors such as saltwater-bearing aquifers provide stronger signals than freshwater aquifers and much stronger signals than dry sand. The signal is the sum of the (secondary) magnetic fields of all induced currents at one frequency. In Fig. 1 the secondary field comes from the three layers and the conductor; the signal is transformed into a voltage by means of a receiver coil.

It should be noted that the induced currents and their magnetic fields in general have a phase shift relative to the phase of the primary field (unlike d.c. fields). Thus, two values are measured at each frequency: the inphase (real) field component R and the out-of-phase (imaginary) field component Q. The R and Q values of all frequencies are sampled 4 to 10 times a second together with positioning data (GPS coordinates, barometric and radar altitudes) and data from the other geophysical methods applied with the BGR geophysics helicopter, namely magnetics (total geomagnetic field) and gamma-ray spectrometry (256 energy channels). All data are stored on magnetic tape (cassette) and on chart paper. A sampling rate of 4/sec corresponds to a sampling distance of about 10 m on the flight line.

Inversion of measured EM data into ground parameters

The measured data originate from ground in which the resistivity distribution is unknown. When beginning evaluation, it is common practice to assume that the ground is uniform around the measurement site, i.e. to use the homogeneous halfspace model. This leads to the "apparent" resistivity ρ_a (or apparent conductivity $\sigma_a = 1/\rho_a$) which is obtained for each measuring frequency.

Over the last 20 years, the airborne EM method has proved to be a very useful tool for mapping the lateral (apparent) resistivity distribution both in detail and at high survey speed (Fraser, 1978). Besides ρ_a, a second parameter (D_a) can be determined from the two input values R and Q, where D_a is the (apparent) distance between the coil system and the surface of the halfspace model. D_a can be compared with the flight altitude of the EM bird and thus can yield preliminary information on the vertical resistivity distribution in the ground. Furthermore, ρ_a and D_a can be used to calculate a depth value z^* called the centroid depth (Sengpiel, 1988), which is a measure of the depth of the center of the induced current system.

The parameters ρ_a and z^*, calculated for a great number of frequencies, define the sounding curve $\rho_a(z^*)$ shown in Fig. 2. This curve is obtained for the three-layer (step) model $\rho(z)$, where $\rho_1 = 200$ Ωm, $\rho_2 = 20$ Ωm, $\rho_3 = 1000$ Ωm, and the layer thicknesses are $d_1 = 30$ m, $d_2 = 40$ m, and $d_3 = \infty$. This sounding curve is closely related to the model, at least in the range of the upper two layers, while the ρ-value of the third layer is only approached very gradually by the curve.

In reality, with only the three frequencies f_1, f_2, f_3 available as indicated in Fig. 2 by asterisks on the curve, we obtain merely a short piece of the sounding curve, yielding the approximate resistivities in the depth range of about 20 to 60 m. An improvement of the inversion capabilities was achieved in 1993 when BGR started using its newly developed "Automatic inversion of AEM data into multilayer parameters" (Sengpiel et al., 1994). This evaluation procedure uses the sounding parameters ρ_a and z^* to develop an individual start model for each set of survey data. An iteration process based on a Marquardt inversion varies the model parameters until an optimum fit is achieved between the survey data and the calculated field data for the inversion model. It is only necessary to define the number of layers of the inversion model. This number can be derived from the $\rho_a(z^*)$ sounding curve or from other information, especially drilling results. With good quality field data, the inversion process can provide accurate step model parameters. In Fig. 2, this case applies for inversion model (1), calculated for $\delta = 0.01$ %, where δ is the residual misfit between model data and (theoretical) survey data. The value δ is adjusted according to the accuracy of the survey data. Allowing for a typical misfit of $\delta \approx 10$ % for survey data, the accuracy of the inversion parameters is reduced; this affects mainly the lower and less conductive layers (layer 3 in Fig. 2). The choice of the number of layers (N) is not critical, provided N is equal or greater than the true number of significant layers.

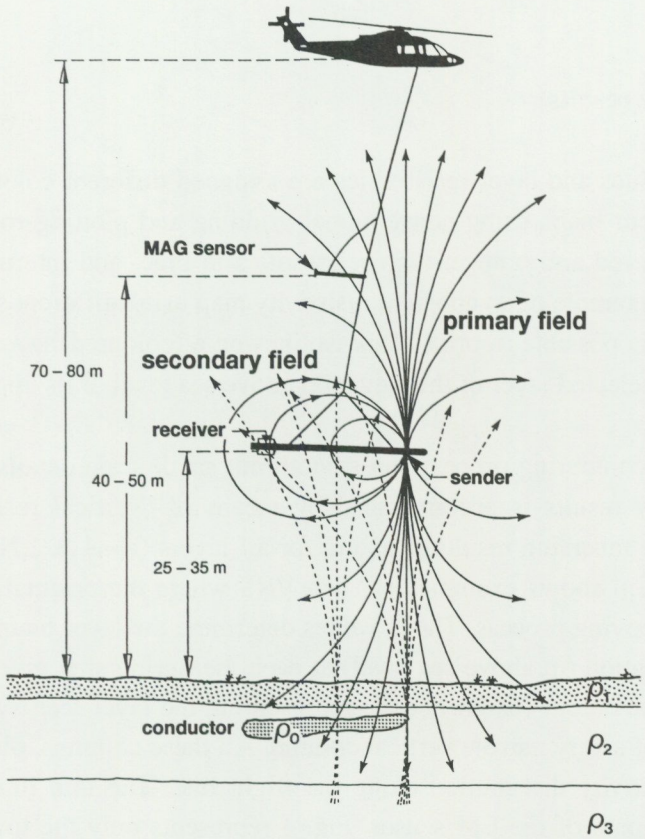


Fig. 1: Sikorsky S 76 B helicopter carrying the EM and magnetometer sensors at the indicated elevations above ground. Geometry of the transmitted primary magnetic field (dipole field) inducing currents in the conductive parts of the ground. Sketch of the secondary magnetic fields of these currents flowing in the three layers (ρ_1, ρ_2, ρ_3) and the conductor (ρ_0); a small portion of the secondary field passes through the receiver coil.

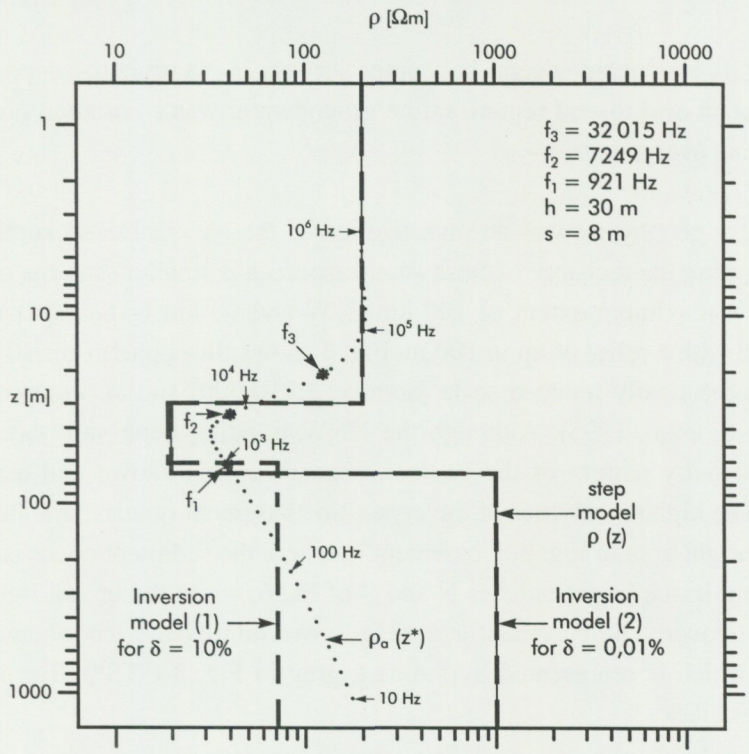


Fig. 2: ρ/z diagram showing resistivities ρ and thicknesses d of a three-layer model ρ(z), where ρ_1 = 200, ρ_2 = 20, ρ_3 = 1000 Ωm, d_1 = 30, d_2 = 40 m, and the results of different inversion methods:
– The sounding curve ρ_a (z*) obtained when a large number of frequencies is used,
– the perfect inversion (model 1) using perfect survey data (δ = 0.01 %),
– a less accurate inversion (model 2) simulating imperfect survey data (δ = 10 %).

Presentation of survey results

Apparent resistivity values and layer resistivities are assigned different colours and presented in the form of coloured contour maps using conventional gridding and plotting routines. Low resistivities are normally plotted in red and orange, high resistivities in blue, and intermediate values in yellow and green. Fig. 3 is an example of an apparent resistivity map using different shades of grey, dark grey for low resistivities. It is possible to print black isolines on a (coloured) layer resistivity map to indicate the thickness of a selected layer or the elevation above sea level of its upper boundary.

As is well known, the contouring process can smooth out small-scale details. A fully detailed representation of the survey results is accomplished by means of "vertical resistivity sections" (VRS) which are based on the inversion results ρ_i and d_i for all layers (i = 1,2,...,N) at each measuring site along a flight line. Fig. 4 shows examples of such VRS where the original colours of ρ_i are reproduced in grey by the copying process. The d_i values determine the layer boundaries which are related to the topographic elevation (m above sea level) at each measuring site, given on the vertical axis of the plots (left side). The colour (or grey) code representing the layer resistivities below a measuring site is plotted in form of a very narrow vertical column. All these columns, plotted side by side, represent a continuous resistivity distribution along the flight line. The thin line above the topographic relief shows the flight path of the EM sensor. Fig. 4 represents only the lower parts of the original VRS; the upper part normally contains the measured R and Q values along the line and data from the two other methods, such as the magnetic anomalies and the total gamma radiation (in uranium equivalents).

Examples of groundwater investigation results

In 1992 and 1993 BGR conducted several helicopter surveys in Namibia to support groundwater investigations. In this semi-arid to arid region, saline groundwater was a common problem, not only in coastal areas but almost everywhere.

A special challenge for geophysics was an investigation in the Namib Desert south of the important port of Walvis Bay, where the recharge of freshwater resources is smaller than the increasing demand. The survey area has a maximum extent of 100 km E–W and 90 km N–S and is almost completely covered by dune sand with a relief of up to 100 m. Fig. 3 shows the apparent resistivity distribution in the whole area at an drastically reduced scale (approx. 1:710 000) and at a measuring frequency of 921 Hz (Sengpiel & Siemon, 1995). Although the NNW trending dune valleys and ridges are still recognizable, the resistivity pattern of the bedrock beneath is also shown and reveals a number of crossing structures. The high resistivities of the crystalline basement (gneiss, granite, schist, quartzite) are indicated by the bright area in Fig. 3, ("basement"), where the sediment cover is thin. Outcropping basement is also found in the bright patches N and S of PC 6, while the broad, light grey strip in the W is due to the sand cover. The basement is generally overlain by the (conductive) Tsondab Sandstone (Ward, 1987) which is represented by the dark grey in Fig. 3 ("TS"). The lowest resistivities (around 1 Ωm) appear black.

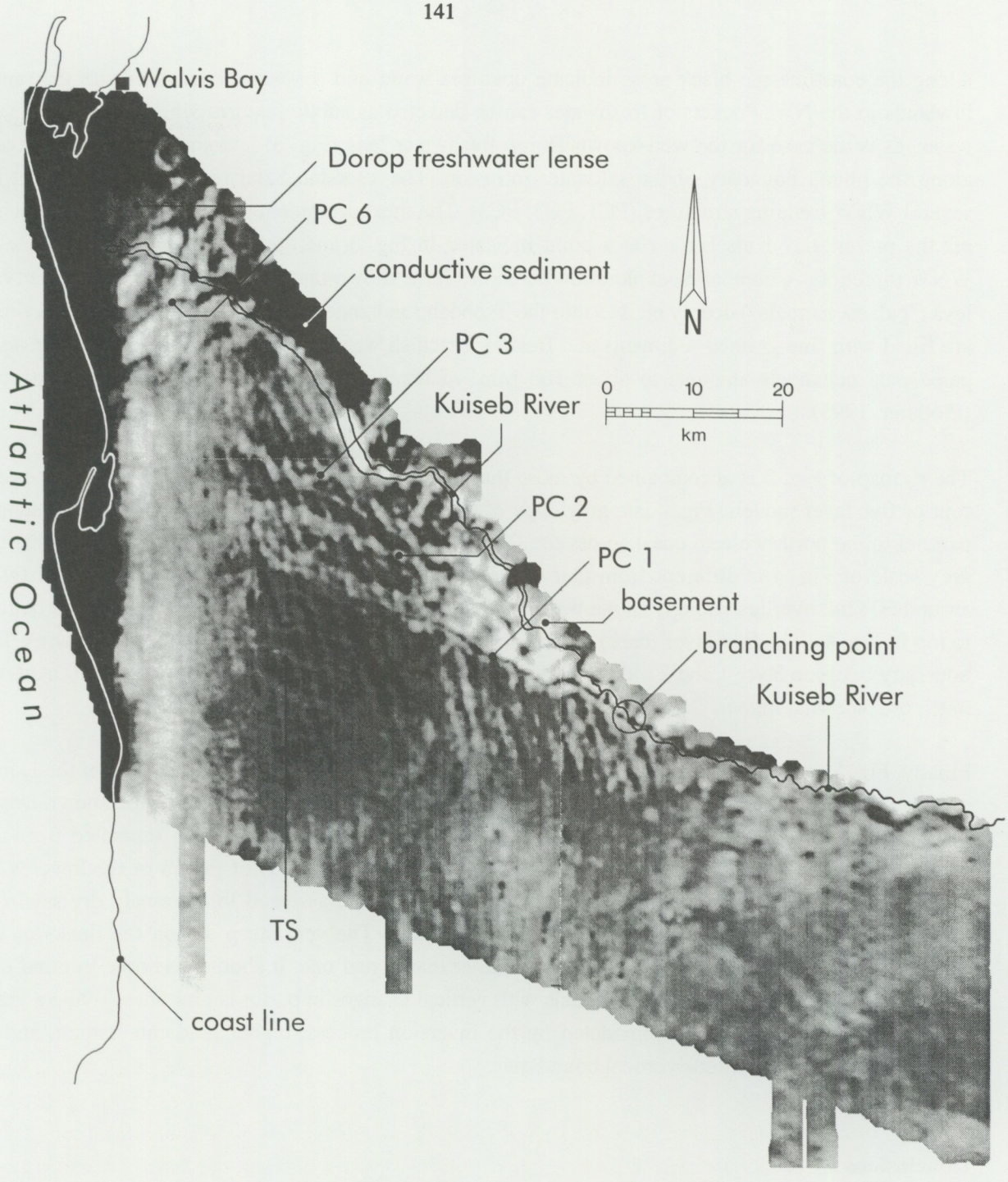


Fig. 3: Grey scale representation of apparent resistivity ρ_a (at 921 Hz) in the Kuiseb Dunes area of Namibia, showing mainly the resistivity pattern of the bedrock below a thick sand cover; only the NNW-trending features originate from dune ridges and valleys. The structures PC 1 to PC 6 were identified as palaeochannels of the Kuiseb River, which has shifted its course stepwise from PC 1 to the north. The palaeochannels are cut into basement rock (light-coloured areas) and/or conductive Tsondab Sandstone (medium dark areas, TS). The black area along the coastline indicates highly conductive saltwater intrusion. Along its eastern edge it is overlain by freshwater pockets (subtle dark-grey features).

Along the coastline the black areas indicate open sea water and sea-water intrusions into the sandy lowlands in the NW. Pockets of freshwater can be detected as subtle features which overlie the salt-water, as is the case for the well-known Dorop freshwater lens (Fig. 3) and similar, smaller pockets along the inland boundary of the saltwater intrusion. The Tsondab Sandstone Formation is cut by several WNW trending structures (PC1, PC2, PC3). The most prominent one is PC 1 which branches off the present-day Kuiseb river at a point indicated in Fig. 3 and continues as a thin dark line in WNW direction. A number of exploration boreholes have shown that these structures are former valleys ("palaeochannels") deeply incised into the Tsondab sandstone and/or the basement. These valleys are filled with fine-grained sediments and fresh or brackish water. The water potential of the investigated palaeochannels amounts to about 100 Mm^3 of brackish and 280 Mm^3 of fresh groundwater (Plöthner, 1995).

The ρ_a map of Fig. 3 is accompanied by more than 12 000 line km of vertical resistivity sections for four or five layer models. Fig. 4 is a grey copy of three coloured VRS which extend over 20 line km, parallel to the north-western coast across the Dorop freshwater lens indicated in Fig. 3. Note that the grey scale of Fig. 4 is different from that of Fig. 3. The Dorop aquifer has a formation resistivity around 30 Ωm, overlies strongly saline water (~ 1 Ωm), and thins out towards the coast (from bottom to top in Fig. 4). The first layer (dark) represents the highly resistive sand cover ($\rho_1 > 1000$ Ωm). The boundary between layer 1 and 2 indicates the approximate groundwater table and occurs at 0 m above m.s.l. or somewhat higher.

Finally, Fig. 5 shows two VRS along flight lines (tie lines) which cross the northern part of the Dorop aquifer (line 927.9) and its southern part (line 926.9), both from SE to NW. Besides the known Dorop aquifer, more fresh water is expected in PC 6b (line 927.9 and 926.9) which is separated from the Dorop aquifer by a bedrock high. Above the water table (w.t. in Fig. 5) of PC 6b of the lower VRS there are three layers of somewhat higher resistivity, which are assigned to extremely dry sand (on top) and underlying sand with a residual moisture content. The very steep dip on the flanks of the bedrock highs is probably an apparent feature rather than a real one. It should be borne in mind that the one-dimensional layer model only deals with vertical changes in ρ, not lateral ones. While a gradual lateral change can be accommodated by the inversion process, higher gradients cannot, and in some cases produce fictitious vertical boundaries.

Conclusions

In addition to the survey results presented here, many thousand line km were surveyed and evaluated using the techniques described above. This demonstrates that groundwater salinity can be reliably mapped in three dimensions by airborne EM, preferably in areas where unconsolidated sediments prevail. The water table can be determined under favourable conditions, i.e. if there is a significant resistivity contrast between unsaturated cover and the aquifer. The airborne survey should be followed immediately by a test drilling program; a few boreholes may provide the key to understanding the relationship between resistivity and hydrogeology of a whole region. BGR is trying to increase the resolution and the reliability of the survey results by the development of a new five-frequency EM sensor, which is expected to be in operation in 1996.

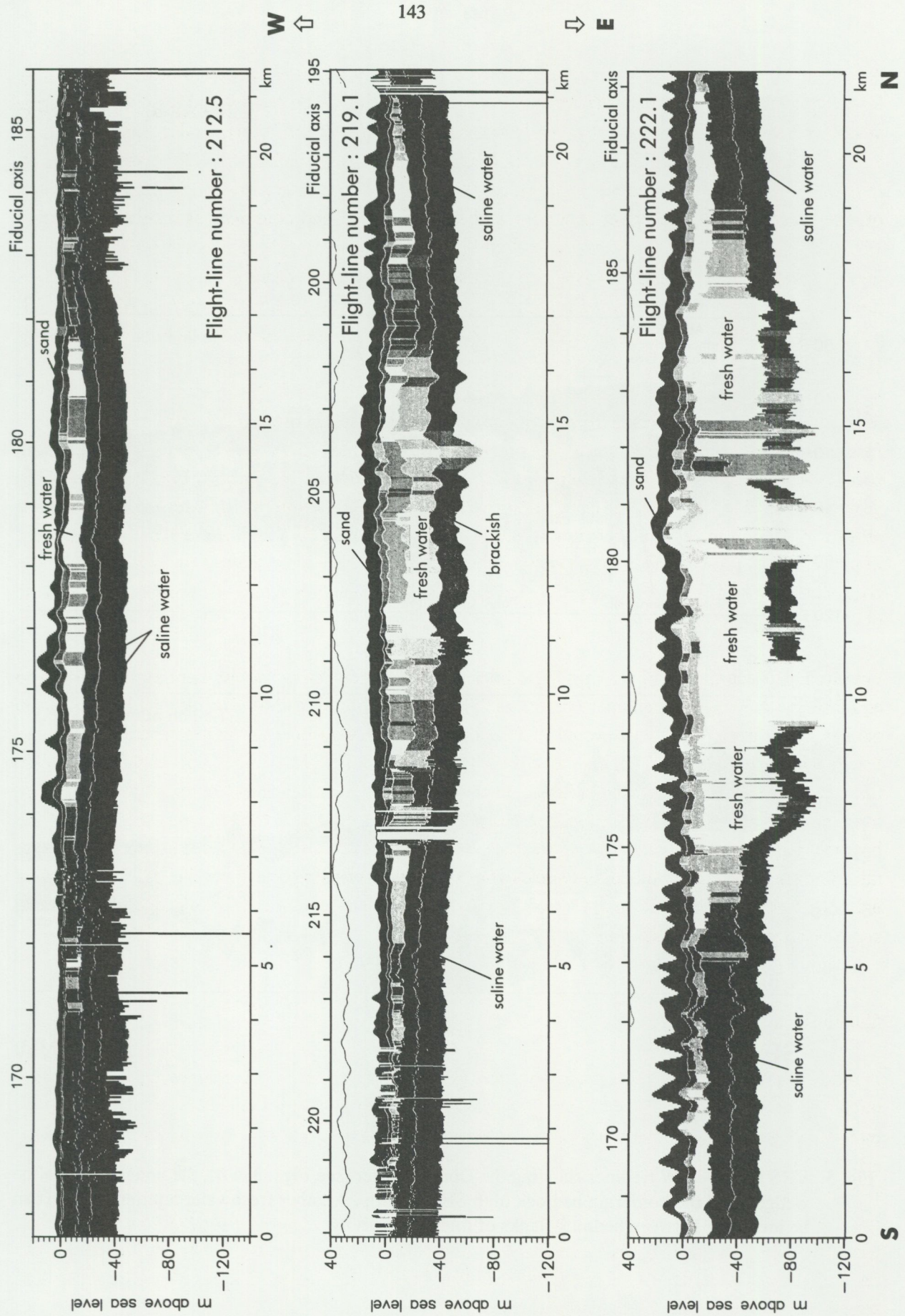


Fig. 4: Vertical resistivity sections (VRS) from airborne EM data provide a three-dimensional picture of a freshwater lens surrounded by saline water in a sandy environment (Dorop freshwater lens in Fig. 3). Flight lines are oriented N–S; line 212.5 is the westernmost, situated about 4 km E of the coast, the others follow 2.4 km and 3.6 km further inland. Resistivities are represented by grey shading and correspond to the types of groundwater indicated, known from drillings.

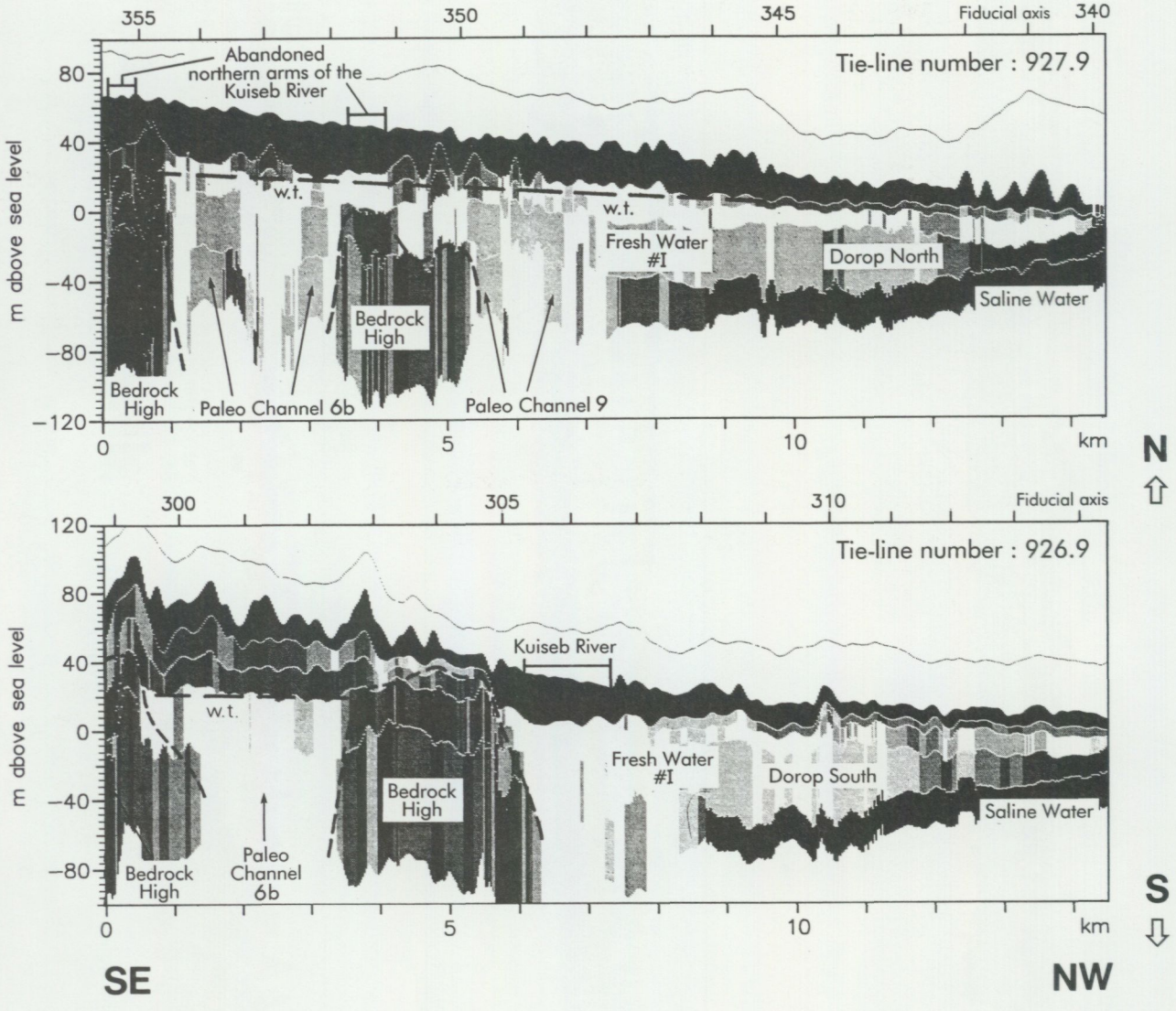


Fig. 5: VRS for SE–NW tie-lines showing the Dorop aquifer (see Figs. 3 & 4), the underlying "saline wedge", and the bordering bedrock high SE of Dorop. Another freshwater aquifer (PC 6b) can be identified between bedrock flanks of higher resistivity.

References

FRASER, D.C., 1978: Resistivity mapping with an airborne multicoil electromagnetic system. - Geophysics, v. 43, pp. 144-172.

PLÖTHNER, D., 1995: Status report of the German-Namibian groundwater exploration project (GNGEP), Jan. 1994 - Feb. 1995. - BGR archives no. 112 764 (unpublished), Hannover.

SENGPIEL, K.-P., 1988: Approximate inversion of airborne EM data from a multilayered ground. - Geophysical Prospecting 36, pp. 446-459.

SENGPIEL, K.-P., FLUCHE, B., LENZ, R., RÖTTGER, B., AND VOSS, W., 1994: Automatic inversion of AEM data into multilayer parameters and its application to groundwater exploration in the Namib Desert. Extended Abstracts Book of the International Meeting in Vienna. EAEG, Zeist.

SENGPIEL, K.-P. & SIEMON, B., 1995: The BGR helicopter survey in the Kuiseb Dune Area (Central Namib Desert) 1992; Interpretation of Geophysical Data. Vol. B-III. BGR archives no. 113 810 (unpublished), Hannover.

WARD, J.D., 1987: The Cenozoic succession in the Kuiseb Valley, Central Namib Desert. Geol. Surv. Namibia Memoir, 9, Windhoek.

Interaction of Salt/Fresh-water Flow and Hydrochemical Zoning in an Aquifer of Pyrmont Area, SW Lower Saxony

Johann-Peter Groetzner[1], Axel Rogge[1], & Peter-Christoph Scherler[2]

[1] Institut für Geologie und Paläontologie der Universität Hannover, Callinstr. 30, D-30167 Hannover
[2] Niedersächsisches Landesamt für Bodenforschung, Stilleweg 2, D-30655 Hannover

Abstract

The hydrodynamics and hydrochemistry of salt water and fresh water, including intermediate types, in solid rock aquifer systems in the area of Pyrmont are described on the basis of the latest research results (geoelectrics, isotop hydrology, soil air analysis). Theories on the source of the springs in this area are developed, which explain the different compositions of the springs and make it possible to protect them.

Bad Pyrmont is situated on a broad dome of Triassic rocks in the southern part of the Lower Saxony uplands. Inversion of the relief has caused the development of an erosion basin surrounded by a prominent ridge. Deep faults developed at the crest of the dome because this part of the structure was subjected to the strongest tectonic stress. Underground solution or subrosion of the Zechstein salts in the western part of the dome has caused the main salt bed to wedge out westwards along a N-S zone across the Pyrmont dome; this zone is reffered to as the "Salzhang" (salt slope). West of the "Salzhang", where subrosion has removed the salt bed that prevents gas rising from below, carbon dioxide of deep volcanic origin can now rise to the surface.

Extensive and deep-seated groundwater flow takes place within the entire Pyrmont dome and is illustrated by means of hydraulic sections. Groundwater flow is directed vertically downwards in the area of the surrounding ridge, centripetal horizontal flow predominates in the intermediate area, and the groundwater rises in the center of the basin to join the River Emmer, the main receiving stream.

The depth of the saltwater/freshwater interface is determined by the weight of the superimposed freshwater body. Hydrochemical sections show the shape and position of this interface and document a certain degree of hydrochemical zonation of the slightly mineralized fresh water. Genetic relationships between the two water types as well as within the hydrochemical zones of the freshwater body are described.

A knowledge of the hydrogeological relationships in the Bad Pyrmont aquifer systems permit wells withdrawing groundwater for different uses (medicinal, mineral, drinking and industrial water) to be sited relatively close together.

1. Introduction

Individual aspects of the geology and hydrogeology of the Bad Pyrmont area have been investigated over the past few decades, but during the last 20 years no comprehensive study has been carried out of the spring systems in the Pyrmont basin. A research project on the hydrogeology of the Bad Pyrmont area is being conducted by the University of Hannover using recently developed methods of investigation. The project is supported by the Lower Saxony Ministry for Science and Culture.

The aims of the project are to bring our knowledge of the geology of the Pyrmont anticline up to date, to investigate the hydrogeology of the Bad Pyrmont area with particular emphasis on the spring system, and to determine the source of the CO_2 in the spring water.

2. Methods used

Initially, an extensive search was carried out of the literature and unpublished records. This included all relevant data on springs, wells, gauges, and streams in the study area.

The update of the geology of the Pyrmont anticline was based on the results of recent drilling and the reinterpretation of older geophysical borehole logs. In the field, new exposures were examined and described. During the project, several boreholes were drilled and the data processed.

Geoelectric soundings were conducted in the study area together with the Joint Geoscientific Research Division of the State Geological Surveys of the FRG (part of the Lower Saxony Geological Survey). This was to obtain information about the shallow geology and the distribution of groundwater salinization of natural origin.
Soil air analyses were carried out to identify CO_2 anomalies, which possibly indicate the presence of fault zones.

A large number of hydrochemical analyses were carried out, which permitted several groundwater types to be recognised. In addition, an extensive hydrological survey based on isotope analyses carried out by the Lower Saxony Geological Survey provided valuable results.

The source and mode of formation of the groundwater were determined on the basis of interpretation and reconstruction of the hydrochemical regime and determination of the hydraulic relationships. These were derived in particular from measurements of the groundwater level and spring levels.

3. Results

The geological, hydrogeological and hydrochemical studies enabled a model of the origin of the Pyrmont springs to be developed. This in turn allowed the causes for the variable compositions of the springs to be postulated and provided data on which to base a scheme for protecting the springs. Before explaining the above model, it is necessary to give a short summary of the geology of the Pyrmont area.

3.1 Geology

Bad Pyrmont lies in the central part of a broad anticline of Triassic rocks about 35 km long and 12 km wide (Fig. 1).

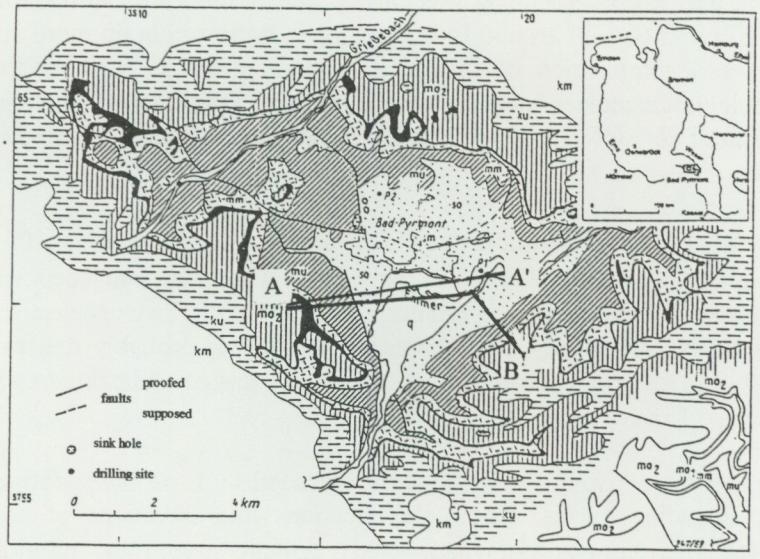


Fig. 1 Geological map of the Pyrmont anticline showing the location of sections A-B and A-A'

The Pyrmont basin, the broadened part of the Emmer valley in which Bad Pyrmont lies, is situated not quite at the centre of the crest of the Pyrmont anticline, which has an area of about 420 km^2. During formation of the anticline, the hinge region, which is the area of maximum strain, underwent deep fracturing. These fractures permitted groundwater to penetrate to considerable depths where the Zechstein salt was extensively dissolved. Underground solution or subrosion of the Zechstein salt in the western part of the Pyrmont anticline has caused the main salt bed to wedge out westwards from the so-called "Salzhang" (salt slope), a N—S zone running across the Pyrmont basin. . Since salt rock is impermeable to gas, its removal on the western side of the anticline permits CO_2 of volcanic derivation to rise towards the surface. Information on the nature of the, Rotliegendes, Zechstein and Buntsandstein in the core of the Pyrmont anticline has mostly been obtained from three boreholes, i.e. Pyrmont 1 (P1), Pyrmont 2 (P2), and Sonneborn (S). Figure 3 shows a geological section through the area.

The Pyrmont 2 borehole, which was drilled to tap thermal groundwater, penetrated the Zechstein and met a sequence of mostly strongly jointed, coarse sandstones, which probably belong to the Rotliegendes Cornberg Sandstone.

The Zechstein has a total thickness of about 600 m where it has not been affected by subrosion. It consists of several cycles, each comprising the sequence claystone, dolomite, anhydrite, and salt.

The lower part of the Buntsandstein consists of about 300 m of Lower Buntsandstein, alternating claystones and sandstones. The oldest rock outcropping in the built-up area of Pyrmont is the Middle Buntsandstein. It is 340—360 m thick and consists of an alternating sequence of sandstone and claystone. In the upper part there is a thick-bedded sandstone sequence (Bausandstein = building sandstone). The transitional beds to the Upper Buntsandstein (the Röt) comprise predominantly homogeneous, fine-grained, finely laminated shales with rare intercalations of thin, quartz-rich layers and sandstone beds. In the basal part of this sequence, there are intercalations of salt, anhydrite, limestone, and dolomite (Röt salt bed). The thickness of the Upper Buntsandstein where no underground solution (subrosion) of the evaporites has occurred is 170—200 m; the basal part mentioned above is about 50 m thick. About 140 m of Upper Buntsandstein was drilled in Pyrmont.

The higher and steeper parts of the hills surrounding Bad Pyrmont are made up of Muschelkalk, about 180—200 m thick and mostly limestones. Outside the hills, these rocks are overlain by the Keuper strata.. The bedrock in and around the Pyrmont area is overlain by superficial deposits of Quaternary age

In the spring of 1995, d.c. electric sounding was carried out by the Joint Geoscientific Research of the German Geological Surveys (GGA) around Bad Pyrmont in order to obtain more accurate information about the thickness and composition of the Quaternary deposits as well as the distribution and movement of geogenic salinization of the groundwater. The results are shown in the form of five vertical sections (BROST & ROGGE 1995) and are summarised shortly below. Fig. 3 shows section A—A´ as an example.

The Quaternary deposits consist predominantly of detritus, i.e. gravel and sand (100—130 Ωm), which is overlain by flood-plain loam (40—80 Ωm) in the valleys. The Quaternary deposits have a relatively uniform thickness of up to 30 m beneath the Emmer River lowlands. Two geoelectric stations where the base of the Quaternary is particularly deep represent exceptions, probably due to the presence of a concealed sinkhole above Röt or Zechstein salt. Alternatively, this could be due to a narrow Quaternary erosion channel.

The differences in specific resistivity and the different depths of various stratigraphic horizons on adjacent geoelectric sounding curves enable the locations and directions of several faults to be confirmed or corrected.

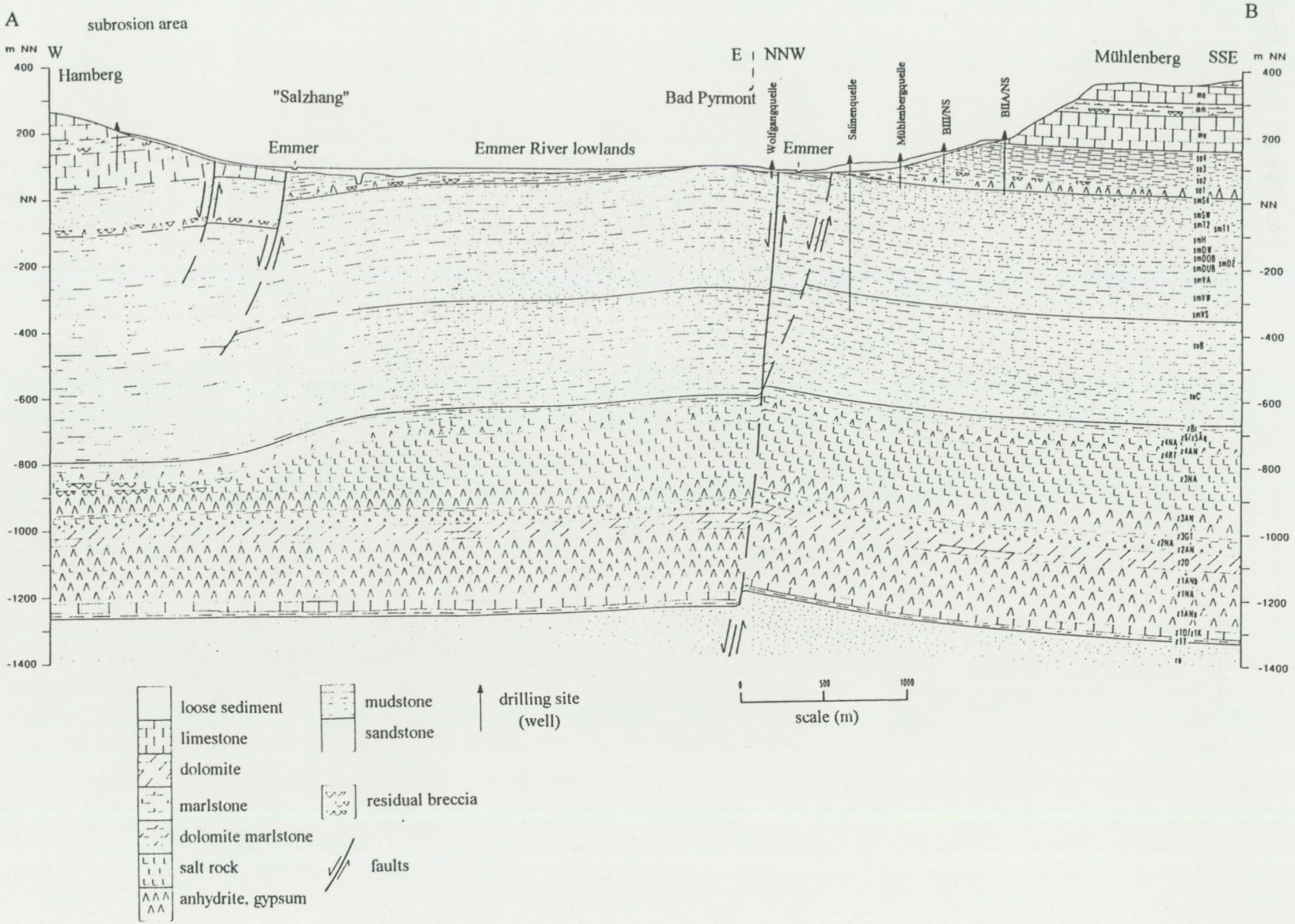


Fig.2 Geological cross section A—B

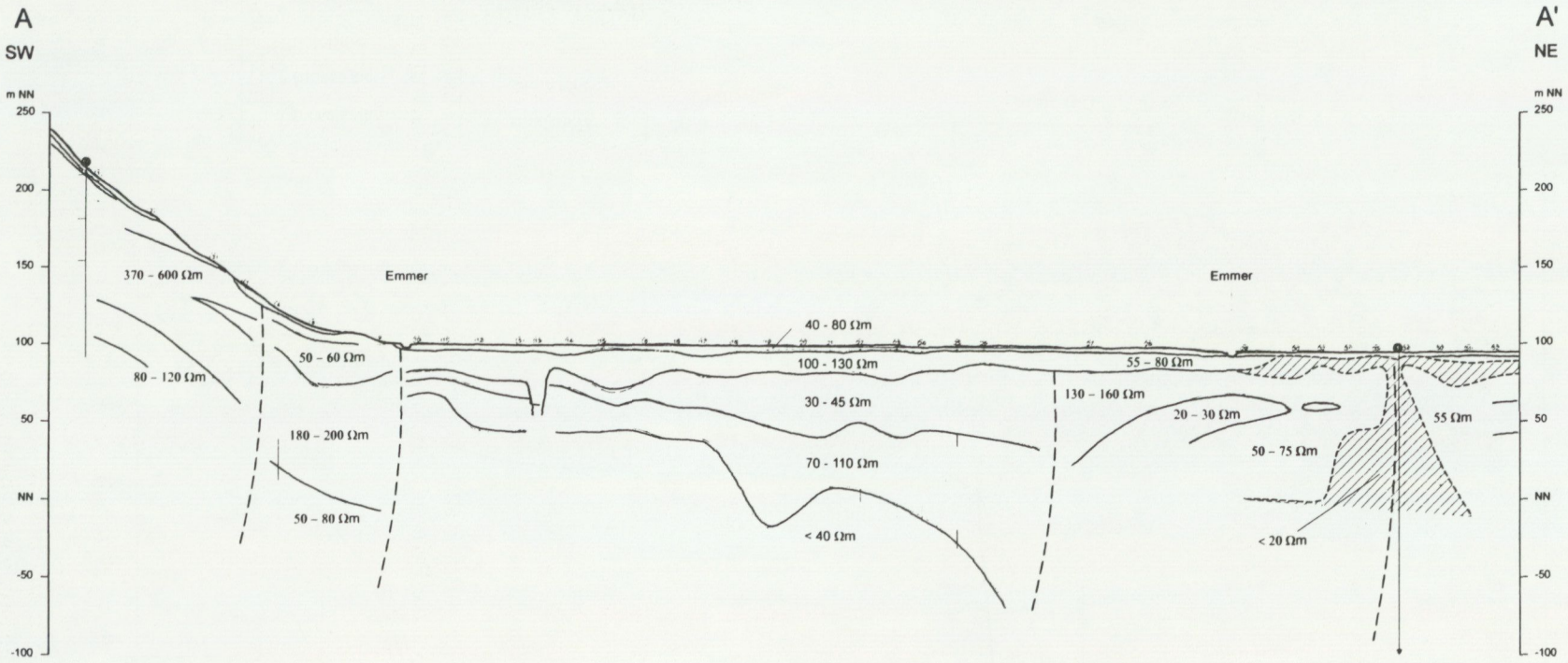


Fig.3. Geoelectric measurements at Bad Pyrmont, Section A—A´

The saline groundwater was demonstrated to be rising in the vicinity of a fault zone; moreover the distribution of salinized groundwater in the Quaternary deposits was plotted accurately. Evidence was found of salinized groundwater near the surface in the Emmer lowlands between Oesdorf and Löwensen within the urban area of Bad Pyrmont, as well as south of the swimming bath.

The geoelectric soundings show that clayey rocks belonging to the Buntsandstein are widely distributed below much of the Emmer lowlands. Below the Quaternary deposits, the low resistivities of 30—45 Ωm suggest claystone or siltstone of Röt age (Upper Buntsandstein) and clay transitional beds (Middle Buntsandstein). Below this the specific resistivity is 70—110 Ωm; this represents sandstones of the Middle Buntsandstein. This information is significant from the point of view of the protection these rocks afford to deeper groundwater (mineral-water aquifer).

The geoelectric soundings confirmed that the rocks above the Zechstein salt in the subrosion area NW of a line between Holzhausen and Lügde are considerably fractured, and also confirmed the position of the "Salzhang" described by HERMANN (1969b).

The positions and trends of several faults in the urban area (town park, "Dünsthöhle"), where it was not possible to carry out geoelectric soundings, were confirmed and corrected with the help of measurements of the CO_2 content of soil air.

The results of the geological studies are displayed in several geological sections. They form the basis of a model of the groundwater flow system supplying the Bad Pyrmont springs.

3.2 Hydrogeology

3.2.1 Hydrogeological structure

The hydrogeological structure is best explained using the semi-schematic cross section A—B (Fig. 4).

Over much of the area of the Pyrmont anticline, the Zechstein salt, which occurs at a depth of about 700 m below sea level, forms an almost impermeable lower boundary for the regional groundwater flow system. The area in which subrosion has taken place, i.e. west of the "Salzhang", represents an exception. In this area the salt bed, an effective barrier to rising water and gas, has been leached away, leaving a path free for rising CO_2 of volcanic origin. It is probable that the rise of CO_2 encourages the rise of groundwater, possibly confined groundwater, from the Rotliegendes into the overlying strata.

The lowest part of the aquifer system comprises the alternating claystones of the Lower Buntsandstein, which are present throughout the Pyrmont anticline. This part of the aquifer system contains slowly flowing or stationary groundwater.

The main aquifer of the mineral-water multiaquifer is made up of the sandstone-rich parts of the Middle Buntsandstein. They are separated by relatively impermeable clay-rich interbeds and alternating claystone-sandstone sequences. The Middle Buntsandstein is about 350 m thick and is also present throughout the study area. The uppermost beds, the Solling Buntsandstein crop out in parts of the Pyrmont basin.

On the limbs of the anticline the Upper Buntsandstein (Röt), a sequence about 100 m thick with a low to very low permeability, forms an aquiclude, which separates the mineral-water aquifer (Middle and Lower Buntsandstein) from the freshwater aquifer (Muschelkalk and Keuper). The permeability of the Röt is much enhanced in fault and fracture zones. The leached zones in the lower part of the Röt contain mineralised water and have a good permeability.

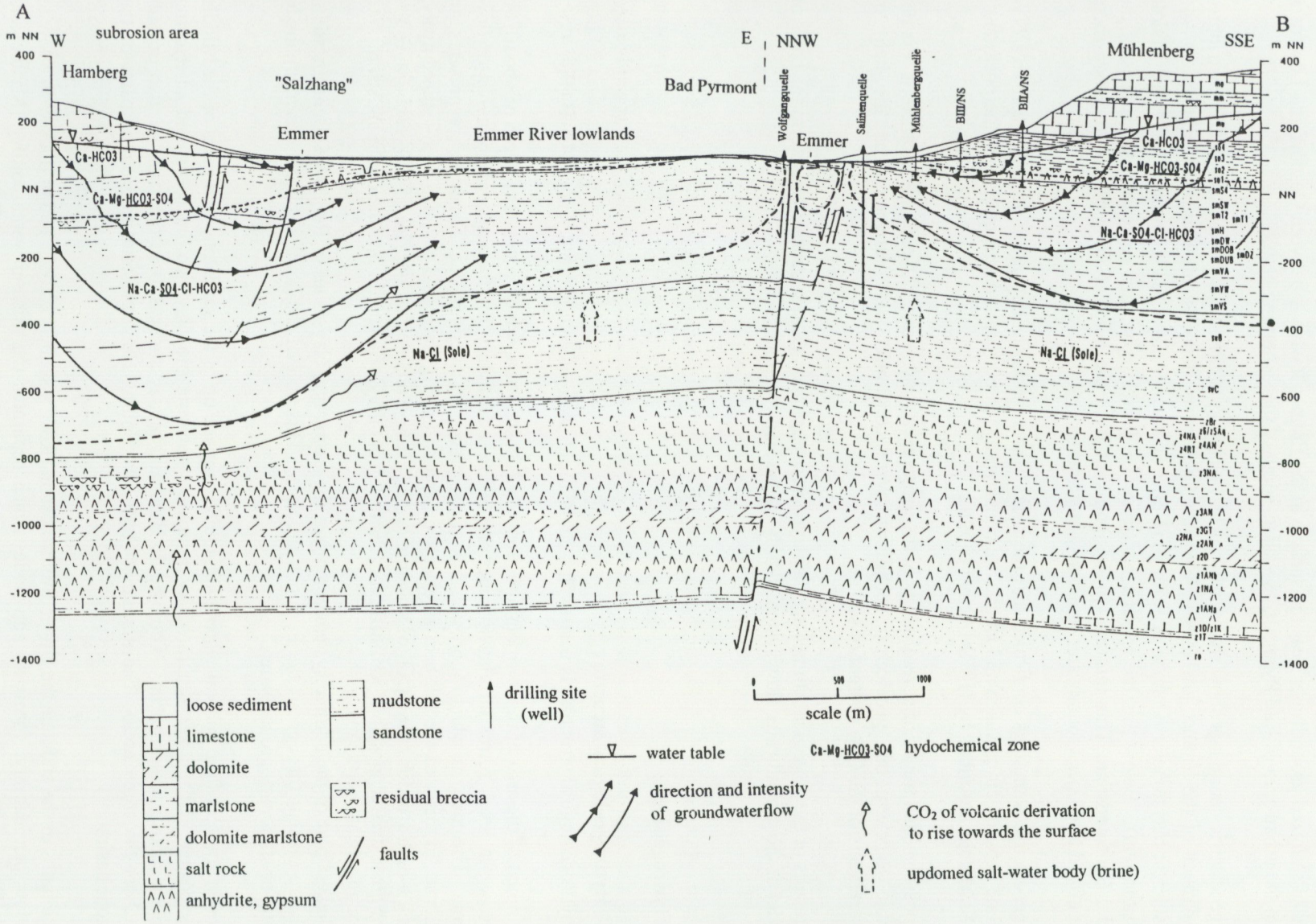


Fig. 4: Hydrogeological section A - B (semischematic)

The Lower and Middle Muschelkalk on the limbs of the anticline are important aquifers; they are separated by low permeability Middle Muschelkalk marls into two distinct aquifer levels.

The Keuper rocks have a predominantly low permeability. They are confined to the plateau in the SE part of the anticline core, and the outer parts of the limbs.

West of a line through Holzhausen and Lügde, subrosion has caused much deformation and fracturing of the strata. It must be assumed that the permeability is therefore considerably higher than in the other areas, in which the strata is almost undisturbed. The faults represent zones of particularly effective hydraulic conductivity.

3.2.2 Groundwater flow system

A model of the groundwater flow system in the Pyrmont pericline has been constructed on the basis of hydraulic data (groundwater levels and spring elevations) and the results of geological and hydrochemical studies. This provides considerably more insight into the hydrogeology of the area than previous descriptions (HERRMANN 1969a, SCHERLER & HAHN 1992). The hydrogeological situation of the Pyrmont springs must be assumed, in analogy to current hydraulic models, to have an extensive and deep-reaching groundwater flow system (Fig. 4) that extends over the whole Pyrmont pericline and can be subdivided into:

- elevated groundwater recharge areas (hills surrounding the area)
- connecting intermediate zones,
- low lying discharge areas (Pyrmont basin, Emmer lowlands)

This system can be divided on the basis of lithological, hydraulic and hydrochemical factors into 3 subsystems:

a) shallow near-surface groundwater flow system in the Quaternary deposits (pore groundwater, freshwater aquifer),
b) deeper groundwater flow system in bedrock (mostly fracture aquifer, freshwater and mineral-water levels),
c) more or less static, deep-groundwater flow system (saline water, brine).

In addition, the hydrogeological system of the Pyrmont anticline contains a large number of sometimes very local and often interconnected aquifers and aquitards, as well as fault zones.

In the hills surrounding the basin (groundwater recharge area), the downward vertical component of flow predominates, in the intermediate area the flow is horizontal and in the Emmer lowlands the groundwater rises (discharge area).

3.2.3 Interplay between rising saline water and near-surface groundwater

The flow velocity of groundwater decreases rapidly with increasing depth. This is partly due to the decrease in permeability of the rocks at depth and to the fact that the deeper groundwater is mineralized and has a higher density than fresh water.

The near-surface groundwater flow system in the Quaternary deposits together with the deeper groundwater flow system in bedrock form a major hydraulic unit. In contrast, the almost static flow system (saline water) plays a different hydraulic role. The fresh and mineralised groundwater is separated from the saline groundwater by a barrier. Diffusion and hydromechanical dispersion through this barrier, and vertical oscillations of the saline groundwater have led to the formation of a mixed zone, whose thickness is unknown, in which water and ion exchange between the two flow systems takes place. The regional flow system of the saline water is not yet known. One can postulate that it is towards the Weser River, being the nearest large receiving stream. The depth of the contact between the freshwater and mineral-water/ saline water depends on the weight of the overlying fresh and mineral-water body. This is highest beneath the peripheral hills. In the Emmer lowlands, where the pressure

from the overlying groundwater is reduced by the groundwater discharging into the receiving stream (the Emmer River), the saline-water body is domed up.

As the results of the geoelectric soundings in the Emmer lowlands (BROST & ROGGE 1995) have shown, saline water migrates along hydraulically effective fault zones into the vicinity of the surface and spreads out laterally in the permeable Quaternary gravels. The rise of saline water is possibly facilitated by a gas-lift effect. This is caused by pressure due to the release of CO_2. The CO_2 of volcanic origin rises in the area in which the Zechstein has undergone subrosion into higher levels and there becomes mixed with saline groundwater and the circulating mineral water. This probably leads to mixing of the saline water and mineral water, but to an unknown extent.

The saline groundwater emerging in the Pyrmont medicinal springs is derived from the Zechstein salt, which is present about 800 - 1100 m deep beneath the springs. The main source is assumed to be the "Salzhang", which is still being leached. In the subrosion area west of the "Salzhang", mineralized groundwater descends to considerable depth as a result of the amount of fracturing which the rocks there have undergone. There, it dissolves the Zechstein salt, sometimes producing brine and sometimes mixed groundwater. It is possible that the leaching process is chemically facilitated by CO_2, which rises in this area from Paleozoic rocks beneath.

As the diagram of the groundwater flow system shows, all the Bad Pyrmont medicinal springs yield a mixture of slightly mineralized groundwater that flows down towards the valley and more mineralized groundwater rising from much deeper levels. Differences in the total dissolved solids (mineralization) are a result of differences in the hydraulic conductivity of the fault zones and different spring heights or abstraction depths. The proportion of rising deep groundwater tends to decrease with height of spring or abstraction level. In other words, the total mineralization decreases upwards.

3.3 Hydrochemistry

The Bad Pyrmont medicinal springs fall into three groups of different kinds of mineralization:

A. mineral-poor and mineral-rich hydrogen carbonate water

Ca-Mg- $\underline{HCO_3^-}$-$SO_4^=$ acidulous type

B. mineral-rich

Na-Ca-$SO_4^=$ Cl-HCO_3^- type

C. very highly mineralized chloride water

Na-$\underline{Cl}$- $SO_4^=$ and Na-Cl (brine) acidulous types

In spite of the fact that the transition from strongly circulating, little mineralized groundwater to deeper, almost static, highly mineralized groundwater may be very variable and irregular (DVWK 1987, 1983), it is still possible to subdivide the Bad Pyrmont area into hydrochemical zones. This can be shown to be genetically related to the groundwater flow system. The composition of the water from the individual zones is dealt with shortly below (see above Fig. 5).

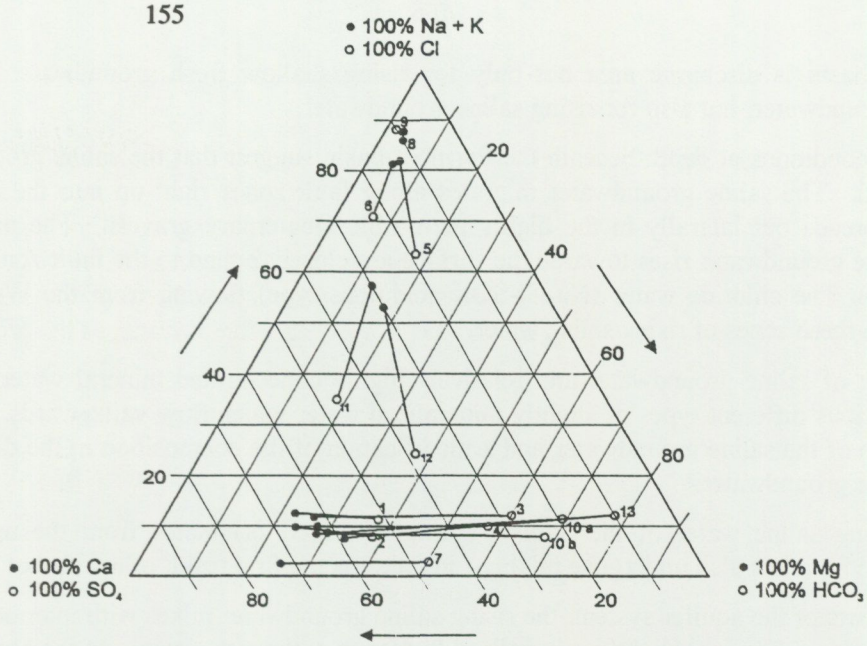


Fig. 5: Anion-cation diagram for the Bad Pyrmont medicinal springs.

Groundwater recharge takes place in the hills surrounding Bad Pyrmont. The groundwater then mostly flows over a long period of time down to a depth of about 1000 m. There is some interreaction between the aquifer and various kinds of groundwater. The composition of the water is the result of various physicochemical processes such as:

- solution and precipitation,
- adsorption, desorption and ion exchange,
- diffusion,
- oxidation and reduction,
- mixing.

Below the hills surrounding Bad Pyrmont, a hydrochemical zonation can be demonstrated on the basis of the different types of groundwater in the springs and wells of that area (BII/NS, Mühlenberg spring, and saline spring). Hydrogen carbonate water is underlain by sulphate water and this in turn by chloride water.

Infiltrating water from precipitation (groundwater recharge) takes up CO_2 while it passes through the soil. The action of the CO_2 on the carbonate in the Muschelkalk (mu) causes Ca and HCO_3^- ions to go into solution in the near-surface groundwater. This slightly mineralized hydrogen carbonate water circulates fairly rapidly and is usually oxygen-bearing. Solution of gypsum and anhydrite in the Middle Muschelkalk (mm) and Upper lower Röt (so4 to so2) gives the groundwater an elevated $SO_4^=$ content.

During its downward passage into deeper parts of the aquifer system, the groundwater dissolves considerable amounts of gypsum and anhydrite from the relict salt beds in the Röt. $SO_4^=$ now assumes a dominant role in the composition of the groundwater. Free oxygen disappears as a result of the oxidation of sulphide and decomposition of organic matter. The HCO_3^- is considerably reduced on account of the strong increase in total mineralisation.

The high NaCl concentration in more or less static groundwater at deep levels is probably due to solution (subrosion) of Zechstein salt, particularly at the Zechstein "Salzhang".

Diffusion and hydrochemical dispersion at the interface between the almost static, highly mineralized, chloride water (brine) and the clearly circulating sulphate water causes mixing in these two types of groundwater. The resulting mixed water flows towards the discharge area, the Bad Pyrmont basin, and as it rises, it mixes with slightly mineralized water of various compositions.

The Pyrmont basin is discharge area not only for rising shallow fresh groundwater and relatively mineralized groundwater, but also for rising saline groundwater.

The hydraulic conditions at depth beneath the Pyrmont basin suggest that the saline groundwater body is dome shaped. The saline groundwater migrates along fault zones right up into the rocks near the surface and spreads out laterally in the highly permeable Quaternary gravels. The pathways along which the saline groundwater rises towards the surface are closely bound to the fault zones (BROST & ROGGE 1995): The chloride water (Na-Cl-$SO_4^=$ acidulous type) flowing from the Wolfgang spring originates from these zones of rising saline water.

During the rise of saline groundwater and relatively highly concentrated mineral water, they become mixed with various different types of slightly mineralized water which flow valleywards. This causes a general dilution of the saline groundwater and a modification of the composition in the direction of that of the shallower groundwater.

The CO_2-bearing saline water of the Salinen springs I and II originates from the updomed saline groundwater body; it has also undergone mixing - in fact it is the first result of a series of mixings.

In the higher parts of the aquifer system, the rising saline groundwater mixes with intermediate sulphate water and downward-flowing, slightly mineralized hydrogen carbonate water. At the abstraction depth of the Mühlenberg spring, mixing (in this case dilution) has produced a mineral water belonging to the Na-Ca-$SO_4^=$-Cl-HCO_3^- type.

As it rises further, the proportion of chloride water decreases in favour of the hydrogen carbonate water with which it is mixed. This produces a mineral water belonging to the Ca-Mg-HCO_3^--$SO_4^=$ acidulous type, which is characteristic of many of the springsand wells in the town area of Bad Pyrmont.

References

BROST, E. & ROGGE, A. (1995): Geoelektrische Messungen zur Erforschung der Quartärbasis und der geogenen Grundwasserversalzung im Raum Pyrmont.- Archiv NLfB: 7 S., 6 Anl.; Hannover.- (Unveröff.)

DVWK (1983): Beiträge zu tiefen Grundwässern und zum Grundwasserwärmehaushalt.- DVWK-Schriften **61**: 166 S.; Hamburg, Berlin.

DVWK (1987): Erkundung tiefer Grundwasser-Zirkulationssysteme.- DVWK-Schriften **81**: 223 S; Hamburg, Berlin.

HERRMANN, R. (1969a): Die Heilquellen von Bad Pyrmont, ihre Beschaffenheit und ihre Herkunft.- N. Arch. f. Nieders., **18:** 3-14; Göttingen.

- (1969b): Die Auslaugung der Zechsteinsalze im niedersächsisch-westfälischen Grenzgebiet bei Bad Pyrmont. - Geol. Jb., **87:** 277-294, 6 Abb., 2 Tab., 1 Taf.; Hannover.

SCHERLER, P.-Chr. & HAHN, J. (1992): Balneogeologische Nutzung von Solequellen in Niedersachsen.- Nds. Akad. Geowiss. Veröfftl., **8**: 44-57; Hannover.

Quality evolution of the fresh and salt groundwater pumped near a drainage canal in the Western Flemish coastal plain

L. Lebbe[1,3], E. Van Houtte[2], F. Vanlerberghe[2] en W. De Breuck[1]

[1] Laboratory of Applied Geology and Hydrogeology (LTGH), University of Ghent, Krijgslaan 281 - S8, B-9000 Gent

[2] Intermunicipal Water Company of Veurne-Ambacht (IWVA) Doornpanne 1, B-8670 Koksijde

[3] National Fund of Scientific Research, Belgium

INTRODUCTION

Until now, 65 % of the water supplied by the Intermunicipal Water Company of the Veurne Region (IWVA), is pumped from the fresh water lens in the dune belt of the western Flemish coastal plain. Because this extraction has reached its maximum capacity, the IWVA plans to optimize the water production by recharging water into the dunes. During winter, a large amount of fresh surface water is available in the polder area south of the dune belt. Especially the Avekapelle region is a potential intake region, because of the presence of a sandy creek ridge. This Avekapelle creek ridge is drained by two canals, the Kromme Gracht in the west and the Oude A-vaart in the east. The drainage water is of relatively good quality. Until now it is evacuated to the sea, as quickly as possible.

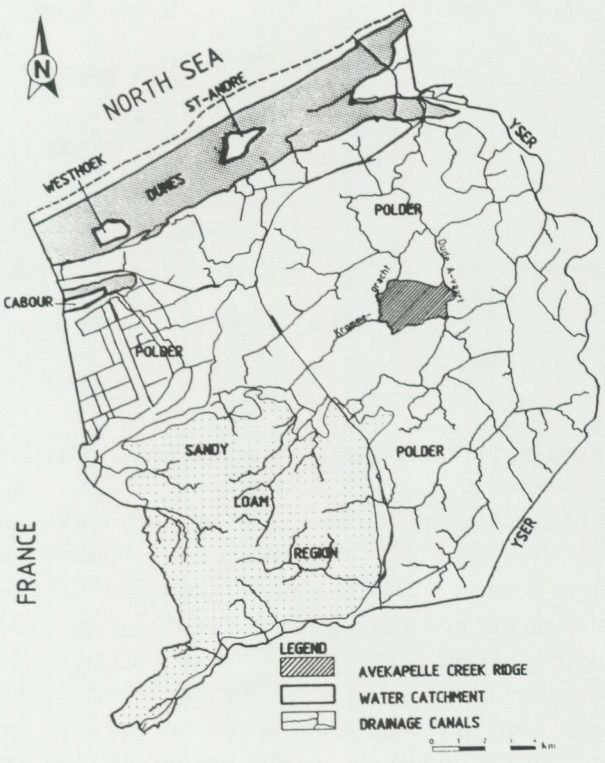


Figure 1. Location of the investigation area

DESCRIPTION OF THE PROJECT

In the dune water catchment of St-André, the IWVA plans to increase its water production by creating an infiltration basin with a capacity of 2 to 2,5 million m^3/year. To prevent propagation of the recharged water, the total amount of this water will be extracted by production wells in the vicinity of the basin. The minimum residence time of the recharged water in the phreatic aquifer will be in the order of six weeks. This is to ensure that the produced water will be bacteriologically safe.

The project will allow a total production rate of 3,5 to 4 million m^3/year in St-André, which means that the netto-groundwater production in these dunes will diminish by 0,5 million m^3/year. The production of drinking water from a combination of groundwater and surface water has a lot of advantages. The existing production system can be used. The recharge will restore natural groundwater levels and will also prevent salt water encroachment in the phreatic aquifer from the beach and from the polder area, respectively north and south of the water catchment.

The quality of the recharge water will improve so that it will approximate dune water quality. In case of pollution the recharge can be stopped while the production can still continue for a short period. Furthermore, the produced groundwater will be bacteriologically clear and no disinfection is needed (Van Houtte et al., 1995).

The recharge water could be produced in the central part of the Avekapelle creek ridge. Extraction wells alongside an intake canal, connecting the Kromme Gracht and the Oude A-vaart and crossing the creek ridge, would make it possible to capture the surface water. Because the aquifer under the creek ridge is filled with fresh water in the upper part and salt water in the lower part, it will be necessary to construct extraction well pairs. One of the wells of a pair should be screened in the upper part of the aquifer. This well will withdraw infiltrating surface water and fresh water from the aquifer. The other well of a pair should be screened in the lower part of the aquifer and will produce salt water. This system will prevent an upward flow of brackish and salt water to the fresh water wells. In order to smoothen the effect of different qualities of intake water, the well pairs must be constructed at various distances from the intake canal. After treatment, the fresh water will be pumped to the dune area. The pumped salt water will be piped to the sea.

HYDROGEOLOGY OF THE AVEKAPELLE CREEK RIDGE

The permeable Quarternary sediments form the phreatic aquifer. The thickness of this aquifer varies between 12 and 30 m. Under the central part of the Avekapelle creek ridge, the aquifer consists of a succession of fine and medium sands with shells. The top of the aquifer generally contains sandy clays. Closer to the Oude A-vaart the lower part of the Quarternary sediments become clayey. The reservoir is bounded below by Tertiary clay (Fig. 2), which can be considered as an impervious substratum.

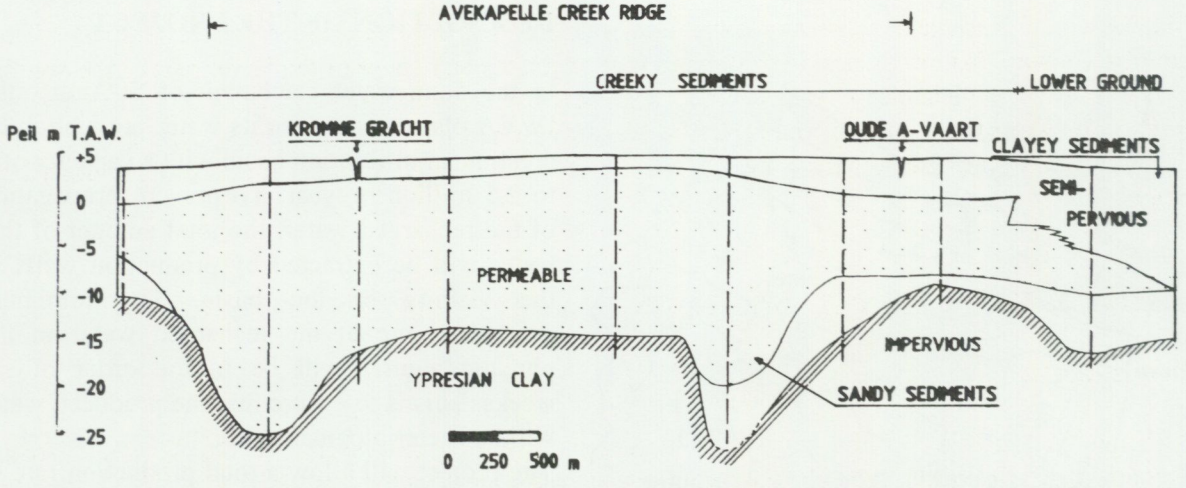


Figure 2. Lithological WE-section through the central part of the Avekapelle creek (Zeuwts, 1991)

The quality of the groundwater in the central part of the Avekapelle creek ridge varies from top to bottom (Fig. 3). According to the classification of Stuyfzand (1986), Zeuwts (1991) observed a succession of the following types of water from top to bottom : (1) fresh water of the F-$CaHCO_3$, F-CaMix and F-$CaSO_4$-types; (2) fresh-brackish water of the F_b-$CaHCO_3$ and F_b-$NaHCO_3$-types; (3) brackish water of the B-$CaHCO_3$ and B-$NaHCO_3$-types; (4) brackish water of the B-NaCl-type; (5) brackish-salt water of the B_s-NaCl-type and (6) salt water of the S-NaCl-type. In the vicinity of the Kromme Gracht and the Oude A-vaart the fresh/salt water interface rises because of the drainage activity of those canals (Zeuwts, 1991). The groundwater movement in the central part of the Avekapelle creek ridge is dominated by the drainage canals, which means that the groundwater under the creek ridge flows towards the Kromme Gracht and the Oude A-vaart.

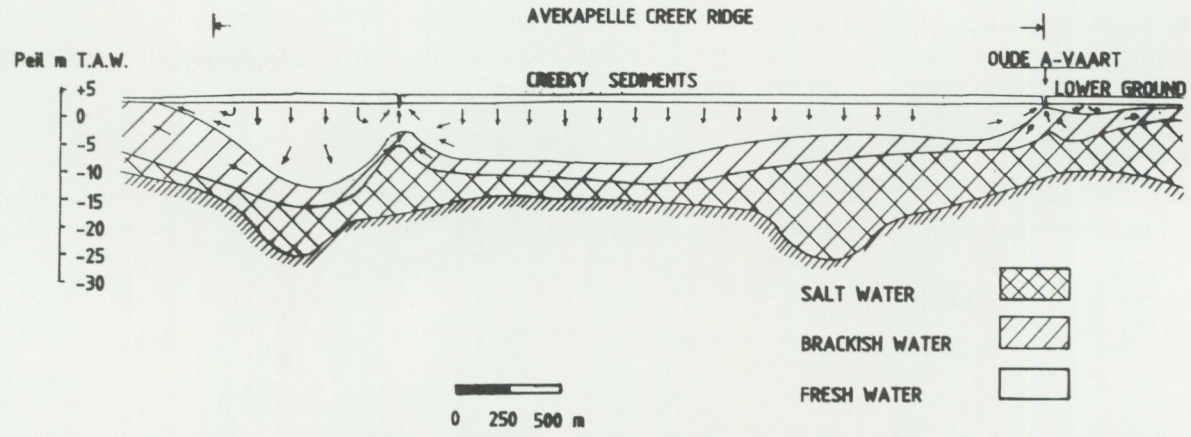


Figure 3. Fresh/salt water distribution in the aquifer of the Avekapelle creek (Zeuwts, 1991)

A double pumping test in the Avekapelle creek ridge (Lebbe et al., 1995) showed that the hydraulic resistance between the intake canal and the upper part of the aquifer is low (in the order of 9 days). During this test, the salt water from the lower part of the aquifer was discharged during 3 days at a rate of 144 m^3/day. After the first day of pumping, the fresh water from the upper part of the aquifer was extracted at a rate of 59 m^3/day. Despite the small hydraulic resistance between the upper and lower part of the aquifer (6 days), the water pumped from the upper well did not become brackish, because the hydraulic head in the lower part of the aquifer was lower than in the upper part. The sediments in the upper part of the aquifer have a horizontal hydraulic conductivity of 5,54 m/d; the sediments of the lower part 5,70 m/d. The specific elastic storage of the Quarternary sediments is 1.9 10^{-4} m^{-1}; the specific yield 0,022.

Simulation of fresh and salt water extraction, respectively from the upper and lower part of the aquifer, showed that after a period of three to four years, the salt water of the lower part of the aquifer would freshen, which means that it could also be used to recharge the dunes. To investigate the relation between the quality of the produced fresh water and the quality of the surface water, it was decided that a long-term double pumping test had to be done. The results of this test are described below.

LONG-TERM DOUBLE PUMPING TEST IN THE AVEKAPELLE CREEK RIDGE

Description

Although the location of the test site is not optimal due to the vicinity of the Kromme Gracht (upconing of salt water), the existing pumping and observation wells were used. There is no suitable location available more to the centre of the creek ridge at a certain distance from the canals. The pumping wells (PP1 en PP2) are at 1 m distance from one another. The shortest distance between the Kromme Gracht and the upper pumping well (PP2) is 8 m. Four observation wells are placed in a WSW-ENE direction (Fig. 4) : two in the upper part of the aquifer (2.3 and 2.4) and two in the lower part (1.3 and 1.4). Another four observation wells, two in the upper (2.1 and 2.2) and two in the lower (1.1 and 1.2) part of the aquifer, are located on a line perpendicular to the first mentioned direction.

The pumping test started on December 11th, 1995 and lasted until April 22nd, 1996. The mean discharge rate until March 11th, 1996 was 5,09 m^3/h for PP1 and 2,64 m^3/h for PP2. On this day the discharge rate from well PP2 was reduced to 2,04 m^3/h. It remained constant until April 22nd. However, from March 11th, on the discharge rate from well PP1 gradually declined to 4,6 m^3/h and averaging 4,83 m^3/h for the period March 11th - April 22nd. The drawdown in the wells was recorded

by a datalogger from December 11th until December 20th, 1995. During the rest of the time the drawdown was measured manually.

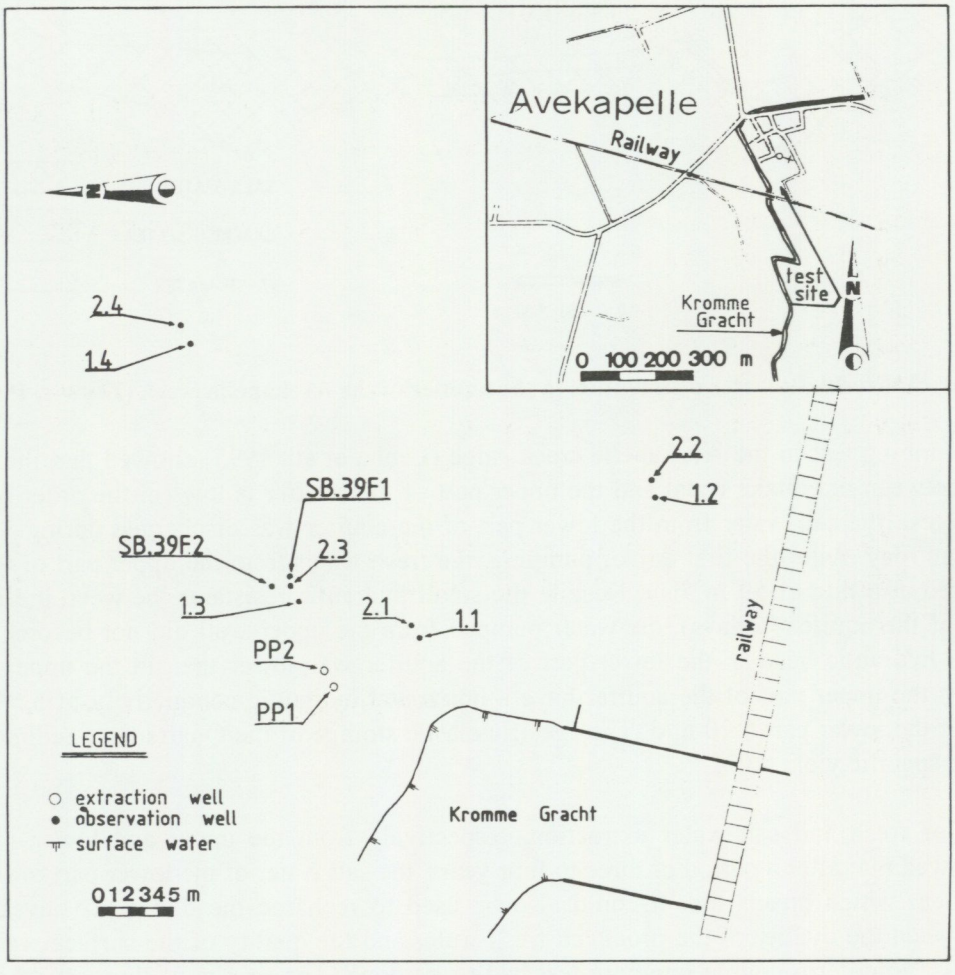


Figure 4. Configuration at the test site

The quality of the fresh groundwater (well PP2) and of the surface water was monitored by automatic registration of the electrical conductivity during the first month of the test. Also the following parameters were analysed on a regular basis (Fig. 5) : electrical conductivity, pH-value and temperature; the anions chloride, nitrate, nitrite, sulphate and bicarbonate; the cations sodium, potassium, calcium, magnesium, ammonium, total iron and total phosphorus. The bacteriological contamination was controlled by counting total coliforms.

Quality of the surface water

The water of the Kromme Gracht is fresh. The mean chloride content is 236 mg/l, varying between 147 and 545 mg/l. The electrical conductivity varies from 1056 µS/cm to 1770 µS/cm, and the sodium content from 66 to 318 mg/l with an average of 146 mg Na^+/l. There is a good relationship between those parameters : high electrical conductivity corresponds with high contents of chloride and sodium (Fig. 5). The potassium content is relatively stable averaging 19,8 mg K^+/l and varying from 13 to 26 mg K^+/l. The surface water caries an important load of contaminants with mean levels for nitrate of 29,1 mg/l, nitrite of 0,43 mg/l, ammonia of 2,72 mg/l, total phosphorus of 0,84 mg/l and sulfate of 248 mg/l.

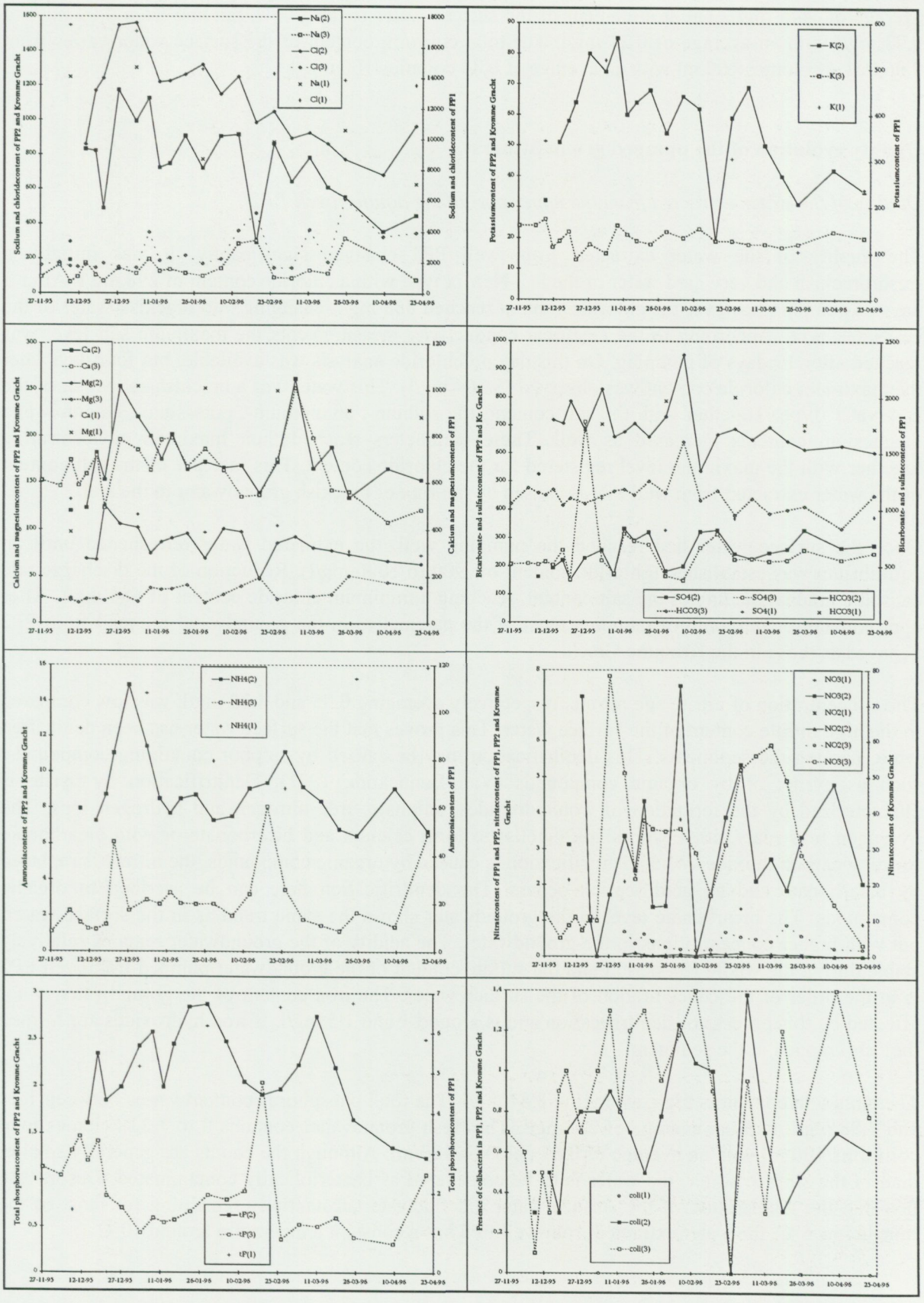


Figure 5. Chemical quality of the extracted salt (PP1, 1) and fresh (PP2, 2) groundwater and of the surface water (Kromme Gracht, 3)

The surface water is hard : the calcium content varies between between 108 and 252 mg/l with an average of 164 mg/l; the magnesium content varies between 22 and 51 mg/l with an average of 32,2 mg Mg^{2+}/l. The bicarbonate content is relatively stable and ranges between 334 and 641 mg/l with an average of 445 mg/l. The iron content of the surface water is fairly low, ranging from 0,09 mg/l to 0,73 mg/l with an average of 0,24 mg/l. The total coliform content of the surface water varies from 0,06 to 1,4 colonies/100 ml with an average of 0,84 colonies/100 ml.

Quality evolution of the pumped groundwaters

Quality of the water extracted from the upper part of the aquifer (well PP2)

The quality of the water extracted from well PP2 changed significantly. It was initially a fresh/brackish and very hard water of the F_b3-NaMix type with a chloride content of 298 mg/l. After 3 days of pumping however the chloride content reached 858 mg/l, changing into brackish water of the B3-$NaCl^+$ type. According to the electrical conductivity measurements the maximum salt level was reached after 19 days of pumping. On this day no chloride analysis was available, but four days later the maximum chloride content was observed (1.564 mg/l). This water was a brackish/salt water of the B_s4-$NaCl^+$ type. Together with the salt content, the sodium-, ammonium-, potassium-, calcium- and magnesium contents increased as well. These parameters reached their maximum concentration together with the maximum level registered for the chloride content. This increase of the salt content of the water extracted from well PP2 is caused by the flux of brackish groundwater to the well.

Once the surface water had reached the pumping well, the extracted water refreshened until an equilibrium was established (chloride content of 900 to 1000 mg/l). Reduction of the discharge rate caused a gradual decline of the salt content, reaching a minimum chloride content of 684 mg/l. After approximately one month of pumping most of the parameters in the groundwater pumped from PP2 behaved as those in the Kromme Gracht.

The concentration of nitrite and nitrate, respectively averaging 0,05 and 3,23 mg/l, was low compared to the high nitrate content of the surface water. This proves that the surface water has been denitrified while passing the sediments. This denitrification may be caused by sulphur containing compounds, such as pyrite, or by organic compounds (Van Bennekom, 1991). Denitrification by pyrite is characterized by the formation of ironhydroxides, sulphate, free nitrogen and hydrogen ions. The hydrogen ions react either with chalk (shells) to form calcium and bicarbonate or with bicarbonate forming carbon dioxide. When denitrification is caused by organic compounds, the nitrate is replaced by bicarbonate and no acidification occurs. The denitrification here can be ascribed to organic compounds. The bicarbonate level in the groundwater shows the same trend as in the surface water, but with higher concentrations in the groundwater. The acidity of the groundwater remains relatively stable during the whole test period and the sulfate content of the groundwater pumped from well PP2 is in the order of the concentration of the surface water. The iron content of the groundwater is not affected by this process of denitrification and is around 1 and 1,5 mg/l. If iron hydroxides are formed they are trapped in the sediment.

The ammonia content is high, averaging 8,84 mg/l. The total phosphorus content varies between 1,24 and 2,88 mg/l, with an average of 2,1 mg/l. The fresh groundwater contains 0 to 1,23 colonies total coliforms/100 ml with an average of 0,69 colonies/100 ml. Although the counts are generally smaller than in the surface water, the water is to be considered as bacteriolically contaminated. Despite the fact that the temperature of the surface water did fluctuate substantially remaining for most of the time below 5°C, the water extracted from well PP2 has a constant temperature around 10°C.

Quality of the water extracted from the lower part of the aquifer (well PP1)

The water extracted from well PP1 was a salty and very hard water of the S6-$NaCl^+$ type with an initial chloride content of 17.434 mg/l. The salt content gradually diminished as the pumping went on, but the water was still salty and of the S6-$NaCl^-$ type. The final chloride content was 13.532 mg/l, which is 77,6 % of the initial content. Similar to the decrease of the electrical conductivity and the chloride content, a decrease of the sodium-, potassium-, calcium- and magnesium content is observed. The salt water is rich in iron and ammonia. The nitrite and nitrate content is low. The total phosphorus content increases as pumping goes on. The water extracted from well PP1 is bacteriologically safe with a constant temperature of about 11°C.

SIMULATION OF GROUNDWATER QUALITY EVOLUTION

A first attempt is made to simulate the groundwater quality evolution near a drainage canal by means of the adapted MOC model. This model of Konikow and Bredehoeft (1978) was adapted so that density differences are taken into account (Lebbe, 1981 and Lebbe, 1983). Fig. 6 shows the geometry and subsoil parameters of the cross-section. By means of a double pumping test the hydraulic conductivities of the groundwater reservoir have been determined (Lebbe et. al, 1995). Four different layers have been identified: a lower pervious layer (k^h=5.7 m/d), a middle less pervious layer (k^h=2.4 m/d), an upper pervious layer (k^h=5.4 m/d) and an upper semi-pervious layer (k^h=0.6 m/d). The ratio vertical versus horizontal conductivity is 0.4. According to the results of the modeling regression of the salt water lens on the shore of De Panne (Lebbe, 1996) the longitudinal and the transversal dispersivity have small values (α_L=0.061 m and α_T/α_L=0.25). The effective porosity n_e is 0.38. No storage changes are considered in the model.

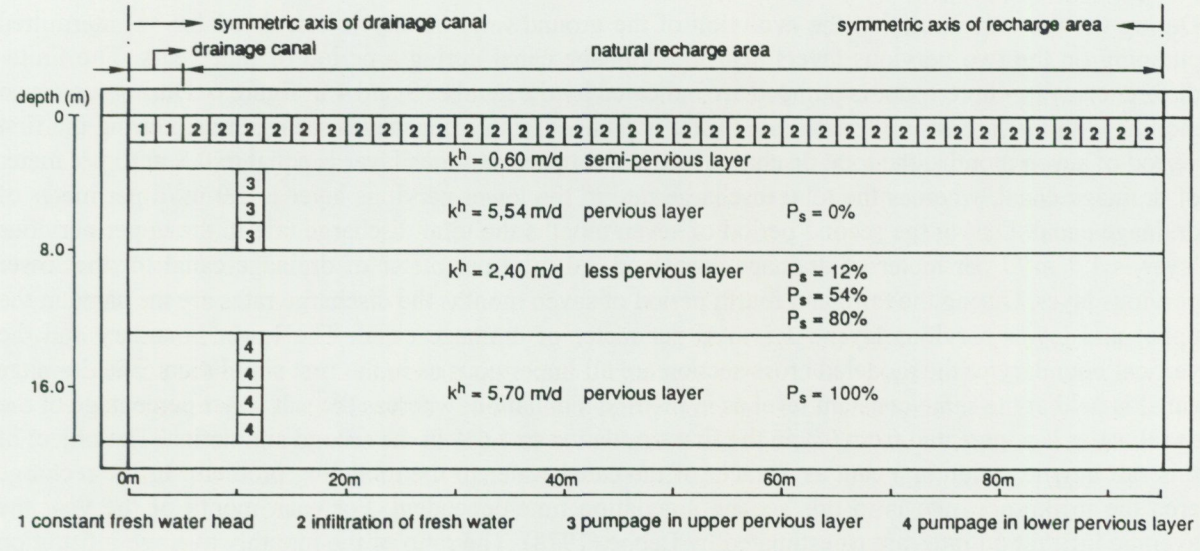


Figure 6. Geometry and subsoil parameters of the modeled cross-section

The modeled cross-section is subdivided in 12 layers and 38 columns. All columns have the same width (2.5 m) and all the layers the same thickness (1.6m). The lower boundary of the modeled cross-section coincides with the top of the 100 m thick Tertiary clay layer and is impervious in the model. The two vertical boundaries of the cross section are supposed to be impervious because they coincide with water divides. One vertical boundary is located under the middle of the drainage canal, the other vertical boundary in the middle of the recharge area. The upper boundary is a constant flux boundary under the natural recharge area and a constant head boundary (fresh water head is 1.9 mTAW).

The initial salt water distribution is first calculated by means of a first simulation. During this first simulation a constant infiltration of 0.069 m^3/d of pure fresh water per meter of drainage canal (280 mm/year) is assumed whereas the head in the drainage canal is constant. Because of this boundary condition a groundwater flow arises which deforms the transition zone which was here initially assumed to be horizontal (see salt water percentages in Fig. 6). After 20 years of simulation the transition zone reaches a new dynamic equilibrium and consequently, a new stable position. Under the drainage canal is an upconing of salt water and the transition zone has the largest thickness. Under the centre of the recharge area the transition zone is situated on the largest depth. In figure 7 the salt water distribution is represented along with the fresh water head configuration and the flow velocity field. This salt water distribution is now used as initial distribution in the second simulation.

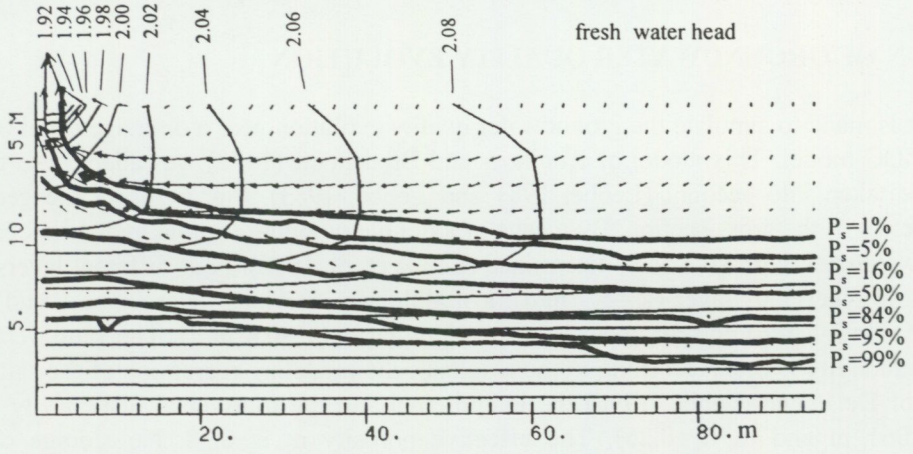


Figure 7. Salt water distribution along with the fresh water head configuration and flow velocity for the dynamic equilibrium reached after the simulation of 20 years of steady-state

During the second simulation the evolution of the groundwater quality is calculated for an intermitted pumping on the two pervious layers near the drainage canal during a period of four years. The finite-difference cells where water is pumped are indicated by the number 3 and 4 in figure 6. During the seven months with the largest infiltration rate, water is pumped with a constant discharge rate. During the first period of seven months, the total discharge rate in the upper pervious layer is equal to 0.8 m^3/d per meter of drainage canal, whereas the total discharge rate in the lower pervious layer is 2.0 m^3/d per meter of drainage canal. During the second period of seven months the total discharge rate in the upper pervious layer is 1.2 m^3/d per meter of drainage canal and 2,0 m^3/d per meter of drainage canal for the lower pervious layer. During the third and fourth period of seven months the discharge rates are the same in the upper and lower pervious layer : 1.5 m^3/d per meter of drainage canal. The lower boundary and the vertical boundary of the modeled cross-section are all impervious as in the first simulation. The drainage canal is held at the same constant level as in the first simulation, whereas the salt water percentage of the canal water is augmented from 0% in the first simulation to 1.6% in the second simulation. The object of this salt augmentation is meant as a tracer of the canal water in the modeling problem. In the recharge area the infiltration rate is in this second simulation time-dependent. For each month of the year the average infiltration rates are as estimated by Lebbe (1978). The ratio of the monthly average infiltration rates to the yearly average infiltration rate (280 mm/year) is given in table 1. During each month of pumping the total amount of infiltration is only a fraction of the total pumping amount. The largest part of the pumped water is provided by artificial recharge through the canal bottom.

Table 1. Ratio of the monthly average recharge rate versus the yearly average recharge rate.

April	May	June	July	Aug	Sept	Oct	Nov	Dec	Jan	Feb	Mar
.1429	.0951	.0563	.0346	.1487	.4241	1.292	3.063	2.445	1.884	1.744	.6827

In figure 8 the calculated salt water percentage fluctuations are represented for the different pumped cells. One can see that the fluctuation of the salt water percentage is strongly level dependent in the lower pervious layer. Already after the first seven months of pumping the salt water percentage at the top of the lower pervious layer reaches the salt concentration of the drainage canal while the salt water percentage at the base only shows a slight decrease. During the first pumping period the salt water percentage in the pumped cells of the upper pervious layer is also level dependent. In this first pumping period the salt at the base of this layer is pumped away. The salt water content in the upper part of the upper pervious layer is initially lower than at its base. After somewhat less than two months of pumping the salt content in the upper pervious layer reaches its lowest value. After three and a half months of pumping the salt water percentage of the three pumped cells in the upper pervious layer reaches 1.6 %, the assumed salt percentage of the canal. After the first pumping period the salt content stays in these cells approximately at the same salt content of the canal. At the start of the second, third and fourth pumping period the salt content changes only slightly after which it reaches again the salt content of the canal.

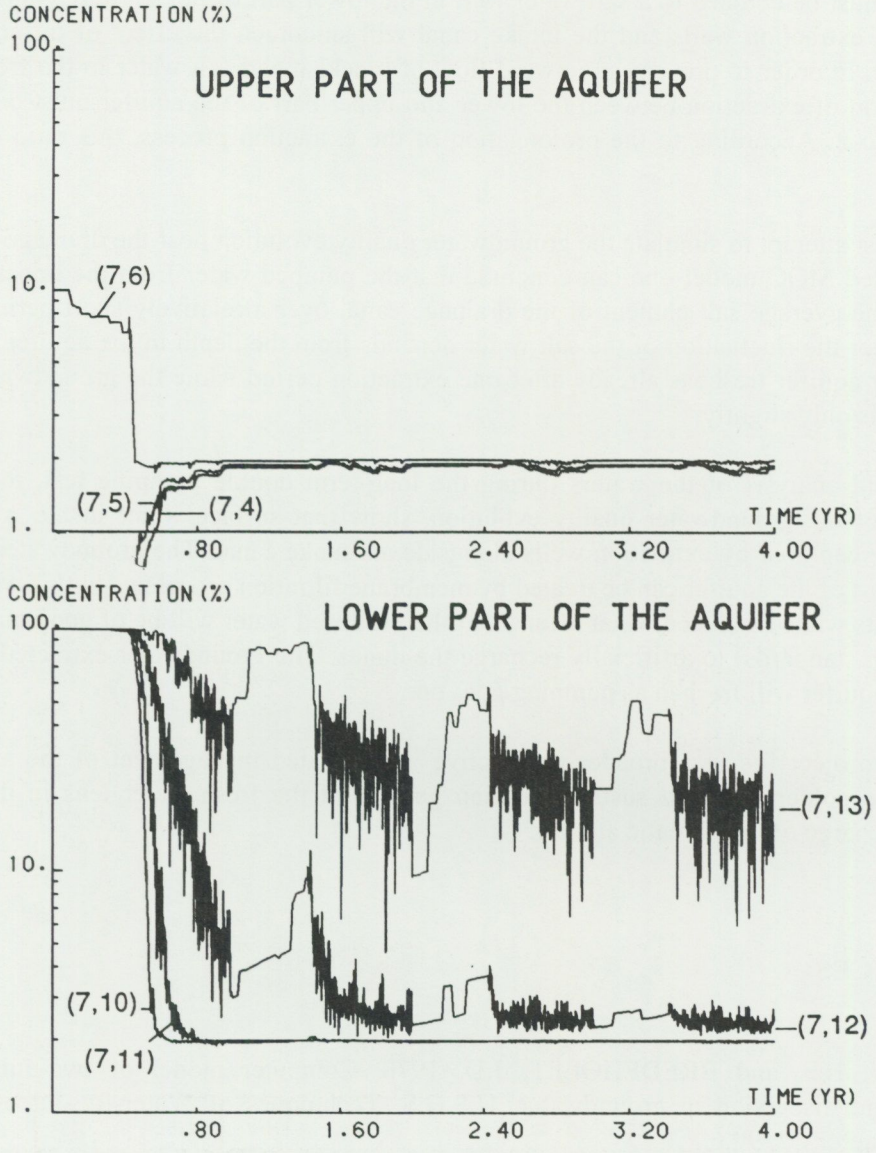


Figure 8. Salt water percentage fluctuation for the pumped cells

CONCLUSION

Due to the location of the test site at only 8 m distance from the Kromme Gracht, the quality of the water extracted from the upper part of the aquifer was influenced by the upconing of salt water near this drainage canal. Reduction of the volume extracted from the upper pumping well reduced the salt content in a significant way.

The water in the Kromme Gracht is fresh and hard. The mean chloride content was 236 mg/l, the mean sodium content 146 mg/l. However the water is nutrient-rich with mean levels for nitrate of 29,1 mg/l, ammonia of 2,72 mg/l, sulfate of 248 mg/l and total phosphorus of 0,84 mg/l. Although the nitrate content in the surface water is important, the content in the groundwater extracted from the upper part of the phreatic aquifer (PP2) is fairly low averaging 3,23 mg/l. This is caused by denitrification into the sediments by organic compounds. The salt content of the water extracted from the lower part of the aquifer gradually decreases, reaching 77,6 % of the initial content.

As a result from the evaluation of the quality of the waters, the extraction wells in the upper part of the aquifer will have to be located at some distance from the existing drainage canals. Each fresh water well must be coupled to a salt water well in the lower part of the aquifer. Varying the distance between the extraction wells and the intake canal will smoothen the effect of different qualities of intake water. In order to prevent an upward flow of brackish and salt water to the fresh water wells, the proportion of extraction between the lower and upper part of the aquifer must be initially in the order of 5 to 2. According to the prolongation of the extraction process, this ratio can decrease in time.

From the first attempt to simulate the groundwater quality evolution near the drainage canal by means of the adapted MOC model one can conclude that the pumped water from the upper pervious layer will reach the average salt content of the drainage canal over a relatively short period. In the lower pervious layer the fluctuation of the salt water depends from the depth in the aquifer. The upper half of the lower aquifer freshens already after one extraction period while the groundwater in the lower half freshens only slightly.

The chemical analysis of the waters during the long-term double pumping test, together with the simulation of the groundwater quality evolution, show that surface water in the Avekapelle creek ridge can be captured by extraction wells alongside an intake canal. The groundwater extracted from the upper part of the aquifer can be treated by membrane filtration processes. In this way more than 80 % of the salts will be reduced, what means that the produced water will be of good quality (according to the Dutch standards) to artificially recharge the dunes. The groundwater extracted from the lower part of the aquifer will freshen as pumping goes on.

The whole project fits in a broader perspective : integrated management of the available surface water in the polder area and sustainable management of the fresh water lens in the dune belt by artificial recharge of the phreatic aquifer.

REFERENCES

KONIKOW, L.F. and BREDEHOEFT, J.D. 1978. Computer model of two-dimensional solute transport and dispersion in groundwater. U.S.G.S. Techniques of Water-Resources Investigations, Book 7, Chapter C2, 90 p.

LEBBE, L., 1978. Hydrogeologie van het duingebied ten westen van De Panne. Geological Institute, Ghent University, Ph. D. dissertation, 164 p.

LEBBE, L., 1981. The subterranean flow of fresh and salt water underneath the western Belgian beach. Proceedings 7th Salt Water Intrusion Meeting, Uppsala. Sveriges geologiska undersökning, Rapporten och meddelanden, 27, pp. 193-218.

LEBBE, L., 1983. Mathematical model of the evolution of the fresh water lens under the dunes and beach with semi-diurnal tides. Proceedings 8th Salt Water Intrusion Meeting, Bari. Geologica Applicata e Idrogeologia, Volume 18, parte 2, pp. 211-216.

LEBBE, L., TARHOUNI, J., VAN HOUTTE, E. and DE BREUCK, W., 1995. Recharge of an artificial recharge test and a double pumping test as preliminary studies for optimizing water supply in the Western Belgian coastal plain. Hydrogeology Journal, volume 3, Number 3, 1995, pp. 53-63.

LEBBE, L., 1996. Regression modelling of fresh and salt water heads and borehole resistivities observed on the shore. Proceedings of ModelCARE '96, Golden, Colorado, IAHS Publication (in print).

STUYFZAND, P.J., 1986. A new hydrochemical classification of water types : principles and application to the dunes aquifer system of the Netherlands. Proceedings 9th Salt Water Intrusion Meeting, Delft. pp. 641-655.

VAN BENNEKOM, C.A., 1991. Beïnvloeding grondwaterwinning- en zuivering door uitspoeling van stikstofverbindingen. H_2O 1991, nr. 25, pp. 619-622.

VAN HOUTTE, E., VANLERBERGHE, F., LEBBE, L. and DE BREUCK, W., 1995. Optimization of the drinking-water production in the dune area of the western Flemish coastal plain. International Symposium on Environmental Impact Assessment in Water Management, Bruges, pp. 302-309.

ZEUWTS, L., 1991. Hydrogeologie en hydrochemie van de IJzervlakte tussen de Frans-Belgische grens en Avekapelle-Pervijze (Westelijke kustvlakte). Geological Institute, Ghent University, Ph. D. dissertation, 389 p.

Salinization of drinking water in the Netherlands: anamnesis, diagnosis and remediation

Pieter Jan Stuyfzand
Kiwa Ltd, Research and Consultancy Division, Groningenhaven 7, P.O. Box 1072,
3430 BB Nieuwegein, The Netherlands.

ABSTRACT: Recent and ancient data on all 365 pumping stations which existed in the period 1853-1996 (most of them well fields), are combined in order to reconstruct historical trends in drinking water supply in the Netherlands. These trends include geographical, hydrological and hydrochemical information. The purpose is to: (a) get a better definition of the salinization problem (size, location, trends), (b) identify stations with salinization phenomena and classify their origin as either continental (related to agriculture, evaporation, bank infiltration, artificial recharge, local pollution or sea spray) or maritime (recent North Sea intrusion or upconing of ancient North Sea water), and (c) give a list of remedial or preventive measures for both types of salinization.
A rapid screening method is proposed and used (Table 3) to assign the salinization cause and scale to each pumping station. The following parameters are required for each pumping station: type of water resource and state (closed or active), Cl^- concentration at start of operation and in 1992 (or year of close down), and the most recent concentrations of NO_3^-, SO_4^{2-} and ^3H, and $\delta^{18}O$ only in dubious cases of Rhine bank infiltrate.
It is shown that 61 pumping stations (17%) of a total of 365 pumping stations are classified as salinized due to continental causes, and that 33 stations (9%) salinized for maritime reasons. From a total of 102 abandoned stations, 42 (41%) closed with salinization phenomena, of which 17 (5%) suffered from maritime salinization and were probably closed for that reason. Salinization is therefore a wide-spread problem in the Netherlands, which in about 50% of its cases is due to either continental or maritime reasons. The most susceptible areas are situated along the coast (intrusion and artificial recharge) and in the fluvial plain (bank infiltration and upconing).

Introduction

There is a definite increasing trend for the Na^+ and Cl^- concentrations of drinking water in the Netherlands (derived from data in Van Beek et al., 1990) and about 17 well fields are likely to salinize due to upconing of brackish groundwater (Peters & Meijer, 1993). This salinization is worrying for the following reasons: it may affect the potability of water (maximum permissible concentrations resp. 120 and 150 mg/l in the EU), it surely increases corrosion of pumping wells and the distribution network, reduces the effectiveness of detergents (and thereby raises their consumption) and lowers the diuretic activity on the consumer whose blood-pressure will rise too.
The centralized monitoring of raw and purified water for public drinking water supply is considered a task for both the government (mainly for national health protection) and the drinking water supply companies (mainly for safeguarding their water resources).
Data are therefore collected by both: the RIVM (the governmental institute for public health and environmental protection) and VEWIN (Netherlands' Waterworks Association). Both institutes suffer from the same problem: data prior to the mid 1980s are not readily available as digital data files, they scatter around in annual reports and 'fugitive sources', like unpublished project reports, governemental agency file documents, memoranda, old hand-written data files etc.
It was therefore a challenge to dive into this 'data-grave-yard', in order to (a) get a better anamnesis of the problem, (b) combine data for identification (the diagnosis) of the causes of salinization, using some of the tracers discussed during the previous SWIM (Stuyfzand & Stuurman, 1994), and (c) assign the right remediation (and prevention) for the different types of salinization. The various sources of data that were consulted, are listed in the references.

Anamnesis: historical developments in water supply and salinization

A centralized public drinking water supply started in the Netherlands in 1853 with the pumping of phreatic dune groundwater (Leeflang, 1974). The hygienic advantages (reduction of cholera epidemies) and better taste of groundwater gradually conduced to the national change over from surface to groundwater as the main source of drinking water. The increasing population and water consumption per capita raised the water demands from 70 Mm^3/y in 1900 to 335 Mm^3/y in 1950 to 1,250 Mm^3/y in 1992 (VEWIN, 1895-1996). This necessitated an expansion of water abstraction sites (pumping stations, in case of groundwater well fields).

The 1,250 Mm^3 of drinking water prepared in 1992, is composed of 7 types of water resources (Table 1), in decreasing order:

- 440 Mm^3 of (semi)confined groundwater from sandy aquifers (type B),
- 335 Mm^3 of phreatic groundwater from sandy aquifers (type A),
- 232 Mm^3 of directly purified surface water, mainly from the rivers Rhine and Meuse (type O),
- 161 Mm^3 of artificially recharged river Rhine and Meuse water (type I),
- 55 Mm^3 of Rhine bank infiltrate (type U), and
- 27 Mm^3 of groundwater from Cretaceous limestone (type K).

This water was abstracted in 1992 on 262 pumping stations (Fig.1). Further details on the characterics of the 7 types of pumping stations (water resources) are given in Tables 1 and 2.

A very important facet is the record on the close-down of pumping stations, because it constitutes a sensor of environmental problems. The location, type and size of abandoned pumping stations are shown in Fig.1, their distribution over the various types in Table 1 and the development in the course of time in Fig.2. In 1992 a cumulative total of 102 abandoned pumping stations was reached, with the highest closure rate for pumping stations using (semi)confined groundwater, and the lowest for those using recharged surface water. The highest percentage of closed stations (the lowest persistence) is observed for stations that used Rhine bank infiltrate.

TABLE 1. General characteristics of the 7 types of water resources for public drinking water supply in the Netherlands, anno 1992.

Type:	A	B	I	K	O	U
Diagnostic features	phreatic ground-water	(semi) confined ground-water	artificial recharge and recovery	ground-water from limestone	surface water	Rhine bank infiltrate
First year of operation of first station‡	1853	1893	1940	1904	1881	1890
No. of active pumping stations	103	104	9	15	16	15
No. of closed pumping stations	31	34	1	8	13	15
Percentage of closed stations*	23	25	10	35	45	50
Mean closure rate** (N/y)	0.22	0.34	0.02	0.09	0.11	0.15
Mean raw water production (Mm^3/y)	3.3	4.2	17.9	1.8	38.8	3.6
Amount of drinking water produced (Mm^3/y)	335	440	161	27	232†	55
Percentage of total amount of drinking water	27	35	13	2	19†	4
Mean number of wells/collection points	13	16	94	6	1	14
Mean surface Level = SL (m+MSL@)	18.1	13.1	8.6	76.0	2.1	1.8
Mean abstraction level (m-SL)	32-65	63-125	8-30	23-74	0	28-69
Mean depth to brackish water## (m-SL)	166	194	62	170	-	128
Age spectrum (y)	2-200	20-25,000	0.1-0.3	2-200	0-1	1-50

* = 100*closed/(active + closed); ** = closed/(1993-first year); @ = Mean Sea Level; ## = 150 mg Cl^-/l interface;
† = excluding the amount of surface water which is (a) pretreated for artificial recharge and industrial water supply (246 Mm^3/y, 9 stations), and (b) posttreated elsewhere (148 Mm^3/y, 2 stations); ‡ = still active.

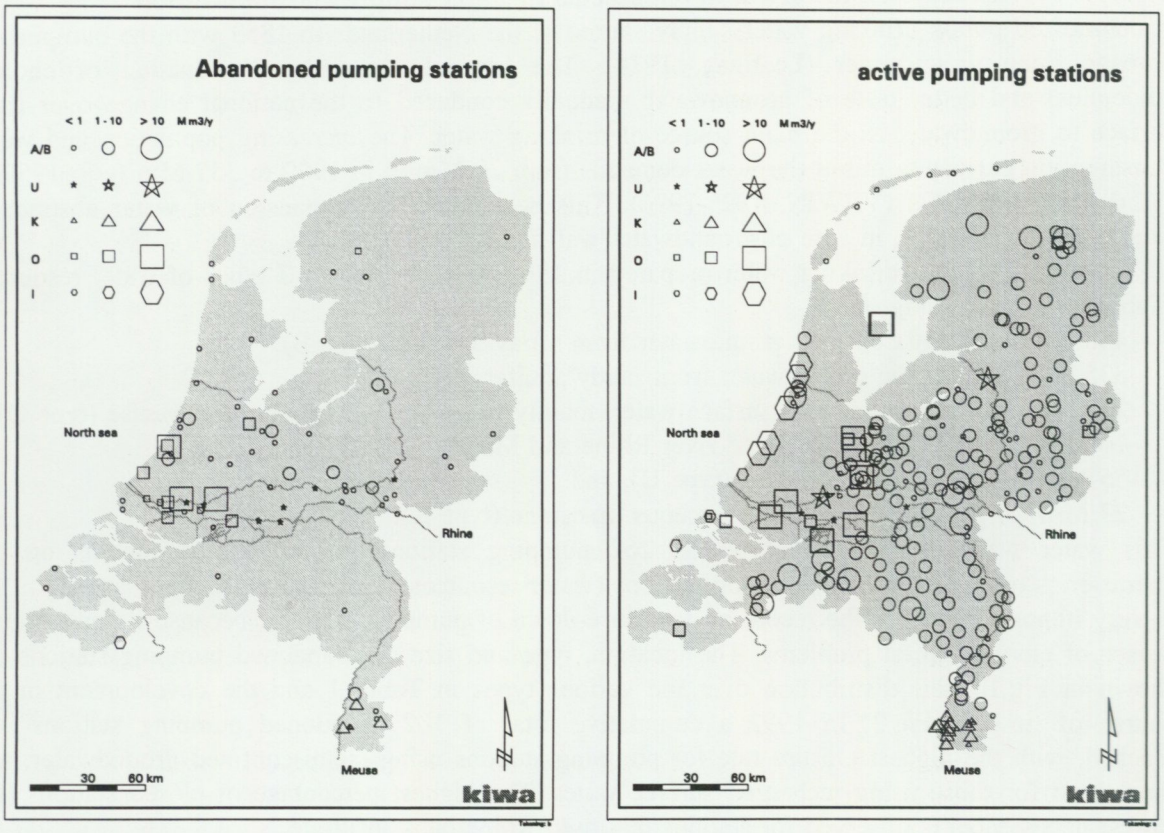


FIG. 1 The active and abandoned (closed) pumping stations for public drinking water supply in the Netherlands in 1992, with indication of type (A/B, I, K, O, U; see Table 1) and annual production.

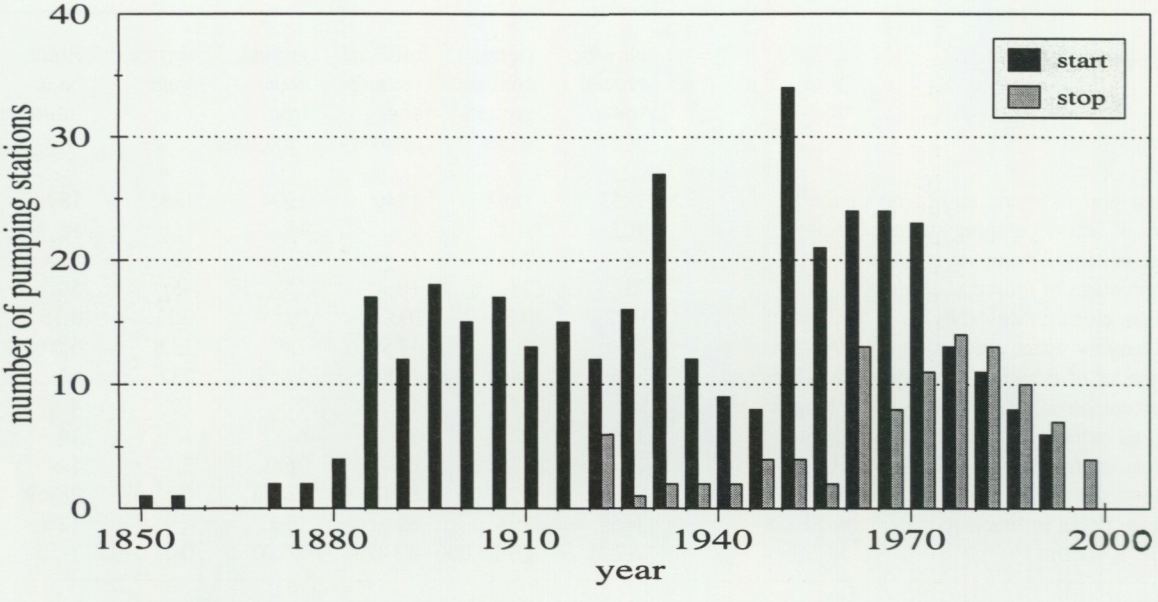


FIG. 2 Historical development of the total number of resp. new and closed pumping stations during 5-years periods from 1850 till 1995.

Reasons for close down were not always registered, but are clearly related to clogging, too serious environmental damage (like subsidence), salinization and other water quality problems, like 'anoxia' (too high methane, colour and ammonia), nitrate and micropollutants (mainly pesticides).

The size of the salinization problem is depicted in Figs.3-5, and quantified in Tables 2 and 4. It can be concluded from the chloride increase (ΔCl^-) and salinization rate (v_{Cl}) in Table 2 (regarding all active pumping stations), that on average:
(a) all types except for type O show some salinization, (b) type O (surface water) does not show any salinization (most of them started after 1955 when the salinization of surface water already had reached a high level), and (c) the types I and U exhibit most salinization of all (due to the change over from autochthonous groundwater to saltier surface water in case of I, and due to a strong salinization of river Rhine water in the period 1900-1975 in case of U).
The data in Table 4 show that 26% of a total of 365 pumping stations suffers or suffered from serious salinization (>20 mg Cl^-/l increase since the first production year), and that at least about 5% had to be closed due to salinization (salinization scale 5). The spatial distribution of the salinization process in Fig.5 shows that the most seriously affected areas are located along the North Sea coast (intrusion and artificial recharge) and along branches of the rivers Rhine and Meuse (bank infiltration and upconing). Typical salinization rates for pumping stations range in between 1 and 5 mg Cl^-/l/y, in only 2 out of 94 cases higher rates were observed (Fig.5). The salinization rates of 'bad' individual pumping wells normally is substantially higher (5-50 mg Cl^-/l/y), and in individual piezometers rates as high as 500 mg Cl^-/l/y are not rare in coastal aquifers.

TABLE 2. Chemical characteristics of the 7 types of water resources for public drinking water supply in the Netherlands, anno 1992.

Type:	unit	A	B	I	K	O	U
Diagnostic features		phreatic groundwater	(semi) confined groundwater	artificial recharge and recovery	groundwater from limestone	surface water	Rhine bank infiltrate
No of active pumping stations		103	102	9	15	14	15
Cl^-	mg/l	33	29	114	31	98	116
SO_4^{2-}	mg/l	38	14	76	68	65	47
NO_3^-	mg N/l	1.72	0.11	1.32	2.89	3.00	0.26
HCO_3^-	mg/l	166	217	189	355	158	244
B *	µg/l	24	56	170	20	105	76
Ba	µg/l	34	31	26	73	56	95
EOCl	µg/l	0.13	0.14	0.25	0.11	0.25	0.37
F	µg/l	83	102	239	151	223	130
I #	µg/l	5	7	12	5	8	20
Li #	µg/l	6	5	11	-	-	7
^3H **	Bq/l	2.43	0.95	6.93	2.29	7.43	6.07
^{226}Rn **	mBq/l	1.8	1.8	1.3	9.0	0.6	1.8
Cl^-, start	mg/l	22	20	41§	15	102	49
ΔCl^-	mg/l	11	9	73	14	-15	67
$v_{Cl} = \Delta Cl/\Delta t$	mg/l/y	0.21	0.18	0.88	0.48	-0.81	0.87

$\Delta Cl^- = Cl^-_{1992} - Cl^-_{start}$; v_{Cl} = salinization rate = ΔCl^-/(1993 - start year).
** = total iodine in drinking water in 1978 (based on data in Reijnders et al., 1980); * = in drinking water in 1984 (unpubl. results from RIVM, obtained from A.J. van den Eshof); ** = in drinking water in period 1981-1984 (based on data in Glastra et al., 1989); § = at the start, prior to the introduction of artificial recharge.

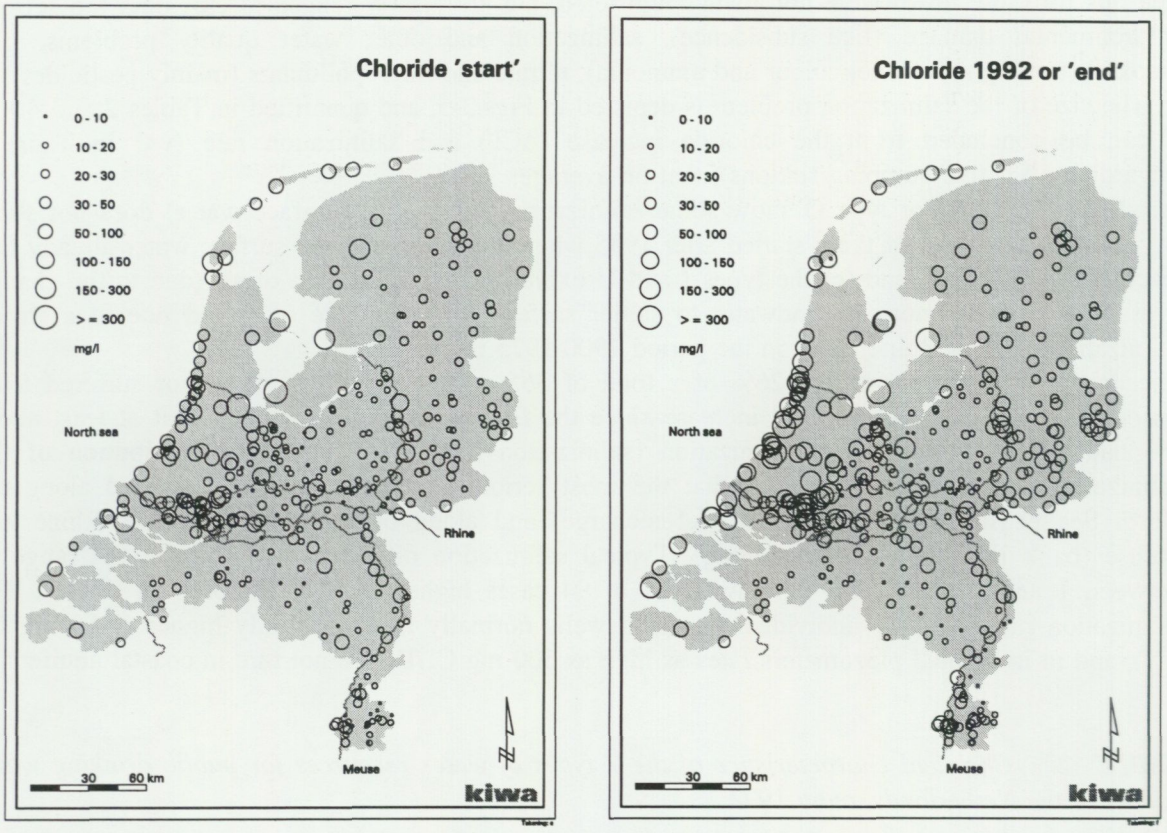


FIG. 3. Areal distribution of the chloride concentration of raw water from pumping stations in the Netherlands, at their start (first year of operation) and in 1992 (or for the closed stations, in the year of closure).

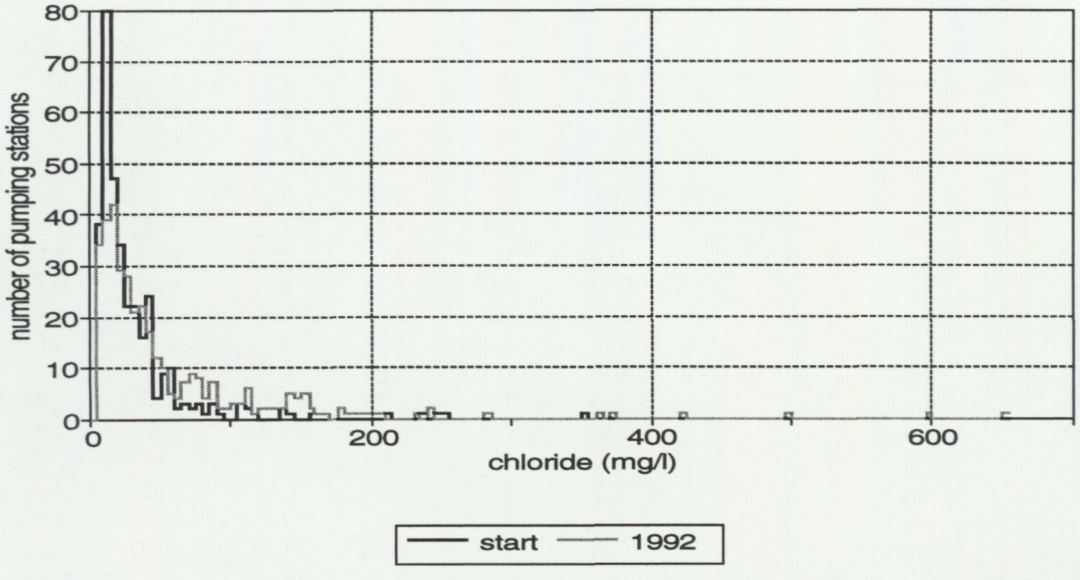


FIG. 4. Histogram showing the frequency distribution of the chloride concentration of raw water from all pumping stations, at their start (first year of operation) and in 1992 (or for the closed stations, in the year of closure).

Diagnosis: looking for the causes

METHODS: In this survey of the raw water produced by 365 pumping stations in the period 1853-1992, salinization is defined as a net rise in chlorinity superior to 20 mg Cl^-/l in 1992 (or in the year of close-down) since the pumping station became active. Stuyfzand & Stuurman (1994) recognized 11 sources of salinization of groundwater in the Netherlands, and recommended several tracers for identifying them. In the case of water abstracted for drinking water preparation, 2 main groups of salinization are discerned for simplicity:

- the continental salinization type, which is related to either agriculture, evaporation, bank infiltration, artificial recharge, local pollution sources and sea spray; and
- the maritime salinization type, which is related to direct North Sea intrusion, and ancient North Sea water (which transgreded during the Holocene or was trapped during sedimentation of marine, fine-grained deposits during the Holocene and Lower Pleistocene and Upper Tertiary).

The criteria for both types of salinization are given in Table 3: the continental type was assigned in any case to surface water (O), artificially recharged surface water (I) and Rhine bank infiltrate (U). Pumping stations were a priori classified as such on the basis of their water resource and previous research, including ^{18}O isotopic data for difficult cases of Rhine bank infiltrate (Stuyfzand, 1989; Stuyfzand, 1993). The continental type was also assigned in case of the other types of pumping stations (the true groundwater stations: A, B or K), on the condition that in 1992 either nitrate was ≥5 mg N/l, or the SO_4^{2-}/Cl^- ratio was ≥0.5 (on mg/l-basis), or tritium was ≥4 Bq/l (= ≥34 TU). In all other cases the maritime salinization type was assigned.

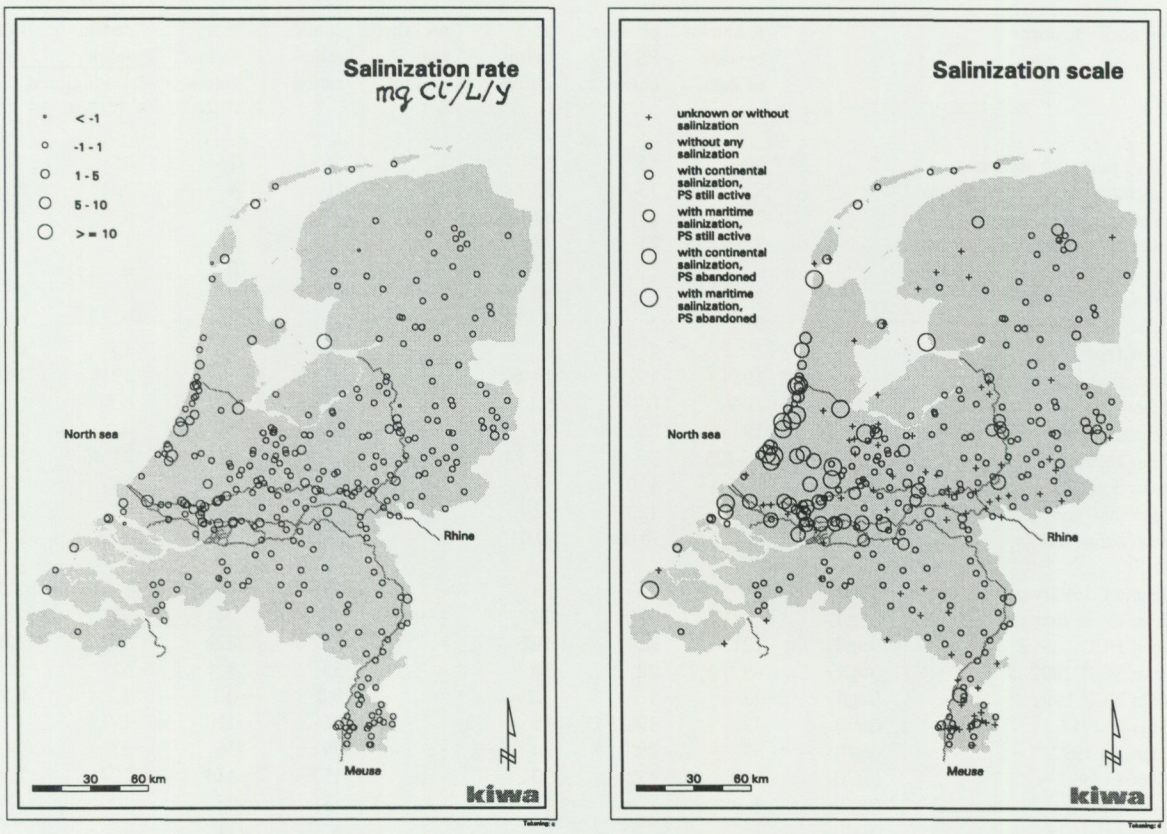


FIG. 5. Salinization rate and scale for pumping stations of raw water for drinking water supply in the Netherlands. The salinization rate (v_{Cl}) is defined as $\Delta Cl^-/\Delta t$ (see foot notes in Table 3), the salinization scale is fully explained in Table 3 (scales - and -1 combined into '+ sign').

TABLE 3. The salinization scale for drinking water, with its criteria.

description of scale No		state of pumping station (PS)	ΔCl^- [§] mg/l	vCl [##] mg Cl/l/y	ΔH [**] m	Continental or Maritime types of PS	NO_3 mg N/l	SO_4/Cl mg/l	^3H Bq/l
-	undefined	act./closed	{? or	? or	? or	? or	? or	? or	?}
-1	no salinization	closed	<20	-	-	all	-	-	-
0	no salinization, no risk	active	<20	<1	-	all	-	-	-
1	no saliniz., risk present	active	<20	{>1 or	<20}	all	-	-	-
2	continental salinization	active	≥20	-	-	{I,O,U or	{≥5 or	≥0.5 or	≥4}}
3	maritime salinization	active	≥20	-	-	{A,B,K and	{<5 and	<0.5 and	<4}}
4	cont. saliniz., PS closed	closed	≥20	-	-	{I,O,U or	{≥5 or	≥0.5 or	≥4}}
5	marit. saliniz., PS closed	closed	≥20	-	-	{A,B,K and	{<5 and	<0.5 and	<4}}

[§] = if active: $Cl^-_{1992} - Cl^-_{start}$, if closed: $Cl^-_{closure\ year} - Cl^-_{start}$; [##] = if active: ΔCl^-/(1992 - start year), if closed: ΔCl^-/(1992 - closure year); [**] = vertical distance between lower side of well screen and the brackish water interface (150 mg Cl^-/l).

TABLE 4. Survey of the salinization scale of raw water for public drinking water supply in the Netherlands, with the mean characteristics of each group.

Salinization scale:		-	-1	0	1	2	3	4	5
Diagnostic features		unknown by lack of data	no salin, PS closed	no salini-zation	no salin, risk present	contin. salini-zation	marit. salini-zation	contin. salin. PS closed	marit. salin. PS closed
No. of pumping stations		30	56	184	1	36	16	25	17
Percentage of all 365 stations		8	15	50	0.3	10	4	7	5
No of type A stations		7	**22**	**82**	0	8	6	4	5
No of type B stations		**9**	**21**	**79**	0	6	**10**	1	**12**
No of type I stations		0	1	1	0	8	0	0	0
No of type K stations		3	8	10	0	2	0	0	0
No of type O stations		**9**	3	8	**1**	2	0	7	0
No of type U stations		2	1	4	0	**10**	0	**13**	0
Mean first year of operation		1964	1925	1946	-	1921	1929	1914	1910
Mean raw water production	(Mm^3/y)	10.9	0.7	5.1	-	7.4	5.1	6.5	0.43
Mean surface Level = SL	(m+MSL[@])	18	25	19	-	11	5.4	4.0	2.1
Mean abstraction level	(m-SL)	66-123	35-56	45-94	-	22-54	53-100	21-40	26-40
Mean depth to brackish water[##]	(m-SL)	206	170	187	-	97	140	88	52
Mean dist. screen to brack. water[†]	(m)	118	123	92	-	45	41	29	17
Mean salin. rate (v_{Cl})	(mg Cl/l/y)	-	-0.03	-0.01	-	1.03	1.07	1.52	3.59
Mean Cl^- 1992/year of closure	(mg/l)	50	36	28	-	98	84	132	217
Mean Cl^- in first year	(mg/l)	-	38	26	-	35	24	49	73
Mean HCO_3^- 1992	(mg/l)	221	224	192	-	232	229	302	320
Mean SO_4^{2-} 1992	(mg/l)	49	28	30	-	33	8	52	30
Mean NO_3^- 1992	(mg/l)	2.0	1.7	1.2	-	0.8	0.1	1.1	0.2
Mean B 1984	(µg/l)	79	19	36	-	76	110	191	-
Mean Ba 1992	(µg/l)	59	29	34	-	59	36	57	34
Mean F^- 1992	(µg/l)	160	122	104	-	137	114	224	250
Mean I 1978	(µg/l)	9	9	5	-	13	25	18	18
Mean Li^+ 1978	(µg/l)	-	7	5	-	8	11	11	7
Mean ^{226}Rn 1981-84	(mBq/l)	4.4	2.5	1.9	-	3.0	1.8	2.3	0.6
Mean ^3H 1981-84	(Bq/l)	1.4	3.2	1.9	-	5.8	0.5	2.4	0.7

[*] = 100*closed/(active + closed); [**] = closed/(1993-first year); [@] = Mean Sea Level; [##] = 150 mg Cl^-/l interface;
[†] = from lower side of well screen to the fresh-brackish water interface (150 mg Cl^-/l).

The philosophy behind the fences posed by nitrate, sulphate/chloride-ratio and tritium is, that actual and ancient North Sea groundwaters normally do not contain nitrate and tritium, and normally have a SO_4^{2-}/Cl^-ratio ≤0.14 on mg/l-basis (Stuyfzand, 1993; Stuyfzand & Stuurman, 1994). And in addition, low levels of these quality parameters for groundwater generally point at a negligible contribution of shallow fresh groundwater to the mixture pumped.
Obviously, the criteria used for classifying a pumping station as salinized and the further ranking of it according to Table 3 may seem rather subjective. However, the results were verified for many cases where detailed field investigations had been carried out in the past, and the rapid screening method (the salinization scale) proved to work very well. Certainly there are some cases with both a continental and a maritime salinization process, like in case of several stations pumping both Rhine bank infiltrate and very deep autochthonous groundwater. In those cases the salinization type is to be considered as the dominant one.

RESULTS: The results of classifying all pumping stations according to their salinization scale (incl. their salinization type) are depicted in Fig.5. Additional mean characteristics for each salinization scale, viz. number and type of pumping stations, hydrological and hydrochemical data, are presented in Table 4.
The data in Table 4 show that 61 pumping stations (17%) of a total of 365 pumping stations are classified as salinized due to continental causes, and that 33 stations (9%) salinized for maritime reasons. From a total of 102 abandoned stations, 42 (41%) closed with salinization phenomena, of which 17 (5%) suffered from maritime salinization and were probably closed for that reason. Salinization is therefore a wide-spread problem in the Netherlands, which in about 50% of its cases is due to either continental or maritime reasons. Station type B (pumping (semi)confined groundwater) is most susceptible to maritime salinization (67% of all cases with scale 3 and 5) and close down (71%), probably for that reason. Station type U (Rhine bank infiltrate) is most susceptible to continental salinization (38% of all cases with scale 2 and 4) and close down (52%), probably for other quality reasons than salinization ('anoxia' and micropollutants).
Water with continental salinization shows, as compared to water without salinization, on average higher concentration levels of HCO_3^-, B, Ba, EOCl, F, and especially I and Li, but lower levels of NO_3^-. This is explained by a very high contribution of station types I and U (see Table 2 for their mean chemical composition).
The spatial distribution of the salinization process in Fig.5 and hydrological data in Table 4 reveal that the most susceptible stations are located in the lowest parts of the Netherlands (mean surface level ≤11 m+MSL) with the shallowest position of the fresh-brackish water interface below the lower side of the pumping screen: along the North Sea coast (intrusion and artificial recharge) and along branches of the rivers Rhine and Meuse (bank infiltration and upconing).

Remediation: how to lower salinization

The pumping of large amounts of water showing continental salinization (the mild variety), in general means for drinking water supply that the pumping station (or well field) does not need to be abandoned or pinched, but that additional purification of the raw water is or soon will be required. Further treatment is necessary to remove organic micropollutants and to reduce the nitrate and calcium (or aluminium) concentrations, as the salinization is associated in most cases with environmental pollution or the change-over from autochthonous to allochthonous groundwater (like in case of artificial recharge and bank infiltration).
Preventive measures are composed of sanitation of land-use and point sources of pollution within the contributing area of the well field or fluvial basin.
The pumping of small amounts of water showing maritime salinization (the more severe variety), normally implies that the well field has to be closed or rigorously pinched, unless desalinization techniques become economically feasible. Preventive measures consist of extensifying the well field (increasing the distance between wells), horizontal in stead of vertical wells, translocation of

hazardous wells to less susceptible areas within the concession (outside the upconing area or one aquifer higher), and artificial recharge (for instance just below the pumping well, one aquifer deeper).

In looking for new well fields, a low chance on salinization seems to be associated with the following hydrological conditions: (1) a high initial distance in between the fresh-salt water interface and the lower side of the pumping screen; (2) the presence of an aquitard in between the well screen and the initial fresh-salt water interface; (3) the absence of an aquitard with high vertical flow resistance and a large areal extent in between the well screen and groundwater table; (4) no restrictions in lateral flow due to other well fields upgradient or the presence of vertical semi-pervious boundaries (like glacial basins filled with varve clays, and faults); (5) position in the infiltrating parts of the groundwater flow domain; (6) no other human interferences (afforestation, urbanisation, intensive drainage, land reclamation); and (7) no other natural interferences (coastal erosion).

The mixing of fresh and salt groundwater should be prevented as much as possible, as this means a serious loss of potable water. This can be achieved to some degree, by pumping as continuously as possible. Strong fluctuations in the pumping rate may create the alternation of upconing and gravitational subsidence of the brackish upconing. In a frequently changing flow domain this contributes to the mixing of fresh and brackish water.

Concluding remarks

Pumping stations for drinking water supply constitute a powerful monitoring system for environmental pollution, including salinization. It requires, however, that ancient historical data be retrieved from dusty paper-archieves which were loaded in the pre-floppydisk-age. Data on the close-down, changes in water resources (from surface to groundwater, from autochthonous to allochthonous groundwater, etc.), changes in pumping depth, pumping rate and analytical methods need consideration as well for obtaining the right interpretations.

In this desk study attention focused mainly on chloride, but some other chemical parameters clearly show interesting distribution patterns: relatively high ^{226}Rn levels are mainly restricted to the limestone areas in the south (Table 2), and tritium activity was in the 1980s highest in surface water and groundwater derived from surface water (Table 2; contribution of nuclear power plants).

Acknowledgements

The Netherlands' Waterworks Association (VEWIN) financed this study. Carla Gommer and Frans Lüers (both Kiwa) assisted in resp. preparing the maps and statistical elaboration.

References

GLASTRA, P., R. VAN ZANTEN, R.M.S. DROST & F.C.M. MATTERN 1989. Onderzoek naar de radioactiviteit van drinkwater over de periode 1981-1984. RIVM-rapport 248201001, Bilthoven, 30p.

FONDS, A.W. 1989. De som van adsorbeerbare organische halogeenverbindingen (AOX) in het Nederlandse drinkwater. RIVM-rapport 218108007, 17p.

LEEFLANG, K.W.H. 1974. Ons drinkwater in de stroom van de tijd. VEWIN, Rijswijk, 228p.

PETERS, J.H. & J.A. MEIJER 1993. Will upconing be a problem in the Netherlands? Water Supply 11, 157-163.

REIJNDERS, H.F.R., J. STOLTENKAMP & M.J. STOLTENKAMP-WOUTERSE 1980. Het totaal jodium, jodide en organisch-jodiumgehalte in drinkwater in Nederland in 1978. RIVM-rapport 87/80LMC, Bilthgoven, 12p.

REIJNDERS, H.F.R., J.J. VAN STADEN & N.W. NAGTEGAAL 1983. Voorkomen en trend van enige chemische bestanddelen in uitgaand water van drinkwaterpompstations in Nederland. RIVM-rapport 218108001, 71p.

STUYFZAND, P.J. 1989. Hydrology and water quality aspects of Rhine bank ground water in The Netherlands. J. Hydrol. 106, 341-363.

STUYFZAND, P.J. 1993. Hydrochemistry and hydrology of the coastal dune area of the Western Netherlands. KIWA Publication, also Ph.D Thesis Vrije Univ. Amsterdam, ISBN 90-74741-01-0, 366 p.

STUYFZAND, P.J. 1994. The impact of land reclamation on groundwater quality and future drinking water supply in The Netherlands. Water Sci & Technol. 31, 47-57.

STUYFZAND, P.J. & J.W. KOOIMAN 1996. Elimination of pollutants during artificial recharge and bank infiltration: a comparison. In 'Artificial recharge of groundwater' (A.L. Kivimäki & T. Suokko, eds), Proc. Int. Symp., Helsinki, June 3-5 1996, NHP-report 38, 223-231.

STUYFZAND, P.J. & R.J. STUURMAN 1994. Recognition and genesis of various brackish to hypersaline groundwaters in The Netherlands. Proc. 13th Salt Water Intrusion Meeting, June 1994 Cagliari, Italy, in press; also Kiwa-rapport SWI-95.133, 12p.

VAN BEEK, C.G.E.M., F.A.M. HETTINGA & P.K. BAGGELAAR 1990. Onderzoek naar trendmatige veranderingen in de kwaliteit van het grondwater onttrokken door de Nederlandse waterleidingbedrijven. Kiwa-rapport SWE 90.013, 48p.

VAN DUIJVENBOODEN, W. & G.T. BUSZ 1978. Overzicht van de grondwaterwinplaatsen voor de openbare drinkwatervoorziening op basis van een classificatie van de geëxploiteerde watervoerende pakketten. RID-rapport hy.h-78/01, 25p.

VEENENDAAL, G., C.G.E.M. VAN BEEK & L.M. PUIJKER 1986. Het voorkomen van organische stoffen in het grondwater onttrokken door de Nederlandse waterleidingbedrijven. KIWA-Meded. 97, 99p en KIWA-rapport SWO-86.267 (de analyseresultaten).

VERSTEEGH, J.F.M. & F.J. WETSTEYN 1994. De kwaliteit van het drinkwater in Nederland, in 1992. RIVM-rapport 731011002, VROM-rapport 1994/58, 60p.

VERWEIJ, W., T. VAN DER VELDE-KOERTS, J.L.M. DE BOER & W. MENNES 1994. Zeldzame aarden in drinkwater en drinkwaterbronnen. RIVM-rapport 734301003, 58p.

VEWIN, 1895-1996. Statistische overzichten van de waterleiding in Nederland, met uitkomsten van het fysisch en chemisch onderzoek. Jaarrapporten 1895-1939 (elk jaar), 1943, 1949, 1952, 1957, 1966, 1968, 1973, 1981, 1986, 1992.

VOGELAAR, A.J. 1993. Indeling van winplaatsen voor onderzoek naar sporenelementen. Kiwa-rapport SWI 92.162, 15p.

Degradation of groundwater quality in the Güzelyurt basin, Northern Cyprus

Hüseyin Gökçekuş
Department of Civil Engineering, Near East University, Northern Cyprus

Vedat Doyuran
Department of Geological Engineering, Middle East Technical University, Ankara, Turkey

In Northern Cyprus the Güzelyurt groundwater basin constitutes the only aquifer which is presently exploited for irrigation and municipal water supply. In the Güzelyurt basin the groundwater occurs under unconfined conditions within the fanglomerates (Pliocene) and the surficial clastic deposits (Holocene). The Tertiary and pre-Tertiary rocks constitute the impervious and semi-pervious basement and the boundaries of the aquifer.

In arid and semi-arid regions, due to the thirst of vegetation and greater demand for human consumption, more water is withdrawn from the aquifer. Where natural recharge is limited, such excessive withdrawals produce considerable reduction in the aquifer storage, which results in progressive decline of the groundwater levels. In coastal aquifers, such as the Güzelyurt basin, excessive withdrawals do not only cause shortage of water supply but also degradation of water quality.

In the Güzelyurt groundwater basin degradation of groundwater quality occurs as a result of sea water intrusion and bedrock contamination. Excessive withdrawals from the aquifer have caused the groundwater levels to decline well below the mean sea level, which resulted in sea water intrusion extending for a distance of 2 km to 4 km inland from the coast. The lithological units exposed in the northern part of the watershed contain evaporites. These soluble rocks are the main causes of bedrock contamination.

Evaluation of hydrochemical data helped to distinguish the sources and areal distribution of the contaminants throughout the aquifer. The modified double-mass curve approach was particularly effective in delineating historical trends of the sea water intrusion.

Introduction

The Güzelyurt groundwater basin is located within a semi-arid coastal plain of Northern Cyprus. Since 1957 increasing rates of pumpage have caused progressive decline in the groundwater levels, locally reaching to 35-50 m below mean sea level (Gökçekuş and Doyuran, 1993). Limited natural recharge and excessive withdrawals from approximately 650 active municipal and irrigation wells have not only produced considerable reduction in the aquifer storage but also degradation of groundwater quality due to salt water intrusion and bedrock contamination.

In this paper the causes of groundwater degradation are described. A total of eighty water samples were collected from municipal water supply, irrigation and observation wells. Selection of sampling points was based on the degree and nature of contamination of the groundwater. Water sampling stations are concentrated along the coastal zone to determine the extent of the sea water intrusion. For bedrock contamination wells located at the northern part of the groundwater basin, where evaporites are exposed, are considered. The groundwater samples were analyzed for major ions, specific conductance, pH, and total dissolved solids. The results of hydrochemical data are presented in the form of tables, contour maps and water quality diagrams.

Hydrogeology

In the Güzelyurt basin the groundwater occurs under unconfined conditions within the surficial deposits (alluviums, talus, beach deposits, slopewash deposits, and river terrace deposits) and semi-consolidated and poorly cemented fanglomerates. The consolidated rocks of Pre-Tertiary (mostly pillow lavas) and Tertiary (limestone, conglomerate, marl, sandstone, chalk and evaporites) (Gökçekuş and Olgun, 1993) constitute the semi-pervious to impervious basement and the boundary of the aquifer (Fig. 1).

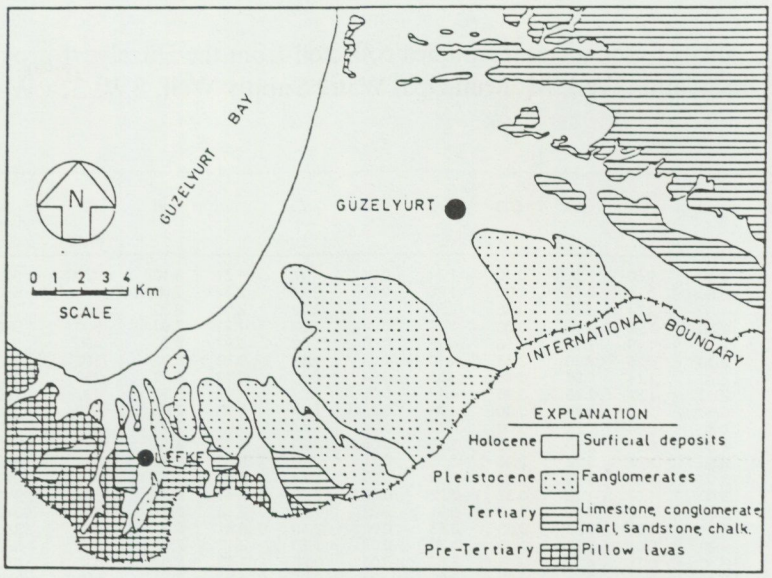


Fig. 1. Simplified geological map of the Güzelyurt groundwater basin

The transmissivities of the surficial deposits range between 250 m^2/day and 1500 m^2/day, whereas the fanglomerates have transmissivities in the range of 10 m^2/day and 250 m^2/day. The thickness of the surficial deposits ranges between 10 m and 120 m. The maximum thickness of the fanglomerates is estimated as 80 m. Only a few wells tap fanglomerates, however, they serve as avenues for subsurface recharge to the alluvial aquifer.

Hydrochemistry

CONTAMINATION DUE TO SEA-WATER INTRUSION: Table 1 depicts the chemical quality of the groundwater collected from selected wells of the Güzelyurt groundwater basin (Gökçekuş and Doyuran, 1995). Based on the salinity classification proposed by Robinove and others (1958) wells with sequence number 1 thru 51 and also including 54-56 show no salinity problem (for the location of wells refer to Fig. 2). Wells with sequence number 52 and 53, as well as 57 thru 71 yield slightly saline water. Those with sequence number 72 thru 77 yield moderately saline water and the rest are highly saline.

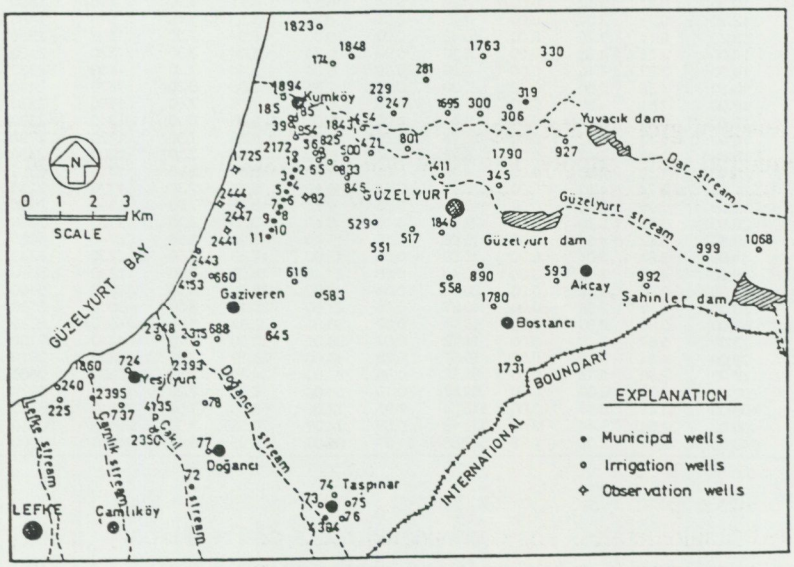


Fig. 2. Distribution of wells within the Güzelyurt plain.

Table 1. Chemical quality of groundwater samples collected from the Güzelyurt groundwater basin (Ir: Irrigation Well; O: Observation Well; M: Municipal Water Supply Well; SW: Sea Water).

Seq. No:	Well No:	Remarks	Cl	SO4	HCO3	CO3	Na	K	Ca	Mg	pH	TDS	SC	%Na	SAR
						Ions as meq/lt						mg/lt	uS/cm		
1	992	Ir	1.40	0.60	2.32	0.40	1.74	0.01	1.76	1.21	8.10	320	520	37.08	1.43
2	74	Ir	1.60	0.98	3.58	0.00	1.70	0.02	2.20	2.34	7.00	440	660	27.48	1.13
3	75	Ir	1.80	2.04	3.36	0.48	2.35	0.03	2.72	2.58	8.30	520	720	30.99	1.44
4	411	Ir	1.80	1.99	4.00	0.00	4.70	0.04	1.84	1.21	7.90	560	860	60.85	3.81
5	1790	Ir	2.00	1.49	2.92	0.56	4.78	0.02	1.20	0.97	8.30	480	670	68.87	4.59
6	345	Ir	2.10	1.36	3.20	0.48	4.70	0.03	1.52	0.89	8.30	500	830	66.25	4.28
7	72	M	2.20	1.14	6.96	0.16	3.83	0.04	2.80	3.79	8.30	750	950	37.00	2.11
8	4	M	2.40	1.59	2.48	0.96	4.17	0.05	1.28	1.93	8.50	490	720	56.80	3.29
9	56	Ir	2.60	1.42	4.16	0.00	4.78	0.03	1.44	1.93	7.50	580	780	58.80	3.68
10	2172	Ir	2.80	0.54	4.24	0.00	4.17	0.04	1.44	1.93	7.90	530	760	55.54	3.21
11	2395	M	2.80	6.34	5.36	1.76	3.26	0.05	3.20	9.75	8.30	1040	1730	20.36	1.28
12	737	Ir	3.00	3.21	6.72	0.96	2.52	0.11	2.96	8.30	8.50	920	1220	18.93	1.06
13	240	Ir	3.00	4.65	6.08	0.00	3.39	0.05	3.84	6.45	7.70	940	1170	25.05	1.49
14	4135	Ir	3.00	1.64	4.72	0.32	3.22	0.03	2.32	4.11	8.30	650	910	33.57	1.80
15	2	M	3.00	0.32	4.08	0.32	3.91	0.03	1.60	2.18	8.30	530	1010	51.04	2.84
16	225	Ir	3.20	3.30	5.60	0.80	3.83	0.06	2.40	6.61	8.30	860	1320	30.16	1.80
17	834	Ir	3.20	0.91	3.92	0.00	4.70	0.03	1.20	2.10	7.90	560	830	58.90	3.66
18	593	Ir	3.40	0.72	4.40	0.48	6.87	0.04	0.96	1.13	8.20	630	830	76.78	6.72
19	1854	Ir	3.40	2.40	3.44	0.00	3.65	0.04	0.96	4.59	7.50	610	910	39.94	2.19
20	801	Ir	3.40	3.02	4.56	0.00	8.00	0.09	2.00	0.89	8.10	780	990	73.68	6.66
21	999	Ir	3.50	2.15	3.60	0.00	3.04	0.03	3.68	2.50	8.00	620	870	33.19	1.73
22	558	Ir	3.50	0.49	2.96	0.00	4.26	0.04	1.36	1.29	8.10	470	720	61.87	3.70
23	1846	Ir	3.60	1.68	3.04	0.16	4.96	0.06	1.28	2.18	8.30	570	810	59.20	3.77
24	1856	Ir	3.60	1.83	3.52	0.00	2.74	0.03	3.20	2.98	7.50	590	960	30.95	1.56
25	78	Ir	3.60	0.64	5.52	0.00	5.48	0.07	1.23	2.98	8.10	680	1030	56.86	3.78
26	583	Ir	4.00	0.08	3.60	0.00	4.43	0.04	1.44	1.77	8.10	520	940	58.20	3.50
27	65	Ir	4.00	0.96	3.68	0.48	4.52	0.03	2.64	1.93	8.30	610	1110	49.89	2.99
28	1068	Ir	4.00	2.16	4.32	0.00	4.26	0.04	3.68	2.50	8.00	710	970	41.03	2.42
29	2350	Ir	4.20	1.29	4.48	0.32	3.65	0.04	1.60	5.00	8.50	670	1010	35.86	2.01
30	77	Ir	4.60	1.62	5.20	0.48	6.70	0.06	1.84	3.30	8.50	810	1160	56.81	4.18
31	4153	Ir	4.60	2.85	0.64	0.00	1.98	0.25	3.20	2.66	6.80	490	1020	27.56	1.16
32	832	Ir	4.80	0.96	5.28	0.00	5.87	0.03	2.96	2.18	6.90	760	1530	53.44	3.66
33	645	Ir	5.20	0.98	3.04	0.48	6.52	0.05	1.84	1.29	8.30	640	1020	67.73	5.21
34	39	Ir	5.20	3.11	4.56	0.00	4.96	0.04	3.68	4.19	8.10	850	1210	38.85	2.50
35	1731	Ir	5.40	1.29	3.76	0.00	8.70	0.06	0.76	0.93	8.00	710	1010	83.83	9.46
36	833	Ir	5.40	0.74	3.68	0.48	5.04	0.04	2.80	2.42	8.30	670	1090	49.32	3.12
37	9	M	5.40	0.98	3.36	0.80	6.09	0.03	2.08	2.34	8.30	680	1320	58.06	4.10
38	616	Ir	560	0.55	2.96	0.64	6.17	0.04	1.36	2.18	8.50	620	1010	63.69	4.64
39	517	Ir	5.80	0.78	3.20	0.00	7.39	0.07	1.76	0.56	8.00	650	910	76.28	6.86
40	890	Ir	6.00	0.45	3.92	0.48	8.48	0.04	1.00	1.33	8.20	780	1010	78.53	7.86
41	1780	Ir	6.00	0.80	3.76	0.48	8.70	0.05	1.16	1.13	8.20	730	1090	79.26	8.13
42	825	Ir	6.20	1.06	3.76	0.00	4.17	0.03	3.60	3.22	7.70	710	1170	38.11	2.26
43	824	Ir	6.20	1.32	3.76	0.00	4.17	0.04	3.44	3.63	7.50	720	1140	37.32	2.22
44	76	Ir	6.40	2.73	3.84	0.64	6.96	0.06	2.48	4.11	8.30	870	1320	51.58	3.83
45	724	Ir	6.60	2.01	7.60	0.00	3.70	0.05	4.48	7.98	7.50	650	1730	23.13	1.48
46	551	Ir	7.00	0.48	2.40	0.48	6.30	0.05	1.76	1.77	8.30	610	1120	64.27	4.74
47	73	Ir	7.00	2.22	3.92	0.64	5.87	0.03	3.04	4.84	8.20	870	1470	42.82	2.96
48	846	Ir	7.20	0.57	2.80	0.48	4.52	0.03	3.60	2.90	8.10	680	1260	41.18	2.51
49	4304	M	8.00	2.06	4.48	0.32	8.70	0.05	2.40	3.71	8.30	960	1450	58.88	4.98
50	660	Ir	8.00	2.77	3.60	0.00	6.52	0.06	3.84	3.95	8.00	910	1400	45.79	3.30
51	82	O	8.20	0.31	5.60	0.00	5.22	0.06	4.56	4.27	7.50	910	1690	37.42	2.48
52	529	Ir	8.20	3.72	3.84	0.00	9.91	0.06	1.76	4.03	7.50	1020	1500	63.26	5.82
53	823	Ir	8.60	4.07	3.68	0.00	4.35	0.02	4.48	7.50	7.60	1010	1240	26.73	1.78
54	11	M	10.20	0.40	3.68	0.64	8.69	0.04	2.56	3.63	8.20	920	1600	58.51	4.94
55	454	Ir	10.80	0.81	3.12	0.00	4.25	0.04	6.32	4.11	7.10	890	1690	29.19	1.87
56	229	Ir	12.20	0.75	3.04	0.00	7.83	0.05	4.56	3.55	7.10	970	1480	49.28	3.89
57	927	Ir	13.20	8.14	5.20	0.00	10.43	0.07	10.00	6.04	7.80	1690	2330	39.56	3.68
58	247	Ir	14.00	3.25	4.32	0.00	6.30	0.04	9.20	6.04	7.30	1320	2160	29.38	2.28
59	281	Ir	14.80	3.83	4.16	0.00	8.25	0.09	9.00	5.44	7.30	1400	2380	36.64	3.07
60	1763	Ir	15.60	4.25	5.60	0.32	21.30	0.26	1.36	2.86	8.20	1670	2480	83.63	14.66
61	319	Ir	16.00	7.51	4.80	0.00	15.00	0.26	6.00	7.05	7.60	1780	2530	53.90	5.87
62	1855	Ir	16.80	0.86	3.04	0.64	5.44	0.05	10.00	5.85	8.10	1240	2390	25.73	1.93
63	300	Ir	18.40	6.13	3.52	0.00	16.74	0.26	4.80	6.25	7.30	1730	2790	60.61	7.12
64	1894	Ir	18.80	1.48	2.40	0.00	6.78	0.04	7.80	8.06	7.50	1300	2330	30.07	2.41
65	500	Ir	20.40	1.50	2.80	0.00	4.78	0.05	11.00	8.87	8.00	1410	2380	19.55	1.52
66	1823	Ir	21.60	2.74	4.80	0.00	13.91	0.18	8.80	6.75	7.30	1770	2110	47.54	4.99
67	330	Ir	22.00	7.05	4.00	0.00	12.61	0.56	9.20	10.68	7.70	1990	2950	39.85	4.00
68	306	Ir	26.00	3.71	5.28	0.00	22.61	0.15	8.40	3.83	7.30	2160	3620	65.05	9.14
69	1848	Ir	33.60	8.22	4.64	0.00	15.00	0.16	17.40	13.90	6.90	2740	5060	32.63	3.79
70	7	M	41.60	3.84	3.04	0.00	16.09	0.06	15.00	17.33	7.60	2730	4240	33.31	4.00
71	471	Ir	48.80	4.72	2.72	0.00	10.43	0.08	27.40	18.33	7.50	2940	5060	18.69	2.18
72	1860	Ir	48.80	2.10	3.04	0.96	20.43	0.08	9.00	25.39	8.30	3010	5160	37.36	4.93
73	2348	Ir	50.00	1.79	2.88	0.00	10.87	0.05	23.60	20.15	8.00	3000	5590	19.97	2.32
74	1843	Ir	67.00	3.88	2.80	0.00	13.04	0.07	38.00	22.57	8.00	4070	6320	17.79	2.37
75	688	Ir	73.00	5.67	2.40	0.00	14.78	0.07	36.00	30.00	7.70	4440	7100	18.37	2.57
76	2315	Ir	79.00	4.64	3.20	0.00	19.57	0.08	42.00	25.19	7.70	4820	7610	22.63	3.38
77	2441	O	110.00	2.90	0.72	0.00	56.52	0.85	22.00	34.25	7.50	6280	9660	50.49	10.66
78	2447	O	200.00	4.32	2.00	0.00	69.57	0.19	60.00	76.56	7.20	11170	16270	33.81	8.42
79	2444	O	400.00	55.61	0.88	0.00	313.04	2.95	72.00	68.50	7.00	26510	28480	69.22	37.35
80	1725	O	400.00	34.54	5.84	0.00	339.13	0.69	24.00	76.56	7.50	25450	30510	77.17	47.83
81	SEA W	SW	640.00	73.09	2.08	1.28	547.83	11.67	28.00	128.95	8.40	41580	43000	78.09	61.84

Areal distribution of saline water throughout the aquifer may be seen from the isochloride contour map (Fig. 3). Here the chloride concentrations expressed in mg/l provide invaluable clues about the extent of salt water intrusion into the aquifer. High chloride concentrations are observed along the coastal strip of approximately 2 km wide. Around Kumköy, due to overdrafts from irrigation well field the isochloride contours extend considerably inland from the shore line. Similar anomaly may be observed between Yeşilyurt and Gaziveren. Here, the shape of the isochloride contours suggest upconing phenomenon resulting from overpumping of the irrigation wells.

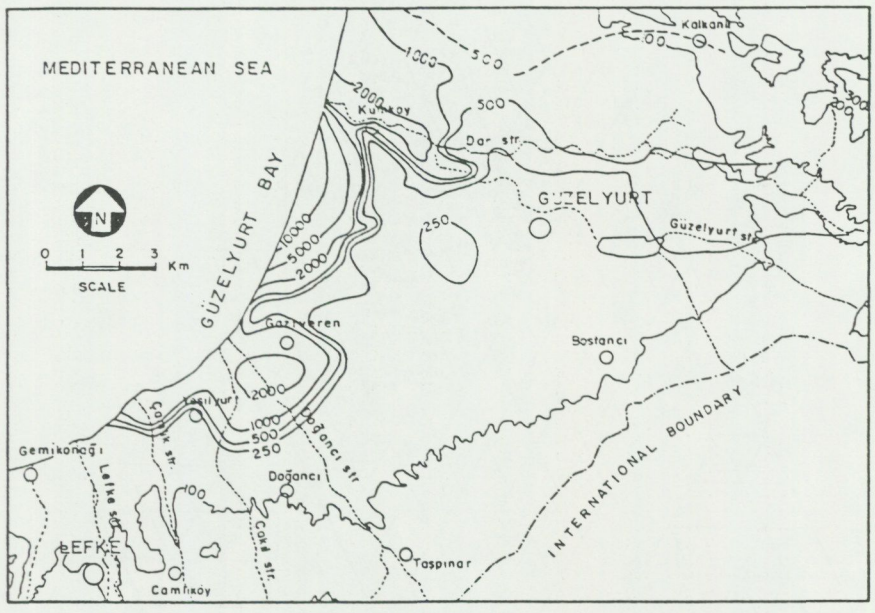


Fig. 3. Isochloride contour map.

An attempt is made to group the wells according the their degree of contamination. The major ion given in Table 1 are entered to the trilinear diagram (Fig. 4). From the figure four distinct groups may be distinguished. The wells represented by solid triangles form Group A, which are located close to the shore line. They are characterized by high suphate and chloride (80%-100%) concentrations. Group B wells (squares) are mostly located between Kumköy and Yuvacık dam. In these wells moderately high sulphate and chloride (50%-80%) concentrations are noted. Group C wells (circle and triangle) are mostly located around Yeşilyurt. In these wells chloride concentrations range between 15% and 45%, and they are characterized by bicarbonate and carbonate type water. Group D wells (circles) are mostly located at the central and western part of the groundwater basin. They are characterized by variable chloride concentrations and high bicarbonate and carbonate ions.

A number of researchers (Chapelle, 1983; Mercado, 1985; and Şen and Al-Dakheel, 1986) attempted one-to-one correlation between anions and cations to establish the hydrochemical pattern of the groundwater. Relationships between chloride and selected ions are given in Fig. 5. Here Na^+/Cl^- molar ration of 0.95, as suggested by Richter and Kreitner (1987), is also indicated. This ratio increases in fresh water and decreases in saline water. From Fig. 5 it is clearly seen that almost all wells of Groups A and B lie below molar ratio of 0.95.

The double-mass curve is used to check the consistency of hydrological data by comparing data for a single station with that of a pattern composed of the data from several other stations in the area (Searcy and Hardison, 1960). This technique is adopted to the study area to explain the historical trends of the sea water intrusion.

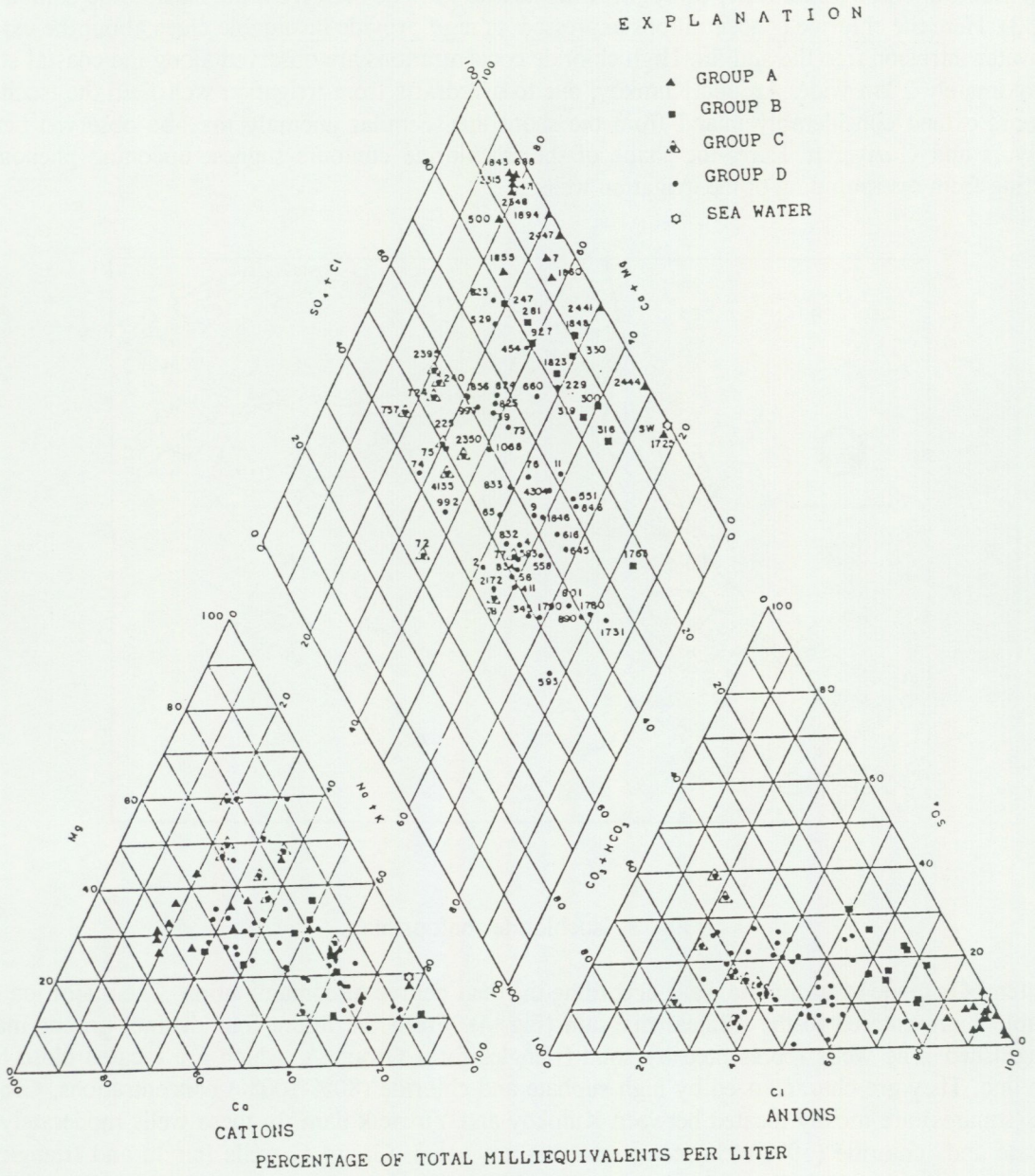


Fig. 4. Trilinear diagram for the group of wells.

The wells affected from sea water contamination (2444, 688, 2447, and 1725) were selected as single stations and twenty wells with constant chloride concentrations, which are located in the central part of the basin, were taken as pattern. Average annual and cumulative chloride values were calculated for the period 1977 thru 1987. For the double-mass curve the cumulative chloride values of each selected well are plotted against cumulative chloride values of the pattern (Fig. 6). The slope of the line represents constant of proportionality between the quantities. The breaks in the slope of the double-mass curve mean that a change in the constant of proportionality between the two variables has occurred. The chloride concentration of the contaminated wells show significant variations with time. Fig. 6 suggests that depending upon the distance from the shore line each well reflects historical fingerprints of the salt water intrusion.

BEDROCK CONTAMINATION: The chemical composition of the groundwater is controlled by the lithology of the catchment area and of the aquifer . In the Güzelyurt groundwater basin major source of recharge is through infiltration of precipitation. During this process some of the soluble minerals are leached from the bedrock and introduced to the groundwater reservoir.

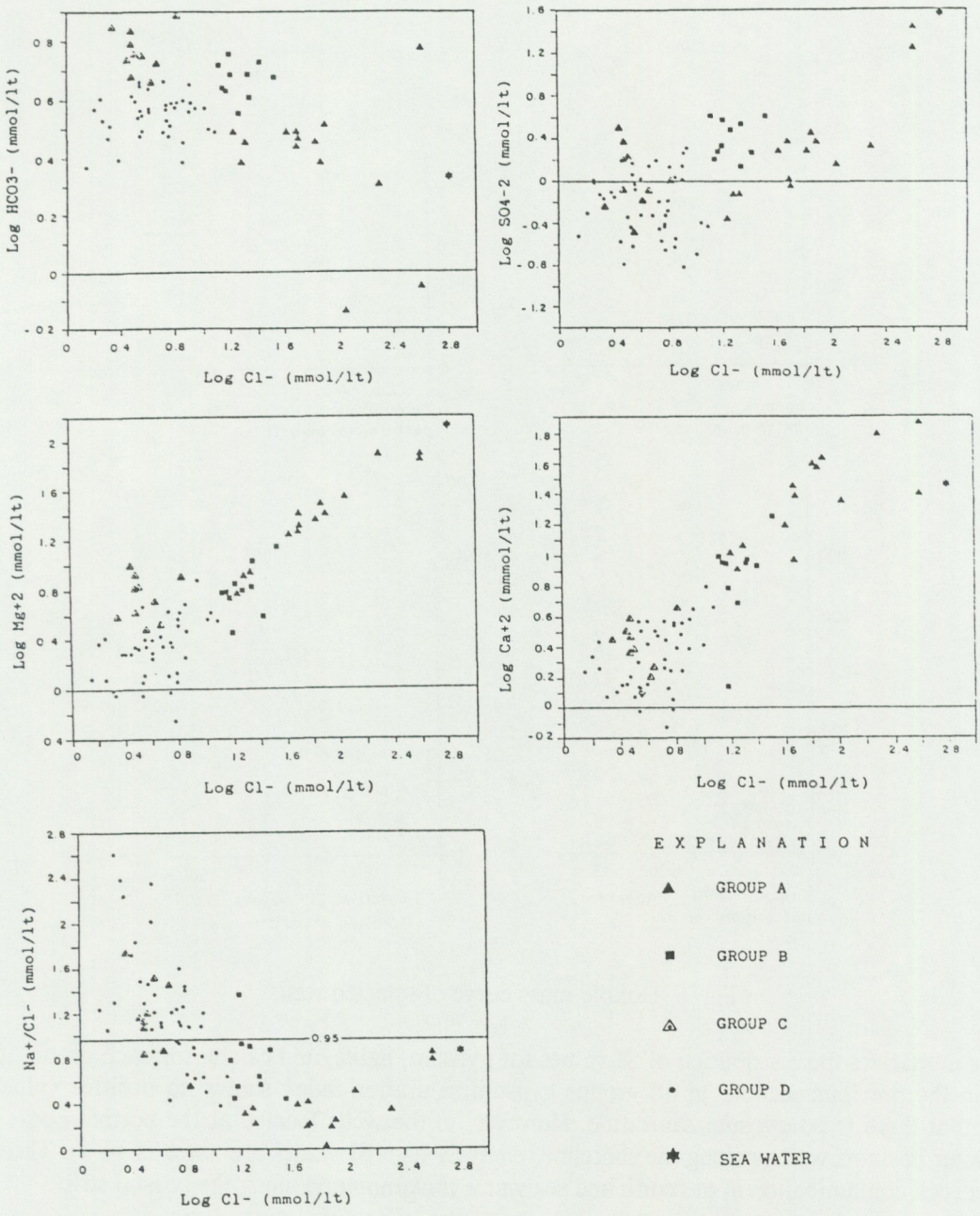


Fig. 5. Relationship between Cl^- and selected ions

Different types of soluble rocks are exposed in the groundwater basin and its watershed. Carbonate and evaporite containing Tertiary rocks crop out at the northern and eastern part of the basin. The fanglomerates (Pliocene) contain carbonate cement and caliche deposits. In order to assess the influence of bedrock contamination the saturation index of certain minerals are evaluated using the computer program WATEQB (Arıkan, 1988). The saturation index (SI) is widely used by a number of researchers, such as Langmuir (1971), Chapelle (1983) and Lee (1985). Langmuir (1971) stated that the sample is saturated if SI falls within the range of -0.1 and 0.1. Lee (1985) classified the SI values as follows: For SI>0.1, the specific mineral is oversaturated and precipitation is possible; for SI=±0.1, the specific mineral is saturated and precipitation or dissolution is possible; for SI<0.1, the specific mineral is undersaturated and dissolution is possible.

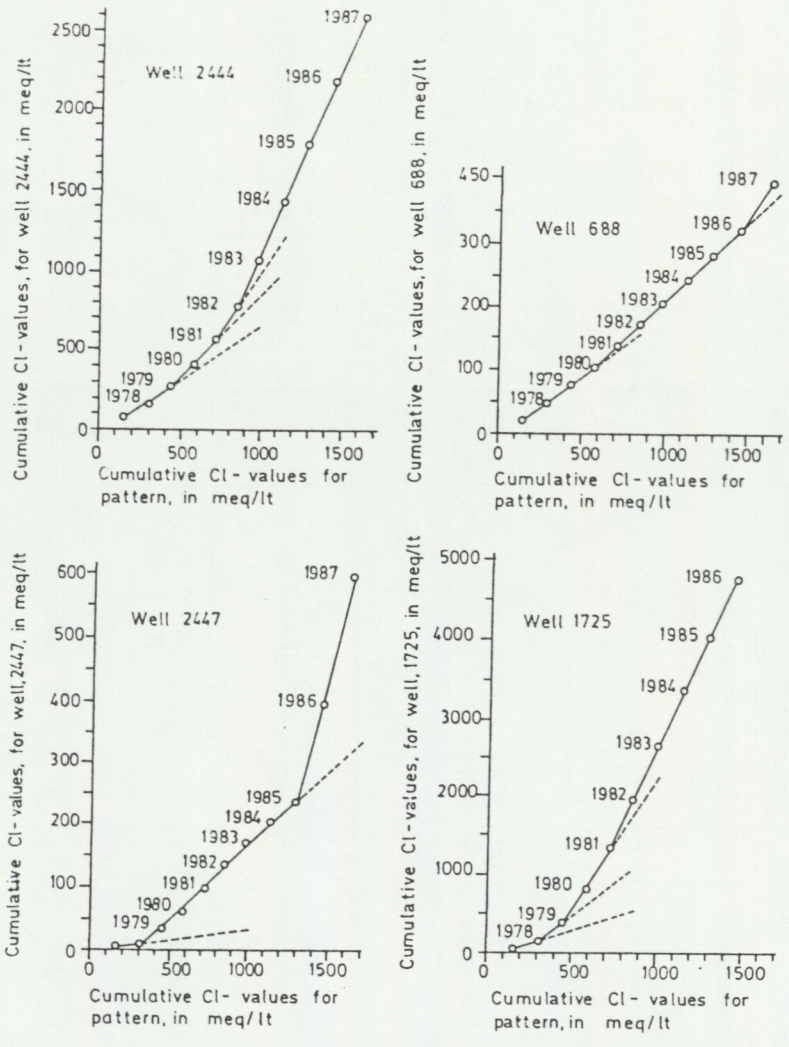


Fig. 6. Double-mass curve of selected wells

Table 2 summarizes the distribution of SI values for gypsum, halite, and calcite for each group of wells defined in the previous section. In all groups gypsum saturation index shows no positive value. This suggests that there is no gypsum saturation. However, in the wells located at the northern part of the groundwater basin as well as along the shoreline relatively high SI values are noted (Fig. 7). These may imply bedrock contamination in the north and sea water contamination along the coastal strip.

$SO_4^{=}/Cl^-$ ratios given in Table 2 are used to compare $SO_4^{=}$ enrichment of the groups A and B. In group B wells more than four-fold increase in the ratio is noted. This may be attributed to bedrock contamination at that part of the aquifer. In group C and D wells an increase in the $SO_4^{=}/Cl^-$ ratio is attributed to low Cl^- content of the groundwater.

All groups show calcite oversaturation. The increasing calcite saturation index in the northeast and in the east (Fig. 8) directly correlate with the distribution of the carbonate sequences of the groundwater basin.

Conclusions

Grouping of wells on the basis of their degree of their contamination is accomplished through salinity data and trilinear diagrams. The wells of group A and B yield groundwater of high and moderately high sulphate and chloride concentrations, respectively. Isochloride contour map suggests that the sea water front has advanced 2 km to 4 km inland from the sea. The wells of group C and D are less affected from the sea water intrusions and they yield carbonate-bicarbonate type water.

Historical fingerprints of sea water intrusion are well distinguished through double-mass curves. Depending on the distance to the shore line the selected wells show significant goundwater degradation in late 1970's and early to middle 1980's.

The saturation index of minerals such as gypsum, halite, and calcite provided valuable clues for bedrock contamination. Increasing calcite saturation in the northeast and east of the groundwater basin correlate well with the distribution of carbonate sequences of the Tertiary units.

Table 2. Gypsum, halite, and calcite saturation indices and $SO_4^{=}/Cl^{-}$ for group of wells.

Seq. No:	Well No:	SO4/Cl	SATURATION INDEX GYPSUM	HALITE	CALCITE
GROUP A					
62	1855	0.05	-1.78	-5.76	1.00
64	1894	0.08	-2.03	-5.60	-0.22
65	500	0.07	-1.54	-5.74	0.87
70	7	0.09	-1.18	-4.94	0.56
71	471	0.10	-0.91	-5.07	0.64
72	1860	0.04	-1.67	-4.77	0.96
73	2348	0.04	-1.38	-5.04	1.08
74	1843	0.06	-0.95	-4.86	1.21
75	688	0.08	-0.84	-4.77	0.82
76	2315	0.06	-0.87	-4.62	0.99
77	2441	0.03	-1.36	-4.03	-0.13
78	2447	0.02	-1.01	-3.72	0.32
79	2444	0.14	-0.01	-2.81	-0.27
80	1725	0.09	-0.65	-2.77	0.60
MIN		0.02	-2.03	-5.76	-0.27
MAX		0.14	-0.01	-2.77	1.21
AVG		0.067	-1.155	-4.607	0.601
STD		0.03	0.50	0.92	0.48
GROUP B					
57	927	0.62	-0.87	-5.59	0.86
58	247	0.23	-1.24	-5.77	0.32
59	281	0.26	-1.19	-5.64	0.33
60	1763	0.27	-1.91	-5.20	0.50
61	319	0.47	-1.12	-5.35	0.43
63	300	0.33	-1.27	-5.24	-0.08
66	1823	0.13	-1.38	-5.26	0.34
67	330	0.32	-1.02	-5.30	0.61
68	306	0.14	-1.28	-4.97	0.34
69	1848	0.24	-0.79	-5.06	0.11
MIN		0.13	-1.91	-5.77	-0.08
MAX		0.62	-0.79	-4.97	0.86
AVG		0.302	-1.207	-5.338	0.375
STD		0.14	0.29	0.24	0.24
GROUP C					
7	72	0.52	-2.03	-6.75	1.05
11	2395	2.26	-1.38	-6.74	0.90
12	737	1.07	-1.66	-6.81	1.17
13	240	1.55	-1.38	-6.69	0.50
14	4135	0.55	-1.94	-6.69	0.82
16	225	1.03	-1.70	-6.60	0.85
25	78	0.18	-2.58	-6.38	0.46
29	2350	0.31	-2.21	-6.49	0.82
30	77	0.35	-2.06	-6.20	0.95
45	724	0.30	-1.70	-6.31	0.47
MIN		0.18	-2.58	-6.81	0.46
MAX		2.26	-1.38	-6.20	1.17
AVG		0.812	-1.864	-6.565	0.798
STD		0.64	0.36	0.20	0.23
GROUP D					
1	992	0.43	-2.34	-7.27	0.34
2	74	0.61	-2.09	-7.22	-0.53
3	75	1.13	-1.73	-7.04	0.75
4	411	1.11	-1.73	-6.25	0.57
5	1790	0.75	-2.16	-6.68	0.40
6	345	0.65	-2.11	-6.67	0.55
8	4	0.66	-2.13	-6.66	0.53
9	56	0.55	-2.14	-6.58	-0.17
10	2172	0.19	-2.53	-6.60	-0.83
15	2	0.11	-2.73	-6.60	0.67
17	834	0.28	-2.40	-6.49	0.13
18	593	0.21	-2.59	-6.31	0.41
19	1854	0.71	-2.14	-6.58	-0.46
20	801	0.89	-1.73	-6.25	0.55
21	999	0.61	-1.62	-6.65	0.62
22	558	0.14	-2.58	-6.49	0.31
23	1846	0.47	-2.13	-6.42	0.43
24	1856	0.51	-1.74	-6.68	0.09
26	583	0.02	-3.34	-6.42	0.40
27	65	0.24	-2.07	-6.42	0.81
28	1068	0.54	-1.63	-6.45	0.70
31	4153	0.62	-1.54	-6.71	-1.33
32	832	0.20	-2.05	-6.23	-0.37
33	645	0.19	-2.20	-6.15	0.59
34	39	0.60	-1.53	-6.28	0.79
35	1731	0.24	-2.46	-6.01	0.02
36	833	0.14	-2.18	-6.24	0.83
37	9	0.18	-2.18	-6.16	0.65
38	616	0.10	-2.58	-6.13	0.62
39	517	0.13	-2.30	-6.04	0.32
40	890	0.08	-2.80	-5.97	0.36
41	1780	0.13	-2.50	-5.97	0.41
42	825	0.17	-1.95	-6.27	0.35
43	824	0.21	-1.88	-6.27	0.13
44	76	0.43	-1.74	-6.04	0.74
46	551	0.07	-3.29	-6.03	0.48
47	73	0.32	-1.75	-6.08	-0.83
48	846	0.08	-2.20	-6.17	0.63
49	4304	0.26	-1.88	-5.85	0.79
50	660	0.35	-1.57	-5.98	0.61
51	82	0.04	-2.43	-6.06	0.41
52	529	0.45	-1.77	-5.79	-0.21
53	823	0.47	-1.40	-6.13	0.26
54	11	0.04	-2.54	-5.74	0.65
55	454	0.08	-1.90	-6.04	-0.10
56	229	0.06	-2.05	-5.72	-0.26
MIN		0.02	-3.34	-7.27	-1.33
MAX		1.13	-1.40	-5.72	0.83
AVG		0.357	-2.137	-6.321	0.278
STD		0.28	0.43	0.35	0.49
sw	1111	0.11	-0.42	-2.37	0.88

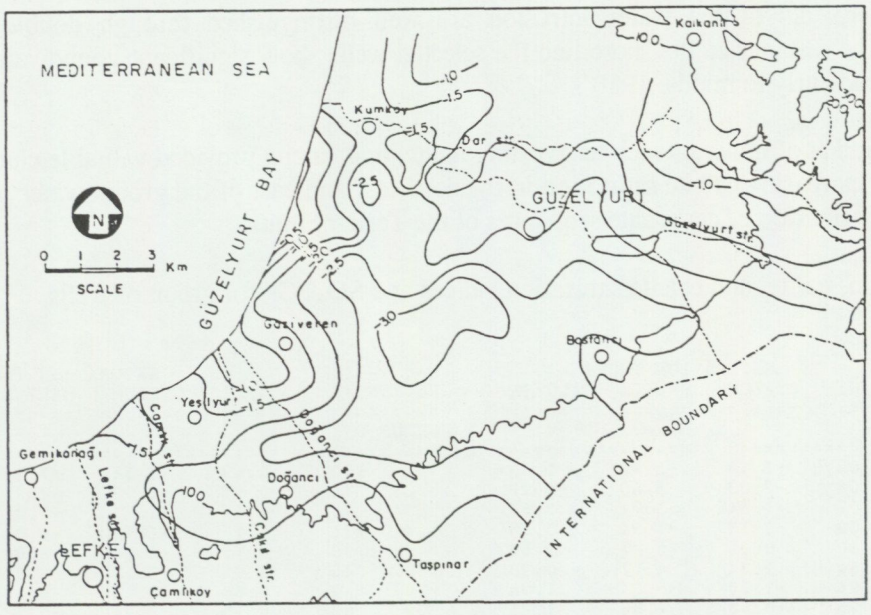


Fig. 7. Areal distribution of gypsum saturation index.

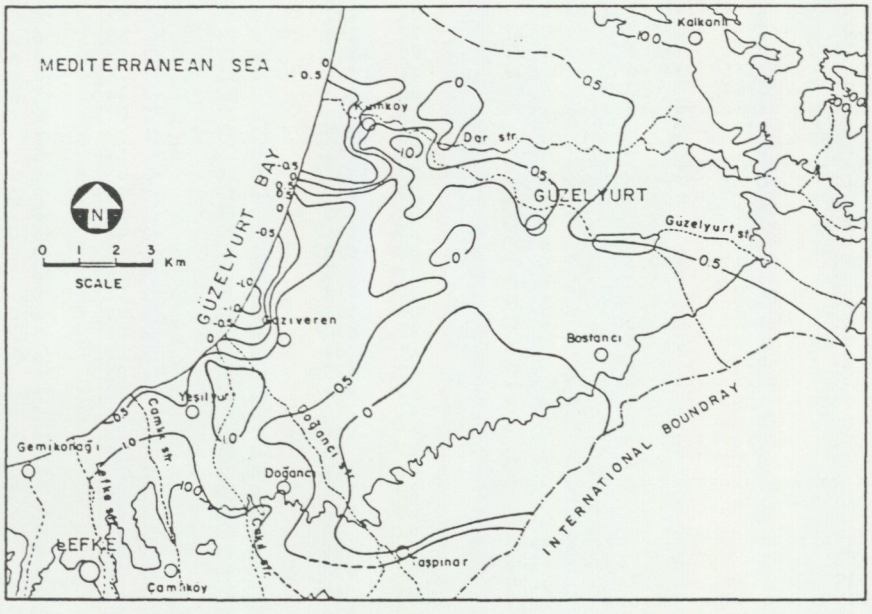


Fig. 8. Areal distribution of calcite saturation index.

REFERENCES

ARIKAN, A., 1988: Wateqb-basica revision of Wateqf for IBM personal computers-Groundwater, 26, 2, 222-227.

CHAPELLE, F.H., 1983: Groundwater geochemistry and calcite cementation of the Aguia aquifer in Southern Maryland-Water Resources Research, 19,1, 545-556.

GÖKÇEKUŞ, H. & OLGUN, E., 1993: Cenozoic stratigraphy of the Güzelyurt basin, Turkish Republic of Northern Cyprus-TAPG Bulletin, 5, 1, 57-68.

GÖKÇEKUŞ, H. & DOYURAN, V., 1993: Mining groundwater: A case study from Northern Cyprus-Advances in Civil Engineering, First Technical Congress, vol. II, Gazi Mağusa, Northern Cyprus, 819-829.

GÖKÇEKUŞ, H. & DOYURAN, V., 1995: Evaluation of hydrochemical data from Güzelyurt aquifer (Turkish Republic of Northern Cyprus) through cluster analysis-Turkish Journal of Earth Sciences,4, 1-10.

LANGMUIR, D., 1971: The geochemistry of some carbonate groundwater in central Pennsylvania-Geochim. Cosmochim. Acta, 35, 1023-1045.

LEE, R.W., 1985: Geochemistry of groundwater in Cretaceous sediments of the southern coastal plain of eastern Mississippi and western Alabama-Water Resources Research, 21, 10, 1545-1556.

MERCADO, A., 1985: The use of hydrochemical patterns in carbonate sand and sandstone aquifers identify intrusions and flushing of saline water-Groundwater, 23,5,635-645.

RICHTER, B.C. & KREITLER, C.W., 1987: Geochemistry of salt water beneath the rolling planes, North Central Texas-Groundwater, 24, 6, 735-742.

ROBINOVE, C.J., LANGFORD, R.H. & BROOKHART, J.W., 1958: Saline-water resources of North Dakota-U.S. Geol. Survey Water-Supply Paper 1428, 72pp.

SEARCY, J.K. & HARDISON, C.H., 1960: Double-mass curves; with a section on fitting curves to cyclic data-U.S. Geological Survey Water-Supply Paper, 1541-B, 31-36.

ŞEN, Z. & AL-DAKHEEL, A., 1986: Hydrochemical facies evaluation in Umm Er Radhuma limestone, eastern Saudi Arabia-Groundwater, 24, 5, 626-635.

Risk Mapping of Groundwater Salinization Using Geographic Information Systems

Johan Lindberg, Bo Olofsson and Thomas Gumbricht
Division of Land and Water Resources, Royal Institute of Technology, S-100 44 Stockholm, Sweden

Abstract

Due to the increased withdrawal of groundwater in many areas in Sweden, the risk for groundwater salinization is increasing. As a tool for municipal planners to assess the risk the Risk Variable Method (the RV-method) has been developed. The method is an expert system where a number of statistically processed parameters are assigned weights and added together to a final risk value. When estimating the spatially distributed uncertainty for each specific parameter and adding the values together, after weights have been assigned, the final uncertainty value is a help to validate the risk value. An implementation of the RV-method into a GIS environment makes it possible to perform a study over extended areas. The major problem when working with the GIS implementation is the database creation, both the collection of data and the assurance of a proper database quality. If these problems are solved the RV-method implemented in a GIS is a powerful tool in assessing the risk for salt groundwater in municipal areas. However, the method has so far been developed for the natural conditions prevailing in eastern Sweden and adapting to other areas needs a careful selection of variables and their ratings.

Introduction

Salt groundwater is a widespread and serious problem in large areas of southern and central Sweden, especially along the coastal zone. The problem is described by Lindewald (1985) and Olofsson (1992 and 1994). Various sources of the salts have been proposed such as intrusion of seawater, fossil salt groundwater from ancient seas and anthropogenic sources such as de-icing salt along roads and leachates from waste deposits. The salinization problem has increased within the last decades mainly due to an increased discharge of groundwater particularly during the summer season along the coastal areas. The groundwater supply in these areas is today mainly based on limited water resources in crystalline rock and the water is usually extracted from private drilled wells, with depths sometimes exceeding 100 m. The rocks usually show a strongly heterogeneous and anisotropic character. The flow occurs along fractures and is strongly depending of their genesis, mineral filling and probably of the prevailing rock stress pattern. The heterogeneous hydraulic conditions can be illustrated by the situation in the archipelago of Stockholm, where drilled wells located close to the shore may be totally fresh, whereas wells far from the coastline may exhibit clear effects of salt water intrusion.

Risk assessments for salt groundwater

Up to today, no judicial tools for control of construction of wells and extraction of groundwater for ordinary households, have been available outside detailed planned areas in Sweden. However, the increased salinization problem in many municipalities of Sweden has raised the necessity for some types of permission for extraction of groundwater in areas with limited freshwater resources (Grundvattenutredningen, 1994). Hence, it has been necessary to develop methods for quantitative as well as qualitative risk assessments for salinization of groundwater. Since the assessment should be used within municipal planning among decision makers, it must be clear, easy understandable and reliable. Several approaches have been tested. Numerical methods using finite elements or finite differences, which is commonly applied to coastal zones, can hardly be reliable within the strongly heterogeneous and anisotropic hydraulic conditions prevailing in crystalline rock areas of Sweden.

One method, which frequently have been used in Sweden, is the *Water Balance Method*, in which the discharge of groundwater from wells is compared to an estimation of the groundwater recharge, calculated as a fraction of the annual precipitation (Sund & Bergman, 1980, Tilly-Leander, 1990). When the discharge equals or exceeds the recharge, salinization will occur in the long run. However, the method is incorrect since it does not take into consideration the storage capacity of the aquifer. The crystalline rock itself is a very small reservoir with a kinematic porosity usually less than 0.05% (Carson & Oslo, 1981, Olofsson, 1991), which can only store a minor part of the potential recharge. The main part of the annual precipitation is also usually restricted to the summer period (July-August) when the groundwater recharge probably is very small or negligible.

Several qualitative vulnerability assessments using information of the geological and hydrogeological conditions have been developed, such as the well known DRASTIC method (Aller et al 1987) and the LeGrand-method (LeGrand, 1983). However, these methods are static, developed for pollution sources placed on the land surface within geohydrological conditions which significantly differ from the conditions prevailing in Sweden. Moreover, they do not take into account the uncertainty within the assessments, as would be desirable within decision making situations. Therefore, a new method, the *Risk Variable Method* (the RV-method) was developed with inspiration from the DRASTIC method. It has been manually tested within the Värmdö municipality, in the archipelago east of Stockholm (Bucht & Larsson, 1995). This paper describes the first attempt to adopt the RV-method over extended areas within the Norrtälje municipality, north of Stockholm, using the GIS technique.

The Risk Variable Method - a short description

The RV-method is an expert system which takes into account and evaluates topographical, hydrological, geological and technical variables (Figure 1). The expert parts of the method (the preparation stage) comprise selection of variables and their ratings. This is done once within a region (such as for eastern Sweden). The selection of variables in Sweden was carried out by statistical analyses of water chemistry in drilled wells from the Well Record Section at the Geological Survey of Sweden (SGU) and from local municipal archives. The variables include topography, hydrology (precipitation etc.), geology (type of soil and rock, soil depth) and technical variables (degree of land utilisation, well depths etc.). Finally, zonation factors are added, such as distance to the shoreline and distance to roads on which de-icing salts are used. The variables are subdivided into classes with variable risk values between +2 and -2 (where positive values mean that the variable decreases the risk for salinization). The variables have ratings varying between 1 and 3.

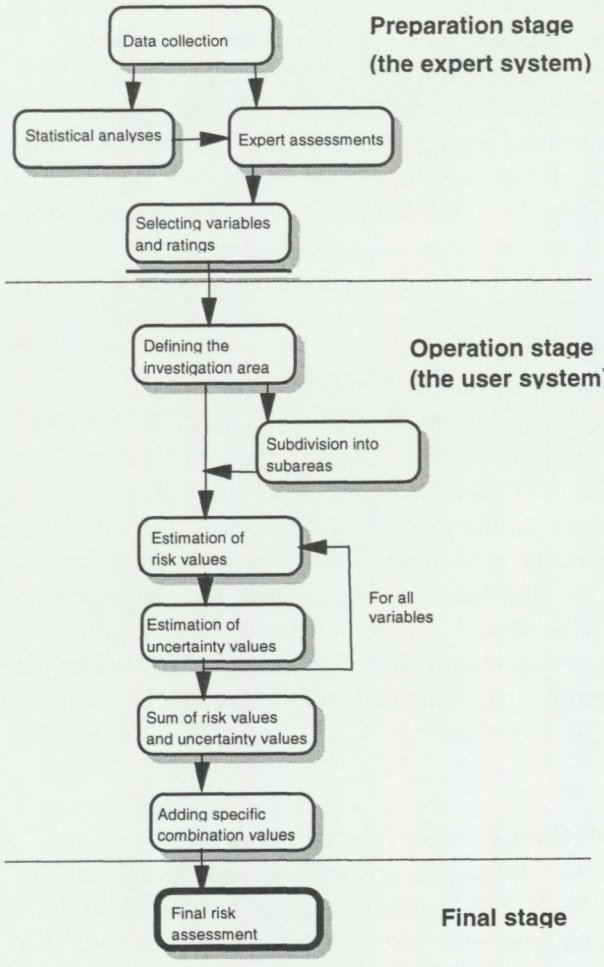
$$V_1 \times R_1 + V_2 \times R_2 + V_3 \times R_3 + \ldots + V_n \times R_n = \sum_{i=1}^{n} V_i \times R_i = FRV \textit{ (Final Risk Value)}$$

where V_i = a risk value for a specific variable (-2 to +2) and R_i = the rating of the variable (1 to 3).

For each variable the operator also gives a value of the uncertainty within the classification of the variable. The uncertainty values vary between -1 and +1, where negative values represent a high degree of uncertainty. The uncertainty values are handed in a similar way as the variable values.

$$U_1 \times R_1 + U_2 \times R_2 + U_3 \times R_3 + \ldots + U_n \times R_n = \sum_{i=1}^{n} U_i \times R_i = FUV \textit{ (Final Uncertainty Value)}$$

where U_i = an uncertainty value for a specific variable (-1 to +1) and R_i = the rating of the variable (1 to 3).



Name of variable	*Rating*
Natural variables	
Precipitation	1
Slope	3
Soils	2
Thickness of soil cover	2
Regional fracture zones	1
Local fracture frequency	1
Technical variables	
Well depth below sea level[a]	2
Degree of land utilisation	2
Localisation of discharge wells	2
Sanitary standard	3
Zone factors	
Distance to shore[a]	3
Distance to lakes	2
Distance to wetlands	1
Distance to main road	2
Distance to other salt sources	2

[a] not used in this study

Figure 1. Principal sketch of the Risk Variable Method and a tabulation of the different variables used in eastern Sweden.

Summation of the risk values and the uncertainty values gives the final risk value (FRV) and the final uncertainty value (FUV). However, some combination effects occur, which significantly increase or decrease the salinization risk. Hence the final risk value is adjusted for such effects, by using Specific Combination Values. The FRV and the FUV values can be plotted within the scattered bi-plot in Figure 2, where the axis represent the salinization risk and the uncertainty.

It must be clearly pointed out that the variables and ratings selected within this project and presented in Figure 1, only represent the most important factors for eastern Sweden. Adapting the RV-method to other areas with significantly different natural as well as technical conditions, needs careful selection of variables and ratings.

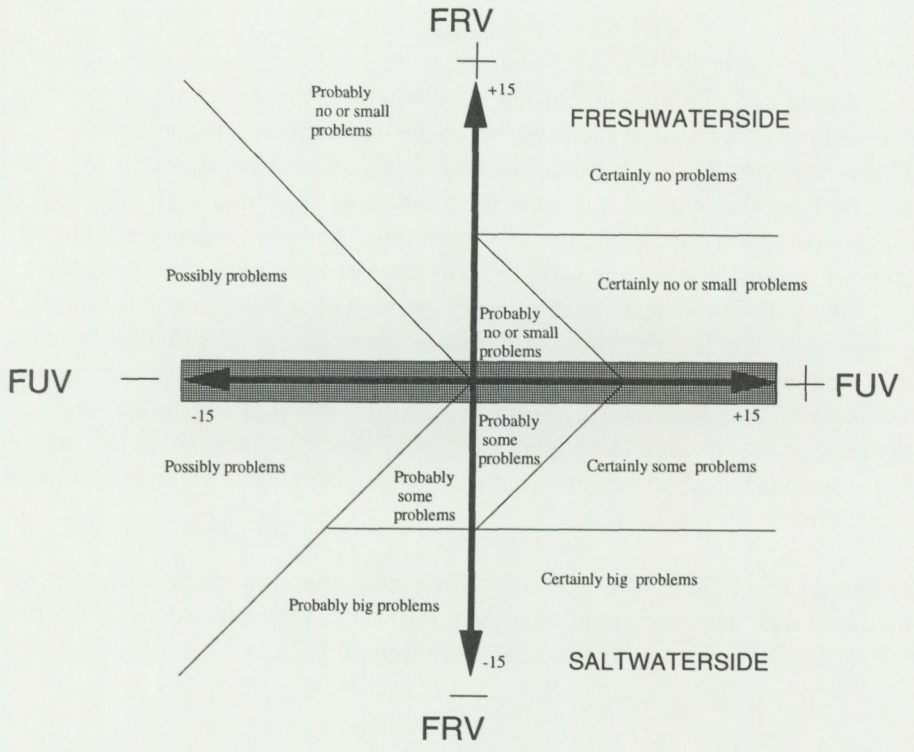


Figure 2. Principal graph for salt water risk analysis

The investigated area

The study was carried out within the south-eastern part of the Norrtälje municipality, in the County of Stockholm, Sweden (Figure 3). The study area has a size of 341 k^{m2}. The geology in the study area is representative for the region with hard crystalline rock which forms a hilly topography and soil layers of varying thickness. In the bottom of the narrow valleys a layer of post-glacial clay is overlaying the till that is found along the slopes. On the tops there are outcrop or just very thin layers of till. The area was covered by ice during the latest glacial period and has since then been surged by waves while the land has progressed from the sea. The area is sparsely populated with single houses and farms spread all over the area. There are also a few places or gatherings of houses within the area. The water supply is mainly based on private dug or drilled wells.

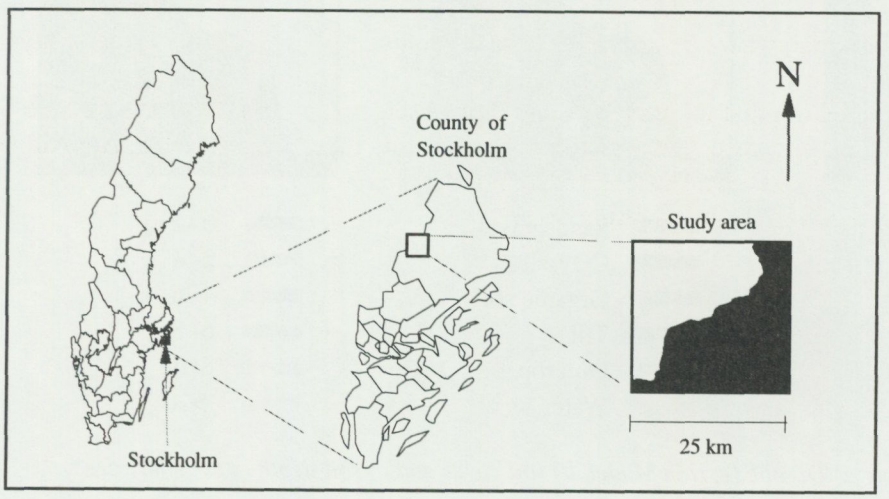


Figure 3. The study area.

The GIS-technique

Geographic Information Systems (GIS) is a tool for input, storage, resampling, analysing and presentation of spatial distributed digital data. During the last ten years the technique has developed very quick, mainly as a result of the progress in the development of computers. Another reason, and pre-requisite, for the rapid development of GIS is the availability of databases. This has so far been the major bottle neck for most people working with GIS, as it is expensive and tedious to transform data into digital form, but also because of problems due to transformation between different data storage formats. GIS software can be divided into two major categories that principally differ from each other in the way of storing and handling data. In a *raster based* system each map layer is built up of picture elements (pixels) that are small squares with a specific spatial resolution (the length of the square side), oriented in a regular grid. Each pixel is assigned a value that describes the property (e.g. soil class) or magnitude (e.g. altitude in a topographic map) of the area that is represented by that specific pixel in the map layer. A *vector based* system is based on vectors (points, lines or polygons) to which data bases with attribute data are coupled.

In this study a raster based GIS (IDRISI) has been used for implementation of the RV-method. The major part of the input data has been supplied as MapInfo files (vector based GIS). All data has been transformed to IDRISI-format with a spatial resolution of 50 m.

Database creation

For this project data has been supplied by SGU (soil map and data from the Well Record Section, e.g. well localisation, well depth and thickness of soil layers in the drilled wells), the National Land Survey of Sweden (Digital Terrain Model (DTM) and landuse map) and the Norrtälje municipality (data about sanitary standard, degree of land utilisation and delineation of areas with municipal responsibility for fresh water and waste water). The way to create the database for the project is described in the following. Figure 4 shows three different maps used in, or produced by, the process; a) DTM, b) soil map, c) map showing soil depth.

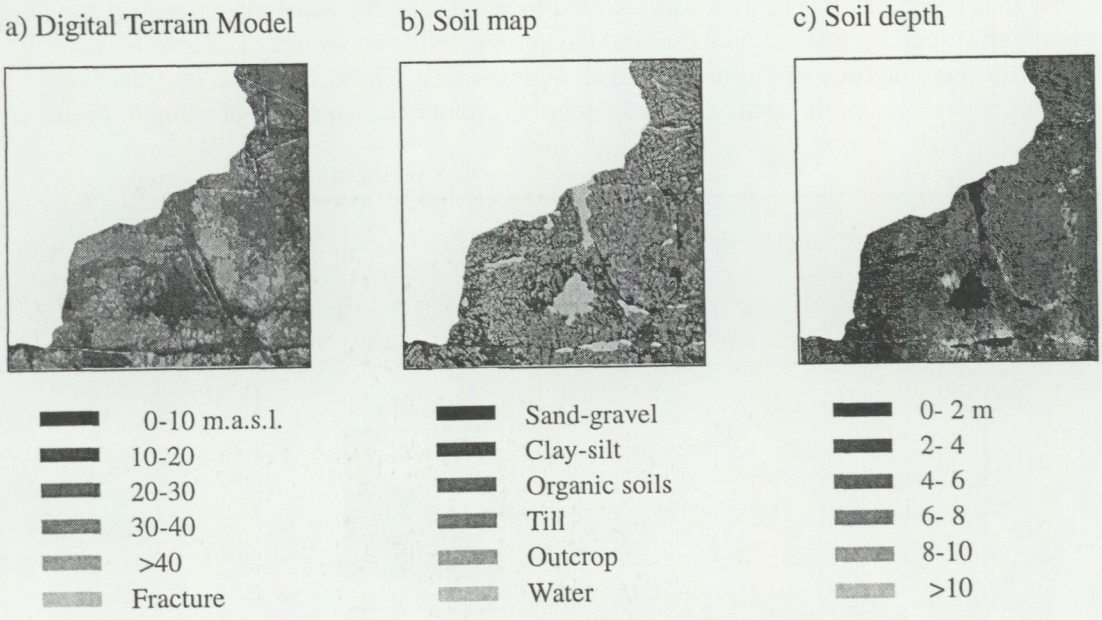


Figure 4. Maps showing a) Digital Terrain Model, b) soil cover and c) soil depth in the study area.

To calculate the *slope*, IDRISI has been used to process the DTM. The *soil* map has been reclassified to match the classes defined for the RV-method. To model the *soil depth* the soil map has first been classified into five classes (sand-gravel, clay-silt, organic soils, till and outcrop). Secondly, statistics about well depth has been extracted for wells situated in the different soil classes. This statistics has acted as a rule to assign a value of soil depth to each soil class. Parallel to this, an aerial interpolation has been performed using IDRISI with well depth as input data. These two maps has finally been combined by calculating the arithmetic mean value for each pixel to be used as a value for soil depth. The *regional fracture zones* have been digitised into IDRISI from the hydrogeological map (Engqvist & Fogdestam, 1984). To get a map layer describing the *local fracture frequency* a rock map has been digitised in the same way as for regional fracture zones and reclassified with respect to local fracture frequency according to information in the description to the hydrogeological map.

To produce a map for the *degree of land utilisation*, areas classified as built-up areas (high and low exploited) and industrial areas have been extracted from the landuse map and reclassified according to the RV-method. The input data for the *spatial distribution of discharge wells* has been the Well Record Section at SGU. On-screen digitising has been performed to sort out areas with a homogeneity in the spatial distribution of wells. A map for *sanitary standard* has been created by using and reclassifying the landuse map in combination with information about areas where the municipality is responsible for delivery of fresh water and treatment of waste water. *Distance to lakes* and *distance to wetlands* have been estimated by buffer analyses. Separate maps have been created for the *distance to roads* (that are treated with de-icing salt during the winter) and the *distance to other salt sources* (a landfill).

Two important parameters (in general) when assessing the risk for salt groundwater that do not affect the result in this study is the *precipitation* and the *distance to shore*. As there is no difference in precipitation within the area this parameter does not affect the result and as the study area is not a coastal area that variable has been excluded in this study.

Results

The resulting risk map from the RV-method implemented in a GIS is presented in Figure 5.

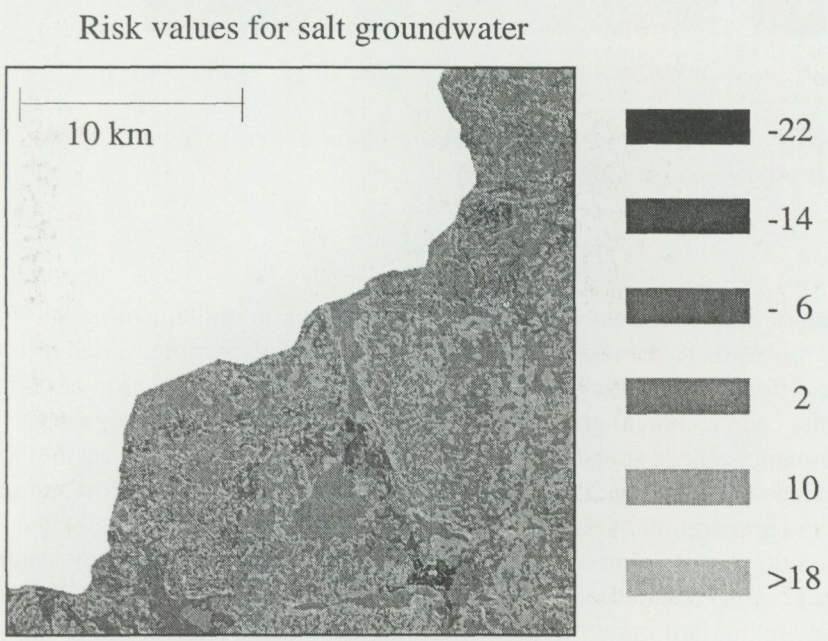


Figure 5. Risk map for salt groundwater.

This resulting map is simply produced by assigning the specific weight to each parameter before adding them together. The RV-method is a dynamic method in the sense that it allows the user to add or take away parameters that is not relevant for the actual study. In this study a parameter describing the well depth has been excluded as it is a site specific parameter without spatial distribution. In some cases it may though be interesting to take this parameter into consideration, for instance if the risk for salt groundwater will depend on the well depth when planning for drilling or dugging of new wells. Such an example is presented in Figure 6, where the risk value is presented for three different well depths; b) 40-70m, c) 0-10m and d) >90m.

From Figure 6b-6d it can be seen, using (b) as a reference that the risk in general decreases with smaller depth and increases with larger depth. In the shallow well (c) the increased risk along the diagonal linear structure in the centre of the image, that in practice is a road treated with de-icing salt during the winter and located on a sandy soil, is a result of a specific combination of parameters. Due to the conservative salt and the high hydraulic conductivity of the sand, the risk for finding salt groundwater in a shallow well in areas close to the road increases. In the other parts of the image the risk is lower due to the decreased withdrawal of groundwater from the rock aquifer. In a deep well (d), the risk is higher (in general) to find fossil salt groundwater and also to get an intrusion of seawater, and so the RV-method come up with a higher risk value.

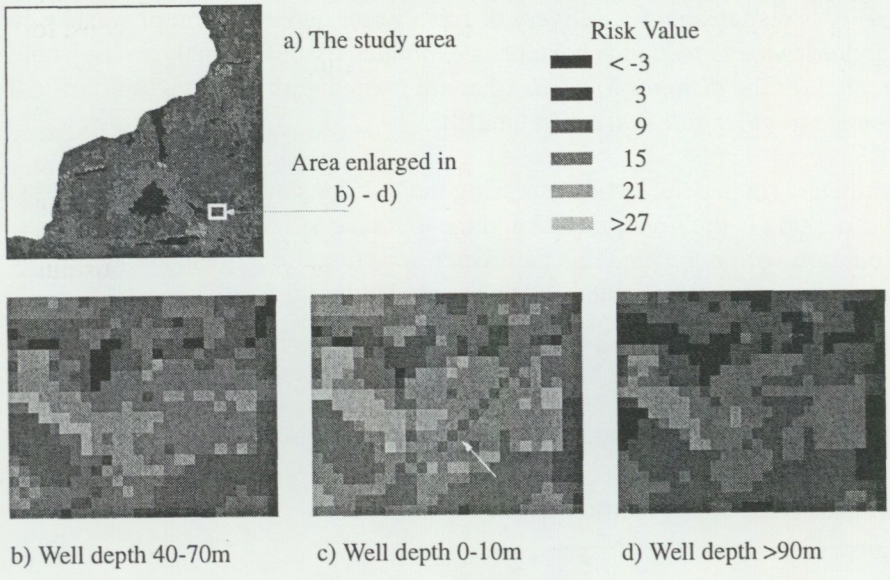


Figure 6. The risk value as a function of well depth. Figure 6b-6d are enlargements of the marked area in Figure 6a (pixelsize = 50 m).

Discussion

As expected, the creation of databases has been the major bottle neck in implementing the RV-method into a GIS. The problems have been of two major characteristics; problems due to transformation between different data storage formats and problems due to collection of data. In the first case it has mainly been technical problems including struggling with software and searching for existing modules able to transform a data set from one format to another. In the last case the problems have been related to questions of database quality. How much effort should be put in the construction and preparation of databases? The database quality is essential when working with GIS as the output will never be of higher quality than the input. This may sound basic but is important to keep in mind, especially when the risk map is to be used by politicians and decision makers that are not familiar with the new technology and its possibilities and limitations. When determining the quality of the input data, there are mainly two factors affecting

the result; the reliability of the input data source and the spatial resolution, as it decides the proper scale for the decision support tool.

Another problem that is still to be solved is how to model the soil depth for an area. This parameter is important for the analysis as it is limiting for the storage of groundwater. If the input point data (as point vectors) is dense enough and evenly spread all over the area it would be possible to use the GIS for a simple area interpolation or kriging, but as this is not the case in the data used for this project, as well as for most other projects, the problem must be solved in an other way. One attractive way is to develop some kind of knowledge based/ruled system that combine knowledge about the regional topographical structures with detailed elevation data and data about thickness of soil. If it is possible to construct a filter for image processing that could recognise major structures in the topography, information about soil depth in different parts of the terrain (valleys, slopes and hills) could be coupled to it, and a final map of soil depth could be produced.

A coupling of the risk value to an uncertainty value is a way to improve and secure the quality and the reliability of the result. It is also a way to make users not familiar with the information technology aware of the uncertainties that is included in the result. Another advantage with the uncertainty value is that it can be used as a support for planning further investigations, for instance collecting of new data or improving the quality of existing data.

When working with collection of input data, it is of course important to make use of all different kinds of information available (maps, technical reports, municipal plans etc.). Another important source of information is people with local knowledge as officials at the local authorities and people living in the study area. Their knowledge about site specific parameters like sanitary standard (water consumption) and degree of land utilisation can normally not be substituted by other information sources.

The raster based technique has proved to be powerful in the analysis as in many other applications coupled to management of natural resources. Anyhow, in a further development of the technique and as a final product, it must be possible to use a vector based GIS as ArcInfo or MapInfo instead of IDRISI, as they are totally dominating the market, especially among local and regional authorities.

Conclusion

To combine the RV-method and GIS-technique is a good way for analysing the risk for salt groundwater over a spatially extended area, for instance as a tool for municipal comprehensive planning. In combination with the uncertainty value, the risk value can be a good support in making decisions about how to go on with further studies and investigations or where to put restrictions about groundwater discharge. As the RV-method is an expert system, it should be possible for officials at local authorities to perform the analyses by their own without needing support of experts in hydrogeology, geology and hydrochemistry, as long as they are supported with relevant and high-quality databases.

Further studies

The first thing to go on with in the project is to finish the implementation of the RV-method into the GIS environment, including both the risk value and the uncertainty value. A transformation of the resulting risk map to ArcInfo and/or MapInfo is also included in the task. The final step is to couple the qualitative RV-method to a quantitative water balance model. This integrated system could be a powerful tool for the authorities in their planning process answering questions not

only where the risk is high or low for finding salt water in drilled or dug wells, but also how much groundwater that could be extracted before problems arise.

Acknowledgement

The data for this project were kindly supplied by the Geological Survey of Sweden (SGU) and the municipality of Norrtälje. MSc Jenny McCarthy has taken part in the project in the initialising stage and has also contributed to the result with fruitful discussions throughout the work. The project has been financially supported by the Council of the Stockholm County.

References

Aller, L., Bennet, T., Lehr, J.H., Petty, R.J., 1987: DRASTIC - a standardised system for evaluation groundwater pollution potential using hydrogeological settings. Report, US Environmental Protection Agency.

Bucht, M., Larsson, P-O., 1995: Risk assessment for salt groundwater - proposal for a new methodology (Riskbedömning för salt grundvatten - förslag till ny metodik.). MSc degree report 1995:6, 106 pp. Div of land and water resources, Royal Institute of Technology, Stockholm.

Carlsson, A., Olsson, T., 1981: Hydraulic Properties of a Fractured Granitic Rock Mass at Forsmark. Geological Survey of Sweden (SGU), Ser C, no 783, 67 pp, Uppsala.

Engqvist, P., Fogdestam, B., 1984: Hydrogeological Map of Stockholm County. Geological Survey of Sweden (SGU), Ser Ah, no 6, Uppsala.

Grundvattenutredningen, 1994: Reglering av vattenuttag ur enskilda brunnar. Statens Offentliga Utredningar (SOU) 1994:97.

LeGrand, H.E., 1983: A Standardized System for Evaluation Waste-Disposal Sites. Report, National Water Well Association, second edition.

Lindewald, H., 1985: Salt grundvatten i Sverige (Saline groundwater in Sweden). Geological Survey of Sweden (SGU), Rapporter och Meddelanden no 39, Uppsala.

Olofsson, B., 1991: Groundwater conditions when tunnelling in hard crystalline rocks - a study of water flow and water chemistry at Staverhult, the Bolmen tunnel, S Sweden. Swedish Engineering Research Foundation (BeFo), Research report 160:4/91, 165 pp, Stockholm.

Olofsson, B., 1992: Saline Groundwater - A Complex Water Planning Problem. *in* Lopes, H., Jergman, K., Aswathanarayana, U., (eds): Environment, Technology and Sustainable Development. Proceedings of the Africa International Conference, Maputo, Mozambique, Nov. 25-29, 1991, pp 99-105.

Olofsson, B., 1994: Salt groundwater in Sweden. *in* Olofsson, B.,(ed) Salt groundwater in the Nordic countries. Proceedings of a workshop, Saltsjöbaden, Sept. 30 - Oct. 1, 1992. Nordic Hydrological Programme (NHP) Report no 35, pp 17-35.

Sund, B., Bergman, G., 1980: Salt water intrusion into drilled wells (Saltvatteninträngning i bergborrade brunnar). Swedish Environment Research Institute (IVL), Report no B584.

Tilly-Leander, L., 1990: Salt groundwater in coastal areas in Sweden. Methods of investigations and estimations (with examples from the county of Stockholm). Report. The county of Stockholm and Dept. of land- and water resources, Royal institute of Technology, Stockholm.

The method of pollution-tracer to measure lowest groundwater velocities in the city of Bremen

Dieter Ortlam
Department of Bremen of the Geological survey of Lower Saxony /Germany,
D-28199 Bremen, Werderstr. 101

In 1886 was the beginning of the installation of pottash-mines in the drainage area of the river Weser. Up to the first world war many discharges of potashium waste water were derivated into the river Werra/Weser and its eastern affluents Ulster/Leine/Aller (Fig. 1).

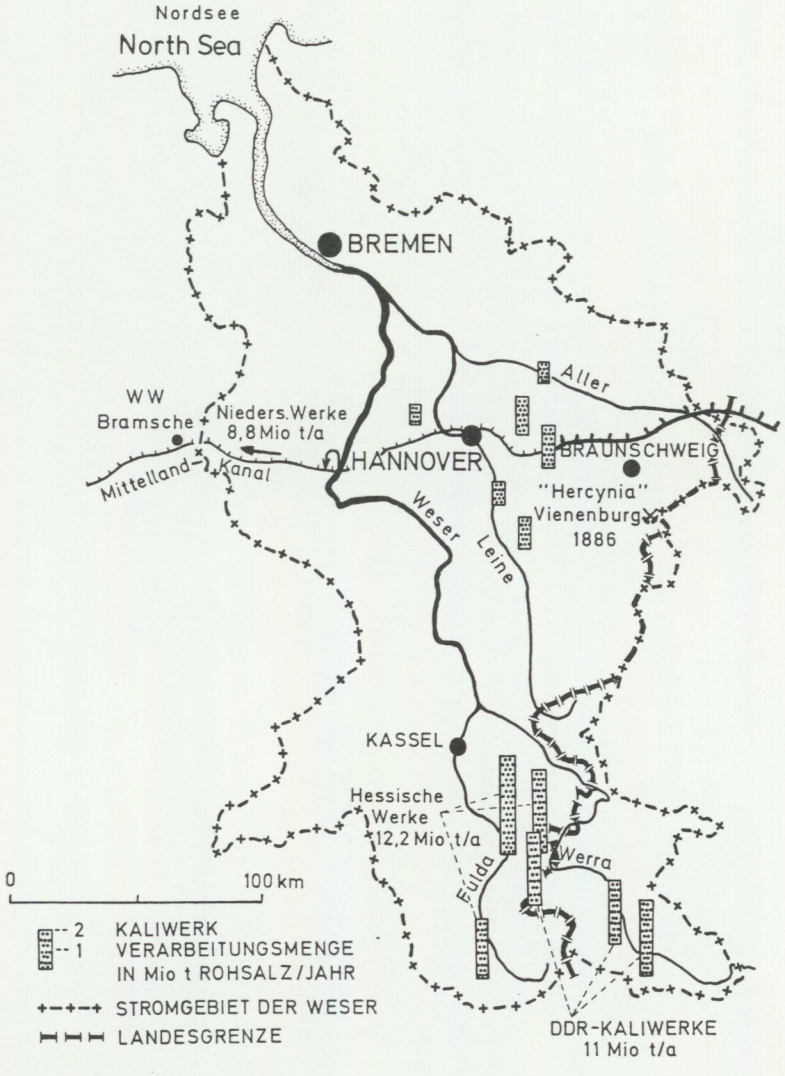


Fig. 1. Area of research (= drainage area of the river Weser) with the outputs of the different potash-mines in nothern Germany (Date: 1987)

Therefore the taking out of river water for the water authorities and the breweries of Bremen and of other towns along the river Weser was very problematical (LÜTTIG & FRICKE 1967). An arrangement between the thuringian potash-mines and the Government of Bremen guarenteed a maximum concentration of chlorides of 350 mg/l in the water of the river Weser in Bremen (Fig. 3).

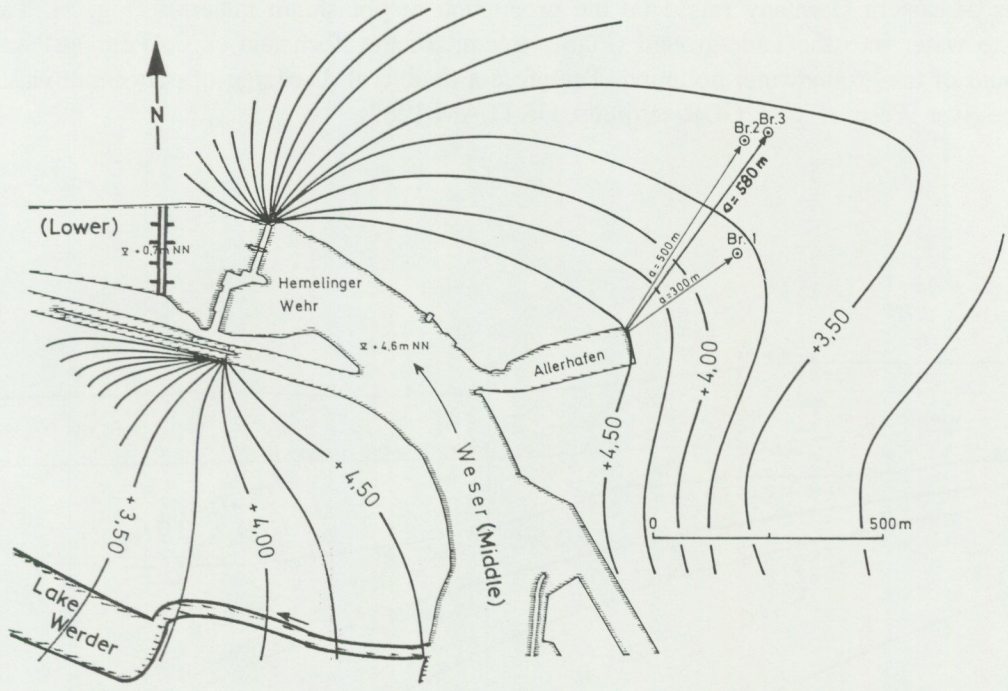


Fig. 2. Siteplan of the wells 1, 2 and 3 (non-tidal region) above the barrage of the river Weser at Bremen-Hemelingen (border Lower to Middle Weser) with the counter lines of the level of groundwater of the upper aquifer (=Wesersande).

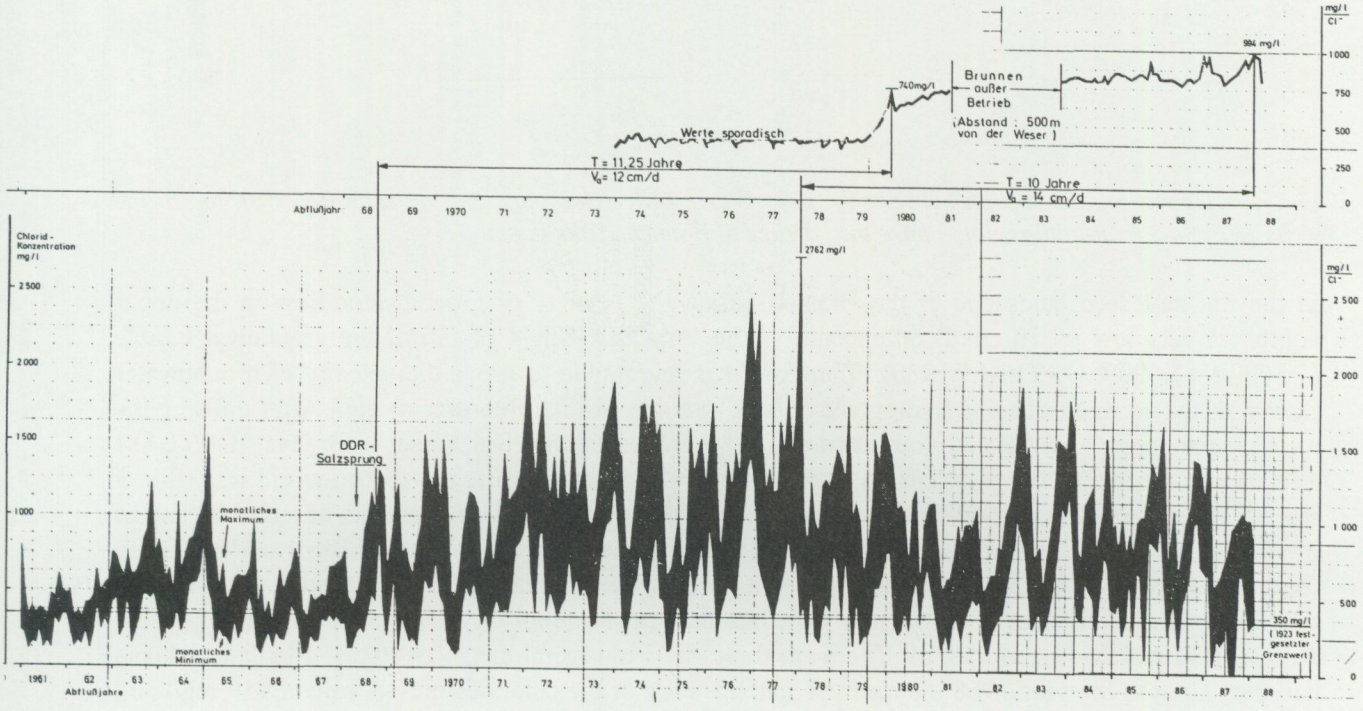


Fig. 3. Temporal correlation of the contents of chlorides in the water of the river (Middle)Weser (between 1960 and 1988) and in the well 2, (non-tidal region) above the barrage of Bremen-Hemelingen

After the second world war the eastern part of Germany (=GDR) allowed their potash-mines to increase this discharge of potashium waste water into the rivers Ulster/Werra/Weser after the year 1950. In 1968 the potash-mines of eastern Germany raised up the production of potashium minerals (Fig. 1). The injection of waste water into the underground (Plattendolomit of the Zechstein, Z 3, Permian) was stopped on account of the groundwater pollution. Therefore a double of discharge of potashium waste water ran into the river Weser (Fig. 3, GDR-saltjump, ORTLAM 1989).

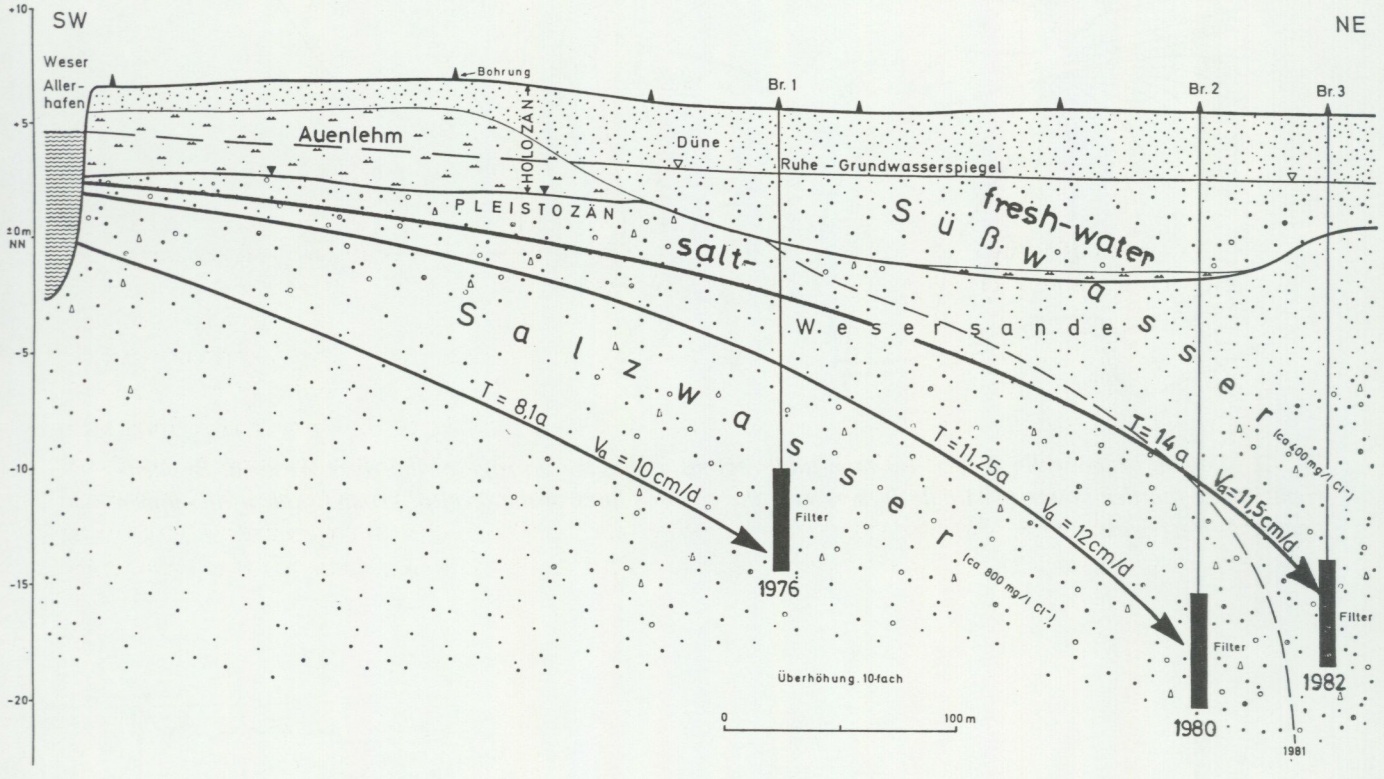


Fig. 4. Hydrogeological section between the river Weser (Aller-Harbour) and the saltwater intrusion to the wells 1, 2 and 3,(non-tidal region) above the barrage of Bremen-Hemelingen

In the flat and deep landscape of the Bremen bassin the velocity of groundwater flow in the upper aquifer is very low (< 10 cm/d) on account of the very little height of fall of the groundwater table (1:1000 to 1:6000, ORTLAM 1980). Therefore it is impossible to prove the velocity of groundwater flow with the normal tracers in hydrogeology (salt, uranine, eosine, fluorescëine etc.).After drawing the monthly maximum and minimum concentrations of the water in the river Weser in Bremen (ORTLAM 1983a) you can see very typical curves in the pollution by chlorides after the second world war (Fig. 3 and 6). Beyond 1980 many wells nearby the river Weser showed increasing contents of chlorides and of iron/manganese in the groundwater (ORTLAM 1989). Upstream of the barrage of Bremen-Hemelingen (built 1910) the river water ist dammed up about 4 m. In view of this highwater situation the saltwater intrusion of the river Weser permanently went into the upper aquifer of the river flanks (Fig.2, HOLZ 1971, ORTLAM 1980 and 1983b). There are three wells in several distances to the Allerhafen (Aller-harbour).Until to the year 1968 the medium concentration of the chlorides moved around 450 mg/l and after 1968 the double with 900 mg/l (= GDR-saltjump) was reached (Fig. 3). Now we are able to compare this typical curve of the river chlorides with the curve of the groundwater chlorides of three wells nearby. You can see the GDR-saltjump of 1968 after 11,25 years in the year

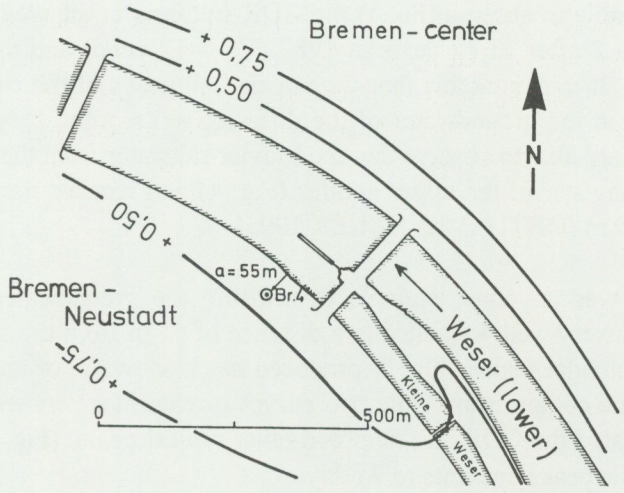


Fig. 5. Siteplan of the well 4 in the tidal region of the river Weser in the center of Bremen with contour lines of the level of the groundwater of the upper aquifer (=Wesersande).

1979/80 (Fig. 3) at the well 2 in a distance of 500 m from the river Weser. The flow velocity of the saltwater intrusion in the groundwater is about 12 cm/d. Well 2 was closed in the years 1981-1983. After this time the groundwater recharge of well 2 and the lowering of the groundwater level were started again and you can observe several typical peaks of chlorides between the curves of the Weser and the well 2 in the years 1976/77 and 1987/88 with a flow velocity of 14 cm/d. It is very interesting that the concentration of chlorides in the groundwater reached 50% of the salt concentration of the water in the river Weser. The groundwater recharge of this region is very low on account of many town settle-

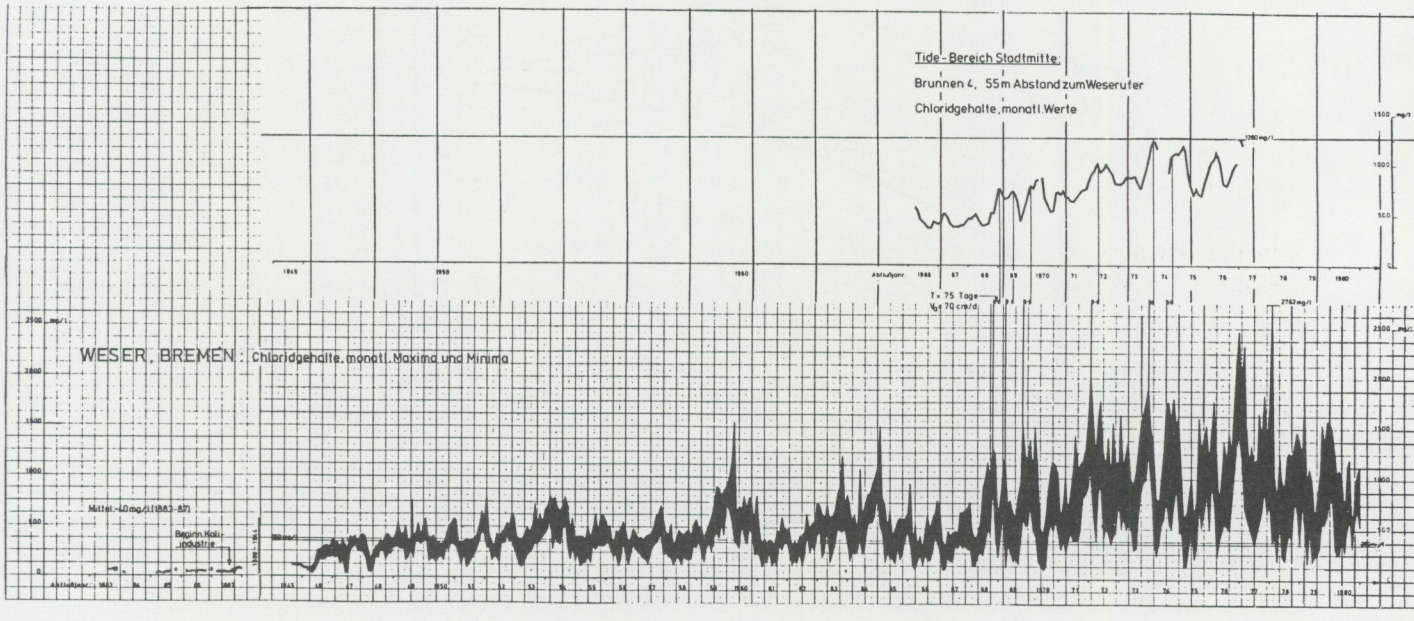


Fig. 6. Temporal correlation of the contents of chlorides in the water of the river (Lower)Weser (between 1945 and 1980) and in the well 4, tidal region of Bremen-Center.

ment and streets and of the holocene loam of the valley in the underground (Fig.4). In the hydrogeological section you are able to observe (Fig.4) the GDR-saltjump in the well 1 after 8,1 years in 1977 (V_a = 10 cm/d), in well 2 after 11,25 years in 1980 (V_a = 12 cm/d) and the well 3 after 14 years in 1982 (V_a = 11,5 cm/d). It is remarkable that we can find all peaks of the chlorides as well in the water of the river Weser as in the groundwater of the different wells, after 15 years of detention period in the upper aquifer. You are able to observe that the heavier saltwater from the river Weser went down after1968 beneath the freshwater of the upper aquifer (Fig. 4) and reached now a distance from the river Weser about 800 - 1000 m (ORTLAM & SAUER 1993).

In the center of Bremen there was an other example to measure the groundwater velocity by the pollution-tracer "chloride". A brewery well 4 situated in a distance of 55 m from the southern border of the river (Lower)Weser and in the tidal region (Fig. 5) produced much saltwater of unknown origin and with bacteriological problems.The comparison of the two curves of chlorides between the river Weser and the well 4 exactly demonstrated the GDR-saltjump and other typical peaks (Fig. 6). The temporal difference between the comparable peaks amounts to 75 days.

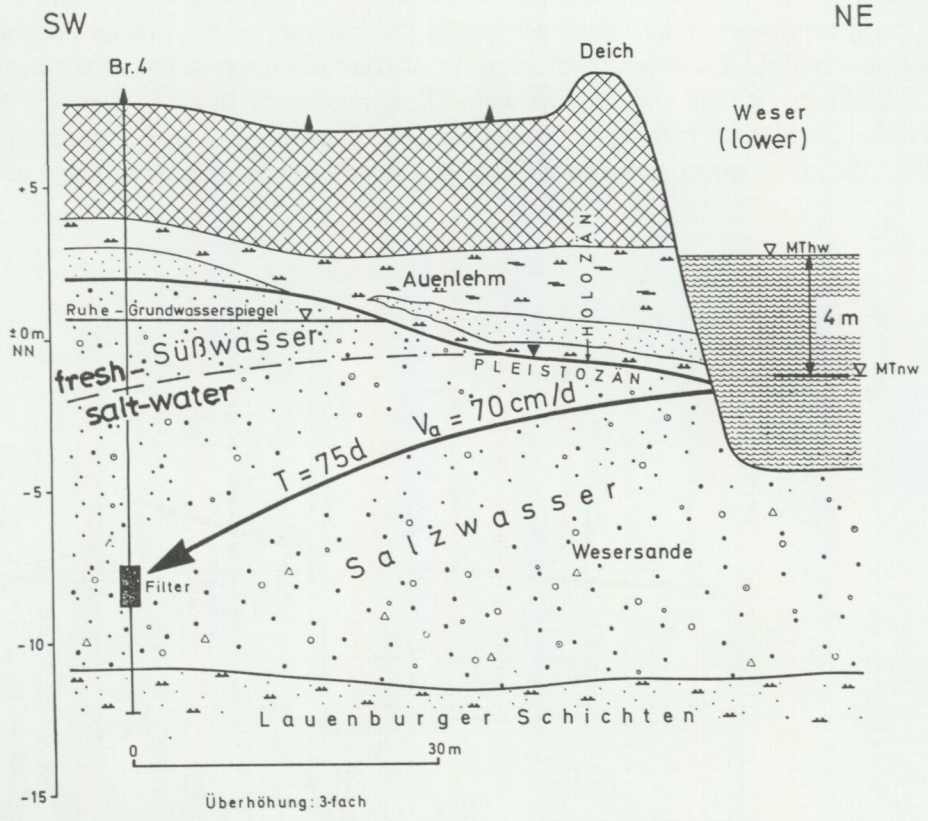


Fig. 7. Hydrogeological section between the river (Lower)Weser (tidal region) and the saltwater intrusion by tidal pumping to the well 4 (pilgrim step method), Bremen-Neustadt

In the hydrogeological section (Fig. 7) we are able to watch the pumping effect of the river Weser with a tidal difference of 4 m, the covering holocene loam of the valley (= Auenlehm), the upper aquifer (= Wesersande) and the active well 4. The flow velocity of the saltwater from the river Weser amounts to 70 cm/d (V_a), in consideration of the pilgrim step flow of the groundwater by tidal movements. Corresponding to the detention time of 75 days the bacteriological influence of the groundwater of the well 4 did not come from the river Weser as the first idea but from other local influences.

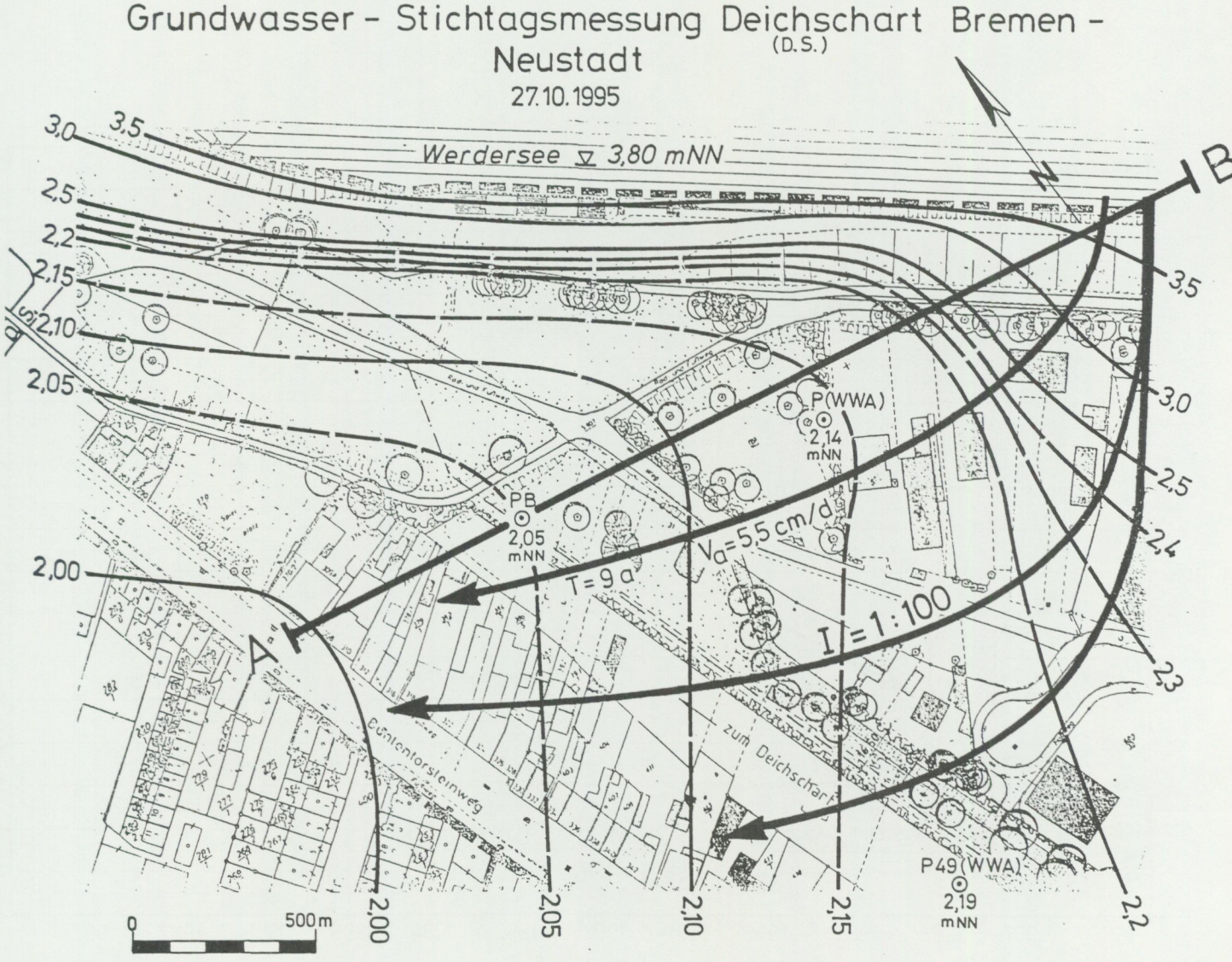


Fig. 8. Siteplan of the southern border of the Lake Werder, water input from the river (Middle) Weser (see Fig. 2), of the different depth gauges, of the section line and the counter lines of the groundwater level of the upper aquifer (= Wesersande)

In Bremen-Neustadt the (artificial) Lake Werder is situated south of the river Weser. The water of this lake comes from the river (Middle)Weser above the barrage of Bremen-Hemelingen (Fig. 2). The lakewater is dammed up to 3.80 m NN (Fig. 8). Considering the local groundwater level of 1.30 m NN there is a saltwater intrusion from the lakewater into the groundwater at the southwestern border of the Lake Werder (Fig. 8 and 10). In the years 1981-1986 the Lake Werder was empty because of a catastrophical act of highwater. In April 1986 the Lake Werder was filled up again with saltwater from the river (Middle)Weser and the saltwater infiltration into the groundwater began. Two times a year we observed the conductivity of the water of the Lake Weser in comparison with the groundwater at the depth gauge PB in a distance of 80 m from the southwestern border of the lake (Fig. 8). The groundwater flow is very irregular due to the hydrogeological situation (Fig. 10) and shows a western direction with a dipping of the groundwater level of 1:100. In comparison of the two curves of conductivity of the water of the Lake Weser and the groundwater in the depth gauge PB you are able to observe that in the year 1995 higher conductivities reached the depth gauge after 9 years (Fig. 9). The flow velocity of the saltwater intrusion amounts to 5.5 cm/d (V_a).

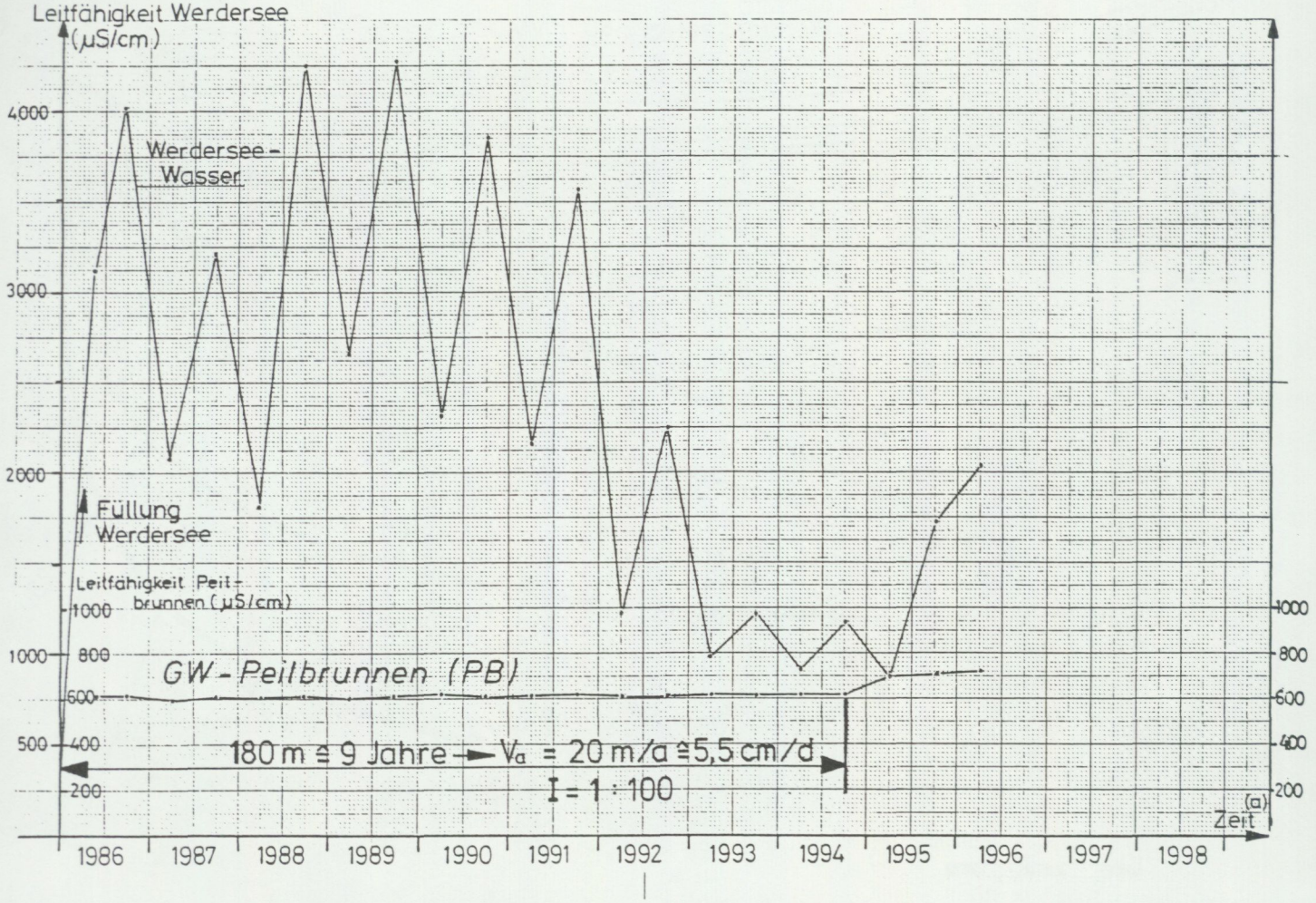


Fig. 9.Temporal correlation of the conductivity (µS/cm) in water of the Lake Werder (non-tidal region) and the depth gauge PB, near Deichschart of Bremen-Neustadt

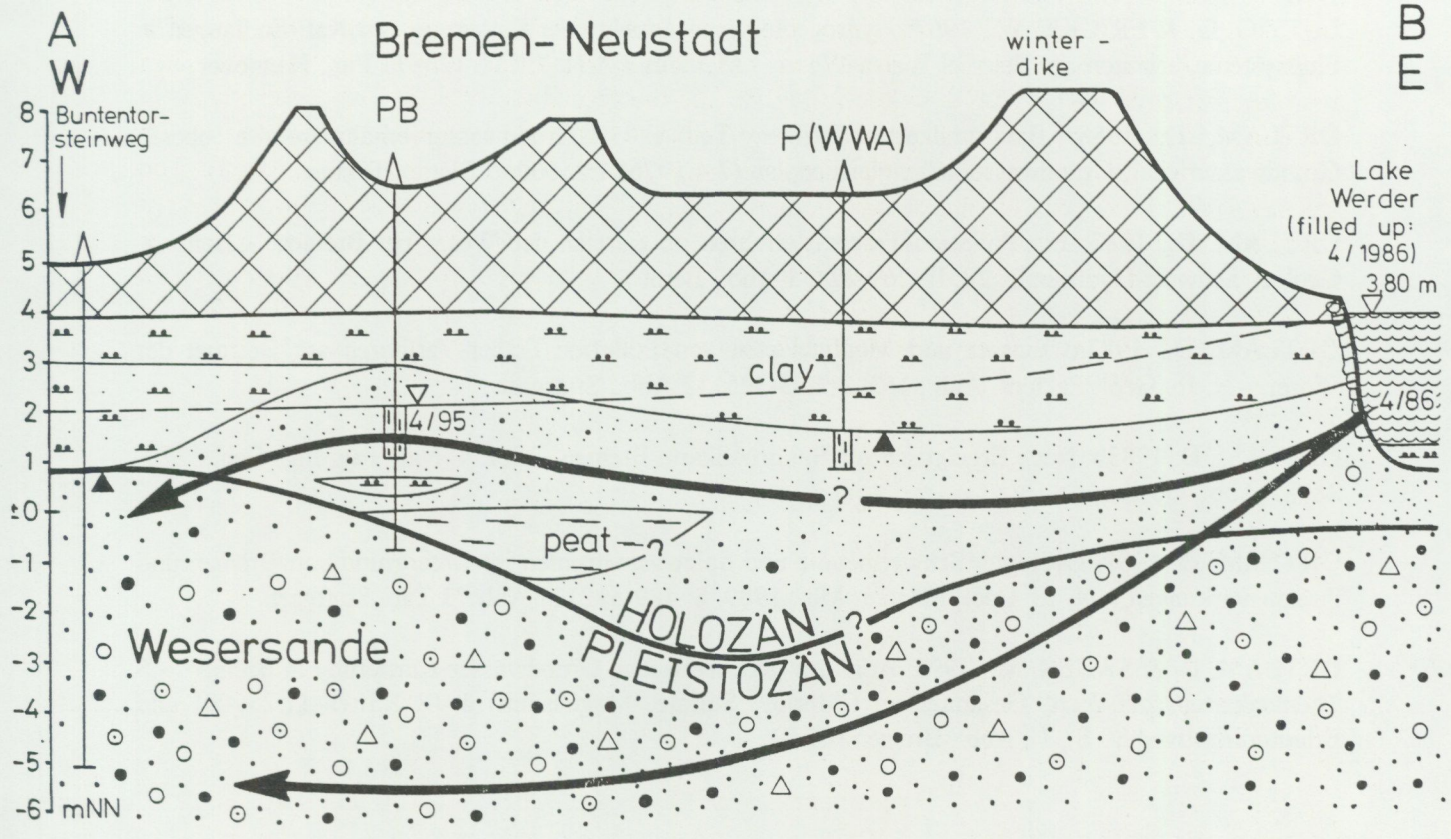


Fig. 10. Hydrogeological section between the Lake Werder and the depth gauge PB, near Deichschart of Bremen-Neustadt

These three examples demonstrate the possibility to measure the groundwater velocity by the pollution-tracer "chloride" with good results after long times (ORTLAM 1982, 1983a), because the chlorides have no retardation and adsorption effect in the aquifer. The different concentrations of chlorides are not mixed during the intrusion. The different peaks are very good recognizable in the several curves.

An application of the pollution-tracer method was the clarification of the origin of saltwater in several wells of the water works of Bramsche, situated nearby the Mittelland-Kanal (Mittelland-canal). The water of the Mittelland-canal was permanently pumped up from the river Weser near the town of Minden, 100 km south of Bremen (Fig. 1). Therefore the typical curves of the chlorides go in the canal, too. The canalwater flows to west in a few days and leaks in the groundwater flow above the wells of the water works of Bramsche. Therefore we are able to observe all peaks of chlorides of the water of the river Weser in the groundwater of several wells of the water works of Bramsche. This clarification proved the leakage of the canal (salt)water into the groundwater by the pollution-tracer method, developed in the town of Bremen.

REFERENCES

HOLZ, H.W.,1971: Groundwater recharge by dammed-up rivers. - Memoirs I.A.H., **9**: 72-79, Tokio.

LÜTTIG, G. & FRICKE, W., 1967: Hydrogeologische Aspekte der Einleitung von Kali-Endlaugen in Flußsysteme, erläutert am Beispiel Werra-Weser. - Memoirs I.A.H. **7**: 111-120, 11 Fig., Hannover.

ORTLAM, D, 1980: Baugrundkarte Bremen, Teil E 1. Grundwasserverhältnisse im oberen Grundwasserleiter, Grundwasserhöhengleichenplan (7.4.1976) 1:25000, 6 Blätter, Bremen.

ORTLAM, D., 1982: Ein Pollution-Tracer-Verfahren im Bereich der Weser bei Bremen. - Beitr. z. Geol. d. Schweiz-Hydrologie, **28**, II: 269-274, 1 Abb., Bern.

ORTLAM, D., 1983a: Einsatz und Möglichkeiten von Pollution-Tracer-Verfahren am Beispiel der Weser. - N. Jb. Geol. Paläont. Abh., **165**, 2: 303-325, 12 Abb., Stuttgart.

ORTLAM, D. 1983b: Neue Ergebnisse zur Baugrundkarte Bremen. - Ber. 4. Nat. Tag. Ing. Geol.: 273-280, 7 Abb., Goslar.

ORTLAM, D. 1989: Geologie, Schwermetalle und Salzwasserfronten im Untergrund von Bremen und ihre auswirkungen. - N. Jb. Geol. Paläont. Mh., **1989**, 8: 489-512, 11 Abb., 3 Tab.,Stuttgart.

ORTLAM, D. & SAUER, M., 1993: Atlas zur geochemischen Grundwasser-Kartierung in Bremen. - 5 Themenkarten (pH-Wert, Gesamteisen, Chloride, Sulfate, Magnesium) à 12 Karten (1:25000) und Erläuterungsband 30 S., 10 Abb., Bremen (BEB).

Geogene and anthropogene salinization-phenomenons in the groundwater of Bremen (northern Germany)

Dieter Ortlam [1] & Michael Sauer [2]

[1] Department of Bremen of the geological survey of Lower Saxony, Werderstr. 101, D-28199 Bremen

[2] Roggenkamp 26, D-28259 Bremen

Motivation for this presentation is the first time square covered groundwater-mapping in Germany. From 1989 until 1992 the procedure of the „Rollendes Peilrohr" was realized in the city of Bremen. It allows a quick, environmentally careful and low-priced research of groundwater especially contaminated by geogene salt sources and waste deposits. The elaborated background results of the groundwater chemism are published in the atlas „Geochemische Grundwasser-Kartierung Bremen" (ORTLAM & SAUER 1993) and are an important contribution for an efficient risk valuation of waste deposits.

Location and geology

Bremen is settled along the river Weser 80 km south of the coast of the North Sea, where Bremerhaven is situated (Fig. 1). The two towns are parts of the fossil valley of Weser and Aller, which stretched to the Bremen basin. This basin (=region with freshwater depression) is surrounded by the geest of northern Bremen, the geest of Zeven, Achim and of Delmenhorst-Syke (=regions with freshwater recharge, Fig.1).

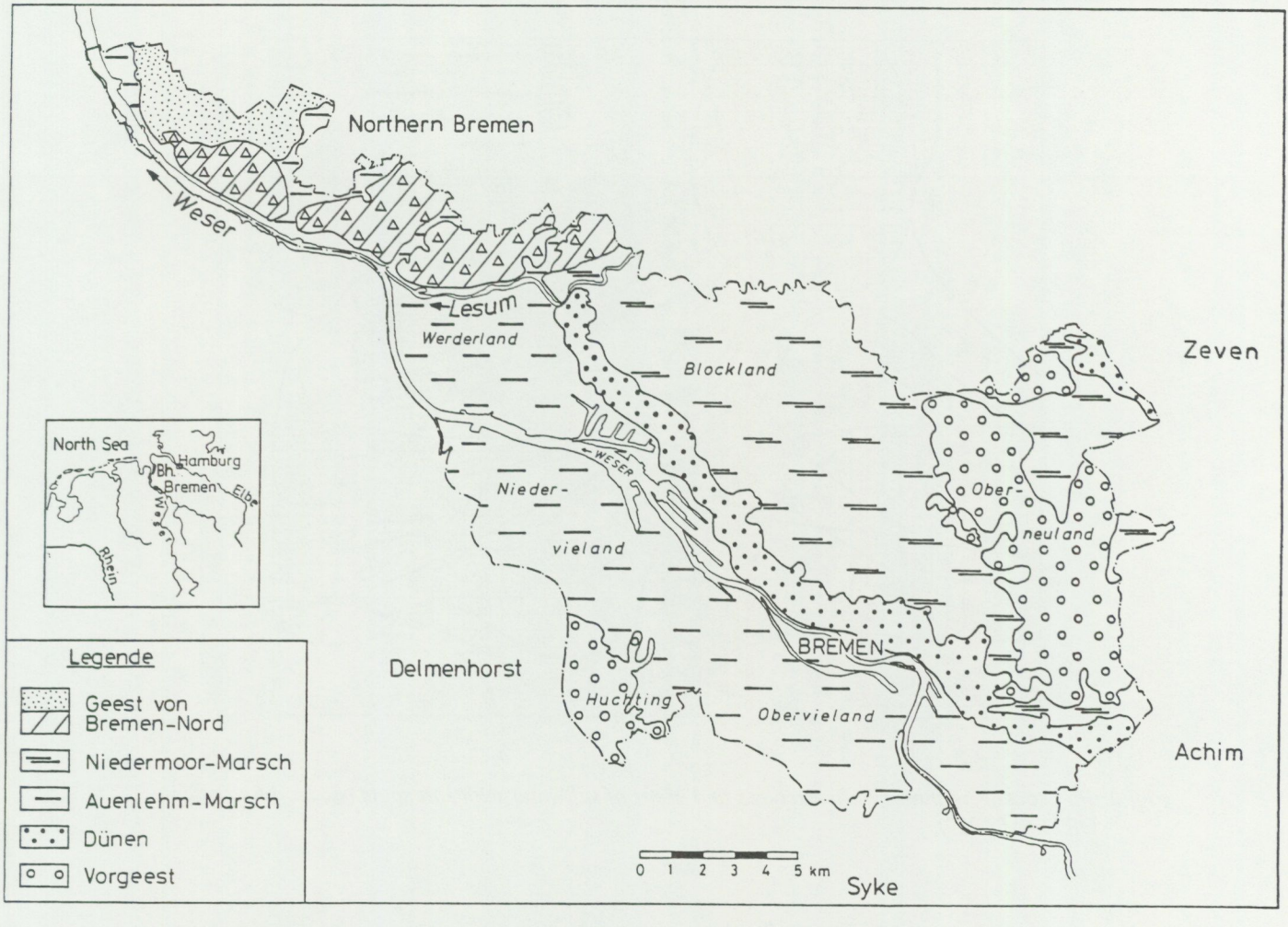


Fig. 1: Geological situation of the basin (=marsh) of Bremen and its surrounding (=geest); Bh.=Bremerhaven.

The geest of northern Bremen is generally covered by Saalian tills (up to 18m thickness), underlayed by the Lauenburger Schichten (=Elsterian glaciation). The sandy facies (sands of Ritterhude) represents the upper aquifer. A silty clay (clay-facies of the Lauenburger Schichten) or the silty layers of the higher miocene (tmi) are the basis of the upper aquifer (ORTLAM & SCHNIER 1980, ORTLAM et al. 1981, ORTLAM 1983b, 1989, ORTLAM & SAUER 1995b).

In the marsh of Bremen generally we have an upper aquifer consisting of glaziofluviatile sands of Saalian and Weichselian glaciation with a thickness between 5m to 50m, medium 15m. He is covered by holocene sediments of the river-marsh (loam of the valley) and peat with a thickness of 1m to 4m (maximum: 12m; ORTLAM & SAUER 1995b, 1995c). The city of Bremen is situated on a dune (Fig. 1) with a thickness up to 16m (ORTLAM & SAUER 1995b). The basis of the upper aquifer consists of the Lauenburger Schichten (Elsterian glaciation) in silty or sandy facies (ORTLAM et al. 1981, ORTLAM 1983b, 1989,).

Salinization-phenomenons in the groundwater of Bremen

The geochemical maps of groundwater show the geogene charakter of groundwater-chemistry which is defined by different geological cover of the upper aquifer, the structures of saltdomes, the deep pleistocene channels and the areas of saltwater with saltspots. Beyond that the chemistry of groundwater changes anthropogenically by water-infiltration of the river Weser, leakage of the sewage system and waste deposits (ORTLAM & SAUER 1995b). The following salinization-phenomenons are important for the different groundwater-chemistry in Bremen.

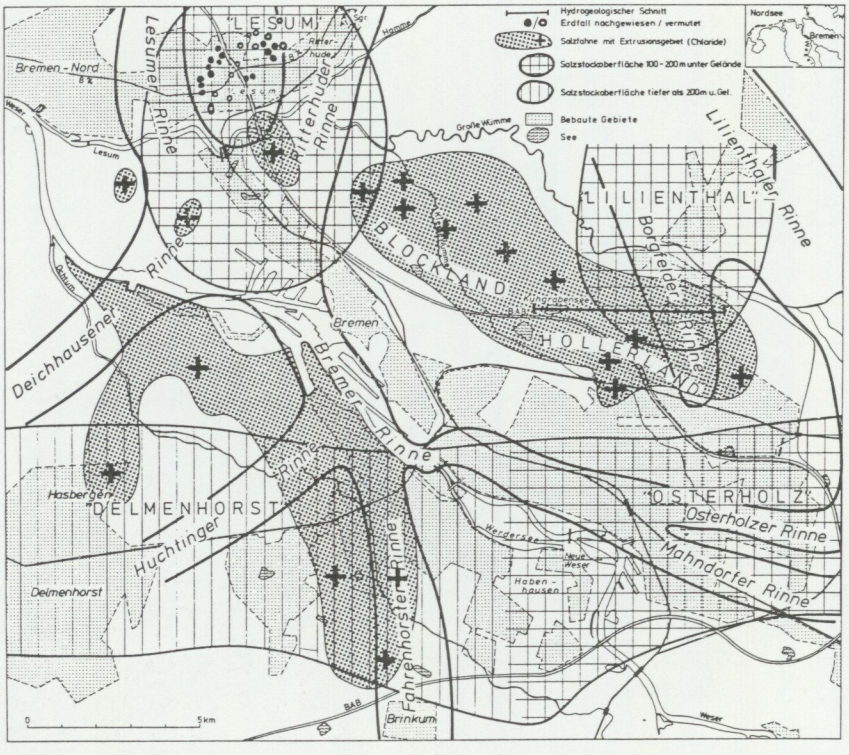


Fig. 2: Pleistocene channels, saltstructures and areas of saltwater with salt spots (+, modified after ORTLAM 1989).

1. Principle of salt/mineral spots

The swelling of high mineralized deep groundwater into the upper aquifer is responsible for large salinizations in the Bremen basin. This is caused by three structures of Permian salt in Bremen: the saltdome of „Lesum", the saltdome of „Lilienthal" and the saltwall of „Delmenhorst-Osterholz" (Fig. 2; ORTLAM 1989). Zechsteinian salt swelled up from a depth of 4500m to 130m up to 400m under the surface (ORTLAM 1989). Pleistocene channels have eroded the tertiary layers up to 350m depth like a wide-branch-system in the underground of Bremen (Fig. 2; ORTLAM & SAUER 1995b). The pleistocene channels cut salinar structures, too. For example the channel of „Borgfeld" (Fig. 3; ORTLAM 1984) eroded the saltdome of „Lilienthal" and the channel of „Lesum", the saltdome of „Lesum"(ORTLAM 1989).

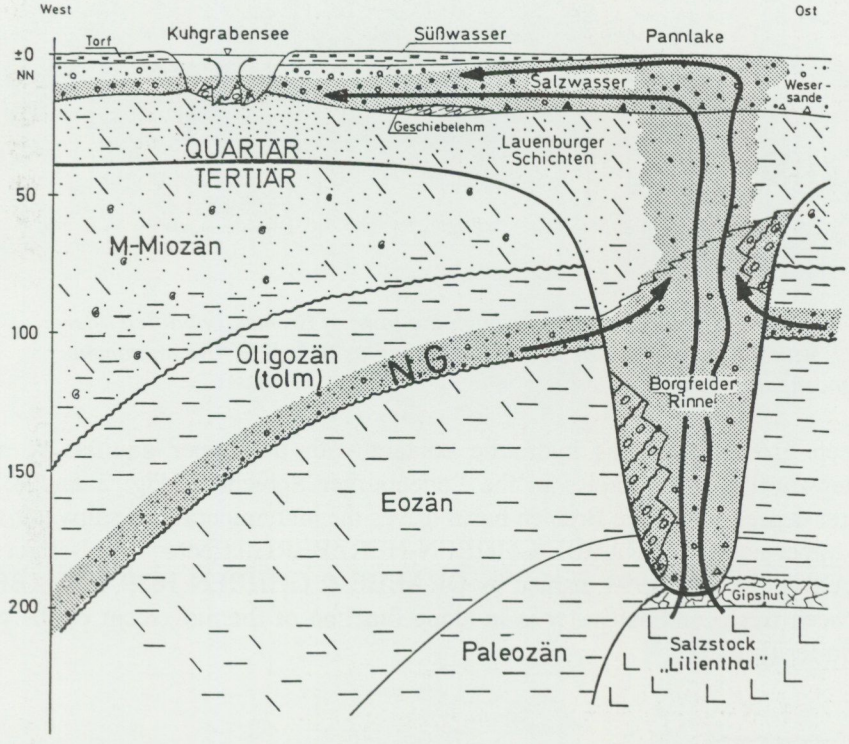


Fig. 3: Hydrogeological section through the Hollerland of Bremen (modified after ORTLAM 1989); position of the hydrogeological section see Fig. 2 and Fig. 6; N.G.=Neuengammer Gassand (Oligocene, tolm).

The salinars were solved and therefore this deep-groundwater of the channels is highly mineralized. On account of the solution of salt on the top of the different salinars in northern Germany the groundwater normally contents high concentration of chlorides and further lower concentrations of sulphates and magnesium. This demonstrates the possibility to solute the different salt-materials in the groundwater: the saltdome of „Lilienthal" as **donator of chlorides**. In the area of the saltdome of „Lesum" especially sulphates are solved out of the caprock (up to a maximum concentration of 1700 mg/l, Fig. 4). The chlorides are kept back by residual-clay along the salt-mirror. Therefore the saltdome of „Lesum" represents a **donator of sulphates** with important aspects on the density of the clayic salt-mirror (=enclosure of waste materials in saltdomes). In the geest of northern Bremen many (30) sinkholes are situated on the top of the saltdome „Lesum" on account of the solution of the caprock (Fig. 2 and 4; ORTLAM & SCHNIER 1981). A large gypsum cavern was found in the caprock „Lesum" (diameter >50m). This large druse was formed by recristallisation of gypsum as Marienglas in pre-oligocene time by down-streaming groundwater (Fig. 4; ORTLAM 1989, ORTLAM & SAUER 1995b). The Neuengammer Gassand (tolm) is filled up with fossil saltwater now in contact with the channel of „Lesum" (Fig. 4; ORTLAM 1989, ORTLAM & SAUER 1995a).

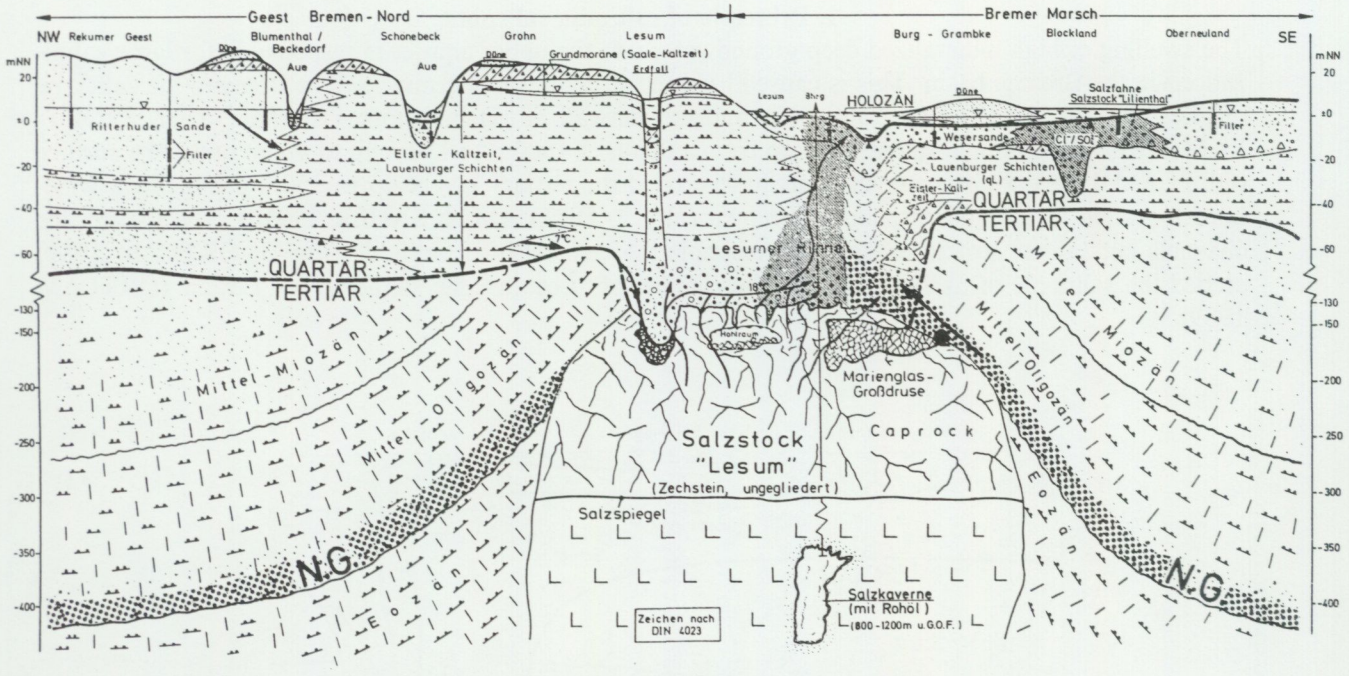


Fig. 4: Half-schematical hydrogeological section through the town of Bremen (modified after ORTLAM 1989) with the position of the druse of Marienglas (●); N.G.=Neuengammer Gassand (Oligocene, tolm).

The mineralized deep groundwater has hydraulic contact with the upper aquifer by a „window-situation" of the step-formed sandy facies in the Lauenburger Schichten (Fig. 3 and 4; ORTLAM 1989). The freshwater depression of the Bremen basin drives the high mineralized saltwater like a motor to swell up into the upper aquifer (DRABBE-GHIJBEN-HERZBERG-effect = DGH-effect after ORTLAM 1989, ORTLAM & SAUER 1993; named by DRABBE & GHIJBEN 1889, HERZBERG 1901). The border line between fresh- and saltwater is in slope function of the movement of the groundwater level in the upper aquifer (Fig. 5).

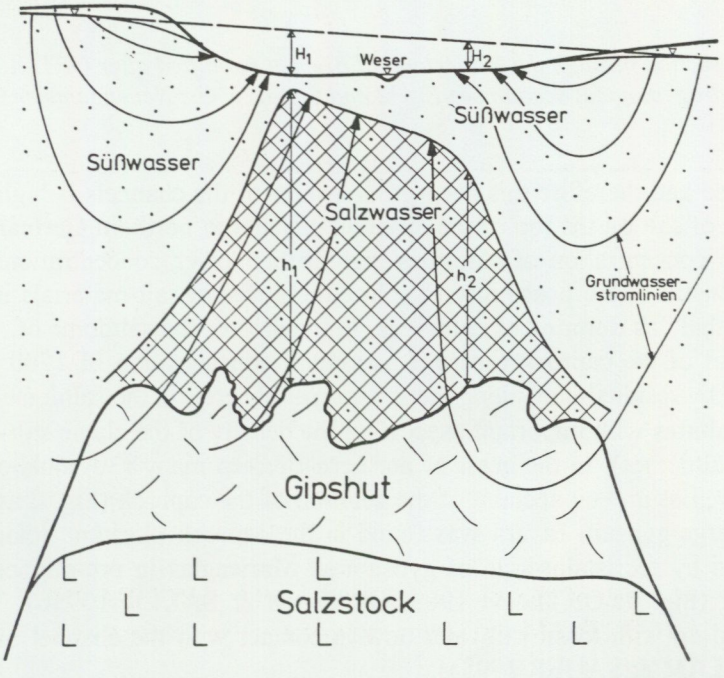


Fig. 5: The conditions of deep saltwater intrusion in large areas of groundwater depression in the Bremen basin (=DGH-effect).

During the „Geochemische Grundwasser-Kartierung Bremen“ (ORTLAM & SAUER 1993, 1995b, 1995c) we took the groundwater in a homogeneous depth of approximately 7m below the surface. On account of the DGH-effect we found areas with freshwater nearby areas with saltwater in slope function of the different freshwater-charge. The upstreaming zones coming from the salinars are narrow. Therefore we call them „mineral-spots“ or „salt-spots“ (Fig. 6; ORTLAM & SAUER 1993, 1995b). If the freshwater-charge is very low (<1m) the deep saltwater is swelling up to the surface. For that reason we find high mineralized ditch water and plants of halophytes in several regions of the Bremen basin (Fig. 2; ORTLAM 1982, 1984, 1989).

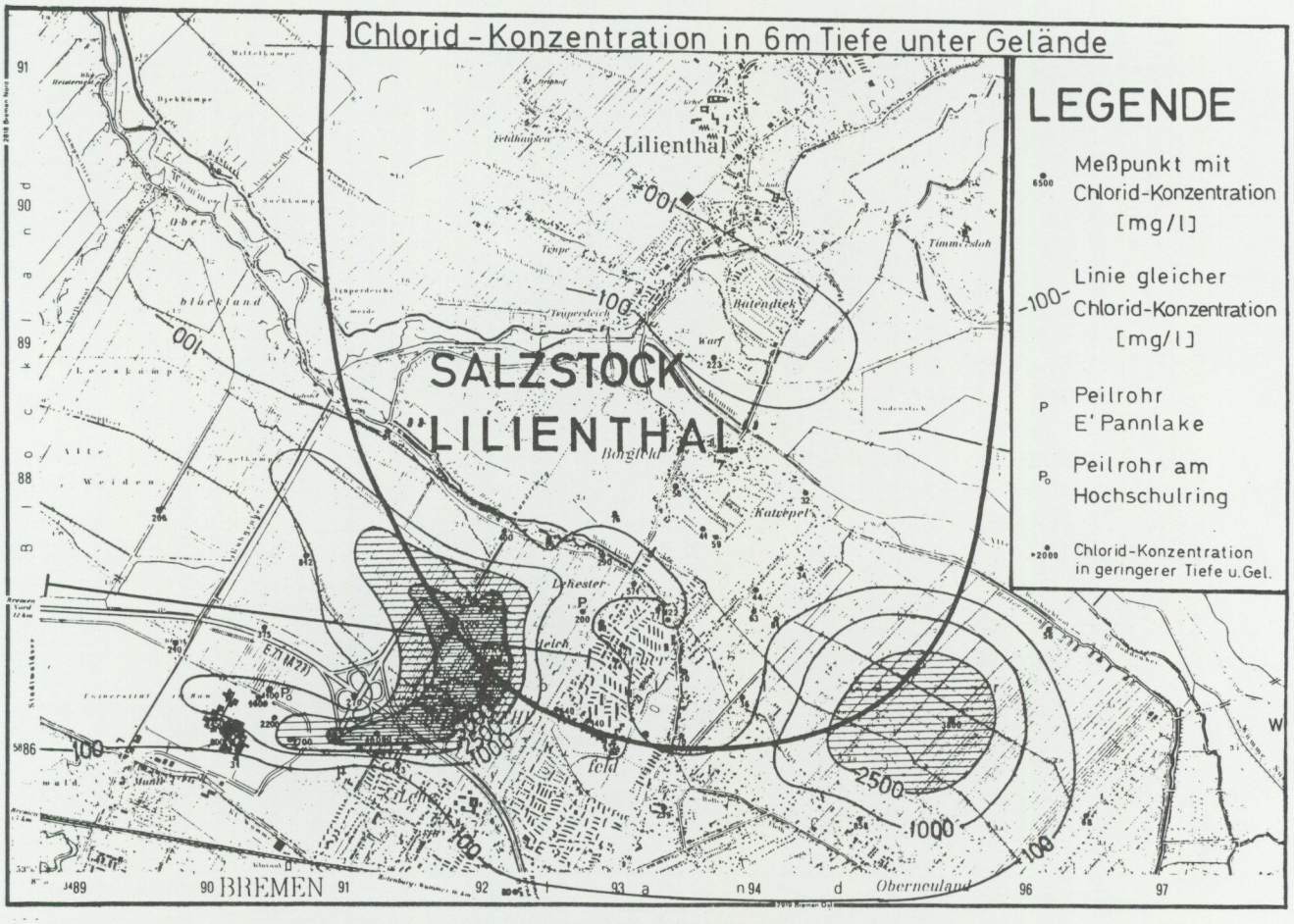


Fig. 6: Concentration of chlorides in the higher part of the upper aquifer (=Wesersande) in the Hollerland of Bremen and the position of the hydrogeological section (Fig. 3).

In the Pannlake area of Bremen-Hollerland an experiment was started in the year 1982 to investigate the fresh-/saltwater-zone and its variability (Fig.6; ORTLAM 1982, 1984). Therefore the depth gauge P was total filtered (Fig. 7a). Between march and october 1982 we measured in a depth between 1m to 18m under surface freshwater with a conductivity of less than 500 µS/cm. Below of 18m the conductivity jumped up very quick about 2000 µS/cm. The fresh-/saltwater-zone is situated in 18m and consists of a very narrow border line about 10 cm. During the year 1982 the border line between fresh- and saltwater variated in slope function of the movement of the groundwater level (Fig. 7b) on account of the several rainfalls: the border line between fresh- and saltwater moved reverse proportionally to the groundwater level. The quotient of the dive equilibrium (after ARCHIMEDES) of fresh-/saltwater amounts at this locality 1:15 (ORTLAM 1982) in comparism to the quotient of the North Sea 1:37.

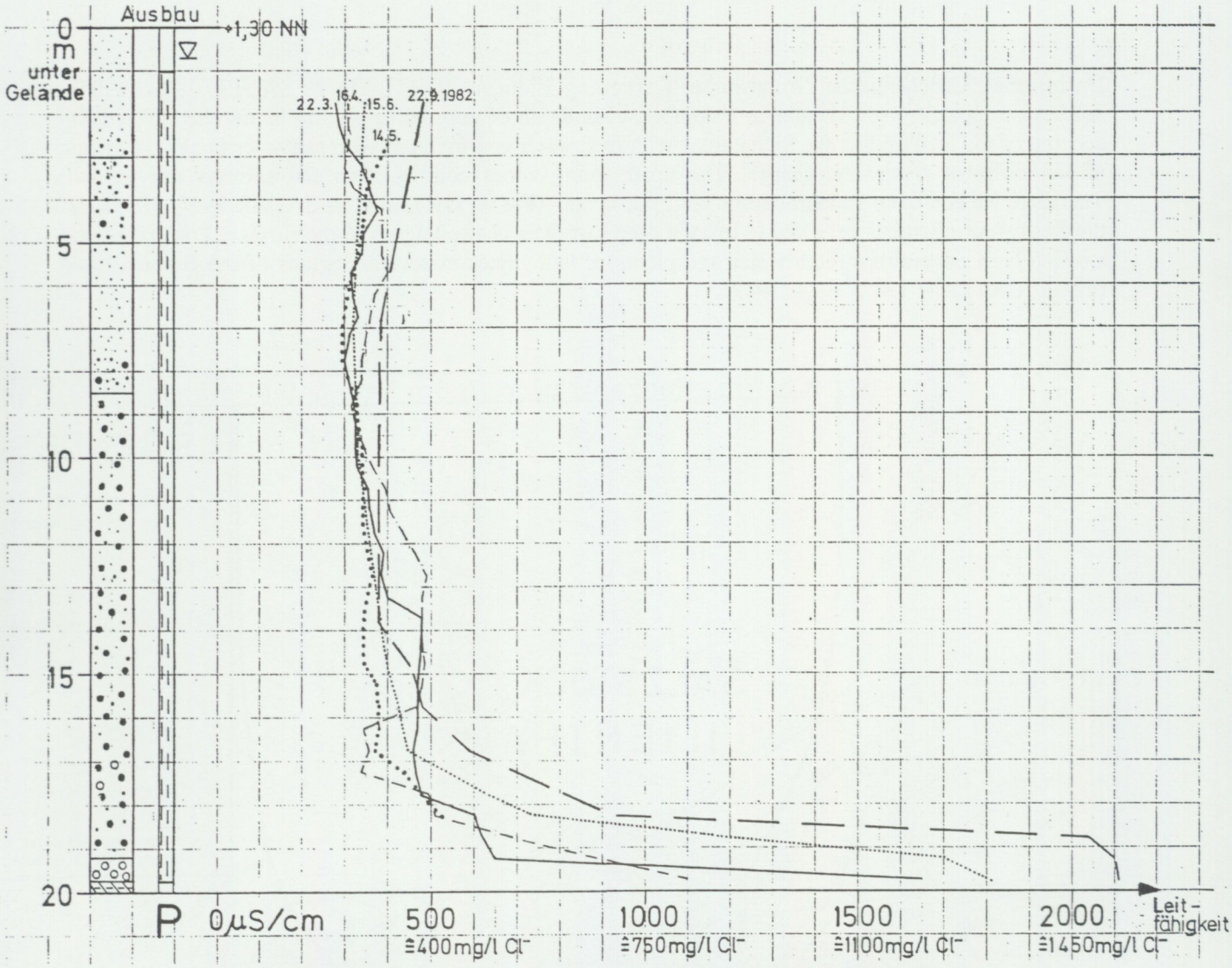


Fig. 7a: Variations of the border line between fresh- and saltwater in the depth gauge P (position see Fig. 6) under meteorological influences during the year 1982, Bremen-Hollerland.

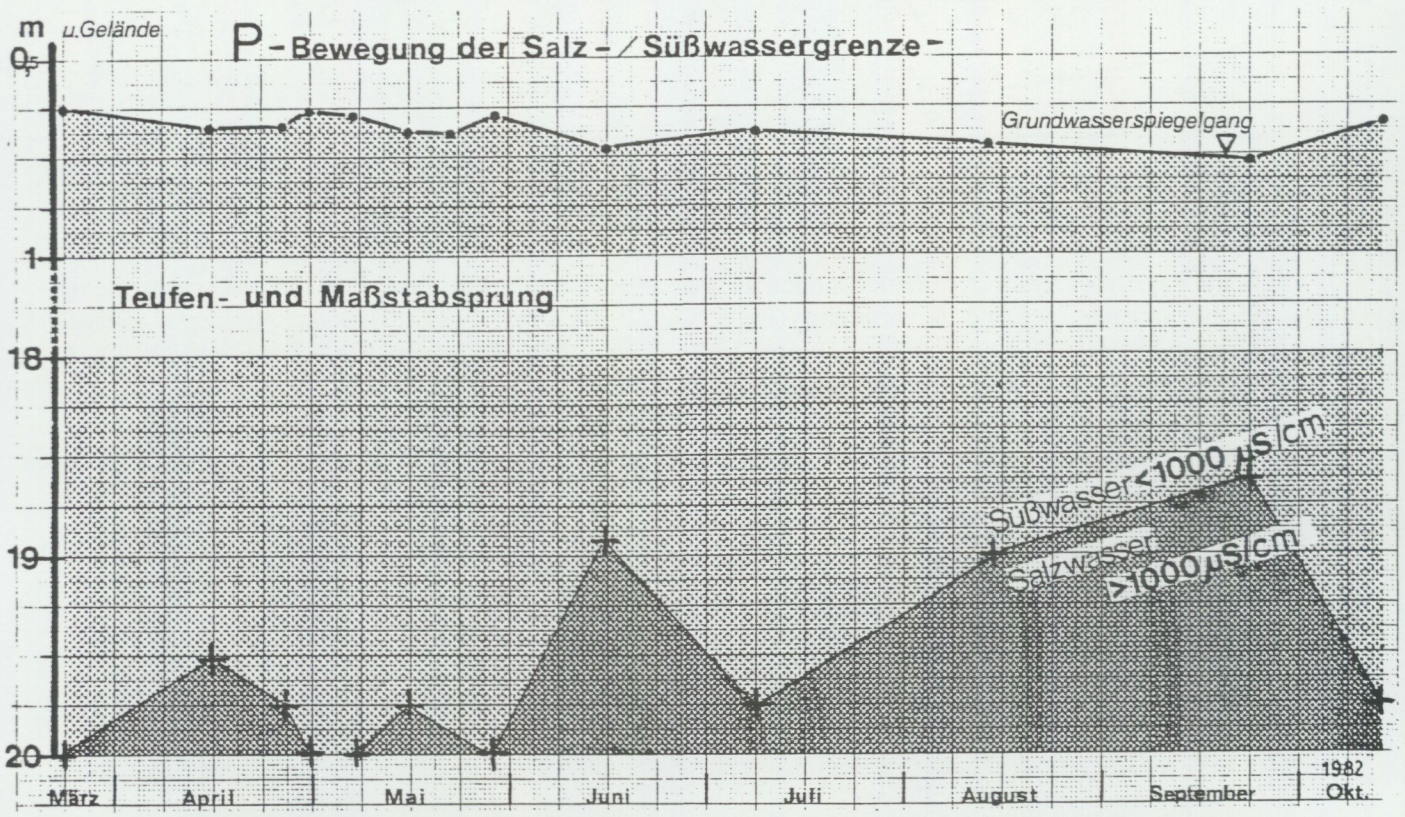


Fig. 7b: Variations of the border line between fresh- and saltwater in slope function of the movement of the groundwater level (=charge of freshwater) during the year 1982, Bremen-Hollerland.

At another depth gauge P_0 the conductivity of groundwater started on 6m under surface with 700 µS/cm and jumped up to high conductivities nearby 2500 µS/cm (first border line) in 7m under surface and increased to 3500 µS/cm in 18m under surface (Fig. 8; ORTLAM 1982). By pumping of groundwater (19.2. - 5.3.1982) nearby (2m) the depth gauge P_0 a second border line with different concentrations of saltwater raised up from an unknown depth to 10m under surface. After this artificial conditions of the freshwater-charge by lowering and raising the groundwater level the second border line felt down during two month (march/april 1982) at a depth of > 16m under surface (=end of the depth gauge; Fig. 8). The quotient of the dive equilibrium of fresh-/saltwater amounts at this locality 1:12 (ORTLAM 1982).

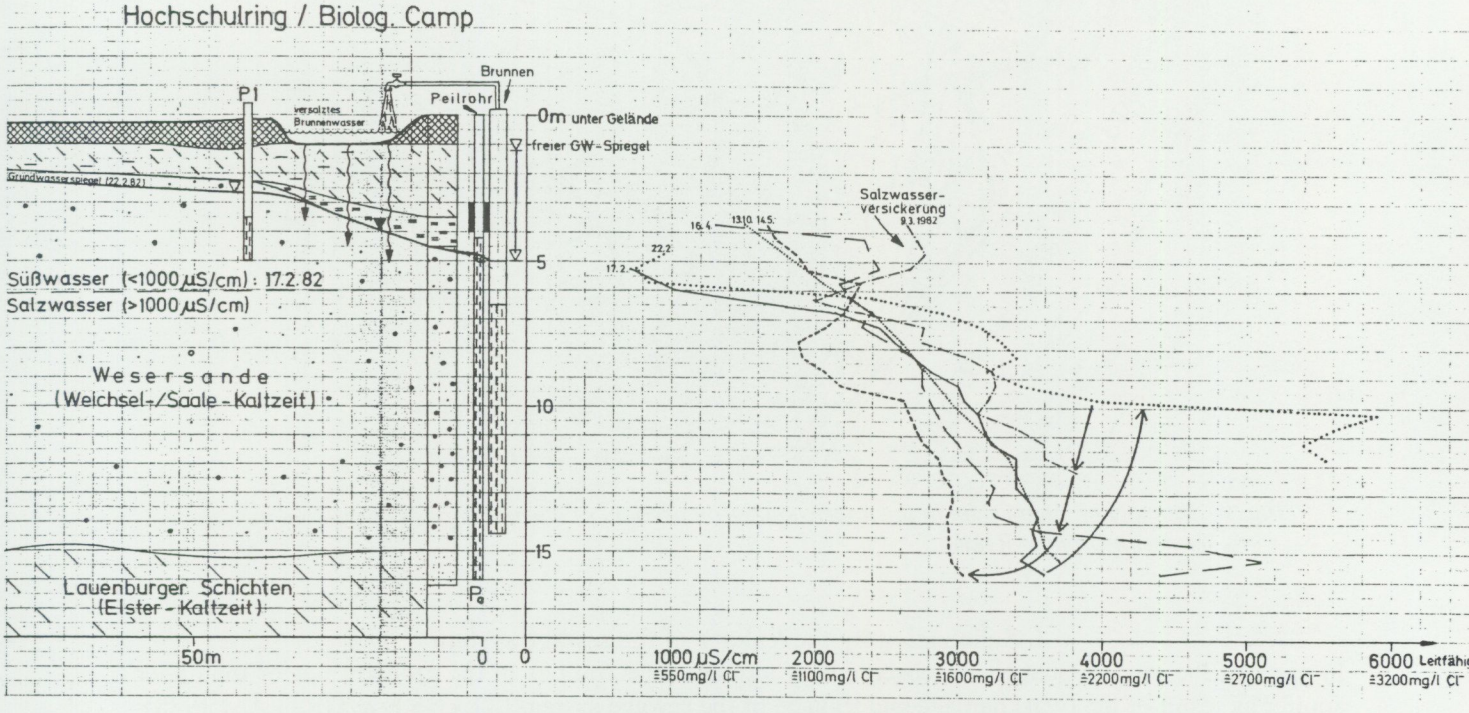


Fig. 8: Variations of the border line between fresh- and saltwater in the depth gauge P_0 (position see Fig. 6) under artificial conditions (=lowering of the groundwater level by pumping) during the year 1982, Bremen-University.

On account of the DGH-effect the saltwater was pumped up nearby in a polder with natural underground (sandy loam and peat). This saltwater infiltrated into the upper aquifer during 15 days the holocene layers (3,5m thick). Therefore one is able to measure a permeability of the local underground layers $K_f=3x10^{-6}$ m/s by pollution tracer.

2. Salinization by infiltration of the water of the river Weser

Between the groundwater of the upper aquifer and the surface water of the river Weser exists a hydraulic contact. The saltwater of the river Weser infiltrates the upper aquifer around the locked ports in Bremen and above the barrage of Bremen-Hemelingen (see the paper ORTLAM in this book).

3. Salinization by waste deposits

We can observe several contaminations of the groundwater by waste deposits in the geest and in the marsh of Bremen. If we have a low geogene background of the groundwater-chemistry we can recognize the contaminations by regional untypical concentrations of one or more groundwater-parameters in the downstreaming areas of waste deposits (ORTLAM & SAUER 1993, 1995b, 1995c). For example in Fig. 9 we see an anomaly of magnesium in the upper aquifer which is situated nearby a waste deposit of pit-coal ashes in Bremen-Rekum.

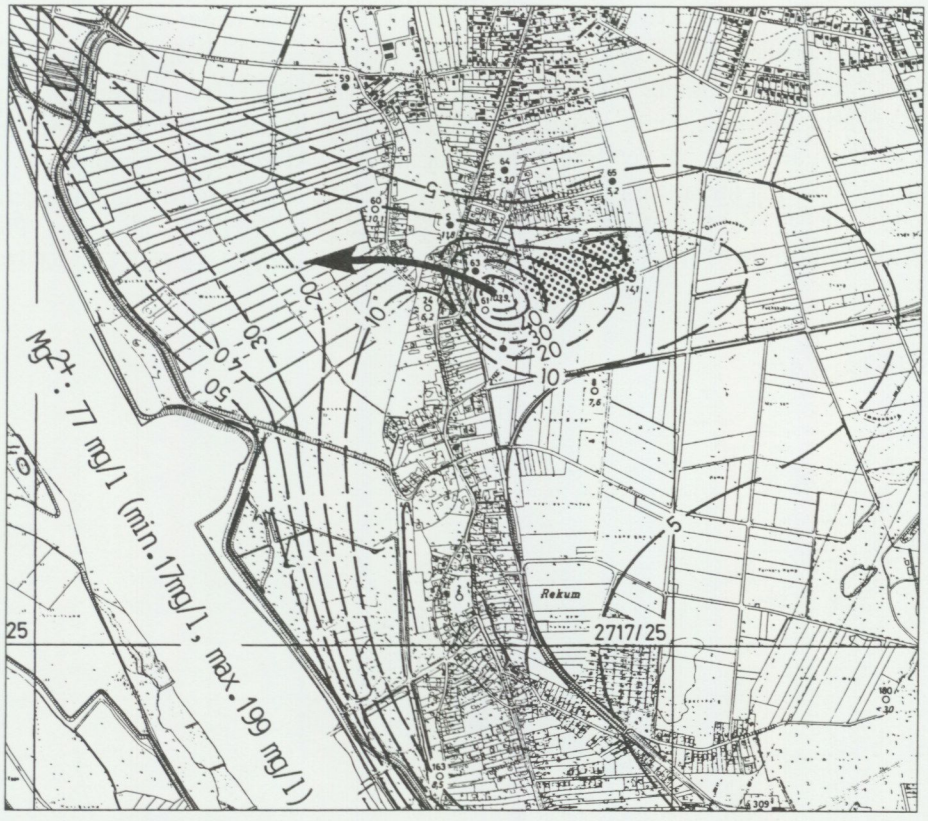


Fig. 9: Anomaly of magnesium in the upper aquifer on account of a waste deposit of pit-coal ashes (screen), Bremen-Rekum.

4. Salinization by the leakage of the sewage system

In parts of the city of Bremen we observe high nitrate-concentrations in the groundwater of the upper aquifer as result of the (war) damage and leakage of the sewage system (KLENKE & ORTLAM 1988). Only along the large dune of Bremen the seawage system is situated above the groundwater level. Therefore the nitrification processes need many oxigene in the percolation zone and many iron in pyrite/markasite around the grains of the upper aquifer. On account of this chemical and bacteriological processes many anomalies of sulphates, iron, protons and nitrates were produced (Fig. 10; KLENKE & ORTLAM 1988, ORTLAM 1989, ORTLAM & SAUER 1993, 1995b).

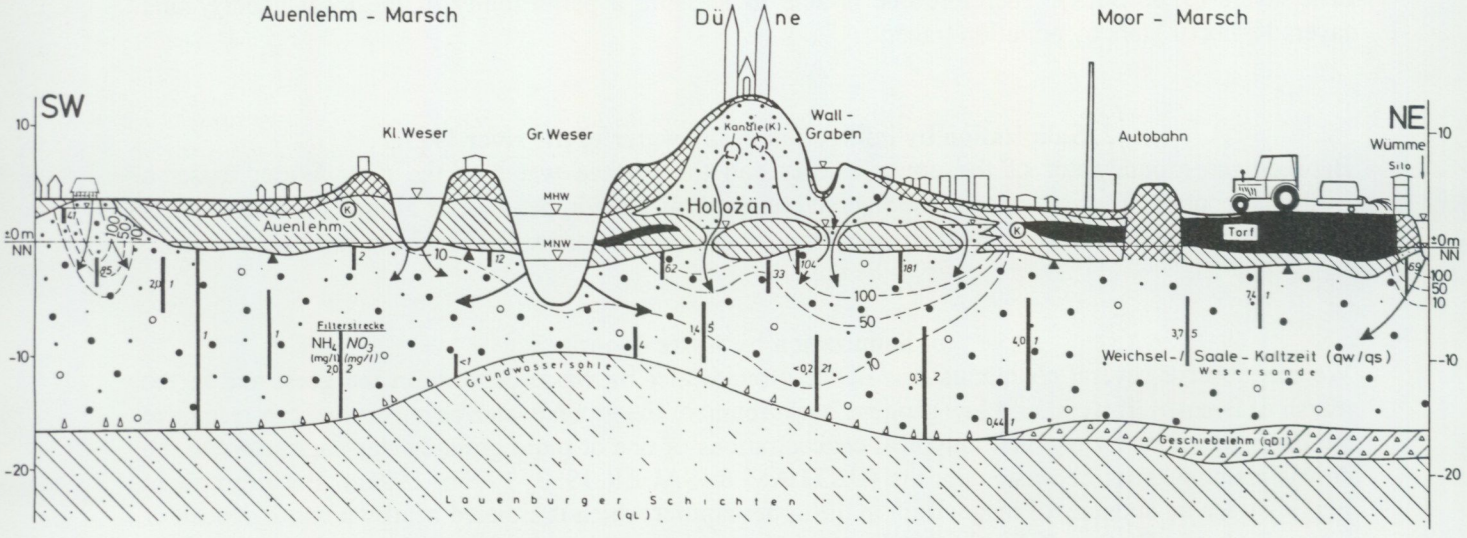


Fig. 10: Schematical hydrogeological section through the center of Bremen showing the input of nitrogene into the upper aquifer: fertilizing and leakage of the sewage system.

5. Intrusion of Seawater

At the coast of the southern North Sea in Bremerhaven we observe different intrusion zones of seawater in the upper aquifer on account of the different hydraulic pressure coming from the higher freshwater level in the geest areas (Fig. 1). The border line of fresh- and seawater is variable during the hydrological year about a distance of > 100m. On account of the higher specific weight of the saltwater and the different permeability in the upper aquifer the border line dips under the freshwater and toothes with the freshwater. At some localities the geest areas have contact with the coastline. Therefore one is able to observe some freshwater springs at the southern coast of the North Sea (p.e. Bremerhaven, Cuxhaven, Esens).

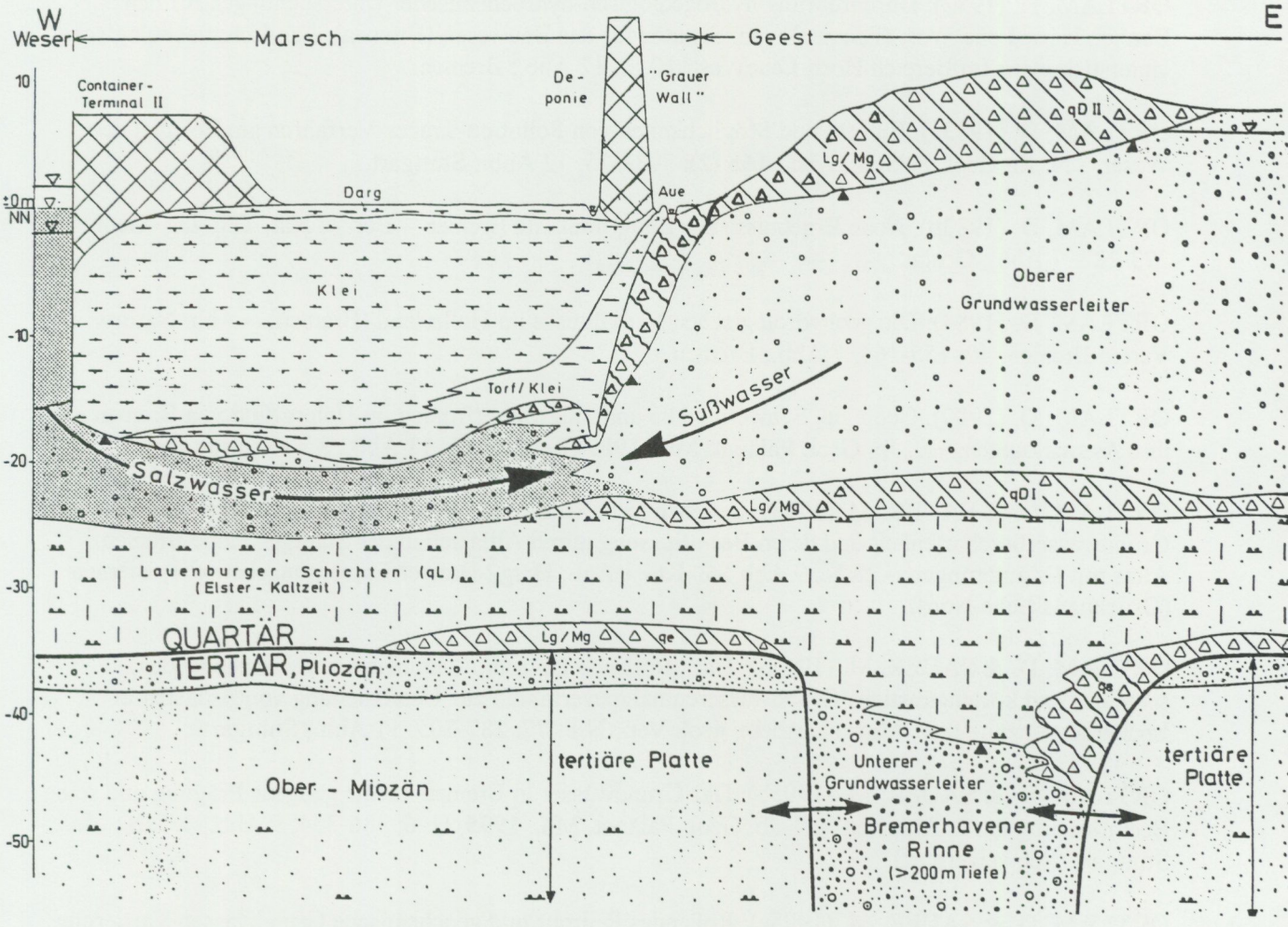


Fig. 11: Schematical hydrogeological section showing the hydraulic connection between seawater intrusion and freshwater in the upper aquifer and deeper aquifers with freshwater of Bremerhaven.

REFERENCES

DRABBE, J. & GHIJBEN, W.B. (1889): Nota in Verband met de voorgenomen putboring nabij Amsterdam. - Kon. Inst. Ing. Tijd-schr., **1888/89**: 8-22, 11 Abb.; Amsterdam.

HERZBERG, A. (1901): Die Wasserversorgung einiger Nordseebäder. - Gasbeleuchtung u. Wasserversorg., **44**: 815-819 u. 842-844, 1 Abb.; München.

KLENKE, Th. & ORTLAM, D. (1988): Beobachtungen zur Nitratverteilung im oberen Grundwasserleiter der Stadt Bremen. - Z. dt. geol. Ges., **139**: 485-492, 3 Abb., 1 Tab.; Hannover.

ORTLAM, D. (1982): Durchführung hydrogeologisch-hydrochemischer Untersuchungen für den Bereich Horn-Lehe-West (Bremen). - In: Senator für das Bauwesen (Bremen), Landschaftsökologische Untersuchungen im Bereich Horn-LeheWest, 10 S., 12 Abb.; Bremen.

ORTLAM, D. (1983a): Einsatz und Möglichkeiten von Pollution-Tracer-Verfahren am Beispiel der Weser. - N. Jb. Geol. Paläont. Abh., **165** (2): 303-325, 12 Abb.; Stuttgart.

ORTLAM, D. (1983b): Neue Ergebnisse zur Baugrundkarte Bremen. - Ber. 4. Nat. Tag. Ing.-Geol.: 273-280, 7 Abb.; Goslar.

ORTLAM, D. (1984): Die geohydrologischen Verhältnisse im Hollerland (Bremen). - Abh. Naturw. Verein Bremen, **40**: 155-164, 7 Abb.; Bremen.

ORTLAM, D. (1989): Geologie, Schwermetalle und Salzwasserfronten im Untergrund von Bremen und ihre Auswirkungen. - N. Jb. Geol. Paläont. Mh., **1989** (8):489-512, 11 Abb., 3 Tab.; Stuttgart.

ORTLAM, D. & SAUER, M. (1993): Geochemische Grundwasser-Kartierung Bremen. Darstellung der Grundwasserbeschaffenheit und deren Beeinflussung durch Altlasten in der Stadtgemeinde Bremen. - Atlas mit Erläuterungen. - 28 S., 9 Abb., 60 Kt., 1 Anl.; Hrsg.: Bremer Entsorgungsbetriebe; Bremen (Druckhaus Lehe-Nord).

ORTLAM, D. & SAUER, M. (1995a): Das „Rollende Peilrohr" - ein neues umweltschonendes, schnelles und kostengünstiges Grundwasserentnahmeverfahren zur Untersuchung von Altlasten in Lockergesteinen. - Jber. Mitt. oberrhein. geol. Ver., N.F. **77**: 287-305, 11 Abb.; Stuttgart.

ORTLAM, D. & SAUER, M. (1995b): Das Grundwasser in Bremen - seine geogene Prägung und seine Beeinflussung durch Altlasten. - N. Jb. Geol. Paläont. Mh., **1995**, H. 6: 336-354, 9 Abb., 1 Tab.; Stuttgart (Schweizerbart).

ORTLAM, D. & SAUER, M. (1995c): Rollendes Peilrohr und geochemische Grundwasser-Kartierung in Bremen. - gwf-Wasser/Abfall, **09/1995**: 478-481, 6 Abb.; München (Oldenbourg).

ORTLAM, D. & SCHNIER, H. (1980): Erläuterungen zur Baugrundkarte Bremen. - 41 S., 12 Abb., 3 Tab.; Bremen (Schmalfeld).

ORTLAM, D. & SCHNIER, H. (1981): Erdfälle und Salzwasseraufstieg in Bremen - Typbeispiel für Süßwasserdepressionsgebiete. - N. Jb. Geol. Paläont. Mh., **1981** (4): 236-256, 9 Abb.; Stuttgart.

ORTLAM, D., SCHNIER, H., SEYLER, E. & WEMPE, H. (1981): Baugrundkarte Bremen, Teile A-D (1:10000 und 1:25000). - Bremen.

Repeatability of Geoelectrical Investigations

Jaana Aaltonen & Göran Blomqvist, Division of Land and Water Resources,
Royal Institute of Technology, S-100 44 Stockholm

Introduction

The use of geophysical methods, especially geoelectrical investigations, in observations of e.g. saltwater intrusion or leakage from waste deposits, has increased during the last years (Stierman, 1984; Chapman & Bair, 1992; Frohlich et. al., 1994). In the field of monitoring in time, however, this use have not been fully implemented, due to i.a. lack of knowledge of how the results from the geoelectrical resistivity investigations varies during the year and from year to year.

Within a larger project, investigating the surroundings of a waste deposit, the repeatability of resistivity measurements has been examined as one objective. The investigation area is situated in Småland, South Sweden and is rather complex and heterogeneous, with assorted sandy and gravely soil layers. There is also possible till layers on top of the bedrock which is found at a depth of approximately 15 metres beneath the soil surface.

This paper presents some of the results from these investigations and give a short discussion of the impacts from natural variations on the measuring results.

Method

The method used in this investigation is direct current resistivity profiling. It results in a profile which will show the lateral distribution of apparent resistivities in the ground. Electrical resistivity is the reciprocal value to electrical conductivity and hence, we will be able to detect areas with different electrical properties.

Since dissolved chloride ions in the ground water increases the electrical conductivity, dc-resistivity methods have proven to be suitable to detect areas with raised chloride content, as for instance, leachate plumes at waste deposits or salt water intrusion in coastal areas.

However, the natural variations, both in time and space, can be in the same magnitude as the anthropogene anomalies and by that conceal the expected results of anthropogene effects. In this investigation the aim is to compare the natural variation of resisitivity by time in the same profile under different climatic circumstances during the year (summer and autumn) and from year to year.

The repetition of the measurements has been ongoing twice a year since June 1994. The occasions when the measurements has taken place are:

- 1994-06-07
- 1994-10-07
- 1995-06-26
- 1995-09-16

The topical profile was measured with an electrode configuration according to Wenner (Fig. 1) with a constant electrode separation (a) of 20 m (Kofoed, 1979). The whole array was moved forward in 20 metres steps. This configuration then enables us to measure the apparent resistivity within a depth of approximately 10 m (Barker, 1989) and every 20 metre.

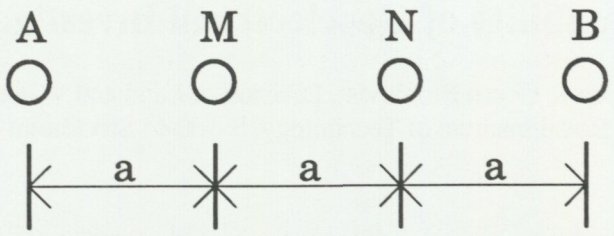


Figure 1. *The Wenner electrode configuration.*

A current (I) is put into the ground by the two outer electrodes, A and B. Then the potential gradient (U) is measured between the two inner electrodes, M and N. The formula

$$\rho_{\alpha} = 2 \cdot \Pi \cdot a \cdot \frac{U}{I}$$

will give the apparent resistivity (ρ_{α}) in a half sphere volume of the ground with the centre at the mid point of the electrode array.

Results

The repeatability of the DC-resistivity profile is, as seen, good (Fig. 2). The shape of the different parts in the profile is fairly well repeated from one year to another. However, there is a quite clear difference between the measurements made during the summer (dotted line) compared to those made in the autumn (solid line). The latter have been shifted toward higher resistivities by approximately 225 Ohm-m. It is also possible to distinguish between the years. In 1994, the mean upshift was 160 Ohm-m, while in 1995, the mean upshift was 280 Ohm-m.

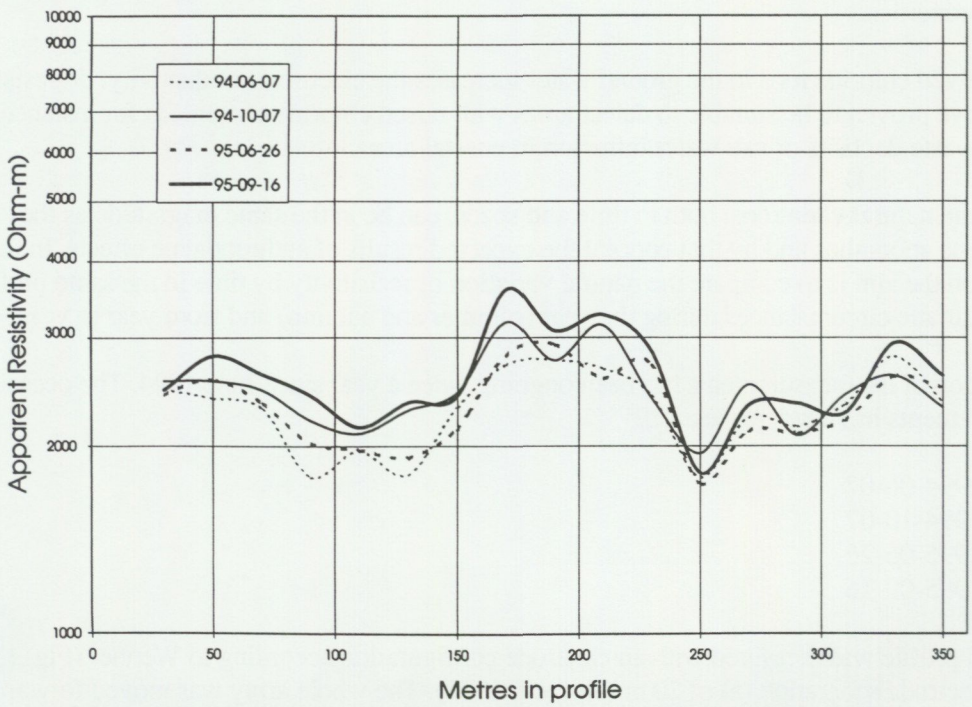


Figure 2. *Results from the investigated profile.*

The differences between the seasons and between the years are undoubtedly an effect of different ground water levels and soil moisture content within the measured volumes. In the autumn investigation the result of a dry summer season is reflected, when the measurments where done before the intense autumn rain started. The lower resisistivity values in summer, on the other hand, still reflects the foregoing spring with snowmelt and higher groundwater levels.

The variations in the apparent resisitivity which gives the general shape of the profile, is mainly due to the distances to the ground water level in different parts of the profile. This makes the resisitivty values clearly reflect the topography of the investigated profile.

By taking these variations between seasons and even years into account the dc-resistivity profiling method would be an easily manageable reconnaissance tool in mapping and monitoring ground water contamination, as for instance increased chloride content.

References

BARKER, R.D., 1989. Depth investigation of Collinear Symmetrical Four-electrode Arrays. Geophysics, no. 54, pp.1031-1037.

CHAPMAN, M. J. and BAIR, E. S., 1992. Mapping a Brine Plume Using Surface Geophysical Methods in Conjunction with Ground Water Quality Data. Groundwater Monitoring Review, v.12, no. 3, pp.203-209.

FROHLICH, R.K., URISH, D. W., FULLER, J. AND O`REILLY, M., 1994. Use of geoelectrical methods in groundwater pollution surveys in a coastal environment. Journal of Applied Geophysics, no. 39, pp. 139-154.

KOFOED, O., 1979. Geosounding Principles. Elsevier Scientific Publishing Co., Amsterdam, The Netherlands.

STIERMAN, D. J., 1984. Electrical Methods of Detecting Contaminated Groundwater at the Stringfellow Waste Disposal Site, Riverside County, California. Environmental Geological Water Science, no. 6, pp. 11-20.

Salinization of private wells from de-icing chemicals - A pilot project in central Sweden

Charlott Fabricius and Bo Olofsson
Division of Land and Water Resources, Royal Institute of Technology, S-100 44 Stockholm, Sweden

Abstract

Road salt consisting of sodium chloride is a commonly used de-icer in Sweden. Many wells are situated close to major roads and thereby in risk of contamination. The area chosen for the present investigation is located in the central part of Sweden. Well records from eight counties were collected from the Geological Survey of Sweden (SGU) and, using GIS, wells located within a distance of 500 m from major roads were selected. Groundwater sampling and analysing was carried out in 93 wells located within 300 m from major roads in the county of Västmanland. The correlation between the chloride content and various natural and technical variables, such as geology, topography, proximity to road and elevation related to the road, were statistically analysed through variance analysis (ANOVA). The project showed that almost 40 % of the collected water samples in the county of Västmanland had a raised content of chloride. A comparison between well records close to major roads in central Sweden and all well records from the same area stored at SGU, showed that wells close to roads had a harder (Ca+Mg) and more chloride rich water than the other wells. Increasing chloride content indicates the presence of NaCl, in this case probably road salt. The increased hardness is then a result of ion exchange processes due to addition of sodium to the soil. The amount of chloride is positive correlated to the depth of the wells. In the data from the county of Västmanland as well as in well records from SGU, wells with depths of 0-10 m show an increase of chloride that goes against the general trend, indicating an external salt source from the surface. The distance to the roads and the elevation of the well compared to the road surface were found as the primary risk factors for contamination. An increased amount of wells with an enhanced chloride content (>50 mg Cl/l) in the county of Västmanland were encountered among the wells situated close to major roads compared to all well records stored at SGU, within the same area. The project indicates that de-icing salts on roads may be an important source of chloride in groundwater, especially in shallow groundwater storages.

Introduction

Maintenance of roads and in particular de-icing chemicals may be one important cause to groundwater contamination. In the southern parts of Finland several municipal waterworks are believed to be contaminated by road salt (Soveri 1994). This has also been shown in Sweden (Bäckman 1980, Maxe et al. 1994) and in Canada (Howard & Haynes1993). However, the situation according to the private wells and their salinization due to road salt is of a unknown extension. This investigation is a first attempt to study the degree of salinization of private wells along major roads in Sweden at a regional scale. The aim was also to relate the salinization to the natural conditions of the wells such as geology, topography and hydrology. The investigation area is situated in the central part of Sweden.

In Sweden natural content of chloride in the groundwater is 1-20 mg/l (Aastrup 1979), depending on the geographical location. Waters with a chloride content exceeding 50 mg/l is in this investigation regarded as *salt affected* waters. Saline groundwater may have various sources e.g. marine (seawater intrusion, fossil seawater), geological (fluid inclusions, evaporites) or anthropogenic (leakage from waste deposits, road salt, sewers) which complicate the analysis of the origin of the saline water. Fossil seawater may be found below the highest marine shore level in Sweden where the land has been covered with salt or brackish water after the latest glaciation period. The occurrence and origin of salt water in Sweden is discussed by Olofsson (1994).

Well construction and sensitivity to contamination

The most common types of wells in the investigation area are drilled wells, dug wells and tube wells. The natural protection against contamination may not be enough if high permeable soils such as sand or gravel, or a highly fractured bedrock exists from the surface to the groundwater table. Unfortunately many old wells are situated in for groundwater contamination vulnerable areas. The vulnerability of the groundwater storage depends of its extension and capability, groundwater level, groundwater flow, geology, precipitation, the distance between the road and the aquifer and the amount of road salt used in the area (Bäckman 1980). The greatest risk is when the water storage has a high groundwater level, a plane topography and a slow groundwater flow (Bäckman 1994).

Runoff water from roads

The composition of Runoff water from roads depends on e.g. the intensity of traffic, the length of the dry periods and the intensity and duration of the precipitation (Lundberg & Lindmark 1994). The most important pollutants are suspended material, BOD and COD, nutrients (N,P), heavy metals (Pb, Cd, Zn, Cu, Fe, Ni), hydrocarbons (HC), micro-organisms, chemical de-icers, (Lundberg & Lindmark 1994). The runoff from a road section in a region with the mean precipitation of 700 mm/year in Sweden is estimated to 2.8×10^6 m^3 / m^2, year (Lundberg & Lindmark 1994).

The effect of road salt on soil and groundwater

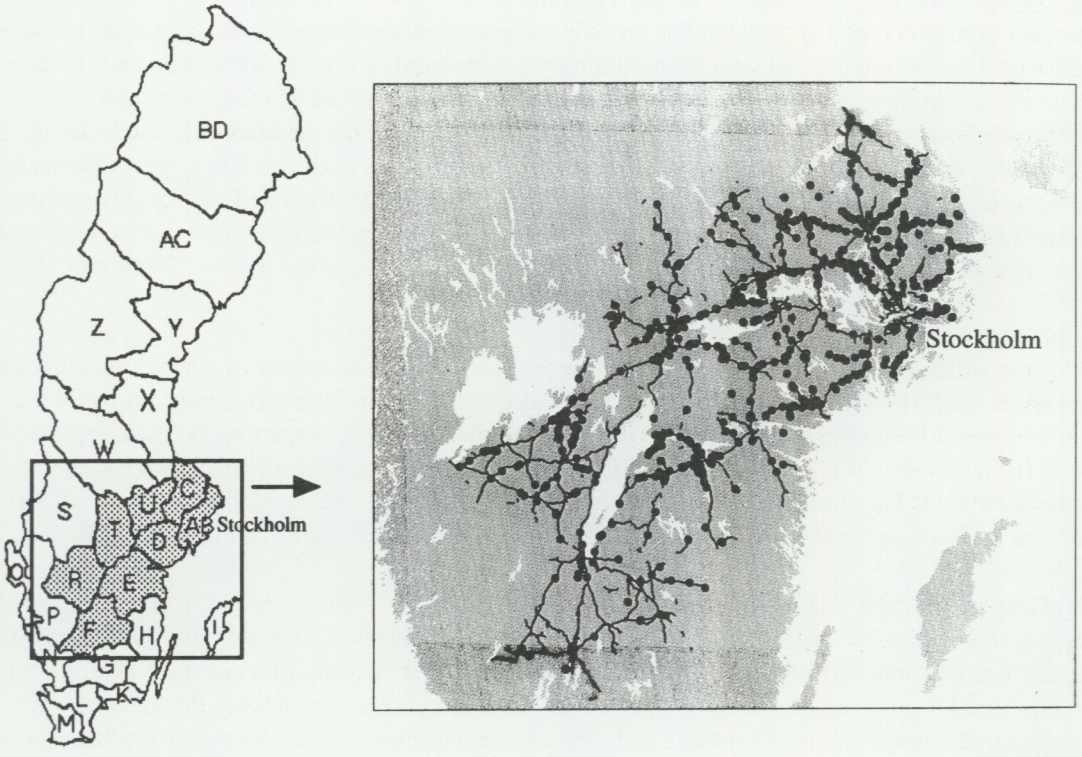
Road salt has generally been spread in Sweden since the nineteen-sixties. About 100 kg salt is spread per year and per vehicle (Falukuriren 1994). During the snow melting process the NaCl dissociates into Na^+ and Cl^-. Investigations have shown that NaCl effects the ground and the groundwater through an increased chloride content , sodium content, hardness, alkalinity and dissociated bound compounds (O'Brien & Majewski 1975). Chloride is a conservative ion, which does not react with the soil particles but instead leaches to the groundwater (Knutsson 1995). This characteristics makes it to an excellent tracer. The sodium ion tends to react with the soil e.g. through ion exchange:

$$2\ Na^{+}_{(aq)} + Ca_{(ad)} \rightarrow Ca^{2+}_{(aq)} + 2\ Na_{(ad)}$$

This ion exchange makes the water harder when the sodium ions change places with the calcium and magnesium ions which are adsorbed on the soil particles. Another effect of sodium ions is that it may disperse organic matters and clay minerals when the content of exchangeable sodium is high and the electrolytic concentration is low (Amhrein et al, 1992). This dispersion may release the heavy metals which are adsorbed on the organic matters or the clay minerals. I addition polyaromatic hydrocarbons (PAH), which are sorbed on the humus, may be released and thereby easily transported to the groundwater (Jacks et al. 1995).

Description of the investigation area

The county of Västmanland was chosen as the main field area due to its varying geological conditions and the presence of major roads parallel to or intersecting the many great eskers in the county. The bedrock in central Sweden consists mainly of hard crystalline rocks. The bedrock surface, which is slightly undulating, is covered by till and in topographical lower parts by glacial or postglacial clays. The eskers, which consist of glaciofluvial deposits of sand and gravel, are major groundwater reservoirs. The investigation area is located below the highest marine shore level.



AB= The county of Stockholm
C= The county of Uppsala
D= The county of Södermanland
E= The county of Östergötland
F= The county of Jönköping
R= The county of Skaraborg
T= The county of Örebro
U= The county of Västmanland

Figure 1 *Investigated area in central Sweden and the distribution of selected wells along major roads (data from SGU). A specific study was carried out in the county of Västmanland.*

Investigation methods

Specific study of the county of Västmanland

Water sampling was carried out in private wells situated within 300 m from major roads in Västmanland. In total 93 samples were collected, among which 45% were drilled wells in rock. The samples were collected directly from the water tap. In addition information regarding technical well parameters, the location of the well compared to the road as well as the geological environment close to and in the surrounding of the well, were collected.

The chemical analyses comprised content of chloride, sodium, magnesium and calcium, pH-value and electric conductivity. These analyses were made on wells which are presently in use.

Regional study in eight counties based on data from SGU

Chemical data from private wells in eight counties (see figure 1) were selected from the well record database at SGU using the GIS program MapInfo with the criteria that the wells should be located within a distance less than 500 m from roads which are at least 7 m wide. However, the accuracy regarding the exact position of the wells in relation to the roads were insufficient for detailed studies, hence the analysis can only give a rough picture of the chemical variations along the roads.

Statistical analysis

Statistical analyses were made based on results from the county of Västmanland in order to evaluate how various geological, topographical and hydrological factors influence on the chloride content. The statistical analyses comprised principal component analysis (PCA) and variance analysis (ANOVA). Primarily PCA was applied in order to gain a general view of the relationship between the components. ANOVA was used to investigate the influence on the chloride content by technical and natural, often non numerical, variables.

Results

Water chemical analyses

Median values for the chemical data of wells situated close to major roads in four counties, based on data from SGU, were chemically compared to the total amount of wells stored in the same database. For some of the counties, in which hydrogeological mapping has been carried out, the selected wells were compared with results from compilations made within the hydrogeological mappings. Although these two populations are not completely comparable since they represent different wells, the result may indicate the trend.

The compared parameters are chloride content and hardness. Soil and bedrock wells have been analysed separately in order not to mix the different water characteristics (see figure 2 and 3). The figures show that the hardness and chloride content for both soil and bedrock wells are usually higher in the wells located close to the road than the general values of the counties.

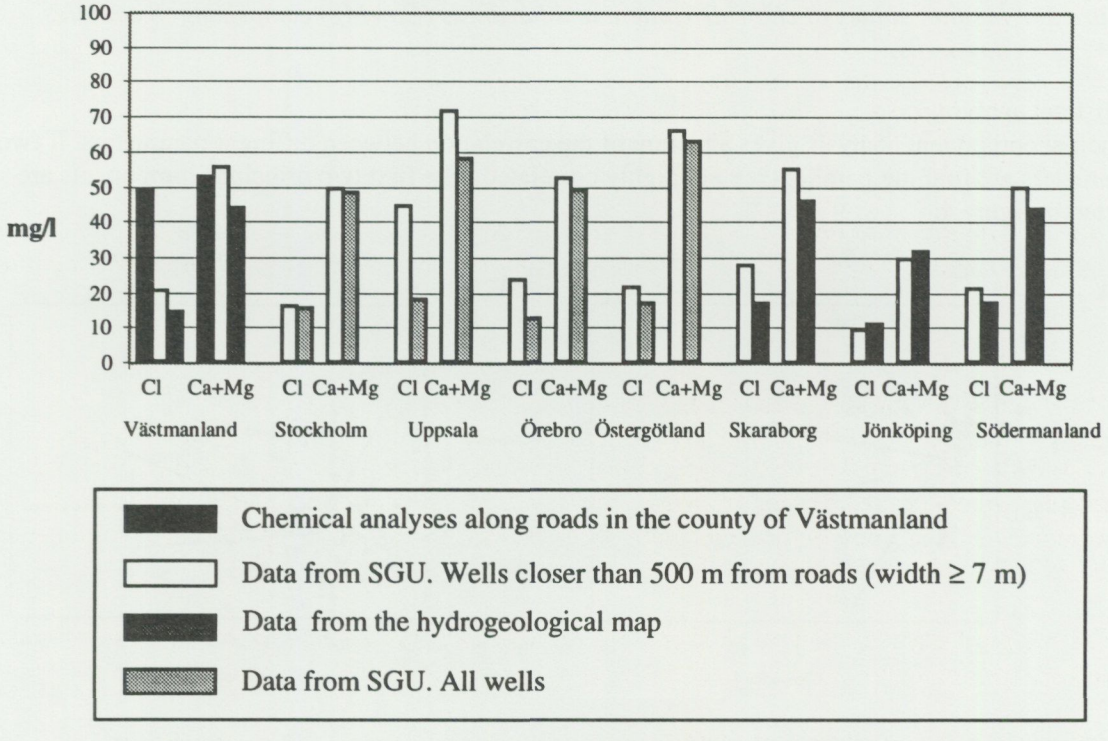


Figure 2 Median values of chloride content and hardness (Ca+Mg) comprising 8 counties, drilled wells

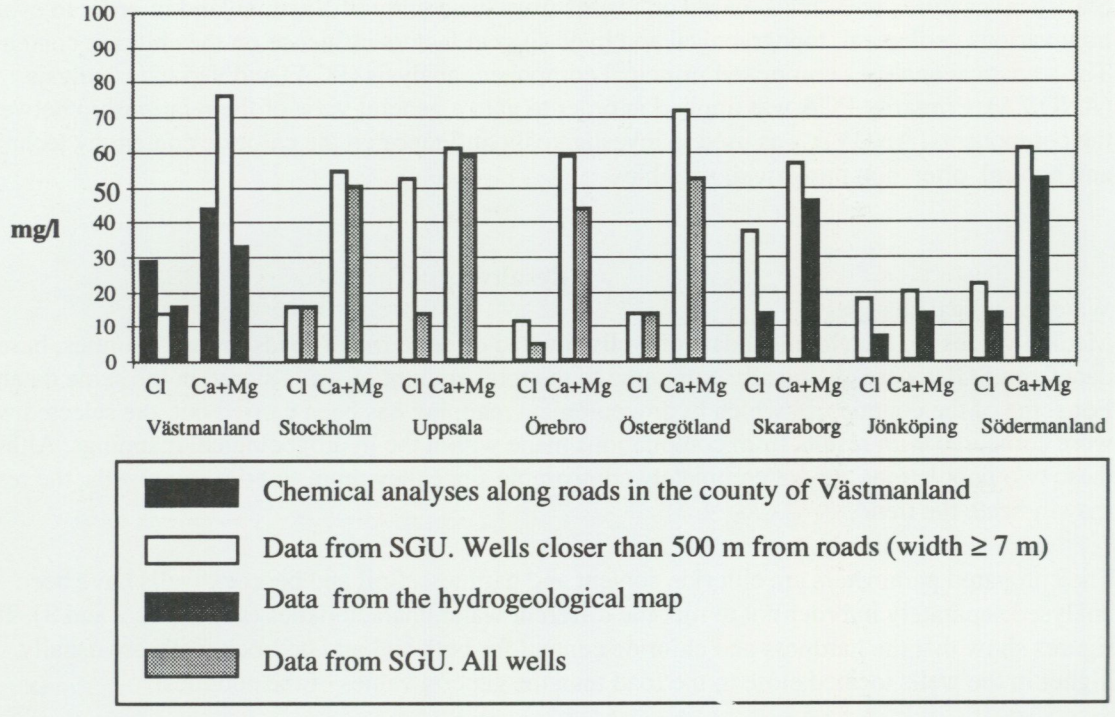


Figure 3 Median values of chloride content and hardness (Ca+Mg) comprising 8 counties, dug wells.

Statistical analyses

Principal component analysis gives a picture of the correlation between different parameters. If two parameters are running parallel they are highly correlated. The first two principal components are plotted in figure 4.

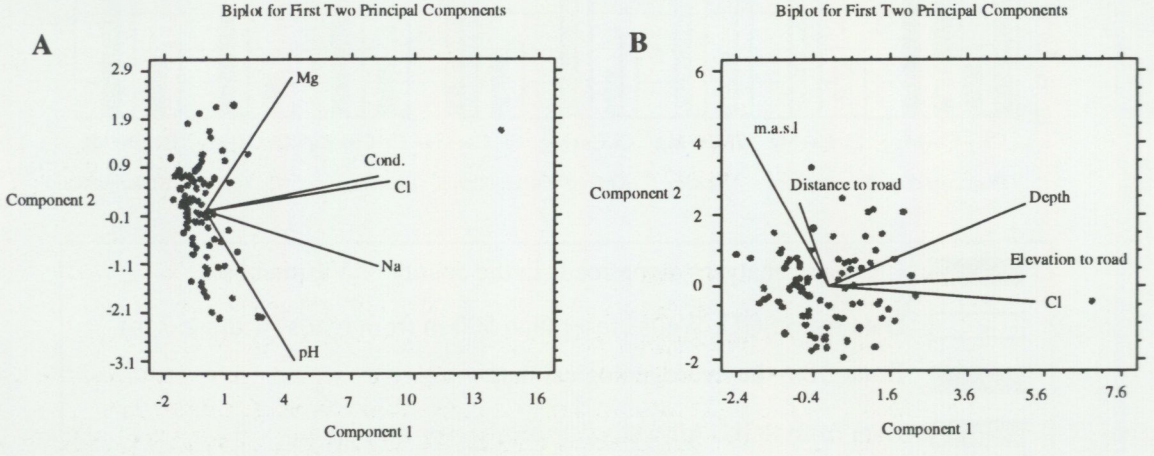
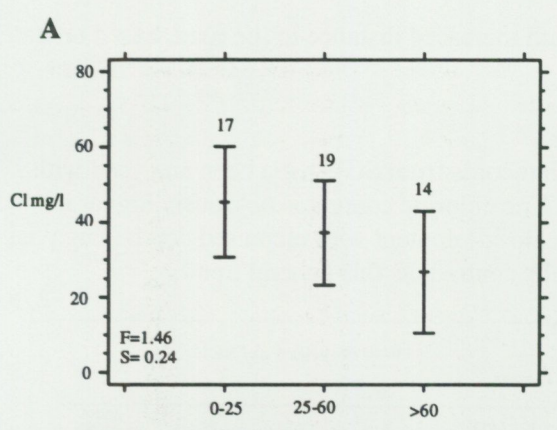


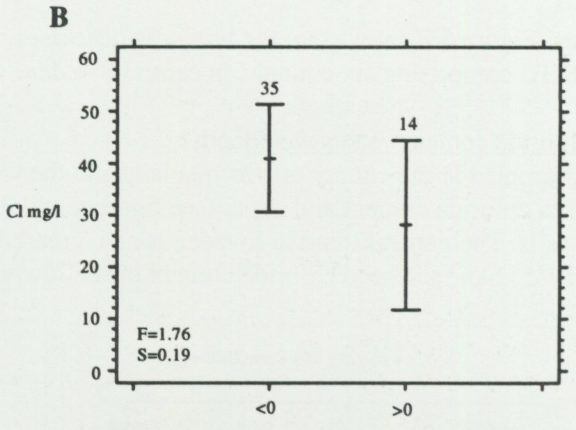
Figure 4 PCA - results from wells along roads in the county of Västmanland, 93 wells.

Figure 4A shows that the conductivity and the chloride content are highly correlated. In figure 4B, the depth and the elevation related to the road are relatively well correlated to the chloride content.

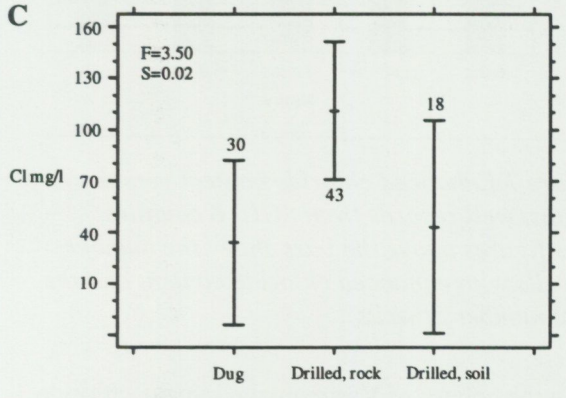
The results from the variance analysis (ANOVA) are presented in figure 5 A-F.



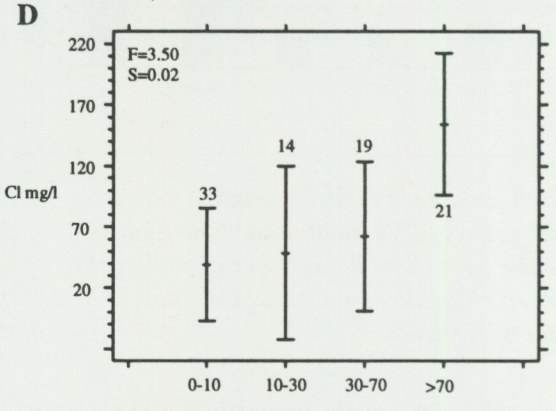
The chloride content versus the distance (m) to the road, soil wells.



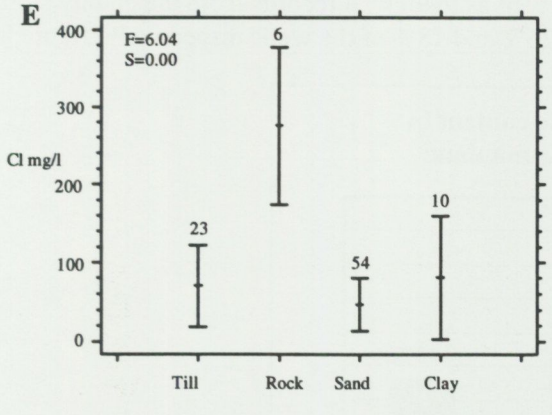
The chloride content versus the elevation (m) in relation to the road, soil wells.



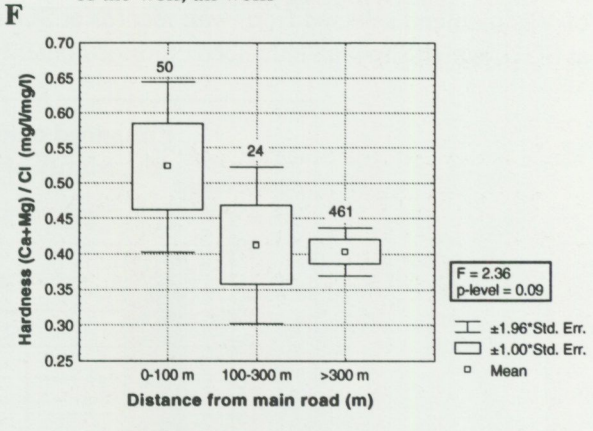
The chloride content versus type of well



The chloride content versus the depth (m) of the well, all wells



The chloride content versus the geology at the well, all wells.



The Ca+Mg / Cl quota versus the vicinity to the road.

Figure 5 A-E Results from ANOVA carried out on wells along roads in the county of Västmanland (Median values are presented with 95 % confidence intervals). Figure. 5 F is based on data from SGU, comprising six counties.

The variance analysis showed that the chloride content decreases with increased distance to the road. Wells situated below the road surface have an enhanced chloride content compared to wells situated above the road surface. Figure 5 C shows that drilled rock wells have a higher chloride content than soil wells. Deep drilled wells have a significantly higher chloride content than superficial soil and rock wells. This is also shown in figure 5 E, in which wells situated in rock have a higher chloride content than the rest, due to that most rock wells are drilled to a relatively greater depth than wells in other geological

settings. Figure 5 F shows that the hardness decreases with increased distance to the road, based on data from SGU comprising six counties in central Sweden.

The chloride content versus well depth

Wells sampled in the county of Västmanland and the well records from SGU have been analysed with regard to chloride content and depth (see figure 6 and 7). The chloride content is obviously higher in deep wells. The general trend in Sweden is an increased chloride content with increased depth (Engqvist et al. 1985). An increased chloride content in shallow wells contradicts this general trend.

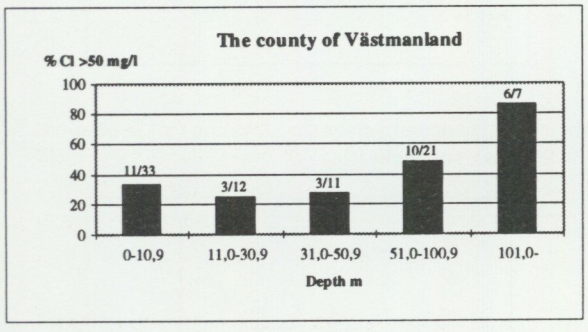


Figure 6 Enhanced chloride content versus. depths, county of Västmanland. (The figures above the bars show the number of wells with enhanced chloride content and the total number of wells).

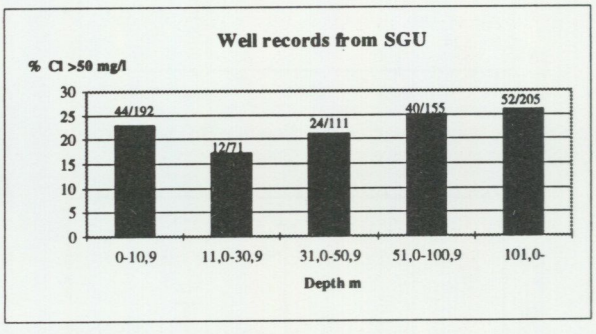


Figure 7 Enhanced chloride content versus. depths, well records from SGU, 8 counties. (The figures above the bars show the number of wells with enhanced chloride content and the total number of wells).

In total, 39% of the wells, presently in use along roads in the county of Västmanland, have a chloride content exceeding 50 mg/l. This figure can be compared to analyses of wells close to roads in the county of Västmanland selected from well records at SGU as well as to all well records from the county stored at SGU, which show an enhanced chloride content in 25% and 18% of the wells respectively, figure 8.

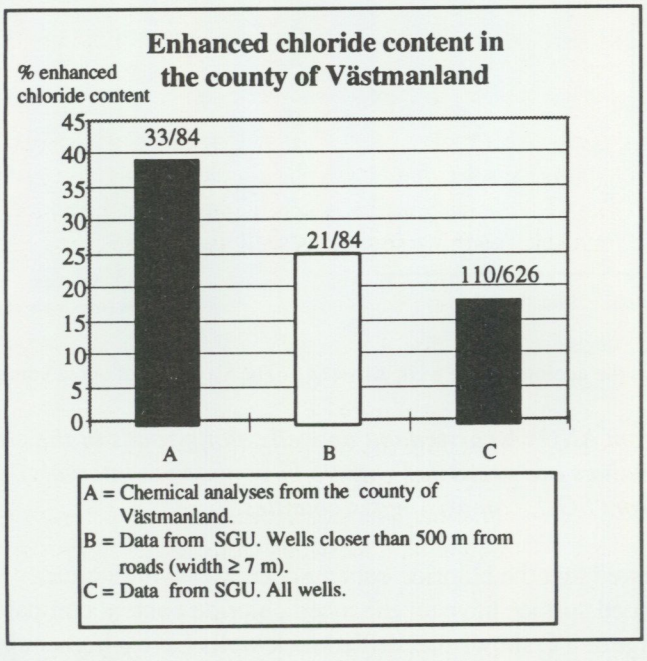


Figure 8 Enhanced chloride content of wells in the county of Västmanland. (The figures above the bars show the number of wells with enhanced chloride content and the total number of wells).

Discussion

A comparison between soil and rock wells shows that rock wells have a higher conductivity, pH-value, chloride content and usually a harder water. This is in agreement with for Sweden common situation. The conductivity and the pH-value increase with increasing depth of the well. When the chloride content raises the hardness (Ca+Mg), the pH-value and the conductivity tend to increase (Engqvist et al. 1985).

For the counties of Stockholm, Uppsala, Örebro and Östergötland (figure 2 and 3) it has been possible to compare a selected part of the well records with all well records stored at SGU. The results showed that wells close to roads had a higher hardness and in general a higher chloride content than the natural values. This is valuable for soil wells and for rock wells.

By ion exchange processes sodium may change place with adsorbed magnesium and calcium ions, which become released increasing the hardness of the groundwater. An increase of the chloride content in the groundwater close to roads is also obvious. The raised hardness in the groundwater as well as the increased chloride content can be explained by influence of road salt.

In the other investigated counties (figure 2 and 3) similar situation can be seen when wells close to roads are compared to well records compiled in connection to the hydrogeological mapping within these counties. However, the groups comprise two different populations which are not completely comparable. Also in this analysis an influence of road salt seems to have raised the hardness and the chloride content of the groundwater.

According to the results from the county of Västmanland, the vicinity and the elevation compared to the road are the major factors which influence on the vulnerability of the well for contamination of road salt. Wells situated at an altitude lower than the road surface and close to the road show a higher risk for contamination. This has previously been clarified by Canadian investigations (Howard & Beck 1993). De-icing salt on the road is transported to the surroundings as spray or as runoff water. Measurements have shown that 98 % of all the salt that is transported from the road surface is found within 50 m from the road borders (Demers & Sage 1989). Where the salt reaches the ground it may infiltrate to the groundwater, and hence contaminate wells situated close to the road.

Shallow wells (0-10 m) comprise a higher amount of salt affected wells than slightly deeper wells (10-50 m). The general trend ought to give an increasing chloride content with increasing depth (Engqvist et al. 1985). The superficial sources of salt, which can explain the high chloride content in shallow wells, include road salt, leaching sewers as well as leakage from waste deposits and industries.

Wells located close to roads in the county of Västmanland show an enhanced chloride content compared to the median content calculated from all wells in the county. The comparison between groundwater sampled along roads in the county of Västmanland and well record data from SGU as well as from well records compiled within the hydrogeological mapping are not completely comparable due to a higher amount of soil wells among the collected water samples. Soil wells have generally a higher risk for contamination. The significant difference regarding amount of salt affected wells in the county of Västmanland, between wells located close to roads (25-39%) and all wells in the same county (18%) can hardly be explained by other chloride sources than road salt. The minimum difference (7%) is probably underestimated because the selection of wells along major roads covers a distance of 500 m from the road, which probably is a much broader zone than can be affected by the road. A plausible assumption is that 10-20 % of the wells close to roads (within 100 m from the road) may be affected by road salt

Conclusions

The present investigation indicates that there is a general salinization of private wells along major roads in the central part of Sweden. As much as 40% of all the wells along major roads in the county of Västmanland showed an increased content of chloride. Wells located close to roads often show a higher median value of chloride and an increased hardness compared to the natural situation, which may be an effect of an external salt source, probably road salt.

The statistical analyses of wells in the county of Västmanland show that drilled rock wells generally have a higher chloride content than soil wells. The distance from the well to the road and the elevation of the well in relation to the road surface are the most important factors affecting the vulnerability to contamination. If the well is situated lower than, or close to the road, the risk for pollution increases significantly.

Acknowledgement

This study could not have been carried out without support from Sten Sandström at the Geological Survey of Sweden. The project was partly granted by the Swedish National Road Administration.

References

AASTRUP, M.,1979 : Nederbördens betydelse för klorid och sulfat i Sverige (The dependence of precipitation on chloride and sulphate in Sweden). SGU Rapporter och meddelanden no. 14. Särutgåva av Vannet i Norden no: 1, 1979.

AMHREIN, C., STRONG, J. E & MOSHER, P. A, 1992:Effect of deicing salts on metal and organic matter mobilization in roadside soils. Environ. Sci. Technol., vol 26, No.4 1992. p 703-709.

BÄCKMAN, L. ,1980: Vintervägsaltets miljöpåverkan (Environmental effects of chemical de-icing). VTI report no. 197.

BÄCKMAN, L. ,1994: Environmental effects of chemical de-icing.Technical Report vol. 2, IX th PIARC International Winter Road Congress. p 486-490.

DEMERS, C. L. & Jr SAGE, R.W. , 1989: Effect of road deicing salts on chloride levels in four adirondack streams. Water, air and soil pollution 49. p 369-376 ,1990.

ENGQVIST, P., FAGERLIND, T., LUNDSTRÖM, A. & SANDSTRÖM, S. ,1985: Svenskt vattenarkiv, Grundvattenkvalitet (Swedish water archive, groundwater quality). SGU Rapporter och meddelanden no. 44.

Falukuriren, Dalarna. 1994-09-14.

HOWARD, K.W. F. & BECK, P.J ,1993: Hydrogeochemical implications of groundwater contamination by road de-icing chemicals. Journal of contaminant hydrology, 12 (1993), p 245-268.

HOWARD, K. W. F. & HAYNES, J., 1993: Groundwater contamination due to road de-icing chemicals - salt balance implications. Urban geology 3. Geoscience Canada Volume 20 No. 1.

JACKS, G, NORRSTRÖM, A-C & ÖMAN, C ,1995: NaCl-Me-PAH- en farlig kombination för grundvattnet omkring tätorter? (NaCl-Me-PAH- a dangerous combination for groundwater around cities?) Unpublished report at the Div. of Land and Water Resources, KTH and IVL.

KNUTSSON, G.,1995: Vägunderhållsåtgärders inverkan på grundvattnet (Effect on the groundwater due to maintenance of roads) Unpublished report at the Div. of Land and Water Resources, KTH

LUNDBERG, K. & LINDMARK, P.,1994: Sammansättning av vägdagvatten (The composition of runoff from roads). Rening av vägdagvatten, Vägledning 7, Swedish Geothecnical Institute.

MAXE, L., KNUTSSON, G., OLOFSSON, B. & JACKS, G. ,1994: Analys och utvärdering av saltets ursprung i grundvatten från Hammarby reservvattentäkt (Analysis and evaluation of the origin of salt in the groundwater at Hammarby waterworks), Report to the municipalities of Upplands Väsby, county of Stockholm. Div. of Land and Water Resources, KTH.

OLOFSSON, B., 1994: Salt groundwater in Sweden. *in* Olofsson, B., (ed) Salt groundwater in the Nordic countries. Proceedings of a workshop, Saltsjöbaden, sept. 30 - Oct. 1, 1992. Nordic Hydrological Programme (NHP) Report no 35, pp 17-35.

O'BRIEN, J.E. & MAJEWSKI, J.C. ,1975: Effects of de-icing salt on groundwater characteristics. Environmental letters, 8(4). p 303-313.

SOVERI, J., 1994: The effects of de-icing salts on groundwater quality in Finland. Nordic Hydrological Programme Report no. 35. Salt groundwater in the Nordic countries. p 117-126.

Regional flow of intruding sea water in the carbonate aquifers of Apulia (Southern Italy)

Maria Dolores Fidelibus*, Luigi Tulipano**
*Istituto di Geologia Applicata e Geotecnica, Politecnico di Bari, 4 Via Orabona, 70125 Bari, Italy
**Dipartimento di Idraulica Trasporti e Strade, Università di Roma "La Sapienza", 20 Via Eudossiana 00184 Roma, Italy

Apulian coastal carbonate aquifers suffer from salinization that only in the coastal areas is connected with modern sea water intrusion. Salt groundwaters sampled inland show chemical characteristics variably modified with respect to those of modern sea water. To the west of the emerged platform, carbonate formation, sunk as a graben, is covered by thick argillaceous deposits of Plio-Pleistocene age: salt waters deeply diagenised have been recognised there. Beside observation wells, only a few drillings reach salt groundwaters: information about their occurrence and mobility was thus indirectly obtained through the hydrochemical study of brackish coastal spring waters. Using major, minor and trace ions as natural tracers of the different salt water end-members, salt water components of the brackish coastal spring waters were hypothesised, thus allowing a scheme of the occurrence and the mobility of salt groundwaters within the Apulian territory to be outlined.

Geological and hydrogeological setting

The Apulian carbonate platform of Mesozoic age elongates from Gargano Promontory to Salentine Peninsula (Fig. 1). The present structural setting of Mesozoic carbonate series was originated by an ample synclinal which was later transformed, due to faulting, into a huge Horst, corresponding to the present outcropping formations, Gargano Promontory and the Murgia-Salento system. Faulting began during Cretaceous and the Horst reached an almost definitive order at the end of the tectonic phase which occurred between Pliocene and lower Pleistocene. To the W the Mesozoic rocks sank as a graben: the consequent Plio-Quaternary transgression filled the graben of mainly argillaceous sediments, having a maximum thickness of about 6000 m, in connection with the more depressed part of Mesozoic basement. While Murgia and Salento can be considered stable areas, the Gargano is still affected by active tectonics: the main fault which separates Gargano from Tavoliere (Candelaro fault) is seismo-genetic. The structural setting of the whole platform allows the identification of four hydrogeological units: Gargano, Tavoliere, Murgia and Salento (Fig. 1).

Gargano aquifer does not correspond to the whole extension of the Promontory, owing to the existence of carbonate facies almost impermeable, as limestone and marly limestone with interbedded flint-stones, beside facies very permeable due to fissuring and karstification, constituted by limestone and dolomitic limestone (Cotecchia & Magri, 1966). Salt water of marine origin is found in coastal areas under fresh groundwater. In the central area of the Promontory fresh groundwater show piezometric heads between 30 and 50 m: salt waters should be at depths of about 1000 m under m.s.l. and more, however no drillings are available to control their occurrence, owing to high elevations (reaching 1000 m above m.s.l.). Two main aquifers are recognised in the Tavoliere. The Quaternary shallow porous aquifer, having a thickness of a few tens of meters, is limited at the bottom by the top of the Plio-Pleistocene formation: it consists of strips of regressive deposits (sands and conglomerate) and of alluvial material. Mesozoic carbonate rocks at the bottom of transgressive deposits constitute the deep aquifer, where groundwaters are in hydraulic continuity with those of Gargano and Murgia. Normally fresh or slightly brackish groundwaters flow in the shallower part of the basement, at depths lesser than a few hundred meters under m.s.l.: going inland, approaching the central part of foreland, groundwater becomes progressively more saline. Fresh groundwater is recognised only when the hydraulic head is able to maintain salt water at a depth lower than that of the basement top. The hydrogeological units of Murgia and Salento can be considered as a single aquifer, since great part of Murgia groundwater discharges into the Salento aquifer (Tulipano et al., 1990).

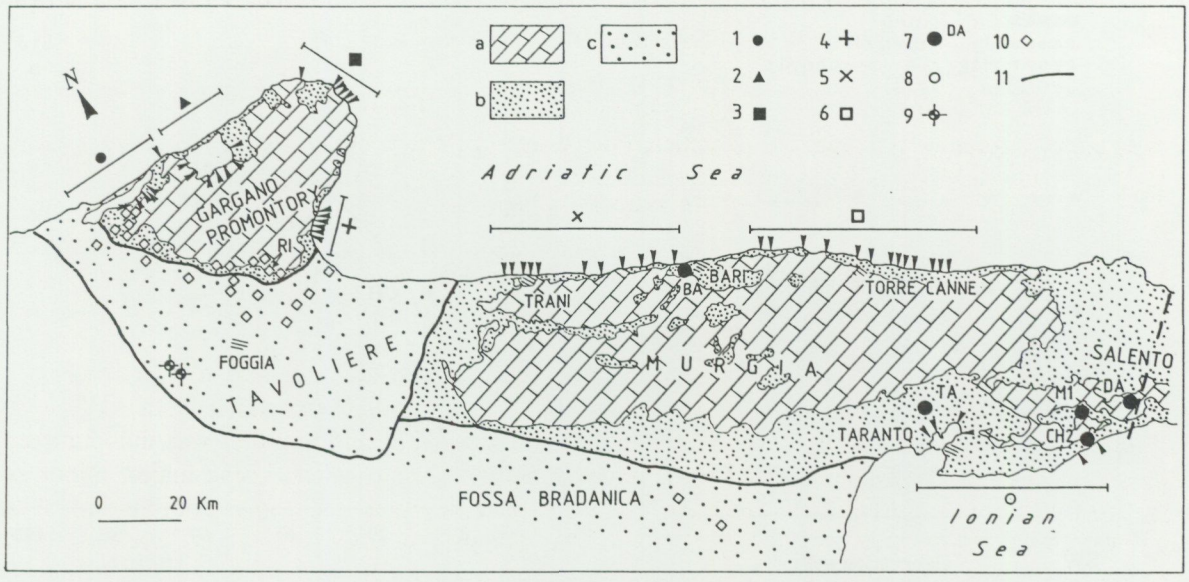


Fig. 1. Map of the Apulia region: a) outcropping Mesozoic carbonate formation; b) thin Quaternary deposits; c) Plio-Pleistocene formation of the Tavoliere and Fossa Bradanica; 1) Lesina springs; 2) Varano springs; 3) Vieste springs; 4) Manfredonia springs; 5) NW Bari springs; 6) SE Bari springs; 7) observation-wells; 8) Taranto springs; 9) oil-exploration wells; 10) drilled wells reaching the carbonate basement; 11) boundary of hydrogeological units.

In the Murgia fresh groundwater floats on salt water, certainly in the coastal zone, where it is recognised through observation- or deep wells. Inland, salt water should occur at depths of thousands of meters below sea level, due to the values of fresh water hydraulic heads, higher than 200 m. a.s.l.: however, permeability characteristics of rocks at these depths are unknown. In Salento fresh groundwater floats everywhere on intruding sea water, due to very low piezometric heads, not higher than 4 m above m.s.l..

Peculiar aspects of sea water intrusion in the territory

Previous researches (Tulipano & Fidelibus, 1984, Fidelibus & Tulipano, 1986 and 1990) dealt with the chemical characteristics of salt groundwaters sampled in Murgia and Salento carbonate aquifers. These salt waters represent diagenetically modified sea water: they are typically dominated by Na^+ and Cl^-, but exhibit Ca^{2+} enrichment and a variable degree of Mg^{2+} depletion with respect to modern sea water. The low Mg/Ca ratios (if no otherwise specified, concentrations in the ratios are expressed in meq/l), ranging from 4 to 1.5, allowed to differentiate the salt groundwaters from sea water, having average ratio of 5: the other major constituents showed less sensible changes, while minor and trace constituents as strontium and lithium were distinctly enriched (Fig. 2). ^{14}C contents (Fig. 3) measured in a few salt groundwaters of Apulia region indicated that the decrease of Mg/Ca ratio could be connected to increasing residence times (Fidelibus, 1992). Corrected ages were not calculated: however, if the 50% of ^{14}C is considered of biogenic origin, the apparent ages are of thousands of years (for example about 18.000 years for the CH1 well).

However these findings were not enough to define the mobility of salt waters within the considered carbonate aquifers. Thus an attempt was made in order to recognise if some of them took part in the coastal discharge, mixed with fresh groundwaters. Recognition of the characteristics of salt water component of coastal brackish springs of Murgia and Salento was attained using calcium, strontium and particularly lithium, as capable to trace the connection with the different salt end-members. These natural tracers showed the maximum range of variation in salt groundwaters compared to other constituents (Fig. 2). Ca^{2+} and Sr^{2+} gave only general indication, being involved in water-rock interaction due to mixing (Fidelibus & Tulipano, 1990). Lithium was considered, instead, to be a specific tracer able to differentiate the salt water end-members.

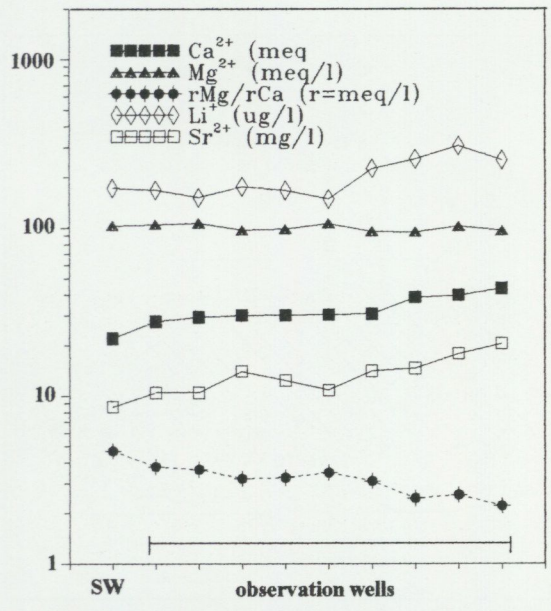


Fig. 2. Variation of major and minor ions concentrations (normalised to 19.000 ppm of chloride) and Mg/Ca ratio in salt groundwaters sampled in Murgia and Salento aquifers with respect to sea water.

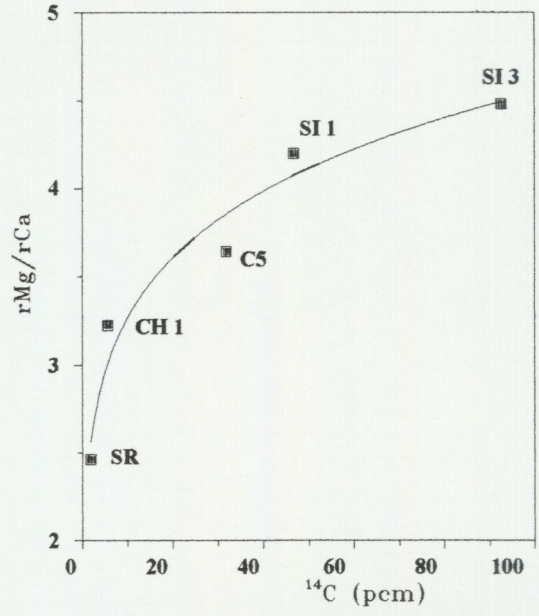


Fig. 4. Cross plot of rMg/rCa (r stands for meq/l) versus ^{14}C contents for some salt groundwaters sampled in the observation wells of Salento aquifer.

A salt water component older than modern sea water could be ascribed to most of Murgia springs, while almost all the coastal springs of Salento Peninsula exhibit a salt water component quite similar to sea water. The study of a few coastal springs discharging near to the submerged part of Murgia carbonate formation, implied that a salt water more ancient than those already known, should be involved in the mixing. Joined interpretation of both the geographic distribution of salt groundwaters of different age and the recognition of different salt water components in the brackish springs, allowed to put forward initial hypotheses upon the underground pathways followed by sea water from intrusion fronts to the coastal discharge in Murgia and Salento aquifers (Fidelibus & Tulipano, 1986 and 1990).

Further information about salt waters was provided by the analysis of a sample coming from the shallower part of carbonate basement of Tavoliere close to Gargano unit. This salt water appeared to be the most drastically altered salt water found in Apulia: it showed extremely high Ca^{2+} enrichment and exhibit remarkable changes in some major and minor constituents. The very low value of Mg/Ca ratio occurred with appreciable depletion of sodium, magnesium, potassium and sulphate and the greatest observed enrichment in strontium and lithium. The hydrochemical study of the coastal brackish springs of Gargano (Fidelibus, 1992) established that most of them had a salt water component very similar to that sampled in the Tavoliere carbonate basement: the same salt water could satisfy the required characteristics of the salt water component hypothesised for the coastal springs of Murgia close to the boundary with Tavoliere and Fossa Bradanica. These last findings suggested more ancient waters than those found in coastal zones, and likely existing in the basement, could reach the coastal discharge, following pathways that presupposed very large distances to be covered.

Wells reaching the shallower part of the basement provide mostly fresh and brackish waters: unfortunately not enough facts are known concerning either the occurrence of salt waters in the deepest part of the carbonate basement or their principal chemical constituents. Only a few oil-exploration wells have seldom reached the basement, the interest of investigation being ordinarily limited to Plio-Pleistocene formation due to the presence of oil or gas reservoirs: consequently, just a few data on salinity are available. Waters found between 1000 and 2000 m in the basement showed salinity in the range 20-30 g/l. Even if waters have been found in oil drilling operation, normally sampling conditions are unknown: given that innumerable possibilities exist for errors in sampling of this sort, the only two chemical analyses available must be considered with caution.

The hypothesis which will be discussed, is that salt waters existent into the carbonate basement of Tavoliere and Fossa Bradanica could actively mix with fresh waters of outcropping aquifers, at least in the zones close to the outcropping formation. The study aims at recognising the role played by these fluids in the salinisation of coastal springs, in order to contribute at clarifying, on a regional scale, the complex behaviour of all the salt water end-members.

Data presentation

The study is based on the chemical analyses of salt and brackish waters sampled in the whole Apulia region. Salt water samples (Cl > 300 meq/l) are represented by: (1) sea water of the Adriatic and Ionian side sampled far from the coast; 2) salt groundwaters from the observation-wells pertaining to the Murgia aquifer (namely TA, SR, CH2, M1, DA, BA) and 3) salt groundwaters from drilled wells reaching the carbonate basement of Tavoliere close to Gargano unit (RI, PG). One salt water sample (L1) comes from the carbonate formation reached by an oil-well at 1600 m of depth in the Tavoliere; another salt water sample (MZ1) comes from the sandy Pliocene levels intercepted in the 1172-1213 m of depth range in a close oil-well. For these last samples no information about minor and trace elements is available. Brackish groundwaters were sample in some wells reaching the shallower part of carbonate basement.

Furthermore, waters from numerous brackish coastal springs have been sampled. Springs outflowing along the Gargano coastline belong to four main groups, namely Lesina, Varano, Vieste and Manfredonia (Fig. 1), having a total discharge rate of 5 m^3/sec. Salinity ranges from 0.5 to 14 g/l. Temperature ranges from a minimum of 14 °C for the Varano springs to maximum values of 27 °C of some springs of Lesina group. Coastal springs outflowing along Adriatic and Ionian coastlines of Murgia region are divided in three main groups, Bari NW, Bari SE and Taranto (Fig. 1), which include, respectively, the big concentrated springs of Trani, Torre Canne and Taranto. Average total discharge rate of concentrated springs is higher than 5.5 m^3/sec: this figure do not takes into account submarine and minor spring discharge. Salinity ranges from 2 to 21 g/l and temperature from 17 to 19 °C. Southernmost coastal springs of Salento aquifer, due to a little involvement in coastal discharge of salt waters different from modern sea water, will not be included in the study.

Chemical characteristics of salt waters in relation to their diagenetic history.

Fig. 4 shows the cross-plots of Ca^{2+} Mg^{2+}, Na^{+}, K^{+}, Li^{+}, Sr^{2+}, $SO_4^{=}$, HCO_3^{-} versus Cl^{-} for coastal springs waters, brackish and salt groundwaters and modern sea water. Because of its generally conservative behaviour, chloride has been used to infer the origin of the waters. The salt waters exhibit distinct behaviour: dispersion in the diagrams defines the domain of the possible end-members of the mixing.

Salt waters from observation-wells show a general Ca^{2+} enrichment (Fig. 4a) and Mg^{2+} and K^{+} depletion (Fig. 4b and 4d), while sulphates are only occasionally depleted (Fig. 4e). Salt waters from carbonate basement and from Pliocene sands show marked chemical variation with respect to sea water: they show Mg^{2+}, K^{+} and $SO_4^{=}$ depletion and Ca^{2+} and HCO_3^{-} enrichment. Na^{+} depletion is observed in RI and L1 samples from carbonate formation, while MZ1 in Pliocene sands shows higher Na/Cl ratio with respect to sea water. The enrichment and depletion of major, minor and trace constituents follow the tendency of more striking changes usually recognised for the same constituents in subsurface waters of marine origin enclosed in different sedimentary rocks of ancient basins (Chave, 1960). Major reactions recognisable as responsible of salt waters diagenesis are: (a) Ca^{2+}-Mg^{2+} exchange due to water-carbonate rocks interaction, (b) Na^{+}-Ca^{2+} or Na^{+}-Mg^{2+} base exchange and (c) SO_4^{2-} reduction.

In carbonate environments, simultaneous enrichment of Ca^{2+} and depletion of Mg^{2+} have been explained as mainly due to water-rock interaction processes as dolomitisation, dissolution and

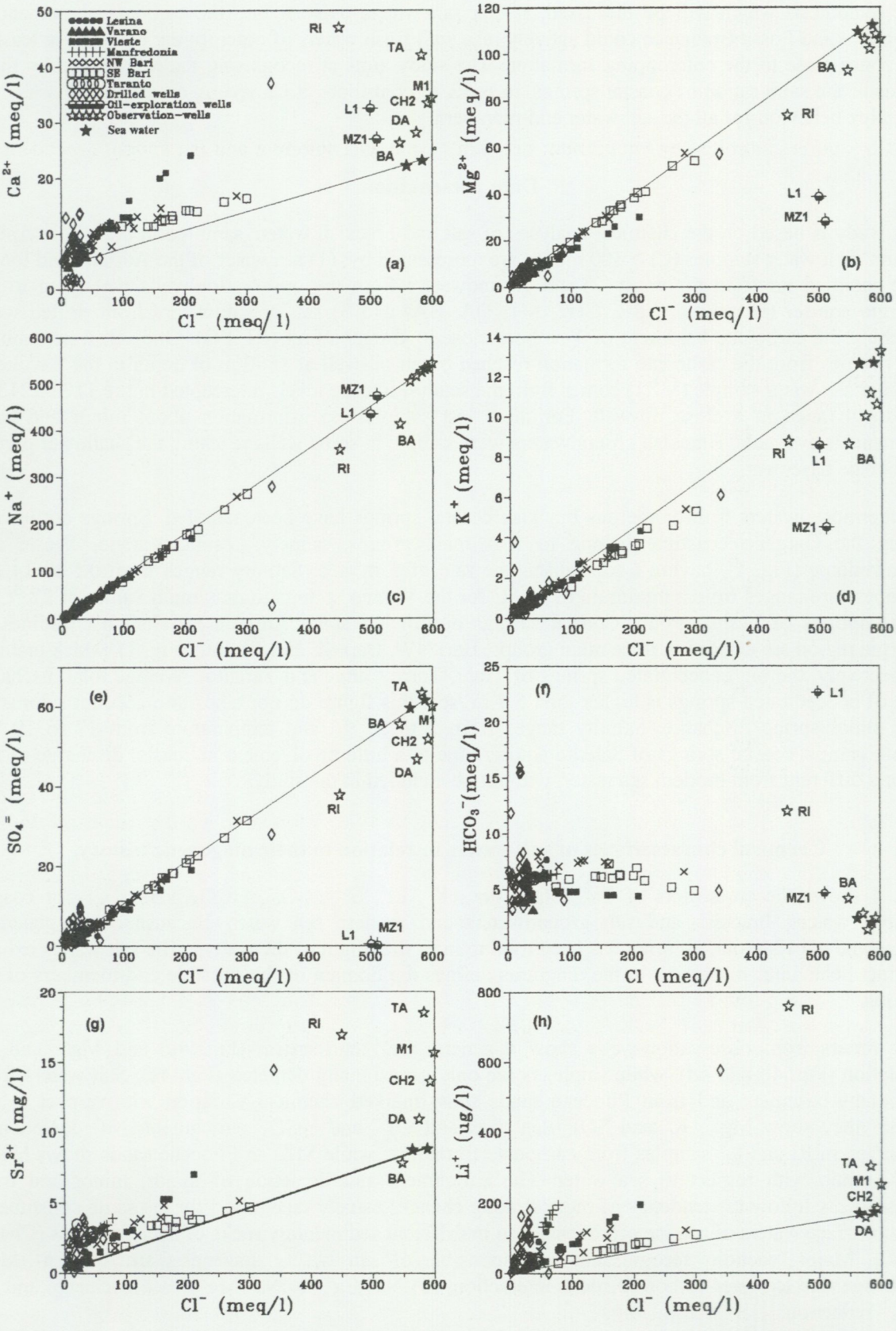


Fig. 4 - Cross - plots of Ca^{2+}, Mg^{2+}, Na^{+}, K^{+}, $SO_4^{=}$, HCO_3^{-} concentrations versus Cl^{-} contents for the coastal spring waters, brackish and salt groundwaters, and sea water. Lines stand for fresh water-sea water conservative mixing.

precipitation (Tulipano & Fidelibus, 1984, Fidelibus & Tulipano, 1986). Ca^{2+}-Mg^{2+} exchange reaction (dolomitisation) has been reported as cause of Mg/Ca ratio decrease in salt waters of ancient carbonate basins (Land, 1987): progressive decrease of Mg/Ca ratio was observed according to increasing age of aquifer rocks. The same reactions can also take place in brackish conditions (Folk & Land, 1975, Hanshaw et al., 1971, Matthews, 1971, Magaritz et al., 1980). Land (1987) stated that the decrease of Mg/Ca ratio is controlled by equilibrium between calcite and dolomite and is strongly dependent on temperature.

Sulphate reduction clearly affects salt waters of CH2, DA and RI wells. The average SO_4^{2-} /Cl ratio (Fig. 4e) of modern sea water is 0.1, while in subsurface waters of ancient basins it rarely exceeds 0.07 (Chave, 1960): according to this values, old salt waters of L1 and MZ1 oil-exploration wells have very low sulphate concentration, respectively of 20 and 4 mg/l. SO_4^{2-} can be reduced by anaerobic bacteria at temperatures lower than 80°C, while thermo-chemical reduction prevails at higher temperatures. In these processes CO_2 and H_2S are produced: salt waters from Tavoliere basement near Candelaro fault (RI) show very high bicarbonate concentrations (Fig. 4f) and, in the same zone, recurring presence of H_2S is observed in connection to the highest temperatures. The reduction process can produce either high or lower pH, depending on conditions and materials involved. A reductive environment and a pH decrease should favour dissolution of carbonate minerals: this way sulphate reduction could be ascribed of further changes of Mg/Ca ratio.

The feasibility of Na^+-Ca^{2+} or Na^+-Mg^{2+} base exchange was demonstrated in the coastal carbonate aquifer of Garraf by Pascual & Custodio (1990). Nadler et. al (1980), following laboratory experiments, stated that small amounts (a few percent) of clay in the carbonate rocks could be sufficient to produce appreciable changes in Na^+, Ca^{2+} and Mg^{2+} concentrations in salt waters by base exchange. The wells BA and RI show in fact appreciable depletion of Na^+. Moreover, K^+ depletion is generally observed. MZ1 sample, from Pliocenic sands, shows the maximum depletion; in the same sample, as well as in the L1 sample from the upper part of the deep carbonate basement, very high depletion of Mg^{2+} is detected (Fig. 4b). K^+ and Mg^{2+} depletion can be probably put in connection with diagenetic conversion, due to compaction of buried sediments, respectively of montmorillonite to illite and kaolinite to chlorite: it would mean that the effect of processes taking place in the transgressive deposits surrounding carbonate reservoirs might be felt in adjacent formations. Pelitic or siltitic-argillaceous levels, sometime of appreciable thickness, have been found within the carbonate Apulian formation. Furthermore, *terra rossa*, originated by alterations of limestone and constituted mainly by kaolinite and enriched with iron and aluminium hydroxides, is disseminated in cavities and fractures of the whole carbonate platform. A few stratigraphies of wells drilled in the basement in the SE part of Fossa Bradanica show argillaceous materials in the fractures. This way clays can be considered as responsible of part of observed chemical variations.

Sr^{2+} and Li^+ are abundant in all analysed salt waters. Sr^{2+} content (normalised to 19.000 ppm of chloride) in sea water is of 7 to 8 ppm, while salt waters show higher normalised values (maximum 19 ppm). Sr/Cl ratio in subsurface waters of ancient basins is always higher than that of modern sea water: however, the increase in strontium is sometimes higher than could be justified by dissolution of carbonate, unless, as observed in fresh karst groundwater (Tulipano et al., 1990), strontium concentration rises in liquid phase at each dissolution-precipitation cycle, owing to incongruent dissolution of strontium-rich skeletal aragonite.

Lithium is commonly enriched in sampled salt waters: RI sample shows lithium enriched up to 700% with respect to sea water. A very low Li/Cl weight ratio ($\cong 10^{-6}$) characterises modern sea waters, while in many oil-field waters the ratio increases up to the value of 10^{-3}. Lithium cannot enter the lattice structure of the minerals of other alkali-metals, thus its presence in carbonate can only be linked to clay fraction. Clay minerals selectively remove lithium from natural waters, becoming lithium-enriched: however lithium is unstable in the lattice structure due to its charge. A small rise in temperature is enough to cause lithium to leave the mineral: a very small difference in temperature at which the rock-water interaction takes place brings about an increase of lithium content in water of a factor of 100 to

10.000 times, allowing to consider lithium an useful pathfinder in hydrogeochemical exploration of hydrothermal systems (Brondi et al., 1973). Contents in thermal waters are in fact extremely high: 1000 ppb are normal for thermal springs, reaching 10 ppm as well. Besides temperature, other processes are likely to produce an increase of lithium content in groundwaters of sedimentary basins: for instance, laboratory experiments (Kharaka et al., 1973) indicated that, under compaction, the filtering through clays, acting as semi-permeable membranes, could produce squeezed fluids selectively richer in lithium than hyper-filtrate solutions, being lithium the species which passes preferentially with respect to the other monovalent and divalent cations.

The significance of chemical diagenesis seems roughly in relation with the increasing sampling depth and/or the temperature: salt waters in the carbonate basement or in the transgressive deposits surrounding carbonate formations show the more remarkable modifications.

Recognition of salt water component in brackish spring waters

Concentrations of major, minor and trace constituents were measured in coastal spring waters and compared with those in modern sea water, brackish and salt groundwaters. As shown in Fig. 4. the cross-plots of Ca^{2+}, Li^{+}, Sr^{2+} versus Cl^{-} yield data arrays which fall above the Ca-Cl, Li-Cl and Sr-Cl trends expected for waters derived from dilution of sea water. Cross-plots of Mg^{2+}, Na^{+}, K^{+}, $SO_4^{=}$ versus Cl^{-} show data arrays which fall under or on the respective dilution trends. The more diluted spring waters can barely be observed at the scale of the graphs: however, a distinct behaviour can be noticed for the springs of high salinity, belonging to two different data arrays, roughly identifying the Gargano and Murgia springs. For sake of clarity the springs pertaining to the two hydrogeological units will be discussed separately.

Gargano springs follow a general trend which inclines to RI water characteristics. Enrichment and depletion calculated for major, minor and trace constituents with respect to concentrations determined by conservative mixing were considered meaningful when higher than respective analytical error. The deficits and the excesses, expressed as $\Delta ion = C_m - C_{ex}$ (C_m = measured concentration and C_{ex} = concentration expected by fresh water-sea water conservative mixing) are shown in Fig. 5a and 5c: data are ordered, within each spring group, according to increasing TDS. Almost all springs show changes in major constituents (Fig. 5a) in the same direction of the modifications observed in the salt water sampled in the carbonate basement (RI well) and the changes appear to be, in general, and within each group, in accordance with salt content increase. Δions of the more diluted spring waters are not easily decipherable: at very low salinity, oscillation of the concentration of the real fresh end-member with respect to the chosen one, prevails on the effect of mixing; moreover Δions include the effects of water-rock interaction processes brought into action by mixing. This way the salt water component of Varano Lake springs, due to very low salinity, cannot be easily outlined: Δ values of most elements are only slightly higher than analytical error. However, the tracing effect of a salt end-member deeply modified predominates at higher salinity. In Fig. 5c lithium and strontium excesses rise according to the salinity increase within each group (with the exception of some springs of Lesina group); however, lithium highest enrichment is observed in some Lesina and Manfredonia spring waters, having a lower salinity with respect to Vieste springs. Temperature variations are in accordance with lithium changes.

Murgia spring waters show less remarkable ion enrichment and depletion with respect to those observed in Gargano (Fig. 5b and 5d): Δ values are shown following the geographical order, going from NW Bari to Taranto. Several Δion were not considered, since of the same order of related analytical error. The Bari SE group shows very light depletion in magnesium and sulphates, being calcium enrichment practically constant while salinity markedly varies; the same occurs for lithium and strontium excesses. On the contrary, the Bari NW and Taranto spring groups show calcium excess and sodium depletion in accordance with salinity variations: lithium and strontium follow salinity as well. The Bari NW group evolves from NW to SE showing, in the central springs, the most remarkable effects of an altered salt water; Taranto springs show enhancement of the ion excess and depletion

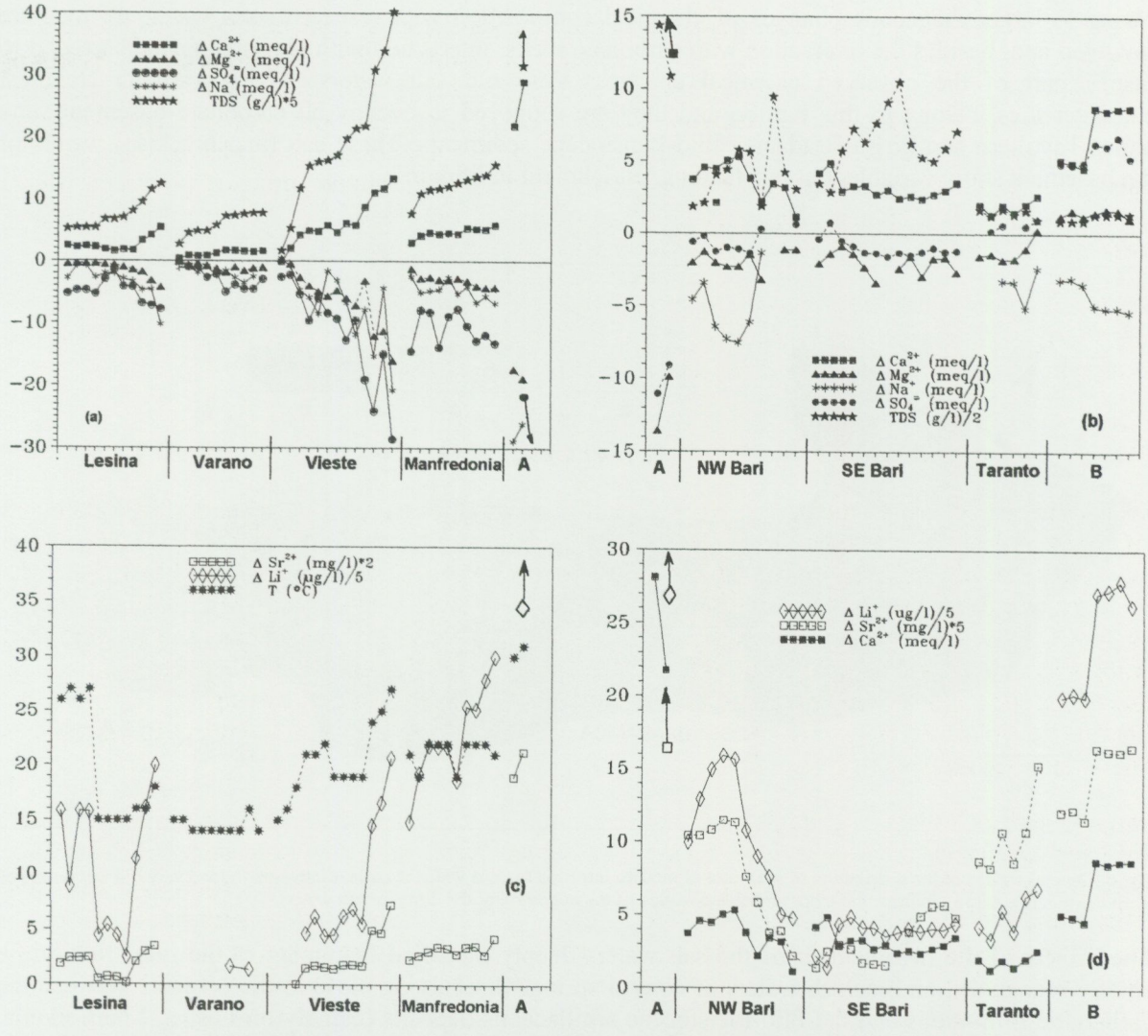


Fig. 5. Enrichment and depletion related to major (a) and minor constituents (c) for coastal spring waters of Gargano Promontory with respect to conservative mixing between fresh and sea water (zero line); data are ordered within each spring group according to TDS increase; A: salt waters of RI well. - (b) and (d) refer respectively to enrichment and depletion of major and minor constituents for coastal spring waters of Murgia aquifer; data are shown in geographical order; B: brackish waters of drilled wells of carbonate basement of Fossa Bradanica.

approaching to the Fossa Bradanica border. In Figs. 5b a 5d the first two samples represent the salt waters sampled in the basement of Tavoliere, while the last seven samples represent brackish waters sampled in the basement of Fossa Bradanica: both groups of waters show an outstanding excess of lithium and diagenetic modifications amplified with respect to those observed in the NW Bari and Taranto spring groups.

Conclusions

Some conclusions can be drawn on the basis of chemical data interpretation. The whole Apulia territory hosts different types of salt waters which can be grouped in three broad families. The first family includes sea water of recent intrusion which is recognised in limited coastal areas of the carbonate aquifers (Fig. 6). The second family gathers the salt waters of ancient intrusion which diagenesis developed essentially in a carbonate environment: mainly calcium, magnesium and strontium concentrations turn out modified with respect to sea water, due to water-rock interaction, roughly being Mg/Ca ratio decrease and strontium enrichment in connection with increasing residence times: this family should occupy a great part of the Murgia aquifer and, even if not directly recognised, in Fig. 6 its presence is outlined also in its central part. The third family differentiates from the second

owing to larger diagenetic changes of chemical composition with respect to sea water: all ions are involved and, besides the interaction with carbonate rocks, interaction with clay sediments is needed to justify part of the observed chemical changes. Very old salt waters, having variable chemical characteristics, belong to this family, and they are supposed to occupy all carbonate basement sunk under Tavoliere and Fossa Bradanica Plio-Pleistocene sediments. These salt (and brackish) waters of the basement show variable, but outstanding, enrichment in lithium.

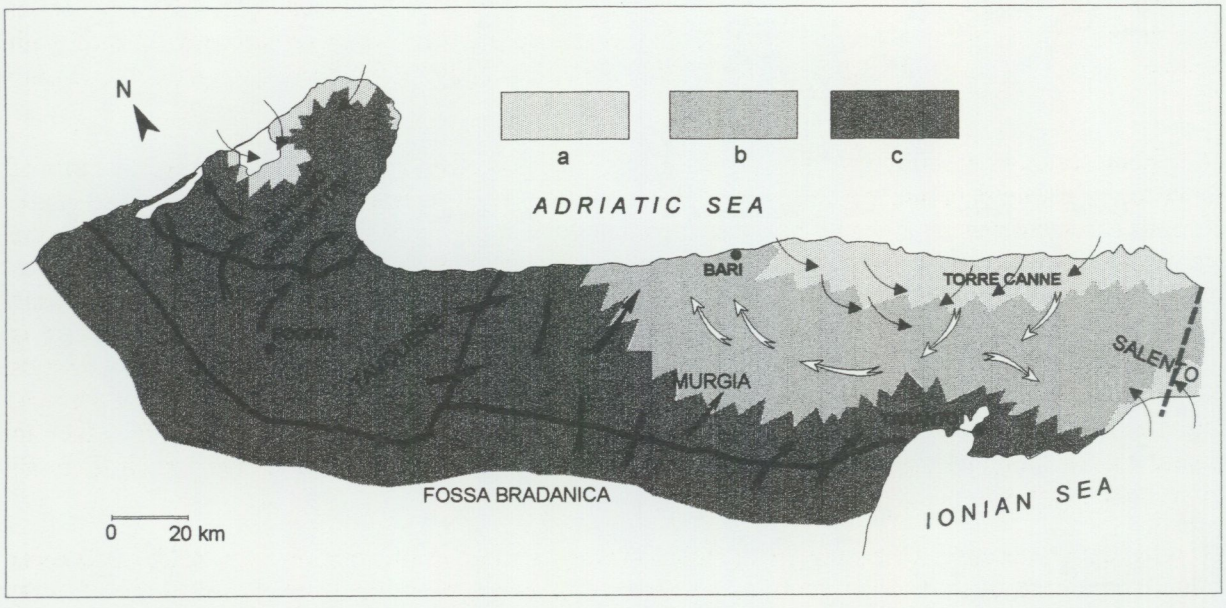


Fig. 6. General outline of the distribution of sea water of modern intrusion (a), sea water of ancient intrusion (b) and very old salt waters of marine origin (c). Arrows indicate the more probable direction of the migration of the different salt waters.

The effects of the involvement of the salt waters deeply modified belonging to the third family are chiefly recognised on brackish waters of coastal springs discharging close to the contacts between the carbonatic formations and the Plio-Pleistocene argillaceous deposits (namely on Lesina, Manfredonia, NW Bari and Taranto spring groups). If only slight, but significant, differences on the characteristics of salt water component are recognised as far as major constituents are concerned, when lithium excesses are evaluated, a more clear distinction of the different situations is obtained.

At the contact between Gargano and Tavoliere, along Candelaro fault, outstanding and localised increases of geothermal gradient (up to 10 °C/100 m) have been recognised by numerous investigations. Part of Lesina and all Manfredonia springs show a remarkable enrichment in lithium, according to the temperatures of the spring waters (of 27 °C maximum): this can be explained by the influence of convective upward flows, rising through the tectonic fault, which convey towards spring discharge deep salt waters enriched in lithium. The influence of these upward flows is not recognised in the Varano lake springs, which are probably slightly salinised due to direct sea water intrusion. Even though the salt water component of Vieste springs, which locate far from the fault, could be considered deeply modified by major chemical data, it is not marked by high lithium excess: this should mean that salt waters present in Vieste brackish springs do not come from the basement, being their diagenetic environment closer to the discharge zones.

NW Bari springs show the clear mark of a salt water similar, as diagenetic modifications on major constituents are concerned, to that involved in the Gargano springs: lithium enrichments are here, in absence of geothermal anomalies, in accordance with total salt increase, indicating an homogeneous old salt end-member to be involved in spring discharge. Approaching Bari town, due to the increasing influence of recent intruded or slightly modified sea water, a progressive decrease of the lithium effect is noticed.

At the contact between Murgia carbonate formation and Fossa Bradanica sediments, high lithium excesses are found in the brackish water of the basement and, in minor extent, in Taranto spring waters. No information about deep salt waters of the zone is available. Extrapolation of the characteristics of analysed brackish waters to a higher salinity, leads to a salt end-member of Ca-Cl-SO_4 type. The possible existence of this type of salt water should be in accordance with the findings of geological exploration drillings which found thick Messinian gypsum strata on the top of carbonate basement in the Fossa Bradanica: these evaporite deposits should be able to originate Ca-Cl-SO_4 brines. As far as the brackish waters of the basement are concerned, they are naturally involved in the groundwater circulation of this part of Murgia aquifer, due to the accordance of their piezometric heads with regional piezometric trend, indicating the natural discharge of the groundwater towards the Taranto Gulf.

A hypothesis about mobility and flow direction of deep salt waters can be put forward on the basis of both the available data and the following considerations. When interpreting the characteristics of the various basement waters, it should be considered that thick argillaceous deposits are in contact with the carbonate basement rocks. In a sedimentary basin it can be assumed that the compaction of argillaceous sediments is the principal cause for flows which, in the course of geological periods, can move large quantities of water. The existence of such flows, caused by compaction in recent sedimentary basins, is evidenced, for instance, by the presence of super hydrostatic pressures in formation waters of sands surrounded by layers of clay. So, in the Plio-Pleistocenic deposits of Tavoliere and Fossa Bradanica, compaction could be challenged for arising flow of interstitial solutions, which, due to intercommunicating porosity, could penetrate through the sedimentary rocks and thus participate in all diagenetic processes.

Besides the compaction by simple gravitational loading, a more drastic compression of the sediments can be produced by horizontal compressive stresses of tectonic origin: Hubbert and Rubey (1959) stated that water-filled clays or shales would respond to deformational stresses by an increase of the fluid pressures. Some geological evidences indicate that a tectonic compression, owing to the convergence of thrust sheets of Apennine towards foreland and having direction from W to E, could originate over-pressures in Fossa Bradanica and Tavoliere basins. This would cause the migration of deep fluids which should be forced to rise, emerging as springs, or could be expelled towards permeable sediments of the foreland basin and platform.

As previously discussed, squezeed interstitial solutions would be highly enriched in lithium: this occurrence could explain high lithium excesses in basement waters also in absence of geothermal anomalies; moreover, even if based on a few chemical data, it can be outlined that the salt waters coming from oil-exploration wells drilled in different formations seem to have been subject to very similar diagenesis.

The fact itself that very old salt end-members reach the coastal discharge indicates that these waters are moving, though their migration velocity should be very low. As an example, $6 * 10^6$ m^3 of old salt water are outflowing per year through the Trani and Taranto springs. These volumes must be replaced by other salt water, which, owing to the particular characteristics, can only come from contact areas. An hypothesis about regional circulation has been outlined in Fig. 6: this circulation has to be intended in the wider sense, owing to the fact that migration velocity is very slow, probably of the order of a few centimetres per year, as calculated hypothesising the flow through a broad section contact between Murgia and Plio-Pleistocene sediments.

We do not pretend to have fully understood this huge system, most of which is inaccessible, and conclude our remarks with the recommendation that more data are surely needed to reach reliable conclusions.

REFERENCES

BRONDI, M., DALL'AGLIO, M. & VITRANI, F., 1973: Lithium as pathfinder element in the large scale hydrochemical exploration for hydrothermal systems. Geothermics, 2:3, pp. 142-153.

CHAVE, K. E., 1960: Evidence of History of Sea Water from Chemistry of Deeper Subsurface Waters of Ancient Basins. Bull. Amer. Assoc. Petrol. Geol., 44:3, pp. 357-370.

COTECCHIA, V. & MAGRI, G., 1966: Idrogeologia del Gargano. Geol. Appl. e Idrog., I, pp. 1-86.

FIDELIBUS, M. D., 1992: Origine ed evoluzione delle acque salate sotterranee della Murgia Nord-Occidentale e del Gargano - Atti del II Conv. Naz. dei Giovani Ricercatori di Geol. Appl., Viterbo, 1992. Geologica Romana, XXX, pp. 439-449.

FIDELIBUS, M. D. & TULIPANO, L., 1986: Mixing phenomena owing to sea water intrusion for the interpretation of chemical and isotopic data of discharge waters in the Apulian coastal carbonate aquifer (Southern Italy). Proc. of 9th SWIM, 1986, Delft, Boekelman R.H. & al. (Eds), Water Management Group, Department of Civil Engineering, Delft, The Netherlands, pp. 591-600.

FIDELIBUS, M. D. & TULIPANO, L, 1990: Major and minor ions as natural tracers in mixing phenomena in coastal carbonate aquifers of Apulia. Proc. of 11th SWIM, 1990, Gdansk, Kozerski B. & Sadurski A. (Eds.), Technical University of Gdansk, Department of Hydrogeology and Water Supply, Gdansk, Poland, pp. 283-293.

FOLK, R. L. & LAND, L. S., 1975: Mg/Ca ratio and Salinity: two controls over Crystallisation of Dolomite. Bull. of Am. Assoc. Petrol. Geol., 59, pp. 60-68.

HANSHAW, B. B., BACK, W. & DEIKE, R. G., 1971: A geochemical hypothesis for dolomitization by groundwater. Economic Geology, 66, pp. 710-724.

HUBBERT, M. K. & RUBEY, W. W., 1959: Role of fluid pressure in mechanics of overthrust faulting. Bull. of the Geol. Soc. of America, 70, pp. 115-166.

KHARAKA, Y. K. & BERRY, F. A. F., 1973: Simultaneous flow of water and solutes through geological membranes - I. Experimental investigation. Geoch.. et Cosmoch.. Acta, 37, pp. 2577-2603.

LAND, L. S., 1987. The major ion chemistry of saline brines in sedimentary basins. In J. R. Banavar, J. Koplik & Winkler W. (eds), Physics and Chemistry of Porous media II, Riegfield, Conn., American Institute of Physics Conference Proceedings, 154, pp. 160-179.

MAGARITZ, M., GOLDENBERG., L., KAFRI U. & ARAD A., 1980: Dolomite formation in the seawater-freshwater interface. Nature, 287: 5783, pp. 622-624.

MATTHEWS, R. K., 1971: Diagenetic environments of possible importance to the explanation of cementation fabrics in subaerially exposed carbonate sediments. In O. P. Bricker (ed.), Carbonate Cements, The Johns Hopkins University Studies in Geology, 19, John Hopkins Press, pp. 127-132.

NADLER, A., MAGARITZ, M. & MAZOR, E., 1980: Chemical reactions of seawater with rocks and freshwater: experimental and field observations on brackish waters in Israel. Geoch. et Cosmoch. Acta, 44, pp. 879-886.

TULIPANO L., COTECCHIA V. & FIDELIBUS M. D., 1990: An example of multitracing approach in studies of karstic and coastal aquifers. Proc. of Int. Symp. and Field Seminar on Hydrogeological Processes in Karst Terranes, Gunay G., Johnson A. I. & Back W. (Eds.), IAHS Publ. No. 207, pp. 381-390. Antalya 90

TULIPANO, L. & FIDELIBUS, M. D., 1984: Geochemical characteristics of Apulian coastal springs (Southern Italy). Proc. of 5th Int. Conf. on Water Resources Planning and Management, Athens, 1984, G. Tsakiris (Ed.), Div. of Water Resources, Nat. Tech. University of Athens, pp. 2.55-2.67.

WHITE, D. E., 1957: Magmatic, connate and metamorphic waters. Geol. Soc. America Bull., 68, pp. 1659-1682.

The combination of the Stuyfzand-classification and Fuzzy C-Means clustering in a Hydrogeochemical System Analysis of the IJssel valley, The Netherlands (a case study)

S.J.A. van Baalen
Institute for Inland Water management and Waste Water Treatment (RIZA), P.O. box 17, 8200 AA Lelystad, The Netherlands

J.C. de Ruiter
Drinking Water Company of Overijssel (WMO), P.O. box 10005, 8000 GA Zwolle, The Netherlands

In the eastern part of The Netherlands problems arise with the production of good quality drinking water because of upconing relict salt water underlying the deep fresh water aquifer.
Instead of making a laborious hydrological modelling, we choose to make a hydrogeochemical system analysis on a regional scale. Based on the results of this analysis, a decision on the necessity of a more detailed hydrological modelling could be made.
The objective of the hydrogeochemical system analysis is to find and characterize, using a qualitative analysis, different types of groundwater and their origin. Classification of water types is the main theme. This classification was made by means of the Fuzzy C-Means clustering and Non-Linear Mapping, in combination with the classification of water types according to Stuyfzand [13,14].
With the results of the classification, the regional pattern of groundwater quality could be described very well, and the cause of the salinization could be determined.
*The use of **FCM in combination with the Stuyfzand-classification** is very much recommended for the analysis of hydrochemical data, as these methods make it possible to get a good and interpretable picture of a complex matter such as chemical analyses scattered over many dimensions.*

Introduction

A hydrological system analysis, as described by Engelen & Jones [6], is an excellent way for getting insight into a regional hydrological system. The main aim of a hydrological system analysis is the mapping of nested groundwater flow systems of different orders, each connecting a recharge area with one or more discharge areas. When executing a hydrological system analysis, different kinds of interrelated data are used, such as geological (formations, sedimentology), (geo)hydrological (properties, flow patterns), topographical (surface levels, landuse), geochemical (soil) and hydrochemical (groundwater) data.

In the present study, the emphasis is on geohydrochemical interpretation. The problem with hydrochemical data however, is how to describe the properties of one sample point in a simple but meaningful way. Matthes [9] distinguishes about 10 different ways that can be used for solving this problem. However, as pointed out by Stuyfzand [15], each method is intended for a specific purpose and has its own merits, but all of them lack a more "holistic view on water quality". Therefore Stuyfzand [13, 14, 15] developed a procedure to map and diagnose the major factors accounting for regional variations in the hydrochemistry. In this procedure, a classification system to determine water types plays an important role.

An alternative way of classifying water samples is to make use of statistical methods. If any *a priori* knowledge of the processes responsable for the inhomogenity of the dataset is known, conventional multivariate statistics like discriminant function analysis can be used [4, 20, 21]. When there is no such *a priori* knowledge, conventional cluster techniques are commonly used to reorganize the data set into homogeneous groups, which can only be interpreted afterwards [8, 20, 21].

Both discriminant function analysis and conventional cluster techniques have the disadvantage of being rigid, i.e. they assign a sample unambiguously to a group or cluster [8]. However, the spatial variation in hydrochemical data is usually gradual instead of abrupt. Therefore, some overlap between groups is needed to describe the hydrochemical pattern in a sufficient way. A method using fuzzy or continuous classes is thus more appropriate, as it allows overlap between classes [1, 5, 20].

In this paper, we make a comparison between the classification system proposed by Stuyfzand [13, 14, 15] and the Fuzzy C-Means clustering in combination with Non-Linear Mapping used by Vriend et al. [20] and Frapporti et al. [8]. It is not our intention to qualify one of these methods as best, but we want to show how these methods can supplement each other to get a better result than with either single method.
After a brief introduction into the theoretical background of the two methods, a case study in the eastern part of The Netherlands is used to show the applicability of this combination. In the end, some general conclusions will be drawn.

Theoretical Background

In this paper we only summarize the relevant information of both methods. A complete overview is found in the original publications and the handbooks mentioned in the list of references [1, 5, 8, 13, 14, 15, 20].

The classification of water types according to Stuyfzand [13,14]
The classification system combines four essential aspects in a logical code (see Figure 1): the chlorinity (main type), alkalinity (type), most important cation and anion (subtype) and a base exchange index (class). By calculating these four aspects of a certain water sample, the water type is determined in a hierarchical way.

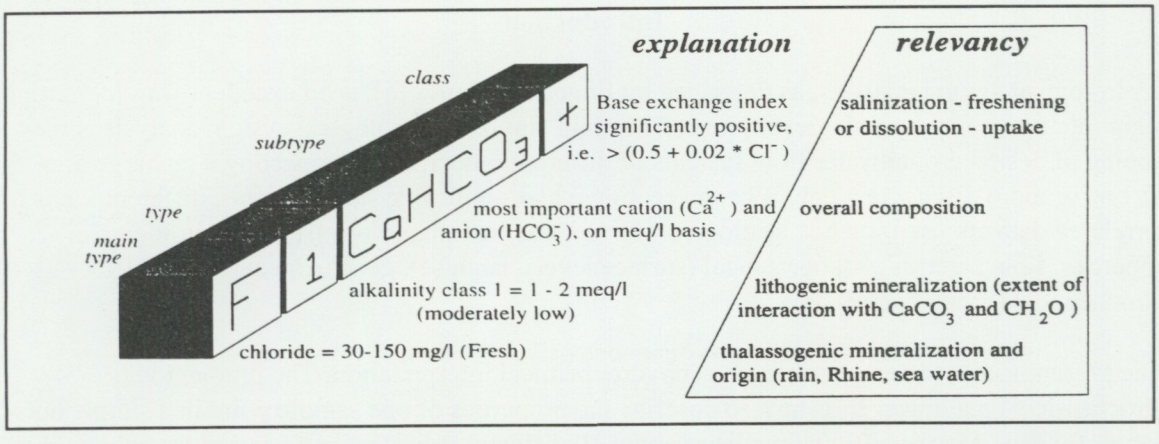


Figure 1: *The hydrochemical classification system of water types by Stuyfzand [14], with its coding in 9 positions. The example is called "a fresh, moderately low alkalinity, calciumbicarbonate water with a positive base exchange index" [15]*

The main advantage of this classification system is that diagnosis of different chemical processes is possible and that the resulting water type of a sample is always the same, because of the predetermined boundaries. Its differentiating power is however in principle always the same, because of those predetermined boundaries. Stuyfzand recognizes the stiffness of the classification system and proposes ways to associate or differentiate within the system. Association takes place by combining two or more main types or by leaving away class and/or subtype. Differentiation can be done by dividing some levels in a more subtle way or by adding new parameters. This flexibilisation however, is still based on presuppositions.

The Fuzzy C-Means clustering in combination with Non-Linear Mapping [8, 20]
This clustering is a powerful tool for separating datasets in homogeneous groups, without any *a priori* knowledge. The technique allows some vagueness in the description of the cluster model. Likeness or similarity of a sample with a cluster group is indicated by a continuous function (membership) between zero (completely different) and one (exactly the same). The memberships of a case to all clusters sum up to 1. Hence, it is possible for a sample to "belong" to more than one cluster, which allows some flexibility in the interpretation of the data set. This flexibility is an important difference with so-called "hard" statistical techniques.
An important issue in executing this clustering is the choice of the number of clusters. Several runs [19] are made, each time with a different number of clusters. A definite choice is based on various criteria. In the present study, our criteria were based on the regional distribution, the hydrochemical interpretability and the "structure" as displayed in a two-dimensional image made by Non-Linear Mapping [8].
The Non-Linear Mapping determines a 2- or 3-dimensional image of a X-dimensional data cloud, such that the interdata distances are minimally distorted [20].
Although the compositional overlap of the different cluster groups is an advantage while interpreting the results, for presentational purposes some "hardening" of the clustering is needed. This "defuzzication" takes place based on the criterium that a sample point is assigned to a certain cluster if the highest membership of that case is 1.67 times higher than the one-highest membership.

Comparison of the Stuyfzand-classification and the Fuzzy C-Means clustering.
As with all classification systems, both methods have their advantages and disadvantages.
With regard to the Stuyfzand-classification and the Fuzzy C-Means clustering, the following can be said.
The advantage of the **Stuyfzand-classification** is that the resulting water type of a sample is always the same because of the predetermined boundaries and that diagnosis of different chemical processes is possible. Its main disadvantage is its stiffness, because of these predetermined boundaries.
The advantage of **Fuzzy C-Means clustering** is that it makes homogeneous groups within the dataset without *a priori* knowledge, while the differences between the groups are relevant for the specific data set. This means that the cluster groups are sometimes coarser and sometimes finer than the water types found by the classification. The main disadvantage of the clustering method is its lack of direct interpretability and its dependency of the specific data set; cluster groups of different data sets are not comparable with each other.

By means of the following case study, we will show that both methods supplement each other, thus taking away the disadvantages of each single method while keeping the advantages of both.

Case Study: Hydrogeochemical System Analysis of the IJssel valley, The Netherlands

Introduction
The Drinking Water Company of Overijssel (WMO) is active in the eastern part of The Netherlands. Recently it took over a groundwater extraction site in the city of Deventer. This site has problems with an increasing chloride-content in the collected water. For example, in the period 1970 to 1993, the chloride-content rose on average from 86 mg/l to 117 mg/l.
In order to find a new, optimal structure of the well field, the WMO wanted to know more about:
- the position of the well field in the regional hydrological system
- the processes that are responsible for the increasing salinization of the well field

We decided to do a regional hydrogeochemical system analysis, with the emphasis on geology, (geo)hydrology and hydrochemistry. Geological and hydrological data were found in literature [3, 7, 10, 11, 12, 16, 17, 18, 22]. It should be mentioned, that in this study no hydrological modelling has

been done. However, one of the results of the study is a list of boundary conditions that can be used in an eventual hydrological modelling of the area.
The hydrochemical data used in this study were mostly existing data, with which we wanted to do a qualitative analysis, with classification of water types as the main theme.

Study Area
The study area is located around the city of Deventer, measuring some 32 km from west to east and 40 km from north to south. It comprises the valley of the river IJssel in between the city of Zwolle in the north and the city of Zutphen in the south. The west- and east-borders are formed by two ice-pushed ridges, respectively the Veluwe and the Sallandse Heuvelrug (see Figure 2). These ridges form the borders of the regional groundwater system of the IJssel valley.

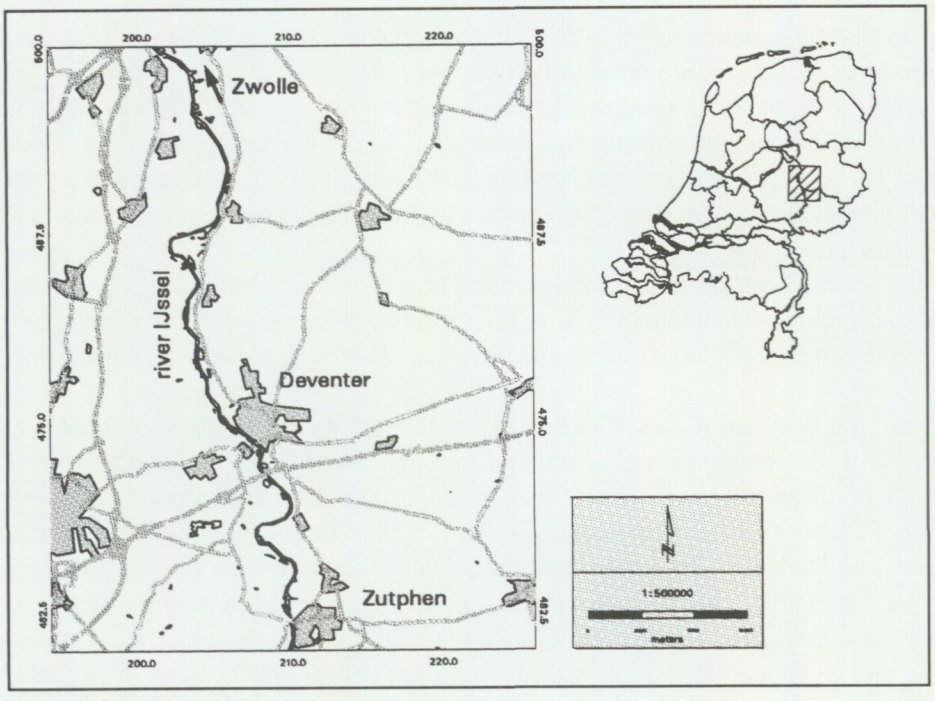


Figure 2: *Location of the study area*

Geology
In the study area, the formations containing the drinking water consist of late-Tertiary and early-Quaternary sediments (Figure 3). The older, deepest formations contain brakish-salt water; the younger formations contain fresh water.
The IJssel valley was formed during the Saale-ice age, in which the ice in The Netherlands reached its outmost extension. An ice-tongue made its way down south through the study area, pushing aside the Tertiary and Quaternary sediments. It so formed an up to 120 m deep basin, flanked by ice-pushed ridges of some 100 m. When the ice regressed, the basin filled with water. In this glacial lake, a thick packet of fluvioglacial material (basin-clay) sedimented. These sediments were during the late-Quaternary covered by fluvial and eolian deposits.

(Geo)hydrology
The two ice-pushed-ridges serve as infiltration areas while the basin-clay forms the principal division between shallow and deep aquifers in the IJssel valley. There is almost no exchange between the shallow groundwater, which is influenced by man and river, and the very old (up to 20.000 years), deep groundwater. Under the city of Deventer the division between fresh and salt water (150 mg/l Cl^-) is found at approximately 130 m below sea-level.

In this study, the main focus was on the deep groundwater, as there is relatively little known about it and because its importance as a source of drinking water.

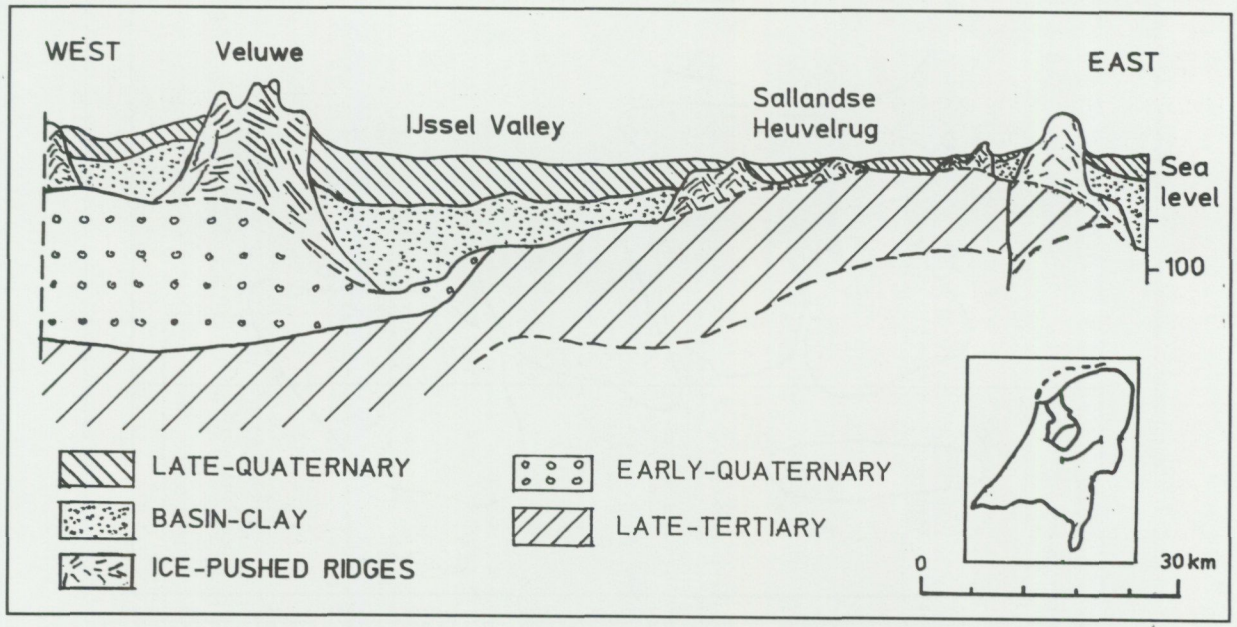


Figure 3: *Geological cross section from west to east across the IJssel valley [after 11]*

Methods of investigation

As mentioned in the introduction, we mainly used existing data. So as in the previous section is described, information about the geology and (geo)hydrology was obtained from literature. The necessary hydrochemical data were collected from the On Line Groundwater Archive (OLGA), operated by TNO-GG, and from internal WMO-archives.

The following criteria have been used by the selection of the data:

- data used should not have been collected before 1970
- analyses should contain at least Na^+, Cl^-, Ca^{2+}, HCO_3^-, Mg^{2+}, SO_4^{2-}, Fe^{2+}, NO_3^{2-}, pH and EC
- only data from monitoring wells with at least one filter below 50 m -N.A.P. (= the minimal depth of the lower side of the basin-clay formation) were used

This selection resulted in a data set of 189 analyses. 17 New analyses were added to this, resulting in a total dataset of 206 analyses located at 33 sites.

The water type was calculated using the program *ChemProc v.4.0* [2]. The clustering was executed using the program *FNX* [19].

Results and discussion

In this study, all elements apart from pH, which is intrinsically logarithmic, were lognormally distributed and therefore logarithmically transformed. Three samples were left out of the analysis, because there were indications that they were unreliable. The clustering may in principle be executed with an unlimited number of parameters, but the result is not always better when using a lot of parameters because of possible correlation between two or more parameters. The parameters ultimately chosen for the clustering were Na^+, Cl^-, Ca^{2+}, HCO_3^-, Mg^{2+}, pH and K^+. They had the highest segregational power. A seven-cluster model appeared best to describe the data set. Cluster centres of the fuzzy clusters and geometric means of the hardened clusters are given in Table 1. The clusters are arranged in order of chlorinity, i.e. cluster 1 has the lowest chlorinity and cluster 7 the highest. The Non-Linear Mapping plot in Figure 4 shows the consistency of the partitioning. The samples indicated by the number "10" are intermediate, i.e. they could not be hardened because of their low memberships.

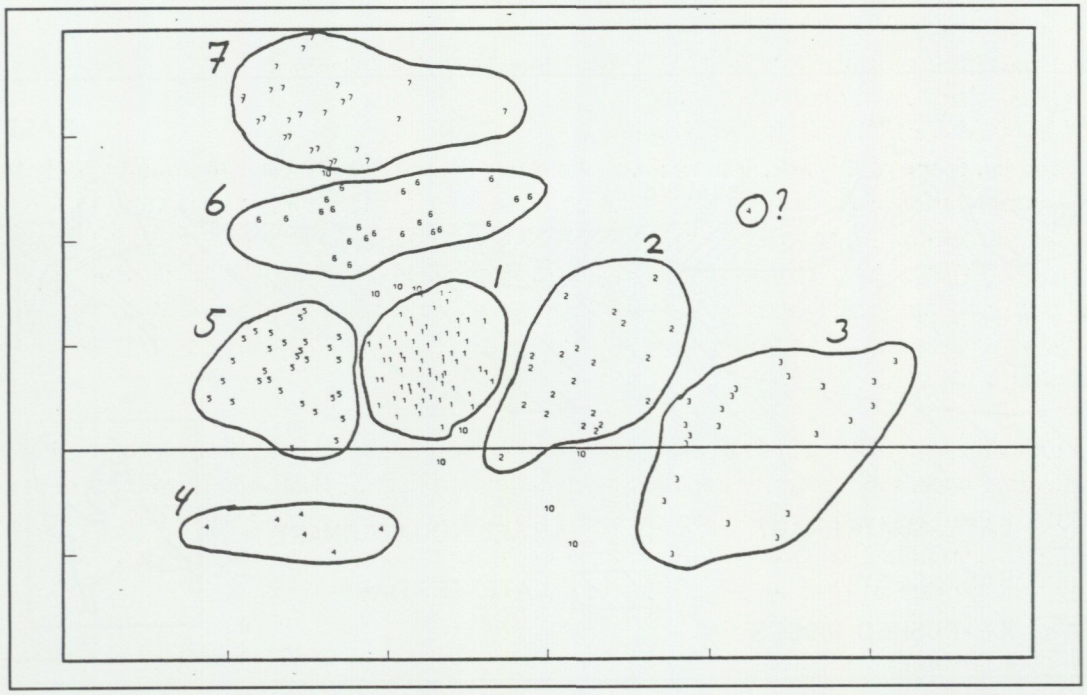


Figure 4: *Fuzzy C-Means classification represented in a Non-Linear Mapping plot. The numbers indicate the hardened cluster numbers.*

	Cluster 1 (n = 66)		Cluster 2 (n = 21)		Cluster 3 (n = 21)		Cluster 4 (n = 7)	
Variable	CC	GM	CC	GM	CC	GM	CC	GM
Na^+	21.5	23.5	14.9	17.9	11.8	30.9	20.5	52.7
Cl^-	13.5	16.3	13.6	13.7	16.3	46.9	25.4	32.1
Ca^{2+}	36.3	36.8	15.4	15.4	9.2	10.8	51.0	54.0
HCO_3^-	169.8	172.9	66.7	74.4	14.8	14.7	210.6	269.7
Mg^{2+}	4.4	4.6	2.7	2.8	1.4	3.0	7.7	8.4
pH	7.7	7.7	7.1	7.3	6.4	6.3	7.5	7.5
K^+	2.6	3.1	1.5	1.6	1.1	1.5	0.0	0.0

	Cluster 5 (n = 30)		Cluster 6 (n = 23)		Cluster 7 (n = 26)	
Variable	CC	GM	CC	GM	CC	GM
Na^+	23.7	24.4	202.4	231.4	1152.0	1290.0
Cl^-	32.6	35.3	257.0	304.0	1822.9	2068.0
Ca^{2+}	87.8	92.5	28.0	30.7	37.9	50.4
HCO_3^-	262.6	277.6	258.4	276.6	391.0	397.0
Mg^{2+}	8.9	9.3	11.6	12.3	52.0	58.0
pH	7.3	7.3	7.9	7.9	8.0	8.0
K^+	1.9	2.3	16.4	17.6	50.3	53.0

Table 1: *Cluster centers (CC) of the fuzzy clusters and geometric means (GM) of the hardened clusters for the adopted cluster model. Nine samples could not be hardened. The differences between the CC's and the CM's are a result of the effect of outliers (samples with a low membership). In calculating the CC, membership is used as weighing factor, so the effect of outliers on the CC is less than on the GM. All variables are expressed in mg/l, except pH. The total number of samples is 194 (206 minus 3 unreliable samples and 9 intermediate samples).*

A description of the clusters was made in several ways, using:

- several statistical parameters for every cluster (geometric mean, median, quartiles, minimum and maximum)
- Stiff-diagrams for the samples with the highest membership for every cluster
- the spatial distribution for every cluster
- the Stuyfzand-classification for all samples

It is beyond the scope of this article to evaluate the water type of every cluster thoroughly, only the ultimate interpretation is given. This interpretation is based on the foregoing descriptions together with information from literature. Next to the interpretation of every cluster, the spatial distribution pattern of the different clusters had to be determined. Horizontal sections at different depths and vertical cross-sections were constructed. In drawing the boundaries between the clusters, the memberships of all samples were used, together with geological data and hydrological (model)results from literature.

Table 2 gives for every cluster a short description of the interpretation of the water type, together with the dominating water type, according to the Stuyfzand-classification. This table shows that in the present study the combination of the two methods results in an association of water types according to the Stuyfzand-classification. Every cluster comprises one or two water types according to the Stuyfzand-classification. Thus, an association of water types is executed without any *a priori* knowledge.

Cluster 1 comprises the water type g2-$CaHCO_3$+: a oligohaline (rainwaterlike), moderate alkalinity, calciumbicarbonate water with a low positive base exchange index. The water in this class is rain water, infiltrated at least some 2500 years ago [3]. As a result of a complex of soil forming processes (reduction of iron and sulfate, weathering of silicates, dissolution of calciumbicarbonate) this water has changed, but is still recognizable as Old Infiltrated (rain)water (OI).

Cluster 2 comprises the water types g1-$CaHCO_3$+ and g2-$NaHCO_3$+: oligohaline, moderately low alkalinity, calcium/natriumbicarbonate water with a low positive base exchange index. The water in this class is rain water, infiltrated between the present and some 2500 years ago [3]. Because of the very low amounts of macro-ions, this water is interpreted as Young Infiltrated (rain)water (YI).

Clusters 3 till 5 comprise a mixture of different water types, ranging from very poor to very rich water, but all with high amounts of nitrate and/or sulfate. The maximum sample depth is 70 m below sea level. Agricultural and surface water influences dominate these clusters. They are therefore all interpreted as Shallow, Man-influenced water (SM).

Cluster 6 comprises the water types f3-NaCl+ and B3-NaCl+/o: fresh-brackish to brackish, moderately high alkalinity, sodiumchloride water with variable base exchange indices. Under the city of Deventer, the lowest base exchange indices point at salinization. Just outside Deventer, the high base exchange indices in this water point at freshening. These samples are interpreted as Relict Brackish water (RB).

Cluster 7 comprises the water types b3/b4-NaClo: a brackish-salt, moderately high to high alkalinity, sodiumchloride water, with a very low base exchange index. The interpretation is Relict Salt water (RS) without any freshening or salinization.

Figure 5 shows an example of a profile, crossing the IJssel valley from west to east. In this figure, the different types of water are easily recognizable and it shows that the salinization is caused by upconing salt water.

When looking at Table 2 and Figure 5, the following conclusions can be drawn:

- by using hydrochemical data together with geological and (geo)hydrological data from literature, it was possible to create a well structured picture of the different kinds of water present in the deep aquifers of the IJssel valley
- the cause and extension of the salinization in the well fields of the city of Deventer are clearly visible in the horizontal and vertical sections

FCM-cluster	Interpretation	Description	Stuyfzand-classification
1	Old Infiltrated (rain)water (OI)	Water in deep aquifers, influenced by processes like reduction and calcite dissolution	g2-$CaHCO_3$+
2	Young Infiltrated (rain)water (YI)	Slightly altered rain water in infiltration areas, lying above type 1	g1-$CaHCO_3$+ g1-$NaHCO_3$+
3,4,5	Shallow, Man-influenced water (SM)	Water above the basin-clay, strongly influenced by surface water and agricultural activities	g*-CaMiClo, g*-CaMISo (3) F2-$CaHCO_3$o (4) g2-$CaHCO_3$+ (4) F3-$CaHCO_3$o/+ (5) g3-$CaHCO_3$+/o (5)
6	Relict Brackish water (RB)	Boundary zone between deep fresh water and marine salt water	f3-NaCl+ B3-NaCl+/o
7	Relict Salt water (RS)	Marine salt water, captured in Tertiary marine sediments	b3-NaClo b4-NaClo

Table 2: *Interpretation of the different clusters, together with a short description and the dominating water type according to the Stuyfzand-classification. Note that the water types according to the Stuyfzand-classification are all unique for one Fuzzy C-Means (FCM) cluster, except g2-$CaHCO_3$+.*

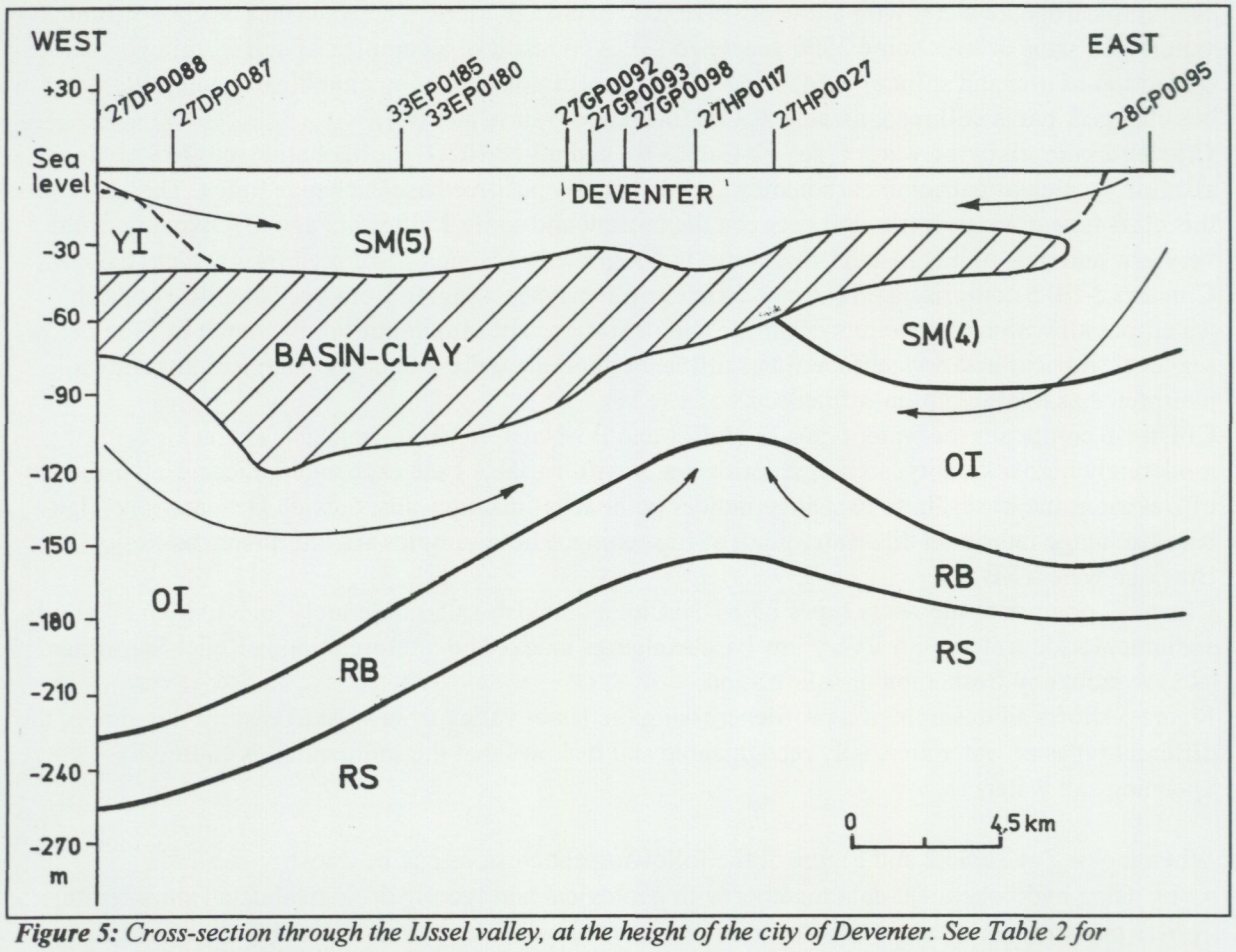


Figure 5: *Cross-section through the IJssel valley, at the height of the city of Deventer. See Table 2 for explanation of the codes.*

- It is shown in Table 2 that a combination of the clustering with the classification gives good results. The homogeneous groups within the data set, found using the Fuzzy C-Means clustering, have differences in an order of magnitude that is relevant for the data set in question. The water types according to the Stuyfzand-classification make it possible to recognize chemical processes, and to compare the clusters with other studies.

General Discussion and Conclusions

In this article, we wanted to show the applicability of the combination of the Fuzzy C-Means clustering together with the Stuyfzand-classification. The result is an easy interpretable hydrochemical classification at the appropiate level, as shown in the presented case study.
Stuyfzand [15] formulated some possible problems with applying a cluster analysis when classifying water samples. He points out that:

1. the boundaries of the clusters are not clearly defined and adjacent maps are incomparable
2. (log)normality and statistical independence have to be assumed
3. extremes have to be excluded
4. a discriminant function analysis is required to reveal the relative importance of all hydrochemical variables

There is, of course, some truth in these points, especially when already a lot is known about the specific area. But in our view the combination of the clustering and the classification method neutralizes part of these problems and is therefore very useful in a new study area with unknown processes.

ad 1. Some vagueness of the boundaries between clusters represents very well the gradual change present in nature, and is therefore greatly approved of by geographers. Adjacent cluster maps are comparable when the water types according to the Stuyfzand-classification are used.

ad 2. Multivariate (log)normality and statistical independence are not required [20] but it is good to keep these features in mind when choosing the variables for executing the clustering.

ad 3. Extremes contribute equally to all clusters and are no problem for the clustering. However, the scale of a Non-Linear Mapping plot is influenced by extremes [20] and some critical view to these extremes is still needed.

ad 4. When using water types according to the Stuyfzand-classification, no discriminant function analysis is needed to interprete the clusters.

Our conclusion is therefore that the great advantage of a statistical technique like Fuzzy C-Means clustering is its possibility to divide a data set in homogeneous groups at the appropriate level. The combination with the Stuyfzand-classification makes a good interpretation of the clusters possible.

Acknowledgements

The valuable contributions of dr. P.F.M. van Gaans are gratefully acknowledged. J. Bell, M.Sc, is thanked for her linguistic comments.

REFERENCES

[1] BEZDEK, C.J., 1981: Pattern recognition with Fuzzy Objective Function algorithms. -Plenum Press, New York

[2] BIESHEUVEL, A., 1991: ChemProc v. 4.0 -Vrije Universiteit Amsterdam, The Netherlands

[3] BROKS, 1992: Geohydrologische onderzoek winbare hoeveelheid "Salland-diep", projectno. 11.250, 4 delen

[4] DAVIS, J.C., 1986: Statistics and data analysis in geology. -John Wiley & Sons, New York, 2nd ed.

[5] DE GRUIJTER, J.J. & McBRATNEY, A.B., 1988: A modified fuzzy k-means method for predictive classification. -Classification and Related Methods of Data Analysis, H.H.Bock (ed.), Elsevier Science Publishers, The Netherlands, pp. 97-104

[6] ENGELEN, G.B. & JONES, G.P., 1986: Developments in the analysis of ground water flow systems. -IAHS Publ. 163, 365 pp.

[7] ENGELEN, G.B. et al., 1989: Grondwaterstromingsstelsels in Nederland. Ministerie van LNV, SDU-uitgeverij, Den Haag

[8] FRAPPORTI, G., VRIEND, S.P. & VAN GAANS, P.F.M. (1993): Hydrogeochemistry of the shallow dutch groundwater: interpretation of the National Groundwater Quality Monitoring Network. -Water Resources Research, Vol. 29, No. 9, pp. 2993-3004

[9] MATTHESS, G. , 1982: The properties of groundwater. -John Wiley & Sons, New York, 406 pp.

[10] RGD (National Geological Survey), 1973: Geologische opbouw van Salland en het aangrenzende randgebied, rapport no. 844 "Schalkhaar".

[11] RGD (National Geological Survey), 1975: Geologische overzichtskaarten van Nederland. Kaarten, profielen en toelichting.

[12] RGD (National geological Survey), 1990: Geologische en Hydrogeologische opbouw waterwingebied Zutphenseweg te Deventer, rapport no. BP 10804

[13] STUYFZAND, P.J., 1986: Een nieuwe hydrochemische classificatie van water typen, met Nederlandse voorbeelden van toepassing. -H_2O, Vol. 19, no. 23, pp. 562-568

[14] STUYFZAND, P.J., 1989: A new hydrochemical classification of water types. -IAHS Publ. 182, pp. 89-98

[15] STUYFZAND, P.J., 1993: Hydrochemistry and Hydrology of the Coastal Dune area of the Western Netherlands. -KIWA-report I11, Nieuwegein, The Netherlands, 366 p., also published as thesis Vrije Universiteit, Amsterdam, The Netherlands

[16] TNO-DGV, 1983: Hydrochemie van Oost-Nederland. OS 83-38, Auteur: J.H. Hoogendoorn

[17] TNO-DGV, 1986: Grondwaterstromingssystemen Salland/O-Veluwe. OS 86-36. Auteurs: G.K.Brouwer & J.H. Hoogendoorn

[18] TNO-DGV, 1990: Grondwatersysteemonderzoek Salland I en II. OS 90-48. Auteur: J.H.Hoogendoorn

[19] VAN GAANS, P.F.M. & VRIEND, S.P., 1995: FNX, a program for Fuzzy C-Means clustering and Non-Linear Mapping. -Universiteit Utrecht, The Netherlands

[20] VRIEND, S.P., VAN GAANS, P.F.M., MIDDELBURG, J. & DE NIJS, A., 1988: The application of fuzzy c-means cluster analysis and non-linear mapping to geochemical datasets: examples from Portugal. -Applied Geochemistry, Vol. 3, pp. 213-224

[21] WEBSTER, R. & OLIVER, M.A., 1990: Statistical methods in soil and land survey. -Oxford University Press, Oxford, 316 pp.

[22] WMO (Water Company of Overijssel), 1981: Grondwaterwinning diepe pakket in de omgeving van Schalkhaar (inventarisatieonderzoek)

Ground Water Salinization in Northern Germany - New Developments in Research -

Knut Wichmann & Alf Grube
DVGW-Forschungsstelle Technische Universität Hamburg-Harburg,
Dampfschiffsweg 11, 21079 Hamburg, F.R.G.

Abstract

Northern Germany shows different forms of geogenic groundwater salinization of which the intrusion of sea water, dilution from salt diapirs and upconing of deeper ground waters from different geological units (possibly Permian to Tertiary) are the most prominent. These salinized waters are a permanent potential threat for the extraction of fresh groundwater and a large number of waterworks is faced with the presence and especially the upconing of salinized ground water; some smaller catchment areas even had to be shut down. A regional scientific working group covering the North German Lowlands has been formed, in which the Geological Surveys, the Watermanagement authorities, Water Supply authorities and universities and private scientists are involved. The work of the group is focused on geogenic and anthropogenically influenced salinizations in soft rock aquifers of Tertiary and Quaternary age. Emphasis is put on the problems of longterm sustainable public water supply. The research areas and the working scope of the group are presented.

Introduction

The hydrological and hydrogeological conditions in Northern Germany (Fig. 1), including the states and larger cities Schleswig-Holstein, Mecklenburg-Vorpommern, Hamburg, Niedersachsen, Bremen, Brandenburg, Berlin and Sachsen-Anhalt, generally offer favourable possibilities for an efficient supply for population and industry with high quality drinking and industrial water. Altogether around 1.4 - 1.5 x 10^9 m^3/a of water are consumed in North Germany, of which around 90% are taken from ground water resources. The use of the ground water however is restricted by geogenic as well as manmade pollutions.

Ground water salinization is a latent threat to ground water utilization in large parts of North Germany. Despite a reduction in the ground water production, which was a result of water saving strategies (since the 80ies) and the strong recession with a resulting decline of industrial production as well as water saving strategies in the former German Democratic Republic (since the end of the 80ies), a slow increase of salinization can be observed in many areas. This give hints that no stable system has been reached yet.

Therefore an estimation of the utilizable ground water resources, the distribution of salt water and the hydrochemical composition of the salinized areas and the surroundings as well as the dynamics of the salt-/freshwater interface is important and has to be intensified.

Ground water salinization in Northern Germany

The main reasons of geogenic salt contamination of ground water resources in North Germany are the intrusion of sea water, dilution from salt diapirs and the upconing of deeper ground waters (CARLÉ 1975). Subrosion and upconing deeper ground waters are here called „inland salinization". The relevance of injected wastewaters from oil- and gasproduction is difficult to estimate, since up to now only little information exists about their influence. Other geogenic sources of salinization, as the

Geogenic background concentrations for chloride in fresh ground water range between 10 and 20 mg/l and sulphate concentrations are even lower. In areas with concentrations higher than 50 mg/l an influence of salinization can be stated. Maximum concentrations reach some hundred g/l. In general chloridic and sulfatic ground water salinizations can be differentiated. Types of salinized ground water and ground waters influenced by salt water occuring in Northern Germany as well as classifications are described by MÜLLER (1966), LÖHNERT (e.g. 1967), CARLÉ (1975), GERHARDY et al. (1976) and others. In contrast to high chloridic concentrations sulfatic salinizations are restricted to the vicinity of caprocks of salt diapirs and generally only have a minor extension.

Maps of ground water salinization exist for all parts of North Germany, but an overview is missing (see Fig. 3). In the German Democratic Republic (today representing the states Mecklenburg-Vorpommern, Brandenburg and Sachsen-Anhalt) a map series in 1:50.000 included detailed information on salinization in relationship to the different aquifers, the depth of the interface and the location of salt spots. Recent largescaled maps in different scales have been drawn for the former German Democratic Republic (REINSCH et al. 1990), Niedersachsen (HAHN 1991b) and Schleswig-Holstein (GRUBE et al. 1996). The existing maps use different definitions for salinization and salinization categories and so cannot directly be compared to one another. Detailed maps (1:25.000) of the concentration and hydrochemical composition in the upper aquifers have recently been published for the area of the town of Bremen, which allow a thorough interpretation of geogenic sources of salinization as subrosion, river bank infiltration and salt water intrusion as well as man made influences (ORTLAM & SAUER 1993).

Our newly drawn map of which a part is shown in Fig. 2 can be used to illustrate the general distribution of ground water salinization as a result of geohydrological structures and processes. Geogenic salinizations are found in the following main natural situations:

- salt water intrusion at the coast (mainly lowland areas)
- large discharge areas (large valleys and lowland areas) with upconing as a result of upward directed potential gradients
- large Tertiary Basins and other geological depressions, with decending salt waters (gravity effect), probably mainly due to subrosion of salt structures
- local hydraulic connections of deeper salinized to higher aquifers through eroded or primary missing aquitards (e.g. Elsterian dorrs) in aquifers with ascending ground waters
- upconing of deeper ground water along faults or equivalent hydraulic pathways through aquitards
- discharge of ground water with higher salt concentration (possibly connate waters) from outcropping older strata.

Investigation Areas

Recent research is carried out in different regions of the north german lowlands with its softrock aquifers (Fig. 1). Three large areas have been choosen as main research fields: Hamburg, Potsdam and Lübeck. These show varied forms of salinizations (see below) and are representative for large parts of the North German Lowlands. Besides that a number of other areas will be investigated, e.g. in Bremen and at places at the North Sea and the Baltic Sea coast. In the following a brief description of the research areas will be given.

The investigation area Hamburg is situated in the marshes of the Elbe valley, a large ice marginal spillway, which represents a large extrusion area. To the north and south of the valley pleistocene till

flooding during tidal waves, the deposition of salts via sea spray in coastal areas, the concentration of shallow subsurface waters by evaporation processes as well as the influence of naturally high salt concentrations of rivers only play a minor and local role.

A number of detailed investigation programs on the distribution and the quality of salinization were carried out in the former German Democratic Republic (e.g. VOIGT 1972, GLANDER et al. 1975, REINSCH 1976). Possibly the most detailed investigations on ground water salinization in North Germany have been carried out on possible nuclear disposal sites in salt domes (e.g. OCHMANN & FIELITZ 1993, VOGEL et al. 1993). Actual examples of research on advanced modelling techniques on salt water upconing in the former East Germany are shown in DIERSCH & NILLERT (1990) and NILLERT et al. (1988). In the coastal area intensive investigations in Niedersachsen since the sixties have to be mentioned (see HAHN 1991a for details and literature), a recent example of a typical coastal ground water salinization in Niedersachsen is shown in ROGGE & JOSOPAIT (1993). In Schleswig-Holstein intensive studies were carried out in the western coastal region (e.g. NEUMAYR 1979; see also literature in GRUBE et al. 1996). Altogether hundreds of scientific papers have been published on numerous areas and many specific aspects of ground water salinization problems in Northern Germany. These are at the moment summarized and evaluated to establish a state-of-the-art report.

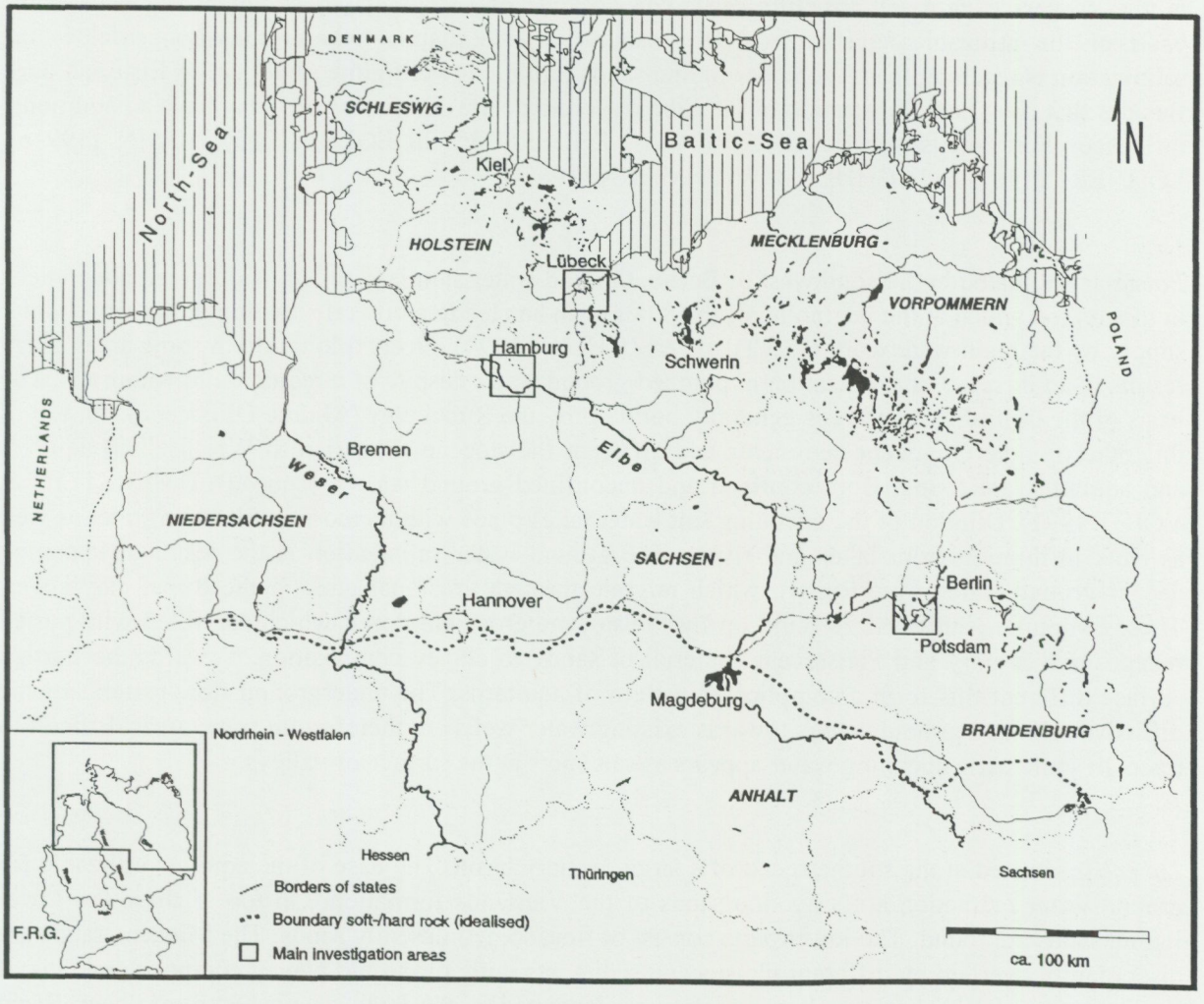


Fig. 1. North German lowland areas and main investigation areas

areas are found. The basis of the aquifer system is build up by silty fine sands of the Vierlande-formation (Lower Miocene). The lowest usable aquifer are the lower lignite sands (Braunkohlensande) which are separated from the upper lignite sands (both Miocene) by the Hamburg clay. The lower lignite sands comprise a series of Miocene fluvial sediments that show dispersed browncoal components and browncoal horizons as well as silty to clayey layers. The Hamburg clay is an aquitard of a few meters in thickess that is present over large area. Nevertheless it shows erosional gaps also, e.g. large Elsterian dorrs cut through this aquitard. The extended silt-horizons in the lignite sands make the hydraulics much more complicated. Above this series Saalian tills and sands occur and on top of these Weichselian fluvial sands reach a thickness of some tens of meters. Holocene perimarine silts, peats and fluvial sediments build up the surface layers. In the western part of the investigation area (Wilhelmsburg) the geological conditions are similar but here a large dorr is plugged by pleistocene clayey sediments and the neighbouring upper mica clay. The distribution of the ground water salinzation is rather complicated. In the eastern part it occurs mainly in the lower lignite sands, but reaches into the Elsterian to Weichselian aquifers also. Salt spots in the highest aquifers reach some thousand mg/l chloride. The salinizations are probably due to subrosion, possible source salt diapir for the eastern part of the area are the structures Meckelfeld or Reitbrook. Recently an increasing of salinization in the city´s aquifers has been stated (FREIE UND HANSESTADT HAMBURG 1996). The higher mineralized ground waters are connected to a large salinization area following the Elbe valley upstream southeast of Hamburg. One of the main questions is if saltwaters from a salt structure can ascend despite of a large clayey sediment sequence at the basis of the utilizable aquifer. In Wilhelmsburg (source diapir: Othmarschen-Langenfelde) the salinization is reaching from the upper lignite sands into the lower lignite sands via an Elsterian dorr. Besides that river bank infiltration of the Elbe river and deepwell reinjections may have an additional influence. For details see BAUHUS (1986), EHLERS & GRIEGER (1985), HAHN (1991b), LÖHNERT (1981) and SCHULZ & WICHMANN (1985).

Potsdam is situated in the southwest of Berlin. Ground water salinization is a widespread phenomena in this region which at the beginning of the 80ies even has led to a critical situation in the city´s water supply by the main waterwork (RECHLIN & ZÜHLKE 1994). Overexploitation in some areas today results in an increase of salinization in pumped ground water despite of a reduction in withdrawl. The basis of the utilizable aquifers is generally build up by the Rupel clay (Middle Oligocene). On top of this other middle Oligocene sediments and different Pleistocene (Elsterian to Weichselian) aquifers and aquitards are found. Both confined and unconfined ground waters occur (BLUMENSTEIN & VOIGT 1991). Dilution of the upconing salt water takes place with meteoric infiltration water as well as bank infiltration from lakes and rivers. The ground water salinization is the result of upconing deeper ground waters (pre-Rupel), which migrate through erosional gaps in the Rupel clay cover. These hydraulic pathways are build up by Pleistocene erosional dorrs, which are filled with varied redeposited Tertiary and Pleistocene material of sandy to clayey composition. Towards the Earth´s surface different tills form a complicated pattern of aquitards. The underground flow patterns of the diffusive salinized ground waters towards existing water wells are therefore in some areas difficult to trace. In some parts upconing water appears as salt spots at the surface of valleys.

Lübeck is situated at the southern end of a large Tertiary basin. The base of the aquifers utilizable for ground water extraction are silty fine sands of the Vierlande-formation. On top of these the lower lignite sands are found. The lower parts consist of fine, sometimes silty sands. The Miocene sands are discordantly overlain by different pleistocene sediments with a sandy to clayey composition. Tills of Saalian age and Weichselian clays which were deposited in the large glazilacustrine Lübeck Basin form widespread aquicludes (JOHANNSEN 1980). Ground water salinization which occurs in the lignite sands as well as in the Quaternary sands is probably due to subrosion (source salt diapir still in discussion) and upconing deeper waters, possibly older formation waters. The fine grained lower parts of the lignite sands in some parts show higher salt concentrations which might result from

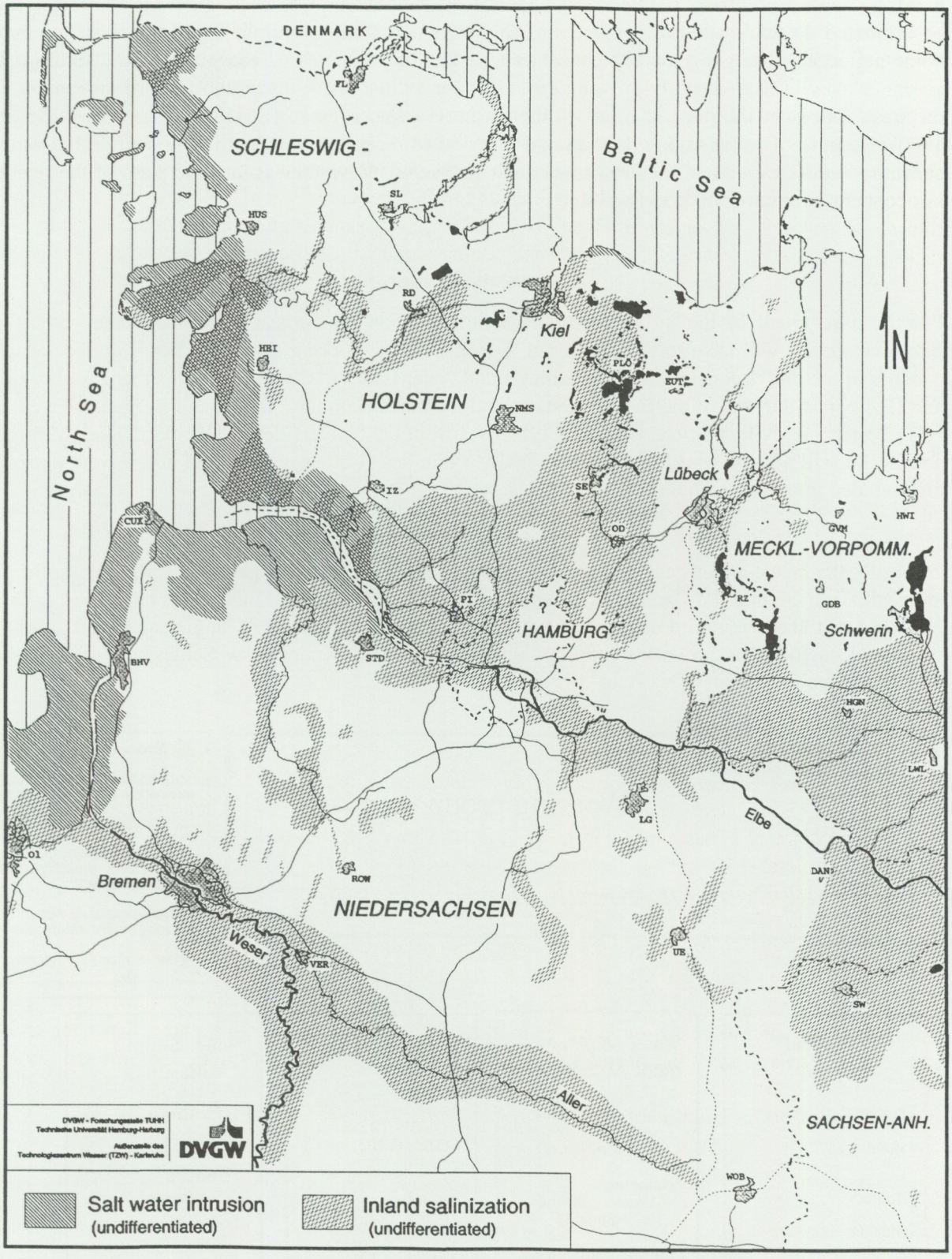


Fig. 2. Ground water salinization in the western part of Northern Germany (draft map; source: GRUBE et al. 1996, HAHN 1991b, REINSCH et al. 1990). The criteria used to define the distribution of salinizations vary in the different sources used for the map. The final map will cover North Germany as a whole and will in the future be developed towards (i) a homogeneous definition on what will be shown as salinization, (ii) the distribution of salinization in different aquifers and depths, (iii) differentiation between subrosion and upconing deeper ground water and (iv) the position of salinization areas towards water works.

grainsize dependend effects. At the coast a small scaled intrusion of seawater from the Baltic Sea can be estimated. Possible additional sources of salinization are the salts from the Trave river and man made pollutions. The geogenic salt concentrations in Lübeck increased especially in the sixties and seventies as a result of steadily growing ground water extraction. A maximum upward movement of the fresh-/saltwater interface of up to 40 meters in 35 years occured (SCHENCK in JOHANNSEN 1980). Because of water saving policies and a period of recession in industrial production the water consumption decreased and the drawdown areas recovered. Nevertheless in some parts of the region salt concentrations are still slowly rising.

Investigation Program

For the assessment of the influence of the salinization on the utilizable ground water resources intensive studies will have to be carried out. For this task a working group has been formed, which consists of the professionals concerned with ground water issues in the Watermanagement Authorities and Geological Surveys of the five large states and the cities Hamburg, Berlin and Bremen, as well as large Water Supply Institutions (Fig. 3). Colleagues from the Universities of Hamburg, Kiel, Münster and Berlin will also be working together. Finally a number of other institutional and private persons are included into the regional research projects.

Generally the investigations can be differentiated into three levels: (I) largescaled screening (softrock areas of North German Lowlands), (ii) regional research of hydrological units (Hamburg-Elbe valley; Untertrave / Lübeck region; Potsdam) as well as (iii) local detail studies of single catchment areas or waterworks settings (waterwork Hamburg-Curslack, waterwork Kuden in W´Schleswig-Holstein and others).

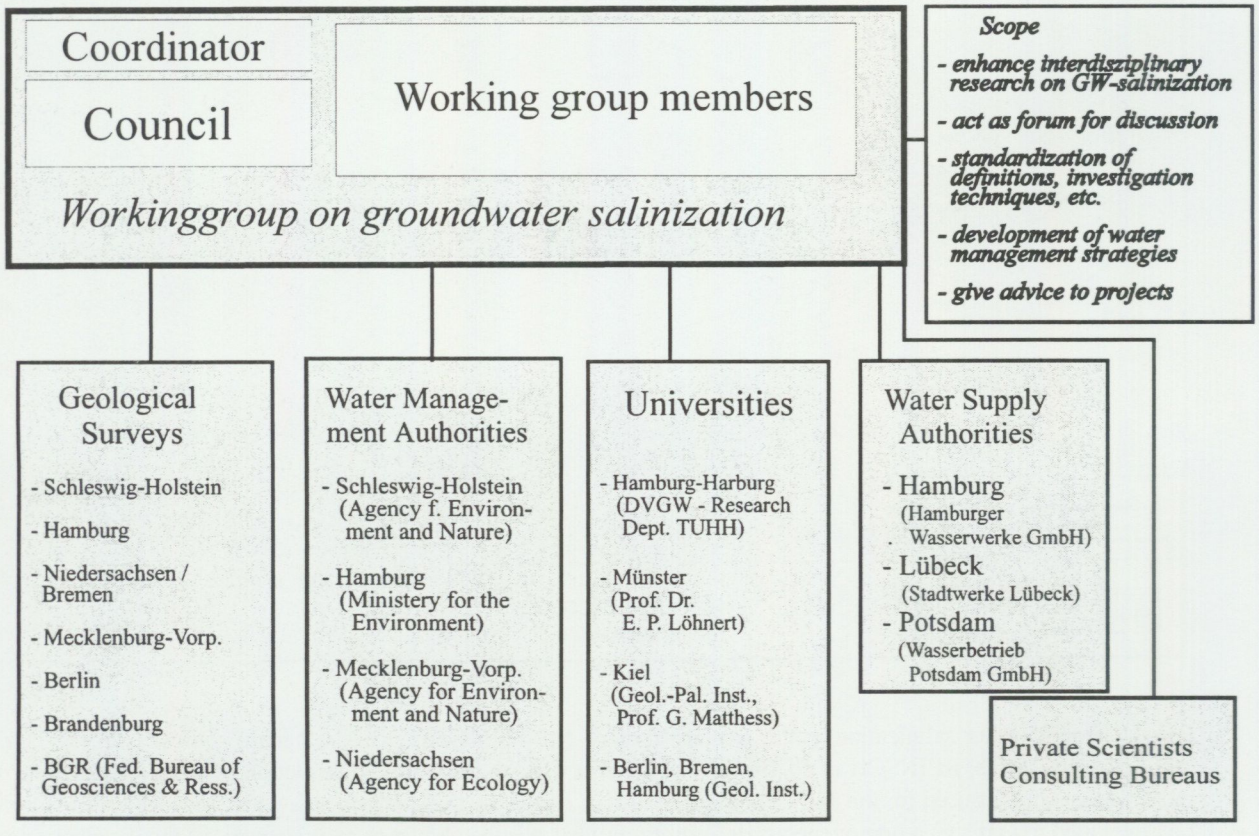


Fig. 3: Structure of the Working Group on Ground Water Salinization

The scope of the working group can be summarized as follows:

- As a basic need the existing data have to be validated and verified (correlation of filterposition and aquifers, ground water level data, geophysical measurements, hydrochemical data etc.). Because of the large amount of data automatic procedures (e.g. numeric and graphical approaches) will have to be enhanced or developed.
- Work on genetical aspects and type classification of salt water and salinized water
  a. methodical questions of genesis
  b. type classification and presentation
  In this context a scope for the classification has to be defined. Based on this the development of models / diagrams has to be carried out. Aspects of salt water genesis, rock-water interaction and manmade influences have to be considered
- The saltwater-/freshwater interface, for which a standardized definition is needed, will have to be worked on towards its configuration and its time and space dependent behaviour. These largely depend on regional ground water dynamics, the petrographical composition of the aquifer as well as manmade influences (e.g. drainage or ground water withdrawal).
- Another important scope is the systematic work on the dynamics of saltwater bodies in its relation towards physical parameters like density, temperature and potential flow direction as well as the structure of the aquifer systems
- Distribution pattern of salinized and fresh waters in regional hydrological units in which the temporal development and influencing factors represent central questions
- To distinguish aspects of salt water genesis and the occurrence of mixture of different ground waters (e.g. upconing deeper ground waters of different origin with fresh water) also hydrochemical models and classifications of fresh waters and mixed waters in the vicinity of ground water salinizations play an important role
- An important aim of the work is the development, standardization and further improvement of (a) measurement techniques (e.g. density problem during water table measurements), observation well configuration, geophysical surveying etc., (b) data evaluation/statistics and (c) ground water monitoring
- These results will be used in water management strategies in the vicinity of fresh-/saltwater bodies with the aim of a sustainable use of ground water resources
- Map presentation of salinized ground waters and salt water bodies requires the development of adjusted and standardized legend, scale and nomenclature
- An additional aspect is the necessity for an increased consideration of paleohydrological and paleohydrogeological issues.

An interdisciplinary research approach is needed to solve salinization issues that are becoming even more important because of a tendency to intensify the utilization of deeper aquifers. A better understanding of geogenic ground water salinization phenomena can also add to an objective discussion on man made interference with our shallow aquifers. New water management methods have to be developed for the Watermanagement Authorities in the relevant areas, replacing older „strategies“ (e.g. relocation of wells) which will allow for a longterm sustainable use of our ground water resources.

REFERENCES

BAUHUS, W., 1986: Hydrogeochemische und isotopenphysikalische Untersuchungen an Grundwässern tieferer Aquifers im Raum Hamburg.- Thesis Univ. Münster, 151pp. Münster.

BLUMENSTEIN, O. & VOIGT, I., 1991: Aspekte geoökologischer Prozeßmechanismen und der Belastbarkeit eines Aquifers im Postdamer Raum - dargestellt am Beispiel eines Wassereinzugsgebietes.- Wissenschaftliche Zeitschrift, 35:395-405, Potsdam.

CARLÉ, W., 1975: Die Mineral- und Thermalwässer von Mitteleuropa - Geologie, Chemismus, Genese.- 643 pp. Wiss. Verl.-Ges., Stuttgart.

DIERSCH, H. J. & NILLERT, P., 1990: Salt-water intrusion processes in groundwater; novel computer simulations, field studies and interception techniques.- IAHS Publ. 173: 319-329.

EHLERS, J. & GRIEGER, J., 1985: Groundwater chemistry in the Hamburg region.- IAHS Publ., 146:285-293, Wallingford (U.K.).

FREIE UND HANSESTADT HAMBURG, 1996: Wasserversorgungsbericht für Hamburg.- Mitteilung des Senats an die Bürgerschaft, Drucksache 15/4715, 16pp, Hamburg.

GERHARDY, H., HOFFMANN, B., MEYER, H.-H. & WICHMANN, K, 1976: Wasserhaushalt der Ostfriesischen Inseln - geologische und hydrologische Datenbestandsaufnahme für die Insel Norderney.- Technische Berichte 9; 30 pp.; SFB 79, Techn. Univ. Hannover

GLANDER, H., W. GOHLKE & SCHIRRMEISTER, W., 1975: Hydrochemische Rayonierung und Erfassung der Gesamtmineralisation der gegenwärtig genutzten Grundwasserleiter in der DDR.- Zeitschrift angewandte Geologie 21 (4) 153-160; Berlin.

GRUBE, A., NACHTIGALL, K. H. & WICHMANN, K., 1996: Zur geogenen Grundwasserversalzung in Schleswig-Holstein.- Meyniana, 48:, Kiel [in press].

HAHN. J., 1991a: Aspects of groundwater salinization in the Wittmund (East Friesland) coastal area.- Int. Contr. to Hydrogeology, 11:251-289; Hannover.

HAHN. J., 1991b: Grundwasser in Niedersachsen.- Veröffentlichungen Niedersächsische Akademie der Geowissenschaften, 7:13-27; Hannover.

JOHANNSEN, A., 1980: Hydrogeologie von Schleswig-Holstein.- Geologisches Jahrbuch., C28:3-586; Hannover.

LÖHNERT, E. P., 1967: Grundwassertypen tieferer Stockwerke in Hamburg.- Neues Jahrbuch Geologie Paläontolgie (Abh.), 129:113-136, Stuttgart.

LÖHNERT, E. P., 1981: Praktische Beispiele komplizierter Zusammenhänge am Kontakt Salz-/Süßwassergrenze im Stadtgebiet von Hamburg.- Münster. Forsch. Geol. Paläont., 54:161-174, Münster.

MÜLLER, E.P., 1969: Zur Geochemie der Tiefenwässer und der organischen Substanz im Nordteil der DDR.- Zeitschrift Angewandte Geologie 15(3):114-124; Berlin

NACHTIGALL, K. H., 1983: Hydrochemical aspects of the interface.- In: Proceedings of the 8th Salt Water Intrusion Meeting, Bari, Italy: 41-48, Bari.

NEUMAYR, V., 1979: Schwermetallspuren und Ursachen ihrer Verbreitung in Grundwässern an der Westlküste von Schleswig-Holstein.- Diss., Math.-Naturw. Fak. Christian-Albrechts-Univ., 282pp, Kiel.

NILLERT, P., DIERSCH, H.-J., GÜNTHER, M. & LEHMANN, H.-W., 1988: Feldtest zum Salzwasseraufstieg unter Brunnen.- Zeitschrift angewandte Geologie, 34(6):161-169, Berlin

OCHMANN, N. & FIELITZ, K., 1993: Estimation of horizontal and vertical groundwater flow from well-logging and pressure data in groundwater of variable density above a salt dome.- Proc. 12th Saltwater Intrusion Meeting, Barcelona, Nov., 1992. CIHS.:599-613, Barcelona CIMNE .

ORTLAM, D. & SAUER, M., 1993: Geochemische Grundwasserkartierung Bremen.- Erläuterungsband und Karten 1:25.000; Bremer Entsorgungsbetriebe [Hrsg.], Bremen.

RECHLIN, B. & ZÜHLKE, K., 1994: Hydrogeologie und Wasserwirtschaft Potsdams.- Kurzfassung, 61. Tagung der Arbeitsgemeinschaft Nordwestdeutscher Geologen 24.-27.5.1994, Potsdam [unpubl.].

REINSCH, D., 1976: Hydrogeologie der mesozoischen und känozoischen Schichten des Küstenbezirkes der Deutschen Demokatischen Republik unter besonderer Berücksichtigung hydrochemischer Anomalien und ihrer Gesetzmäßigkeiten.- Thesis, 233 S., Universität Greiswald, Greifswald (unpubl.).

REINSCH, D., GÄRTITZ, R., ULRICH, A. & MEINKE, I., 1990: Hydrogeologische Übersichtskarte der DDR - Grundwasserversalzung 1: 500.000.- (map), Kombinat Geologische Forschung und Erkundung, Halle [unpubl.].

ROGGE, A. & JOSOPAIT, V., 1993: Salinization caused by groundwater abstraction from an aquifer on the German North Sea coast.- In: Custodio, E. & Galofré, A. (Eds.): Study and modeling of

saltwater intrusion into aquifers; Proc. 12th Saltwater Intrusion Meeting, Barcelona 1992.; S.703-713; CIMNE; Barcelona.

SCHULZ, M. & WICHMANN, K., 1985: Geogenic groundwater pollution in the Hamburg region, FR Germany.- IAHS Publ. 146:285- 293, Wallingford (U.K.).

VOGEL, P., SCHELKES, K. & GIESEL, W., 1993: Modeling of variable-density flow in an aquifer crossing a salt dome - first results.- In: Study and Modelling of Saltwater Intrusion into Aquifers, Proc. 12th Saltwater Intrusion Meeting, Barcelona, Nov., 1992. CIHS.:359-369, Barcelona (CIMNE).

VOIGT, H.-J., 1972: Genese und Hydrochemie mineralisierter Grundwässer.- WTI Wissenschaftlich-Technischer Informationsdienst 13 (Sonderheft 6), 150pp, Berlin.

VOIGT, H.-J., 1977: Hydrodynamische und hydrochemische Probleme am Süß-Salzwasserkontakt.- Geod. Geoph. Veröff., R. IV,22: 48-54.

WURL, J., SOMMER-VON JAMMERSTED, C. & PEKDEGER, A., 1995: Geogene und anthropogene Beeinträchtigungen der Grundwasservorkommen im südwestlichen Stadtgebiet von Berlin.- Zeitschrift deutsche geologische Gesellschaft, 146:243-249, Hannover.

Groundwater salinization in Southern Tuscany (Italy)

Giovanni Pranzini and Alberto Bencini
Department of Earth Sciences, University of Florence, via La Pira, 4, 50121 Firenze, Italy

Nearly all the coastal plains in Tuscany are plagued, to varying extents, by groundwater salinization. In southern Tuscany this creates serious problems for:

- municipal water supplies: during the summer, large numbers of vacationers added to the resident population make water rationing a necessity in some areas;
- farming, the main source of income in the region: the high salinity levels of groundwater used for irrigation has forced lucrative crops to be abandoned and replaced by others that can better withstand the salinity; in some areas, the high level of ground salinity may lead to the total abandonment of agriculture within a few decades;
- the coastal pine groves that are being damaged by groundwater salinity.

The authors of this paper presented a study on groundwater salinization in the Grosseto Plain (Bencini & Pranzini, 1992) at SWIM in Barcelona, 1992. The distribution of the water salinity and chemistry revealed that groundwater salinization was dependent upon various phenomena, not only marine water intrusion. The current study has extended the field of investigation to the nearby Albegna River plain and tackled the issue with several methods: hydrogeological reconstruction of the subsoil of the two plains, chemical and isotopic analyses, and geophysical surveys. The large amount of data findings definitely provided a more accurate picture of the situation and have made it possible to understand the factors involved in groundwater salinization.

Geology and hydrogeology

The coastal plain formed by the Ombrone and Bruna Rivers is a tectonic depression in which a considerable thickness of Quaternary sediments accumulated (at least 200 meters in the central part). The rocks surrounding the plain are primarily sandstone and siltstone with some Mesozoic carbonate outcroppings (Fig. 1).
On the plain there are alluvial sediments and fill deposits while the coastal strip consists of dunes and beaches. Near the Roselle limestones there are recent travertine formations linked to the rise of thermomineral waters.
In order to understand the mechanism of groundwater salinization it is important to take a look at the sedimentary evolution of the plain (Bravetti & Pranzini, 1988). A large amount of sediment (100 meters thick near the seacoast) was deposited during the Holocene transgression, these are both alluvial deposits and non consolidated lagoonal or marine sediments which, therefore, still contain connate salt water. During the past three thousand years the plain has advanced rapidly, especially due to the fact that the introduction of farming combined with deforestation markedly increased the volume of sand transported by the rivers. The Ombrone delta advanced quickly and the river sands formed two bay bars joined to the promontories of Castiglione della Pescaia and Uccellina. The bars enclosed two lagoons that were later reclaimed (the northern one is not completely dried) with sand transported by the Ombrone River.

The geological situation of the Albegna River plain is similar to the Ombrone plain (Fig. 3). The main difference lies in the marked development of the eolic sands attributed to the Wurm. The Orbetello lagoon has not been filled due to the lack of a tributary.
The small Talamone plain was constructed mainly by swamp reclamation.
The area covered by this study is the driest part of Tuscany: mean annual precipitation is approximately 600 mm; the mean temperature ranges from 16° to 15° C.

In both plains there are two main aquifer complexes in the Quaternary sequence (Figs. 2 and 4):

a) fluvial gravel and sand at various depths;
b) coastal sands.
The former are confined aquifers, except for the area where the Ombrone river enters the plain, where the gravel and sand practically reach the surface, and some areas along the edges of the plain where the aquifers are continuous with the hill-slope detritus.

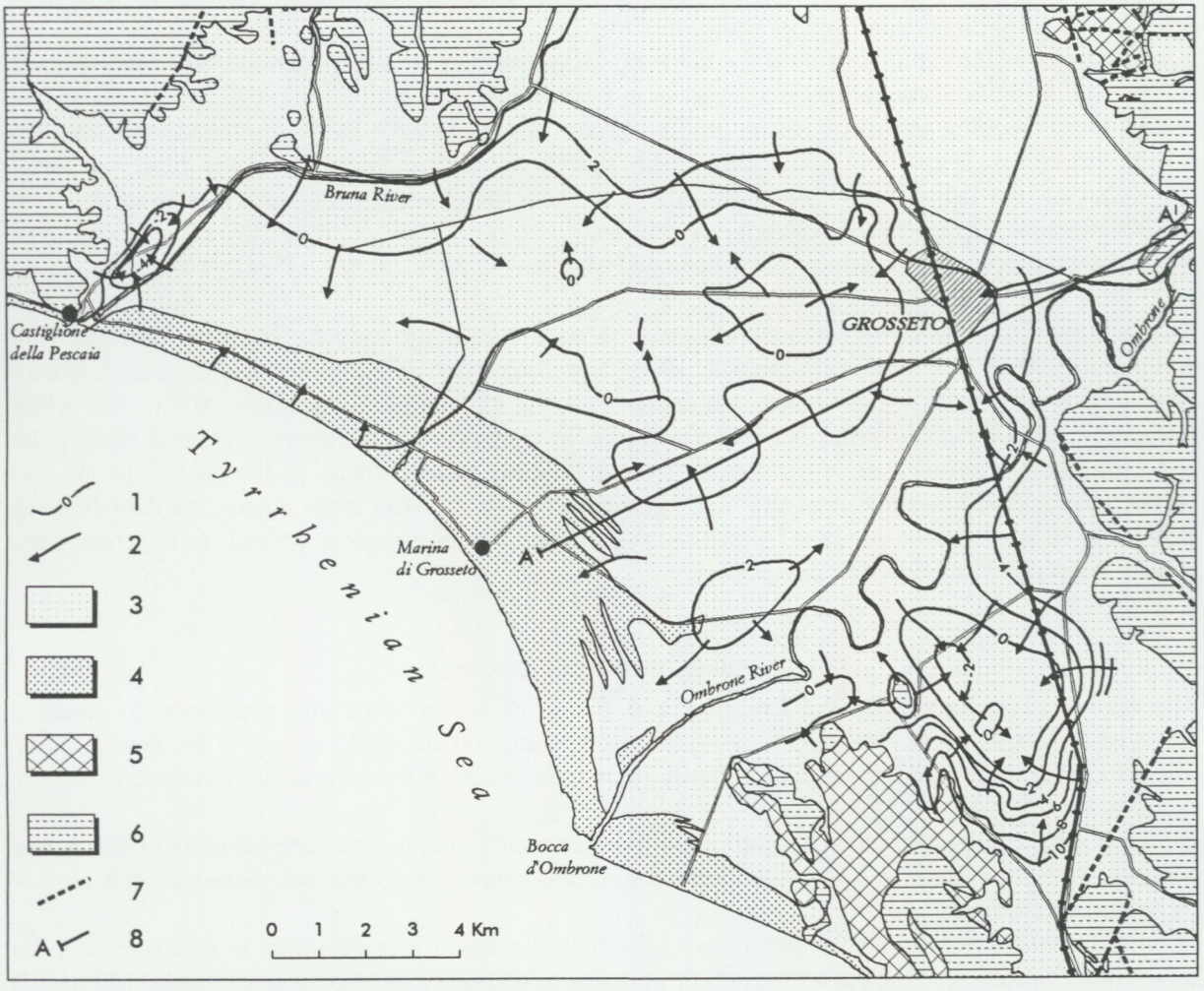


Fig. 1 - Isopiezometric map of the Grosseto Plain, September 1994. 1) Isopiezometric lines, m a.s.l. 2) Flow lines. 3) Alluvial and fill deposits. 4) Dune and beach sand. 5) Mesozoic carbonate rocks, highly permeable because of fracturing and karst. 6) Slightly permeable or impermeable rocks (sandstones, siltstones, marls, marly limestones, shales. 7) Faults. 8) The trace of the cross-section (fig. 2).

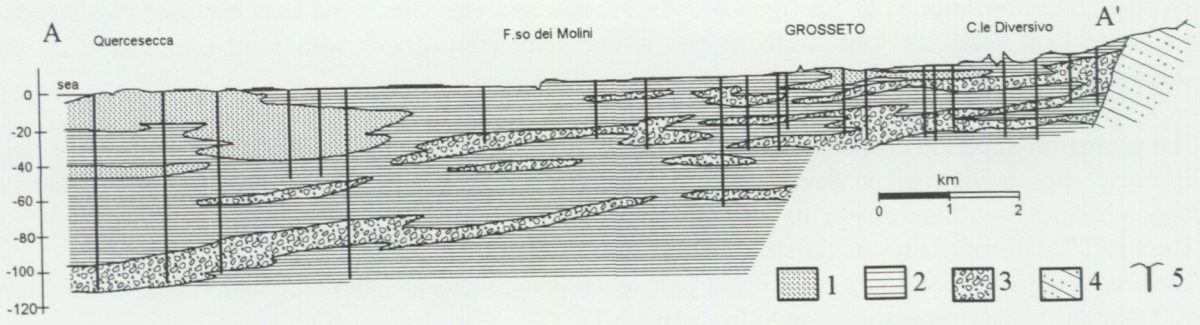


Fig. 2 - Geological cross section of the Grosseto Plain. 1) Sand. 2) Clay and silt. 3) Gravel and sand. 4) Sandstones and siltstones. 5) Wells with lithostratigraphic records.

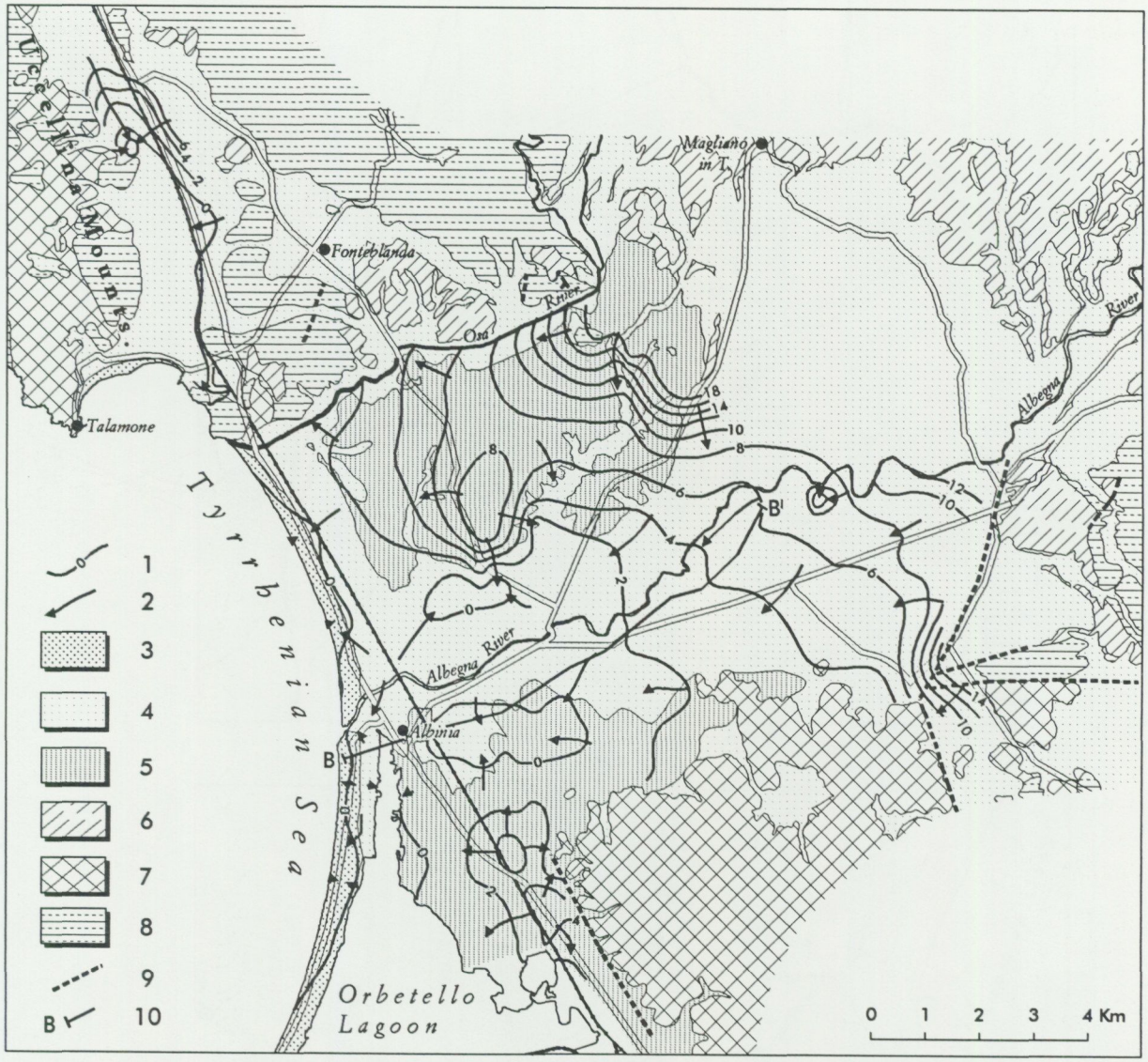


Fig. 3 - Isopiezometric map of the Albegna Plain, September 1994. 1) Isopiezometric lines, m a.s.l. 2) Flow lines. 3) Dune and beach sand. 4) Alluvial and fill deposits. 5) Eolic sand 6) Pliocene clay and sand. 7) Mesozoic carbonate rocks, highly permeable because of fracturing and karst. 8) Slightly permeable or impermeable rocks (sandstones, siltstones, shales). 9) Faults. 10) The trace of the cross-section (fig. 4).

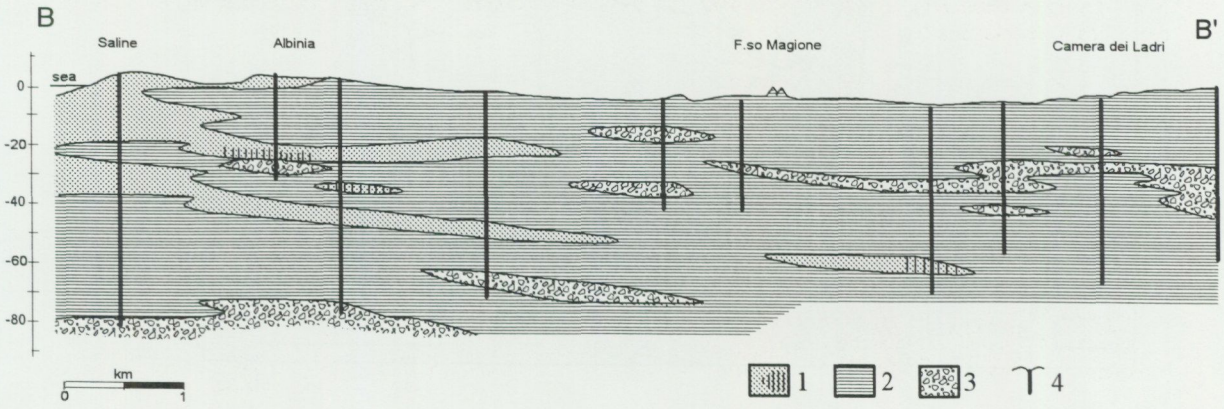


Fig.4 - Geological cross section of the Albegna Plain. 1) Sand. 2) Clay and silt. 3) Gravel and sand, locally cemented 4) Wells with lithostratigraphic records.

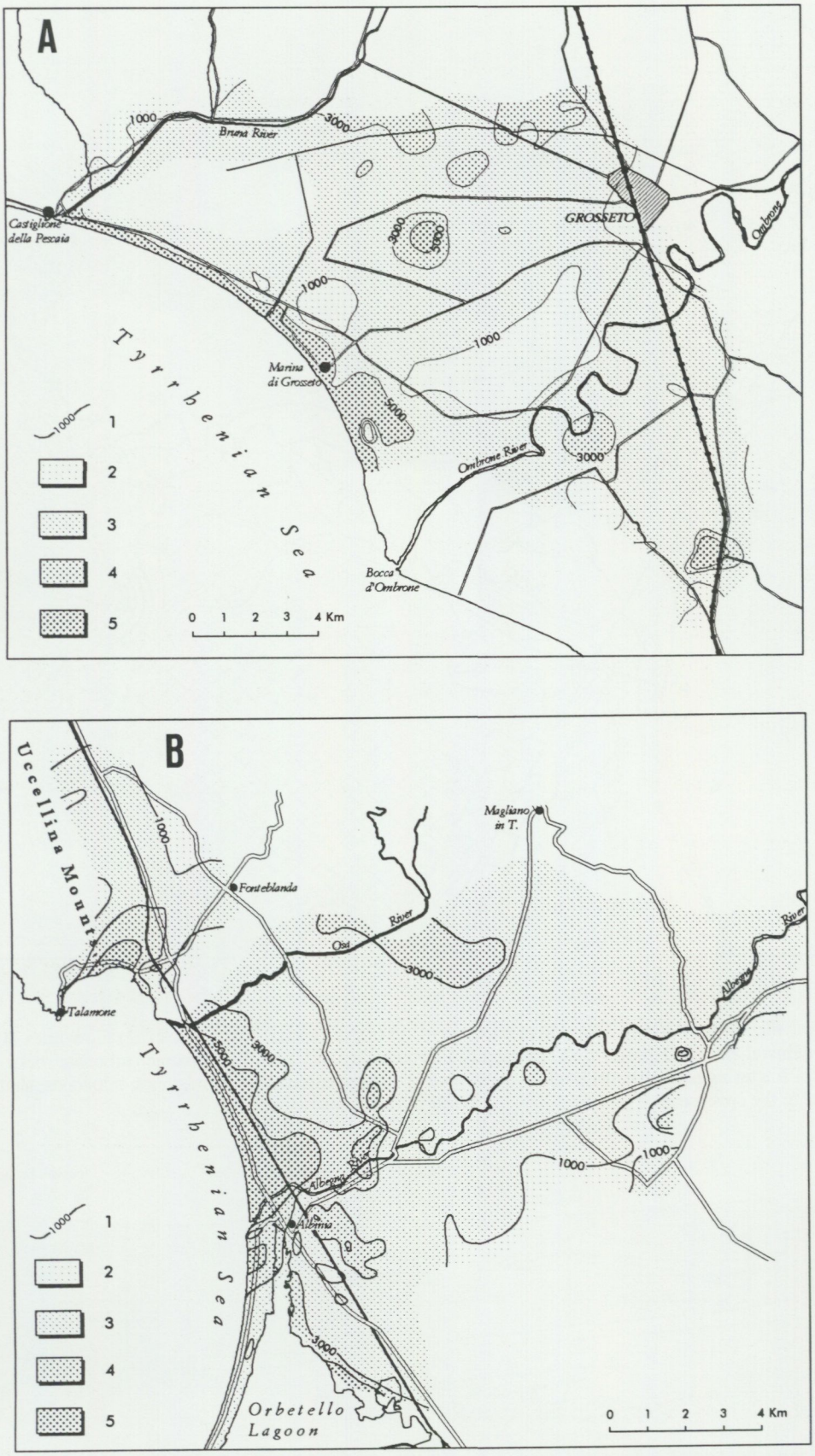


Fig. 5 - Groundwater electrical conductivity in the Grosseto Plain (A), and in the Albegna Plain (B), September 1994. 1) Isoconductive lines, mS/cm. 2) Electrical conductivity less than 1000 μS/cm. 3) E.C. between 1,000 and 3,000 μS/cm. 4) E. C. between 3,000 and 5,000 μS/cm. 5) E. C. over 3,000 μS/cm.

Pumping tests have revealed a transmissivity from 10^{-2} to 10^{-3} m²/s, while the storage coefficient ranges from 1.2 10^{-4} to 6.1 10^{-6}.
The groundwaters are fed by rivers and rain that infiltrate the surrounding hills. These groundwaters are used mainly for farming (over 4,000 wells) and also for municipal water supplies.

The coastal sands form an unconfined aquifer, which is not very productive, and is fed solely by direct rainfall. It is exploited mainly by shallow wells for campsites and summer homes.

The piezometric surface has been reconstructed over several years and seasons. Figs. 1 and 3 show the situation in autumn when areas with the piezometric surface below sea level expand considerably with respect to spring due to the increased summertime pumping. The seasonal variation in the water level is 1-2 meters, on the average, but in some areas, summer pumping cause depressions as deep as 10 meters.

Groundwater Chemistry

Figure 5 shows the distribution of groundwater electric conductivity on the basis of September 1994 measurements. Salinity generally increases between spring and autumn, especially in areas subject to intensive summer pumping.
In addition to the high salinity of the groundwater near the coast, there are also areas with high salinity farther inland which cannot be explained by the phenomenon of marine water intrusion. In this case, the chemistry of the water is the main element for an understanding of the salinization process.
We conducted basic chemical analyses of the water from 185 wells, 6 springs and 2 rivers. On 32 appropriately selected specimens we determined Br, Sr and Li levels. On 18 well water samples we also conducted isotopic analyses (Table 1). We also used 4 ^{3}H and 5 ^{18}O tests on well specimens taken from two small coastal plains north of the Ombrone plain.

A preliminary general evaluation, using the Langelier-Ludwig diagrams identified three main groupings (Fig. 6):
a) alkaline-earth sulfate waters
b) alkaline chloride waters
c) alkaline-earth chloride waters.

We can immediately see that the small quantity of alkaline-earth bicarbonate waters is a major anomaly. The alkaline chloride waters, those with the highest total salinity, are clearly related to marine water intrusion (Fig. 7). This is confirmed by the fact that the respective wells are located mainly along the coast, and that salinity gradually decreases going inland.

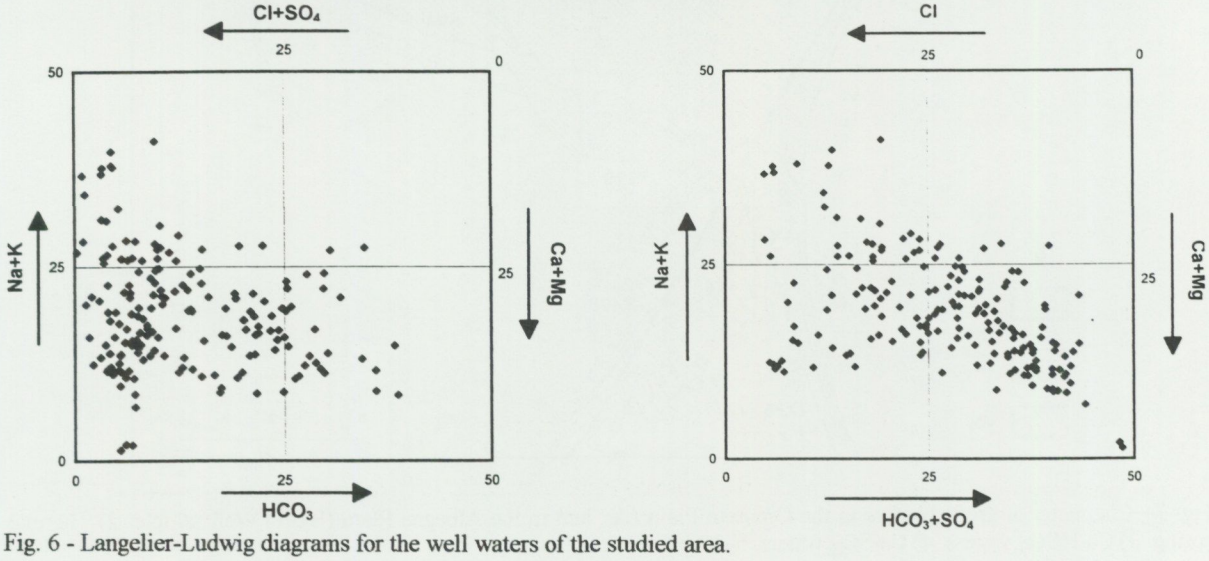


Fig. 6 - Langelier-Ludwig diagrams for the well waters of the studied area.

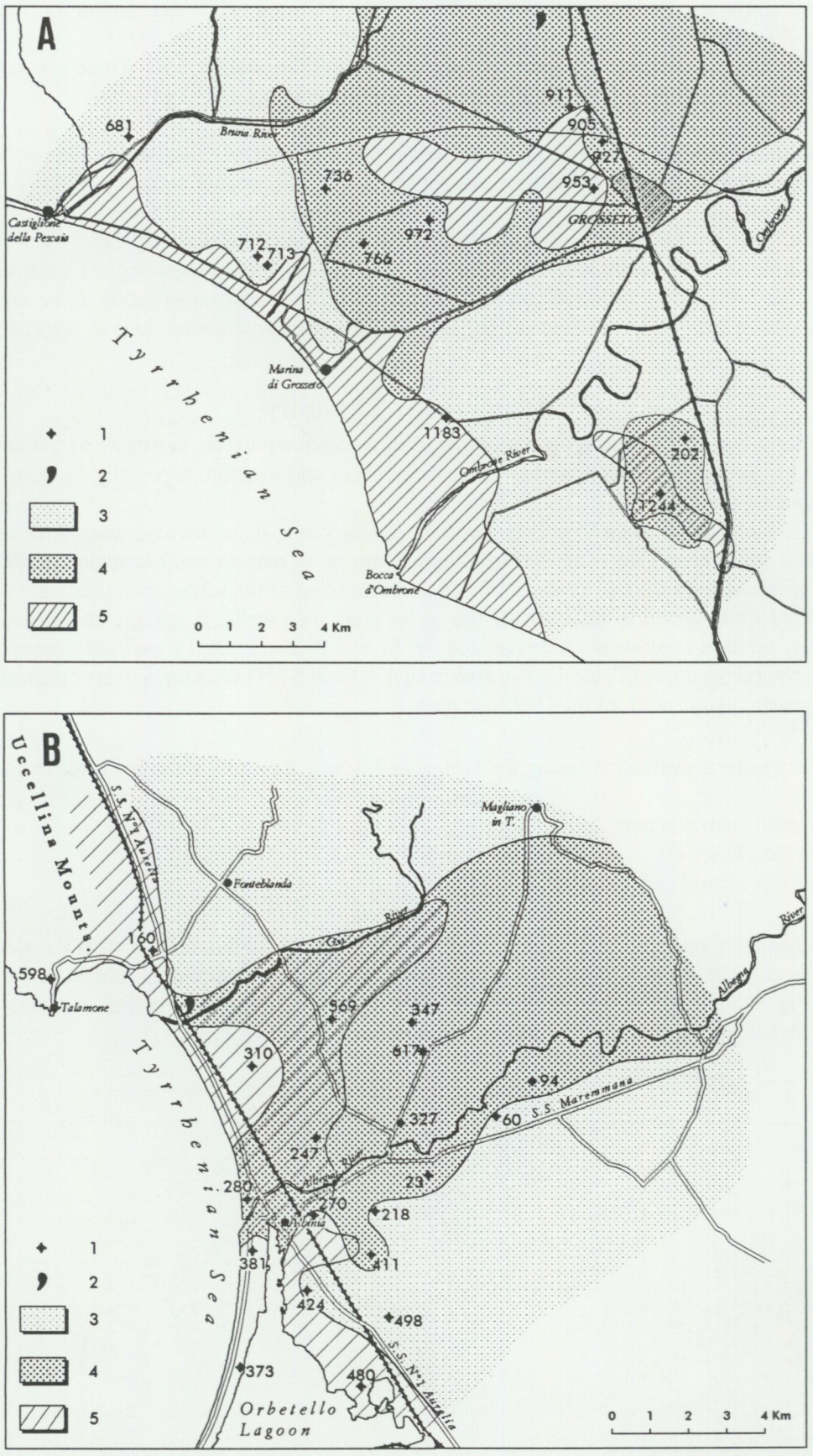


Fig. 7 - Chemistry of groundwaters in the Grosseto Plain (A), and in the Albegna Plain (B). 1) Well sample. 2) Thermal spring. 3) Ca-HCO_3 waters. 4) Ca-SO_4 waters. 5) Na-Cl waters.

The alkaline-earth sulfate waters are the most prevalent, and mainly in the north-central part of the Grosseto plain. The electrical conductivity and hence TDS values are also high. The chemistry of these waters can be attributed to the following mechanisms:

- washing away the gypsum formations in the upper part of both basins: this matches the definite sulfate calcium composition of the rivers, that have salinity levels that are totally abnormal for superficial waters;
- rise of thermal waters from the reservoir of Triassic evaporites (Bencini *et al.*, 1977). In the area there are springs with T>35°C; furthermore the mean temperature of the well waters is 19.5°C, approximately 3° higher than what we would calculate on the basis of the normal geothermal gradient.

The alkaline-earth chloride waters are more difficult to interpret especially since various percentages of other basic elements create a chemical family that is anything but homogenous.
In any event inverse exchange processes between sea and clayey waters (Na^++ Ca-X → Ca^{2+} + Na-X, Appelo & Geirnaert, 1983), and mixing mechanisms and/or aging processes of infiltration waters which evolve according to the well known sequence HCO_3^- → HCO_3^- + SO_4^{2-} → SO_4^{2-} + Cl^- → Cl^- have an evident impact on their composition.

Isotopic analyses performed mainly on the waters from inland wells, where the marine water intrusion does not seem to arrive also made an important contribution to interpreting the findings. For example, the Cl - $\delta\,^2H$ and Cl - $\delta\,^{18}O$ (Figs. 8 and 9) reveal a tetrapolar system with:
a) a local recharging pole: direct infiltration, even from irrigation, or losses from rivers (samples 60, 681, 905);
2) a pole of paleowaters that represent regional recharging and which are vehicled very slowly in the deep confined aquifers (766, 972);
3) a pole of deep thermal waters (911);
4) a "marine" pole, that of current or fossil sea water (1183).
The system seems to be further complicated by the fact that these terms may overlap and some specimens seem related to more than one pole.

Table 1 - Isotopic composition, δ.1000, Cl content, ppm, and Cl/Br of the well waters of the studied area.

samp.	Cl	^3H	^2H	^{18}O	^{13}C	^{14}C	$^{34}S(SO_4)$	$^{18}O(SO_4)$	Cl/Br
60	586.18	7.8±1.2	-35.7	-5.78					158
94		7.6±1.1	-38.3	-5.75					
247	1576		-33.6	-5.46					200
270	1279.95	3.2±1.1	-35.5	-5.57	-11.34	32.1±2.6	16.43	12.22	165
347	249.9	1.0±0.9	-34.9	-5.63	-11.05				223
411	570.15	1.1±1.0	-35.1	-5.8					210
617	145.08		-34.8	-5.45	-12.2	76.4±3.8	6.46	13.28	279
681	97.65	7.0±1.2	-37	-6.1	-12.46				192
738	181.65	<1.0	-39.2	-6.19	-6.91		16.27	16.93	249
766	225.4	<0.5	-40.9	-6.53	-4.97	<2	16.83	16.83	248
905	285.37	3.7±1.0	-31.6	-5.43					352
911	358.05	2.7±0.9	-32.7	-4.87	-12.15	34.4±3.8	15.09	15.85	385
927	272.97		-34.7	-5.51	-13.55	62.3±4.2			290
953	437.81	7.8±1.3	-36.6	-5.79					600
972	178.15	<0.8	-41	-6.47	-6.42				241
1183	1007.84	<1.2	-38.3	-6.45					271
1202	646.96	5.8±1.0	-35.4	-5.59	-10.89				
1244	148.05		-38.2	-5.96					290

An analysis of the Cl/Br ratio (Fig. 10) shows that only few waters exceed the sea water ratio. The high Cl/Br ratio of these waters could be explained by the dissolution of halite. Since there are no halite saturated fluids in Tuscany, the Cl enrichment may be explained by deep geothermal additions, since these are the same waters that in Figs. 8 and 9 appear to be related to the thermal pole.
Most of the samples, however, reveal Br enrichment with respect to sea water (Cl/Br ratio < 290). This

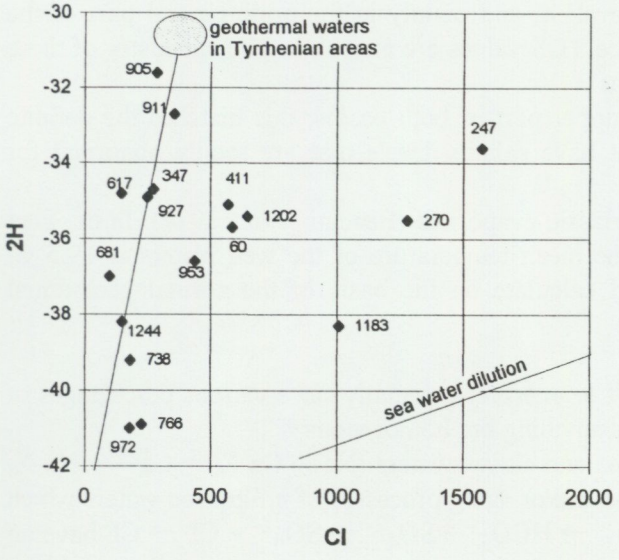


Fig. 8 - Correlation Cl - $\delta^{2}H$ for the groundwaters of the studied area.

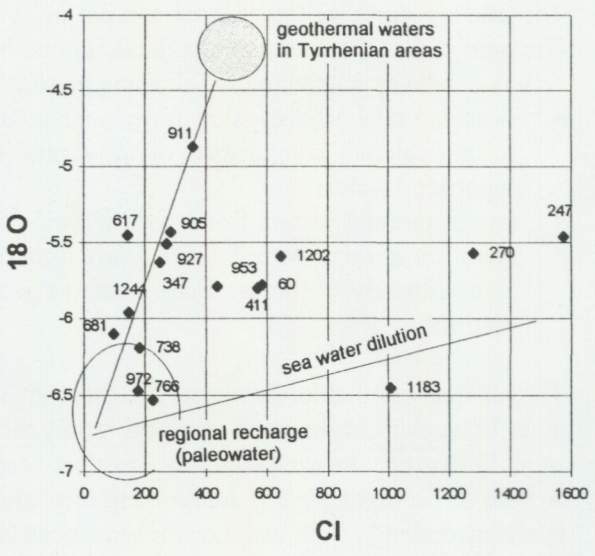


Fig. 9 - Correlation Cl - $\delta^{18}O$ for the groundwaters of the studied area.

feature may be due to precipitation (with rainfall Cl/Br contents that can vary locally), and to two other reasons as well:

a) the effect of a secondary brine that follows halite precipitation (the ratio is approximately 175)

b) remobilization of a residual fluid subject to ultrafiltration phenomena.

Both of these hypotheses seem compatible with a mechanism that mobilizes marine water trapped in the sediments by underground flow. As we mentioned earlier, the sedimentary evolution of the two plains fits in with this hypothesis.

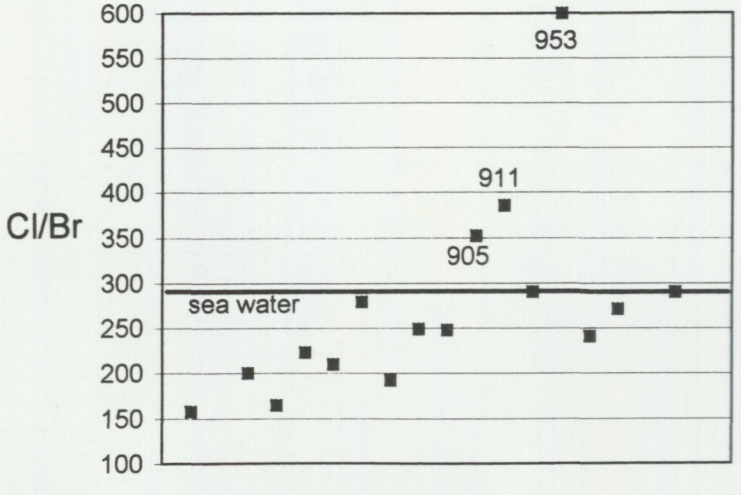


Fig. 10 - Cl/Br ratio for some waters of the studied area.

Groundwater salinization mechanisms and possible remedies

The salinization of groundwater is caused by:

1. marine water intrusion regarding a coastal belt 0.5 - 2.5 km wide. The width is greater in the areas where campsite and summer home wells are concentrated. The fresh water-salt water interface has been reconstructed through electrical conductivity measured with GEONICS electromagnetic equipment (2903 measurements) and through 177 vertical soundings (Fig. 11). The reconstruction

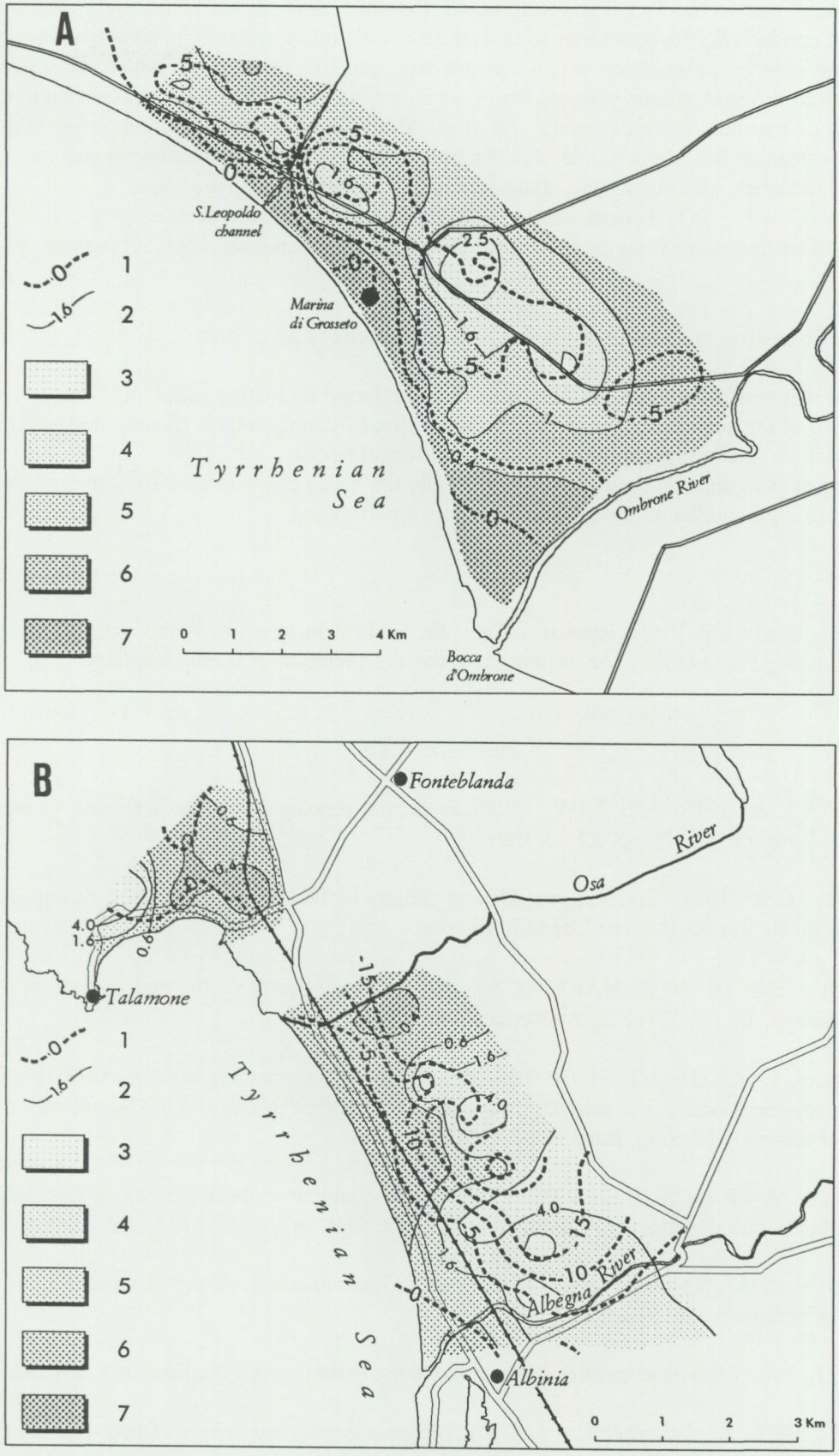


Fig. 11 - Reconstruction of the fresh water - salt water interface in the Grosseto Plain (A), and in the Albegna Plain (B). 1) Lines of equal depth of the interface, m. 2) Electrical resistivity of the layer under the interface, ohm.m. 3) E.R. over 4.0 ohm.m. 4) E.R. between 4.0 and 1.6 ohm.m. 5) E.R. between 1.6 and 0.6 ohm.m. 6) E.R. between 0.6 and 0.4 ohm.m. 7) E.R. less than 0.4 ohm.m.

was difficult due to the fact that going inland, the dune sand passes to lagoonal clay which has electrical conductivity levels similar to that of sand with saline water. The problem was solved by measuring induced polarization which changes from positive to negative values when going from sand with fresh water to sand with sea water, while the inversion does not occur passing to clay;

2. intrusion of marine water into rivers and artificial channels. In the Ombrone River delta marine water also reaches the interdunal depressions which are now pervious due to delta erosion;
3. chemical evolution of groundwater, characterized by cation exchange processes;
4. mixing with Ca-Mg-SO_4 thermal waters rising from the carbonatic reservoirs;
5. seepage of sulfate water from the rivers which flow in the gypsum outcrops of the upper part of the basins.

The following measures are suggested for stopping groundwater salinization:

- dramatic reduction of pumping in the coastal dunes affected by marine water intrusion;
- recharging of the coastal aquifer in the Ombrone River Plain through a channel dug parallel to the coast to which river water can be diverted during winter floods;
- reduction of pumping for agricultural purposes in the areas characterized by a groundwater TDS higher than 2g/l, and the use of superficial waters for irrigation.

Thanks

The authors wish to thank Prof. Gianmaria Zuppi for his help in interpreting the isotopic findings, and Dr. Elena Gimenez Forcada for her contribution to the interpretation of water chemistry.

REFERENCES

APPELO, C.A.J. & GEIRNAERT, W., 1983: Processes accompanying the intrusion of salt water. Geol. Appl. e Idrogeol., 13 (2), pp. 29-40. Bari.

BEEMSTER, J.G.R., 1987: Soil and groundwater salinity in the Grosseto Plain and its implication for irrigation. Inedit Report for Regione Toscana, Firenze.

BENCINI, A., DUCHI, V, & MARTINI, M., 1977: Geochemistry of thermal springs of Tuscany. Chemical Geology, 19, pp. 229-252, Amsterdam.

BENCINI, A. & PRANZINI, G., 1992: The salinization of groundwaters in Grosseto Plain (Tuscany; Italy). In "Study and modelling of saltwater intrusion into aquifers" (Custodio & Galofré editors)" Proc. of Salt Water Intrusion Meeting, Barcelona, 1992, pp. 161-175.

BRAVETTI, L. & PRANZINI, G., 1988: L'evoluzione quaternaria della pianura di Grosseto: prima interpretazione dei dati di sottosuolo. Geogr. Fis. e Dinam. Quatern., 1987, pp. 85-92. Torino.

CUSTODIO, E., 1987: "Hydrochemistry and tracers". Groundwater problems in coastal areas. Studies and reports in hydrology. pp. 212-269, UNESCO.

DREVER, J.I., 1982: The geochemistry of natural waters. Prentice-Hall, Englewood Cliffs, New York.

MAZOR, E., 1991: Applied chemical and isotope groundwater hydrology. Open University Press, Buchingham.

HYDROGEOLOGICAL AND HYDROCHEMICAL STUDY OF THE COASTAL PLAINS OF SAIDIA AND BOU-AREG (NORTH-EASTERN MOROCCO)

K. Walraevens, N. El Halimi, A. Chaouni Alia, E. Beeuwsaert & W. De Breuck
Laboratory for Applied Geology and Hydrogeology, University of Ghent, Belgium

Introduction

North-eastern Morocco has a mediterranean climate, with low rainfall, which is irregularly distributed both within the year and over succeeding years. The climate is very dry in summer, and moderately to weakly humid in winter. Annual rainfall over a 15 year's period has revealed 1983 to be the dryest year, with 116.3 mm, while 1986 was the most humid one, with 412.6 mm. The average over this period amounts to 278.6 mm/year.

The coastal area shows groundwater salinization, which is due to the presence of connate salt water, to sea water intrusion and also to the infiltration of irrigation water, concentrated by evaporation. Low salinity water resources are scarce, and should be carefully managed.

The present study focuses on two aquifer systems in the Mediterranean coastal area of north-eastern Morocco (fig. 1). One is situated in the most easterly coastal plain, up to the Algerian border: the eastern part of Saidia plain. The other one is situated more towards the west, in Bou-Areg plain, behind the lagoon of Bou-Areg Sebkha, which is separated from Mediterranean Sea by a 25 km long, narrow strip of land. A 3-4 km wide gully cutting through it, assures contact between the lagoon and the sea. Saidia plain is mostly dispersely populated, with some agricultural activity, while the city of Saidia is a summer resort. In the western part, outside the studied area, a large sea fish farm is causing extensive groundwater salinization by leakage from sea water filled basins. Bou-Areg plain is largely brought under intensive agriculture and horticulture, thanks to its fertile heavy soils and the implementation of an irrigation system since 1970.

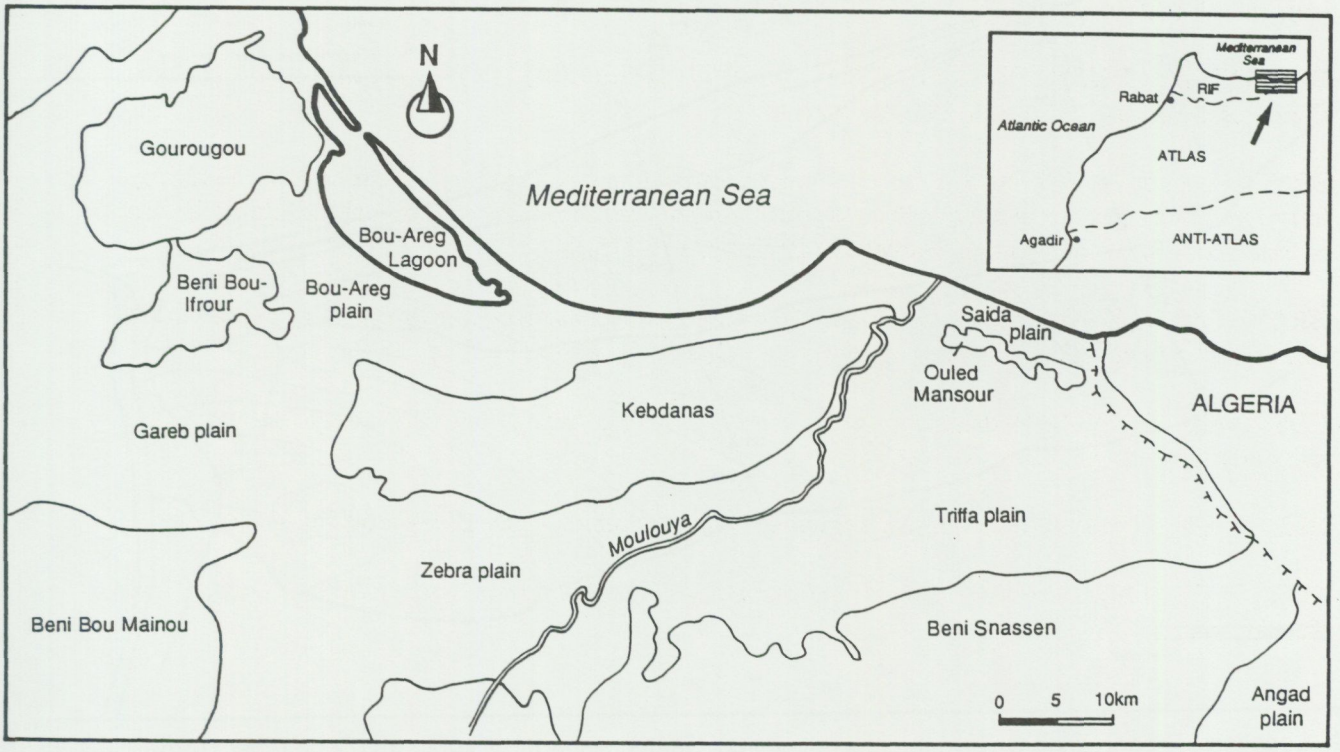


Fig. 1 - Location of study area.

Eastern Saidia plain

Saidia plain (fig. 2) is an elongated area, squeezed in between the Ouled Mansour hills and the sea. To the east, it is bounded by the Algerian border, following the Kiss River. From north to south, several parts, occurring as longitudinal, parallel strips, can be distinguished (e.g. fig. 3): the shore, the northern dunes, the flat of Sareg, the southern dunes, and finally the flat of Merzakan,up to the Ouled Mansour hills.

STRUCTURE OF AQUIFER SYSTEM: The aquifer system has been investigated by means of borings at 13 sites (fig. 2) (El Halimi, in prep.; El Halimi et al., in press). Two transversal SSW-NNE trending cross-sections (AB and CD) have been established (fig. 3 and 4). The aquifer system is composed of Quaternary sediments. Its base is consisting of marls and marly clays, probably of Miocene age. This substratum is overlain by unit X, containing clayey, marly or peaty fine sand with shell fragments. Next follows unit Y, consisting of fine to medium sand with shells. It is overlain by unit Y', consisting of peat and sandy clay to marly sand. The overlying unit Z consists of fine, medium to coarse sand with shell fragments. In most of the area, unit Z reaches the surface. This is the case on the shore and in both dune belts. In the flats of Sareg and Merzakan, a superficial unit Z', composed of silty clay, occurs on top of unit Z.
The units X, Y and Z are considered to be pervious, X showing a lower hydraulic conductivity than Y and Z. Units Y' and Z' are considered to be semi-pervious. Towards the west (profile AB), the pervious character of unit X is still decreasing, with its clay, marl and peat content increasing, as well as its thickness. This causes the hydraulic conductivity of the aquifer system to decrease towards the west.

PIEZOMETRIC MAP: The piezometric map, based on measurements performed in September 1995, is shown in figure 2. The highest heads are recorded in the south-eastern part, where the adjacent Ouled Mansour hills reach the highest altitudes. Groundwater flow occurs towards the north-west. Locally the heads are increased at locations at dune belts. Local lowering of the water table is indicating groundwater abstraction from wells.

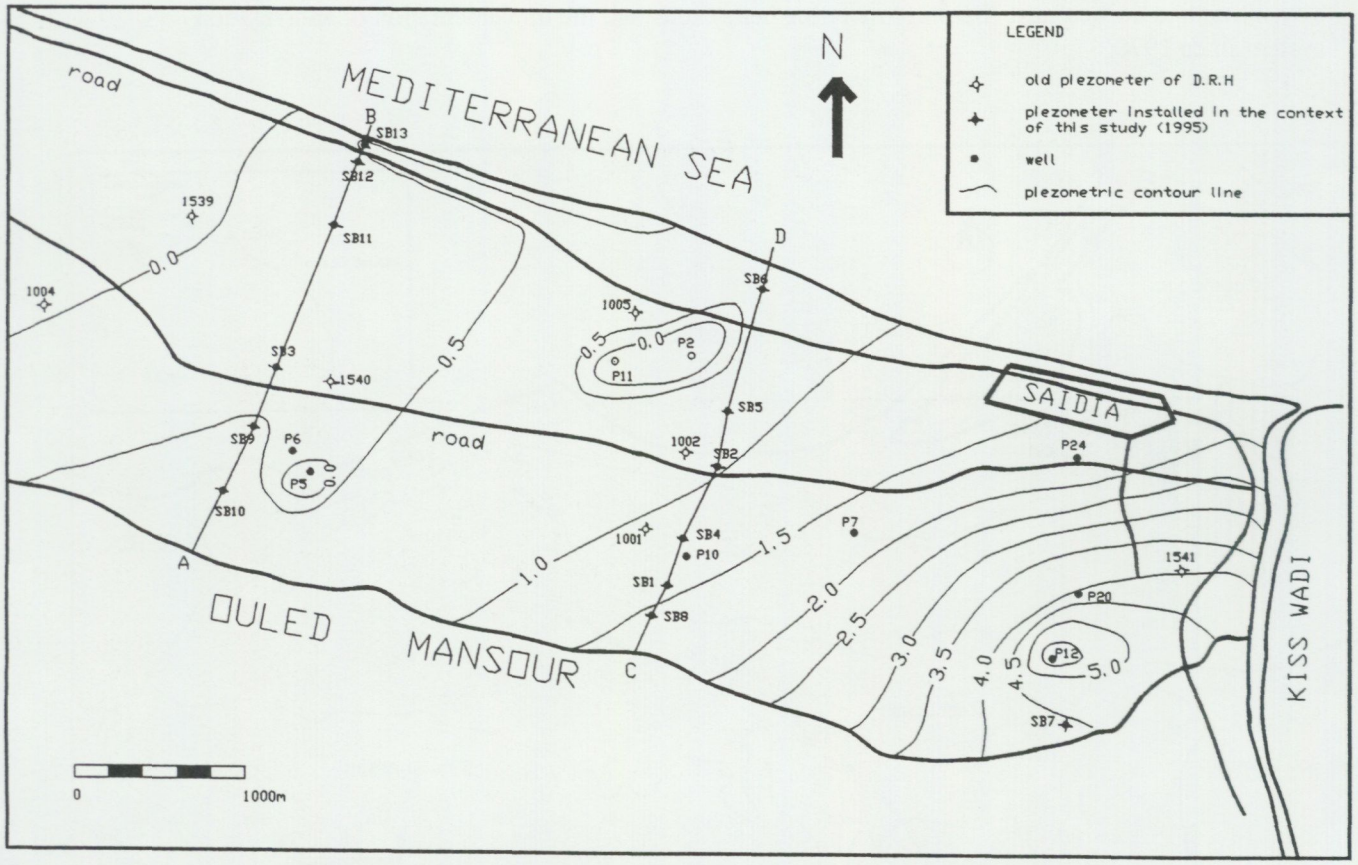


Fig. 2 - Location of observation wells in the coastal plain of Saidia; water table contours (September 1995).

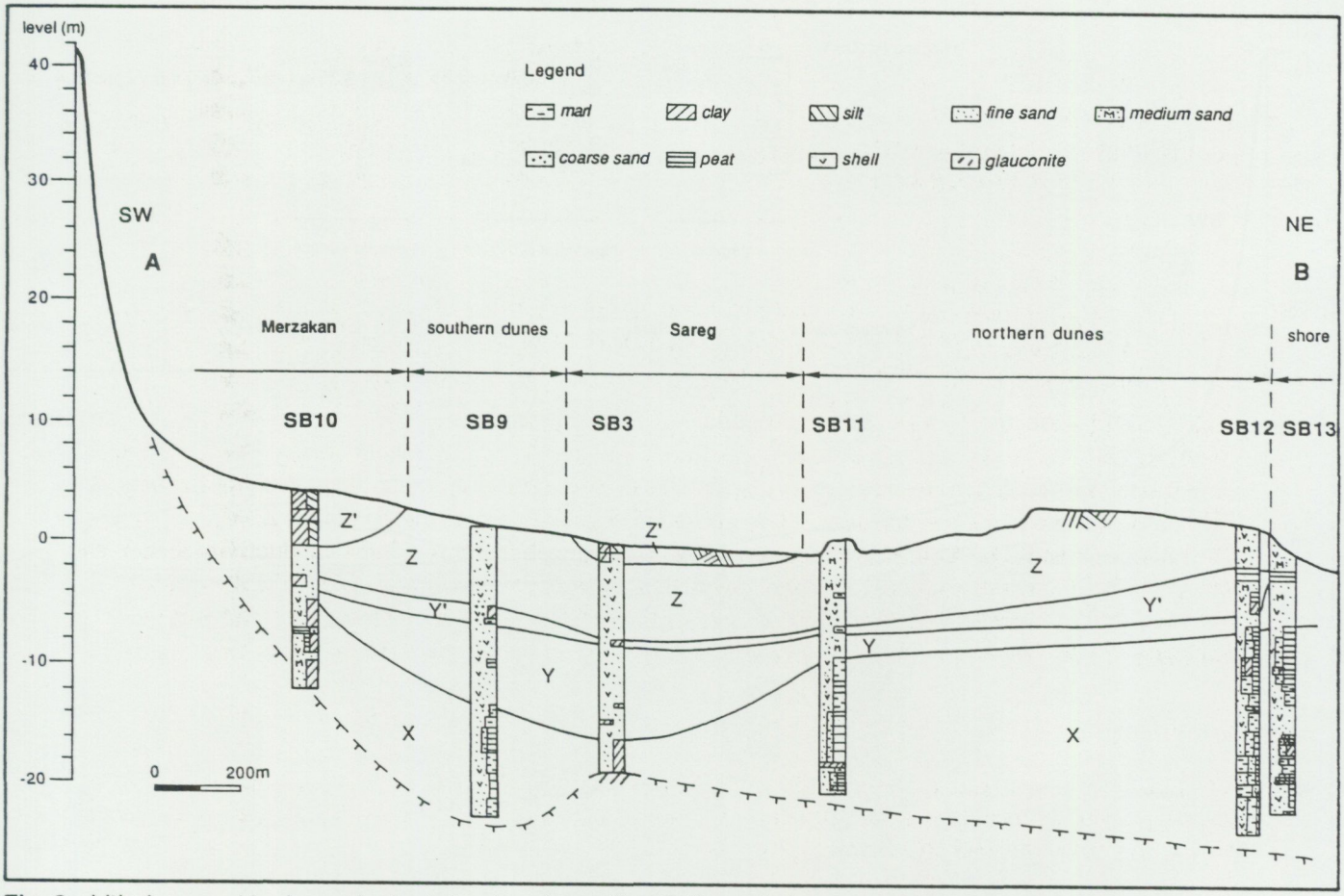


Fig. 3 - Lithology and hydrogeological structure in profile AB through the coastal plain of Saidia.

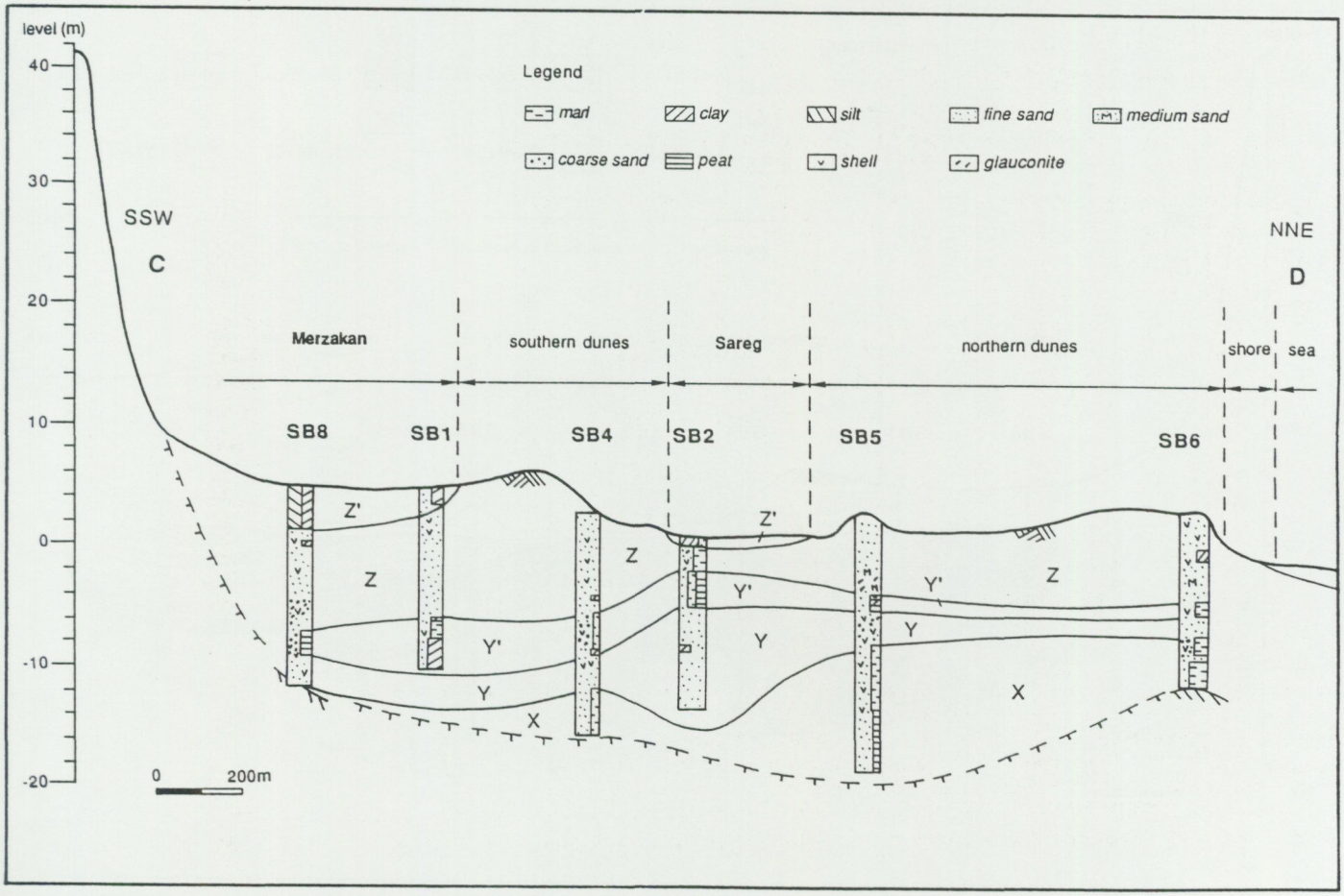


Fig. 4 - Lithology and hydrogeological structure in profile CD through the coastal plain of Saidia.

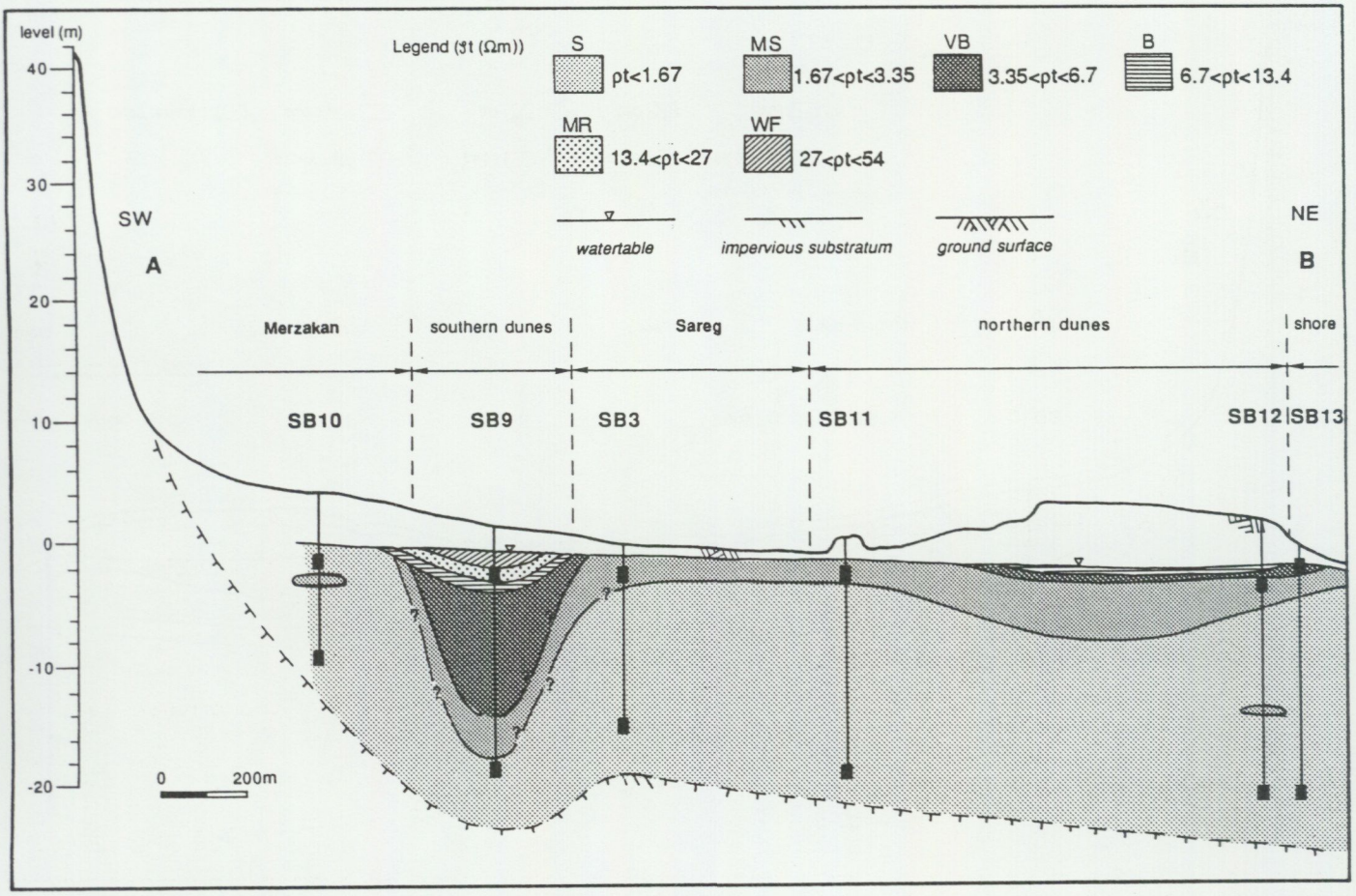


Fig. 5 - Resistivity profile AB through the coastal plain of Saidia.

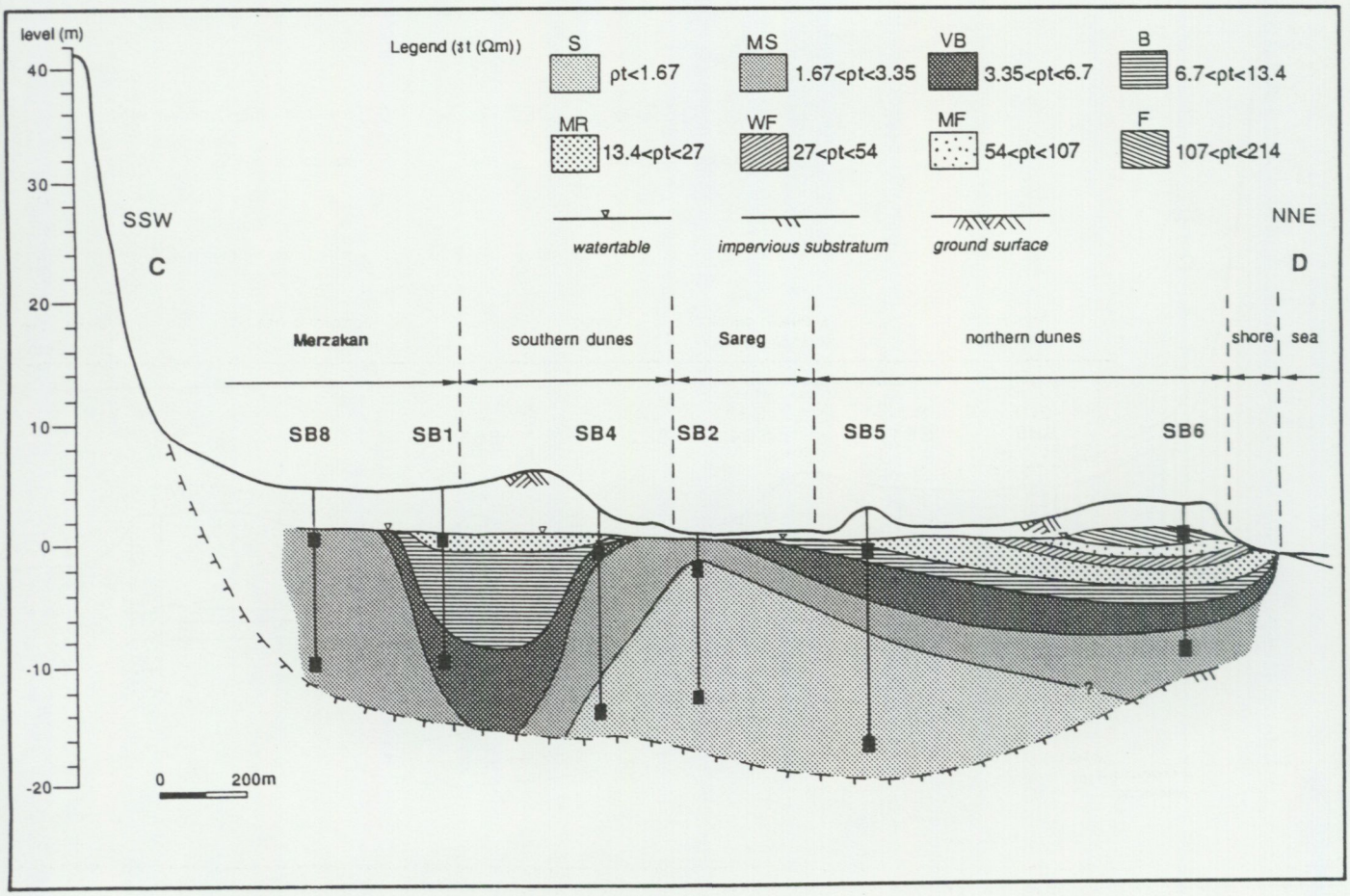


Fig. 6 - Resistivity profile CD through the coastal plain of Saidia.

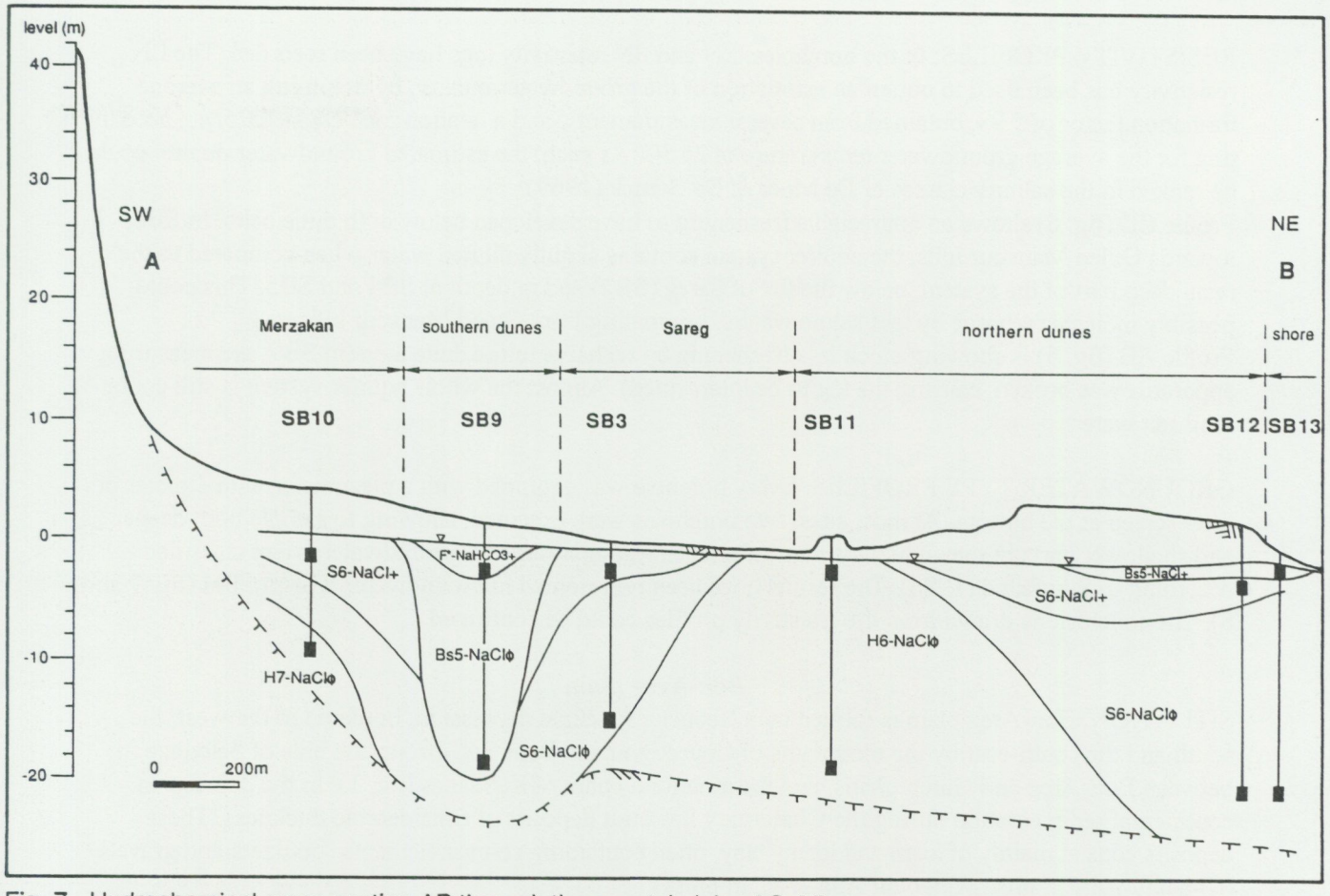


Fig. 7 - Hydrochemical cross-section AB through the coastal plain of Saidia.

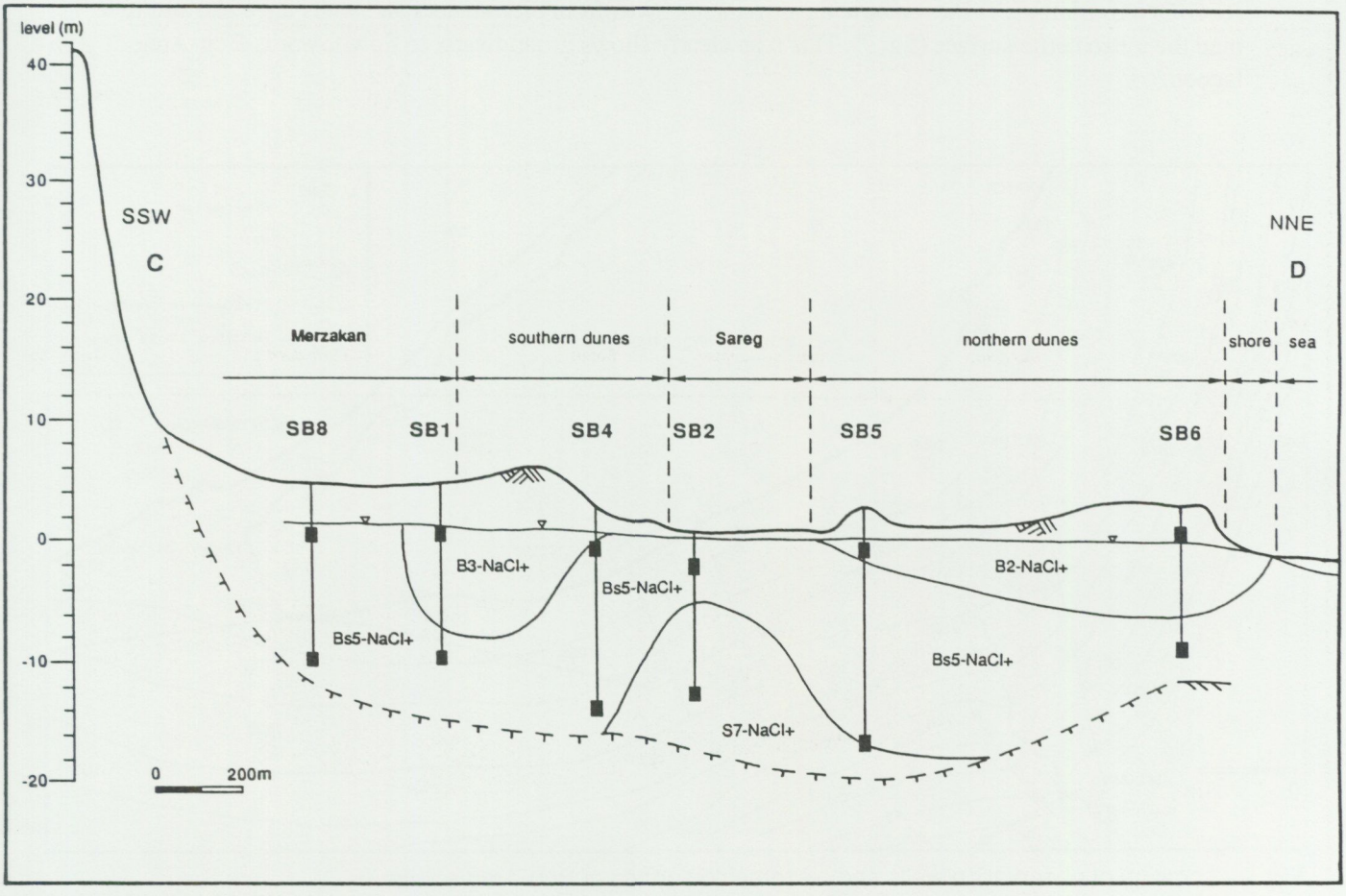


Fig. 8 - Hydrochemical cross-section CD through the coastal plain of Saidia.

RESISTIVITY PROFILES: In the boreholes, LN and SN resistivity logs have been recorded. The LN resistivity has been used to obtain an estimation of the groundwater quality, by assuming an average formation factor of 5.93, obtained from several measurements, and a relation for TDS = $7225/\rho_w$, accounting for the average groundwater temperature of 25 °C. As such, the estimated groundwater quality could be ranked in the salinity classes of De Moor & De Breuck (1969).
Profile CD (fig. 6) shows an appreciable freshening to have developed below both dune belts. In SB8, towards Ouled Mansour hills, the aquifer system contains slightly diluted water when compared to the main deep part of the system, below the flat of Sareg (SB2) and in depth at SB4 and SB5. This could possibly indicate recharge by less saline waters, originating from Ouled Mansour hills.
Profile AB (fig. 5) is showing much less freshening by recharge in the dune area (in SB9, the measuring apparatus was broken, causing the log to be interrupted). Almost the whole aquifer system is still containing salt water.

GROUNDWATER TYPE PROFILES: Every borehole was equipped with a piezometer with 1 meter of filter screen at the bottom. At most sites, two boreholes were executed, allowing to sample both deeper and shallower parts of the aquifer system. After chemical analyses, the groundwaters were classified according to Stuyfzand (1986). The results have been represented in groundwater type profiles (fig. 7 and 8). The conclusions drawn from the resistivity profiles could be confirmed.

Bou-Areg plain

SITUATION: Bou-Areg plain is formed by a Neogene synclinal depression, bordered to the west, the south and the south-east by the mountains of Gourougou and Beni Bou-Ifrour, the hills of Selouane in between Bou-Areg and Gareb plains, and the mountain chain of Kebdanas (fig. 1). In the depression, continental sedimentation during the Quaternary has built deposits of considerable thickness. These deposits consist mainly of loam and loamy clay, often containing coarser elements (boulders and gravels) (Chaouni Alia, in prep.; Chaouni Alia et al., in press).

REGIONAL SURVEY: Piezometric measurements taken from piezometers and wells have allowed to map the piezometric surface (fig. 9). This map clearly shows groundwater to flow towards Bou-Areg lagoon.

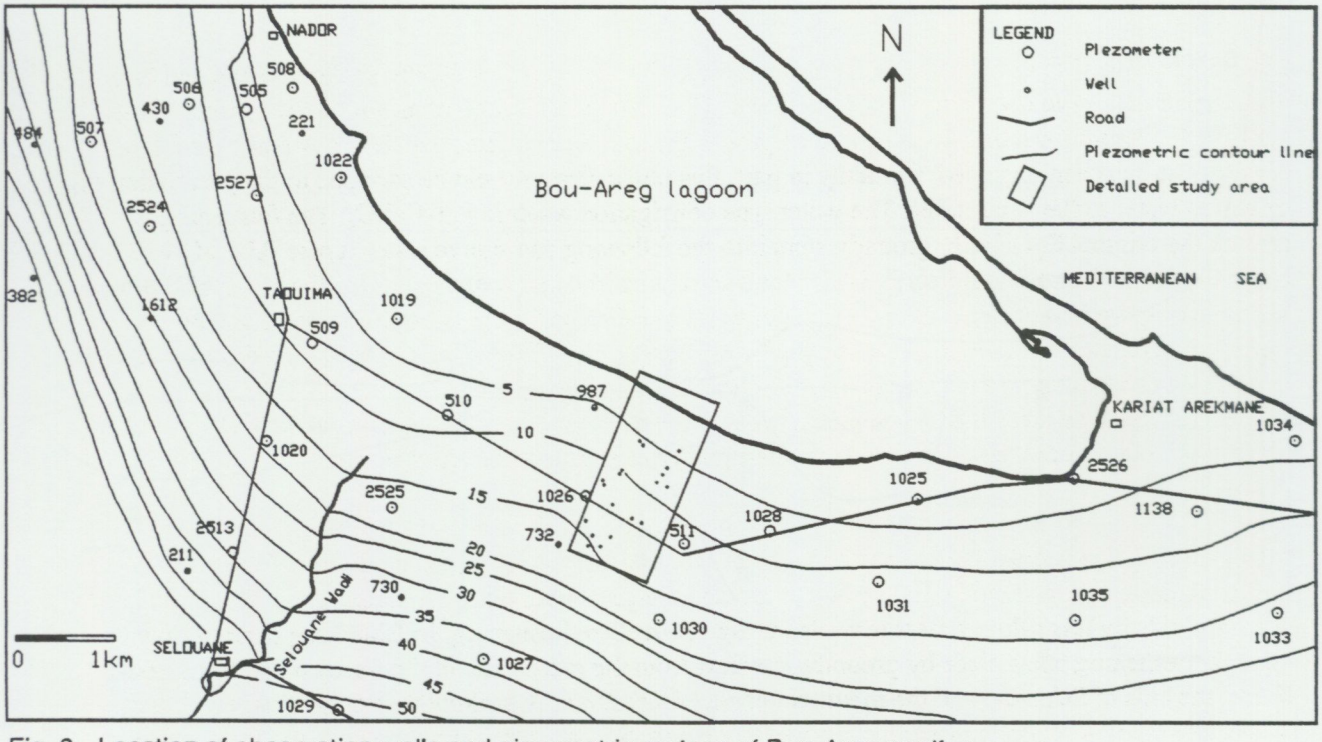


Fig. 9 - Location of observation wells and piezometric surface of Bou-Areg aquifer.

The regional distribution of groundwater types (according to the Stuyfzand, 1986, classification), based on sampling in 1963, has been represented in figure 10. A slow regional freshening is indicated, progressing from the borders in the west, the south and the south-east, towards the lagoon. In the south, along and east of Selouane River, freshening has apparently been more intensive, leading to a cation exchange equilibrium (0) in the water type.

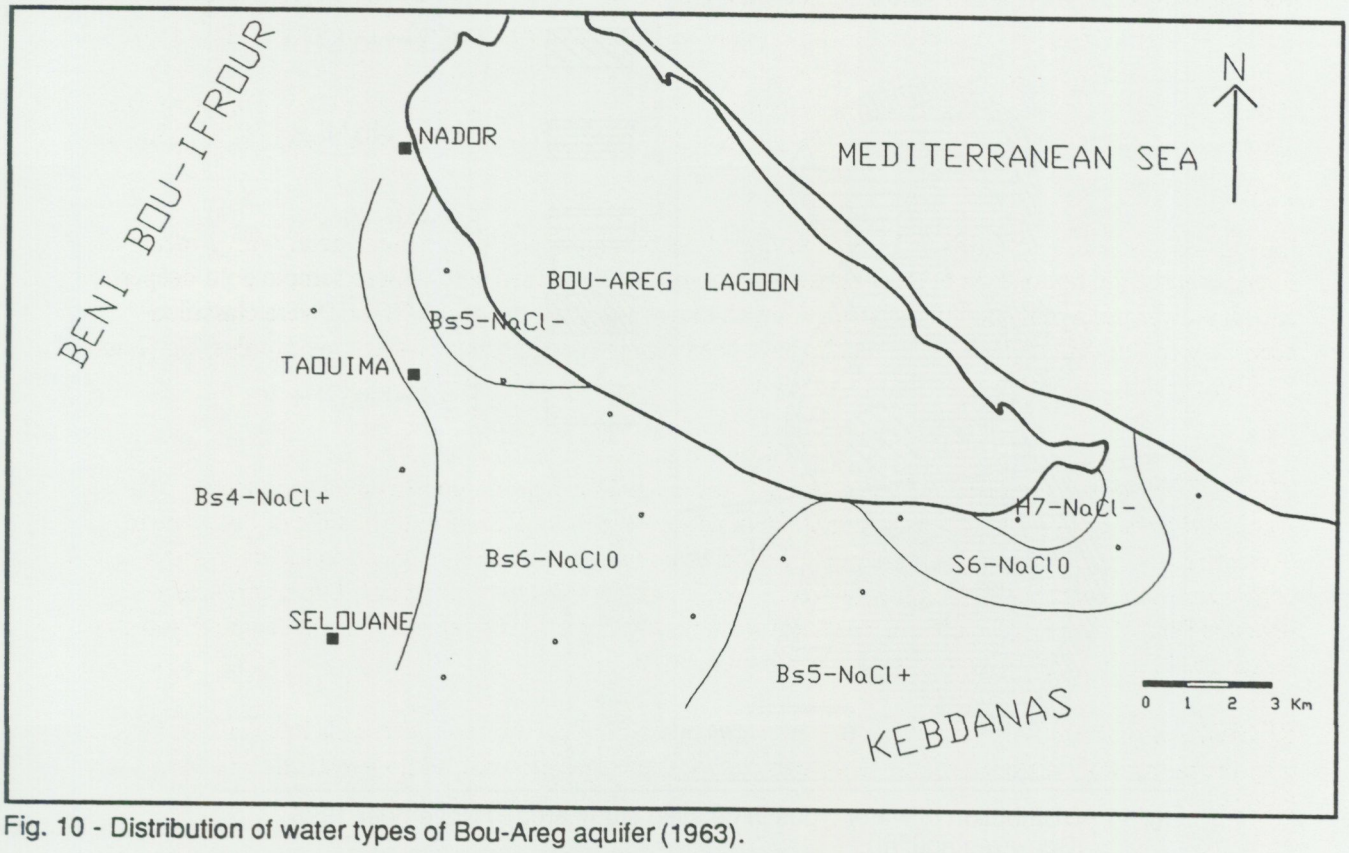


Fig. 10 - Distribution of water types of Bou-Areg aquifer (1963).

DETAILED STUDY: In a detailed study area (indicated in fig. 9), all available (shallow) wells and two irrigation waters have been sampled in November 1995. The distribution of groundwater types is shown is figure 11. Against the background of the regional groundwater quality, which is B_s4-NaCl+, a freshening tongue has been observed. Certainly in part, this phenomenon could be ascribed to the percolation of irrigation water to the water table. The water type of irrigation water is F_b3-$CaSO_4$. The freshening is turning the original B_s4-NaCl+ groundwaters into the following successive water types: B3-NaCl+, B3-NaMix+, F_b3-NaMix+ and finally F_b3-MgMix+. In stead of the last water type, also the F_b3-$NaSO_4$+ type has been observed. Important cation exchange is clearly reflected by the groundwater type and by the magnitude of the cation exchange parameter $(Na+K+Mg)_{measured}$ - 1.061 Cl (in meq/l) (Stuyfzand, 1986), which is ranging in between +6.5 and +50 in the studied groundwaters.
Figure 12 shows the distribution of electrical conductivity, Cl^--content, Na^+-content and HCO_3^--content in the groundwater. These parameters are confirming the freshening tendency of figure 11.

Conclusion

Moderate recharge is inducing a slow freshening in the coastal plains of Saidia and Bou-Areg.
In Saidia plain, this freshening mainly results from recharge in both dune belts. Recharge from Ouled Mansour hills by less saline waters may also bring about some freshening. In Bou-Areg plain, a slow regional freshening takes place by groundwater flow from the mountains of Gourougou and Beni Bou-Ifrour, the hills of Selouane and the mountain chain of Kebdanas. A strikingly stronger freshening is observed locally. It is probably (partly) related to the percolation of irrigation water to the water table.

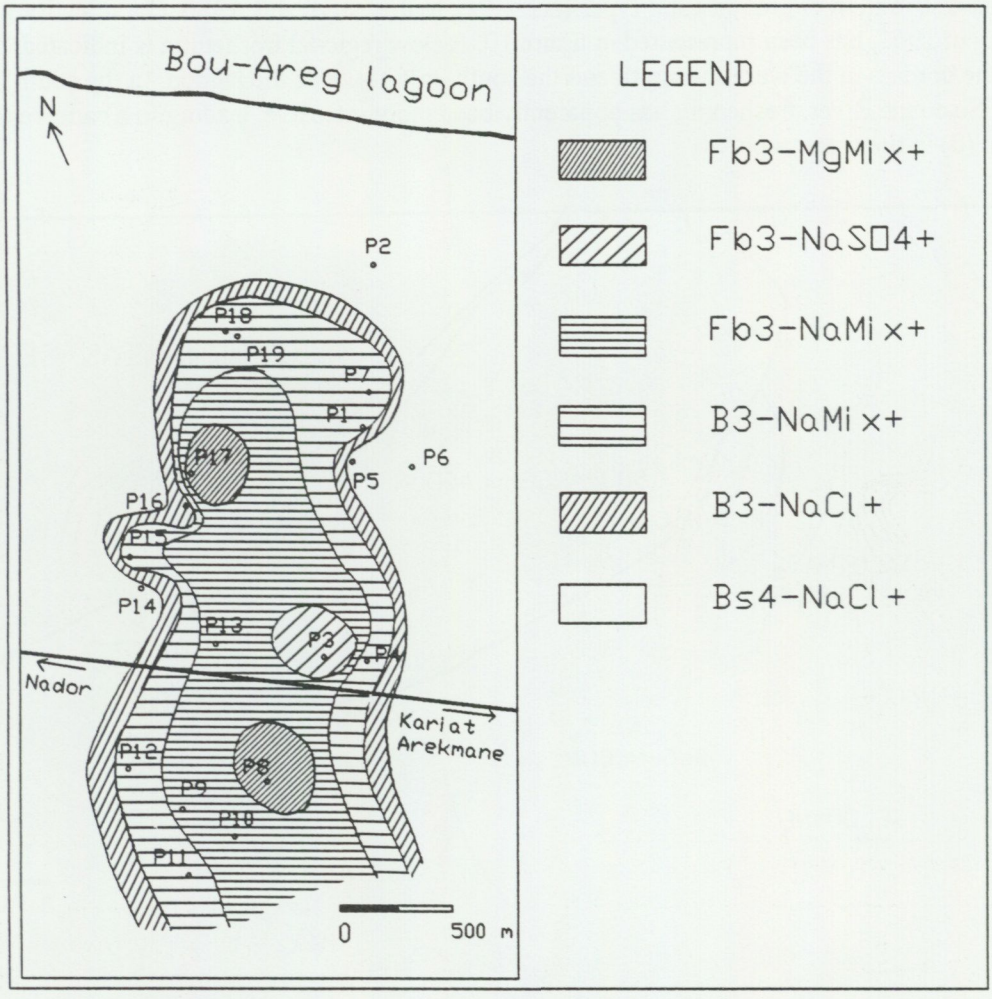


Fig. 11 - Distribution of water types in detailed study area in November 1995 (Bou-Areg aquifer).

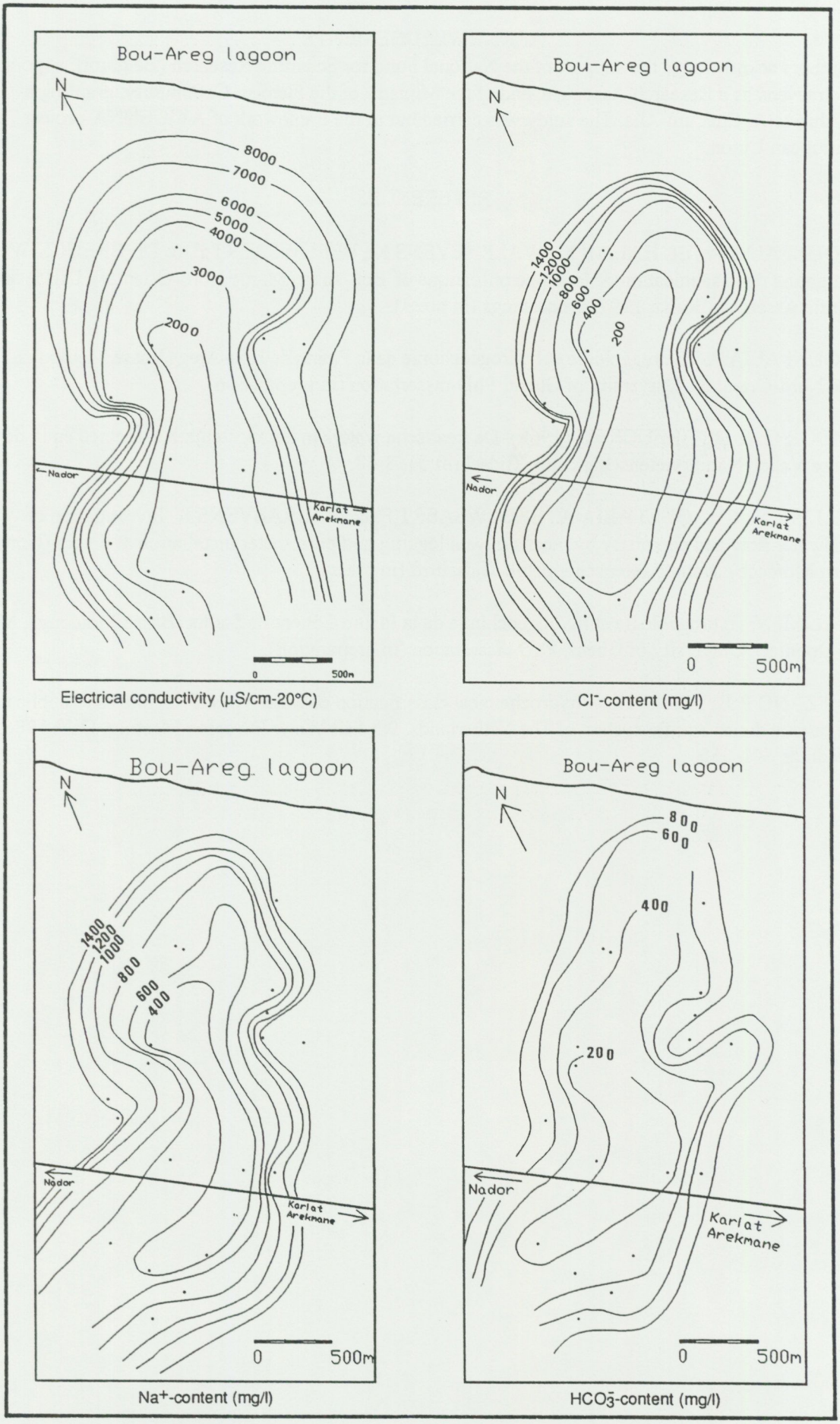


Fig. 12 - Chemical parameters in groundwater of detailed study area in November 1995 (Bou-Areg aquifer).

ACKNOWLEDGEMENTS

The authors acknowledge the support of the National Fund for Scientific Research (Belgium), appointing K. Walraevens as a Research Associate, and of the Ministry of the Flemish Community, granting a fellowship to A. Chaouni Alia. The study was carried out in the framework of AVICENNA-project 73 of the European Union.

REFERENCES

CHAOUNI ALIA A., EL HALIMI N., WALRAEVENS K., BEEUWSAERT E. & DE BREUCK W. Investigation de la salinisation de la nappe phréatique de Bou-Areg (Maroc Nord-Oriental). IAHS, 5th Scientific Assembly, Rabat 1997. Proceedings (in press).

CHAOUNI ALIA A. Hydrogéologie et hydrogéochimie de la Plaine de Bou-Areg (Basse Moulouya, Maroc Nord-Oriental). University of Ghent, PhD-dissertation (in preparation).

DE MOOR G. & DE BREUCK W. (1969). De freatische waters in het Oostelijk Kustgebied en in de Vlaamse Vallei. Natuurwetenschappelijk Tijdschrift 51, 3-68.

EL HALIMI N., CHAOUNI ALIA A., BEEUWSAERT E. & WALRAEVENS K. Investigation of groundwater flow and chemistry by means of well logging and piezometer installation at Saidia (North-Eastern Morocco). Natuurwetenschappelijk Tijdschrift (in press).

EL HALIMI N. Hydrogéologie et hydrogéochimie de la Plaine Côtière de Saidia (Basse Moulouya, Maroc Nord-Oriental). University of Ghent, PhD-dissertation (in preparation).

STUYFZAND P.J. (1986). A new hydrochemical classification of watertypes: Principles and application to the coastal dunes aquifer system of The Netherlands. 9th Salt Water Intrusion Meeting, Delft 1986. Proceedings 641-655.

Simulation of Seawater Intrusion in Libya

Sadeg, S.A. and Karahanoglu, N.
Geological Engineering Department, Middle East Technical University
06531, Ankara - TURKEY

Libya is one of the Southern Mediterranean countries with a shoreline extent of 1900 km where the coastal aquifers are under seawater intrusion risk. The fertile lands of the Gefara plain in the northwest and Jabal Al Akhder in the northeast include more than 80 % of the agricultural activity that entirely depends on rainfall and the groundwater. In recent years, the risk of seawater intrusion is continually threatening coastal part of the Gefara plain that forms one of the most economically significant area in the country.

The potential problem is investigated thoroughly and present position of the seawater intrusion is clearly defined. At present seawater intrusion covers an area of about 250 km2 and is going to extend in the coastal area of the Tripoli region. In order to assess impact of the existing or proposed human activities on the seawater intrusion, this research has been initiated to simulate the problem in the area. A two-dimensional, areal, fully-coupled finite element model is introduced to simulate the flow of freshwater and the diffusion of salt concentration.

Introduction

Due to its semi-desertic climate groundwater is the main source for potable, industrial and irrigation water in Libya. Inevitably, groundwater extraction has been in excess of replenishment due to rapid increase in agricultural and economical activities in the last twenty-five years. This has resulted water level declines and quality deterioration including invasion of seawater along the coastal regions.

It is claimed that seawater contamination in Libya dates back to 1930s after construction of the Salt Canal by Italian occupation. Cedestrom and Bastaiola (1960) were the first researchers who studied water resources in Tripoli area and they stated that saltwater intrusion affected groundwater resources near the Salt Canal constructed by Italian occupation. Later several studies have been performed in order to investigate seawater intrusion in Libya. Kruseman and Floegel (1978) concluded that in the first few kilometers along the coast, the extracted groundwater was partially replaced by intruding seawater. Floegel (1979) conducted a seawater intrusion study along the Gefara coast from Zuarah in the west to Khoms in the east. He collected hydrochemical data along fourteen N-S profiles and defined the intruding wedge and the diffused zone in each profile. Five of the profiles were located in the Tripoli area where the maximum contamination was observed at that time. Meludi and Werynski (1980) studied the seawater intrusion problem in Gargaresh-Swani Well Field, which was considered as a source of water supply to the Tripoli area City since 1976. It was concluded that seawater intrusion into the area progressed and it was accelerated by overpumping of groundwater especially at the well field. Krummenacher (1982) included setting up and operation of a digital simulation model as a part of Gefara Plain Water Management Plan Project undertaken by FAO. The model was based on the Thyson-Weber finite difference method for two-dimensional version of the Laplace's equation. Water quality simulations were incorporated into the model, while the dispersion and molecular diffusion were ignored. The model was used to predict future groundwater levels and water quality distribution in Jefara Plain. Backush (1983) applied a 3-D Trescott model to simulate the aquifer system in Gefara plain for both the steady-state and the transient conditions. He proposed a well field to minimize the saltwater intrusion rate into the upper aquifer. He concluded that maximum drawdown occurs in the middle of the simulated area while the minimum lies towards the shoreline and by this design optimum amount of freshwater may be pumped from the aquifer with minimum saltwater intrusion. Bilal (1987) studied the seawater intrusion in Zanzur area, which is located 10 km west of Tripoli City, and used 23 wells for sampling. As a result of his analysis he concluded that the pumping wells used for industry and domestic uses, were the main causes for seawater intrusion into the area.

Shawi and Philbert (1991) concerned only with the upper aquifer in the Tajura area, located 10 km east of the Tripoli City. He collected 123 water samples and he pointed out that increased water demands for social, agricultural and industrial developments made the seawater intrusion to go farther inland in 1990s than in 1980s.

Upon consideration of these studies a research has been initiated to investigate the seawater intrusion in the Gefara plain, where the seawater contamination is more affective as compared to the other regions in Libya. The study area is located in the north central part of the Gefara Plain and it includes the city of Tripoli (Fig. 1). A finite element model is formulated to simulate the flow and seawater intrusion mechanisms in the area and try to propose optimal management strategies to reduce the rate of seawater intrusion.

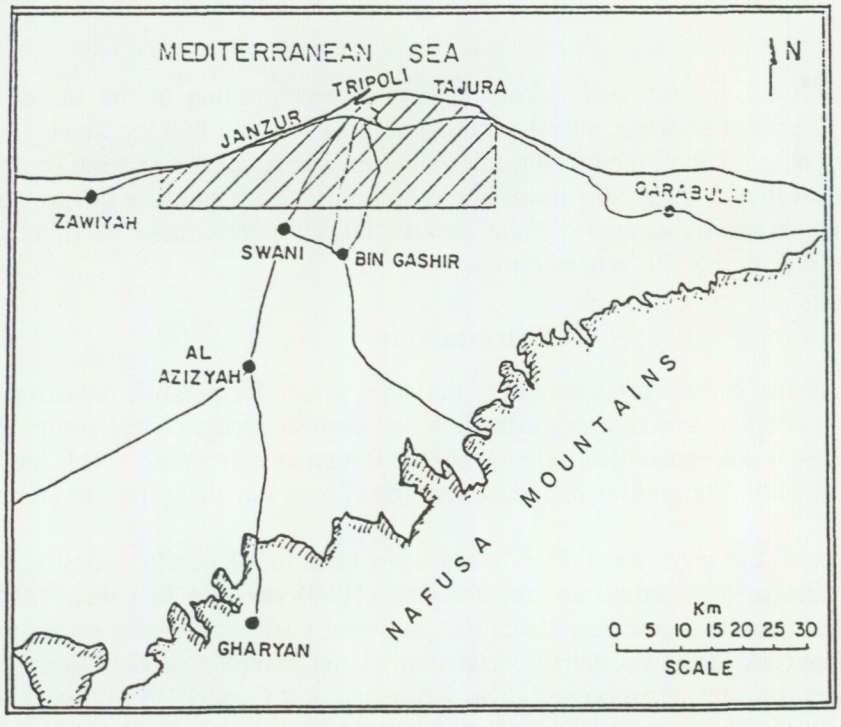


Fig. 1. Location Map of the Study area.

Geological Setting

Gefara Plain forms a flat topography and consists of three parts that are covered by Quaternary deposits. Calcarenites, covered by coastal sandstones and the brown silts of the Gefara Formation form the Coastal strip. Central part of the Gefara Plain stretches from the south end of the coastal strip (10-20 km) to a distance ranging between 60-90 km. Topographic elevation rises gradually toward south and reaches 130 m above mean sea level at the south end. Some of the seasonal streams flow over this region and drain the plateau and they fan out before reaching the sea. Other streams have longer courses and deepen their channels over the plain surface forming Wadis as Wadi Al Majinin, Wadi Ghan and Wadi Zarat. The Central part of the plain is covered mainly by poorly consolidated eolian deposits mixed with brownish silt of the Gefara Formation. The southern border of the Central part interlocks with the Foot Hill strip that is made of fluvial and proluvial coarser sediments. Topography continues to rise in this section and it reaches to elevation of 200 m at the south end of the plain.

Gefara Plain consists of Late Tertiary to Quaternary strata resting on a faulted and tilted Mesozoic basement. Aziziyah fault separates the main Miocene-Quaternary unconfined aquifer from a thin

layer of Quaternary aeolian and wadi deposits in the south. The Ouled Chebbi formation (Permian-Triassic) is the oldest unit in the Gefara plain and is encountered in a few deep groundwater wells in the southern part of the plain. It contains cemented, red, sometimes conglomeratic sandstones with a low permeability at the base and a series of red clays with a few sandstone and dolomitic interbeds at the top. The Ras Hamia formation (Triassic) is known as underlying the whole Gefara plain and its thickness varies in the range of 450-600 m. Ras Hamia formation consists mainly of green, red and black sandy clays and shales with intercalations of red and green, often clayey sandstones. In the study area the formation slopes down to depths far in excess of 1000 m. Aziziyah formation (Fig. 2) consists of dolomitic limestone and limestone and it is present throughout the Gefara plain especially in the western and north central parts. In the area north of Aziziyah fault

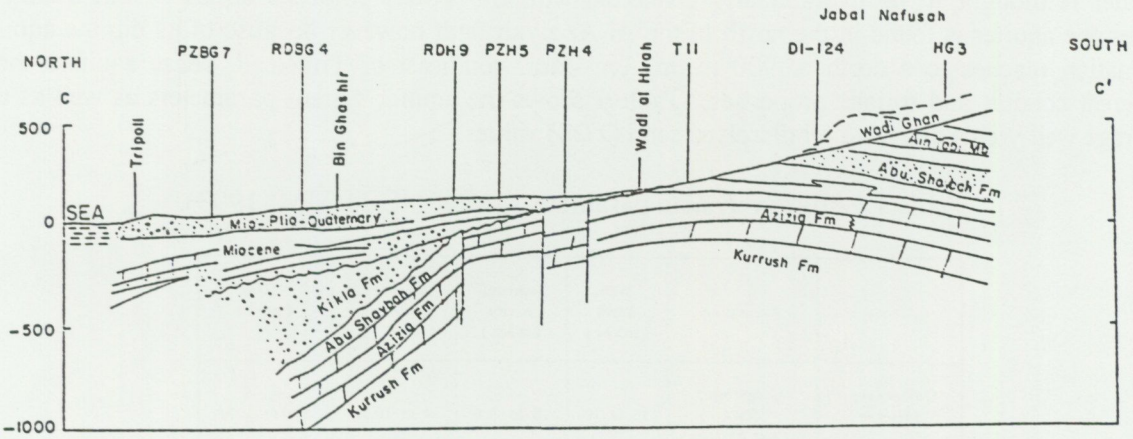


Fig. 2. A Schematic cross section through Gefara plain (Pallas, 1978).

it dips to great depth and reaches to 900 m in the coastal area. Abu Shaybah formation overlies the Aziziyah formation and it is widely distributed over the Gefara plain. It consists of cross bedded sandstone alternating with green and red bands of clays. The Upper Jurassic deposits in the area are represented by the Tokbal, Jawsh and Shakshak formations. They generally consist of sandstones, claystones and dolomites interbedded with black clays and claystones. Kikla and Kabao formations form the Lower Cretaceous units and they consist of light colored, cross bedded, friable quartz sandstone and conglomerates with brown, yellow and red silt and clay intercalations. The Upper Cretaceous formations (Ain Tobi limestone, Yefrin marls and Gharian limestone) form most of the Nafusa escarpment in the south border of the Gefara plain. The Miocene formations are found everywhere in the central and eastern part of the Gefara plain and they cover about two thirds of the northern part. The Quaternary-Miocene series consists of argillaceous sandstone with anhydrite subdivided by clay lens and reaches its greatest thickness in the Tripoli area. Miocene-Pliocene-Quaternary Complex forms the top most series in the northern part of the Gefara plain. This unit consists of fossiliferous detrital limestone and marl formations alternating with yellow clay and sand lenses. The total thickness varies from 40 to 150 m. The Quaternary deposits cover the major part of the Gefara Plain as well as the plateau surface. The Gefara formation consists mainly of fine materials mostly silt and sand occasionally with gravel and caliche bands. In the study area the Gargaresh formation makes steep cliffs along the shore of the Mediterranean Sea. This formation is made up of calcarenite, including shell fragments and minor sand grains, interbedded with silt lenses. The sand dunes and sheets which cover large areas in the region represent the Eolian deposits in the Gefara plain (IRC, 1975; Kruseman, 1977; Krummenacher, 1982).

Hydrogeology

Geology of the area comprises a number of aquifers in the Gefara plain. They are separated by more or less impermeable clay lenses in the north, however they define a single large unconfined aquifer in the inland portion of the plain. The upper aquifer (Quaternary-Miocene-Pliocene) collects water under unconfined conditions and extends throughout the Gefara plain. It is 100-150 m thick and contains good quality water in the central and eastern parts. Along the coastal regions water quality becomes poor where overpumping has led to seawater intrusion. Middle-Miocene aquifer is well developed in the western part of the Gefara plain and it is found 70-120 m below the surface. Thickness of the aquifer varies in the range from 125 to 200 m. Clay layers separate the aquifer from the Quaternary and the Lower Miocene aquifers. The Lower Miocene aquifer consists of sandy limestone and it overlies the sandy facies of the Upper Abu Shaybah formation. Abu Shaybah sandstone aquifer is found in the northern parts, where the Abu Shaybah sandstone is overlain by Miocene units. The aquifer is thought to be hydraulically connected with the Lower Miocene aquifer. The Aziziyah limestone aquifer is found in the north of the Al Aziziyah fault however because of its dip the aquifer formation reaches to a depth of 900 m. in Ayn Zara, southeast of Tripoli. These aquifers show different conduit and storage properties. Table 1 shows the aquifer system parameters as well as the average well yields and the total dissolved solid (TDS) values.

Table 1. Aquifer system parameters (after NCB&MM, 1993).

Group	Formation	Well Yield (m3/hr)	Transmi-ssivity (m2/d)	Storage Coefficient	TDS (mg/l)
Quaternary - Miocene	Gargaresh , Jefara , Qasr Al Haj	15 to 30	20 to 700	4 to 10 %	500 to 2000
Oligocene - Miocene	Al Khums	15 to 70	up to 300	confined	1500 to 3500
Cretaceous / Upper Jurassic	Sidi as Sid Kikla	40 to 90	up to 520	Unconfined Mainly confined	1000 to 1500
Middle Jurassic	Tokbal	< 15	Very variable	-	-
Triassic	Abu Shaybah	about 30	4 to 1555	Confined	-
	Al Aziziyah	30 to 110	up to 450	1 to 5 % confined	1000 to 3000 2000 to 10000
	Kurrush	2 to 10	about 60	Confined	
	Ouled Chebbi	2 to 10	-	Confined	-

The aquifer system in the Gefara Plain is thought to be majorly recharged from precipitation, infiltration from surface runoff, and by inflow from the south (Pallas, 1978; Krummenacher, 1982). In addition to these components NCB and MM (1993) consider the recharge by irrigation returns and by municipal supply losses. The main discharge of the groundwater from the aquifer system in the Gefara plain is by water abstraction by pumping for the irrigation and the domestic purposes.

Seawater Contamination in NW Libya

Cedestrom and Bastaiola (1960) performed a research in the region to quantify the problem of seawater contamination. Their observations for 1957 showed that some of the water wells near the coast started to be contaminated by seawater at that time (Fig. 3). Gefli (1972) obtained a similar distribution for Chloride concentration for 1972, where a slight change can be detected for landward

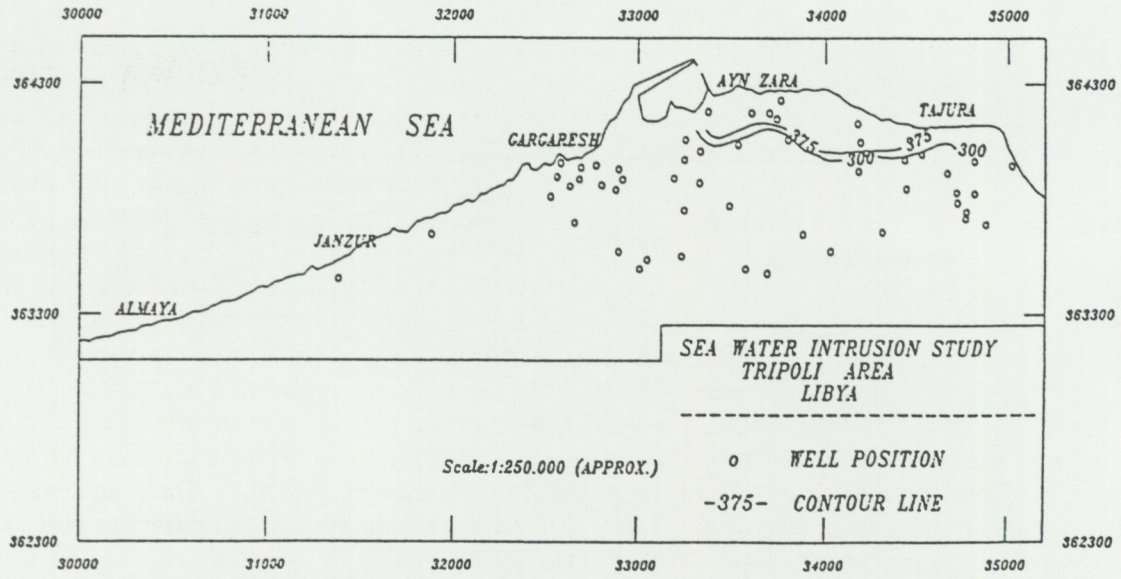


Fig. 3. Chloride concentrations in 1957 (after Cederstrom & Bastaiola, 1960).

movement of the chlorine contours. In recent years, high rate of urbanization and increased agricultural and economical activities have required more water to be pumped from the aquifer. This has continually increased the risk of seawater intrusion and deteriorated the quality of freshwater in the Gefara plain. Observations during this research in 1994 show that 375 mg/l chlorine contour has migrated inland reaching to distances of 10 km from the coast in Gargaresh and Ayn Zara regions (Fig. 4).

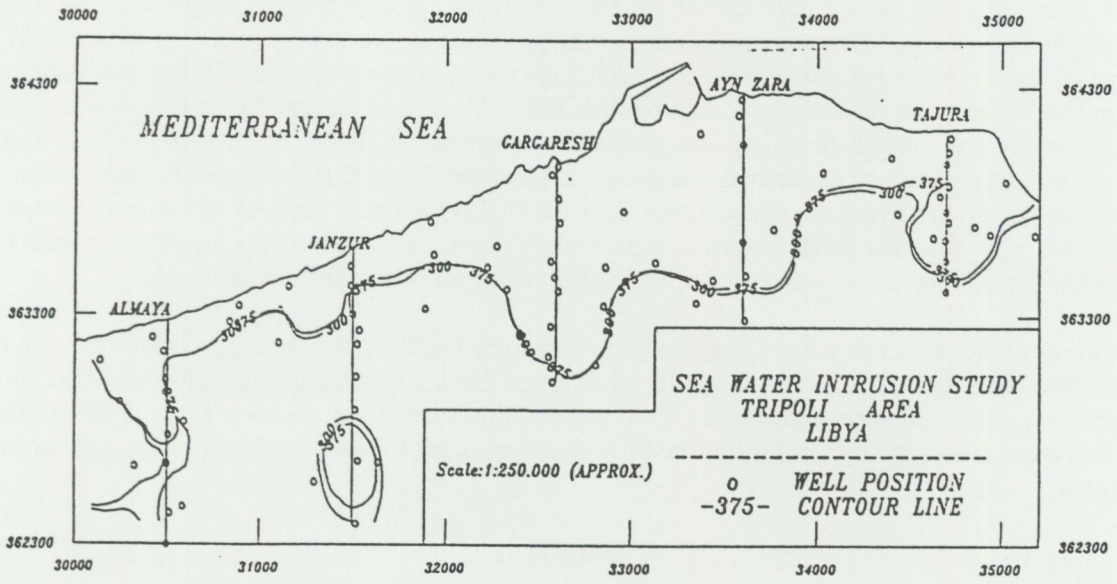


Fig. 4. Chloride concentrations in 1994.

This rapid increase in the seawater intrusion necessitates detailed investigation of the intrusion mechanism for optimum use of the fresh water in the area. For this purpose a finite element model is formed to simulate freshwater flow and salt concentration diffusion in the Quaternary aquifer system. The study area is discretized by means of 4-nodal rectangular elements and a finite element mesh, with 398 elements and 444 nodes, has been constructed (Fig. 5). In the analysis an areal model is

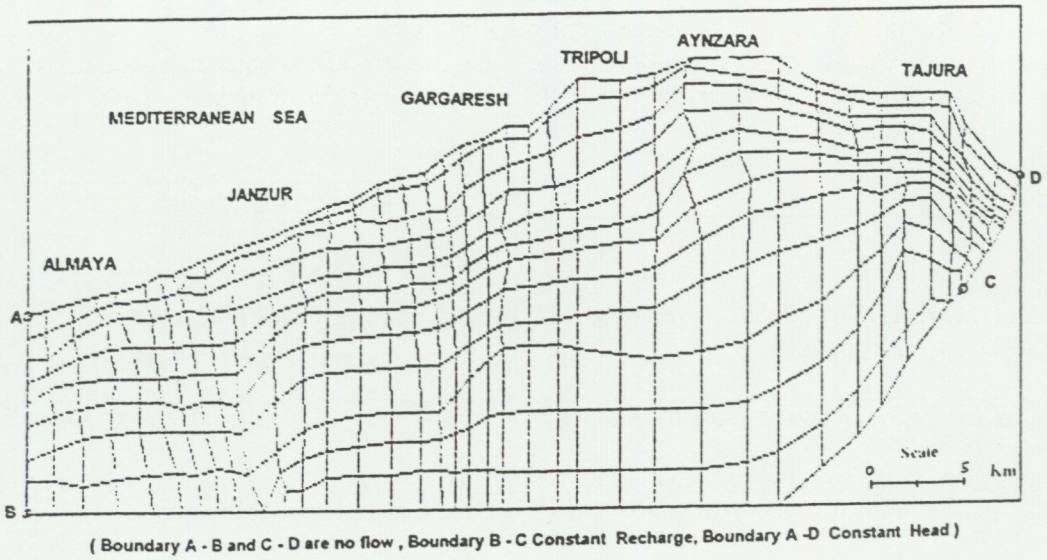


Fig. 5. Finite element mesh and the Boundary conditions.

formulated in order to study the flow and diffusion mechanisms over an areal surface and SUTRA program has been applied for the computer solutions (Voss, 1984). The model was calibrated for the flow equation under steady-state conditions and the hydraulic conductivity values were determined. Along the boundaries, constant-head (sea boundary), no-flow (western and eastern boundaries) and constant-recharge (for the southern inflow) boundary conditions were applied. During calibration runs computed water table values were compared with 1957 observed heads and the procedure was repeated until a minimum squared deviation was obtained. A sensitivity analysis was carried out to test the model against hydraulic conductivity variation. It has been found that the model is more sensitive to lower values of the hydraulic conductivity than the higher values. Squared deviations between the computed and observed heads increase exponentially upon reduction of the hydraulic conductivity values, whereas they follow a smooth increasing behaviour for the higher conductivities.

Modeling studies continue progressively to perform history matching the water level elevations for 1972 and 1994 observations. This step would be followed by solution of the diffusion equation for the calibration of the diffusion parameters. Then the equation system will be solved in a coupled manner for the water levels and the concentration distributions in order to simulate the intrusion mechanism in the area.

Conclusions

This paper presents a research to investigate the problem of seawater intrusion in Gefara plain, NW Libya. The problem has been clearly defined and a method has been introduced to model the seawater contamination in the region. Following conclusions can be withdrawn from the analysis:

- Groundwater is the main source for domestic, agricultural and industrial use in the Gefara plain, where recharge is limited. Previous investigations reveal that seawater contamination has started in 1950s and its migration rate has increased with time under continual risk of seawater intrusion.

- Groundwater is discharged from the aquifer by means of water wells distributed all over the area. In order to reduce migration rate of the intrusion new management policies should be planned for optimal use of the freshwater in the aquifer.

- Intrusion mechanism can be investigated by means of a numerical method in order to clarify the problem in the Gefara plain. Proposed finite element model and the boundary conditions are found to be appropriate for the study area and the model will be successful in making predictions for future behaviour of the intrusion.

REFERENCES

BACKUSH, I.M.,1983: A quantitative model of Gefara plain central part NW Libya. - M.Sc. Thesis, Ohio University, 125 pp. Ohio.

BILAL, W.M., 1987, Seawater intrusion in Janzur. - B.Sc. Thesis, El Fateh University, 35 pp. Tripoli.

CEDESTROM, D.,& BASTAIOLA, H., 1960, Groundwater in the Tripoli area, Libya. - USGS Open File Report.

FLOEGEL, H., 1979, Seawater intrusion study - SARLD Report, 57 pp. Tripoli.

GEFLI, 1972, Soil and water resources survey for hydro-agricultural development, Western Zone - Unpublished Report, GWA. Tripoli.

IRC, 1975, Geological map of Libya, 1:250 000 Sheet Tarabulus, Explanatary Booklet - Industrial Research Center. Tripoli.

KRUMMENACHER, R., 1982, Report on Groundwater Resources of Gefara Plain. - SARLD Report, 110 pp Tripoli.

KRUSEMAN, G.P., 1977, Evaluation of water resources of the Gefara plain.- SDWR Unpublished Report, 20 pp. Tripoli.

KRUSEMAN, G.P., & FLOEGEL, H., 1978, Hydrogeology of the Gefara plain, NW Libya. - 2nd Symposium Geology of Libya. Tripoli.

MELUDI, H., & WERYNSKI, K., 1980, Seawater intrusion study, Gargaresh Swani Well Field area.- SARLD Report, 7 pp. Tripoli.

NCB & MM, 1993, Water management plan. - Great Man Made River Water Utilization Authority by the National Consulting Bureau of GSPLAJ with Mott MacDonald of the UK, 3 volumes. Tripoli.

PALLAS, P., 1978, Water resources of the SPLAJ, - SDWR, 80 pp. Tripoli.

SHAWI, T., & PHILBERT, M., 1991, A study of seawater intrusion in Tajura groundwater.- B.Sc Project, El Fateh University, 58 pp. Tripoli.

VOSS, C.I.,1984, SUTRA: A finite element simulation model for saturated-unsaturated, fluid density dependent ground-water flow with energy transport or chemically reactive single species solute transport. - U.S. Geological Survey Water-Resources Investigations Report 84-4369, 409 pp. Reston.

Impact of sea level rise on Dutch groundwater regimes

G.H.P. Oude Essink
e-mail: g.oude.essink@ct.tudelft.nl
Delft University of Technology, Faculty of Civil Engineering,
Hydrology & Ecology Group, P.O. Box 5048, 2600 GA Delft, the Netherlands

Abstract

The impact of sea level rise on vulnerable coastal groundwater regimes in the Netherlands for the next millennium is investigated. For this purpose, the two-dimensional groundwater flow model MOC of Konikow & Bredehoeft [1978] is applied. It has been adapted by the author to simulate density dependent groundwater flow and solute transport in vertical profiles. The model assesses the propagation of sea level rise in the groundwater regimes. Moreover, it assesses the changes in the salinity distributions of these regimes, the changes in the volumes of freshwater lenses in sand-dunes and the changes in seepage (both quantity and quality) in low-lying polders. It appears that, independent of sea level rise, a severe (irreversible) salinisation process already occurs in the groundwater regimes along the Dutch coast. This present salinisation process is generated by human activities such as the reclamation of the (low-lying) polders during the past centuries. It is to be expected that sea level rise significantly intensifies the salinisation process. Whether or not the impact of sea level rise for a specific polder is significant in terms of seepage quantity, mean chloride concentration and chloride load, depends on the distance to the coast, the phreatic groundwater level and the subsoil parameters.

1. Introduction

Groundwater regimes in the coastal zone of the Netherlands within the zone of influence of mean sea level will be threatened by a rise in sea level even more in the future than they are already threatened today (see figure 1). Salt water intrusion in these regimes will probably accelerate. As such, the salinisation process could result in a reduction of fresh water resources. Furthermore, the seepage quantity may increase in those coastal areas which are situated below *N.A.P.*[1] The present capacity of the discharge systems (pumping stations and water courses) in several low-lying polders near the coast may be insufficient to cope with the excess of seepage water. This seepage will probably have a higher salinity than at present. A substantial increase in volumes of water required for flushing could be necessary to counteract the deterioration of the water quality of the surface water systems in the Netherlands. In addition, crops may suffer from salt damage due to the increased salinity of the soil and fertile arable land might eventually become barren land.

Though the impact of sea level rise on groundwater regimes and consequently on water management can be far-reaching, virtually all relevant literature treats this topic only very superficially. Therefore, a Ph.D. study has been set up to partly fill the gap of knowledge [Oude Essink, 1996]. In this paper, the main objective is to quantify the possible impact of sea level rise on vulnerable coastal groundwater regimes in the Netherlands during the next millennium. To arrive at a comprehensive view over the results of the simulations, a selection of only three scenarios of sea level rise has been made: one with a sea level rise of 0 metre per century (SLR=0 m/c), one with SLR=+0.6 m/c and one with SLR=-0.6 m/c (thus a sea level fall !).

Note that this paper is only a concise summary of Oude Essink's Ph.D. thesis [1996]. Obviously, innumerable cases regarding groundwater flow in coastal geohydrologic systems could be simulated. In the thesis, however, a large number of conceivable cases have been evaluated which are not treated here. For instance, the influence of land-subsidence[2] and changes in groundwater recharge[3] have been considered. Moreover, also the influence of (hypothetical) measures that counteract the negative impact

[1] *N.A.P.* stands for Normaal Amsterdams Peil and is the reference level in the Netherlands. *N.A.P.* roughly equals Mean Sea Level.

[2] Polders subside because of compaction, shrinkage and oxidation of peat as well as man-induced processes such as local mining activities (e.g. oil and gas) and groundwater recovery.

[3] The groundwater recharge can alter due to a change in: (a) the natural component: e.g. change in the present precipitation pattern due to climate change, and (b) the anthropogenic component: e.g. change in artificial recharge or withdrawal of groundwater from the phreatic aquifer.

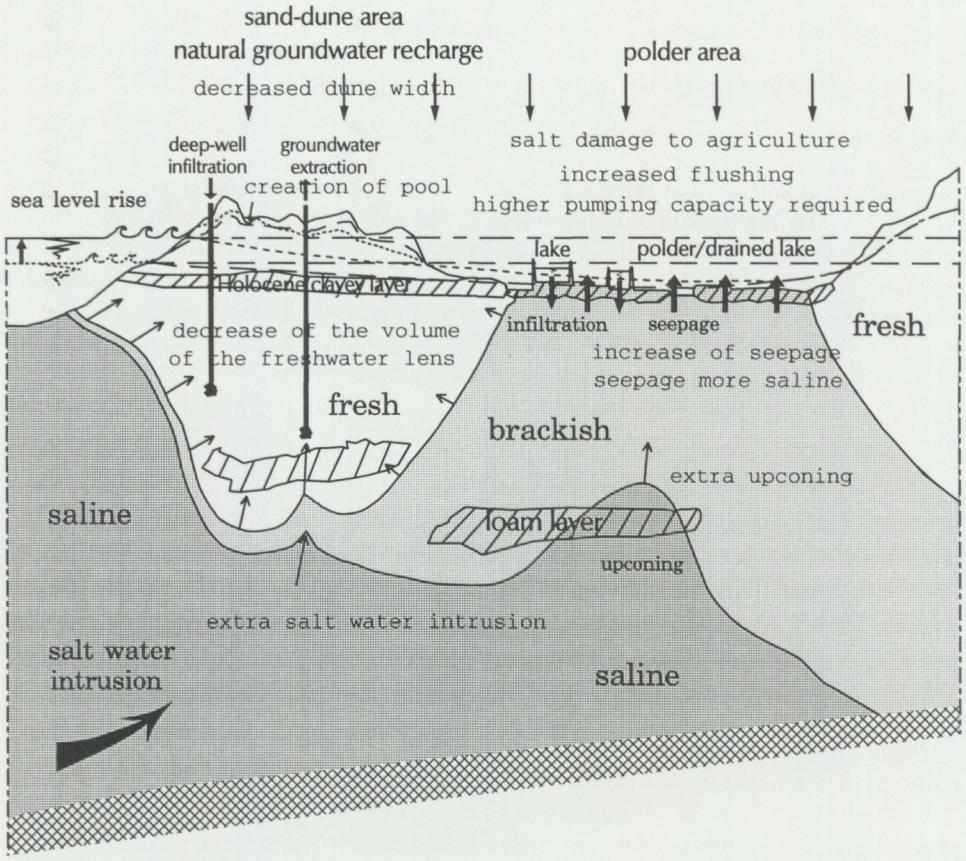


Figure 1: Possible impacts of sea level rise on the groundwater regime in the low-lying western part of the Netherlands.

of sea level rise have been discussed, such as (a) reclaiming land in front of the coast, thus evolving new freshwater lenses; (b) extracting (saline) groundwater, thus decreasing the seepage quantity and chloride load in the polders; (c) infiltrating of surface water (viz. *deep-well infiltration*), thus blocking the salinisation process towards the low-lying hinterland; (d) inundating low-lying polders, thus removing the driving force of the salinisation process; (e) widening existing sand-dune areas, thus generating thicker freshwater lenses; and (f) creating physical barriers, thus blocking the free entrance of saline groundwater and halting the salinisation process. Based on numerous simulations, it appears that, when the sea level rises $+0.6\ m/c$, even the most effective countermeasures cannot stop the salinisation of the subsoil on the long-term. Therefore, it is likely that human interventions can only retard the salinisation of the groundwater regimes in the long-term at the expense of major investments[4]. Finally, also cases with different subsoil parameters have been treated in order to execute a limited parameter sensitivity analysis.

The sensitivity of the groundwater regime in the Netherlands for three scenarios with different rates of sea level rise is analysed[5] by (numerical) modelling of eight representative profiles perpendicular to the Dutch coastline. For this purpose, the model MOC of Konikow & Bredehoeft [1978] is applied, which is adapted for density differences to simulate vertical profiles [Lebbe, 1983; Oude Essink, 1996]. MOC is based on the finite difference method and it uses a particle tracking technique to model (advective) solute transport. In this paper, the objective is focused on the following impacts of sea level rise:

- the propagation of sea level rise in the piezometric level distribution

[4] Whether these investments are considered feasible or not depends on the prevailing economic, environmental and political circumstances at the moment when a (political) decision is taken.

[5] Note that the methodology followed to investigate and to assess the impact of scenarios of sea level rise (and human activities) on Dutch coastal groundwater regimes could also be extended to similar vulnerable coastal groundwater regimes around the world.

- the changes in salt water intrusion in the geohydrologic system
- the changes in the volumes of freshwater lenses in sand-dune areas
- the changes in seepage (both quantity and quality) in low-lying polders

In section 2, the eight representative profiles are described. In section 3, the propagation of sea level rise in each geohydrologic system is considered. In section 4, the salt water intrusion in each geohydrologic system is described. In section 5, the evolution of the freshwater lens in four geohydrologic systems is evaluated. In section 6, the changes in seepage (both quantity and quality) is shortly discussed. Finally, some conclusions are drawn and recommendations are given.

2. Representative profiles along the Dutch coast

As MOC, adapted for density differences, is a two-dimensional model, profiles have been chosen perpendicular to the Dutch coastline. Each *representative profile* characterizes a coastal area in the Netherlands with its own specific subsoil conditions which differ from the subsoil conditions of profiles in the vicinity. The following subsoil conditions have been considered: the length of the geohydrologic system; the thickness of the geohydrologic system down to the geohydrologic base; the hydraulic conductivity; the hydraulic resistance of the Holocene aquitard; the positions and characteristics of loam aquitards; the width of the sand-dune area (if present); and the phreatic groundwater levels in the polders. Strictly speaking, the number of conceivable profiles is infinite. For reasons of simplicity, however, the number of profiles has been limited to eight. Figure 2 shows the position of these eight representative profiles perpendicular to the Dutch coastline. Note that, unfortunately, it is not possible to model the islands of Zeeland by means of a representative profile as they cannot be schematised in two dimensions[6].

Apparently, three-dimensional effects, such as groundwater flow perpendicular to the profile due to groundwater extractions or low phreatic groundwater levels in polders, are left out of consideration. In fact, these effects may be very important for the interpretation of the results, but for the applied profiles, in which subsoil parameters are averaged over areas of several hundred square kilometres, the effects are probably of minor importance.

2.1 Subsoil conditions

Figure 3 shows the schematisation of the geometry, the values of subsoil parameters and the phreatic groundwater levels in the polders of each of the eight profiles. The data of the geohydrological schematisation have mainly been borrowed from numerous sources. As can be seen, there is a great variety of subsoil conditions along the Dutch coast. The following subsoil parameters are applied in MOC: the effective porosity=0.35; the longitudinal dispersivity α_L=0.2 m; and the anisotropy factor=0.1. Sand-dune areas with freshwater lenses occur in the profiles Ber, Haa, Lei and Wad. As can be seen, the phreatic groundwater levels in the polders are below *N.A.P.* in all profiles (except in the profile Vla). Obviously, this situation reveals that a permanent salinisation process must be taking place in the direction of the (low-lying) polders. Figure 4 shows the chloride distributions in 1990 in the eight profiles, derived from several different sources. As concentration measurements at great depths are generally rare, the chloride distribution in some places might be disputable. Specific characteristics of each profile are briefly discussed below:

1. Wie=Wieringermeer: the transmissivity of this geohydrologic system is huge, as the thickness is enormous, some 260 m, and the hydraulic conductivity high. Moreover, the hydraulic resistance of the Holocene aquitard is high. The polder (that is the Wieringermeer polder) in the reach 15,000-29,500 m has a very low phreatic groundwater level: between -4.5 and -5.5 m *N.A.P.* At the inland boundary, the water level in the IJsselmeer is a constant piezometric level boundary. Fresh groundwater, which belongs to the freshwater body of Hoorn, is present in the central part of this profile.

[6]For instance, sand-dune areas occur in the western seaside parts of the islands, which would complicate a proper selection of the orientation of the profile. Moreover, the characteristics of these islands, such as the thickness of the geohydrologic system, the boundary conditions and the phreatic groundwater levels, differ too much from each other to join them together in one representative profile.

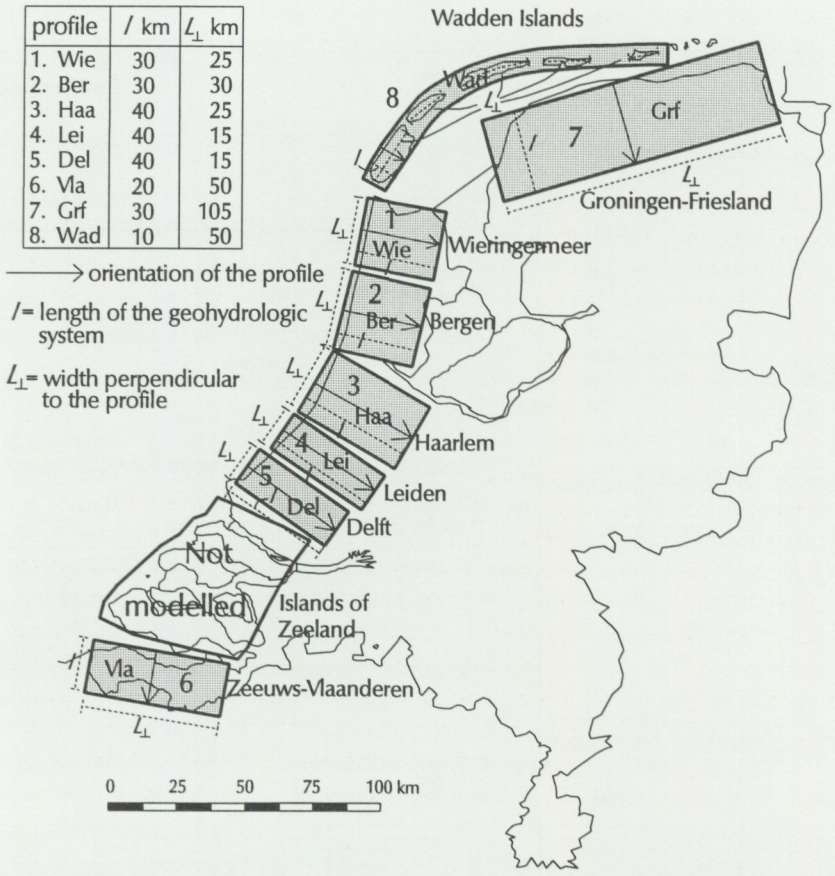


Figure 2: Location of the eight areas in which the eight representative profiles perpendicular to the Dutch coastline are defined. The names of the profiles are arbitrarily chosen: they refer to a city, region or province positioned in that profile. The islands of Zeeland are not modelled.

2. Ber=Bergen: in the central part of this profile, a low-lying polder (-4 m *N.A.P.*) occurs, which represents the areas reclaimed in the seventeenth century: the Beemster (1608-1612), the Wormer (1625-1626) and the Schermer (1633-1635). The main difference with the profile Wie in terms of chloride distribution is caused by the presence of a sand-dune area of 3000 m width under which a freshwater lens has evolved.

3. Haa=Haarlem: the hydraulic conductivity is lower than in the two profiles mentioned above. Various low-lying polders are located at a considerable distance from the coast, such as the Haarlemmermeer polder in the reach 10,000-20,000 m. From the coastline, a broad sand-dune area extends to 3500 m inland. Amsterdam Waterworks has pumped water from this area since the middle of the nineteenth century. The freshwater lens reaches to a depth of at least 80 m below *N.A.P.* Under this lens, saline groundwater flows in the direction of the low-lying Haarlemmermeer polder.

4. Lei=Leiden: this profile resembles the profile Haa to a certain extent. The main differences, however, are that (1) the thickness of the geohydrologic system is 30 m less and (2) the phreatic groundwater level of the polders is a few metres higher. The width of the sand-dune area is 2500 m, and hence, the thickness of the freshwater lens is somewhat smaller than in the profile Haa.

5. Del=Delft: though this profile corresponds to a great extent with the profile Lei, a significant difference can be found in the hydraulic resistance of the Holocene aquitard in the reach 10,000-20,000 m: e.g. 25,000 *days* in the profile Del instead of 3000 *days* and 750 *days* in the profile Lei. The sand-dune area, present in this profile, is too small to be simulated. Relatively low polders at some kilometres inland of the coast (-2.5 m *N.A.P.* from x=5000 m) induce a flow of saline groundwater in the geohydrologic system. Close to the city of Delft, groundwater is extracted for industrial purposes.

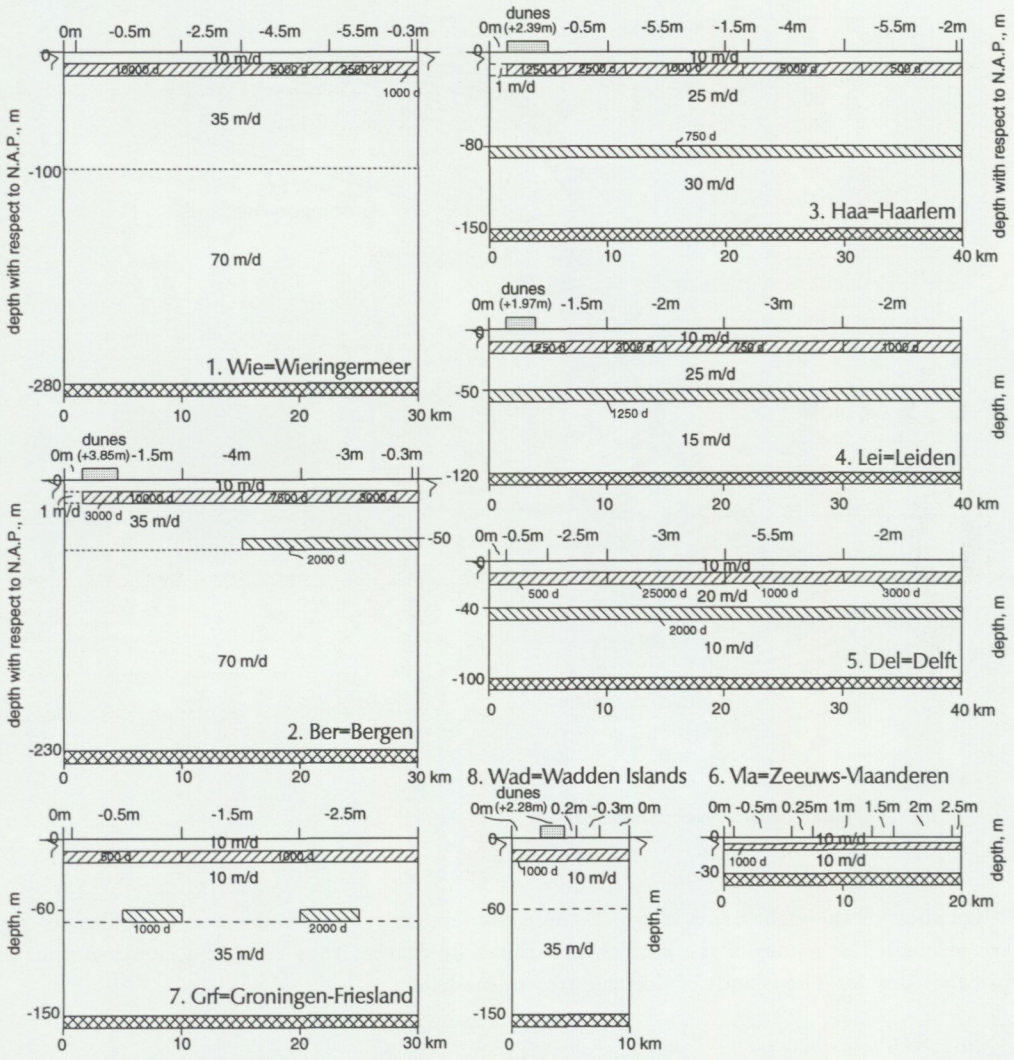


Figure 3: Schematisation of the geometry, the subsoil parameters and the phreatic groundwater levels with respect to $N.A.P.$ in the polders of the eight representative profiles. The groundwater recharge f in the sand-dune area is 360 mm/yr. The highest phreatic groundwater level in the sand-dune areas of the profiles Ber, Haa, Lei and Wad is given in brackets.

6. Vla=Zeeuws-Vlaanderen: the Belgium hinterland is also considered in this profile. The phreatic groundwater levels in the polders at some kilometres inland of the coast are above $N.A.P.$ The thickness of the geohydrologic system is the smallest of all profiles, only some 20 m. In the past, a severe salinisation process has caused high chloride concentrations in this geohydrologic system.

7. Grf=Groningen-Friesland: the phreatic groundwater levels are not very low in this profile. The length of the saline groundwater tongue is limited to some kilometres. More inland of the tongue, brackish groundwater is present in the entire geohydrologic system.

8. Wad=Wadden Islands: at both boundaries, a sea condition is present. At the Waddenzee side, polders are present with phreatic groundwater levels around $N.A.P.$ At the North Sea side, the width of the sand-dune area is 2000 m, under which a freshwater lens has evolved with a thickness of about 80 m. Note that this profile closely corresponds with that of Texel.

2.2 Model parameters in MOC

The following model parameters are applied in the adapted MOC model (see also Oude Essink [1996]). Each grid cell has a length Δx of 250 m and a height Δz of 10 m (only for the profile Vla, the height Δz is equal to 5 m). Each grid cell contains five particles. The convergence criterion TOL is 10^{-5} ft. The flow time step Δt equals 1 $year$. During this step, the velocity field remains constant. The maximum

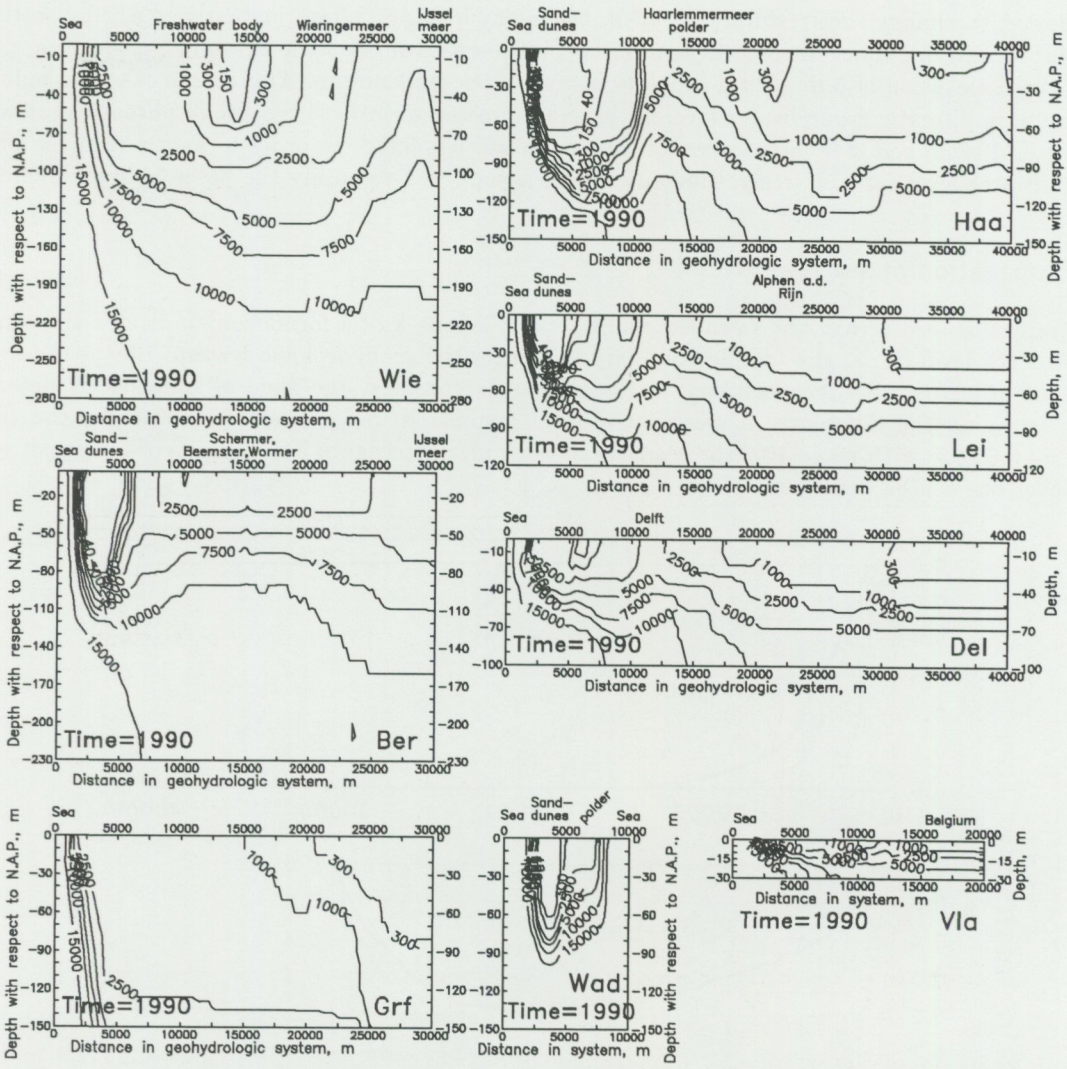


Figure 4: Present fresh-saline distributions (in $mg\ Cl^-/l$) in 1990 in the eight representative profiles.

relative distance in a grid cell is set to 0.9.

2.3 Three scenarios with different rates of sea level rise

The scenario with no sea level rise (SLR=0 m/c) is applied as the so-called *reference case* for all cases. The present situation concerning boundary and initial conditions, phreatic groundwater levels in the polders and groundwater extraction rates is maintained during this scenario. Accordingly, many processes[7] that may affect the geohydrologic system are left out of consideration. The results of this scenario may clarify the effect of (past) human activities, such as land reclamation which has created low-lying polders. Furthermore, the time lag has been determined before a state of dynamic equilibrium regarding the salinity distribution will be reached.

A sea level rise of +0.6 m/c and a sea level fall of -0.6 m/c are considered for a simulation time of one millennium. The change in sea level is added to the freshwater head in the grid cells at the seaside boundary before each calculation time step of 1 *year*. The time lag, in which the freshwater head in the geohydrologic system rises to a new state of dynamic equilibrium due to sea level rise, can be neglected with respect to the time lag in which the salinity distribution changes. Therefore, it

[7]These processes are of a hydrological nature (e.g. less precipitation, more evapotranspiration due to climate change), a morphological nature (e.g. shoreline retreat) or a man-induced nature (e.g. sand-suppletion at the coastal zone to counteract shoreline retreat).

is allowed to change the freshwater head in the geohydrologic system instantaneously by setting the specific storativity equal to zero. Bear in mind that a sea level rise with a rate of e.g. +0.6 m/c means a sea level elevation of 6 m after a simulation time of one millennium. This rise in sea level induces an elevation in phreatic groundwater level in the sand-dune area. In fact, the rise in phreatic groundwater level could be impeded if the position of the land surface is fixed. In order to assure that the phreatic groundwater level can rise freely, sand-suppletion is supposed to nullify the possible impediment.

3. Propagation of sea level rise

In straightforward terms, the so-called characteristic length λ of a formation[8] indicates the zone over which a sea level rise at the seaside boundary influences the geohydrologic system: that is the so-called *zone of influence*. As the geometry of the profiles is complex, the zone of influence is determined by calculating the difference in piezometric level, expressed in freshwater, in 2090 for the scenario SLR=+0.6 m/c with respect to the scenario SLR=0 m/c (see figure 5). Three types of sensitivity for sea level rise can be perceived:

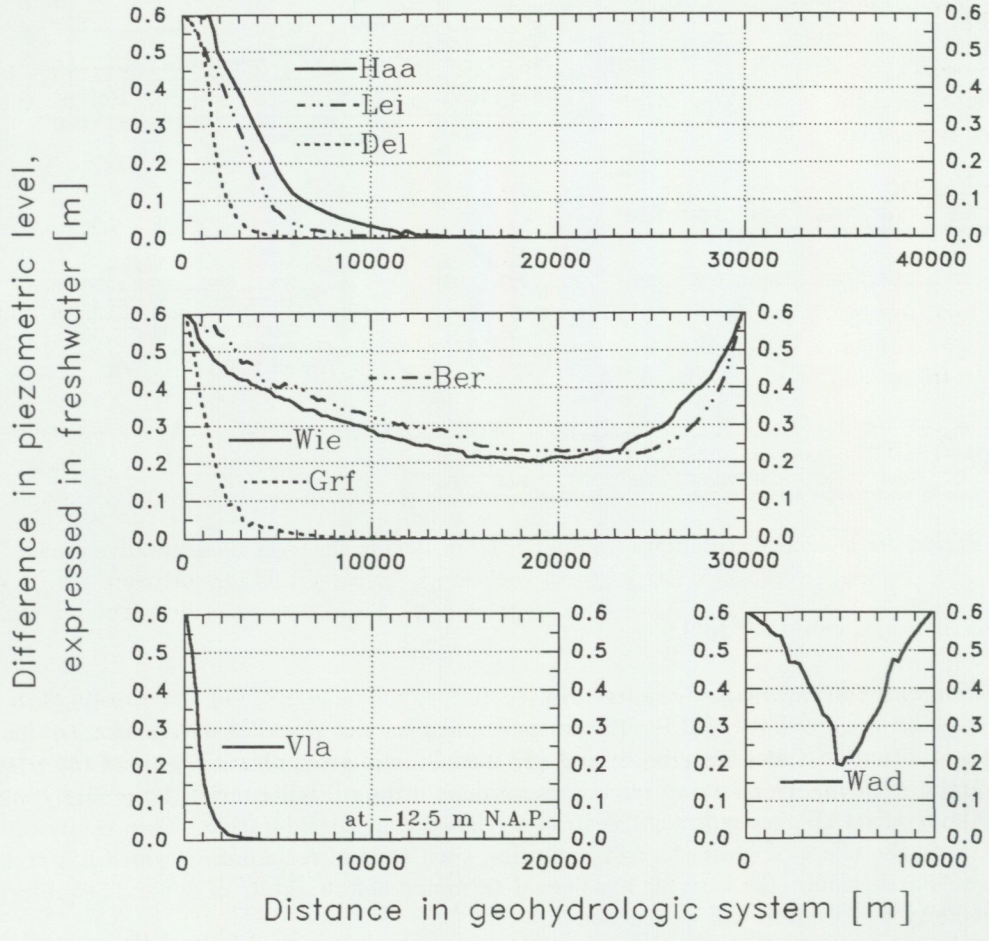


Figure 5: The propagation of a sea level rise in the geohydrologic system: differences in piezometric level, expressed in freshwater, at -25 m *N.A.P.* (in the profile Vla at -12.5 m *N.A.P.*) in 2090 for the scenario SLR=+0.6 m/c with respect to the scenario SLR=0 m/c.

[8] In a simple geohydrological schematisation, which consists of a Pleistocene sandy aquifer overlain by a Holocene (clayey) aquitard, also named the *Holland profile*, the characteristic length λ equals $\sqrt{kDc}$, where k is the hydraulic conductivity of the semi-confined aquifer ($L\,T^{-1}$), D is the saturated thickness of the aquifer (L), and c is the hydraulic resistance of the aquitard (T).

I. High sensitivity to sea level rise: the profile Wad. The zone of influence is very long because: (1) the level of the sea rises at both boundaries of the geohydrologic system; (2) the length of the geohydrologic system is small; and (3) the transmissivity is relatively high.

II. Moderate sensitivity to sea level rise: the profiles Wie and Ber. The zone of influence of sea level rise is significant. Consequently, piezometric levels in the geohydrologic system elevate significantly due to sea level rise. The two causes for this substantial rise in piezometric level are: (1) the transmissivities of the aquifers and the hydraulic resistance of the Holocene aquitard are very high; and (2) the piezometric level at the IJsselmeer side boundary also rises at the same rate as the sea level[9].

III. Low sensitivity to sea level rise: the profiles Haa, Lei, Del, Vla and Grf. The zone of influence of sea level rise is only a few kilometres. Thus, the attenuation of sea level rise is great in these profiles. For instance, the distance in the geohydrologic system, over which a freshwater head elevation of 6 cm (10% of the sea level rise) can still be noticed, is as follows: in Haa 8000 m; in Lei 5300 m; in Del 2800 m; in Vla 1600 m; and in Grf 3000 m.

4. Salt water intrusion in the geohydrologic system

Salt water intrusion in each geohydrologic system is discussed through analysing the chloride distribution in 2990 for the scenario SLR=+0.6 m/c and the time lag before a state of dynamic equilibrium in the salinisation process is reached.

4.1 Chloride distribution in 2990 for the scenario SLR=+0.6 m/c

Figure 6 shows the chloride distributions in 2990 in the eight profiles for the scenario SLR=+0.6 m/c. Through comparison with figure 4 (the situation in 1990), one can deduce the following:

1. Wie=Wieringermeer: two main causes for the severe salt water intrusion of the geohydrologic system are the high transmissivities and the low-lying Wieringermeer polder in the reach 15,000-29,500 m. The entire system will be saline in 2990.

2. Ber=Bergen: also in this profile, a severe salt water intrusion occurs. The freshwater lens remains, though the volume obviously decreases due to sea level rise. The aquifer, which underlies the low-lying polder in the central part of the profile, contains much more saline groundwater in the future than in 1990.

3. Haa=Haarlem: the freshwater lens decreases in such a way that salt water intrusion in the geohydrologic system in the center the low-lying polder (e.g. the Haarlemmermeer polder) will be severe.

4. Lei=Leiden: salt water intrusion is rather limited for several reasons: (1) the thickness of the geohydrologic system is 'only' 120 m; (2) as such, the freshwater lens is obstructing the inflow of saline groundwater to the hinterland; and (3) the phreatic groundwater levels of the polders are not as low as in the profile Haa. Saline groundwater will eventually reach the polder which is located directly behind the decreasing freshwater lens.

5. Del=Delft: the results correspond to some extent with those in the profile Lei. In the first kilometres inland of the coast, a severe salt water intrusion is taking place. Saline seepage occurs in the polder in the reach 5000-7500 m, because there the phreatic groundwater level is relatively low (-2.5 m $N.A.P.$) and the hydraulic resistance is low (500 $days$). Industrial groundwater extractions in the vicinity of Delft cause upconing of brackish groundwater. Meanwhile, surface water infiltrates in the geohydrologic system in the reach 8000-20,000 m, as the extractions create a low piezometric level in the aquifer. From about 10,000 m inland of the coast, the impact of sea level rise is very limited due to the high hydraulic resistance of the Holocene aquitard.

[9] As such, the geohydrologic system is influenced at the seaside as well as at the IJsselmeer side, and consequently, the piezometric level in between rises due to both these rises.

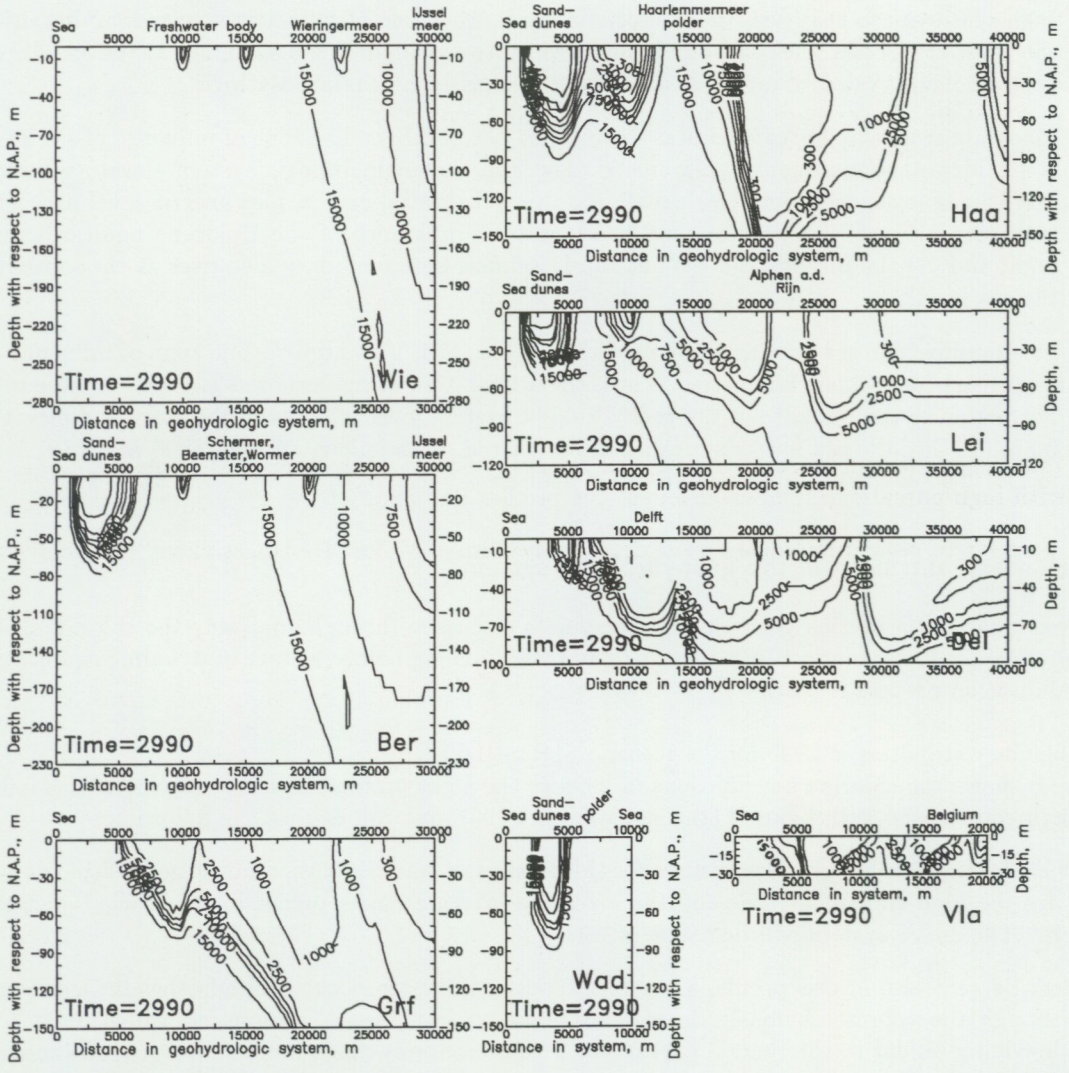


Figure 6: Future fresh-saline distributions (in $mg\ Cl^-/l$) in 2990 in the eight representative profiles for the situation with a sea level rise of $+0.6\ m/c$.

6. Vla=Zeeuws-Vlaanderen: the impact of sea level rise is limited to the first few kilometres from the coast, because the zone of influence is very short and the phreatic groundwater levels of the polders at some kilometres inland are situated above $N.A.P.$ As the thickness of this geohydrologic system is small, groundwater flow is determined by local conditions. Consequently, salt water intrusion from the sea is restricted.

7. Grf=Groningen-Friesland: eventually, the geohydrologic system will be completely saline in the first kilometres inland of the coast.

8. Wad=Wadden Islands: the geohydrologic system underneath the polder becomes more saline at great pace. However, the freshwater lens remains though its volume decreases. Note that the phreatic groundwater level in the sand-dune area is supposed to rise with sea level rise. Sand can be supplied where necessary in order to assure that the phreatic groundwater level can rise freely.

4.2 Time lag before a state of dynamic equilibrium is reached

Based on analyses of the changes in volume distribution of fresh, brackish and saline groundwater in the geohydrologic system for the scenario SLR=0 m/c as a function of 10,000 years[10] [Oude Essink, 1996],

[10] As the state of dynamic equilibrium will not be reached within one millennium in several profiles, the simulation time has been extended to 10,000 years.

it appears that most of the geohydrologic systems along the Dutch coast have at present not yet reached a state of dynamic equilibrium as far as the salinity distribution in the subsoil is concerned. The time lag of a geohydrologic system between the cause of changes and the ultimate effect on the salinisation process is mainly determined by three causes: (a) the driving force of the salinisation process, that is the phreatic groundwater levels in the polders and/or groundwater extractions; (b) the transmissivity and porosity of the geohydrologic system, that is the velocity with which groundwater can pass through the geohydrologic system; and (c) the geometry (size) of the geohydrologic system under consideration. Based on the causes mentioned above, four durations of time lags can be classified:

I. A time lag of several centuries: geohydrologic systems with small geometries: the profiles Vla and Wad.

II. A time lag of a large number of centuries: geohydrologic systems with high transmissivities and low-lying polder areas: the profiles Wie and Ber.

III. A time lag of a few millennia: geohydrologic systems with moderate transmissivities and polder areas with high phreatic groundwater levels: the profiles Haa and Grf.

IV. A time lag of several millennia: geohydrologic systems with low transmissivities and polder areas with high phreatic groundwater levels: the profiles Lei and Del.

Considering the absolute change in the volume of saline groundwater, the salinisation appears to be greatest in the northern part of the Netherlands in the profiles Wie, Ber and Grf. Salt water intrusion is still substantial in the profiles Haa, Lei and Del. The salinisation is limited in the profiles Wad and especially Vla, which is obvious as the geohydrologic system of the profile Vla is small.

5. Freshwater lenses in sand-dune areas

Figure 7 shows the volume of fresh groundwater in the sand-dune areas as a function of time in the four profiles Ber, Haa, Lei and Wad. During the next century, the impact of sea level rise on the fresh groundwater resources along the coast appears to be of minor importance, at most a few percents. After a millennium, however, the changes are (obviously) significant.

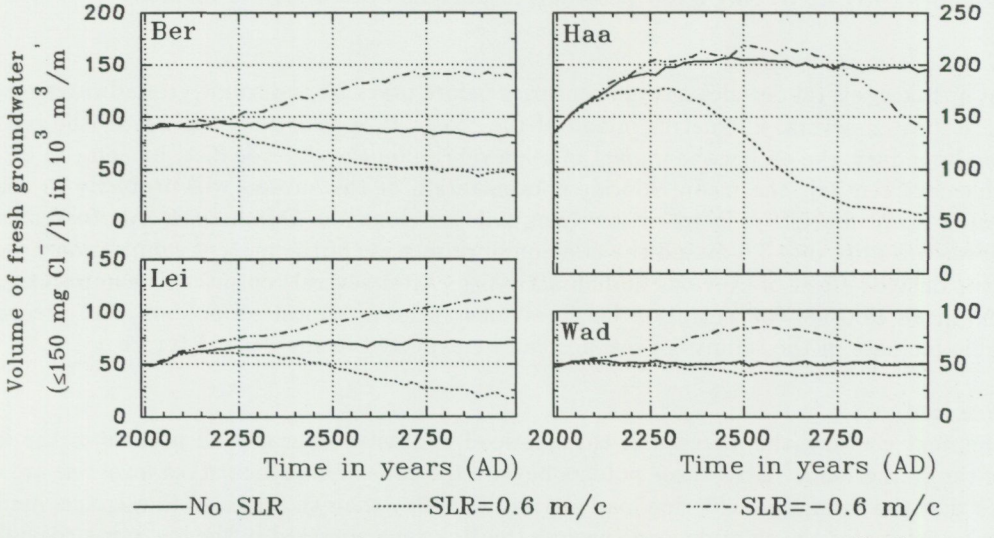


Figure 7: Volume of fresh groundwater ($\leq$ 150 $mg\ Cl^-/l$) in the sand-dune area in $10^3\ m^3/m'$ as a function of time for the three scenarios of sea level rise.

Two phenomena occur in the profile Haa. Firstly, for the scenario SLR=-0.6 m/c, the volume of the freshwater lens drops below the volume for the scenario SLR=0 m/c after some seven centuries. The reason for this phenomenon is that, after some centuries, the groundwater flow in the sand-dune

area alters in the direction of the sea, as the sea level is falling. The shape of the freshwater lens also changes, which results in a decreasing volume of fresh groundwater. Secondly, for the scenario SLR=0 m/c, the volume of fresh groundwater increases significantly (e.g. +23.4 % in 2090 with respect to 1990) because of two reasons: (a) the groundwater extraction rate has been decreased since 1956 and (b) the freshwater lens evolves towards the low-lying polder in the reach 10,000-20,000 m, and as a result, the volume increases. In the profile Wad, the volume of fresh groundwater decreases during the second half of the next millennium for the scenario SLR=-0.6 m/c. The reason is that, from then on, sea level fall causes fresh surface water, which originates from the polder adjacent to the sand-dune area, to infiltrate in the geohydrologic system. This water, which contains a higher chloride concentration than 150 $mg\ Cl^-/l$, supersedes the fresh groundwater that recharges the sand-dune area.

6. Seepage in low-lying polders

The impact of sea level rise in a specific polder can be significant in terms of seepage quantity, mean chloride concentration and chloride load if the following situations occur: the polder is situated directly inland of the coast; the phreatic groundwater level in the polder is low, namely several metres below $N.A.P.$; and/or the zone of influence of sea level rise in the geohydrologic system is long as a result of high transmissivities of aquifers. In this section, the changes in seepage through the Holocene aquitard in low-lying polders are shortly discussed for the three topics: (6.1) seepage quantity; (6.2) mean chloride concentration; and (6.3) chloride load.

6.1 Seepage quantity

The propagation of the sea level rise (see figure 5) already indicates the possible changes in seepage quantity due to sea level rise. Obviously, if the sea level rise is attenuated considerably in the geohydrologic system, the changes in seepage quantity are limited. In general, for Dutch polders at a great distance from the coast, the increase in seepage due to sea level rise appears to be of minor importance with respect to the already existing seepage quantities in those polders. For the scenario SLR=0 m/c, the decrease in seepage quantity through the Holocene aquitard due to changes in density distribution (caused by the salinisation of the geohydrologic system) is not insignificant, and thus remarkable. The impact of a sea level rise of +0.6 m (during the next century) on the change in seepage quantity is considerable (up to several tens of percents) in polders in the first kilometres from the coast, whereas it is marginal (mostly up to only a few percents) in polders located further inland.

6.2 Mean chloride concentration

In general, it takes several decades or even centuries before brackish and saline groundwater reach polders that are located several kilometres inland of the coast. It is clear that the nearer the polder is to the seaside boundary, the earlier the impact of sea level rise on the chloride distribution can be noticed. During the next century, the mean chloride concentration of the subsoil will probably increase with several hundreds of $mg\ Cl^-/l$ in many low-lying polders along the Dutch coast due to the combined effect of a sea level rise of +0.6 m and the non-equilibrium state of the present salinisation process as a result of the delayed effect of previous human activities. After several centuries, the impact of sea level rise on the mean chloride concentration becomes substantial in almost all polders, and accordingly, a considerable increase in the salinity of seepage can be expected in the distant future.

6.3 Chloride load

During the next century, the increase in chloride load is drastic in nearly all polders in the low-lying regions of the Netherlands. Even those polders beyond the zone of influence of sea level rise are affected. It appears that the changes in chloride load are much greater than the changes in seepage quantity. As an indicative estimate: the chloride load through the Holocene aquitard in the low-lying coastal regions of the Netherlands will be doubled in 2090, three fifths of which is caused by a sea level rise of 0.6 m and two fifths by the delayed effect of previous human activities (namely the reclamation of lakes or parts of the sea) on the future salinisation process.

Conclusions

- groundwater flow and solute transport are flow processes,
- most of the groundwater regimes of the eight studied profiles along the Dutch coast have not yet reached a state of dynamic equilibrium as far as the salinity distribution in the subsoil is concerned,
- sea level rise significantly accelerates the salinisation,
- many groundwater regimes will eventually become completely saline due to: (1) the future sea level rise; and (2) the present difference in polder level and sea level caused by previous human activities, such as the reclamation of lakes or parts of the sea.
- when the sea level rises $+0.6\ m$ during the next century, the volumes of the freshwater lenses in the four profiles with existing sand-dune areas hardly decrease. However, a few centuries later, the decrease in volume may reach several tens of percents,
- when the sea level rises $+0.6\ m$ during the next century, the chloride load increases substantially in nearly all polders in the low-lying regions of the Netherlands.

Recommendations

- as the impact of sea level rise could be significant in the coastal groundwater regimes in Zeeland, it is recommended to consider these islands through three-dimensional numerical modelling. For this purpose, a promising three-dimensional model could be an interconnected model of MODFLOW [McDonald & Harbaugh, 1984] (made suitable for simulating density dependent groundwater flow) and the (solute) transport model MT3D [Zheng, 1990],
- to increase the reliability of numerical groundwater modelling, groundwater regimes should be calibrated more accurately through intensifying the data collection of subsoil parameters and time series of hydrochemical constituents.

References

KONIKOW, L.F. & BREDEHOEFT, J.D. 1978. Computer model of two-dimensional solute transport and dispersion in ground water. *U.S.G.S. Techniques of Water-Resources Investigations, Book 7, Chapter C2, 90 p.*

LEBBE, L.C. 1983. Mathematical model of the evolution of the fresh-water lens under the dunes and beach with semi-diurnal tides. *Proc. 8^{th} Salt Water Intrusion Meeting, Bari, Italy. Geologia Applicata e Idrogeologia, Vol. XVIII, Parte II: 211-226.*

MCDONALD, M.G. & HARBAUGH, A.W. 1984. A modular three-dimensional finite-difference ground-water flow model. *U.S.G.S. Open-File Report 83-875, 528 p.*

OUDE ESSINK, G.H.P. 1996. Impact of sea level rise on groundwater flow regimes. A sensitivity analysis for the Netherlands. *Ph.D. thesis. Delft University of Technology. Delft Studies in Integrated Water Management: no. 7 (ISBN 90-407-1330-8). 411 p.*

ZHENG, C. 1990. MT3D. A modular three-dimensional transport model. *S.S. Papadopolous and Associates, Bethesda, Md.*

ON THE SIMULATION OF SALINE INTRUSION FOR REPOSITORY PERFORMANCE ASSESSMENT

Sven Follin, Golder Associates AB, Korta gatan 7, S-171 54 Solna, Sweden, sfollin@golder.se

Abstract

The objective of this paper is to assess the extent and duration of saline intrusion to a coastal nuclear waste repository located at depth in sparsely fractured Baltic Shield rocks. The underlying motive for the study is that long-term changes in the chemical environment associated with saline intrusion may affect the properties of the repository buffer zone material. The reconstruction used in this study of the hydrological conditions during the Holocene between 10,000 BP and today leads to the interpretation that the present occurrence of saline ground water reflects an ongoing but incomplete flushing of the Baltic Shield. The simulations of fifty years of dewatering followed by fifty years of resaturation suggest that the final interface between fresh and saline ground waters may be close to the conditions prior to the dewatering phase.

Introduction

Since the end of the 1970's, the Swedish Nuclear Fuel and Waste Management Company (SKB) has carried out a large number of studies at several study sites in Sweden. The investigations have been carried out from the ground surface and in boreholes down to depths of about 1,000 m. Moreover, a great deal of experimental work has been done at the Stripa mine within the framework of the international Stripa Project. The most recent large-scale project in Sweden is the construction of the Äspö Hard Rock Laboratory (HRL) in southern Sweden. The HRL provides excellent opportunities for a direct verification of the results of surface and borehole investigations by systematic observations from shafts and tunnels down to a depth of 450 m. In addition to the many laboratory and field experiments carried out by the international Task Force at Äspö, the conceptualization of ground water flow and mass transport through sparsely fractured crystalline rocks is also studied by means of numerical modeling.

This study treats the dewatering and resaturation phases associated with the construction, use and closure of a coastal nuclear waste repository located at depth in sparsely fractured Baltic Shield rocks. *Figure 1* shows a schematic cross section of the studied situation. The objective is to assess the extent and duration of saline intrusion for a set of reasonable geohydrological assumptions based on field investigations at the HRL. The underlying motive for the study is that long-term changes in the chemical environment associated with saline intrusion may affect the properties of the repository buffer zone material (bentonite).

Present-day depth-distribution of salt content in fluids residing the Baltic Shield rocks is not well known on the regional scale. For the purpose of this study, the work is therefore divided into two parts; the first part deals with model calibration and finding initial conditions for the second part, which deals with simulation of the dewatering and resaturation phases of a repository. The first part treats changes in the ground water conditions during the Holocene between 10,000 BP and today due to deglaciation and land upheaval, and the second parts treats an anticipated 50 year long period of dewatering followed by 50 years of resaturation.

Method and Limitations

The study uses the US Geological Survey computer code SUTRA (Voss, 1984). The reason for using SUTRA is its documented capability to simulate two-dimensional variable-density flow and mass transfer in saturated and unsaturated porous media under isothermal conditions. For example, Voss and Andersson (1993) used SUTRA in a related study that focused on the historical occurrence of saline ground water and regional flow patterns in the Baltic Shield during the Holocene coastal regression. The main difficulty with using SUTRA in this study, as well as in the study of Voss and Andersson (1993), is above all conceptual. Both studies address flow and transport problems through sparsely fractured crystalline rocks by using a continuum approach composed of several large zones of uniform properties. The homogeneity of each zone provides connection between any two points within a zone and flow is allowed along any pathway, whereas the actual heterogeneous fabric of sparsely fractured crystalline rocks restricts flow to distinct pathways, and hydraulic connections may not always exist between any two points.

The simulations of the dewatering and resaturation phases are approximate for several reasons. First, SUTRA cannot simulate the fully coupled variable-density problem of simultaneous heat transfer, multiphase flow and mass transport. Hence, neither the geothermal gradient nor any production of heat and gas at the repository are considered in this study while simulating the variable-density saline-intrusion problem. Second, the relationships generally considered to govern unsaturated flow are essentially unknown for sparsely fractured rock. The required relationships are the capillary head versus the saturation and the relative permeability versus the saturation. Third, the net change of the rock permeability close to a repository due to various underground activities such as blasting, excavation, grouting, etc. (excavation damaged zone) is uncertain. Fourth, SUTRA is two-dimensional, which implies an infinite extent of the conditions perpendicular to the modeled cross section.

Part 1 - Model Calibration

The purpose of *Part 1* is to provide reasonable initial and boundary conditions with regard to pressure and concentration for the simulation of the dewatering and resaturation phases (*Part 2*). *Part 1* treats the period between 10,000 BP and present.

Fourteen thousand years BP Sweden was covered with ice. The Baltic Shield was isostatically depressed by the weight of the ice cap to over 200 m below sea level, and large areas were subject to marine excursion (SNA, 1994). *Figure 2* shows the Holocene marine limit in Sweden about 10,000 years BP together with the locations of the modeled cross section (solid line) and the major upstream regional run off divide (dashed line). As indicated in *Figure 2*, more than half of the cross section falls outside the region that was inundated by sea water after the latest glaciation.

The initial ground water situation along the modeled cross section 14,000–10,000 years BP is of course unknown and must therefore be assumed. The salinity situation in the Baltic Shield was probably quite complex with high fresh water pressures under the ice cap and a simultaneous extensive marine excursion. For the purpose of this study it was assumed that the initial TDS concentration 10,000 years BP varied linearly with depth. That is, a linear concentration gradient is applied to the entire cross section as an initial condition for *Part 1*.

Figure 3 shows the modeled cross section (shaded area) and the adopted initial and boundary conditions. The cross section is assumed to be impervious at the landward and the bottom sides. This is equivalent to forcing flow to be vertical along the inland boundary, a probably acceptable boundary condition considering the location of the regional run off divide, see *Figure 2*. The chosen location of the bottom boundary at 2,000 m below sea level is found to be beyond major significance for the study.

The boundary conditions at the top and seaward sides are important for this study. A flux boundary condition must be specified at the top side in order to allow for a drawdown of the water table while the repository is depressurized. This study assumes a stationary infiltration rate at the top side. The stationary recharge is spatially adjusted to match the Holocene evolution of the hydraulic head profile of the modeled cross section between 10,000 years BP and today. Present-day heads of lakes close to the run off divide are in the range 200–300 m above sea level (SNA, 1994).

If no fluid flow is allowed across the seaward side of the model, the modeled cross section should be stretched out to the east so that the no-flow boundary is located far enough from the region of interest (cf. Voss and Andersson, 1993). This study replaces a distant boundary by using a fixed concentration profile at the seaward side of the modeled cross section, see *Figure 3*. Thus, the pressure profile at the seaward side is hydrostatic. The reason for this approximation is to allow for an increased discretization of the region close to simulated repository in *Part 2*.

Present-day depth-distribution of salt content in fluids residing the Baltic Shield rocks is not well known on the regional scale. For the purpose of this study, the chloride measurements carried out in the deep core boreholes KLX01 and KLX02 at Laxemar were used for calibrating the simulations in *Part 1*. The locations of these boreholes coincide with the modeled cross section, with KLX01 located 500 m and KLX02 1,500 m from the seashore, respectively. KLX01 is about 1,100 m deep and KLX02 is about 1,700 m deep. The concentration profiles shown in *Figure 4* suggest that the fresh water lens is somewhat thicker in KLX02. Measurements yield that the salinity expressed as Total Dissolved Solids of the borehole fluid in KLX02 above 900 m depth is less than or equal to the present value of the Baltic Sea, which is about 0.7 % by weight (0.007 kg/kg or 7,000 ppm). At 1,700 m depth, the TDS value has increased to almost 7 % by weight, or ten times the present TDS value of the Baltic Sea (Follin, 1994). According to Laaksoharju *et al.* (1995) the bottommost water is very old.

For the simulation of *Part 1* the initial TDS concentration 10,000 years BP was assumed to vary linearly with depth between 0.7 % and 7 % throughout the modeled cross section. For an ambient isothermal temperature of +7 °C the linear TDS profile implies a linear fluid densitity profile ranging between 999,90 kg/m^3 at the top of the model to 1,049.40 kg/m^3 at the bottom.

The representation of the fractured heterogeneous shield rock as a porous medium tacitly implies that values used are in some sense mean or effective values of the heterogeneous fabric. Voss and Andersson (1993) provide a good presentation of continuum approximations and their discussion applies to the present study. For the purpose of this study different flow parameter combinations were tested based on findings from the Äspö HRL. The parameter values chosen for this study are shown in *Table 1*. The considered case consists of a heterogeneous porosity, a heterogeneous and anisotropic permeability, and a homogeneous and anisotropic dispersivity.

Table 1 *Chosen parameter values for Part 1. mbsl = meters below sea level, k = permeability, ϕ = porosity, α = dispersivity (longitudinal and transverse), D_m = molecular diffusivity. The meaning x and z is defined in Figure 3.*

Depth (mbsl)	k_x (m^2)	k_z (m^2)	ϕ (%)	α_L (m)	α_T (m)	D_m (m^2/s)
0 – 100	1.45 E–15	1.45 E–14	0.1–0.075	200	10	5 E–10
100 – 200	7.25 E–16	7.25 E–15	0.075–0.025	200	10	5 E–10
200 – 2,000	1.45 E–16	1.45 E–15	0.025	200	10	5 E–10

The solution to *Part 1* is shown in *Figure 5*. The reconstruction used in this study of the hydrological conditions during the Holocene between 10,000 BP and today leads to the interpretation that the present occurrence of saline ground water reflects an ongoing but incomplete flushing of the Baltic Shield. *Figure 5* provides the desired concentration distribution for the simulations in *Part 2*.

As shown in *Table 1* the values of the effective porosity and permeability values both decrease at depth. There is data from the Äspö HRL area to support this. For instance, Follin (1994) interpreted a long-term multi-packer interference test between KLX02 and KLX01 and concluded that both the transmissivity and storativity decrease at depth. La Pointe *et al.* (1995) analyzed packer-test and fracture data in parallel and concluded that the vertical component of the permeability tensor at Laxemar and the Äspö HRL is probably larger than the horizontal component in the east-west direction. The values of the principal components of the dispersivity tensor in *Table 1* are taken from Follin (1992), who analyzed the heterogeneity of ground water flow by means of particle tracking and Monte Carlo simulations based on the spatial variability of packer-test data from the Äspö HRL. Voss and Andersson (1993) used similar values.

Part 2 – Dewatering and Resaturation

Two cases A and B are studied. In case A the permeability of the model elements adjacent to the simulated repository is unaltered, whereas in case B it is lowered two orders of magnitude. The purpose of case B is to study the effect of a tentative excavation damaged zone close to a repository. Figure 6 shows the discretization of the simulated repository and its near-field. The distance between the center of the simulated repository and the seashore in Figure 6 is 1 km.

The simulation of the dewatering and resaturation phases requires a model for treating flow in the unsaturated zone. Unfortunately, there is no generally accepted model for unsaturated flow in sparsely fractured rock (Evans *et al.*, 1987). For the purpose of this study, van Genuchten's model (van Genuchten, 1980) is adopted. This model is implemented in SUTRA as an option by Voss (1984).

Figures 7 shows a close-up of *Figure 5* between 0–2 km from the seashore. The rectangle in *Figure 7* indicates the assumed location of the repository to be depressurized. *Figures 8 and 9* show the results of cases A and B, respectively, after fifty years of dewatering. The solid line represents zero (atmospheric) pressure (p=0). Ideally, this isobar should coincide with the dashed contour line that represents unit saturation (S=1.0). However, in order to achieve reasonable computation times it was necessary to relax the iterative convergence criterion for the nonlinear equations in SUTRA. In result, the accepted solutions are not perfect. The simulation of 50 years of dewatering required about 13 hours on a 90 MHz Pentium for a maximum model time step of 24 hours.

The extent of the water table decline is considerable for case A. As shown in *Figure 8* the entire region between the top side and the simulated repository is more or less unsaturated at the end of the simulation period. Most of this drawdown develops during the first two years of dewatering. Despite the closeness to the seashore, *Figure 8* suggests that the question of saline intrusion to a coastal repository may be a phenomenon that is dominated by vertical upconing rather than lateral infiltration from the sea. Moreover, in *Figure 8* the occurrence of saline ground water in the unsaturated zone above the repository is notable. The TDS value at the level of the simulated repository has increased about five times.

Field pressure data from the tunnel at the Äspö HRL yields that the hydraulic head at 450 m depth is close to hydrostatic right behind the tunnel wall (Rhén, 1995) and that the drawdown of the ground water table above the tunnel does not exceed 60 m at any location. This implies a low-permeability of the excavation damaged zone around the HRL tunnel. In *Figure 9*, the effective permeability of the most adjacent model elements is lowered two orders of magnitude compared to *Figure 8*. The decrease in drawdown is quite significant. This figure supports the standpoint that the excavation damaged zone has strong skin effect.

Figure 10 shows the simulation results for case A after fifty years of recovery. The location of the closed repository is indicated with a rectangle. Again, the solid line represent zero (atmospheric) pressure and for a perfect numerical solution this isobar should fall on top of the dashed contour line that represents unit saturation. *Figure 10* suggests an extensive residual drawdown of the ground water table for case A. The incomplete recovery may to some extent be due to the small fixed infiltration rate prescribed at the top side of the model. Notwithstanding, the interface between fresh and saline ground waters after fifty years of closure is close to the conditions prior to the dewatering phase (cf. *Figure 7*) despite the incomplete pressure recovery, which is an interesting result considering the objective of the study.

Conclusions

This study treats the question of saline intrusion to a deep coastal repository in Baltic Shield rocks. The motive is that long-term changes in the chemical environment associated with saline intrusion may affect the properties of the repository buffer zone material (bentonite). The reconstruction used in this study of the hydrological conditions during the Holocene between 10,000 BP and today leads to the interpretation that the present occurrence of saline ground water reflects an ongoing but incomplete flushing of the Baltic Shield. The simulations of fifty years of dewatering followed by fifty years of resaturation suggest that the final interface between fresh and saline ground waters may be close to the conditions prior to the dewatering phase.

Aknowledgments

The financial support provided by the Swedish Nuclear Fuel and Waste Management Company is gratefully acknowledged.

References

Evans, D.D & T. J. Nicholson, 1987. Flow and transport through unsaturated fractured rock, Geophysical Monograph 42, American Geophysical Union, Washington D.C.

Follin, S., 1992. Numerical calculations on heterogeneity of ground water flow, Technical Report 92–14, Swedish Nuclear Fuel and Waste Management Company, Stockholm.

Follin, S., 1994. Djupborrning KLX02, Etapp 1, Evaluation of the hydraulic testing of KLX02, Arbetsrapport 94–21, Swedish Nuclear Fuel and Waste Management Company, Stockholm.

La Pointe, P. R., P. Wallmann, P. and S. Follin, 1995. Estimation of effective block conductivities based on discrete network analyses using data from Äspö site, Technical Report 95–15, Swedish Nuclear Fuel and Waste Management Company, Stockholm.

Laaksoharju, M, J. Smellie, A.-C. Nilsson, and C. Skårman, 1995. Ground water sampling and chemical characterization of the Laxemar deep borehole KLX02, Technical Report 95–05, Swedish Nuclear Fuel and Waste Management Company, Stockholm.

Lindewald, H., 1985. Salt grundvatten i Sverige (Saline ground water in Sweden). Geological Survey of Sweden, Report No. 39, Uppsala.

Rhén, I., 1995. Documentation of tunnel and shaft data, tunnel section 2,874 – 3,600 m hoist and ventilation shafts 0 – 450 m, Äspö Hard Rock Laboratory Progress Report 25–95–28, Swedish Nuclear Fuel and Waste Management Company, Stockholm.

SNA, 1994. Sveriges Nationalatlas (The National Atlas of Sweden), Bokförlaget Bra Böcker, Höganäs.

van Genuchten, M. Th., 1980. A closed-form equation for predicting the hydraulic conductivity of unsaturated soils, Soil Science Society of America Journal, 44(5), 892–898.

Voss, C. I., 1984. SUTRA – A finite-element simulation model for saturated-unsaturated, fluid-density-dependent ground water flow with energy transport or chemically-reactive single-species solute transport, Water-Resources Investigation Report 84–4369, US Geological Survey, Reston.

Voss, C. I. and J. Andersson, 1993. Regional flow in the Baltic Shield during Holocene coastal regression, Ground Water, 31(6), 989–1006.

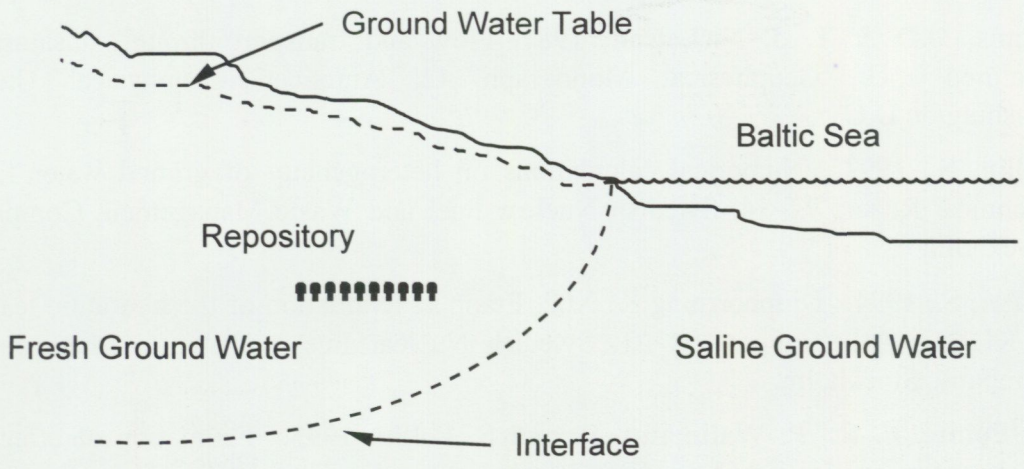


Figure 1 *Schematic cross section of the studied scenario.*

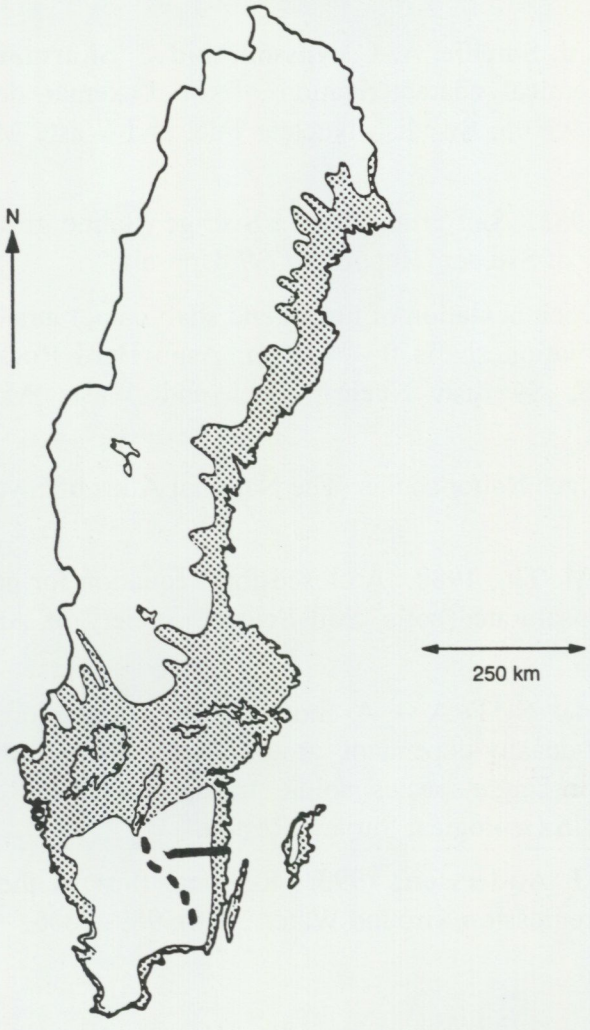


Figure 2 *Holocene marine limit in Sweden, about 10,000 years BP. Shaded region was inundated by sea water. The solid line shows the location of the modeled cross section. The dashed line shows an interpretation of the location of the major run off divide for the region of interest. Modified after Lindewald (1985).*

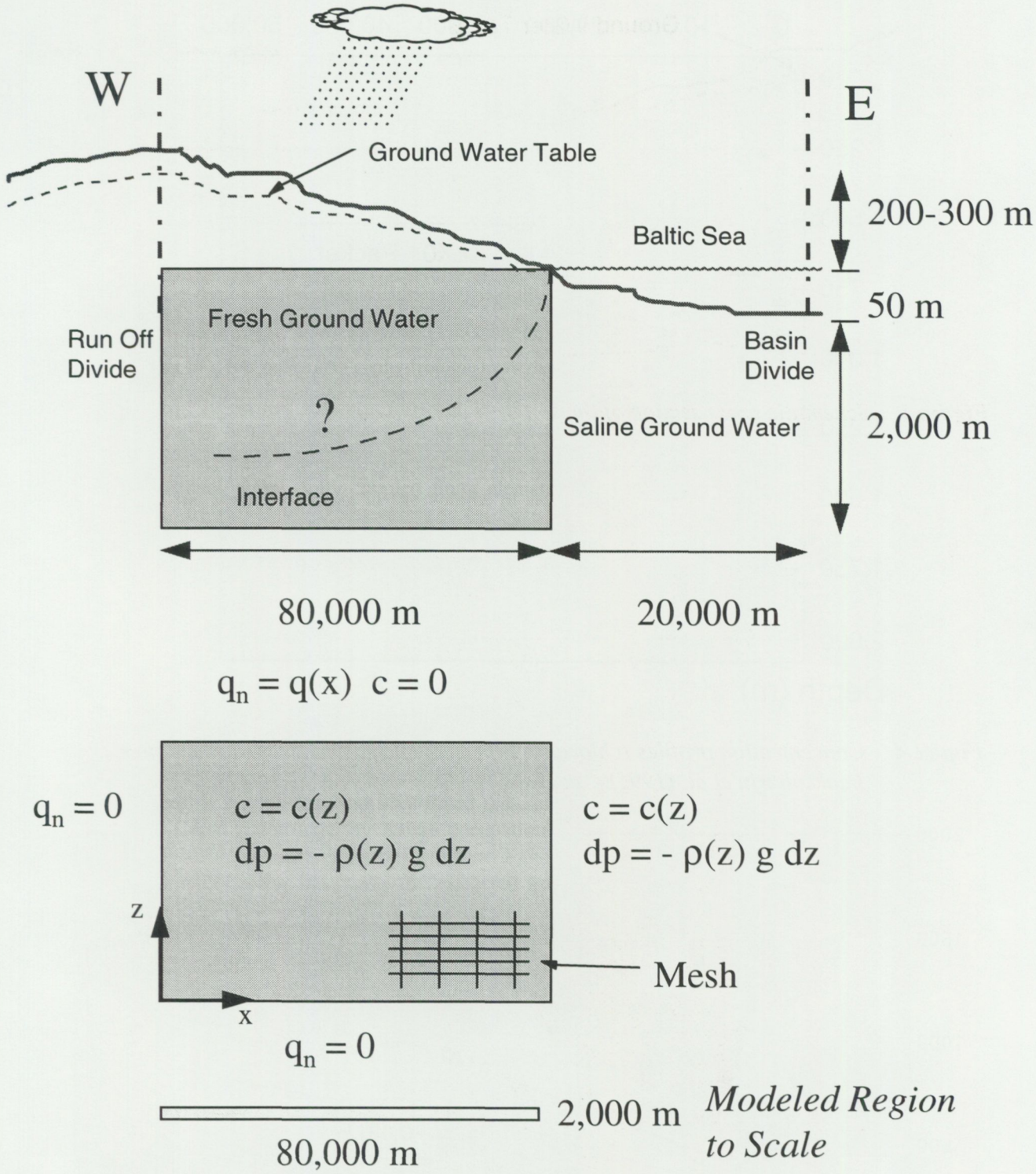


Figure 3 *The conceptual-numerical model used for Part 1. Model discretization mesh has 861 nodes and 800 elements (shaded area). Each element is 2 km long and 100 m deep.*

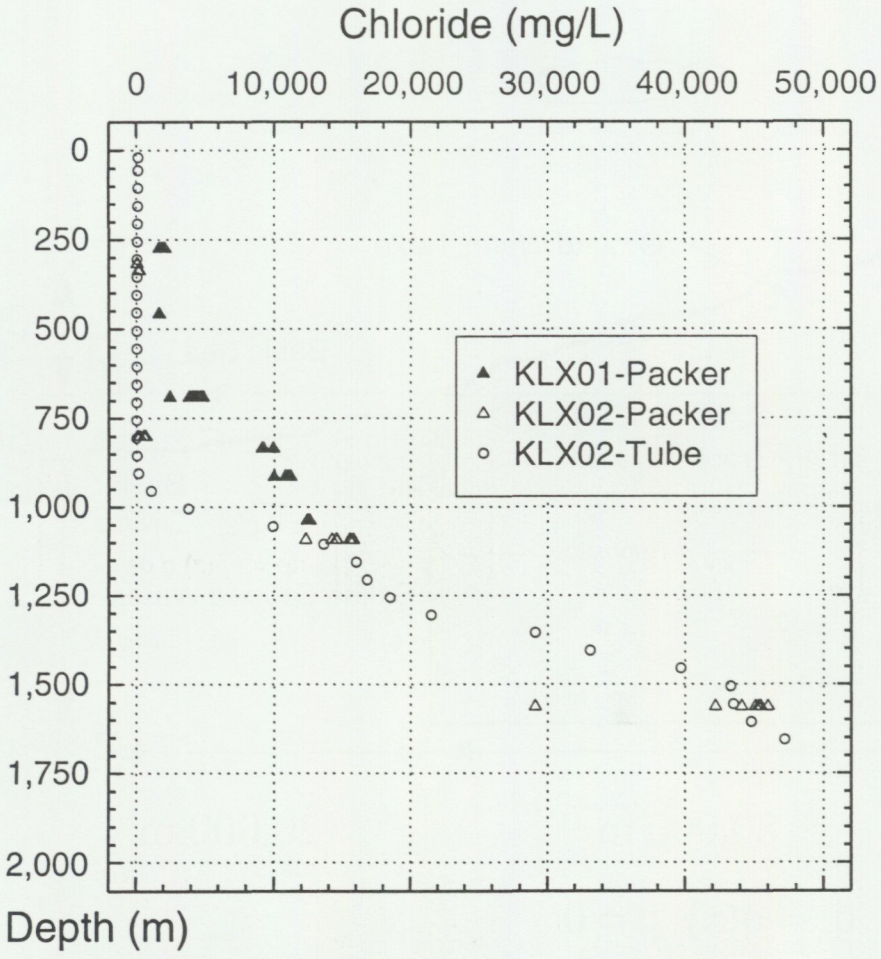


Figure 4 *Concentration profiles (chloride) from KLX01 and KLX02. Modified after Laaksoharju et al. (1995).*

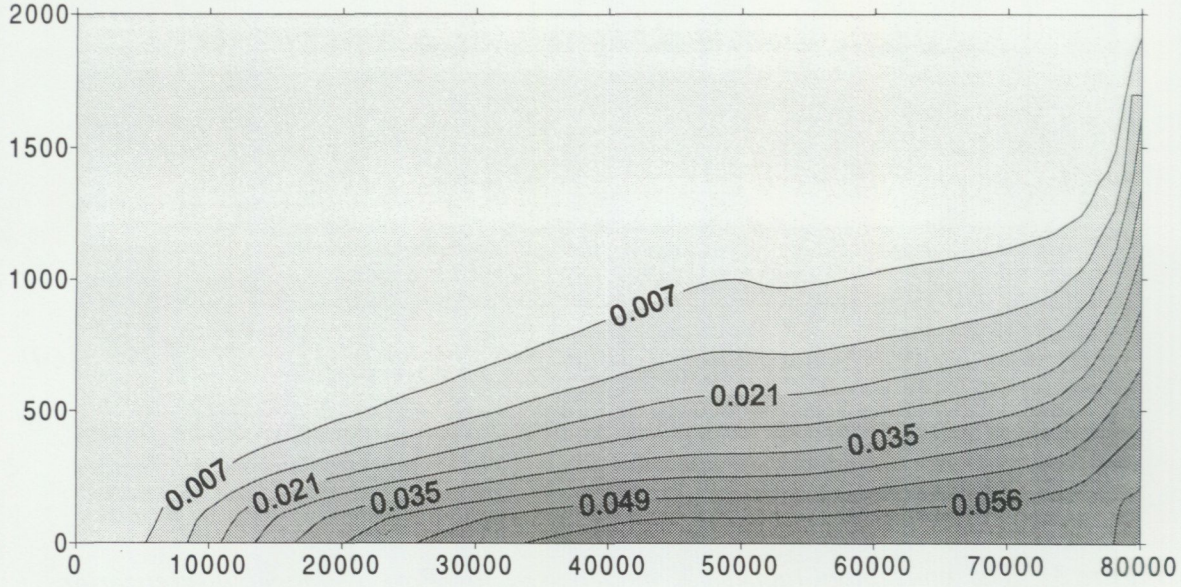


Figure 5 *Result of the model calibration in Part 1 for the parameter values and hydraulic conditions specified in Table 1 and Figure 3. The salinity contours are in kg TDS/kg solution. The conceptual locations of the (Chloride) contration profiles in Figure 4 are at 78,500 m (KLX02) and 79,500 m (KLX01).*

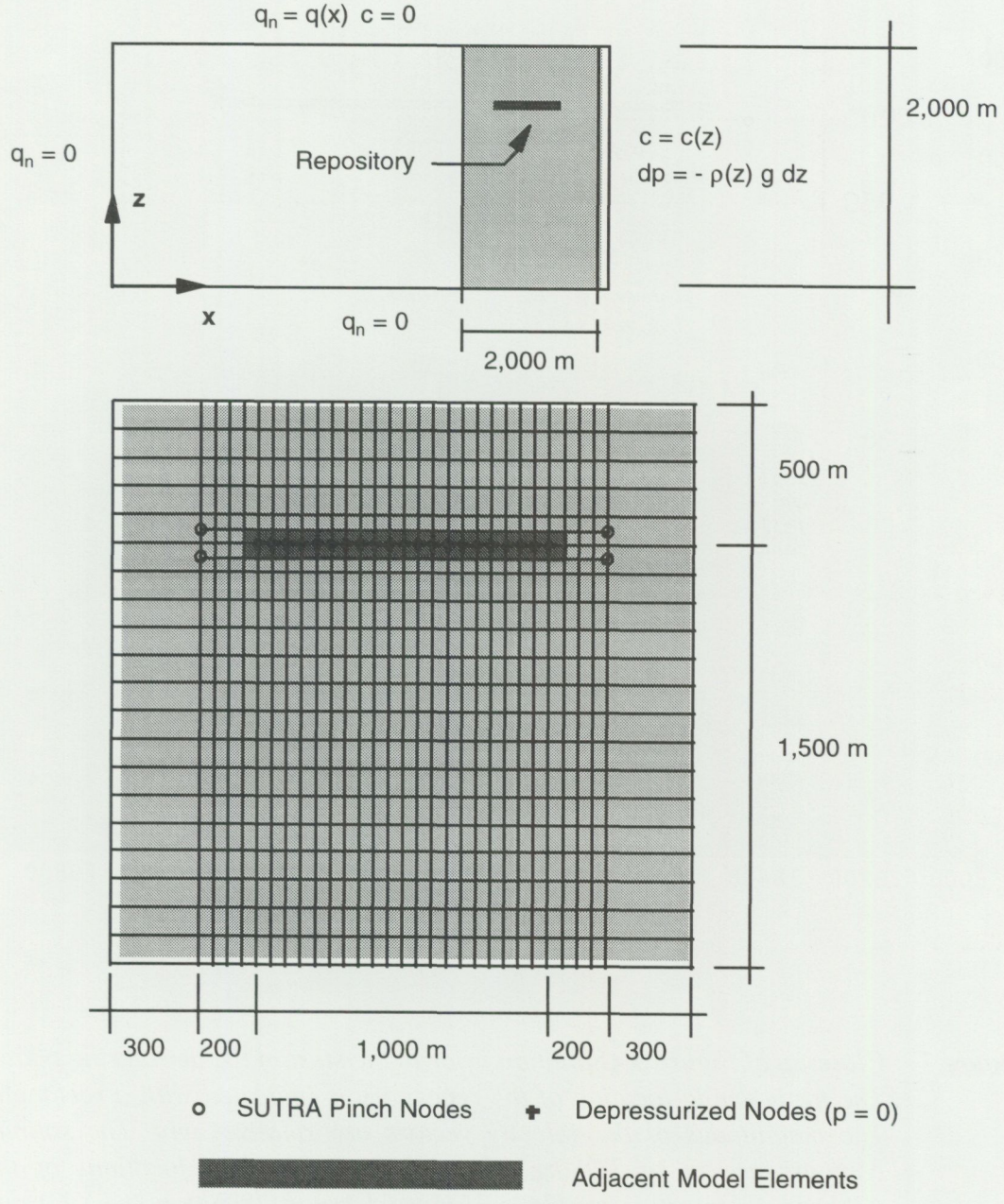


Figure 6 *Finite-element discretization for simulation of saline intrusion to a repository. The complete mesh consists of 1,528 nodes and 1,436 elements.*

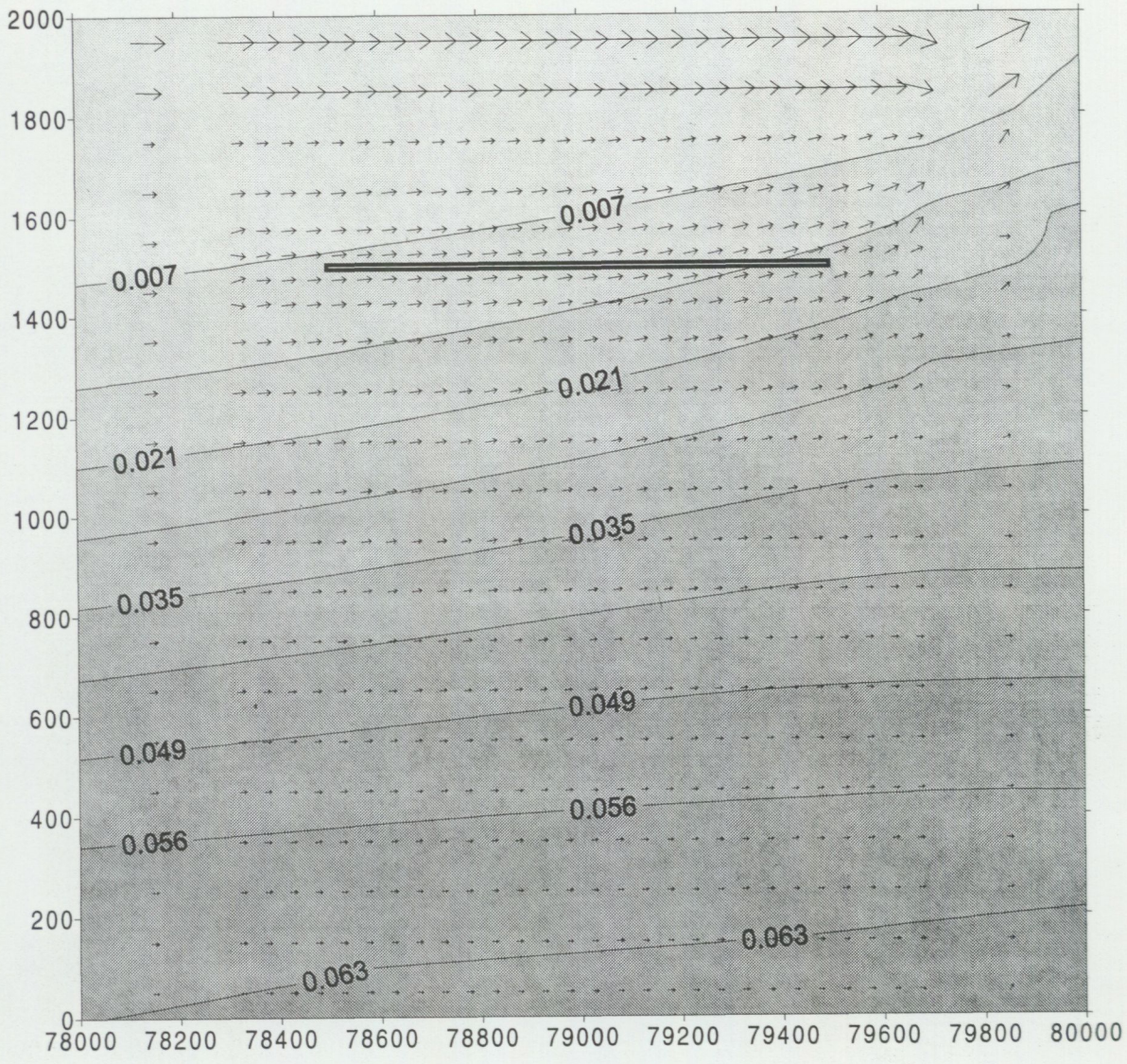


Figure 7 *Close-up of Figure 5 - Situation prior to the start of the dewatering phase. The forthcoming location of the repository is indicated with a rectangle. The magnitudes of the velocity vectors are relative only. The salinity contours are in kg TDS/kg solution. The conceptual locations of the (Chloride) contration profiles in Figure 4 are at 78,500 m (KLX02) and 79,500 m (KLX01).*

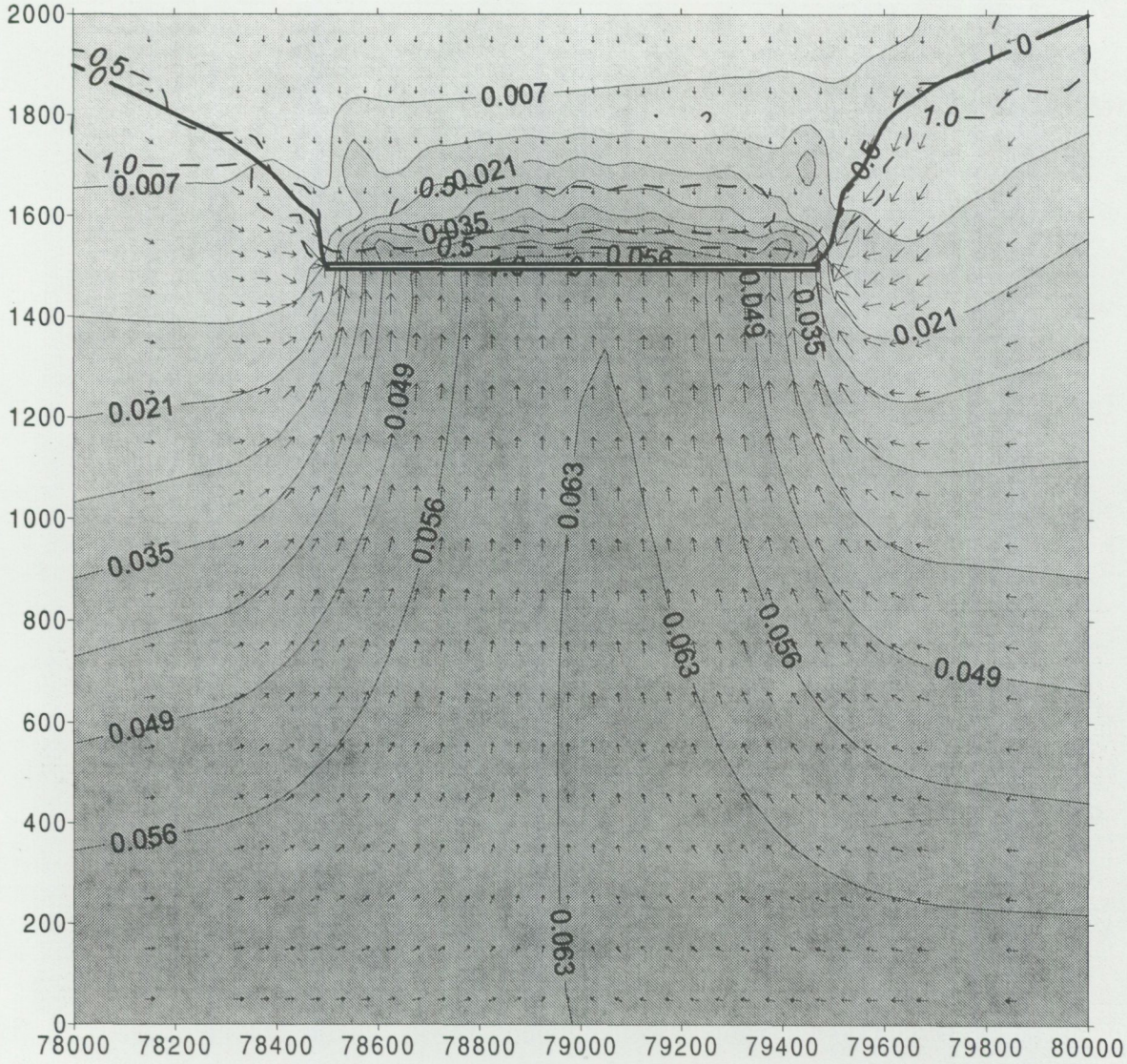


Figure 8 *Situation after 50 years of dewatering for case A (unaltered permeability close to the depressurized repository nodes).*

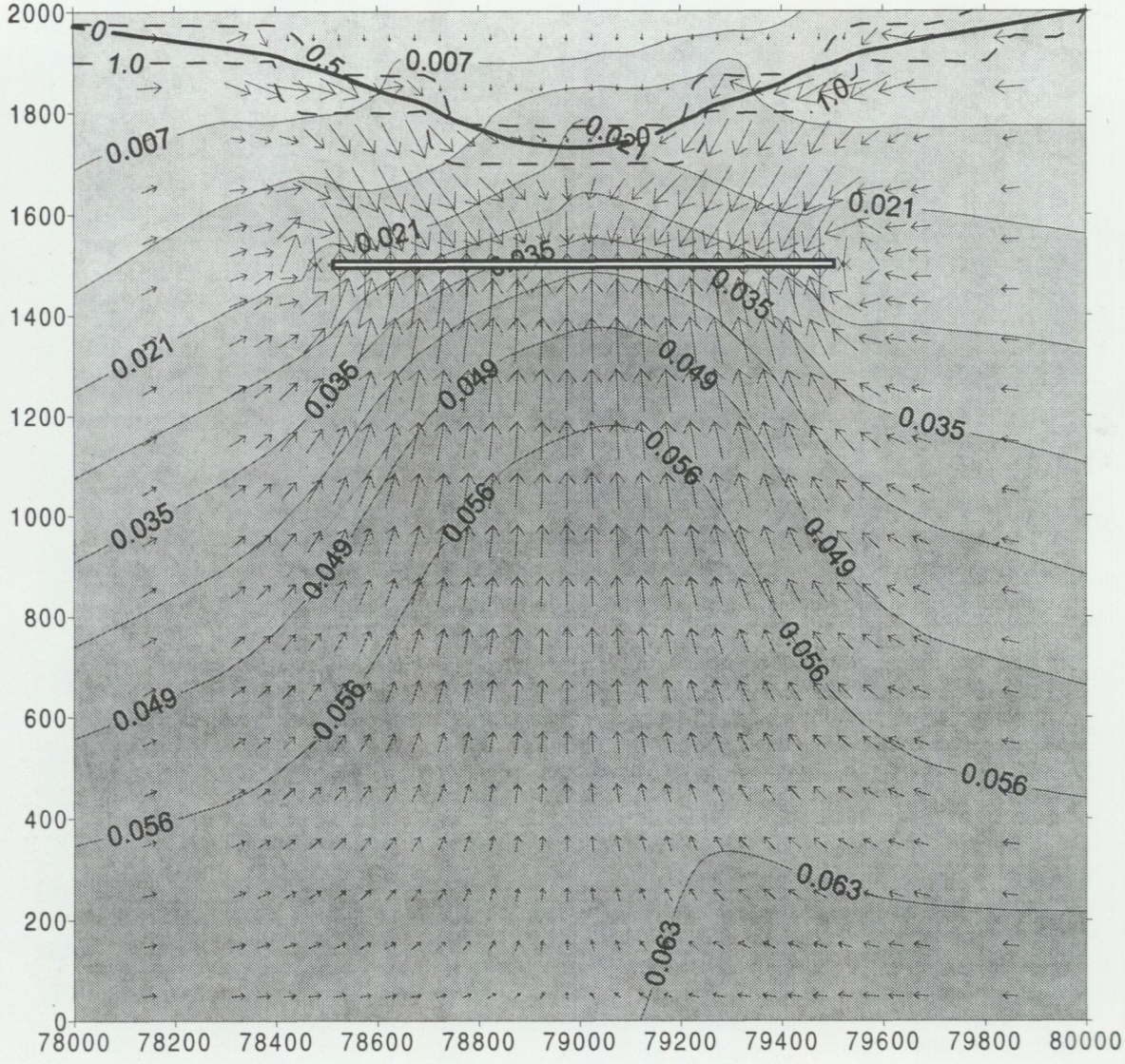


Figure 9 *Situation after 50 years of dewatering of case B (the permeability of the model elements adjacent to the repository is decreased 2 orders of magnitude with regard to case A).*

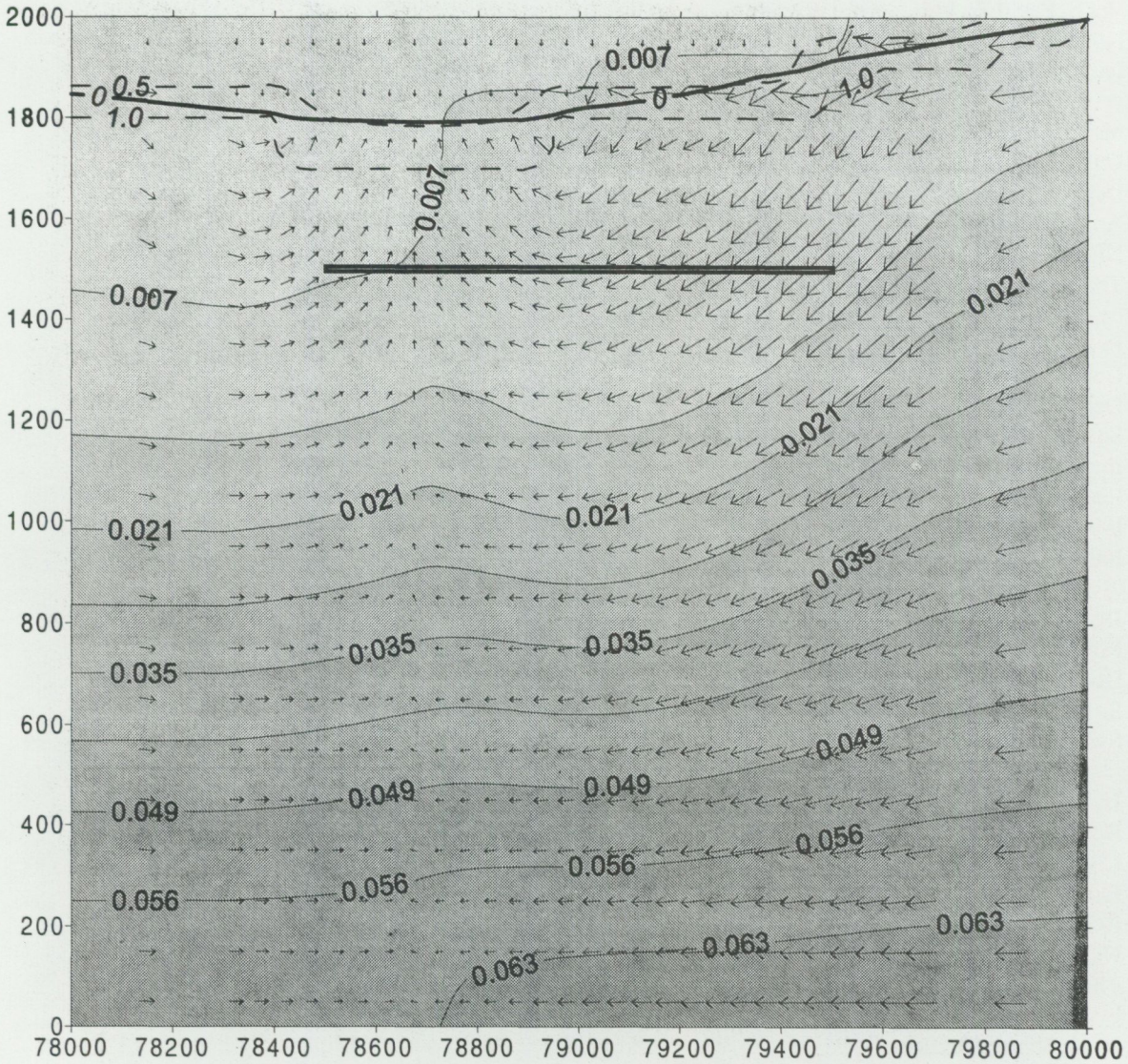


Figure 10 *Situation after 50 years of dewatering and 50 years of resaturation for case A.*

Participants

Prof. Aurelio Aureli
University of Catania
Via S. Paolo W. 66
I–95123 Catania
Italy

Mr. Steef S.J.A. van Baalen
University of Utrecht
Department of Physical Geography
A. Numankade 19
NL–3572 KP Utrecht
The Netherlands

Prof. Giovanni Barrocu
University of Cagliari
Department of Territorial Engineering
Sezione di Geologia Applicata, Facoltà di Ingegneria
Piazza d'Armi
I–09123 Cagliari
Italy

Dr. Göran Blomqvist
Royal Institute of Technology
Division of Land and Water Resources
S–100 44 Stockholm
Sweden

Ir. Reinder H Boekelman
Delft University of Technology
Civil Engineering Department, Hydrology and Ecology
P.O. Box 5048
NL–2600 GA Delft
The Netherlands

Prof., Dr. W. De Breuck
Geologisch Instituut S8
Krijgslaan 281
B–9000 Gent
Belgium

Mr. Gilbert Bruggeman
Nieuwe Weteringsweg 140
NL–3737 Groenekan
The Netherlands

Prof., Dr. Jan C van Dam
van der Horstlaan 9
NL–2641 RT Pijnacker
The Netherlands

Dr. Lars O Ericsson
Swedish Nuclear Fuel and Waste Management Co
P.O. Box 5864
S–102 48 Stockholm
Sweden

Mr. Leif Eriksson
Geological Survey of Sweden
P.O. Box 670
S–751 28 Uppsala
Sweden

Ir. John van Esch
Delft Geotechnics
P.O. Box 69
NL–2600 AB Delft
The Netherlands

Ms. Charlott Fabricius
Royal Institute of Technology
Division of Land and Water Resources
S–100 44 Stockholm
Sweden

Prof. Malin Falkenmark
Swedish Natural Science Research Council
P.O. Box 7142
S–103 87 Stockholm
Sweden

Ms. Dolores Fidelibus
Politecnico di Bari
Instituto Geologia Applicata e Geotecnica
Faculta di Ingegneria
Via Orabona 4
I–70125 Bari
Italy

Dr. Sven Follin
Golder Associates AB
Korta gatan 4
S–171 54 Solna
Sweden

Prof. Franco Francavilla
Universitá di Bologna
Dipartimento di Scienze della Terra
Via Zamboni 67
I–40126 Bolonga
Italy

Mr. Alf Grube
Forschungsgemeinschaft
Wasserwirtschaft und Wasserversorgung an der TU
Hamburg– Harburg
Dampfschiffsweg 11
D–21079 Hamburg
Germany

Mr. Ove Gustafsson
Geological Survey of Sweden
Kiliansgatan 10
S–223 50 Lund
Sweden

Assoc. Prof., Dr. Hüseyin Gökçekus
Near East University
Department of Civil Engineering
Via Mersin 10
Neu Nicosia, North Cyprus
Cyprus

Mr. Hans Jørgen Henriksen
Geological Survey of Denmark
Thoravej 8
DK–2400 København NV
Denmark

Lic. Emmanuel van Houtte
Intercommunale Waterleidingsmaatschppij van
veurne–AMB
Doornpanne 1
B–8670 Koksijde
Belgium

Prof. Gunnar Jacks
Royal Institute of Technology
Division of Land and Water Resources
S–100 44 Stockholm
Sweden

Ms. Eva–Lotta Johansson
Ormsta
Östragården
S–137 91 Västerhaninge
Sweden

Ms. Iréne Johansson
Swedish Natural Science Research Council
P.O. Box 7142
S–103 87 Stockholm
Sweden

Assoc. Prof. Nurkan Karahanoglu
Middle East Technical University
Department of Geological Engineering
06531 Ankara
Turkey

Prof., Dr. Bohdan Kozerski
Technical University of Gdansk
Hydrotechnics Faculty,
Narutowicza 11/12
PL–80 952 Gdansk
Poland

Dr. Marcus Laaksoharju
GeoPoint AB
Sollentunavägen 63
S–191 40 Sollentuna
Sweden

Mr. Gert Laursen
Rambøll
Jernbanevej 65
DK–5210 Odense NV
Denmark

Mr. Bo Leander
VBB
Geijersgatan 8
S–216 18 Malmö
Sweden

Mr. Per Leander
Department of Environmental and Public Health
Protection
S–205 80 Malmö
Sweden

Prof., Dr. Luc Lebbe
Nat. Fund. Scientific Research
Gent University
Geologisch Instituut
Krijgslaan 281
B–9000 Gent
Belgium

Mr. Johan Lindberg
Royal Institute of Technology
Division of Land and Water Resources
S–100 44 Stockholm
Sweden

Prof. George Matthess
Kiel University
Geological–Palaentological Institute and Museum
Olshausenstrasse 40–60
D–24118 Kiel
Germany

Dr. Kazuri Momii
Lund University
Department of Water Resources Engineering
P.O. Box 118
S–221 00 Lund
Sweden

Mr. Carl-Fredrik Müllern
Geological Survey of Sweden
Box 670
751 28 Uppsala
Sweden

Dr. Bo Olofsson
Royal Institute of Technology
Division of Land and Water Resources
S–100 44 Stockholm
Sweden

Ir. Theo N. Olsthoorn
Amsterdam Water Supply
Vogelenszangseweg 21
NL–2114 BA Vogelsenzang
The Netherlands

Dr. Dieter Ortlam
Niedersächsisches Landesamt für Bodenforschung
Aussenstelle Bremen
Werderstrasse 101
D–28199 Bremen
Germany

Mr. Sascha Oswald
Institut für Hydromechanik
UTH Hönggerberg, HIL
CH–8093 Zürich
Schweiz

Prof. Gualbert Oude Essink
Delft University of Technology
Civil Engineering Department, Hydrology & Ecology
P.O. Box 5048
NL–2600 GA Delft, The Netherlands

Prof. Giovanni Pranzini
Universitá di Firenze
Dipartimento di Scienze della Terra
via G. la Pira 4
I–50121 Firenze
Italy

Mrs. Anita Reslow
VBB
Geijersgatan 8
S–216 18 Malmö
Sweden

Dipl.–Geol. Axel Rogge
Universität Hannover
Institut für Geologie und Paläontologie
Callinstrasse 30
D–30167 Hannover
Germany

Drs. Hannie J.C. de Ruiter
WMO (Water Company Overijssel)
Afdeling Onderzoek
P.O. Box 10005
NL–8000 G A Zwolle
The Netherlands

Mr. F. Schaars
Amsterdam Water Supply
Vogelenszangseweg 21
NL–2114 BA Vogelsenzang
The Netherlands

Dr. Klaus–Peter Sengpiel
BRG Hannover
Postfach 510153
D–30631 Hannover
Germany

Prof. Giuseppe Spilotro
Universitá della Basilicata
Via della Resistenan 48/92
I–70125 Bari
Italy

M.Sc. Albert Stakelbeek
nv. PWN Water Supply Company of North Holland
P.O. Box 5
NL–2060 BA Bloemendaal
The Netherlands

Dr. Pieter–Jan Stuyfzand
KIWA
P.O. Box 1072
NL–3430 BB Nieuwegein
The Netherlands

Prof. Tiziano Tadolini
Politecnico di Bari
Facoltá di Ingeneria
Instituto di Geologia Applicata e Geotecnica
Via Orabona 4
I–0125 Bari
Italy

Prof Luigi Tulipano
Politecnico di Bari
Ist. Geologia Applicata e Geotecnica
Faculta di Ingegneria
Via Orabona 4
I–70125 Bari, Italy

Ing. Frans Vanlerberghe
Intercommunale Waterleidingsmaatschappij van veurne–AMB
Doornpanne 1
B–8670 Koksijde
Belgium

Prof. Antonio Vernier
University of Cagliari
Department of Territorial Engineering
Piazza D'Armi
I–09123 Cagliari
Italy

Dr. Peter Vogel
Federal Institute for Geosciences and Natural Resources
PO Box 510153
D–30631 Hannover
Germany

Dr. Josopait Volker
Nds. Landesamt für Bodenforschung
Post fach 510153
D–30631 Hannover
Germany

Prof., Dr. Kristine Walraevens
University of Gent
Lab. Applied Geology and Hydrogeology
Krijgslaan 281
B–9000 Gent
Belgium

Prof., Dr. Knut Wichmann
Technische Universität Hamburg–Harburg
Arbeitsbereich Wasserwirtschaft und Wasserversorgung
Dampfsciffsweg 11
D–21079 Hamburg
Germany

Dr. Alexander Yakirevich
J. Blaustein Institute for Desert Research
Ben–Gurion University of the Negev
Sede Boker Campus 84990
Israel

Dr. Yoseph Yechieli
Geological Survey of Israel
30 Malchei Israel St.
Jerusalem 95501
Israel

Mr. Yuecel Yurtsever
International Atomic Energy Agency
Section of Isotope Hydrology
Wagramerstr. 5
P.O. Box 100
A–1400 Vienna
Austria

The UNESCO Interdisciplinary Working Group for "Coasts and Small Islands"

Mrs Alice Aureli
UNESCO
Division of Water Sciences
1, rue Miollis
F–75732 Paris Cedex 15
France

Mr Said Mouline
1, rue Mhamed Boujendar
Km3, Route des Zaers
Rabat
Morocco

Mr Josep Ma. Serra Majem
Edifici, Z Carrer 60 N 5–27
Sector A, Zona Franca
E–08040 Barcelona
Spain

Ms Brigitte Colin
Habitat Programme
UNESCO
1, rue Miollis
F–75015 Paris
France

Mr Salvador Moreno Peralta
Arquitecto
Malaga

Prof Olof Wärneryd
Lund University
Department of Social and Economic Geography
Sölvegatan 23
S–223 62 Lund
Sweden

Presentations

Monday 17 June

08.00 **Registration** at S:t Gertruds, Bagersgatan 1, room: Bagersalen

Opening ceremony

Chairperson: Bo Leander

09.00 **Welcoming speech** by County Governor **Ann–Cathrine Haglund**

09.15 **Introductions**
Land and water mismanagement as reflected in groundwater degradation
Professor Malin Falkenmark

09.40 Salt water intrusion: Analysis, problems, solutions and research needs
Professor Jan C. van Dam

10.10 *Coffee*

Session 1. *Basic theories – mathematical modelling.*

10.40 **Chairperson: Dr Peter Vogel**

Key note speaker: **Professor Gualbert H. P. Oude Essink**
Modelling sea water intrusion in 3–D — Creating a virtual reality

11.00 Benchmarking in numerical modelling of density driven flow
Mr. Sascha Oswald, Germany
Paper written together with Mr Kinzelbach

11.20 3–dimensional density depended solute transport calculations of brackish groundwater near a deep–well infiltration system in the Dutch dune area
Ir. John van Esch, The Netherlands
Paper written together with M.Sc. Albert Stakelbeek

11.40 Variable density groundwater flow modelling with MODFLOW
Theo N. Olsthoorn, The Netherlands

12.00 Discussion

12.30 ***Lunch***

Session 2. *Hydrochemical characterization, chemical mixing and tracing of salt water.*

13.30 **Chairperson: Professor Gunnar Jacks**
Key note speech: Hydrochemistry and hydraulics of a couple of large South East Asian coastal aquifers — Apparent inconsistencies seen in the light of the climate history

13.50 ^{14}C-dating of sea water intrusion in the coastal aquifer of Israel
Dr. Yoseph Yechieli, Israel
Paper written together with Mr. Ronen and Mr. Vengosh

14.10 Salt groundwater in Sweden — Occurence and origin
Dr. Bo Olofsson, Sweden

14.30 Multivariate mixing calculations used to trace modern Baltic Sea water intrusion at Äspö, Sweden **Dr. Marcus Laaksoharju**, Sweden
Paper written together with Ms Skårman

15.00 ***Excursion***

19.30 ***Dinner***

Tuesday 18 June

Session 2 continues.

Chairperson: Professor Gunnar Jacks

08.30 Use of principal component analysis in hydrogeochemical characterization of an aquifer along the Mediterranean coast of Turkey
Assoc. Professor Nurkan Karahanoglu, Turkey

08.50 Isotope applications in the study of processes and dynamics of water salination **Mr. Yuecel Yurtsever**, Austria

09.10 Discussion

09.30 ***Coffee***

Session 3. *Investigation methodologies.*

10.00 **Chairperson: Professor W. de Breuck**
Keynote speech: Future research in coastal aquifers

10.20 Direct current through saline rock **Mr. Leif Eriksson**, Sweden

10.40 Improved delineation of saline groundwater by airborne electromagnetics — **Dr. Klaus–Peter Sengpiel**, Germany

11.00 Interaction of salt water/fresh water flow and hydrochemical zoning in an aquifer in the Pyrmont area, SW Lower Saxony
Dipl.–Geol. Axel Rogge, Germany
Paper written together with Mr. Groeztner and Mr. Scherler

11.20 Quality evolution of fresh and salt groundwater pumped near a drainage canal in the Western Flemish coastal plain
Lic. Emmanuel van Houtte, Belgium
Paper written together with Professor de Breuck, Professor, Dr. Lebbe and Ing. Vanlerberghe

11.50 How to lower salinization risks for well fields: Lessons from the Netherlands — **Dr. Pieter Jan Stuyfzand**, The Netherlands

12.10 Discussion

12.30 ***Lunch***

Session 4. *Salinization due to irrigation, road salts, waste deposits — its prevention, control and remediation.*

Chairperson: Reinder Boekelman

13.30 Degradation of groundwater quality in the Güzelyurt basin, Northern Cyprus — **Assoc. Prof. Hüsseyin Gökçekus**, Turkey
Paper written together with Prof. Doyuran

13.50 Risk mapping of ground water salinization using Geographical Information Systems — **Mr. Johan Lindberg**, Sweden
Paper written together with Ms McCarthy, Dr Gumbrich and Dr Olofsson

14.10 The method of pollution–tracer to measure lowest groundwater velocities in the city of Bremen — **Dr. Dieter Ortlam**, Germany

14.30 Artificial recharge in the Capoterra coastal aquifer system, Sardinia, Italy — **Professor Giovanni Barrocu**, Italy
Paper written together with Mr Sciabica, Mr Uras, Mr Gallo and Mr Muscas

14.50 Discussion

15.30 ***Coffee***

16.00	Poster presentation. The posters are presented in page 6. *Rapporteur:* **Dr Bo Olofsson**
19.00	***Reception at the Town Hall***
19.30	***Banquet***

Wednesday 19 June, a.m.

Session 5. *Regional and local case studies.*

Chairperson: Professor Giovanni Barrocu

08.30	Regional flow of intruding sea water in the carbonate aquifers of Apulia	**Ms. Dolores Fidelibus**, Italy *Paper written together with Professor Tulipano*
08.50	A hydrogeochemical system analysis to solve a salt water upconing problem	**Mr. Steef S.J.A. van Baalen**, The Netherlands *Paper written together with Drs. de Ruiter*
09.10	Groundwater salinization in Northern Germany – New developments in research	**Professor, Dr. Knut Wichmann**, Germany *Paper written together with Mr Grube*
09.30	Discussions	
09.50	Synthesis and conclusions	
10.30	***Coffee***	
11.30	***Departure for Post–Excursion***	

Posters

Session 1. Hydrochemical characterization, chemical mixing and tracing of salt water

Groundwater flow circuits in the karst aquifer (Apulia, Italy) as defined by the analysis of radon concentrations

Prof Tiziano Tadolini
Instituto di Geologia Applicata e Geotecnica, Italy
Paper written together with Mr Spizzico

Session 2 Basic theories - mathematical modelling

Modeling of brine transport in an aquifer crossing the Gorleben salt dome — Influence of initial conditions and hydrogeological settings

Dr Peter Vogel
Federal Institute for Geosciences and Natural Resources, Germany
Paper written together with Mr Schelkes

A quasi three-dimensional approach for simulating water flow and solute transport in the Vadoze zone and aquifer

Dr Alexander J Yakirevich
Blaustien Institute for Desert Research, Israel
Paper written together with Mr Borisov and Mr Sorek

Session 3. Investigation methodologies

The limited sea water intrusion resulting from the tectonic structural set-up of the Apulian Mesozoic platform in the Gargano

Prof Tiziano Tadolini
Instituto di Geologia Applicata e Geotecnica, Italy
Paper written together with Grassi

Session 4. Salinization due to irrigation, road salts, waste deposits - its prevention, control and remediation

Geogene and anthropogene salinization — phenomenous in the groundwater of Bremen

Dr Dieter Ortlam
Niedersächsisches Landesamt für Bodenforschung, Germany
Paper written together with Mr Sauer

Repeatability of geoelectrical investigations
Dr Jaana Aaltonen
Division of Land and Water Resources, Royal Institute of Technology, Sweden
Dr Göran Blomqvist
Division of Land and Water Resources, Royal Institute of Technology, Sweden

Salinization of private wells from de–icing chemicals — A pilote project in central Sweden
Ms Charlott Fabricius
Division of Land and Water Resources, Royal Institute of Technology, Sweden
Paper written together with Dr Olofsson

Session 5. Regional and local case studies

Groundwater salinization in southern Tuscany
Giovanni Pranzini
Dipartimento di Scienze della Terra, Italy
Paper written together with Mr Bencini

Hydrogeological and hydrochemical study of the coastal plains of Saidia and Bou–Areg (North-Eastern Morocco)
Prof Kristine Walraevens
Laboratory for Applied Geology and Hydrogeology, Belgium
Paper written together with Drs El Halimi, Chaouni Alia, Beeuwsaert and de Breuck

Geohydrological simulation of a deep coastal repository
Dr Sven Follin
Golder Associates AB, Sweden

Simulation of seawater intrusion in Libya
Assoc. Prof Nurkan Karahanoglu,
Middle East Technical University, Turkey
Paper written together with Mr Sadeg

Finite element simulation of saltwater — freshwater interrelations and their optimal management in an aquifer along the Mediterranean coast of Turkey
Assoc. Prof Nurkan Karahanoglu,
Middle East Technical University, Turkey
Paper written together with Mr Yaxicigil, Mr Emekil, Mr Hallaji and Mr Doyuran

Impact of sea level rise on Dutch groundwater regimes
Dr. Ir. Gualbert H.P. Oude Essink,
The Netherlands

I SGUs serie Rapporter och meddelanden har hittills utgivits:

*1. Utredning rörande det svenska jordbrukets kalkförsörjning 1–2. 1931.
*2. **Sahlström, K.E.** Sveriges lodade sjöar. 1945.
*3. **Ödman, O.H.** Rapport över manganmalmsletningen i Jokkmokks socken 1940–48.
4. **Stålhös, G.** Bidrag till kännedomen om den radioaktiva strålningens fördelning inom den svenska berggrunden. 1959.
5. **Johansson, H.G. och Ericsson, B.** Grusutredningen -74. Översiktlig inventering av sand- och grusförekomster – Försöksverksamhet. 1976.
*6. **Knutsson, G., m.fl.** Grustillgångarna i Östersundsområdet. Del 1 inventering. 1976.
*7. **Ericsson, B.** Svallgrustillgångar längs Kilsbergen, Örebro län. 1977.
8. **Gustafsson, O. och De Geer, J.** Skånes större grundvattentillgångar. 1977.
9. **Knutsson, G. och Fagerlind. T.** Grundvattentillgångar i Sverige. 1977.
10. **Modig, S., Knutsson, G., Nordberg, L. och Persson, G.** Särtryck ur Ymer 1978 – Bebyggelsen och vattnet. 1978.
11. **Guy-Ohlson, D.** Jurassic biostratigraphy of three borings in NW Scania. (A brief palynological report.) 1978.
12. **Gustafsson, O., Andersson, J.-E. och De Geer, J.** Sammanställning av hydrogeologiska data från Kristianstadsslätten. 1979.
13. **Hörnsten, Å.** Sand och övriga jordarter i Öresund. Maringeologiska kartor över Öresund. 1979.
*14. Hydrogeologi vid SGU. Särutgåva av Vannet i Norden. 1979.
15. **Knutsson, G., Lindén, A. och Rudmark, L.** Grus- och moräntillgångar i Nybroregionen. 1979.
16. **Wilson, M.R. och Sundin, N.O.** Isotopic age determinations on rocks and minerals from Sweden. 1960–1978.
17. **Karlqvist, L. och Qvarfort, U.** Modell för simulering av utbytesförlopp i ett sand–bentonitskikt. 1980.
18. **Karlqvist, L. och Qvarfort, U.** Gruvhanteringens inverkan på Bersboområdet, Åtvidabergs kommun. 1980.
19. **Wilson, M.R. and Åkerblom, G.** Uranium enriched granites in Sweden. 1980.
*20. **Cato, I och Engdahl, M.** Beskrivning till temakartor utvisande var särskild uppmärksamhet av stabilitetsförhållanden erfordras inom vissa bebyggda eller detaljplanerade områden med lerjord. 1982.
21. **Olsson, T.** Ground-water-level fluctuations as a measure of the effective porosity and ground-water recharge. 1980.
22. **Bergström, J. och Shaikh, N.A.** Malmer, industriella mineral och bergarter i Kristianstads län. Projekt i länsplanering 1980. 1980.
23. **Lilja, A.** Störning av berggrundens temperaturförhållanden vid hammarborrning. 1981.
24. **Agrell, H.** Gotska Sandöns kvartärgeologi. (Summary: The Quaternary geology of the island of Gotska Sandön in the Baltic.) 1981.
25. **Laufeld, S.** (Ed.). Proceedings of Project Ecostratigraphy Plenary Meeting, Gotland, 1981. 1981.
26. **Fredén, C., m.fl.** Tuveskredet, 1977-11-30. Geologiska undersökningar. Särtryck av SGI Rapp. 11 B. 1981.
27. SWIM 81. Intruded and relict groundwater of marine origin. Proceedings of Seventh Salt Water Intrusion Meeting, Uppsala, Sweden, 14–17 September 1981. 1981.
28. **Aastrup, M., Aneblom, T., Henriksson, B. och Persson, G.** PMK-grundvatten. Lägesrapport mars 1982. 1982.
29. Energigeologi. Exempel på verksamhet inom energisektorn vid SGU. April 1982.

30. **Åkerblom, G. and Wilson, C.** Radon – geological aspects of an environmental problem. 1982.
31. **Bergström, J. och Shaikh, N.A.** Malmer, industriella mineral och bergarter i Malmöhus län. 1982.
32. **Ericsson, B. och Grånäs, K.** SGU:s grusdataarkiv. 1983.
33. **Sivhed, U.** Upper Cretaceous Ostracodes from the Malen Limestone quarry and the river Stensån, southern Sweden. 1983.
34. Berggrundsgeokemi som prospekteringsmetod i Sveriges urberg. Föredrag och inlägg från ett symposium i Uppsala den 17–18 mars 1983 anordnat av Sveriges geologiska undersökning och Svenska Gruvföreningen. O. Selinus (Red.). 1983.
35. Vanadin. 1984.
37. **Andersson, M. och Ohlsson, S.-Å.** Geokemisk kartering. 1984.
38. **Lundqvist, Th.** Färg- och teckenschema för SGU:s berggrundskartering. 1984.
39. **Lindewald, H.** Salt grundvatten i Sverige. 1985.
40. **Guy-Ohlson, D. and Malmquist, E.** Lower Jurassic biostratigraphy of the Oppegård Bore No. 1, NW Scania, Sweden. 1985.
41. **Andersson, M.** Geokemisk kartering. Tungmineralanrikad morän. Kartbladen 15–16, C–D och 16–17, G. 1985.
42. **Ressar, H. och Ohlsson, S.-Å.** Geokemisk kartering. Bäcktorv. Bilaga: Beskrivning av de fjorton spårelementens exogena geokemiska kretslopp av John Ek. 1985.
43. Grundvattennätet. Svenskt vattenarkiv. 1985.
44. Grundvattenkvalitet. Svenskt vattenarkiv. 1985.
45. **Shaikh, N.A., Samuelsson, L., Sundberg, A. och Wik, N.-G.** Malmer, industriella mineral och bergarter i Älvsborgs län. 1986.
46. **Fredén, C.** Quaternary marine shell deposits in the region of Uddevalla and Lake Vänern. 1986.
47. **Ahlberg, P.** Den svenska kontinentalsockelns berggrund. 1986.
48. **Ressar, H., Ohlsson, S.-Å. och Ekelund, L.** Geokemiska kartan. Tungmetaller i Bäcktorv. Översiktskartbladen Kalmar, Oskarshamn, Sundsvall och Vilhelmina. 1986.
49. **Ressar, H., Ohlsson, S.-Å. och Ekelund, L.** Geokemiska kartan. Tungmetaller i Bäcktorv. Översiktskartbladen Malmö och Sundsvall. 1987.
50. **Shaikh, N.A., Persson, L., Sundberg, A. och Wik, N-.G.** Malmer, industriella mineral och bergarter i Jönköpings län. 1989.
51. **Ressar, H., Ekelund, L. och Ohlsson, S.-Å.** Biogeokemiska kartan. Tungmetaller i Bäckvattenväxter. Översiktsbladen Göteborg och Borås. 1988.
52. **Gustafsson, O., Jonasson, S.A. och Andersson, C.** Grundvattenundersökningar på Kristianstadsslätten 1976–1987. 1988.
53. **Andersson, M.** Markgeokemiska kartan 18–22, G–I. 1988.
54. **Shaikh, N.A., Karis, L., Kumpulainen, R., Sundberg, A. och Wik, N.-G.** Kalksten och dolomit i Sverige. Del 1. Norra Sverige. 1989.
55. **Shaikh, N.A., Karis, L., Snäll, Sundberg, A. och N.-G. Wik.** Kalksten och dolomit i Sverige. Del 2. Mellersta Sverige. 1989.
56. **Shaikh, N.A., Bruun, Å., Karis, L., Kjellström, G., Sivhed, U., Sundberg, A. och Wik, N.-G.** Kalksten och dolomit i Sverige. Del 3. Södra Sverige. 1990.
57. **Modig, H., Miller, U. och Robertsson, A.-M.** Karbonat i jord. Del 4. Försurning i äldre sedimentlagerföljder med anknytning till och i jämförelse med nutid. 1990.
59. **Andersson, M.** Markgeokemiska kartan 16–18, G–I. 1989.
60. **Ressar, H., Ekelund, L. och Ohlsson, S.-Å.** Biogeokemiska kartan 14–16, G–H. Tungmetaller i bäckvattenväxter. 1990.
61. **Kornfält, K.-A., Samuelsson, L., Sundberg, A., Wik, N.-G. och Wikman, H.** Malmer, industriella mineral och bergarter i Kronobergs län. 1990.
62. **Andersson, M.** Markgeokemiska kartan 18–21, H–J. 1990.

63. **Ressar, H., Ekelund, L. och Ohlsson, S.-Å.** Biogeokemiska kartan 8–10, A–D. tungmetaller i bäckvattenväxter. 1990.
64. **Cato, I.** Sedimentundersökningar i Brofjorden särskilt Trommekilen 1989, samt förändringar efter 1972 och 1984. 1990.
65. **Bruun, Å., Kornfält, K.-A., Sundberg, A., Wik, N.-G., Wikman, H. och Wikström, A.** Malmer, industriella mineral och bergarter i Kalmar län. 1991.
66. **Frietsch, R., Sundberg, A. och Wik, N.-G.** Register över svenska fyndigheter av malmmineral och industriella mineral och bergarter. 1991.
67. **Robertsson, A.-M.** Strandförskjutningen i Eskilstunatrakten för ca 9000 till 4000 år sedan. 1991.
68. **Ressar, H., Ekelund, L. och Ohlsson, S.-Å.** Biogeokemiska kartan 5–7, I–K och 8–10, E–G. Tungmetaller i bäckvattenväxter. 1991.
69. **Selinus, O.** (ed.). 2nd International Symposium on Environmental Chemistry. (Abstracts). 1991.
70. **Andersson, M.** Från Falkenberg till Blomstermåla; nuläge och framtida effekter av syrabelastning. 1992.
71. **Hopsu, V.** Norbergs gruvor på 1960-, 70- och 80-talen. 1992.
72. **Gustafsson, O.** Radonhalten i grundvatten från granitområden i Malmöhus län. 1992.
73. **Andersson, M. och Nilsson, C.A.** Markgeokemiska kartan 3–7, F–H. 1992.
74. **Cato, I.** Sedimentundersökningar längs Bohuskusten 1990 – Göteborgs och Bohus läns kustvattenkontroll. 1992.
75. **Ekelund, L., Nilsson, C.-A. och Ressar, H.** Biogeokemiska kartan 8–10, G–J och 11–12, H–J. Tungmetaller i bäckvattenväxter. 1993.
76. **Stephens, M.B. and Wahlgren, C.-H. (Conveners).** Workshop. Ductile shear zones in the Swedish segment of the Baltic Shield. Abstracts and excursion guide. Uppsala 1993.
77. **Sander, A.** Värderingsmodell för naturresurser. Tillämpning på ballasttillgångar. 1993.
78. **Nilsson, C.-A. och Ressar, H.** Biogeokemiska kartan 11–12, E–H, 12–13, G–J. Tungmetaller i bäckvattenväxter. 1995.
79. **Wahlgren, C.-H. (red.).** Regional berggrundsgeologisk undersökning. Sammanfattning av pågående undersökningar 1994. 1995.
80. **Bruun, Å., Nilsson, C.-A., Sundberg, A., Wik, N.-G. och Wikström, A.** Malmer, industriella mineral och bergarter i Östergötlands län. 1995.
81. **Andersson, M. och Nilsson, C.-A.** Markgeokemiska kartan 7–9, D–E, 7–9, E–H. 1995.
82. **Kornfält, K.-A., Andersson, M., Daniel, E. och Persson, M.** Kadmium i marken i sydöstra Skåne. 1996.
83. **Robertsson, A.-M., Erlström, M., Damell, D., Qvarfort, U. och Fredriksson, D.** Bakgrundsdata för metaller – surhet och landskapsutveckling från sedimentundersökningar. Sammanställning av data från Örebro. 1996.
84. **Wahlgren, C.-H. (red.).** Regional berggrundsgeologisk undersökning. Sammanfattning av pågående undersökningar 1995. 1996.
85. **Andersson, M. och Lax, K.** Markgeokemiska kartan 20–22, J–L. 1996.
86. **Selinus, O. (red.).** Miljögeologi. Kartor för samhällsplanerare och miljövårdare. Exempel från Mittnordenområdet. 1996.

* Utgången



Distribution

SGU
Box 670
S-751 28 Uppsala
Sweden
Tel 018-17 90 00 / + 46 18 17 90 00
Fax 018-17 92 10 / + 46 18 17 92 10

Printed by Gotab, Stockholm 1996

ISBN 91-7158-572-9
ISSN 0349-2176